

# **FINITE ELEMENT METHODE**



## **A projekt keretében elkészült tananyagok:**

Anyagtechnológiák

Materials technology

Anyagtudomány

Áramlástechnikai gépek

CAD tankönyv

CAD book

[CAD/CAM/CAE elektronikus példatár](#)

CAM tankönyv

Méréstechnika

Mérnöki optimalizáció

Engineering optimization

Végeselem-analízis

Finite Element Method



Budapest University of Technology and Economics

Faculty of Mechanical Engineering

Óbuda University

Donát Bánki Faculty of Mechanical and Safety Engineering

Szent István University

Faculty of Mechanical Engineering

# FINITE ELEMENT METHODE

Editor:

**ÁDÁM KOVÁCS**

Authors:

**ISTVÁN MOHAROS**

**ISTVÁN OLDAL**

**ANDRÁS SZEKRÉNYES**



**2012**

COPYRIGHT: © 2012-2017, Ádám Kovács, András Szekrényes, Budapest University of Technology and Economics, Faculty of Mechanical Engineering;  
István Moharos, Óbuda University, Donát Bánki Faculty of Mechanical and Safety Engineering;  
István Oldal, Szent István University, Faculty of Mechanical Engineering

READERS: Ágnes Horváthné Varga, István Keppler, Lajos Pomázi, József Uj

Creative Commons NonCommercial-NoDerivs 3.0 (CC BY-NC-ND 3.0) ©

This work can be reproduced, circulated, published and performed for non-commercial purposes without restriction by indicating the author's name, but it cannot be modified.

ISBN 978-963-687-1

PREPARED UNDER THE EDITORSHIP OF [Typotex Publishing House](#)

RESPONSIBLE MANAGER: Zsuzsa Votisky

GRANT:

Made within the framework of the project Nr. TÁMOP-4.1.2-08/2/A/KMR-2009-0029, entitled „KMR Gépészmechnöki Karok informatikai hátterű anyagai és tartalmi kidolgozásai” (KMR information science materials and content elaborations of Faculties of Mechanical Engineering).

Nemzeti Fejlesztési Ügynökség  
[www.ujszchenyiterv.gov.hu](http://www.ujszchenyiterv.gov.hu)  
06 40 638 638



A projekt az Európai Unió támogatásával, az Európai Szociális Alap társfinanszírozásával valósul meg.

KEYWORDS:

Finite Element Method, ANSYS, COSMOS/M, rods, beam, plane stress, plane strain, beam structure, axisymmetric, plate, shell

SUMMARY:

The history of the finite element model, its mathematical foundation and its role in mechanical engineering design are presented. The necessary basic continuummechanical notions and equations for understanding of the method are also discussed. Element types the most commonly used in design (rod, beam, plane, axisymmetric, thin plate, shell) are described. Starting from the principle of total principle energy the derivation of matrix equilibrium equation related to linear elastic bodies discretized in space and the structure of coefficient matrices for different models are shown. In case of beam structures the structure of equation of motion and the method of eigenfrequency calculation are also presented.

Understanding of theoretical chapters are highly facilitated by the large number of solved examples and the detailed discussion of solution of real problems obtained from industry.

# CONTENTS

|        |  |    |
|--------|--|----|
| 1.     | HISTORY OF FINITE ELEMENT METHOD INCLUDING ITS EVOLUTION, EXTENSION AND ROLE OF APPLICATION IN MECHANICAL ENGINEERING DESIGN.....                          | 11 |
| 1.1.   | Ancient application .....  | 11 |
| 1.2.   | History of variation of calculus, basic definitions .....  | 12 |
| 1.2.1. | <i>Brachistochrone problem</i> .....   | 12 |
| 1.2.2. | <i>Functionals, variations</i> .....   | 14 |
| 1.2.3. | <i>Direct method</i> .....   | 16 |
| 1.3.   | Ritz-method.....   | 18 |
| 1.4.   | Evolution of modern finite element method .....  | 20 |
| 1.4.1. | <i>Force method</i> .....  | 20 |
| 1.4.2. | <i>Motion method</i> .....   | 20 |
| 1.5.   | Finite element method in engineering practice .....  | 21 |
| 1.6.   | Appendix .....   | 22 |
| 1.6.1. | <i>Principals of calculus of variation</i> .....   | 22 |
| 1.6.2. | <i>Euler-Lagrange differential equation</i> .....  | 23 |
| 2.     | FOUNDAMENTAL DEFINITIONS IN CONTINUUM MECHANICS. DIFFERENTIAL EQUATION SYSTEM OF ELASTICITY AND ITS BOUNDARY ELEMENTS PROBLEM. ....                        | 25 |
| 2.1.   | Fundamental definitions in continuum mechanics.....  | 25 |
| 2.2.   | Differential equation system and boundary element problem of Elasticity .....  | 33 |
| 2.2.1. | <i>Equilibrium equations</i> .....   | 33 |
| 2.2.2. | <i>Geometric equations</i> .....   | 36 |
| 2.2.3. | <i>Constitution equations (material equations)</i> .....   | 40 |
| 2.2.4. | <i>Boundary conditions</i> .....   | 41 |
| 2.2.5. | <i>Boundary element method</i> .....   | 42 |
| 3.     | ENERGY THEOREM OF ELASTICITY, CALCULUS OF VARIATION, FINITE ELEMENT METHOD, DETERMINATION OF STIFFNESS EQUATION IN CASE OF CO-PLANAR, TENSED ELEMENT ..... | 43 |
| 3.1.   | Approximate functions.....   | 43 |
| 3.1.1. | <i>Kinematically admissible displacement field</i> .....   | 43 |
| 3.2.   | Principle of virtual energy.....   | 44 |
| 3.3.   | Principle of minimum potential energy .....  | 45 |
| 3.4.   | Principle of Lagrange variation.....   | 47 |
| 3.5.   | Finite element model based on displacement method .....  | 48 |
| 3.5.1. | <i>Introduction of vector fields</i> .....   | 48 |
| 3.5.2. | <i>Elasticity problem and the method of solution</i> .....   | 51 |
| 3.5.3. | <i>Finite element, approximate displacement field</i> .....  | 52 |
| 3.6.   | Definition and solution of stiffness matrix in case of co-planar tensed truss element  | 55 |
| 3.6.1. | <i>Stiffness matrix of 2D, tensed, truss element</i> .....   | 55 |
| 3.6.2. | <i>Example</i> .....   | 60 |
| 4.     | ANALYSIS OF TWO-DIMENSIONAL TRUSSES USING FINITE ELEMENT METHOD BASED PROGRAM SYSTEM .....   | 64 |
| 4.1.   | Two-dimensional bar structures.....  | 64 |

|   |            |
|---|------------|
| 4.2. Finite elements for modeling beams .....   | 64         |
| 4.2.1. <i>The TRUSS element properties</i> .....  | 65         |
| 4.2.2. <i>Beam Element's properties</i> .....   | 66         |
| 4.3. Study solution .....   | 66         |
| 4.4. Remarks .....  | 75         |
| <b>5. TWO-DIMENSIONAL BENT BARS VARIATION PROBLEM, STIFFNESS EQUATIONS AND SOLVING THEM BY FINITE ELEMENT METHOD.....</b>                                       | <b>76</b>  |
| 5.1. Two-dimensional bent beam element variation study .....  | 76         |
| 5.2. Solving the problem using finite element method .....  | 77         |
| 5.2.1. <i>The element stiffness matrix</i> .....  | 78         |
| 5.2.2. <i>The entire structure stiffness matrix</i> .....   | 84         |
| 5.2.3. <i>The complete equations system and the solution</i> .....  | 85         |
| 5.3. Remarks .....  | 86         |
| <b>6. ANALYSIS OF TWO-DIMENSIONAL BENT BARS USING FINITE ELEMENT METHOD BASED PROGRAM SYSTEM .....</b>  | <b>87</b>  |
| 6.1. Planar beam structures .....   | 87         |
| 6.2. The used finite elements in modeling .....   | 87         |
| 6.2.1. <i>Properties of the BEAM element</i> .....  | 87         |
| 6.2.2. <i>The shear deformation</i> .....   | 88         |
| 6.3. The study solution.....  | 90         |
| 6.4. Remarks .....  | 104        |
| <b>7. APPLICATION THE PRINCIPLE OF THE MINIMUM POTENTIAL ENERGY IN FIELD OF THREE-DIMENSIONAL BENT BAR ELEMENTS, RITZ METHOD AND FINITE ELEMENT METHOD.....</b> | <b>105</b> |
| 7.1. Three-dimensional bent bars variational problem .....  | 105        |
| 7.2. Solving the problem using finite element method .....  | 110        |
| 7.3. Remarks .....  | 113        |
| <b>8. ANALYSIS OF THREE-DIMENSIONAL BENT BARS USING FINITE ELEMENT METHOD BASED PROGRAM SYSTEM .....</b>  | <b>114</b> |
| 8.1. Three-dimensional beam structures .....  | 114        |
| 8.2. The used finite elements in modeling .....   | 114        |
| 8.2.1. <i>The properties of the BEAM3D elements</i> .....   | 114        |
| 8.2.2. <i>The special properties of BEAM3D elements</i> .....   | 117        |
| 8.3. The study solution.....  | 119        |
| 8.4. Remarks .....  | 134        |
| <b>9. DYNAMICS OF BEAM STRUCTURES, MASS MATRIX, NATURAL FREQUENCY ANALYSIS .....</b>  | <b>135</b> |
| 9.1. Extending of the finite element method.....  | 135        |
| 9.2. Finite element formulation of the elastic bodies' natural oscillation .....  | 135        |
| 9.3. Natural frequency calculation of two-dimensional bar structures using finite element method.....   | 137        |
| 9.3.1. <i>Determination of the element mass matrix</i> .....  | 138        |
| 9.3.2. <i>Element stiffness matrix</i> .....  | 140        |
| 9.3.3. <i>The system total mass and stiffness matrix</i> .....  | 141        |
| 9.4. Remarks .....  | 143        |
| <b>10. DYNAMIC ANALYSIS OF THREE-DIMENSIONAL BARS, DETERMINATION OF NATURAL FREQUENCY USING PROGRAM SYSTEM BASED ON FINITE ELEMENT METHOD .....</b>             | <b>144</b> |

|  |     |
|--|-----|
| 10.1. Introduction.....  | 144 |
| 10.2. Properties of the used finite elements.....  | 144 |
| 10.3. The study description.....   | 144 |
| 10.4. The finite element solution of the task .....  | 146 |
| 10.5. Remarks .....  | 154 |
| 11. INTRODUCTION TO PLANE PROBLEMS SUBJECT. APPLICATION OF PLANE STRESS, PLANE STRAIN AND REVOLUTION SYMMETRIC (AXISYMMETRIC) MODELS ..... | 155 |
| 11.1. Basic types of plane problems .....  | 155 |
| 11.2. Equilibrium equation, displacement and deformation.....  | 155 |
| 11.3. Constitutive equations .....   | 158 |
| <i>11.3.1. Plane stress state</i> .....  | 158 |
| <i>11.3.2. Plane strain state</i> .....  | 160 |
| 11.4. Basic equations of plane elasticity.....   | 161 |
| <i>11.4.1. Compatibility equation</i> .....  | 161 |
| <i>11.4.2. Airy's stress function</i> .....  | 162 |
| <i>11.4.3. Navier's equation</i> .....   | 162 |
| <i>11.4.4. Boundary value problems</i> .....   | 163 |
| 11.5. Examples for plane stress .....  | 165 |
| <i>11.5.1. Determination of the traction on the boundaries of a square shape plate</i> ... 165   |     |
| <i>11.5.2. Analysis of a tangentially loaded plate</i> .....   | 167 |
| 11.6. The governing equation of plane problems using polar coordinates.....  | 168 |
| 11.7. Axisymmetric plane problems .....  | 172 |
| <i>11.7.1. Solid circular cylinder and thick-walled tube</i> .....   | 172 |
| <i>11.7.2. Rotating disks</i> .....  | 175 |
| 11.8. Bibliography .....   | 179 |
| 12. MODELING OF PLANE STRESS STATE USING FEM SOFTWARE SYSTEMS. MODELING, ANALYSIS OF PROBLEM EVALUATION .....                              | 180 |
| 12.1. Finite element solution of plane problems.....   | 180 |
| 12.2. Linear three node triangle element .....   | 182 |
| <i>12.2.1. Interpolation of the displacement field</i> .....   | 182 |
| <i>12.2.2. Calculation of the stiffness matrix</i> .....   | 185 |
| <i>12.2.3. Definition of the loads</i> .....   | 186 |
| 12.3. Example for the linear triangle element – plane stress state.....  | 188 |
| 12.4. Quadratic six node triangle element .....  | 197 |
| 12.5. Isoparametric four node quadrilateral.....   | 197 |
| <i>12.5.1. Interpolation of the geometry</i> .....   | 197 |
| <i>12.5.2. Interpolation of the displacement field</i> .....   | 201 |
| <i>12.5.3. Calculation of strain components, Jacobi matrix and Jacobi determinant</i> . 201  |     |
| <i>12.5.4. The importance of the Jacobi determinant, example</i> .....   | 204 |
| <i>12.5.5. Calculation of the stress field</i> .....   | 205 |
| <i>12.5.6. Calculation of the stiffness matrix</i> .....   | 206 |
| <i>12.5.7. Calculation of the force vector</i> .....   | 207 |
| 12.6. Numerical integration, the Gauss rule .....  | 209 |
| <i>12.6.1. One dimensional Gauss rule</i> .....  | 210 |
| <i>12.6.2. Two dimensional Gauss rule</i> .....  | 211 |
| 12.7. Example for the isoparametric quadrilateral.....   | 214 |
| 12.8. Quadratic isoparametric quadrilateral.....   | 220 |

|  |     |
|--|-----|
| 12.9. Bibliography .....   | 221 |
| <b>13. MODELING OF AXISYMMETRIC STATE BY FEM SOFTWARE SYSTEMS.</b>   |     |
| <b>MODELING, ANALYSIS OF PROBLEM EVALUATION .....</b>  | 223 |
| 13.1. Finite element solution of axisymmetric problems .....   | 223 |
| 13.2. Axisymmetric linear triangle element .....   | 226 |
| 13.3. Example for the application of axisymmetric triangle element.....  | 228 |
| 13.4. Axisymmetric isoparametric quadrilateral element.....  | 232 |
| 13.5. Example for the application of axisymmetric isoparametric quadrilateral element.....   | 235 |
| 13.6. Bibliography .....   | 243 |
| <b>14. MODELING OF THIN-WALLED SHELLS AND PLATES. INTRODUCTION TO THE THEORY OF SHELL FINITE ELEMENT MODELS .....</b>                      | 244 |
| 14.1. Plate and shell theories .....   | 244 |
| 14.2. The basic equations of Kirchhoff plate theory .....  | 244 |
| 14.2.1. <i>Displacement field</i> .....  | 244 |
| 14.2.2. <i>Strain components</i> .....   | 245 |
| 14.2.3. <i>Stress field, forces and moments in the midplane</i> .....  | 245 |
| 14.2.4. <i>The equilibrium and governing equation of thin plates</i> .....   | 247 |
| 14.3. Finite element equations of thin plates .....  | 250 |
| 14.4. Basic equations of the technical theory of thin shells.....  | 252 |
| 14.4.1. <i>Geometrical equations</i> .....   | 252 |
| 14.4.2. <i>Stress resultants and couples, equilibrium equations</i> .....  | 255 |
| 14.4.3. <i>Displacement field, strain components</i> .....   | 257 |
| 14.4.4. <i>Approximations within the technical theory of thin shells</i> .....   | 258 |
| 14.5. Major steps in the finite element modeling of shells .....   | 259 |
| 14.6. Bibliography .....   | 261 |
| <b>15. MODELING OF IN-PLANE THIN-WALLED SHELLS UNDER IN-PLANE AND TRANSVERSE LOAD BY FINITE ELEMET METHOD BASED SOFTWARE SYSTEMS .....</b> | 262 |
| 15.1. Plate elements subjected to bending .....  | 262 |
| 15.2. Triangular plate bending element or Tocher triangle element.....   | 262 |
| 15.3. Example for the application of the Tocher triangle plate element.....  | 267 |
| 15.4. Incompatible rectangular shape plate element.....  | 270 |
| 15.5. Example for the application of the incompatible rectangle shape element .....  | 274 |
| 15.6. Compatible rectangular shape plate element .....   | 277 |
| 15.7. Plates under in-plane and transverse load.....   | 280 |
| 15.8. Bibliography .....   | 280 |
| <b>16. MODELING OF SPATIAL THIN-WALLED SHELLS BY FINITE ELEMENT METHOD-BASED SOFTWARE SYSTEMS .....</b>                                    | 281 |
| 16.1. Simple flat shell elements .....   | 281 |
| 16.2. Superposition of the linear triangle and Tocher bending plate elements.....  | 281 |
| 16.3. Example for the combination of the linear triangle and Tocher triangle elements....  | 287 |
| 16.4. Bibliography .....   | 294 |
| <b>17. MODELING OF CURVED AND DOUBLY-CURVED SHELLS BY FINITE ELEMENT METHOD BASED SOFTWARE SYSTEMS .....</b>                               | 295 |
| 17.1. Curved shell elements .....  | 295 |
| 17.2. Thin-walled cylindrical shell element .....  | 295 |
| 17.3. Axisymmetric shell problems – conical shell element .....  | 302 |
| 17.4. Thick-walled shell elements .....  | 308 |

---

|   |     |
|---|-----|
| 17.5. A shell-solid transition element .....  | 314 |
| 17.6. Bibliography .....  | 315 |
| 18. ANALYSIS OF 3D PROBLEMS WITH FINITE ELEMENT BASED PROGRAM SYSTEMS. INTRODUCTION OF 3D ELEMENTS .....  | 317 |
| 18.1. Hexahedron elements.....  | 317 |
| <i>18.1.1. Hexahedron element with 8 nodes .....</i>  | 318 |
| <i>18.1.2. Hexahedron element with 20 nodes .....</i>   | 320 |
| <i>18.1.3. Hexahedron element with 32 nodes .....</i>   | 321 |
| <i>18.1.4. Pentagon elements.....</i>   | 323 |
| 18.2. Tetrahedron elements.....   | 323 |
| <i>18.2.1. Tetrahedron element with 4 nodes .....</i>   | 326 |
| <i>18.2.2. Tetrahedron element with 10 nodes .....</i>  | 327 |
| <i>18.2.3. Tetrahedron element with 20 nodes .....</i>  | 329 |
| 18.3. Hierarchic basis functions.....   | 331 |
| 18.4. Definition of stiffness matrix and nodal loads.....   | 331 |
| <i>18.4.1. Numerical Gauss integration method .....</i>   | 331 |
| <i>18.4.2. Definition of stiffness matrix in case of 3D elements.....</i>   | 332 |
| <i>18.4.3. Derivation of nodal loads from distributed force system on volume .....</i>  | 332 |
| <i>18.4.4. Derivation of nodal loads from distributed force system on surfacel .....</i>  | 333 |
| 19. ANALYSIS OF 3D PROBLEMS WITH FINITE ELEMENT BASED PROGRAM SYSTEMS. APPLICATION OF 3D ELEMENTS .....   | 335 |
| 19.1. Creation of geometric model .....   | 335 |
| <i>19.1.1. Editing the original geometry .....</i>  | 335 |
| <i>19.1.2. Modeling sides and corners .....</i>   | 336 |
| <i>19.1.3. Modeling unloaded parts .....</i>  | 336 |
| <i>19.1.4. Modeling symmetric parts.....</i>  | 337 |
| <i>19.2.1. Defining the mesh.....</i>   | 338 |
| <i>19.2.2. Influence of element size .....</i>  | 338 |
| <i>19.2.3. Influence of element type.....</i>   | 340 |
| 19.3. Boundary conditions.....  | 342 |
| <i>19.3.1. Loads .....</i>  | 343 |
| <i>19.3.2. Constraints .....</i>  | 345 |
| 20. PRINCIPLES ABOUT MODELING, ACCURACY AND APPLICABILITY. COMPARISON OF DIFFERENT FINITE ELEMENT MODELS, ANALYSIS OF RESULTS .....   | 348 |
| 20.1. Modeling beams.....   | 348 |
| <i>20.1.1. Analysis of a beam with circular cross section .....</i>   | 348 |
| <i>20.1.2. Modeling of thin-walled beams .....</i>  | 350 |
| <i>20.1.3. Modeling of thin-walled open cross section beams .....</i>   | 352 |
| <i>20.1.4. Modeling of thick-walled cylinders, tubes.....</i>   | 358 |
| 21. EVALUATION AND APPLICATION OF COMPUTATIONAL RESULT IN DESIGN AND QUALIFICATION RELATED MECHANICAL ENGINEERING TASKS. RELATIONSHIP BETWEEN FINITE ELEMENT METHOD AND STANDARDIZED STRENGHT BASED DESIGN..... | 363 |
| 21.1. Precision of Finite Element Method .....  | 363 |
| <i>21.1.1. Estimation of error in case of h-type approximation .....</i>  | 365 |
| <i>21.1.2. Calculation of error in case of h-type approximation.....</i>  | 372 |
| <i>21.1.3. p-type approximation .....</i>   | 375 |

---

|   |     |
|---|-----|
| <i>21.1.4. Convergence in singular locations.....</i> | 376 |
| <i>21.1.5. Modeling mistakes.....</i>                 | 376 |
| 21.2. Evaluation of the calculated results .....      | 376 |
| <i>21.2.1. Stresses beyond yield strength.....</i>    | 376 |
| <i>21.2.2. Singular locations .....</i>               | 377 |
| <i>21.2.3. Standardized methods and the FEM .....</i> | 377 |

# 1. HISTORY OF FINITE ELEMENT METHOD INCLUDING ITS EVOLUTION, EXTENSION AND ROLE OF APPLICATION IN MECHANICAL ENGINEERING DESIGN

## 1.1. Ancient application

Finite elements: complex, and mostly (in case of certain conditions) insolvable problems can be simplified by them. The basic idea is to break up the geometry of the body into finite, simple shaped elements, thus the problem becomes solvable. By this way – instead of applying less but more difficult steps – simple but more mathematical calculation will be carried out in order to find the solution.

Application of discretization on geometrical problems

- Arc length and area of a circle (Fig. 1.1)
- Volume of a cylinder and sphere,
- Other complex geometries.

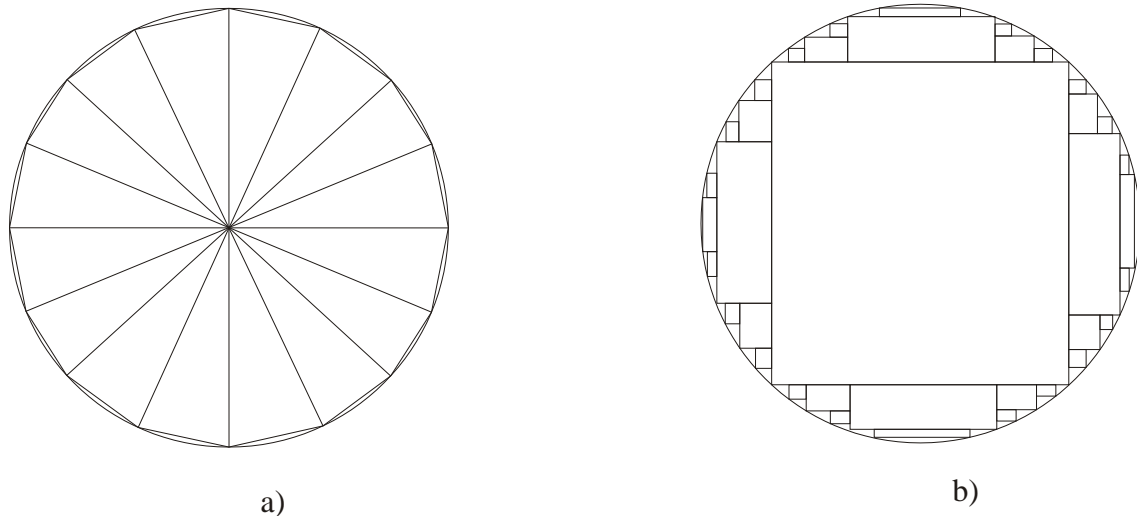


Figure 1.1: Approximation of the area of a circle

In order to calculate the area of a circle plate, the geometry must be broken up to  $n$  identical elements, as it is seen on Figure 1.1.a. The approximated value of  $\pi$ , and its error function related to the discretization is shown on Figure 1.2:

$$\pi \approx n \cos\left(\frac{360^\circ}{2n}\right) \sin\left(\frac{360^\circ}{2n}\right), \text{ and } \text{Error} = \frac{\pi - n \cos\left(\frac{360^\circ}{2n}\right) \sin\left(\frac{360^\circ}{2n}\right)}{\pi} \cdot 100\% .$$

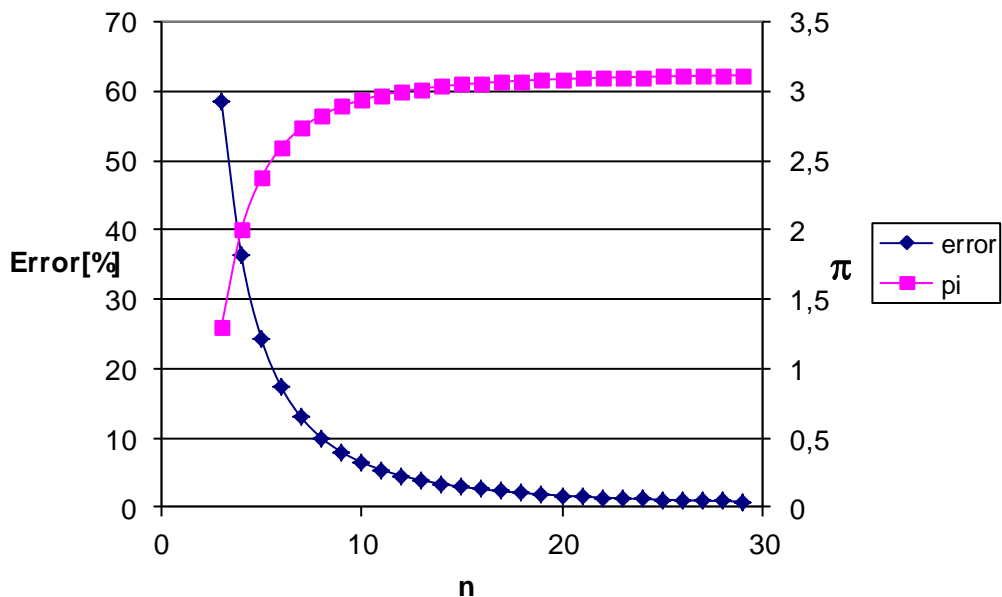


Figure 1.2: Value of  $\pi$  and its error in the function of  $n$  discretization

Tsu Ch'ung-Chih, Chinese engineer (A.D 480) determined by the use of rectangles that the approximated value of  $\pi$  is between 3,1415926 and 3,1415927.

## 1.2. History of variation of calculus, basic definitions

### 1.2.1. Brachistochrone problem

Bernoulli formed a problem in 1696, which initiated the evolution of variation of calculus in order to find the solution.

*The problem:* Two points (A and B) are given on a plane. These points are located at different heights and not on the same vertical line. Let us consider co-planar, vertical curves connecting the two points. If a particle is released from point A, without initial velocity and the effect of friction, on which curve would it descend to point B within the shortest time. The question is, whether such a function (among the curves) exists, which allows the particle to complete the motion in the shortest possible time, and if it does, how is it possible to determine it?

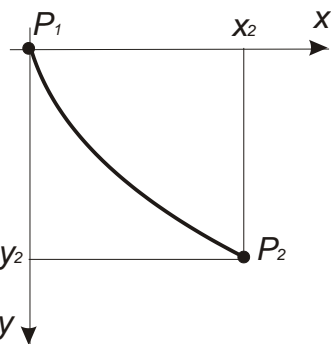


Figure 1.3: Brachistochrone problem

The demanded  $y$  function intersects points  $P_1$  and  $P_2$ , thus:

$$y(0) = 0 \text{ and } y(x_2) = y_2 \quad (1.1)$$

According to the Conservation of Energy:

$$\frac{1}{2}mv^2 = mgy \quad (1.2)$$

The velocity:

$$v = \frac{ds}{dt} \quad (1.3)$$

The infinitesimal arc length:

$$(ds)^2 = (dx)^2 + (dy)^2 \quad (1.4)$$

(1.2) simplifying with the mass and substituting (1.3) and (1.4):

$$\frac{1}{2} \left( \left( \frac{dx}{dt} \right)^2 + \left( \frac{dy}{dt} \right)^2 \right) = gy \quad (1.5)$$

Setting the equation:

$$\left( \frac{dx}{dt} \right)^2 + \left( \frac{dy}{dt} \frac{dx}{dx} \right)^2 = 2gy \quad (1.6)$$

$$\left( 1 + \left( \frac{dy}{dx} \right)^2 \right) \left( \frac{dx}{dt} \right)^2 = 2gy \quad (1.7)$$

By separating the variables, the demanded  $T$  time to run the arc length:

$$T = \int_0^{x_2} \frac{\sqrt{1+y'^2}}{\sqrt{2g \cdot y}} dx. \quad (1.8)$$

Let us find that function which satisfies the (1.1) and provides minimum to (1.8). The solution is a cycloid:

$$y(t) = c_1 \arcsin \frac{x}{c_1} - \sqrt{2c_1 x - x^2} + c_2, \quad (1.9)$$

where  $c_1, c_2$  constants, and can be determined from (1.1) condition.

This problem – which is practically extremizing a scalar quantity – drew the attention of the variation of calculus and started its evolution.

### 1.2.2. Functionals, variations

Similar problems as the „Brachistochrone” often appear in natural- and social science. We frequently face indexes, quantities which are defined by functions. The simplest example is the solution of an indeterminate integral, which depends on the chosen function. At the same time, an arc length, surface, volume or the potential energy of a beam bears the same meaning. These quantities are called as functionals.

*An arbitrary set mapped to the set of real numbers is named **functional** or operator.*

It is a specific case of the general mathematic definition, when a set of functions is mapped to the set of real numbers, and named as functional.

Let:  $f \in R^3 \rightarrow R$  given function, and  $y \in R \rightarrow R$  possible function, which is continuously differentiable on its argument  $y \in C_1[x_1, x_2]$  and intersects  $P_1 = (x_1, y_1)$ , and  $P_2 = (x_2, y_2)$  points which are fixed at the boundary of the domain:

$$y(x_1) = y_1, \quad y(x_2) = y_2. \quad (1.10)$$

Then let us assign all  $y$  to:

$$I[y] = \int_{x_1}^{x_2} f(x, y(x), y'(x)) dx \quad (1.11)$$

real number. Thus we can define  $I$  as a functional.

In most cases the problem is to extremize the values of the functional. The extreme value can be either absolute or local.

If the  $I[y]$  functional is valid on the entire argumentum function  $\tilde{y} \in y$ , and  $I[y] \geq I[\tilde{y}]$ , then  $I[\tilde{y}]$  is **absolute minimum**.

If the  $I[y]$  functional is only valid on a certain part of the argumentum, and  $I[y] \geq I[\tilde{y}]$ , then  $I[\tilde{y}]$  is **local minimum**.

The classical definition of the variation of calculus is analogue with the calculus. Lagrange introduced the variation – denoted by  $\delta$  – and defined the rules, similarly as it is in the calculus. Let us examine the classical definition:

The variation of  $\tilde{y}$  function is  $\delta y$ , and we know that  $\delta y(x_1) = 0$  and  $\delta y(x_2) = 0$ .  $\delta y$  disappears in the  $x_1$  and  $x_2$  points of the domain, while between them is arbitrary.  $y = \bar{y} + \delta y$  provides a sum of (permitted) functions, which includes the solution as well. The variation of the functional is defined as:

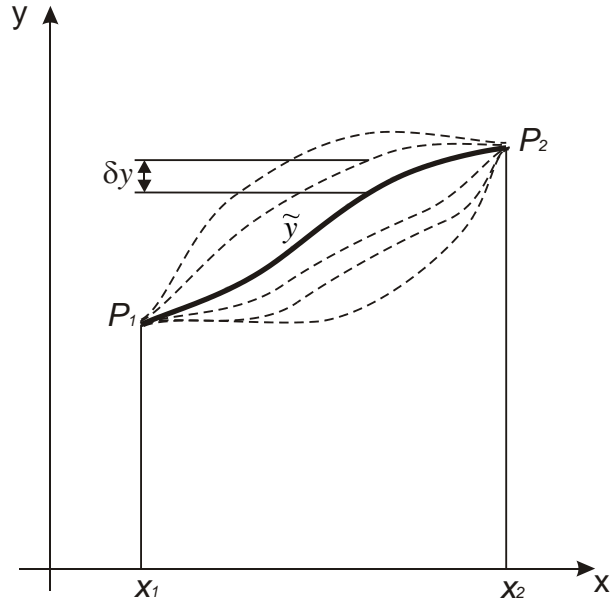


Figure 1.4 : Classical Lagrange definition of variation

$$\delta I = \int_{x_1}^{x_2} \delta f \cdot dx. \quad (1.12)$$

The solution of  $\tilde{y}$  can be obtained if the functional has a minimum. According to the variation definition

$$\delta I = 0. \quad (1.13)$$

This is necessary condition of the extreme value.

In case of a functional-minimum based method the solution of the problem can be defined as an exact or an approximate, which is analogue to the absolute and local minimum theory.

**Exact solution**, if the function – which provides minimum to the functional – is chosen among all possible, existing function.

To find that specific function is only possible in very simple cases. In most cases the exact solution cannot be found, since it is neither possible to solve the equations analytically, nor examining infinite functions to see which one provides minimum. Still the problem must be solved even if we are unable to provide the exact solution. Then an approximate solution must be found.

**Approximate solution**, if the function – which provides minimum to the functional – is not chosen among all possible, existing function.

Direct methods were created to find approximate solution. The so called Euler's broken lines were the elements of Euler's variation method. This method – by wielding the accessories of modern mathematics – gained attention and became the foundation of the direct methods of variation of calculus.

### 1.2.3. Direct method

The first problem of the variation of calculus was the determination of extremizing functions which provides extreme values to the functional.

Fundamentals of Euler's method: let us consider the problem analogue with extrema problem of functions which depend on finite variables. Thus permitted functions have finite ( $n$ ) describing variable, and the integral which is defined as functional (1.11) will be substituted with an approximate value. If  $n$  converges to infinite, then the approximate value converges to the value of the integral.

Euler's solution: the use of linear, continuous „Euler's broken line” functions for each part of the domain. Let us divide the  $[x_1, x_2]$  interval to  $n+1$  identical part, and give arbitrary real numbers  $\eta_1, \dots, \eta_n$ . Then the length of the lines:

$$t = \frac{x_2 - x_1}{n+1}.$$

The points of  $(x_1, y_1), (x_1 + t, \eta_1), (x_1 + 2t, \eta_2), \dots, (x_1 + nt, \eta_n), (x_2, y_2)$  are connected with broken lines, and it creates a continuous function which start and end points are fixed in  $P_1 = (x_1, y_1)$  and  $P_2 = (x_2, y_2)$ .

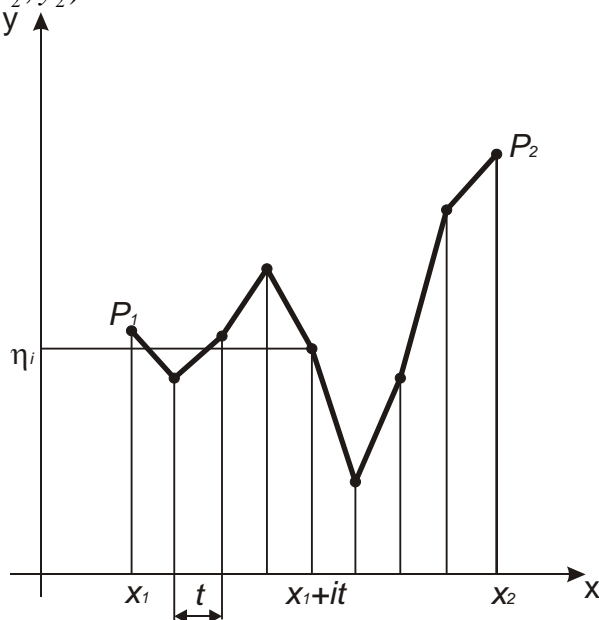


Figure 1.5 : Euler's broken lines

Then the (1.13) functional can be modified as:

$$I_n = \sum_{i=1}^{n+1} f\left(x_1 + i \cdot t, \eta_i, \frac{\eta_i - \eta_{i-1}}{t}\right) t, \quad (1.14)$$

$$(\eta_{n+1} := y_2).$$

If the approximate value of  $I_n$  functional equals to the extreme value of any Euler's broken line, then in the  $(x_1, y_1), (x_1 + t, \eta_1), (x_1 + 2t, \eta_2), \dots, (x_1 + nt, \eta_n), (x_2, y_2)$  points the derivative:

$$\frac{\partial I_n}{\partial \eta_j} = 0, \quad j = 1, \dots, n. \quad (1.15)$$

Let us introduce the partial derivative of a function with respect to the variable denoted by lower index:

$$f_y := \frac{\partial f}{\partial y}, \quad f_{y'} := \frac{\partial f}{\partial y'}, \quad \dots$$

Then another denotation for the basic function is:

$$(f)_j := f\left(x_1 + j \cdot t, \eta_j, \frac{\eta_j - \eta_{j-1}}{t}\right)$$

Thus:

$$\frac{\partial I_n}{\partial \eta_j} = (f_y)_j t + (f_{y'})_j - (f_{y'})_{j+1}. \quad (1.16)$$

Setting the equation of (1.15) and (1.16):

$$(f_y)_j - \frac{(f_{y'})_{j+1} - (f_{y'})_j}{t} = 0. \quad (1.17)$$

If  $n \rightarrow \infty$ ,  $t \rightarrow 0$  and the series of the broken lines converges to a two times differentiable  $y$  function, then from (1.17)

$$f_y(x, y, y') - \frac{d}{dx} f_{y'}(x, y, y') = 0, \quad (1.18)$$

from (1.17), or in another form

$$\frac{\partial f}{\partial y} - \frac{d}{dx} \left( \frac{\partial f}{\partial y'} \right) = 0. \quad (1.19)$$

This is a differential equation which belongs to the  $f$  basic function and named as Euler-Lagrange differential equation. The solution is  $y$ , which provides the minimum of the (1.11) functional. Thus the (1.13) and (1.18) equations mean different definition of an extrema problem in case of a given functional. This equation can be also derived by examining the extrema of a one-parametric sum of functions (1.6. table), however Euler's broken lines theory is the foundation of the direct methods that is why the classical definition was examined in details.

According to the broken lines let us consider the series of the permitted functions – denoted as  $\varphi_k$  – related to the absolute extrema value in the  $k^{\text{th}}$  steps equals to

$$\sum_{i=0}^k a_i \varphi_i \quad (1.20)$$

which provides a function in each step. The obtained function series must be examined (if it is convergent) whether its extrema existence is satisfied or not. This method can be used as:

- An approximate method for problems in variation of calculus,
- If the boundary function has an extreme value and satisfies (1.18), thus the solution of a differential equation can be transform to a variation problem.

This is called as the direct method of variation of calculus.

### 1.3. Ritz-method

In the Ritz-method, the direct method of variation of calculus is applied to find an approximate solution. In contrary with the finite element method, here the complete domain is modeled with one function.

*Definition:* Let  $\varphi_n$  series exist on a norm, and  $a_n$  series on real numbers.  $\varphi_n$  series is **complete**, if to all  $\varphi$  element there is a

$$a_1 \varphi_1 + \dots + a_n \varphi_n$$

series, which arbitrary approximates it.

*Definition:* Let  $I$  be a functional, and  $\varphi_n$  series the argumentum of  $I$ . Let us consider, that  $I$  **minimizable** on the linear combination of  $\varphi_n$  set, if:

- A linear norm exists, which is part of the argumentum  $I$ , and  $\varphi_n$  is complete on it,
- All linear combination of  $\varphi_n$  also part of the argumentum of  $I$ ,
- In all cases of  $n$  exists an  $I_n$  minimal element, where

$$D_{I_n} := \left\{ \varphi = \sum_{i=1}^n a_i \varphi_i \right\}. \quad (1.21)$$

According to Ritz's theorem, if a functional can be minimized on the linear combination of a  $\varphi_n$  set, then  $I$  must have a minimal element which is continuous and in that case,  $y_n$  – which is the series of the minimal function of  $I$  – is the minimizing series of  $I$  functional.

### Ritz method in elasticity

Let us choose the potential energy of a flexible body as a functional. By the use of  $n$ , finite parameter, an approximate function of a kinematically admissible displacement field is created (definitions see at 3.1.1. and 3.3. chapters). According to the theorem of minimum potential energy, the potential energy is minimal in case of real displacement.

The kinematically admissible displacement field is approximated by a function series:

$$\underline{u} = a_1 \underline{\varphi}_1 + \dots + a_n \underline{\varphi}_n = \underline{u}(a_1, a_2, \dots, a_n). \quad (1.22)$$

The derived potential energy includes the same number of  $n$  parameter:

$$\overset{*}{\Pi} = \overset{*}{\Pi}(a_1, a_2, \dots, a_n). \quad (1.23)$$

The potential energy is a functional, thus its extrema is found in case of

$$\delta \overset{*}{\Pi} = 0 \quad (1.24)$$

Thus:

$$\delta \overset{*}{\Pi} = \frac{\partial \overset{*}{\Pi}}{\partial a_1} \delta a_1 + \frac{\partial \overset{*}{\Pi}}{\partial a_2} \delta a_2 + \dots + \frac{\partial \overset{*}{\Pi}}{\partial a_n} \delta a_n = 0. \quad (1.25)$$

Since this integral depends on the parameters, the extrema is obtained by the derivation of the potential energy with respect the parameters and equaling to zero:

$$\frac{\partial \overset{*}{\Pi}}{\partial a_1} = 0,$$

$$\frac{\partial \overset{*}{\Pi}}{\partial a_2} = 0,$$

...,

$\frac{\partial \Pi^*}{\partial a_n} = 0$ , thus we obtain a linear algebraic  $n$  degree system of equation which provides the parameters of  $\varphi_n$  series. Naturally, the function series is arbitrary chosen, the solution is only approximated. The important element of the method, that the (1.22) displacement field must be kinematically admissible, therefore it would satisfy the kinematic boundary conditions. In case of complex problems, the determination of the functions are quite difficult, thus the method is limited to simple problems. The finite element method has the advantage to simplify the geometry of the body to simple elements, thus the approximate functions can be found easily.

## 1.4. Evolution of modern finite element method

### 1.4.1. Force method

In the early '40s the jet planes appeared, and the high terminal and operating velocity demanded more complex structures, such as the swept and delta wings. The earlier methods to design these special wings appeared to be useless, since the unreliability of the calculation could not be compensated by safety coefficients due to the increasing price of the applied materials, operational costs. A sudden need arose for a reliable and precise calculation method for complex geometries.

Levy applied first the force method, which is based on the classic elasticity that the displacements were calculated from the equilibrium of the forces. He published his first paper about the jet planes with swept wings in 1947. In case of Delta wings problems appeared with the force method, thus another approach had to be used for the solution.

### 1.4.2. Motion method

Parallel with the force method, other methods – based on the displacements – were being researched in order to put it into practice. In 1956, a research group of the Boeing Company – led by Turner – published a problem solved by a new method. The method based on the solution of a stiffness matrix derived from a kinematically admissible displacement, which includes the basics of the current modern finite element method.

In the following decades new solutions were found for 2 and 3D problems, with large displacement and various kinds of geometric, material and other non-linearities.

After the recognizing the importance of the analysis of convergence and the parallelism between the matrix equations and elasticity principles, the finite element method was put on a new foundation in the '60s, which was called as: calculus of variation.

The new method – which based on the virtual displacement – became almost the ultimate solution earth wide. The problems of applied mathematics and their solutions are still being developed as computer science is constantly evolving.

The finite element method is widely applied on constructional, thermo- and fluid mechanical problems, including linear- non-linear and FSI problems as well. Since the computers and the programs rapidly developed they became user-friendly and highly useful tools for the engineers. However, the lack of theoretical background resulted inappropriate choice of boundary conditions and models, which failed to provide the solution of the real problem.

### 1.5. Finite element method in engineering practice

The spread of finite element method fundamentally changed the classical process of production, since it was implemented into the production chain (Fig. 1.6).

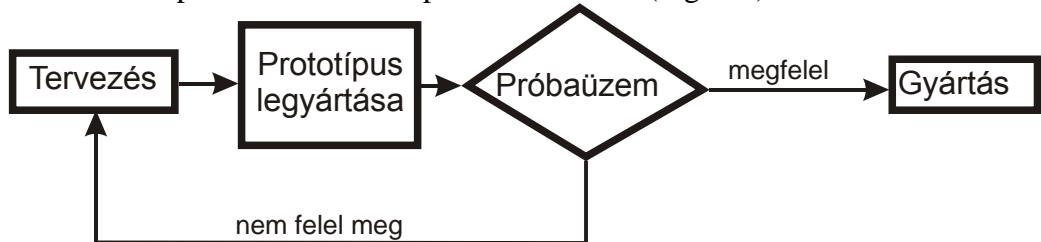


Figure 1.6.: Simplified model of classical production

The production and operation of the prototype consumes considering cost during production. These phases require materials, machining, special conditions for the operation test, experimental tools and rigs. Naturally, assistance with special skills are also demanded to carry out the production and the test of the prototype. These costs are only balanced if the production has either great volume or the manufactured pieces are simply expensive. This cost is relevantly decreased by finite element simulation (Figure 1.7.).

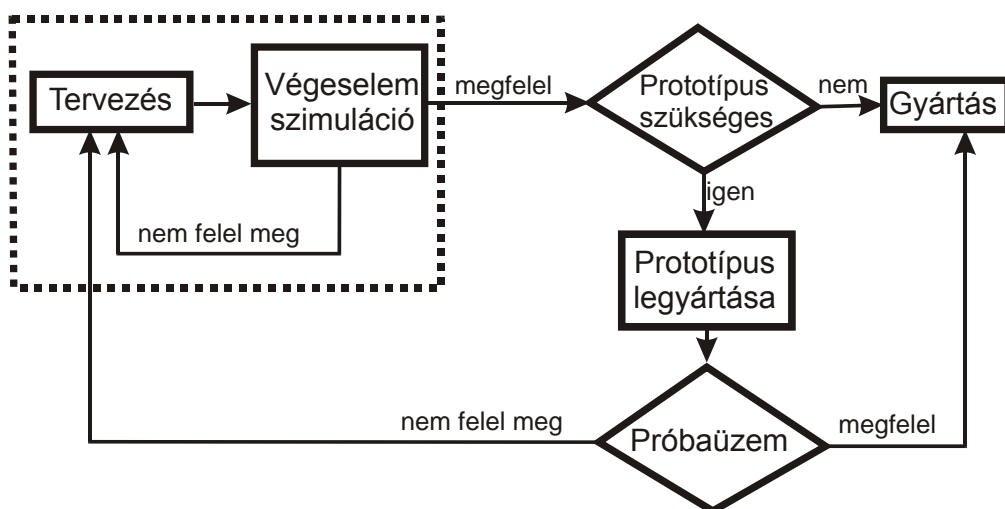


Figure 1.7.: Finite element aided model of production

The required number of prototypes is reduced by the finite element simulation, and in case the problem can be easily modeled, then the prototype production might be even neglected. In such a case, the mass production can begin and only the zero series must be tested during operation.

The simulation provides help during the technological design as well and not only in the strength check. Different software is available to model molding, forging, deep drawing processes, thus the high cost production methods also become cheaper.

We can state that the finite element method – applied in the design – is spread to many fields:

- Strength, thermodynamic, fluid, magnetic examination of the piece during normal operation conditions. This helps to improve the quality of the product and reduce the cost (i.e. reducing weight),

- Real-time simulation of the product during the manufacturing process in order to achieve an optimal cost for a proper manufacturing technique,
- Simulation of tools, which provides additional information about tool life and optimal operation conditions.

The finite element method is not only spread in the production, but in other scientific fields as well. Analogously with the manufacturing, the required prototypes and experiments can be greatly reduced, thus the design is cheaper, faster and more precise.

## 1.6. Appendix

### 1.6.1. Principals of calculus of variation

$u$  function,  $F = F(x, u, u')$  functional.

The variation of the function or its small scale perturbation:  $\delta u$ .

The first variation of the functional:

$$\delta F = \frac{\partial F}{\partial u} \delta u + \frac{\partial F}{\partial u'} \delta u', \quad (1.26)$$

Total derivative:

$$F' = \frac{\partial F}{\partial x} dx + \frac{\partial F}{\partial u} du + \frac{\partial F}{\partial u'} du'. \quad (1.27)$$

In case of  $F_1$ ,  $F_2$  functional the following equations are valid:

$$\delta(F_1 + F_2) = \delta F_1 + \delta F_2, \quad (1.28)$$

$$\delta(F_1 \cdot F_2) = \delta F_1 \cdot F_2 + F_1 \cdot \delta F_2, \quad (1.29)$$

$$\delta\left(\frac{F_1}{F_2}\right) = \frac{\delta F_1 \cdot F_2 - F_1 \cdot \delta F_2}{F_2^2}, \quad (1.30)$$

$$\delta(F^n) = n F^{n-1} \cdot \delta F. \quad (1.31)$$

It is valid to  $u$  function, that:

$$\frac{d}{dx}(\delta u) = \delta\left(\frac{du}{dx}\right), \quad (1.32)$$

$$\delta \int u(x) dx = \int \delta u(x) dx. \quad (1.33)$$

### 1.6.2. Euler-Lagrange differential equation

Let  $f \in R^3 \rightarrow R$  a given function (base function), and  $y \in R \rightarrow R$  is an admissible function, which is continuously derivative along its argumentum  $y \in C_1[x_1, x_2]$ , intersects  $P_1 = (x_1, y_1)$  and  $P_2 = (x_2, y_2)$  fixed points on the boundary and valid to the following statements:  $y(x_1) = y_1$ ,  $y(x_2) = y_2$ .

Let us assign to all  $y$  functions the

$$I[y] = \int_{x_1}^{x_2} f(x, y(x), y'(x)) dx \quad (1.34)$$

real number.

Let us find that certain  $y$  function to which the  $I[y]$  functional stationer. (In case of certain conditions it takes on extreme values).

Let  $\eta \in R \rightarrow R$  arbitrary function with fixed points of

$$\eta(x_1) = \eta(x_2) = 0, \quad (1.35)$$

and  $\varepsilon \in R$  real number. Then we can define an  $\omega \in R^2 \rightarrow R$  parametric set of functions:

$$\omega(x, \varepsilon) = y(x) + \varepsilon \eta(x). \quad (1.36)$$

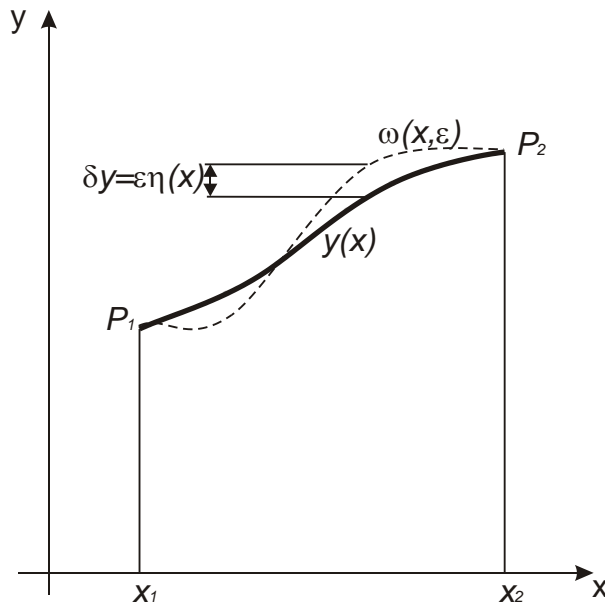


Figure 1.8 : Solution of a variation problem and the varied curve

by substituting (1.36) into (1.34):

$$I = \int_{x_1}^{x_2} f(x, \omega(x), \omega'(x)) dx = \int_{x_1}^{x_2} f(x, y(x) + \varepsilon\eta(x), y'(x) + \varepsilon\eta'(x)) dx. \quad (1.37)$$

In case of a given  $\eta(x)$  function the  $I$  functional only depends on  $\varepsilon$ .  $I(\varepsilon)$  can be only stationer (satisfying the required boundary conditions), if

$$\frac{dI}{d\varepsilon} = 0, \quad (1.38)$$

and

$$\varepsilon = 0. \quad (1.39)$$

According to the differential rules of the parametric integrals:

$$\frac{dI}{d\varepsilon} = \int_{x_1}^{x_2} \left( \eta \frac{\partial f}{\partial y} + \eta' \frac{\partial f}{\partial y'} \right) dx = \int_{x_1}^{x_2} \eta \frac{\partial f}{\partial y} dx + \int_{x_1}^{x_2} \eta' \frac{\partial f}{\partial y'} dx = 0. \quad (1.40)$$

We apply the partial integration rule on  $\eta' \frac{\partial f}{\partial y'} :$

$$\int_{x_1}^{x_2} \eta' \frac{\partial f}{\partial y'} dx = \eta \left( \frac{\partial f}{\partial y'} \right) \Big|_{x_1}^{x_2} - \int_{x_1}^{x_2} \eta \frac{d}{dx} \left( \frac{\partial f}{\partial y'} \right) dx. \quad (1.41)$$

The first member of the right side of (1.41) is zero according to (1.35), thus substituting into (1.40):

$$\int_{x_1}^{x_2} \eta \left[ \frac{\partial f}{\partial y} - \frac{d}{dx} \left( \frac{\partial f}{\partial y'} \right) \right] dx = 0. \quad (1.42)$$

Since  $\eta$  is necessary, the integral can only be zero, if

$$\frac{\partial f}{\partial y} - \frac{d}{dx} \left( \frac{\partial f}{\partial y'} \right) = 0.$$

This is called as the Euler-Lagrange differential equation.

## 2. FOUNDAMENTAL DEFINITIONS IN CONTINUUM MECHANICS. DIFFERENTIAL EQUATION SYSTEM OF ELASTICITY AND ITS BOUNDARY ELEMENTS PROBLEM.

### 2.1. Fundamental definitions in continuum mechanics

**Model:** simplified approximation of reality, which behaves similarly as the examined phenomena.

In order to solve problems in the strength of materials certain models are required as:

- geometrical,
- material-,
- mechanical (load, constraints).

Geometrical models – according to their dimensions – can be:

- 0D: particle model, all the geometrical dimensions are neglected,
- 1D: if two dimensions can be neglected compared to one. Classical beam-truss elements and line elements used in finite element method.
- 2D: if one dimension can be neglected compared to the two others. Plates and membranes.
- 3D: None of its dimensions can be neglected. Although this statement does not always include the complete geometry, since some parts can be still simplified in the mechanical point of view. Only those parts must be ignored which significantly increase the computation but less relevantly the precise of the result.

**Continuum model:** A continuum model can be divided up to finite (or infinite) elements and described by continuous (and continuously derivative) functions. The points of the continuum body can be appointed by a position vector

$$\underline{r} = x\underline{i} + y\underline{j} + z\underline{k} \quad (2.1)$$

in a given coordinate system.

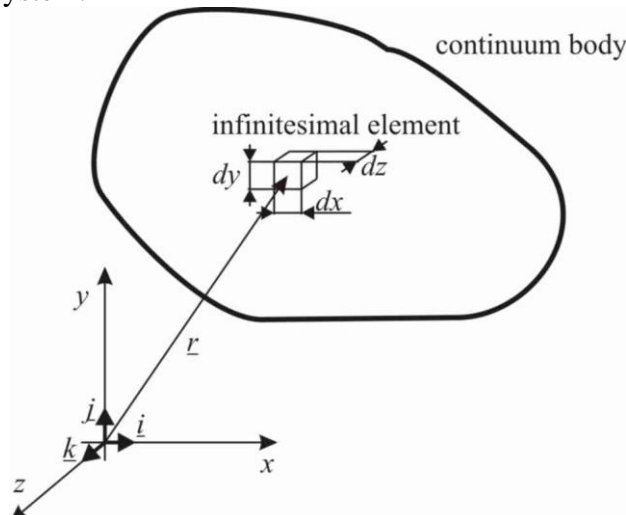


Figure 2.1.: Continuum body and an infinitesimal element

**Infinitesimal element:** an infinitesimally (arbitrarily) small element of a continuum body, depending on the model it can be an infinitesimal mass or volume.

**Rigid body:** the length between two arbitrarily chosen points of a rigid body is always constant, independently the magnitude of the load.

**Elastic body:** the body is capable to deform elastically. The length between its points changes depending on the applied load.

**Linear elastic material model:** the relationship between the load and deformation is linear.

**Non-linear elastic material model:** the relationship between the load and deformation is non-linear.

**Plastic material model:** the subject remains deformed after the removal of the load and does not regain its original form. Several plastic models exist depending on the dominancy of linear, non-linear, elastic or plastic properties.

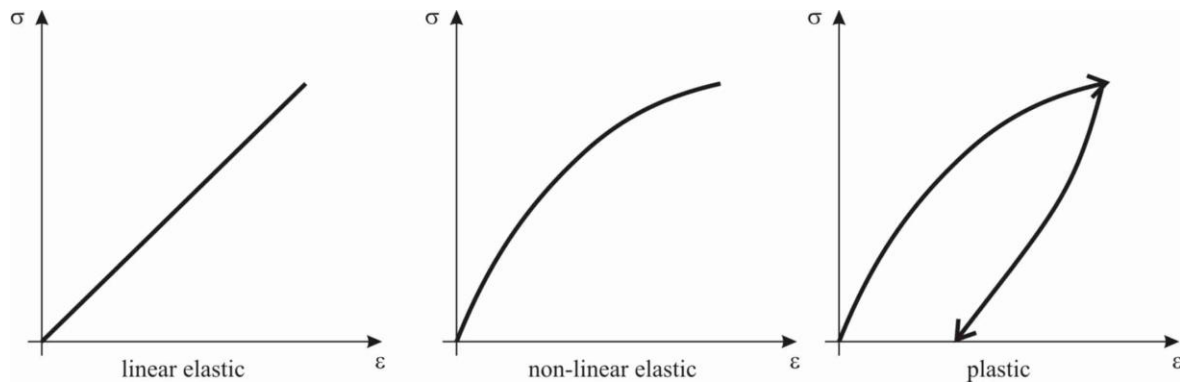


Figure 2.2.: Material models

**Isotropic material:** the behavior of the material does not depend on the direction; all properties are the same independently any arbitrarily direction.

**Displacement vector:** the difference vector between  $P$  and  $P'$  points. The points represent an arbitrary point of an elastic body before- and after applying a load, thus the original – undeformed – and deformed states.

$$\underline{u}_P = u_P \underline{i} + v_P \underline{j} + w_P \underline{k} \quad (2.2)$$

**Displacement field:** displacement vector of all points of the body in the function of the position vector (2.1).

$$\underline{u}(\underline{r}) = u(\underline{r}) \underline{i} + v(\underline{r}) \underline{j} + w(\underline{r}) \underline{k} \quad (2.3)$$

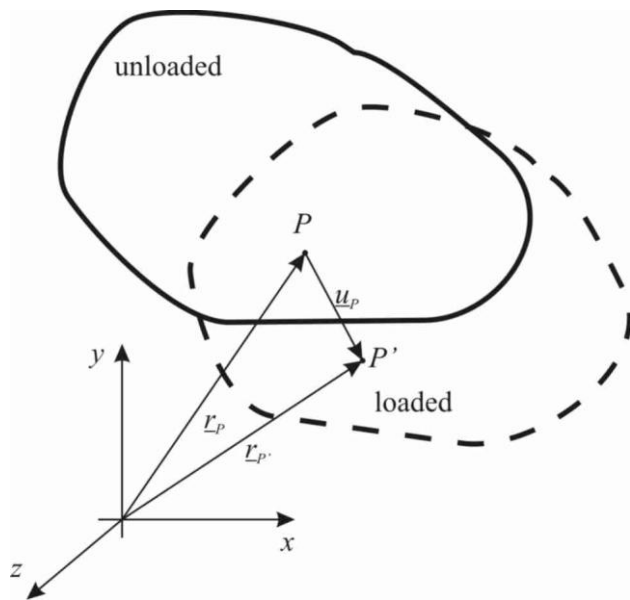


Figure 2.3.: Displacement vector

**Small displacement:** the displacement of the points of the body is irrelevantly small compared to the geometrical dimensions of the body.

**Kinematic boundary conditions:** the given (or admissible) displacements of the body.

**Dynamic boundary conditions:** the given (or admissible) load of the body.

**Deformation:** the proportional displacement of the points of the body (related to a unit length).

- Strain: the gradient of length of  $\varepsilon$  vector,
- Torsion of angle: the  $\gamma$  angle gradient of perpendicular axes (Figure 2.4.b.), the torsion of angle is always symmetric.
- The rigid body motion is not taken into account (Figure 2.4.a.).

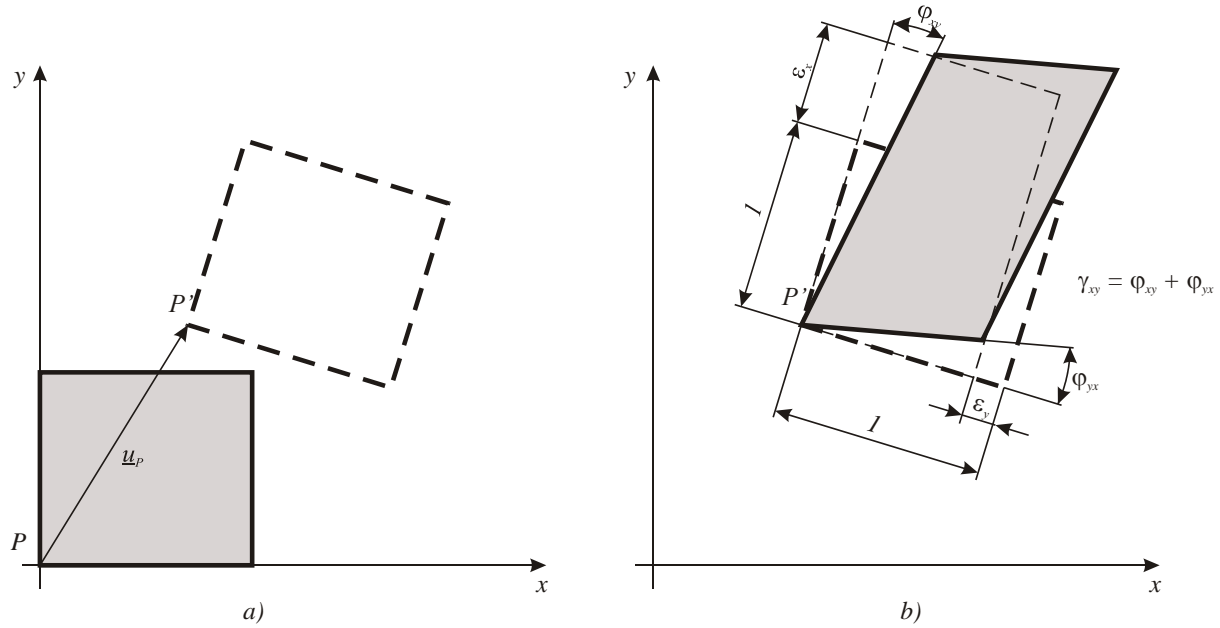


Figure 2.4.: The rigid body motion and deformation in the x-y plane

**Deformation vector:** this vector describes the displacement of a given unit vector. Defining it by  $\underline{i}, \underline{j}, \underline{k}$  unit vectors (tryeder):

$$\underline{a}_x = \varepsilon_x \underline{i} + \frac{1}{2} \gamma_{xy} \underline{j} + \frac{1}{2} \gamma_{xz} \underline{k}, \quad (2.4)$$

$$\underline{a}_y = \frac{1}{2} \gamma_{yx} \underline{i} + \varepsilon_y \underline{j} + \frac{1}{2} \gamma_{yz} \underline{k}, \quad (2.5)$$

$$\underline{a}_z = \frac{1}{2} \gamma_{zx} \underline{i} + \frac{1}{2} \gamma_{zy} \underline{j} + \varepsilon_z \underline{k}, \quad (2.6)$$

where,

$$\gamma_{xy} = \gamma_{yx}, \gamma_{yz} = \gamma_{zy}, \gamma_{xz} = \gamma_{zx}.$$

The property of the vector coordinates:

- Specific strains:  $\varepsilon_x, \varepsilon_y, \varepsilon_z$  properties without dimensions,  
 $\varepsilon > 0$ , the length increases,  
 $\varepsilon < 0$ , the length decreases.
- Angle torsion:  $\gamma_{xy}, \gamma_{yz}, \gamma_{xz}$  the dimension is in radian  
 $\gamma > 0$ , the angle decreases,  
 $\gamma < 0$ , the angle increases.

**Deformation state:** the sum of the deformation vectors related to all directions in a given point. Possible description: infinitesimal unit cube with deformation vectors, deformation tensor, Mohr circle.

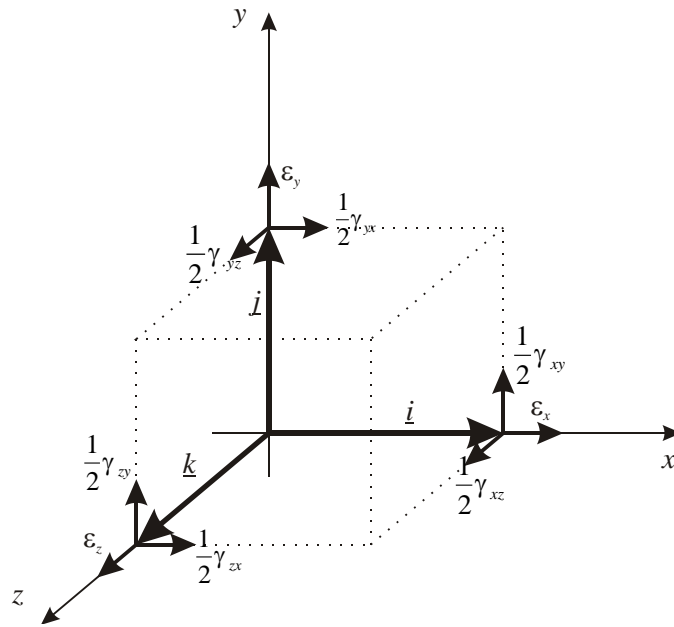


Figure 2.5.: Deformation state with deformation vector coordinates

**Tensor:** linear, homogenous vector-vector function. Description is possible with dyadic form or a matrix defined in a given coordinate system.

**Deformation tensor:** It describes the deformation state of any point of an elastic body by assigning the deformation vector of a given direction to an arbitrary direction. Description is possible with three vectors in matrix or dyadic form in a given coordinate system.

– In dyadic form:

$$\underline{\underline{\varepsilon}} = \underline{a}_x \circ \underline{i} + \underline{a}_y \circ \underline{j} + \underline{a}_z \circ \underline{k}. \quad (2.7)$$

– In matrix form:

$$\underline{\underline{\varepsilon}} = \begin{bmatrix} \varepsilon_x & \frac{1}{2}\gamma_{yx} & \frac{1}{2}\gamma_{zx} \\ \frac{1}{2}\gamma_{xy} & \varepsilon_y & \frac{1}{2}\gamma_{zy} \\ \frac{1}{2}\gamma_{xz} & \frac{1}{2}\gamma_{yz} & \varepsilon_z \end{bmatrix}, \quad (2.8)$$

The deformation vector coordinates of  $x, y, z$ , are in the columns.

The  $\underline{a}_n$  deformation vector related to an arbitrarily chosen  $\underline{n}$  direction is defined as:

$$\underline{a}_n = \underline{\underline{\varepsilon}} \cdot \underline{n}. \quad (2.9)$$

**Deformation tensor field:** the deformation field of all points of the body in the function of position vector.

$$\underline{\underline{\varepsilon}}(\underline{r}) = \begin{bmatrix} \varepsilon_x(\underline{r}) & \frac{1}{2}\gamma_{yx}(\underline{r}) & \frac{1}{2}\gamma_{zx}(\underline{r}) \\ \frac{1}{2}\gamma_{xy}(\underline{r}) & \varepsilon_y(\underline{r}) & \frac{1}{2}\gamma_{zy}(\underline{r}) \\ \frac{1}{2}\gamma_{xz}(\underline{r}) & \frac{1}{2}\gamma_{yz}(\underline{r}) & \varepsilon_z(\underline{r}) \end{bmatrix} \quad (2.10)$$

**Stress:** The intensity of the internal force system distributed on the internal face of the body. Dimension:  $1 \frac{N}{m^2} = 1 Pa$ .

**Stress vector:** the stress is defined by a stress vector. The  $\underline{\rho}_n$  stress vector of a  $dA$  surface related to an arbitrarily chosen  $\underline{n}$  direction is defined as:

$$\underline{\rho}_n = \frac{d\underline{F}}{dA}. \quad (2.11)$$

- On a given surface, the normal coordinate of the stress vector is named as normal stress, and denoted by:  $\sigma$ .  
 $\sigma > 0$ , in case of tension,  
 $\sigma < 0$ , in case of compression.
- The coordinate of the stress vector which is parallel with the surface is named as shear stress, and denoted as:  $\tau$ .

The stress vectors defined by  $\underline{i}, \underline{j}, \underline{k}$  unit vectors on a given surface:

$$\underline{\rho}_x = \sigma_x \underline{i} + \tau_{xy} \underline{j} + \tau_{xz} \underline{k}, \quad (2.12)$$

$$\underline{\rho}_y = \tau_{yx} \underline{i} + \sigma_y \underline{j} + \tau_{yz} \underline{k}, \quad (2.13)$$

$$\underline{\rho}_z = \tau_{zx} \underline{i} + \tau_{zy} \underline{j} + \sigma_z \underline{k}, \quad (2.14)$$

where,

$$\gamma_{xy} = \gamma_{yx}, \gamma_{yz} = \gamma_{zy}, \gamma_{xz} = \gamma_{zx}.$$

**Stress state:** the sum of the stress vectors related to all directions in a given point. Possible description: infinitesimal unit cube with stress vectors, stress tensor, Mohr circle.

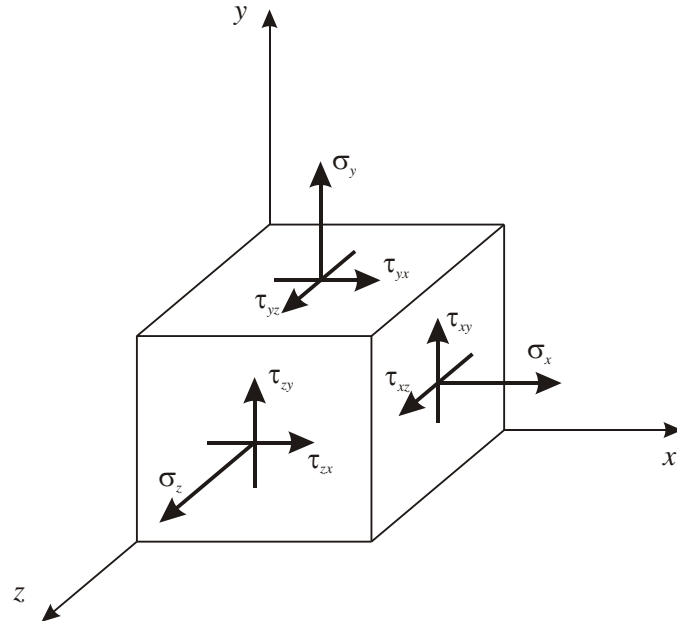


Figure 2.6.: Stress state presented on an infinitesimal cube

**Stress tensor:** It describes the stress state of any point of an elastic body by assigning the stress vector of a given direction to an arbitrary direction. Description is possible with three vectors in matrix or dyadic form in a given coordinate system.

- In dyadic form:

$$\underline{\underline{\sigma}} = \underline{\rho}_x \circ \underline{i} + \underline{\rho}_y \circ \underline{j} + \underline{\rho}_z \circ \underline{k}. \quad (2.15)$$

- In matrix form:

$$\underline{\underline{\sigma}} = \begin{bmatrix} \sigma_x & \tau_{yx} & \tau_{zx} \\ \tau_{xy} & \sigma_y & \tau_{zy} \\ \tau_{xz} & \tau_{yz} & \sigma_z \end{bmatrix}. \quad (2.16)$$

$\underline{\rho}_n$  stress vector defined to an  $\underline{n}$  direction:

$$\underline{\rho}_n = \underline{\underline{\sigma}} \cdot \underline{n}. \quad (2.17)$$

**Stress tensor:** the stress field of all points of the body in the function of position vector.

$$\underline{\underline{\sigma}}(\underline{r}) = \begin{bmatrix} \sigma_x(\underline{r}) & \tau_{yx}(\underline{r}) & \tau_{zx}(\underline{r}) \\ \tau_{xy}(\underline{r}) & \sigma_y(\underline{r}) & \tau_{zy}(\underline{r}) \\ \tau_{xz}(\underline{r}) & \tau_{yz}(\underline{r}) & \sigma_z(\underline{r}) \end{bmatrix} \quad (2.18)$$

The element index of the stress- and strain tensor can be used in a reversed order not only

as it was presented earlier.

**The work of a force:** a force acted along a  $d\underline{r}$  displacement carries out an  $\underline{F} \cdot d\underline{r}$  infinitesimal work (see the geometric description of the scalar multiplication on the Figure 2.7; the force is multiplied by the force directed component of the displacement). The work carried out along a finite displacement is the sum of the infinitesimal works.

$$W = \int_{\bar{r}_1}^{\bar{r}_2} \underline{F}(\underline{r}) d\underline{r} \quad (2.19)$$

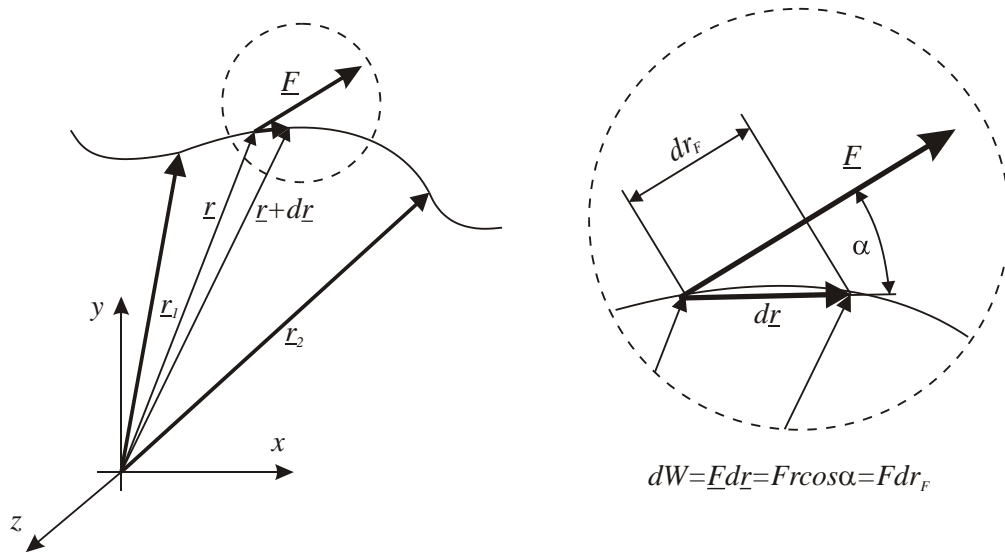


Figure 2.7.: Work of a force

**Internal energy:** (deformation energy) the energy of the internal forces

$$U = \frac{1}{2} \int_V (\sigma_x \varepsilon_x + \sigma_y \varepsilon_y + \sigma_z \varepsilon_z + \tau_{xy} \gamma_{xy} + \tau_{yz} \gamma_{yz} + \tau_{xz} \gamma_{xz}) dV \text{ (Linear case)} \quad (2.20)$$

The internal energy can be derived from the double product of the stress and deformation tensor:

$$U = \frac{1}{2} \int_V \underline{\underline{\sigma}} \cdot \underline{\underline{\varepsilon}} dV \quad (2.21)$$

**Hamilton operator:** (Nabla operator) is a vector, which coordinates are special orders to execute the partial differentiations of the given directions. In a Descartes coordinate system:

$$\nabla = \frac{\partial}{\partial x} \underline{i} + \frac{\partial}{\partial y} \underline{j} + \frac{\partial}{\partial z} \underline{k}. \quad (2.22)$$

In cylindrical (polar) coordinate system:

$$\nabla = \frac{\partial}{\partial R} e_R + \frac{1}{R} \frac{\partial}{\partial \varphi} e_\varphi + \frac{\partial}{\partial z} e_z. \quad (2.23)$$

## 2.2. Differential equation system and boundary element problem of Elasticity

### 2.2.1. Equilibrium equations

The equilibrium equations describe the relationship between the  $\underline{q}(r)$  distributed force system acting on a volume and the  $\underline{\underline{\sigma}}(r)$  stress field tensor.

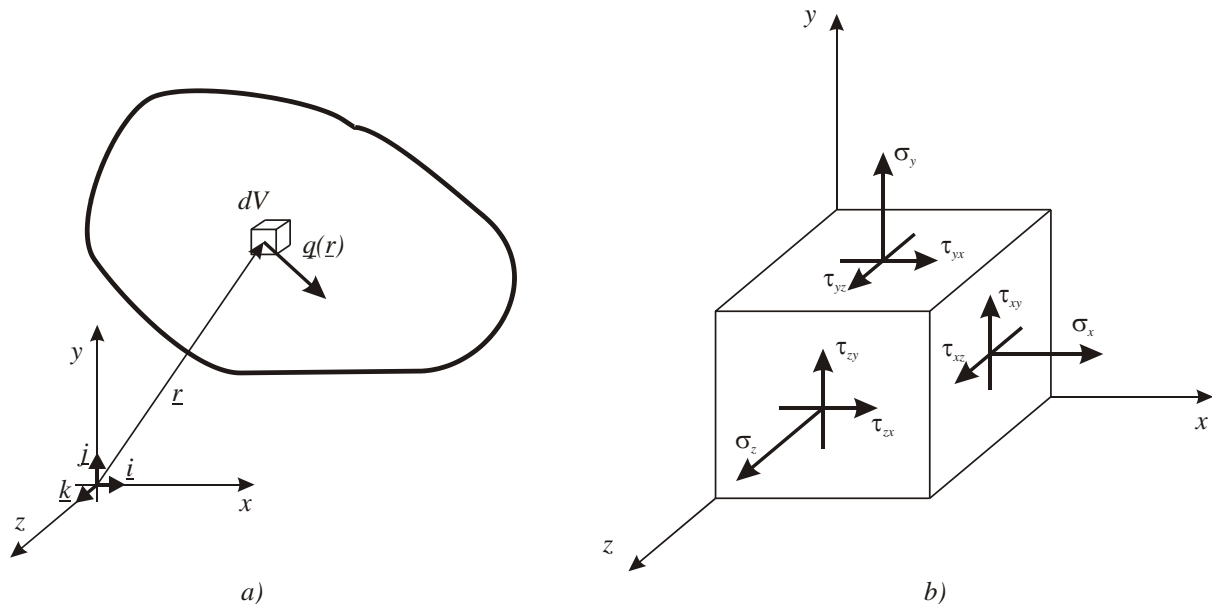


Figure 2.8.: Load case of an infinitesimal body

If an arbitrarily chosen infinitesimal body inside of a body is in steady state, then the external (Figure 2.8.a.) and internal (Figure 2.8.b.) forces are in equilibrium. By investigating the forces along the  $x$  axis (Figure 2.9.a.), it is clearly obvious: if no external forces are acting upon the body, then the internal forces (stresses) have equal magnitude and opposite senses on the proper sides of the body. The change is caused by the external distributed force system acting on the volume. Stress is an internal force distributed on a surface, thus it must be recalculated onto the infinitesimal cube.  $\sigma_x$  appears on the  $dydz$  surface of the cube, and it turns to be a force system acting on a volume if it is divided by  $dx$  side length. Similarly,  $\tau_{zx}$  shear stress must be divided by  $dz$ , while  $\tau_{yx}$  must be divided by  $dy$  side length. Then, all forces acting upon the infinitesimal body along the  $x$  axis are in equilibrium:

$$\frac{\sigma_x + \Delta\sigma_x}{dx} - \frac{\sigma_x}{dx} + \frac{\tau_{zx} + \Delta\tau_{zx}}{dz} - \frac{\tau_{zx}}{dz} + \frac{\tau_{yx} + \Delta\tau_{yx}}{dy} - \frac{\tau_{yx}}{dy} + q_x = 0. \quad (2.24)$$

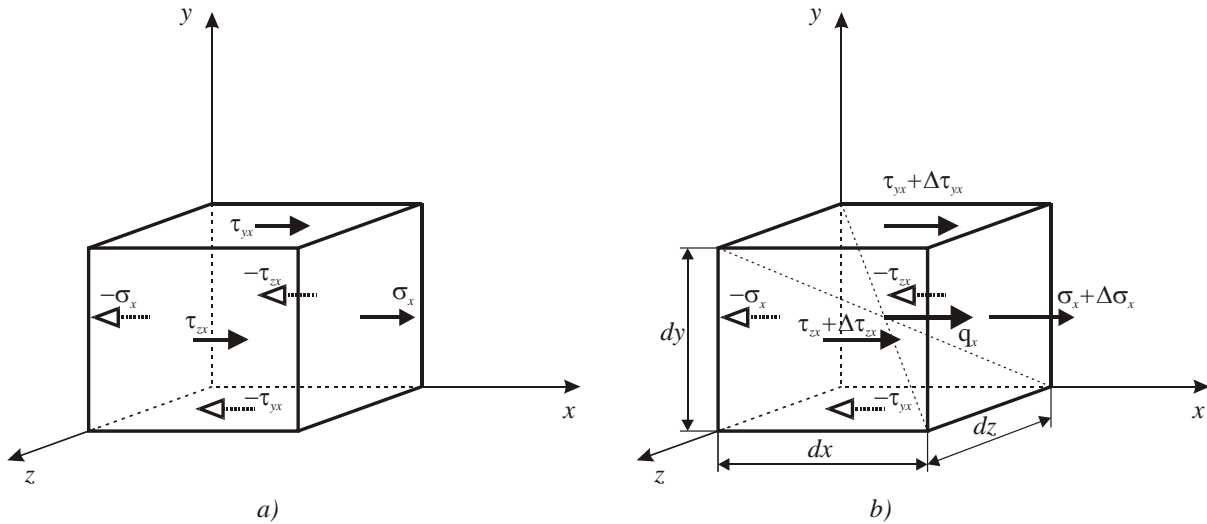


Figure 2.9.: Load case of an infinitesimal body along the x axis

The gradient of the stresses can be described by the partial derivative of the given direction:  $\Delta\sigma_x = \frac{\partial\sigma_x}{\partial x} dx$ ,  $\Delta\tau_{zx} = \frac{\partial\tau_{zx}}{\partial z} dz$ ,  $\Delta\tau_{yx} = \frac{\partial\tau_{yx}}{\partial y} dy$ , which are substituted into (2.24) we obtain:

$$\frac{\partial\sigma_x}{\partial x} + \frac{\partial\tau_{yx}}{\partial y} + \frac{\partial\tau_{zx}}{\partial z} + q_x = 0. \quad (2.25)$$

Analogously to the earlier, the other two directions:

$$\frac{\partial\tau_{xy}}{\partial x} + \frac{\partial\sigma_y}{\partial y} + \frac{\partial\tau_{zy}}{\partial z} + q_y = 0, \quad (2.26)$$

$$\frac{\partial\tau_{xz}}{\partial x} + \frac{\partial\tau_{yz}}{\partial y} + \frac{\partial\sigma_z}{\partial z} + q_z = 0. \quad (2.27)$$

The (2.25)-(2.27) equations are the so called **equilibrium equations** in Descartes coordinate system.

In order to define generally the equilibrium equations let us consider a  $V$  volume inside of a body similarly to Figure 2.10.

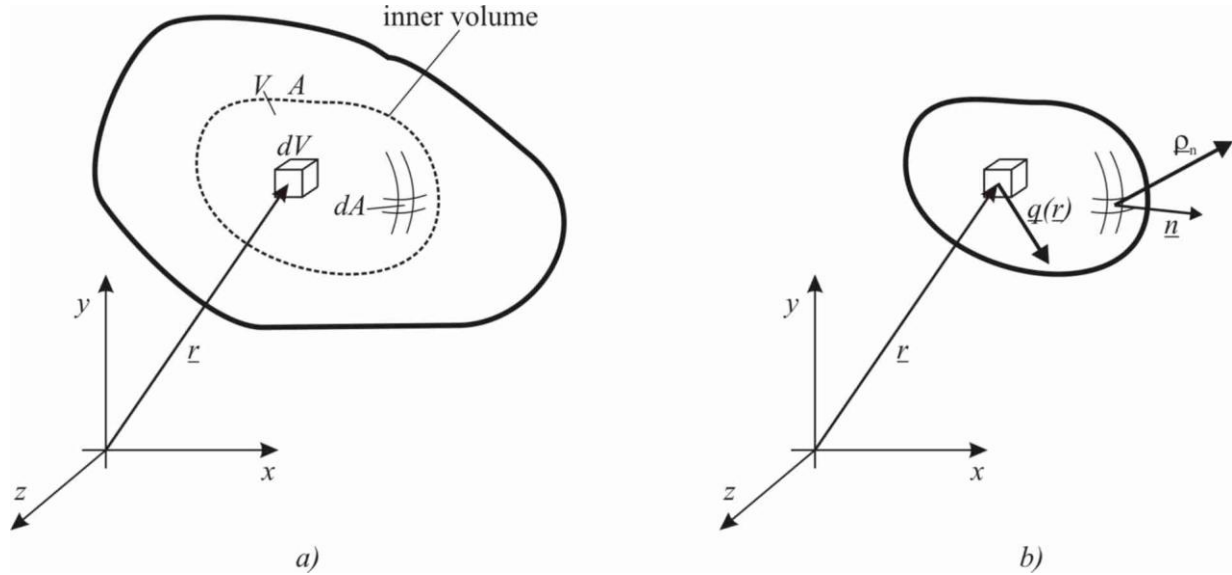


Figure 2.10.:  $V$  volume inside a body with a force system acting on surface and volume

The infinitesimal force acting on a  $dV$  volume of the infinitesimal body:

$$d\underline{F} = \underline{q}dV.$$

The infinitesimal force acting on a  $dA$  surface, and calculated from the  $\underline{\rho}_n$  stress vector:

$$d\underline{F} = \underline{\rho}_n dA = \underline{\underline{\sigma}} \cdot \underline{n} dA.$$

The  $V$  internal body is in equilibrium, thus the sum of the forces acting on the surface and the volume are zero:

$$\underline{F} = 0 = \int_V \underline{q}dV + \int_A \underline{\underline{\sigma}} \cdot \underline{n} dA. \quad (2.28)$$

According to the Gauss-Ostrogradsky integral-transformation theorem:

$$\int_A \underline{\underline{\sigma}} \cdot \underline{n} dA = \int_V \underline{\underline{\sigma}} \cdot \nabla dV.$$

Substituting Gauss-Ostrogradsky into (2.28):

$$0 = \int_V \underline{q}dV + \int_V \underline{\underline{\sigma}} \cdot \nabla dV,$$

Setting the separated parts of the equation into one integral:

$$0 = \int_V (\underline{q} + \underline{\underline{\sigma}} \cdot \nabla) dV \quad (2.29)$$

Since the  $V$  volume is arbitrarily chosen, thus the (2.29) equation is only valid if the integral is zero. This is the *equilibrium equation* of elasticity.

$$\underline{\underline{\sigma}} \cdot \nabla + \underline{q} = 0. \quad (2.30)$$

## 2.2.2. Geometric equations

The geometric (kinematic) equations define the relationship between the  $\underline{u}(r)$  displacement field and the  $\underline{\underline{\varepsilon}}(r)$  deformation tensor field. On Figure 2.8, the deformation of an infinitesimal cube is presented in the  $x - y$  plane of a Descartes coordinate system.

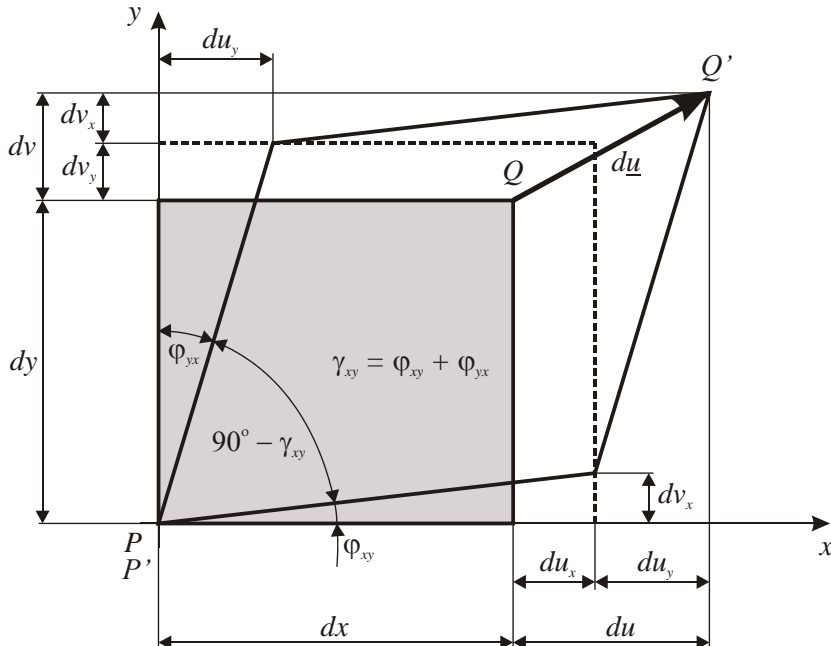


Figure 2.11.: The geometric interpretation of deformation

Let us neglect the rigid-body motion, and let us investigate the relative displacement between point  $P$  and  $Q$ . By plotting  $P$  and  $P'$  points on each other, the gradient of  $\overline{PQ}$  length is the  $\overline{QQ'}$  vector, which is denoted by  $d\underline{u} = du \cdot \underline{i} + dv \cdot \underline{j} + dw \cdot \underline{k}$  infinitesimal displacement vector. It has two coordinates in a plan, namely  $du$  and  $dv$ . Both coordinated can be broken up into two parts:  $du = du_x + du_y$ ,  $dv = dv_y + dv_x$ .

$du_x$ : from the strain of  $dx$  side (in the function of  $x$ ),

$du_y$ : from the strain of  $dy$  side (in the function of  $y$ ), thus

$$\frac{\partial u}{\partial x} = \frac{\partial u_x}{\partial x} + \frac{\partial u_y}{\partial x} = \frac{du_x}{dx} + 0 \text{ and } \frac{\partial u}{\partial y} = \frac{\partial u_x}{\partial y} + \frac{\partial u_y}{\partial y} = 0 + \frac{du_y}{dy}.$$

$dv_y$ : from the strain of  $dy$  side (in the function of  $y$ ),

$dv_x$ : from the strain of  $dx$  side (in the function of  $x$ ), thus

$$\frac{\partial v}{\partial x} = \frac{\partial v_x}{\partial x} + \frac{\partial v_y}{\partial x} = \frac{dv_x}{dx} + 0 \text{ and } \frac{\partial v}{\partial y} = \frac{\partial v_x}{\partial y} + \frac{\partial v_y}{\partial y} = 0 + \frac{dv_y}{dy}.$$

According to Figure 2.11, the strains are:  $\varepsilon_x = \frac{du_x}{dx}$ ,  $\varepsilon_y = \frac{dv_y}{dy}$ ,

While the torsion of angle is:

$$\gamma_{xy} = \varphi_{xy} + \varphi_{yx} = \arctan \frac{dv_x}{dx} + \arctan \frac{du_y}{dy} \approx \frac{dv_x}{dx} + \frac{du_y}{dy}.$$

By the use of the partial derivatives related to the displacement vector:

$$\varepsilon_x = \frac{\partial u}{\partial x}, \quad \varepsilon_y = \frac{\partial v}{\partial y}, \quad \gamma_{xy} = \gamma_{yx} = \frac{\partial v}{\partial x} + \frac{\partial u}{\partial y}.$$

This calculation can be carried out on all planes, which result the **geometric equations** in a Descartes coordinate system:

$$\varepsilon_x = \frac{\partial u}{\partial x}, \quad \varepsilon_y = \frac{\partial v}{\partial y}, \quad \varepsilon_z = \frac{\partial w}{\partial z}, \quad (2.31)$$

$$\gamma_{xy} = \gamma_{yx} = \frac{\partial v}{\partial x} + \frac{\partial u}{\partial y}, \quad \gamma_{yz} = \gamma_{zy} = \frac{\partial v}{\partial z} + \frac{\partial w}{\partial y}, \quad \gamma_{xz} = \gamma_{zx} = \frac{\partial w}{\partial x} + \frac{\partial u}{\partial z}. \quad (2.32)$$

The geometric equations can be defined in a general form. Let us investigate the position of two points on an elastic body before and after applying an external load on it. The distance between the two points – in the undeformed state – is  $d\underline{r} = dx\underline{i} + dy\underline{j} + dz\underline{k}$ .

According to the definition of deformation the gradient of displacement between the two points has to be examined and described.

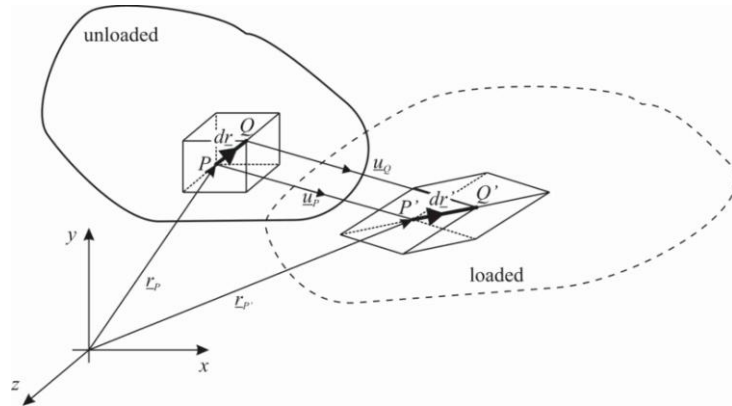


Figure 2.12.: Displacement and deformation

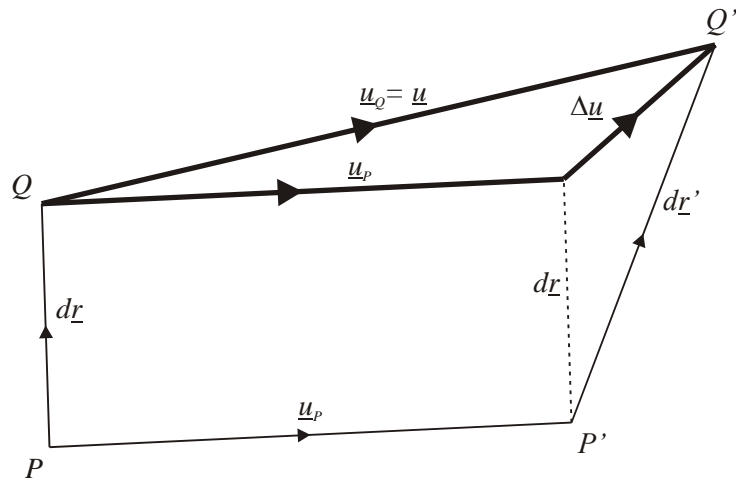


Figure 2.13.: Displacement and deformation vectors

The difference of the two points is defined by the relative displacement of  $P$  and  $Q$  points:

$$\Delta \underline{u} = \underline{u}_Q - \underline{u}_P = \underline{u} - \underline{u}_P .$$

Thus the displacement of  $Q$ :

$$\underline{u} = \underline{u}_P + \Delta \underline{u} . \quad (2.33)$$

Let us approximate the  $\underline{u}(x, y, z)$  displacement function in the close environment of  $P$  point by applying a Taylor-series on  $P$  point:

$$\underline{u}(\underline{r}) = \underline{u}_P + \left. \frac{\partial \underline{u}}{\partial x} \right|_P dx + \left. \frac{\partial \underline{u}}{\partial y} \right|_P dy + \left. \frac{\partial \underline{u}}{\partial z} \right|_P dz + \frac{1}{2} \left. \frac{\partial^2 \underline{u}}{\partial x^2} \right|_P dx^2 + \dots = \underline{u}_P + d\underline{u} . \quad (2.34)$$

From (2.33) and (2.34) can be derived that in the close environment of  $P$  the difference and the derivative are approximately equal. In case of small displacement the higher derivatives can be neglected:

$$\Delta \underline{u} \approx d\underline{u} = \frac{\partial \underline{u}}{\partial x} \Big|_P dx + \frac{\partial \underline{u}}{\partial y} \Big|_P dy + \frac{\partial \underline{u}}{\partial z} \Big|_P dz.$$

Taking into account  $dx = \underline{i} \cdot d\underline{r}$ ,  $dy = \underline{j} \cdot d\underline{r}$ ,  $dz = \underline{k} \cdot d\underline{r}$  equilibriums, and the group theory between the scalar and dyadic product  $\underline{a} \cdot (\underline{b} \cdot \underline{c}) = (\underline{a} \circ \underline{b}) \cdot \underline{c}$ , the infinitesimal gradient of the displacement field is:

$$d\underline{u} = \frac{\partial \underline{u}}{\partial x} \Big|_P (\underline{i} \cdot d\underline{r}) + \frac{\partial \underline{u}}{\partial y} \Big|_P (\underline{j} \cdot d\underline{r}) + \frac{\partial \underline{u}}{\partial z} \Big|_P (\underline{k} \cdot d\underline{r}) = \left( \frac{\partial \underline{u}}{\partial x} \Big|_P \circ \underline{i} + \frac{\partial \underline{u}}{\partial y} \Big|_P \circ \underline{j} + \frac{\partial \underline{u}}{\partial z} \Big|_P \circ \underline{k} \right) \cdot d\underline{r}.$$

By the use of the Hamilton operator:

$$d\underline{u} = (\underline{u} \circ \nabla) \cdot d\underline{r}. \quad (2.35)$$

Where  $\underline{\underline{T}} = (\underline{u} \circ \nabla)$  the derivative tensor of the displacement field, which can be divided to a symmetric and anti-symmetric (skew-symmetric) tensors.

$$\underline{\underline{\underline{T}}} = \frac{1}{2} (\underline{\underline{\underline{T}}} + \underline{\underline{\underline{T}}}^T) + \frac{1}{2} (\underline{\underline{\underline{T}}} - \underline{\underline{\underline{T}}}^T) = \frac{1}{2} (\underline{u} \circ \nabla + \nabla \circ \underline{u}) + \frac{1}{2} (\underline{u} \circ \nabla - \nabla \circ \underline{u}) = \underline{\underline{\varepsilon}} + \underline{\underline{\underline{T}}}_o$$

The symmetric part describes the deformation of the infinitesimal body while the anti-symmetric describes the rotation of the infinitesimal body. Thus the deformation tensor derived from the displacement field is described as:

$$\underline{\underline{\varepsilon}} = \frac{1}{2} (\underline{u} \circ \nabla + \nabla \circ \underline{u}) \quad (2.36)$$

Equation (2.36) is the so-called **geometric equation**.

The identical scalar equations of the tensor form are described in a Descartes coordinate system as it was mentioned earlier in (2.31) and (2.32) equations.

The other type of geometric equations is the so-called Saint-Venant compatibility equation:

$$\nabla \times \underline{\underline{\varepsilon}} \times \nabla = \underline{\underline{0}}.$$

The compatibility is also related to the neighbor infinitesimal elements, since the material is continuous, and the displacement of the neighbor elements have to be identical as well.

### 2.2.3. Constitution equations (material equations)

The constitutional- or material equations determine the relationship between the stress and strain state. The behavior of the material on Figure 2.2 can be described as linear, and the Hooke law is suitable to describe to phenomena. In case of single axis stress state, the simple Hooke law can define the relationship between the strain and the stress:  $\sigma = E\varepsilon$ , where  $E$  (Young-modulus, elasticity modulus) is the coefficient between the stress and strain. In case of tension or compression, the stress has only one principle direction thus component, but strain appears in two directions as it is seen on Figure 2.14. There is positive elongation in the material along the axis of tension, but in the same time, it contracts perpendicularly. The relationship between the elongation and the contraction is described by the dimensionless Poisson-coefficient:  $\varepsilon_y = \varepsilon_z = -\nu\varepsilon_x$ .

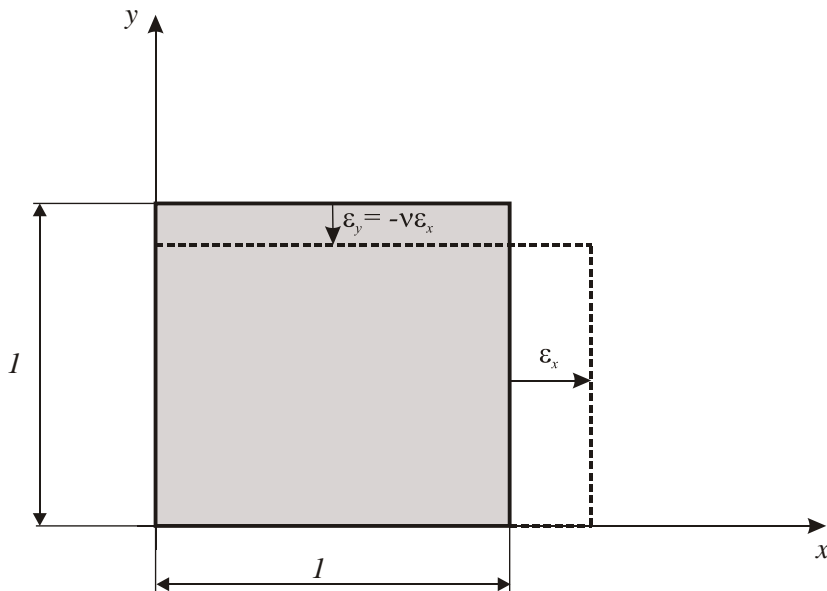


Figure 2.14.: Strains, Poisson-coefficient

In case of multi-axes stress state, the relationship between the stress and strain state can be only described with a tensor equation, the so-called general Hooke law. The law has two isotropic form to linear, elastic materials:

$$\underline{\underline{\sigma}} = 2G \left( \underline{\underline{\varepsilon}} + \frac{\nu}{1-2\nu} \underline{\underline{\varepsilon}_1} \underline{\underline{E}} \right), \quad (2.37)$$

$$\underline{\underline{\varepsilon}} = \frac{1}{2G} \left( \underline{\underline{\sigma}} - \frac{\nu}{1+\nu} \underline{\underline{\sigma}_1} \underline{\underline{E}} \right). \quad (2.38)$$

where,

$G$  : shear elastic modulus, which can be calculated as:  $E = 2G(1+\nu)$ ,

$\underline{\underline{E}}$  : unit matrix,

$\varepsilon_1, \sigma_1$ : the first scalar invariant of the tensors, (the sum of the main row?).

The scalar equations with respect to (2.37) **material equations**:

$$\sigma_x = 2G \left( \varepsilon_x + \frac{\nu}{1-2\nu} (\varepsilon_x + \varepsilon_y + \varepsilon_z) \right),$$

$$\sigma_y = 2G \left( \varepsilon_y + \frac{\nu}{1-2\nu} (\varepsilon_x + \varepsilon_y + \varepsilon_z) \right),$$

$$\sigma_z = 2G \left( \varepsilon_z + \frac{\nu}{1-2\nu} (\varepsilon_x + \varepsilon_y + \varepsilon_z) \right),$$

$$\tau_{xy} = G\gamma_{xy}, \quad \tau_{yz} = G\gamma_{yz}, \quad \tau_{xz} = G\gamma_{xz}.$$

#### 2.2.4. Boundary conditions

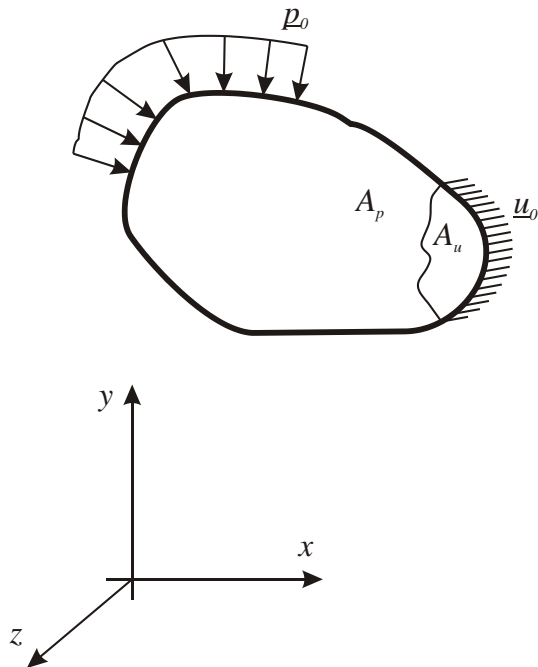


Figure 2.15.: Boundary conditions

In case of an elasticity problem two types of boundary conditions can be defined:

*Kinematic boundary conditions:* the admissible  $\underline{u}_0$  displacements (constraints) on  $A_u$  surface. It stands for the solution that:  $\underline{u} = \underline{u}_0$ .

*Dynamic boundary conditions:* the admissible  $\underline{p}_0$  load on  $A_p$  surface (the unloaded surfaces are included as well, since they have known load which equal to zero). It stands for the solution that:  $\underline{p} = \underline{p}_0$ , or  $\underline{\sigma} \cdot \underline{n} = \underline{p}_0$ .

Other boundary conditions can be defined as well, but these two are the most common.

### 2.2.5. Boundary element method

The boundary element problem of elasticity is consisted the differential equations of elasticity and the boundary conditions:

- $\underline{\underline{\sigma}} \cdot \nabla + \underline{q} = 0$ , equilibrium equations,
- $\underline{\underline{\varepsilon}} = \frac{1}{2}(\underline{u} \circ \nabla + \nabla \circ \underline{u})$ , geometric equations,
- $\underline{\underline{\sigma}} = 2G\left(\underline{\underline{\varepsilon}} + \frac{\nu}{1-2\nu}\varepsilon_1 \underline{\underline{E}}\right)$ , constitutive equations,
- $\underline{u}|_{A_u} = \underline{u}_0$ , kinematic boundary conditions,
- $\underline{\underline{\sigma}} \cdot \underline{n}|_{A_p} = \underline{p}_0$ , dynamic boundary conditions.

With this definition, it is proved that the boundary element problem has solution (existence criteria), and only one solution exist (unicity criteria).

### 3. ENERGY THEOREM OF ELASTICITY, CALCULUS OF VARIATION, FINITE ELEMENT METHOD, DETERMINATION OF STIFFNESS EQUATION IN CASE OF CO-PLANAR, TENSED ELEMENT

#### 3.1. Approximate functions

The approximate solution of an elasticity problem can be obtained by the approximation of displacement or internal forces (stresses). By the use of the elasticity equations the displacement-, deformation or stress field of a body can be determined independently from the way of approach.

##### 3.1.1. Kinematically admissible displacement field

A displacement field  $\underline{\dot{u}} = \underline{\dot{u}}(\underline{r})$  is kinematically admissible if:

- Satisfies the kinematic boundary conditions (Figure 2.15.),  $\underline{\dot{u}} \Big|_{A_u} = \underline{\dot{u}}_0$ ,
- Continuously differentiable (the geometric equations are satisfied).

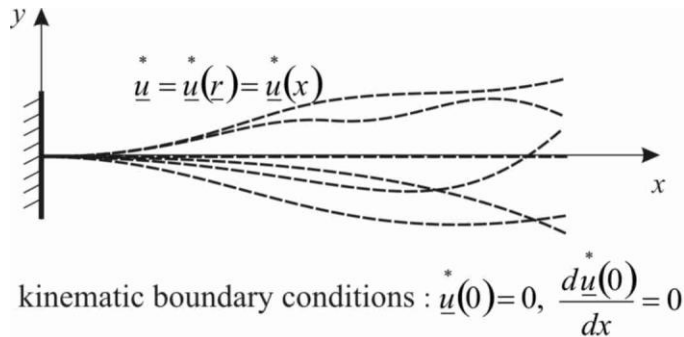


Figure 3.1.: Kinematically admissible displacement field of a fixed beam

The kinematically admissible deformation field can be derived from  $\underline{\dot{\varepsilon}} : \underline{\dot{\varepsilon}} = \frac{1}{2} \left( \underline{\dot{u}} \circ \nabla + \nabla \circ \underline{\dot{u}} \right)$ .

The kinematically admissible stress field can be derived from the displacement field by the use of the constitution equation (material equation, general Hooke law):  $\underline{\dot{\sigma}} = 2G \left( \underline{\dot{\varepsilon}} + \frac{\nu}{1-2\nu} \underline{\dot{\varepsilon}}_1 \underline{\dot{E}} \right)$ . Since an elasticity problem can only have one  $\underline{\dot{\sigma}}(\underline{r})$  solution, while  $\underline{\dot{\sigma}}(\underline{r})$  can have infinite solution thus generally it does not satisfy the equilibrium equations and the dynamic boundary conditions.

##### 3.1.2. Statically admissible stress field

$\underline{\dot{\sigma}} = \underline{\dot{\sigma}}(\underline{r})$  Stress field is statically admissible if:

- Satisfies the dynamic boundary conditions (Figure 2.15.),  $\bar{\underline{\sigma}} \cdot \underline{n}|_{A_p} = \underline{p}_0$ ,
- Satisfies the equilibrium equations:  $\bar{\underline{\sigma}} \cdot \nabla + \underline{q} = 0$ .

The kinematically admissible deformation field can be derived from this stress field by the use of the constitution equation:  $\bar{\underline{\varepsilon}} = \frac{1}{2G} \left( \bar{\underline{\sigma}} - \frac{\nu}{1+\nu} \bar{\underline{\sigma}} \cdot \underline{E} \right)$ . This deformation field and the derived kinematically admissible displacement field generally do not satisfy the geometric equations and the kinematic boundary conditions.

### 3.2. Principle of virtual energy

*Virtual displacement:* small, arbitrary, admissible displacement of the applied constraints, which can be derived from the difference of a kinematically admissible displacement field and the valid displacement field.  $\delta \underline{u} = \underline{u}^* - \underline{u}$ .

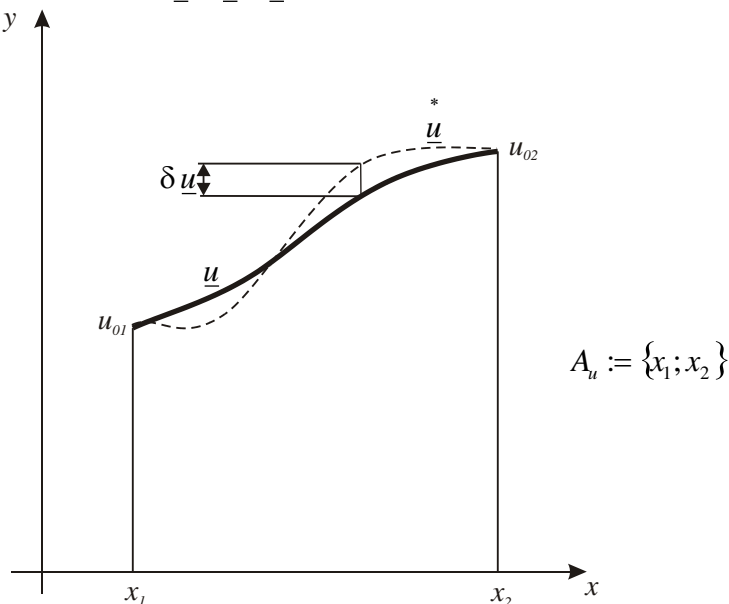


Figure 3.2.: Kinematically admissible and virtual displacement fields

*Principle of virtual work:* if an idyllically elastic system (body) is displaced from its equilibrium state (in case of elasticity the equilibrium is defined by the load and constraints), then the virtual work of the external forces equal to the virtual change of internal energy:

$$\delta W_k = \delta U . \quad (3.1)$$

Work done by the forces on volume and surface:

$$\delta W_k = \int_V \delta \underline{u} \cdot \underline{q} dV + \int_{A_p} \delta \underline{u} \cdot \underline{p} dA \quad (3.2)$$

The virtual internal energy:

$$\delta U = \frac{1}{2} \int_V \underline{\underline{\sigma}} \cdot \underline{\delta \underline{\varepsilon}} dV + \frac{1}{2} \int_V \delta \underline{\underline{\sigma}} \cdot \underline{\underline{\varepsilon}} dV = \int_V \underline{\underline{\sigma}} \cdot \underline{\delta \underline{\varepsilon}} dV \quad (3.3)$$

In (3.3), the  $\underline{\underline{\sigma}} \cdot \underline{\delta \underline{\varepsilon}} = \delta \underline{\underline{\sigma}} \cdot \underline{\underline{\varepsilon}}$  formula (constitution equation) has been already used to describe the relationship between the stress and deformation state.

(3.1) is the theorem of virtual work. Substituting (3.2) and (3.3) equations:

$$\int_V \underline{\underline{\sigma}} \cdot \underline{\delta \underline{\varepsilon}} dV = \int_V \delta \underline{u} \cdot \underline{q} dV + \int_{A_p} \delta \underline{u} \cdot \underline{p} dA. \quad (3.4)$$

### 3.3. Principle of minimum potential energy

The potential energy of a body is the difference of the internal deformation energy and the work done by the external forces:

$$\Pi = U - W_k, \quad (3.5)$$

$$\Pi = \frac{1}{2} \int_V \underline{\underline{\sigma}} \cdot \underline{\underline{\varepsilon}} dV - \int_V \underline{u} \cdot \underline{q} dV - \int_{A_p} \underline{u} \cdot \underline{p} dA. \quad (3.6)$$

The internal deformation energy:

$$U = \frac{1}{2} \int_V \underline{\underline{\sigma}} \cdot \underline{\underline{\varepsilon}} dV,$$

Work done by the external forces:

$$W_k = \int_V \underline{u} \cdot \underline{q} dV + \int_{A_p} \underline{u} \cdot \underline{p} dA.$$

Let us determine the potential energy by using a kinematically admissible displacement field:

$$\overset{*}{\Pi} = \overset{*}{U} - \overset{*}{W}_k \quad (3.7)$$

Work done by the external forces (forces on volume and surface) on an elastic body in case of a kinematically admissible displacement field:

$$\begin{aligned} \overset{*}{W}_k &= \int_V \overset{*}{\underline{u}} \cdot \underline{q} dV + \int_{A_p} \overset{*}{\underline{u}} \cdot \underline{p} dA = \int_V (\underline{u} + \delta \underline{u}) \cdot \underline{q} dV + \int_{A_p} (\underline{u} + \delta \underline{u}) \cdot \underline{p} dA = \\ &= \int_V \underline{u} \cdot \underline{q} dV + \int_V \delta \underline{u} \cdot \underline{q} dV + \int_{A_p} \underline{u} \cdot \underline{p} dA + \int_{A_p} \delta \underline{u} \cdot \underline{p} dA = \end{aligned}$$

$$= \left( \int_V \underline{u} \cdot \underline{q} \, dV + \int_{A_p} \underline{u} \cdot \underline{p} \, dA \right) + \left( \int_V \delta \underline{u} \cdot \underline{q} \, dV + \int_{A_p} \delta \underline{u} \cdot \underline{p} \, dA \right) = W_k + \delta W_k \quad (3.8)$$

The kinematically admissible deformation field:

$$\begin{aligned} \underline{\underline{\varepsilon}}^* &= \frac{1}{2} \left( \underline{u}^* \circ \nabla + \nabla \circ \underline{u}^* \right) = \frac{1}{2} [(\underline{u} + \delta \underline{u}) \circ \nabla + \nabla \circ (\underline{u} + \delta \underline{u})] = \\ &= \frac{1}{2} (\underline{u} \circ \nabla + \nabla \circ \underline{u}) + \frac{1}{2} (\delta \underline{u} \circ \nabla + \nabla \circ \delta \underline{u}) = \underline{\underline{\varepsilon}} + \delta \underline{\underline{\varepsilon}} \end{aligned} \quad (3.9)$$

Internal energy stored in an elastic body due to deformation in case of a kinematically admissible displacement field by applying the constitution equation  $\underline{\underline{\sigma}} \cdot \delta \underline{\underline{\varepsilon}} = \delta \underline{\underline{\sigma}} \cdot \underline{\underline{\varepsilon}}$ :

$$\begin{aligned} U^* &= \frac{1}{2} \int_V \underline{\underline{\sigma}}^* \cdot \underline{\underline{\varepsilon}}^* \, dV = \frac{1}{2} \int_V (\underline{\underline{\sigma}} + \delta \underline{\underline{\sigma}}) \cdot (\underline{\underline{\varepsilon}} + \delta \underline{\underline{\varepsilon}}) \, dV = \\ &= \frac{1}{2} \int_V \underline{\underline{\sigma}} \cdot \underline{\underline{\varepsilon}} \, dV + \frac{1}{2} \int_V \underline{\underline{\sigma}} \cdot \delta \underline{\underline{\varepsilon}} \, dV + \frac{1}{2} \int_V \delta \underline{\underline{\sigma}} \cdot \underline{\underline{\varepsilon}} \, dV + \frac{1}{2} \int_V \delta \underline{\underline{\sigma}} \cdot \delta \underline{\underline{\varepsilon}} \, dV = \\ &= \frac{1}{2} \int_V \underline{\underline{\sigma}} \cdot \underline{\underline{\varepsilon}} \, dV + \int_V \underline{\underline{\sigma}} \cdot \delta \underline{\underline{\varepsilon}} \, dV + \frac{1}{2} \int_V \delta \underline{\underline{\sigma}} \cdot \delta \underline{\underline{\varepsilon}} \, dV = U + \delta U + \delta^2 U \end{aligned} \quad (3.10)$$

The potential energy derived from a kinematically admissible displacement field by the use of (3.7), (3.8) and (3.10):

$$\begin{aligned} \Pi^* &= U^* - W_k^* = U + \delta U + \delta^2 U - W_k - \delta W_k = \\ &= (U - W_k) + (\delta U - \delta W_k) + \delta^2 U = \Pi + \delta \Pi + \delta^2 \Pi, \text{ where} \end{aligned} \quad (3.11)$$

the potential energy of the valid displacement (solution) is:

$$\Pi = U - W_k.$$

The first variation of potential energy:

$$\delta \Pi = \delta U - \delta W_k, \quad (3.12)$$

The second variation of potential energy:

$$\delta^2 \Pi = \delta^2 U. \quad (3.13)$$

The first variation of potential energy is zero according to the theorem of virtual work  $\delta W_k = \delta U$ :

$$\delta\Pi = 0, \quad (3.14)$$

The second variation of potential energy is an energy quantity, thus it is valid to any arbitrary  $\delta u$ :

$$\delta^2\Pi \geq 0. \quad (3.15)$$

Then the difference of a kinematically admissible and a valid displacement field is:

$$\overset{*}{\Pi} - \Pi \geq 0 \quad (= \delta^2\Pi). \quad (3.16)$$

The (3.16) formula is ***the principle of minimum total potential energy***: among all kinematically admissible displacement fields, the potential energy is minimal in case of the valid displacement field.

### 3.4. Principle of Lagrange variation

The variation form of the principle of minimum total potential energy is the principle of Lagrange variation. By using the variation approach, the total potential energy is a functional depending on the displacement field:

$$\Pi[\underline{u}] = U[\underline{u}] - W_k[\underline{u}],$$

Where the kinematic boundary condition in variation form is:

$$\delta\underline{u}\Big|_{A_u} = 0.$$

The condition of the extrema is:  $\delta\Pi = 0$ ,

$$\delta\Pi = \delta U - \delta W_k = 0. \quad (3.17)$$

In case of elastic bodies, this principle is equal with the principle of virtual work (3.1).

If the first variation is zero, then the functional can be stationery, minimum or maximum.

In or case the second variation can be either positive or zero value  $\delta^2\Pi \geq 0$ , thus it can be stationery, or stable minimum.

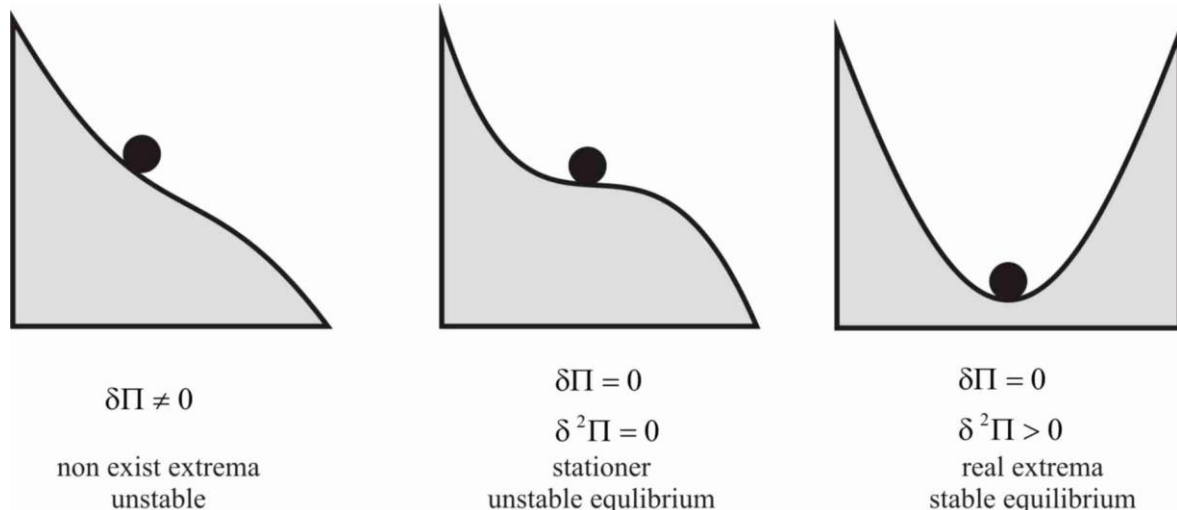


Figure 3.3.: Kinetic example of potential energy

The variations of potential energy describe the stability conditions of a kinetic problem on Figure 3.3.

### 3.5. Finite element model based on displacement method

The most widely spread finite element method is based on the motion method; the commercial programs mostly apply this basic method. The fundamentals of the method are the followings: the body must be divided into elements, and then kinematically admissible displacement fields must be considered on the elements by approximate functions. After that, by applying the geometric and constitution equation alongside with the boundary conditions a linear algebraic equation system is created. The solution of this equation system is the approximate displacement field. The stress field, calculated from the displacement field, will particularly satisfy the equilibrium equations. In the description, vectors (column matrixes) will be used instead of tensors.

#### 3.5.1. Introduction of vector fields

*Vector of stress components (column matrix):* the vector, including the stress tensor compo-

$$\text{nents is described in a spatial system as: } \underline{\sigma} = \underline{\sigma}(r) = \begin{bmatrix} \sigma_x \\ \sigma_y \\ \sigma_z \\ \tau_{xy} \\ \tau_{yz} \\ \tau_{xz} \end{bmatrix} = \begin{bmatrix} \sigma_x(x, y, z) \\ \sigma_y(x, y, z) \\ \sigma_z(x, y, z) \\ \tau_{xy}(x, y, z) \\ \tau_{yz}(x, y, z) \\ \tau_{xz}(x, y, z) \end{bmatrix}, \text{ while in case of co-}$$

$$\text{planar system: } \underline{\sigma} = \underline{\sigma}(r) = \begin{bmatrix} \sigma_x(x, y) \\ \sigma_y(x, y) \\ \tau_{xy}(x, y) \end{bmatrix}.$$

*Strain vector (column matrix):* vector, including the stress tensor components is described

$$\text{in a spatial system as: } \underline{\varepsilon} = \underline{\varepsilon}(r) = \begin{bmatrix} \varepsilon_x \\ \varepsilon_y \\ \varepsilon_z \\ \gamma_{xy} \\ \gamma_{yz} \\ \gamma_{xz} \end{bmatrix} = \begin{bmatrix} \varepsilon_x(x, y, z) \\ \varepsilon_y(x, y, z) \\ \varepsilon_z(x, y, z) \\ \gamma_{xy}(x, y, z) \\ \gamma_{yz}(x, y, z) \\ \gamma_{xz}(x, y, z) \end{bmatrix}, \text{ while in case of co-planar system:}$$

$$\underline{\varepsilon} = \underline{\varepsilon}(r) = \begin{bmatrix} \varepsilon_x(x, y) \\ \varepsilon_y(x, y) \\ \gamma_{xy}(x, y) \end{bmatrix}.$$

If the displacement method is used, then the geometric and constitution equations are also required. These equations have to be reformulated to vector equations. Let us define the scalar components of the geometric equation  $\underline{\underline{\varepsilon}} = \frac{1}{2}(\underline{u} \circ \nabla + \nabla \circ \underline{u})$  in a Descartes coordinate system:

$$\varepsilon_x = \frac{\partial u}{\partial x}, \quad \varepsilon_y = \frac{\partial v}{\partial y}, \quad \varepsilon_z = \frac{\partial w}{\partial z},$$

$$\gamma_{xy} = \gamma_{yx} = \frac{\partial v}{\partial x} + \frac{\partial u}{\partial y}, \quad \gamma_{yz} = \gamma_{zy} = \frac{\partial v}{\partial z} + \frac{\partial w}{\partial y}, \quad \gamma_{xz} = \gamma_{zx} = \frac{\partial w}{\partial x} + \frac{\partial u}{\partial z}$$

and substitute them into the deformation vector. Let us convert them into a product form:

$$\underline{\varepsilon} = \begin{bmatrix} \varepsilon_x \\ \varepsilon_y \\ \varepsilon_z \\ \gamma_{xy} \\ \gamma_{yz} \\ \gamma_{xz} \end{bmatrix} = \begin{bmatrix} \frac{\partial u}{\partial x} \\ \frac{\partial v}{\partial y} \\ \frac{\partial w}{\partial z} \\ \frac{\partial v}{\partial x} + \frac{\partial u}{\partial y} \\ \frac{\partial v}{\partial z} + \frac{\partial w}{\partial y} \\ \frac{\partial w}{\partial x} + \frac{\partial u}{\partial z} \end{bmatrix} = \begin{bmatrix} \frac{\partial}{\partial x} & 0 & 0 \\ 0 & \frac{\partial}{\partial y} & 0 \\ 0 & 0 & \frac{\partial}{\partial z} \\ \frac{\partial}{\partial y} & \frac{\partial}{\partial x} & 0 \\ 0 & \frac{\partial}{\partial z} & \frac{\partial}{\partial y} \\ \frac{\partial}{\partial x} & 0 & \frac{\partial}{\partial z} \end{bmatrix} \cdot \begin{bmatrix} u \\ v \\ w \end{bmatrix} = \underline{\underline{\varepsilon}} \cdot \underline{u}.$$

Thus the deformation vector is derived as product of  $\underline{u}$  displacement vector and  $\underline{\underline{\varepsilon}}$  (including the differential rules) differential operator matrix. The proper elements are substituted into the stress vector by the use of the constitution equation  $\underline{\underline{\sigma}} = 2G\left(\underline{\underline{\varepsilon}} + \frac{\nu}{1-2\nu}\underline{\underline{\varepsilon}}\underline{\underline{E}}\right)$ :

$$\sigma_x = 2G \left( \varepsilon_x + \frac{\nu}{1-2\nu} (\varepsilon_x + \varepsilon_y + \varepsilon_z) \right) = 2G \left( 1 + \frac{\nu}{1-2\nu} \right) \varepsilon_x + \frac{2G\nu}{1-2\nu} \varepsilon_y + \frac{2G\nu}{1-2\nu} \varepsilon_z,$$

$$\sigma_y = 2G \left( \varepsilon_y + \frac{\nu}{1-2\nu} (\varepsilon_x + \varepsilon_y + \varepsilon_z) \right) = \frac{2G\nu}{1-2\nu} \varepsilon_x + 2G \left( 1 + \frac{\nu}{1-2\nu} \right) \varepsilon_y + \frac{2G\nu}{1-2\nu} \varepsilon_z,$$

$$\sigma_z = 2G \left( \varepsilon_z + \frac{\nu}{1-2\nu} (\varepsilon_x + \varepsilon_y + \varepsilon_z) \right) = \frac{2G\nu}{1-2\nu} \varepsilon_x + \frac{2G\nu}{1-2\nu} \varepsilon_y + 2G \left( 1 + \frac{\nu}{1-2\nu} \right) \varepsilon_z,$$

$$\tau_{xy} = G\gamma_{xy}, \quad \tau_{yz} = G\gamma_{yz}, \quad \tau_{xz} = G\gamma_{xz}.$$

Then, let us convert them into product form:

$$\underline{\sigma} = \begin{bmatrix} \sigma_x \\ \sigma_y \\ \sigma_z \\ \tau_{xy} \\ \tau_{yz} \\ \tau_{xz} \end{bmatrix} = \begin{bmatrix} 2G \left( 1 + \frac{\nu}{1-2\nu} \right) \varepsilon_x + \frac{2G\nu}{1-2\nu} \varepsilon_y + \frac{2G\nu}{1-2\nu} \varepsilon_z \\ \frac{2G\nu}{1-2\nu} \varepsilon_x + 2G \left( 1 + \frac{\nu}{1-2\nu} \right) \varepsilon_y + \frac{2G\nu}{1-2\nu} \varepsilon_z \\ \frac{2G\nu}{1-2\nu} \varepsilon_x + \frac{2G\nu}{1-2\nu} \varepsilon_y + 2G \left( 1 + \frac{\nu}{1-2\nu} \right) \varepsilon_z \\ G\gamma_{xy} \\ G\gamma_{yz} \\ G\gamma_{xz} \end{bmatrix} =$$

$$= \begin{bmatrix} 2G \left( 1 + \frac{\nu}{1-2\nu} \right) & \frac{2G\nu}{1-2\nu} & \frac{2G\nu}{1-2\nu} & 0 & 0 & 0 \\ \frac{2G\nu}{1-2\nu} & 2G \left( 1 + \frac{\nu}{1-2\nu} \right) & \frac{2G\nu}{1-2\nu} & 0 & 0 & 0 \\ \frac{2G\nu}{1-2\nu} & \frac{2G\nu}{1-2\nu} & 2G \left( 1 + \frac{\nu}{1-2\nu} \right) & 0 & 0 & 0 \\ 0 & 0 & 0 & G & 0 & 0 \\ 0 & 0 & 0 & 0 & G & 0 \\ 0 & 0 & 0 & 0 & 0 & G \end{bmatrix} \cdot \begin{bmatrix} \varepsilon_x \\ \varepsilon_y \\ \varepsilon_z \\ \gamma_{xy} \\ \gamma_{yz} \\ \gamma_{xz} \end{bmatrix} = \underline{C} \underline{\varepsilon}.$$

Thus the stress vector is derived as a product of the  $\underline{\varepsilon}$  deformation vector and the  $\underline{\underline{C}}$  matrix which includes the material constants. Introducing the vector fields, both the geometric equation:

$$\underline{\varepsilon} = \underline{\underline{C}} \underline{u} \tag{3.18}$$

and the constitution equation:

$$\underline{\sigma} = \underline{\underline{C}} \underline{\epsilon}. \quad (3.19)$$

are obtained as single products. Substituting (3.18) into (3.19):  $\underline{\sigma} = \underline{\underline{C}} \underline{\partial} \underline{u}$ , thus the displacement field is the unknown function, while the stress and deformation can be directly calculated.

### 3.5.2. Elasticity problem and the method of solution

The finite element method is presented on an elasticity problem. The general elasticity problem is the following:

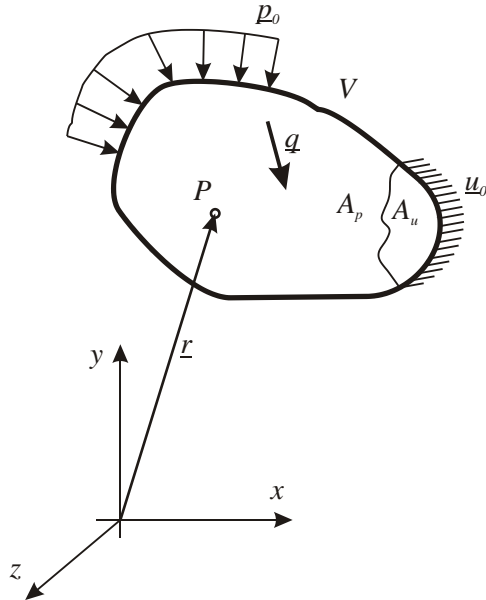


Figure 3.4.: Elasticity problem

According to Figure 3.4, the following data are given:

- The geometry of the body,
- The material constants of the body,
- loads,
- Constraints.

Demand functions:  $\underline{u}(r)$ ,  $\underline{\epsilon}(r)$ ,  $\underline{\sigma}(r)$ .

Steps to solution:

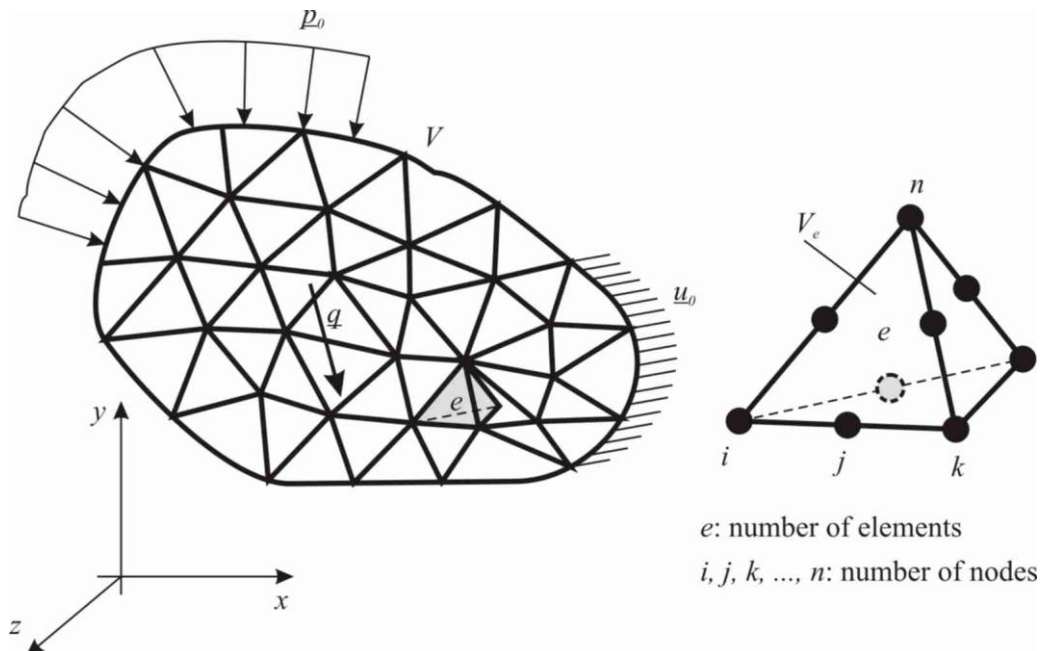
- Firstly, the body is divided to finite domains so-called elements. Special points, nodes are appointed on these elements. The elements cover the total volume of the body, and their geometric representation is a mesh. The single elements are connected to each other by the nodes.
- The displacement field is approximated element by element, generally with polynomials which are fit to the nodes. The displacement fields of the nearby elements are fit to each other through the nodes, and they describe a continuous function on the body.
- The approximate stress- and deformation field can be derived from the displacement field by the use of the geometric- and constitution equation. Then, by the applying the principle of Lagrange variation, a linear, algebraic equation system can be derived with respect to the nodes. This is the so-called ‘stiffness equation’. The algebraic sys-

tem of equation is solvable, if a load or displacement parameter – derived from the kinematic or dynamic boundary conditions – is specified to each nodes on the surface. Thus the unknown values are the displacements of the nodes.

- By solving the system of equation, the approximate nodal displacement field is obtained, thus the approximate stress- and deformation fields can be calculated as well.

### 3.5.3. Finite element, approximate displacement field

The body is divided to arbitrary shaped and sized finite domains, finite elements. Naturally, it is taken into account that the basis functions have to fit to the element.



The displacement field of  $e$  element is approximated by a continuously differentiable function. The type of the function is determined, and according to this function, the demanded numbers of nodes (2 points in case of linear function, 3 points in case of quadratic function) are appointed on the element. Then the displacement field is described by the nodal displacement. The displacement of element node  $i$  on element:

$$\underline{u}_{ei} = \begin{bmatrix} u_{ei} \\ v_{ei} \\ w_{ei} \end{bmatrix},$$

The displacement vector of element  $e$  derived from the displacement of  $i, j, k, \dots, n$  nodes:

$$\underline{u}_e = \begin{bmatrix} u_{ei} \\ v_{ei} \\ w_{ei} \\ \vdots \\ u_{en} \\ v_{en} \\ w_{en} \end{bmatrix} = \begin{bmatrix} \underline{u}_{ei} \\ \underline{u}_{ej} \\ \vdots \\ \underline{u}_{en} \end{bmatrix},$$

while this vector consist  $3n$  number of elements. The  $\underline{u}_e(\underline{r})$  displacement vector (field) of  $e$  element is derived from the interpolation of  $\underline{u}_e$  nodal displacement vector:

$$\underline{u}_e(\underline{r}) = \underline{\underline{N}}_e(\underline{r}) \cdot \underline{u}_e, \quad (3.20)$$

where  $\underline{\underline{N}}_e(\underline{r})$  is the approximate matrix (matrix of the interpolation functions). This matrix is built up by  $(3 \times 3)$  blocks, and each block includes the interpolation function of each node.

The displacement of the element can be derived from the nodal displacement of  $i$  with respect to  $e$  element:

$$\underline{u}_{ei}(\underline{r}) = \underline{\underline{N}}_{ei}(\underline{r}) \cdot \underline{u}_{ei} = \begin{bmatrix} N_{eixx}(\underline{r}) & N_{eixy}(\underline{r}) & N_{eixz}(\underline{r}) \\ N_{eiyx}(\underline{r}) & N_{eiyy}(\underline{r}) & N_{eiyz}(\underline{r}) \\ N_{eizx}(\underline{r}) & N_{eizy}(\underline{r}) & N_{eizz}(\underline{r}) \end{bmatrix} \cdot \begin{bmatrix} u_{ei} \\ v_{ei} \\ w_{ei} \end{bmatrix},$$

Where the elements of  $\underline{\underline{N}}_{ei}(\underline{r})$  are the interpolation functions. Definition of the indexes:

The  $N_{eixz}(\underline{r})$  function defines the displacement along  $x$  direction of element  $e$  related to any arbitrary  $\underline{r}$  location due to the displacement of  $z$  direction of node  $i$ , while the other components of the nodal displacement vector of element  $e$  are zero.

The functions must to satisfy the following conditions:

- The functions must be continuously differentiable,
- $\underline{\underline{N}}_{ei}(\underline{r}_i) = \underline{\underline{E}}$ , the function must provide unit value of displacement in node  $i$ ,
- $\underline{\underline{N}}_{ei}(\underline{r}_j) = \dots = \underline{\underline{N}}_{ei}(\underline{r}_n) = 0$ , the function must equal to zero in the other nodes.

The  $\underline{\underline{N}}_e(\underline{r})$  matrix has  $n$  elements, all the blocks related to the nodes  $\underline{\underline{N}}_{ei}(\underline{r})$ ,  $\underline{\underline{N}}_{ej}(\underline{r})$ , ...,  $\underline{\underline{N}}_{en}(\underline{r})$  has to have the same size  $(3 \times 3)$ :

$$\underline{\underline{N}}_e(\underline{r}) = [\underline{\underline{N}}_{ei}(\underline{r}) \ \underline{\underline{N}}_{ej}(\underline{r}) \ \dots \ \underline{\underline{N}}_{en}(\underline{r})].$$

By the approximation of the element's displacement field, the deformation field can be obtained by substituting (3.20) into (3.18):

$$\underline{\varepsilon}_e(\underline{r}) = \underline{\underline{\partial}} \underline{u}_e(\underline{r}) = \underline{\underline{\partial}} \underline{\underline{N}}_e(\underline{r}) \cdot \underline{u}_e,$$

Introducing  $\underline{\underline{B}}_e(\underline{r})$  nodal-deformation matrix as a product of the differential operator and the approximate matrix:

$$\underline{\varepsilon}_e(\underline{r}) = \underline{\underline{B}}_e(\underline{r}) \cdot \underline{u}_e. \quad (3.21)$$

The stress field of the element:

$$\underline{\sigma}_e(\underline{r}) = \underline{\underline{C}}\underline{\varepsilon}_e(\underline{r}) = \underline{\underline{C}}\underline{\underline{B}}_e(\underline{r}) \cdot \underline{u}_e. \quad (3.22)$$

The potential energy of the element according to (3.6):

$$\Pi_e = \frac{1}{2} \int_{V_e} [\underline{\sigma}_e(\underline{r})]^T \underline{\varepsilon}_e(\underline{r}) dV - \int_{V_e} \underline{u}_e(\underline{r}) \cdot \underline{q} dV - \int_{A_{ep}} \underline{u}_e(\underline{r}) \cdot \underline{p} dA.$$

Rewriting the formula by forming the scalar and double scalar products into matrix products (the constants of the internal energy are replaced) and introducing them as vectors instead of tensors:

$$\Pi_e = \frac{1}{2} \int_{V_e} [\underline{\varepsilon}_e(\underline{r})]^T \underline{\sigma}_e(\underline{r}) dV - \int_{V_e} [\underline{u}_e(\underline{r})]^T \underline{q} dV - \int_{A_{ep}} [\underline{u}_e(\underline{r})]^T \underline{p} dA.$$

Substituting (3.20), (3.21), (3.22) and separating the constants out of the integrals:

$$\Pi_e = \frac{1}{2} (\underline{u}_e)^T \int_{V_e} [\underline{B}_e(\underline{r})]^T \underline{\underline{C}} \underline{B}_e(\underline{r}) dV \underline{u}_e - (\underline{u}_e)^T \int_{V_e} [\underline{N}_e(\underline{r})]^T \underline{q} dV - (\underline{u}_e)^T \int_{A_{ep}} [\underline{N}_e(\underline{r})]^T \underline{p} dA.$$

Let us introduce the stiffness matrix:

$$\underline{\underline{K}}_e = \int_{V_e} [\underline{B}_e(\underline{r})]^T \underline{\underline{C}} \underline{B}_e(\underline{r}) dV, \quad (3.23)$$

And the nodal load vectors with respect to the volume and surface forces:

$$\underline{F}_{qe} = \int_{V_e} [\underline{N}_e(\underline{r})]^T \underline{q} dV, \quad (3.24)$$

$$\underline{F}_{pe} = \int_{A_{ep}} [\underline{N}_e(\underline{r})]^T \underline{p} dA, \quad (3.25)$$

$$\underline{F}_e := \underline{F}_{qe} + \underline{F}_{pe}.$$

Thus the potential energy of the element is:

$$\Pi_e = \frac{1}{2} (\underline{u}_e)^T \underline{\underline{K}}_e \underline{u}_e - (\underline{u}_e)^T \underline{F}_e.$$

The energy theorems can only be applied on the whole body; they are not valid on individual elements. If the body has  $Q$  number of elements, the potential energy of the body is derived from the sum of all elements' potential energy.

$$\Pi = \sum_{e=1}^Q \Pi_e = \frac{1}{2} (\underline{U})^T \underline{\underline{K}} \underline{U} - (\underline{U})^T \underline{F}.$$

According to the principle of Lagrange variation, the first variation of the potential energy is zero:

$$\delta \Pi = 0 = \delta \left( \frac{1}{2} (\underline{U})^T \underline{\underline{K}} \underline{U} - (\underline{U})^T \underline{F} \right) = \underline{\underline{K}} \underline{U} - \underline{F}.$$

Setting the equation we derived the stiffness equation:

$$\underline{\underline{K}} \underline{U} = \underline{F}, \quad (3.26)$$

where:

$\underline{\underline{K}}$  : is the stiffness matrix of the body,

$\underline{U}$  : is the nodal displacement vector of the body,

$\underline{F}$  : is the nodal force vector of the body.

(3.26) equation is linear system of equation, which provides the solution of the elasticity problem. (The elements in the equation are formulated according to a simple static problem, in case of thermal stresses, elastic constraints the stiffness matrix has more elements while in case of dynamic problem even other parts are added as well).

### 3.6. Definition and solution of stiffness matrix in case of co-planar tensed truss element

#### 3.6.1. Stiffness matrix of 2D, tensed, truss element

General property of the tensed-compressed structures (truss elements) that the element are only loaded axially. Let us a coordinate system fix to the axis of a truss element. On Figure 3.6  $\underline{F}_i = (F_i, 0)$ ,  $\underline{F}_j = (F_j, 0)$  are represented as the nodal loads of element  $e$  with length  $L$ .

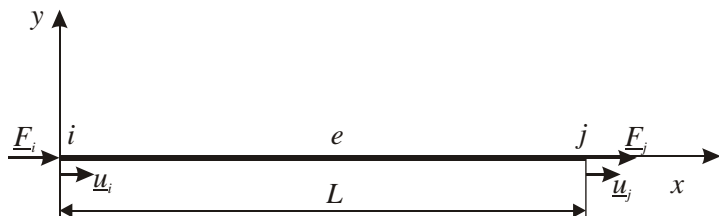


Figure 3.6.: Two nodes on a co-planar element

In node  $i$  the displacement is  $\underline{u}_i = (u_i, 0)$ , while in node  $j$  the displacement is  $\underline{u}_j = (u_j, 0)$ .  
The truss element:

$$\underline{u}_e(x, y) = (u_e(x), 0) \quad (3.27)$$

is approximated by a linear function:

$$u_e(x) = a_{e0} + a_{el}x, \quad (3.28)$$

The displacement field provides the displacement values in the nodes of the element:

$$u_e(x=0) = u_i = a_{e0} + a_{el}0,$$

$$u_e(x=L) = u_j = a_{e0} + a_{el}L.$$

Setting the constants and substituting into (3.28):

$$u_e(x) = u_i + \frac{u_j - u_i}{L}x.$$

Then substituting this equation into (3.27) equation:

$$\underline{u}_e(x, y) = \left( \frac{1-x}{L}u_i + \frac{x}{L}u_j, 0 \right),$$

Forming into matrix product:

$$\underline{u}_e(x, y) = \begin{bmatrix} u_e(x, y) \\ v_e(x, y) \end{bmatrix} = \begin{bmatrix} \frac{1-x}{L} & 0 & \frac{x}{L} & 0 \\ 0 & 0 & 0 & 0 \end{bmatrix} \begin{bmatrix} u_i \\ v_i \\ u_j \\ v_j \end{bmatrix} = \underline{\underline{N}}_e(x, y)\underline{u}_e,$$

where  $\underline{\underline{N}}_e(x, y)$  is the approximation matrix of element  $e$  and  $\underline{u}_e$  is the nodal displacement vector. The approximation matrix is built up from two blocks, with the interpolation functions of node  $i$  and  $j$ :

$$\underline{\underline{N}}_{ei}(x, y) = \begin{bmatrix} \frac{1-x}{L} & 0 \\ 0 & 0 \end{bmatrix}, \quad \underline{\underline{N}}_{ej}(x, y) = \begin{bmatrix} \frac{x}{L} & 0 \\ 0 & 0 \end{bmatrix}.$$

$$N_{eixx}(x, y) = \frac{1-x}{L}, \quad N_{ejxx}(x, y) = \frac{x}{L}$$

These interpolation functions satisfy the required conditions (continuous, provides unit value in its own node, disappears in other nodes) and shown on Figure 3.7.

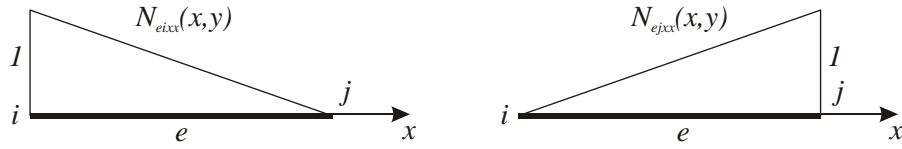


Figure 3.7.: Interpolation functions

In case of truss elements, the only deformation is the elongation, thus the geometric equation:

$$\underline{\varepsilon}_e(x, y) = \begin{bmatrix} \varepsilon_x \\ 0 \end{bmatrix} = \frac{d\underline{u}_e(x, y)}{dx} = \frac{dN_e(x, y)}{dx} \underline{u}_e = \begin{bmatrix} -\frac{1}{L} & 0 & \frac{1}{L} & 0 \\ 0 & 0 & 0 & 0 \end{bmatrix} \begin{bmatrix} u_i \\ v_i \\ u_j \\ v_j \end{bmatrix} = \underline{\underline{B}}_e(x, y) \underline{u}_e .$$

$\underline{\underline{B}}_e(x, y)$  nodal-deformation matrix has constant elements, which results constant strain in the truss. In case of single-stress state, the simple Hooke law can be applied in order to calculate the stress:

$$\underline{\sigma}_e(x, y) = \underline{\underline{C}} \underline{\varepsilon}_e(x, y) = \underline{\underline{C}} \underline{\underline{B}}_e(x, y) \underline{u}_e .$$

The constitution matrix:

$$\underline{\underline{C}} = \begin{bmatrix} E & 0 \\ 0 & E \end{bmatrix} .$$

The stiffness matrix of the element:

$$\begin{aligned} \underline{\underline{K}}_e(x, y) &= \int_{V_e} [\underline{\underline{B}}_e(x, y)]^T \underline{\underline{C}} \underline{\underline{B}}_e(x, y) dV = \int_0^L [\underline{\underline{B}}_e(x, y)]^T \underline{\underline{C}} \underline{\underline{B}}_e(x, y) A dx = \\ &= \int_0^L \begin{bmatrix} -\frac{1}{L} & 0 \\ 0 & 0 \\ \frac{1}{L} & 0 \\ 0 & 0 \end{bmatrix} \begin{bmatrix} E & 0 \\ 0 & E \end{bmatrix} \begin{bmatrix} -\frac{1}{L} & 0 & \frac{1}{L} & 0 \\ 0 & 0 & 0 & 0 \end{bmatrix} A dx = \begin{bmatrix} \frac{E}{L^2} & 0 & -\frac{E}{L^2} & 0 \\ 0 & 0 & 0 & 0 \\ -\frac{E}{L^2} & 0 & \frac{E}{L^2} & 0 \\ 0 & 0 & 0 & 0 \end{bmatrix} A \int_0^L dx \\ \underline{\underline{K}}_e(x, y) &= \frac{AE}{L} \begin{bmatrix} 1 & 0 & -1 & 0 \\ 0 & 0 & 0 & 0 \\ -1 & 0 & 1 & 0 \\ 0 & 0 & 0 & 0 \end{bmatrix} = \underline{\underline{K}}_e . \end{aligned} \quad (3.29)$$

Then the stiffness equation of the element:

$$\underline{\underline{K}}_e \underline{u}_e = \underline{F}_e , \quad (3.30)$$

where

$\underline{u}_e = [u_i \ v_i \ u_j \ v_j]^T$  is the nodal displacement vector of the element,  
 $\underline{F}_e = [F_{xi} \ F_{yi} \ F_{xj} \ F_{yj}]^T$  is the nodal load vector of the element.

In general case, the local coordinate systems fixed to truss elements are different, thus the stiffness equation must be transformed into global (so called absolute) coordinate system in order to summarize the stiffness matrixes of the complete body.

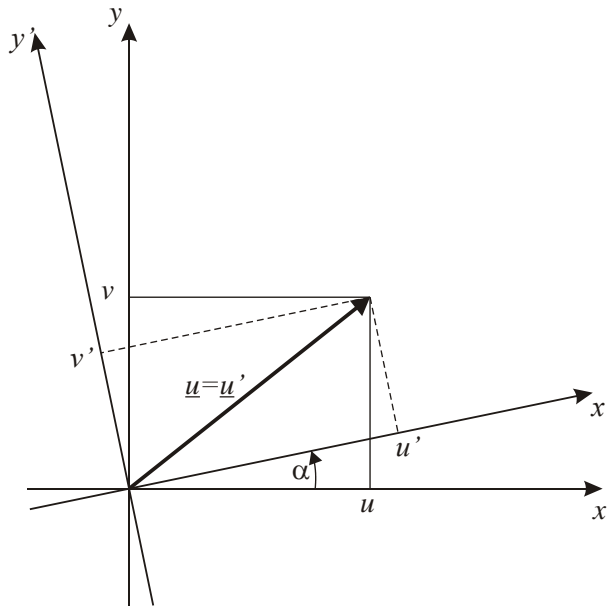


Figure 3.8.: Vector in rotated coordinate system

The vector coordinates show on Figure 3.8 are calculated in a coordinate system rotated by angle  $\alpha$  as follows:

$$u' = u \cdot \cos(\alpha) + v \cdot \sin(\alpha), \quad v' = u \cdot \sin(\alpha) - v \cdot \cos(\alpha).$$

In matrix form:

$$\underline{u}' = \begin{bmatrix} u' \\ v' \end{bmatrix} = \begin{bmatrix} \cos(\alpha) & \sin(\alpha) \\ -\sin(\alpha) & \cos(\alpha) \end{bmatrix} \begin{bmatrix} u \\ v \end{bmatrix} = \underline{T} \underline{u}, \quad (3.31)$$

where  $\underline{T}$  is the transformation matrix. The matrix includes two vectors;  $\underline{u}_e$  and  $\underline{F}_e$  vectors can be described by two blocks, where one block relates to one vector:

$$\underline{\underline{T}} = \begin{bmatrix} \cos(\alpha) & \sin(\alpha) & 0 & 0 \\ -\sin(\alpha) & \cos(\alpha) & 0 & 0 \\ 0 & 0 & \cos(\alpha) & \sin(\alpha) \\ 0 & 0 & -\sin(\alpha) & \cos(\alpha) \end{bmatrix}. \quad (3.32)$$

Let us determine the stiffness matrix in a coordinate system rotated by angle  $\alpha$ ! In order to carry out this calculation, we have to determine the transformed (3.30) equation as well:

$$\underline{\underline{K}}'_e \underline{u}'_e = \underline{F}'_e. \quad (3.33)$$

According to (3.31):

$$\underline{u}'_e = \underline{\underline{T}} \underline{u}_e \Rightarrow \underline{u}_e = \underline{\underline{T}}^{-1} \underline{u}'_e, \text{ similar to this: } \underline{F}_e = \underline{\underline{T}}^{-1} \underline{F}'_e.$$

Substituting this form into (3.30):

$$\underline{\underline{K}}_e \underline{\underline{T}}^{-1} \underline{u}'_e = \underline{\underline{T}}^{-1} \underline{F}'_e.$$

Let us multiply the equation with  $\underline{\underline{T}}$  from the left side:

$$\underline{\underline{T}} \underline{\underline{K}}_e \underline{\underline{T}}^{-1} \underline{u}'_e = \underline{\underline{T}} \underline{\underline{T}}^{-1} \underline{F}'_e,$$

$\underline{\underline{T}} \underline{\underline{T}}^{-1} = \underline{\underline{E}}$   $\Rightarrow \underline{\underline{T}} \underline{\underline{K}}_e \underline{\underline{T}}^{-1} \underline{u}'_e = \underline{F}'_e$ , by the use of (3.33), we obtain the following:

$$\underline{\underline{K}}'_e = \underline{\underline{T}} \underline{\underline{K}}_e \underline{\underline{T}}^{-1}. \quad (3.34)$$

$\underline{\underline{T}}$  is asymmetric, thus  $\underline{\underline{T}}^{-1} = \underline{\underline{T}}^T$ , then:

$$\underline{\underline{K}}'_e = \underline{\underline{T}} \underline{\underline{K}}_e \underline{\underline{T}}^T. \quad (3.35)$$

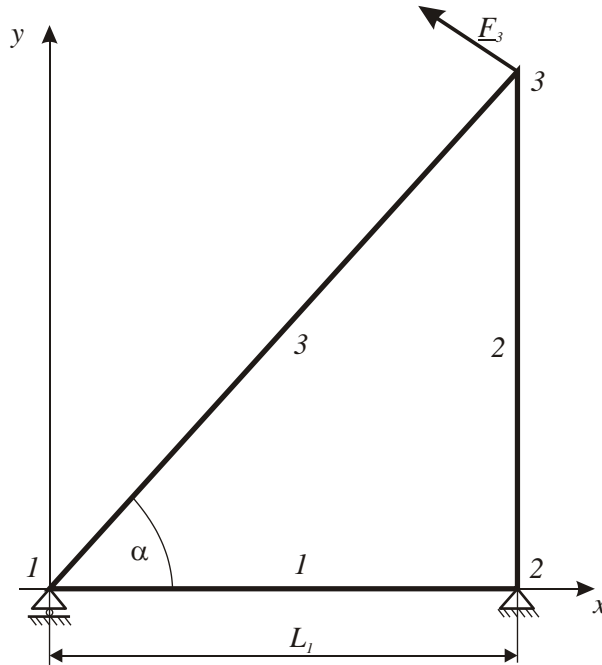
Let us calculate the stiffness matrix of a co-planar truss, defined as (3.35) in a global coordinate system, with respect to formula (3.29) related to the use of the stiffness matrix in local coordinate systems:

$$\underline{\underline{K}}'_e \underline{\underline{T}}^T = \frac{AE}{L} \begin{bmatrix} \cos(\alpha) & -\sin(\alpha) & -\cos(\alpha) & \sin(\alpha) \\ 0 & 0 & 0 & 0 \\ -\cos(\alpha) & \sin(\alpha) & \cos(\alpha) & -\sin(\alpha) \\ 0 & 0 & 0 & 0 \end{bmatrix},$$

$$\underline{\underline{K}}_e = \underline{\underline{T}} \underline{\underline{K}}_e \underline{\underline{T}}^T = \frac{AE}{L} \begin{bmatrix} \cos^2(\alpha) & -\cos(\alpha)\sin(\alpha) & -\cos^2(\alpha) & \cos(\alpha)\sin(\alpha) \\ -\cos(\alpha)\sin(\alpha) & \sin^2(\alpha) & \cos(\alpha)\sin(\alpha) & -\sin^2(\alpha) \\ -\cos^2(\alpha) & \cos(\alpha)\sin(\alpha) & \cos^2(\alpha) & -\cos(\alpha)\sin(\alpha) \\ \cos(\alpha)\sin(\alpha) & -\sin^2(\alpha) & -\cos(\alpha)\sin(\alpha) & \sin^2(\alpha) \end{bmatrix} \quad (3.36)$$

In case of a structure, all stiffness matrixes of the trusses must be transformed into a global coordinate system and there summarized. After then the stiffness equation can be applied on the structure, which provides the solution as displacements and forces in all nodes.

### 3.6.2. Example



3.9. ábra: Trusses

The structure on Figure 3.9 includes three trusses. The given data are:

$$F_{3x} = -1200N$$

$$F_{3y} = 1000N$$

$$L_1 = 1,2m$$

$$\alpha = 50^\circ$$

$$A_1 = A_2 = A_3 = A = 100mm^2$$

$$E = 210GPa$$

Determine the forces and displacements in the nodes!

Lengths of the trusses:

$$L_2 = L_1 \operatorname{tg}(\alpha) = 1430,1mm$$

$$L_3 = \frac{L_1}{\cos(\alpha)} = 1866,87mm$$

The stiffness matrix of truss 1 in the local (which is identical with the absolute) according to (3.29):

$$\underline{\underline{K}}_1 = \frac{AE}{L_1} \begin{bmatrix} 1 & 0 & -1 & 0 \\ 0 & 0 & 0 & 0 \\ -1 & 0 & 1 & 0 \\ 0 & 0 & 0 & 0 \end{bmatrix} = \begin{bmatrix} 17500 & 0 & -17500 & 0 \\ 0 & 0 & 0 & 0 \\ -17500 & 0 & 17500 & 0 \\ 0 & 0 & 0 & 0 \end{bmatrix} \frac{N}{mm}$$

The  $2 \times 2$  nodal blocks (upper index is the number of the element; lower index is the number of the two nodes. The block describes the relationship between nodes):

$$\underline{\underline{K}}_1 = \begin{bmatrix} \underline{\underline{K}}_{11}^1 & \underline{\underline{K}}_{12}^1 \\ \underline{\underline{K}}_{21}^1 & \underline{\underline{K}}_{22}^1 \end{bmatrix}.$$

The stiffness matrix of truss 2 in the local coordinate system:

$$\underline{\underline{K}}_2^\xi = \frac{AE}{L_2} \begin{bmatrix} 1 & 0 & -1 & 0 \\ 0 & 0 & 0 & 0 \\ -1 & 0 & 1 & 0 \\ 0 & 0 & 0 & 0 \end{bmatrix} = \begin{bmatrix} 14684,24 & 0 & -14684,24 & 0 \\ 0 & 0 & 0 & 0 \\ -14684,24 & 0 & 14684,24 & 0 \\ 0 & 0 & 0 & 0 \end{bmatrix} \frac{N}{mm}.$$

Truss 2 is perpendicular in the absolute coordinate system, thus its coordinates have to be recalculated in the absolute coordinate system according to (3.36):

$$\underline{\underline{K}}_2 = \underline{T} \underline{\underline{K}}_2^\xi \underline{T}^T = \frac{AE}{L_2} \begin{bmatrix} \cos^2(\alpha_2) & -\cos(\alpha_2)\sin(\alpha_2) & -\cos^2(\alpha_2) & \cos(\alpha_2)\sin(\alpha_2) \\ -\cos(\alpha_2)\sin(\alpha_2) & \sin^2(\alpha_2) & \cos(\alpha_2)\sin(\alpha_2) & -\sin^2(\alpha_2) \\ -\cos^2(\alpha_2) & \cos(\alpha_2)\sin(\alpha_2) & \cos^2(\alpha_2) & -\cos(\alpha_2)\sin(\alpha_2) \\ \cos(\alpha_2)\sin(\alpha_2) & -\sin^2(\alpha_2) & -\cos(\alpha_2)\sin(\alpha_2) & \sin^2(\alpha_2) \end{bmatrix}$$

where  $\alpha_2 = -90^\circ$ .

$$\underline{\underline{K}}_2 = \frac{AE}{L_2} \begin{bmatrix} 0 & 0 & 0 & 0 \\ 0 & 1 & 0 & -1 \\ 0 & 0 & 0 & 0 \\ 0 & -1 & 0 & 1 \end{bmatrix} = \begin{bmatrix} 0 & 0 & 0 & 0 \\ 0 & 14684,24 & 0 & -14684,24 \\ 0 & 0 & 0 & 0 \\ 0 & -14684,24 & 0 & 14684,24 \end{bmatrix} \frac{N}{mm}$$

The  $2 \times 2$  nodal blocks:

$$\underline{\underline{K}}_2 = \begin{bmatrix} \underline{\underline{K}}_{22}^2 & \underline{\underline{K}}_{23}^2 \\ \underline{\underline{K}}_{32}^2 & \underline{\underline{K}}_{33}^2 \end{bmatrix}.$$

The stiffness matrix of truss 3 in the local coordinate system:

$$\underline{\underline{K}}_3^{\xi} = \frac{AE}{L_3} \begin{bmatrix} 1 & 0 & -1 & 0 \\ 0 & 0 & 0 & 0 \\ -1 & 0 & 1 & 0 \\ 0 & 0 & 0 & 0 \end{bmatrix} = \begin{bmatrix} 11248,78 & 0 & -11248,78 & 0 \\ 0 & 0 & 0 & 0 \\ -11248,78 & 0 & 11248,78 & 0 \\ 0 & 0 & 0 & 0 \end{bmatrix} \frac{N}{mm}$$

Truss 3 is rotated by angle  $\alpha$  in the absolute coordinate system, thus its coordinates have to be recalculated in the absolute coordinate system:

$$\underline{\underline{K}}_3 = \underline{T} \underline{\underline{K}}_3^{\xi} \underline{T}^T = \frac{AE}{L_3} \begin{bmatrix} \cos^2(\alpha) & -\cos(\alpha)\sin(\alpha) & -\cos^2(\alpha) & \cos(\alpha)\sin(\alpha) \\ -\cos(\alpha)\sin(\alpha) & \sin^2(\alpha) & \cos(\alpha)\sin(\alpha) & -\sin^2(\alpha) \\ -\cos^2(\alpha) & \cos(\alpha)\sin(\alpha) & \cos^2(\alpha) & -\cos(\alpha)\sin(\alpha) \\ \cos(\alpha)\sin(\alpha) & -\sin^2(\alpha) & -\cos(\alpha)\sin(\alpha) & \sin^2(\alpha) \end{bmatrix}$$

where  $\alpha = -50^\circ$ .

$$\underline{\underline{K}}_3 = \begin{bmatrix} 4647,73 & 5538,94 & -4647,73 & -5538,94 \\ 5538,94 & 6601,06 & -5538,94 & -6601,06 \\ -4647,73 & -5538,94 & 4647,73 & 5538,94 \\ -5538,94 & -6601,06 & 5538,94 & 6601,06 \end{bmatrix} \frac{N}{mm}$$

The  $2 \times 2$  nodal blocks:

$$\underline{\underline{K}}_3 = \begin{bmatrix} \underline{\underline{K}}_{11}^3 & \underline{\underline{K}}_{13}^3 \\ \underline{\underline{K}}_{31}^3 & \underline{\underline{K}}_{33}^3 \end{bmatrix}.$$

The stiffness matrix is summarized by adding the identical describing blocks of the nearby nodes together, thus the stiffness matrix of the structure is:

$$\underline{\underline{K}} = \begin{bmatrix} \underline{\underline{K}}_{11}^1 + \underline{\underline{K}}_{11}^3 & \underline{\underline{K}}_{12}^1 & \underline{\underline{K}}_{13}^3 \\ \underline{\underline{K}}_{21}^1 & \underline{\underline{K}}_{22}^1 + \underline{\underline{K}}_{22}^2 & \underline{\underline{K}}_{23}^2 \\ \underline{\underline{K}}_{31}^3 & \underline{\underline{K}}_{32}^2 & \underline{\underline{K}}_{33}^2 + \underline{\underline{K}}_{33}^3 \end{bmatrix} =$$

$$= \begin{bmatrix} 17500 + 4647,73 & 5538,94 & -17500 & 0 & -4647,73 & -5538,94 \\ 5538,94 & 6601,06 & 0 & 0 & -5538,94 & -6601,06 \\ -17500 & 0 & 17500 & 0 & 0 & 0 \\ 0 & 0 & 0 & 14684,24 & 0 & -14684,24 \\ -4647,73 & -5538,94 & 0 & 0 & 4647,73 & 5538,94 \\ -5538,94 & -6601,06 & 0 & -14684,24 & 5538,94 & 14684,24 + 6601,06 \end{bmatrix} \frac{N}{mm}$$

The stiffness equation of the structure:

$$\underline{\underline{K}}\underline{U} = \underline{F}$$

$$\begin{bmatrix} 22147,73 & 5538,94 & -17500 & 0 & -4647,73 & -5538,94 \\ 5538,94 & 6601,06 & 0 & 0 & -5538,94 & -6601,06 \\ -17500 & 0 & 17500 & 0 & 0 & 0 \\ 0 & 0 & 0 & 14684,24 & 0 & -14684,24 \\ -4647,73 & -5538,94 & 0 & 0 & 4647,73 & 5538,94 \\ -5538,94 & -6601,06 & 0 & -14684,24 & 5538,94 & 25285,3 \end{bmatrix} \begin{bmatrix} u_1 \\ v_1 \\ u_2 \\ v_2 \\ u_3 \\ v_3 \end{bmatrix} = \begin{bmatrix} F_{1x} \\ F_{1y} \\ F_{2x} \\ F_{2y} \\ F_{3x} \\ F_{3y} \end{bmatrix}$$

By substituting the known force and displacement boundary conditions:

$$\begin{bmatrix} 22147,73 & 5538,94 & -17500 & 0 & -4647,73 & -5538,94 \\ 5538,94 & 6601,06 & 0 & 0 & -5538,94 & -6601,06 \\ -17500 & 0 & 17500 & 0 & 0 & 0 \\ 0 & 0 & 0 & 14684,24 & 0 & -14684,24 \\ -4647,73 & -5538,94 & 0 & 0 & 4647,73 & 5538,94 \\ -5538,94 & -6601,06 & 0 & -14684,24 & 5538,94 & 25285,3 \end{bmatrix} \begin{bmatrix} u_1 \\ 0 \\ 0 \\ 0 \\ u_3 \\ v_3 \end{bmatrix} = \begin{bmatrix} 0 \\ F_{1y} \\ F_{2x} \\ F_{2y} \\ -1200 \\ 1000 \end{bmatrix}.$$

The product is the solution of a linear system of equations with six unknown values:

$$u_1 = -0,068571mm$$

$$u_3 = -0,523986mm$$

$$v_3 = 0,16549mm$$

$$F_{1y} = 1430,1N$$

$$F_{2x} = 1200N$$

$$F_{2y} = -2430,1N$$

## **4. ANALYSIS OF TWO-DIMENSIONAL TRUSSES USING FINITE ELEMENT METHOD BASED PROGRAM SYSTEM**

### **4.1. Two-dimensional bar structures**

In several chapters of the mechanics, we meet structures, which consist of static bars. Their main properties are that they are loaded only at the two ends, and then only axial forces, consequently, drawn or pressed. Such structures are called trusses. In this chapter we deal with two-dimensional trusses only. These structures are defined so that:

- Axis of the bars lie in a common plane,
- The bars are connected in an ideal plane joint,
- The bars geometric axes intersect at one point,
- The structure are linked to the ground by ideal joint constraints,
- The external forces can act in the nodes and the lines of action of the forces are in the plane of the bars.

During the examination of the trusses we usually look for the answer to the following questions:

- magnitude and direction of the reaction forces
- magnitude and direction of forces resulting in bars,
- the forces and stresses generated in bars
- the resulting displacements of each point of the structure and the deformation of each bar

More structures, which generally contain bending bars (simply supported and cantilever beams, frame structure, curved bars etc) may be tested for the stability of the structure and dynamic behavior (the critical forces of compressed bars and natural frequencies). We deal these problems in chapters 5-8 and the instability of compressed bars in the chapter 9-10.

In determining the reactions forces important issue is whether the beam is externally statically determined or indetermined. This is influence the used methods.

In determining the bar forces an important issue whether the beam is internally statically determined or indetermined

The calculation of displacements and deformations are very simply for both internally and externally determined structures. In this case we use geometric approach. For solve complicated structures and statically indeterminate structures we use principles of energy (Castigliano and Betti's theorem).

As we shall see, it is irrelevant whether the structure externally or internally indetermined, the procedure will not be affected, when we use the finite element method-based solution.

### **4.2. Finite elements for modeling beams**

Generally there are two types of element available for modeling of beams in FEA (finite element analysis) programs. For modeling of trusses TRUSS elements and, for the bent, sheared, twisted bars BEAM elements may be used. In both cases, the finite-element two-dimensional and characterized by a single line.

#### 4.2.1. The TRUSS element properties

The TRUSS elements are grouped according to use them for two- or three-dimensional modeling. We distinguish two types of element, TRUSS2D (see Figure 4.1) and TRUSS3D (see Figure 4.2).

The TRUSS2D elements are two-nodes, uniaxial elements, with two displacement degrees of freedom in both nodes. The element local coordinate system x-axis is defined by a vector that starts at the first node and points towards the second node. The y-axis is parallel the global coordinate system XY plane and perpendicular to the x-axis.

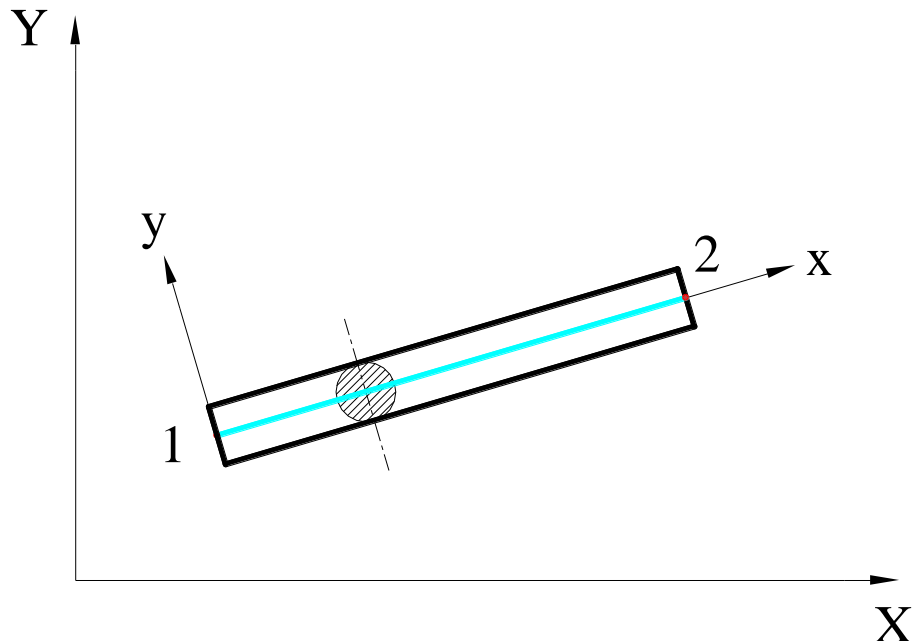


Figure 4.1 TRUSS2D elements

The linear static analysis requires more constants to specify the real three-dimensional element properties. In this case that is the cross-sectional area of the beam. This is not used only to calculate elastic properties of elements, but also it is needed for determination the tare weight.

We will also need the material properties of the bars. In this case, it is sufficient to determine the elastic modulus. The calculations of the own weight of structures requires to determine the material density.

We can perform buckling and heat transfer analysis using TRUSS2D elements.

The BEAM3D is a two-node, uniaxial element too. For structural analysis, six degrees of freedom (three translations and three rotations) are considered per node. The x and y axis of the element coordinate system same as described above, and a third node is required to assign the element orientation.

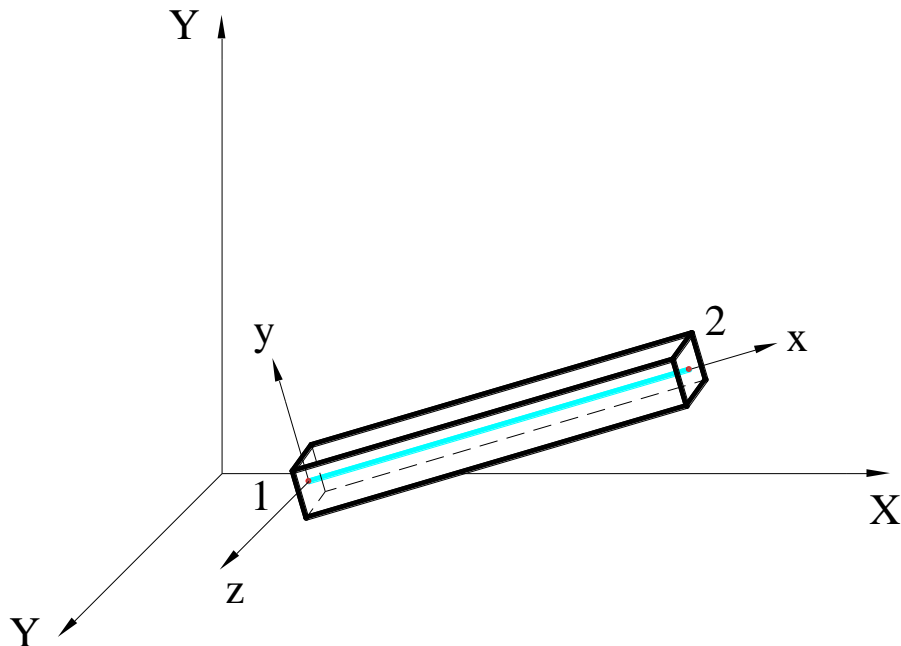


Figure 4.2 TRUSS3D element

The necessary real constants and material properties are the same as given as for TRUSS2D elements.

The TRUSS3D elements can also be used in stability, and thermal analysis problems

#### 4.2.2. Beam Element's properties

The BEAM2D element is a two-node uniaxial element, but unlike the truss elements, at both two-nodes there are three-degrees of freedom (two displacements and a rotation), so these are suitable for two-dimensional modeling of bent bars.

The BEAM3D element is a two-node uniaxial element also, but unlike the truss elements, at both two-node are six-degrees of freedom (three displacement and three rotation). These elements are suitable for modeling three-dimensional bar structures. More detailed description of these elements is in chapter 4-6.

### 4.3. Study solution

The finite element study procedure:

1. problem analysis,
2. create a geometry for generate a finite element mesh,
3. define properties of finite elements (element type, real constant, material properties),
4. determine boundary conditions, and loads,
5. solve the model,
6. evaluation of the results

At both ends supported trusses are loaded at two nodes. The forces are 120-120 kN each. (see Figure 4.3). The bars are steel pipes 100x10.

To be determined:

- deflection of the structure,
- stresses generated in the bars,

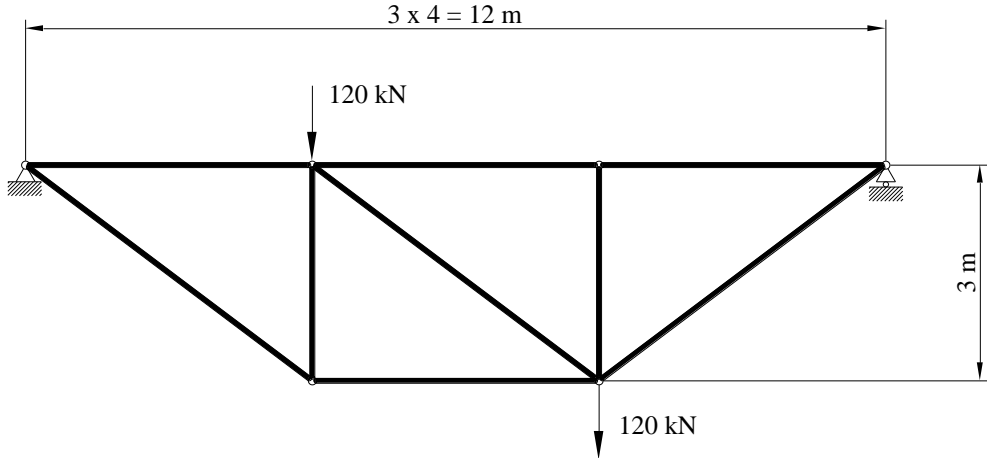


Figure 4.3 The tested trusses

The finite element programs usually contain built-in 3D geometric modeler, graphics pre- and postprocessor. Thus, we can prepare the geometric model in its (see Figure 4.4)

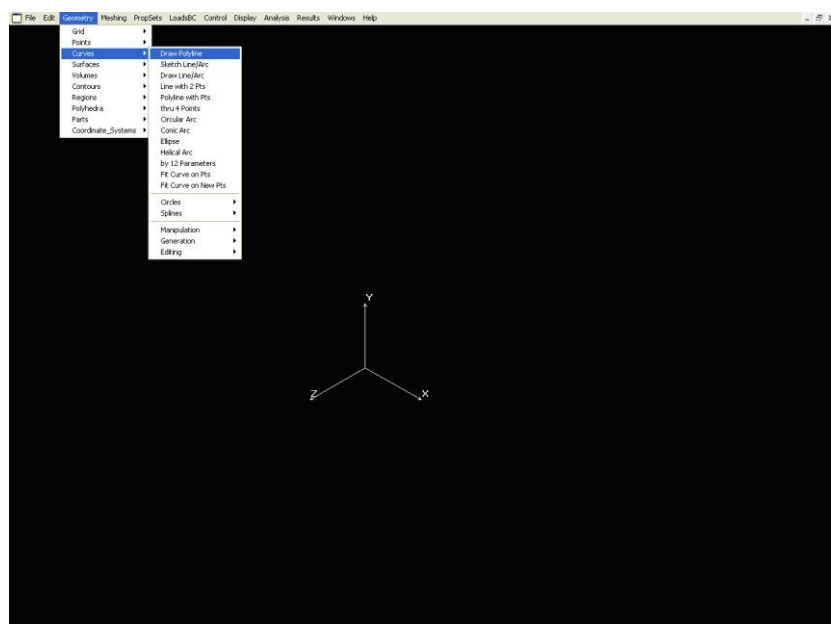


Figure 4.4. Geometric modeler in the finite element program

These built-in geometric modelers do not always offer you the convenience of modern CAD systems. Often we have to analyze existing models. In this case, the data exchange procedure with other CAD systems can be convenient and efficient by any available standard file format such as SAT, IGS, DXF, etc.. (see Figure 4.5).

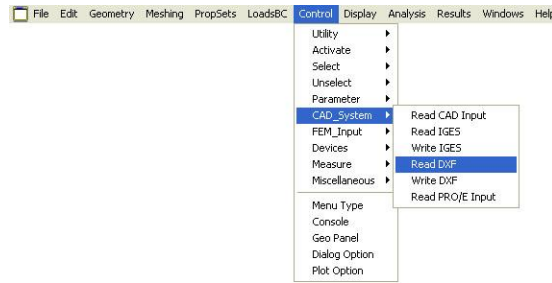


Figure 4.5. Import geometric model

Do not forget, in this case the geometric model only helps to create a finite element mesh. It does not comply with the rules of a technical drawing, and has no relevance to the real shape of the structure. It is true in this exercise, because the 100 mm diameter pipes appear only lines (see Figure 4.3). Thus, we have to transform (simplify and extend) the technical documentation before the finite element analysis. This is shown in Figure 4.6, which shows the imported geometric model. The one piece chord bars are divided at nodes, because it helps the finite element mesh generation.

It should be remembered, that we have to choose a unit system for finite element modeling. If the SI is selected, one drawing unit will be a meter during the data exchange of geometric models.

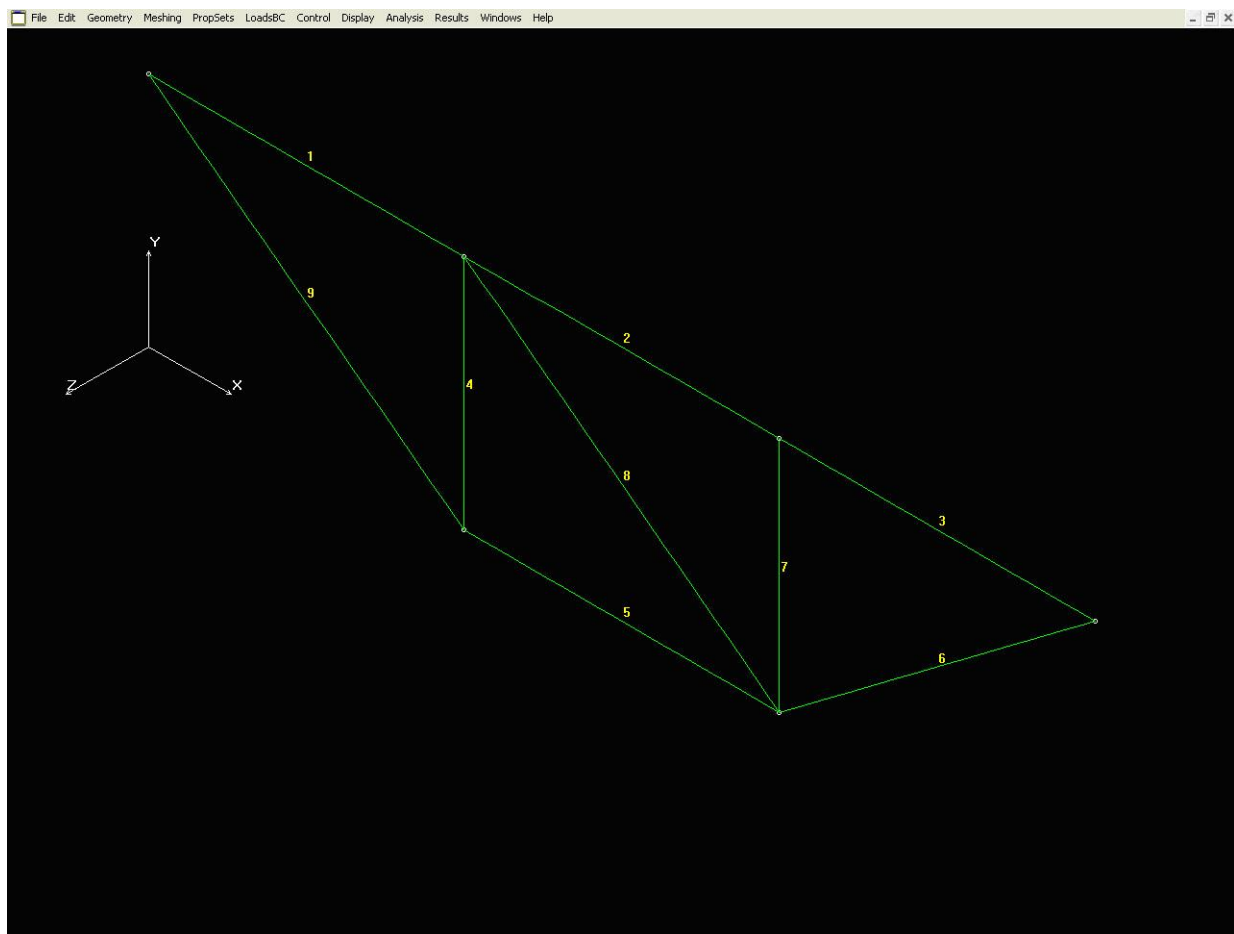


Figure 4.6. The imported geometric model

It is also shown that the elements lie in the XY plane.

In the next step we determine the element group (see Figure 4.7).

We have clarified that we use linear behavior, TRUSS2D elements.

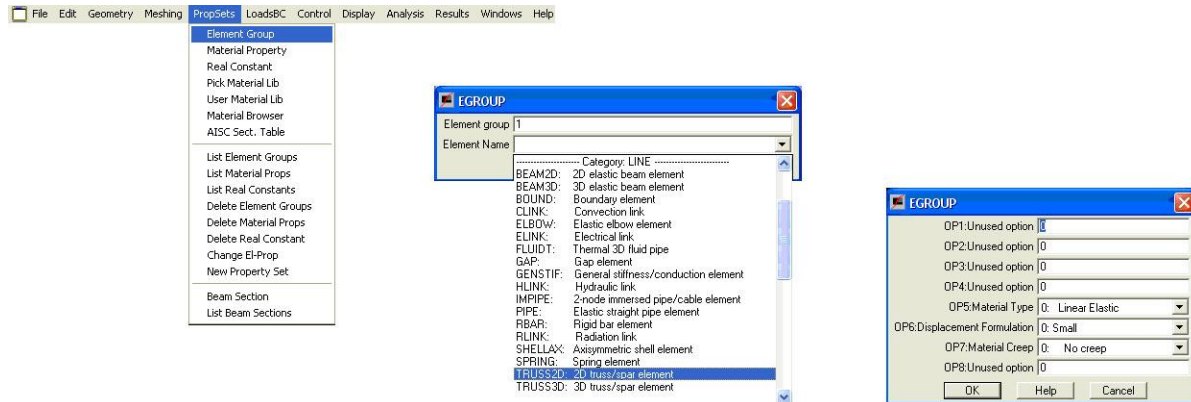


Figure 4.7. Determination of element group

It is also necessary to determine the material properties of finite elements. It is sufficient to specify the value of the modulus of elasticity for the truss element (see Figure 4.8). Making sure to use the selected unit system. In this case, it is the SI system, where the dimensions are determined in meters, and the modulus of elasticity in Pa, (N/m<sup>2</sup>).

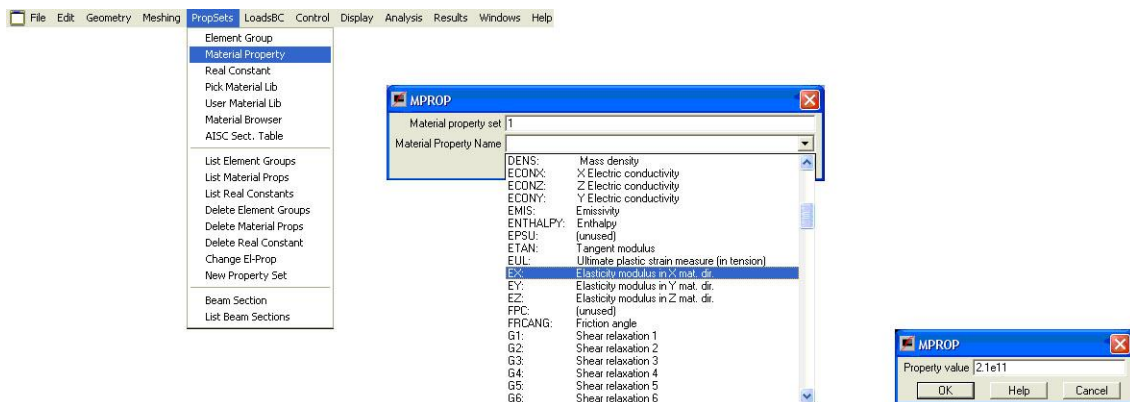


Figure 4.8. Determination of material properties

Next task is determine the real constants of the elements. (see Figure 4.9).

A complex finite element models contain various types of elements, so we have to also determine the associated element group.

As previously described, the real constant is only the cross-sectional area for TRUSS2D elements. Do not forget, we have to use the selected unit system in this case too.

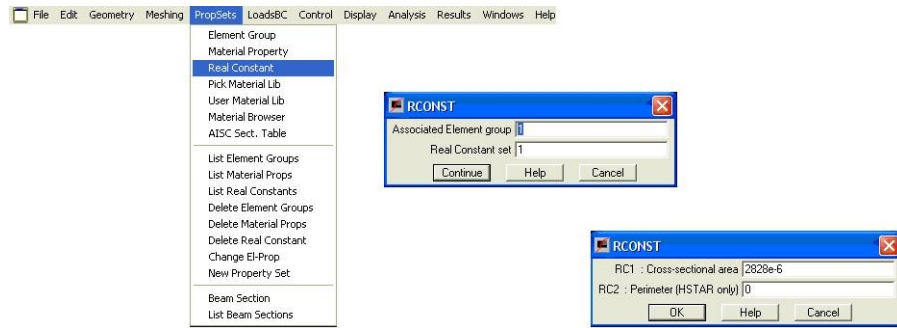


Figure 4.9. Real constants determination

After defining the the mesh properties, may follow the finite element mesh generation. The FEM programs offer several methods for this (see Figure 4.10).

Because the bar forces do not change along the length of the bars, it is sufficient to be placed one element in each objects.



Figure 4.10. Parametric mesh generation

Because, the finite element mesh created each geometry object separately, it is necessary to merge the nodes in each end of the bars (see Figure 4.11). The redundant nodes are removed from the finite element model.

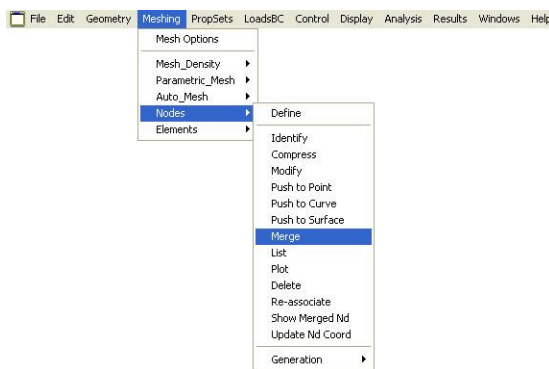


Figure 4.11. Merge of the end of bars

In the next step the boundary conditions should be given. In this case, these are two, 0 displacement constrains on the ends of the trusses.

The left side two degrees of freedom are fixed x and y directions and the other end only the y direction is fixed (see Figure 4.12).

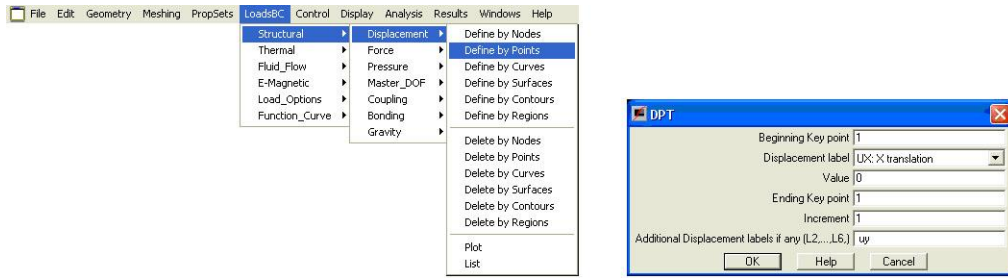


Figure 4.12. Specify displacement constraints

Finally, it should be given the loads (which shown in Figure 4.3), two 120 kN concentrated force (see Figure 4.13). The direction of forces must be given in the global coordinate system, so the downward forces are negative sign.

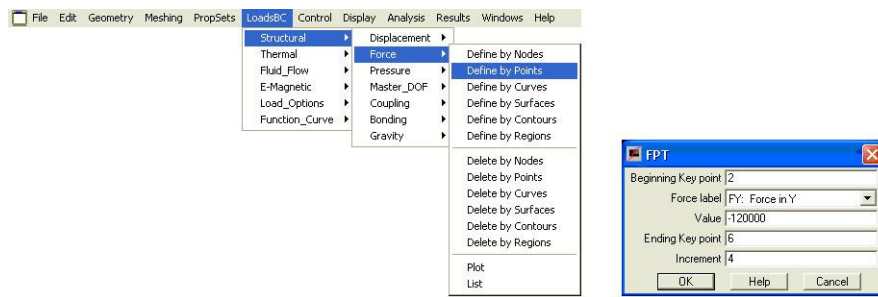


Figure 4.13 Defining the concentrated forces

By the finite element model is built. The calculation follows (see Figure 4.14).

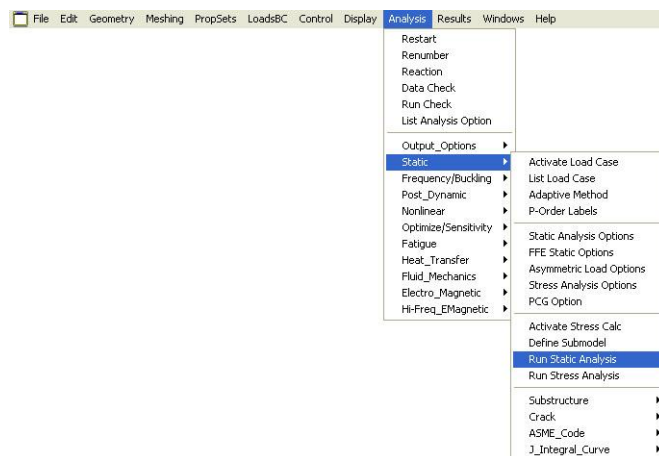


Figure 4.14 Run a linear static analysis

After the successfully solving, the display and evaluation of the results follows.

The displaying stresses generated in bars (see Figure 4.15) can be done in several ways.

The stresses are interpreted on the element and in the element local coordinate system.

There is a possibility that the results display on deformed shape. The deformation is not real of course, the program generates a specific scale factor, so that data can be evaluated.

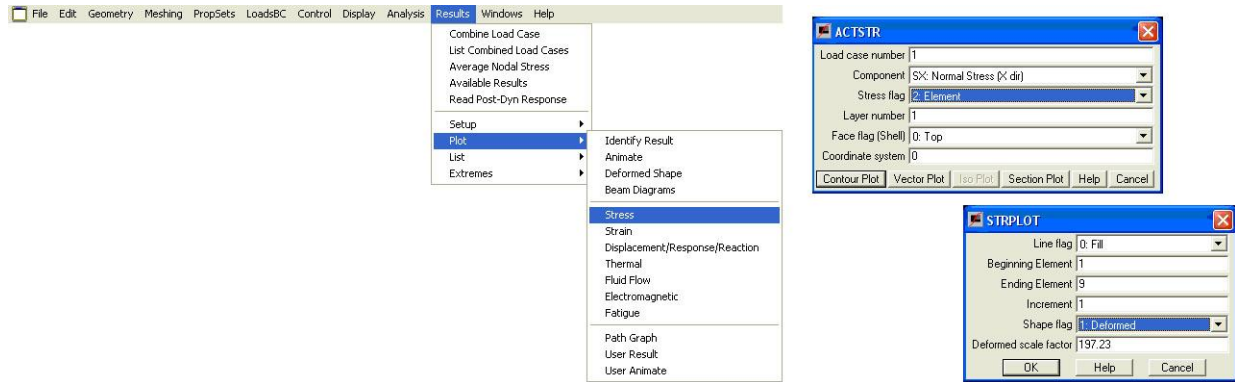


Figure 4.15 Display stresses

The results (see Figure 4.16) must be evaluated. The negative sign indicate compressive stress.

Notice, that the bars were straight, can be interpreted no bending moment generated in them.

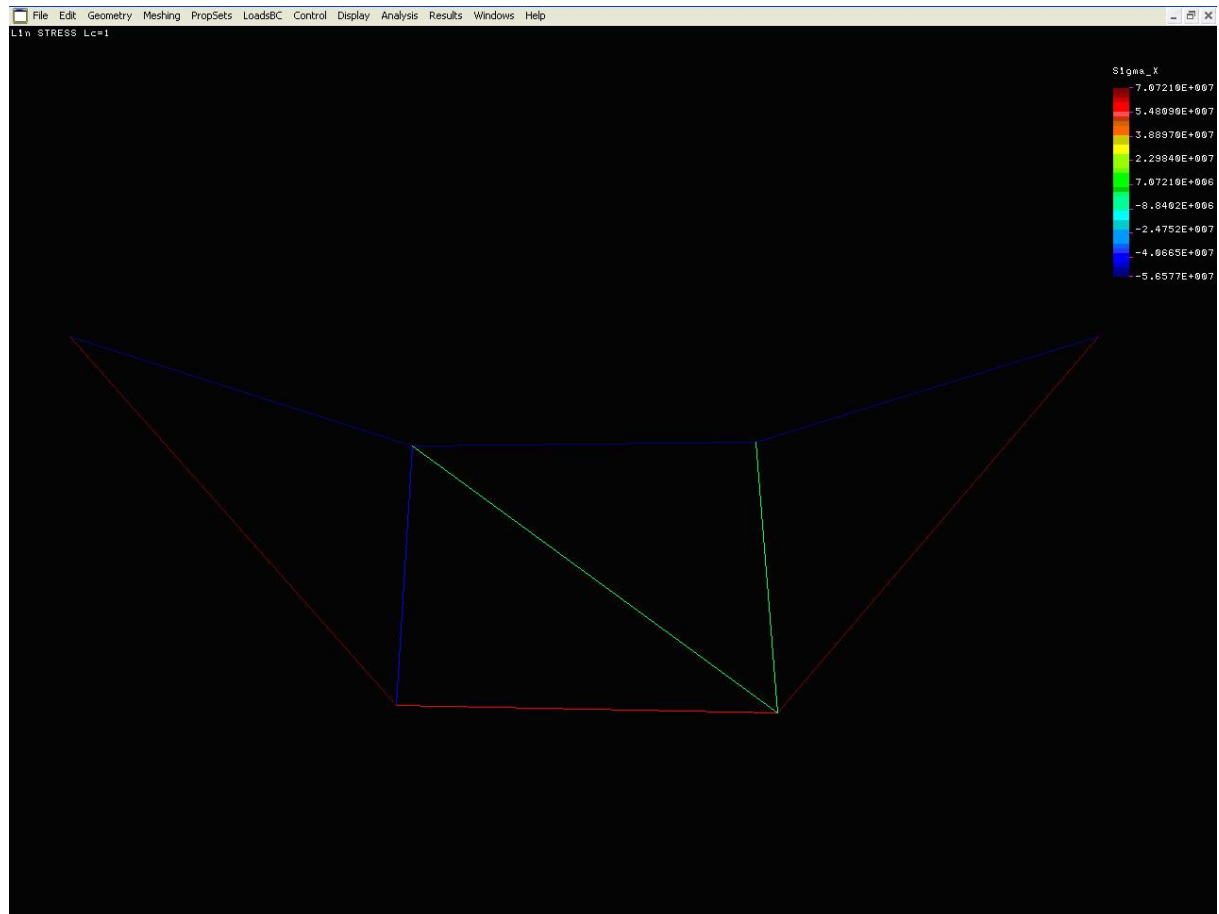


Figure 4.16. Stresses on deformed shape

Our aim was to examine the deflection (see Figure 4.17).

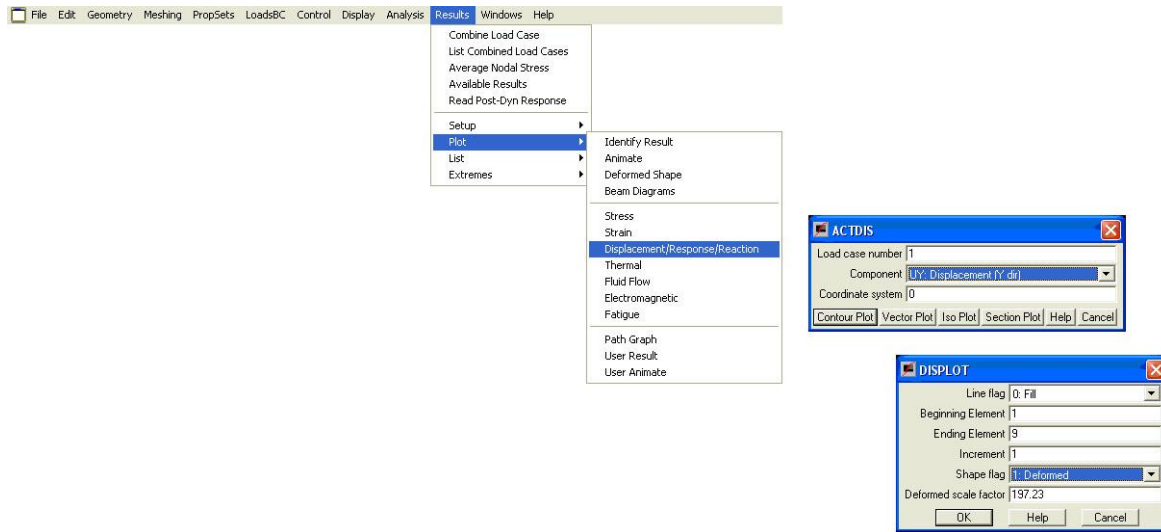


Figure 4.17 Deformed shape

The deformations can be bi-directional displacement of nodes. The deflection is the y displacement in the global coordinate system (see Figure 4.18). The negative sign of results represent a downward displacement. The value of the scale according to SI unit system.

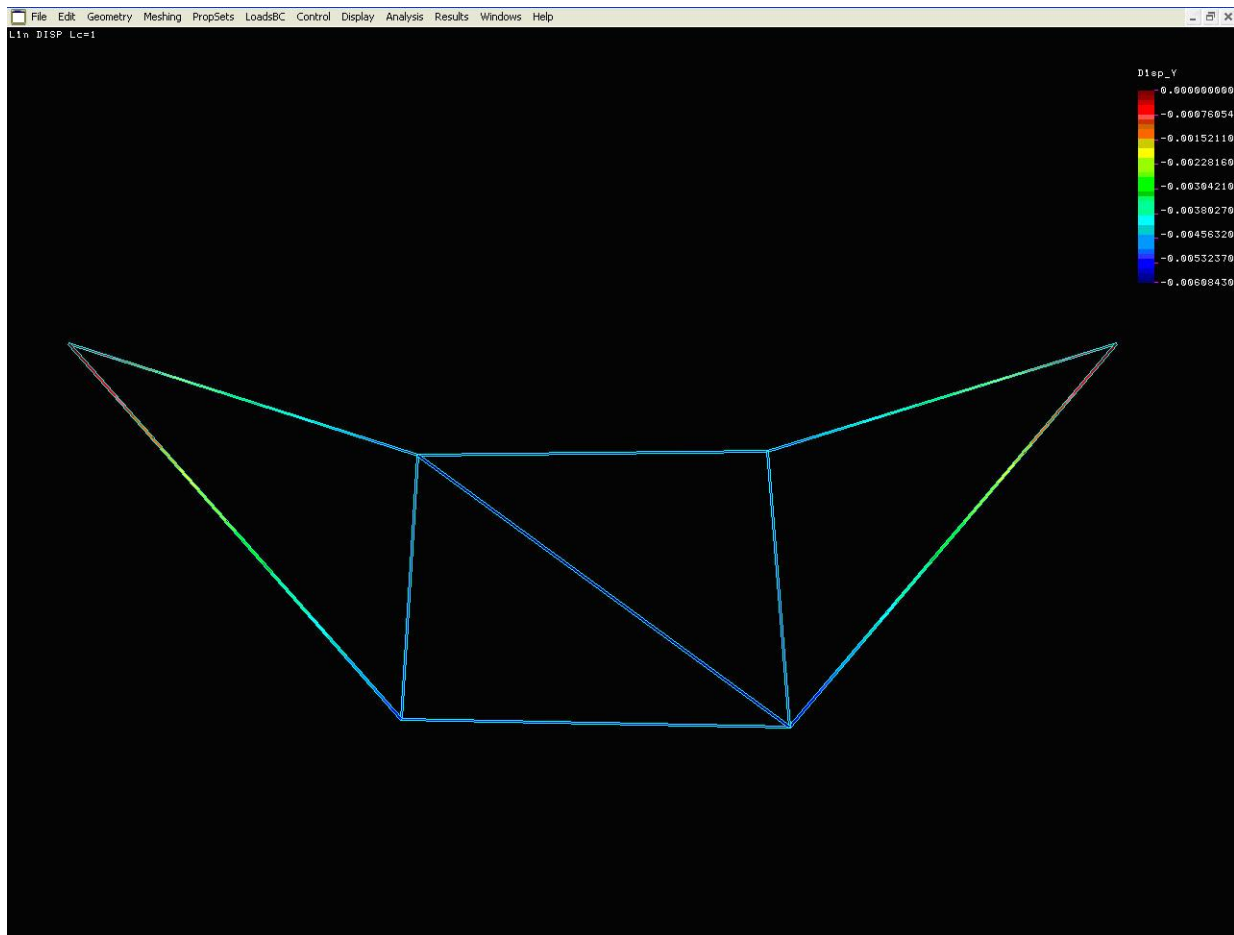


Figure 4.18 Displacement in y direction

It is possible to display the exact numerical results at nodes, forces generated in bars and displacement components (Figure 4:19 to 4:20).

Because the truss elements are loaded only by tension-compression stresses, so the table include only these stresses, interpreted in the element local coordinate system

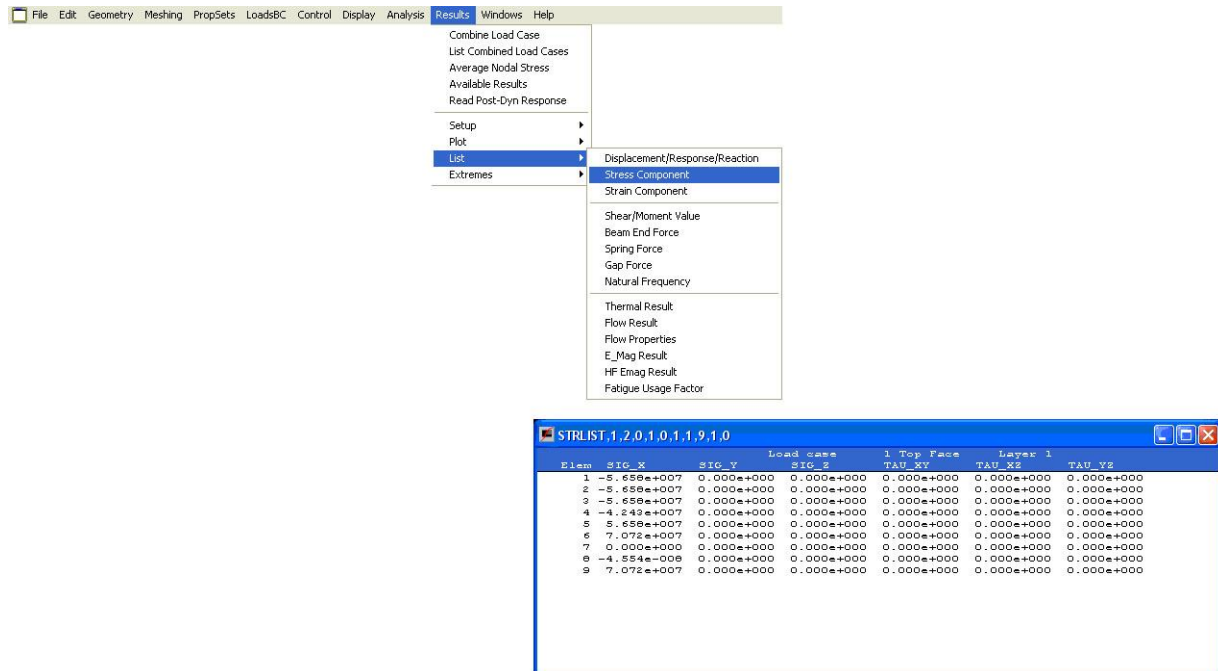
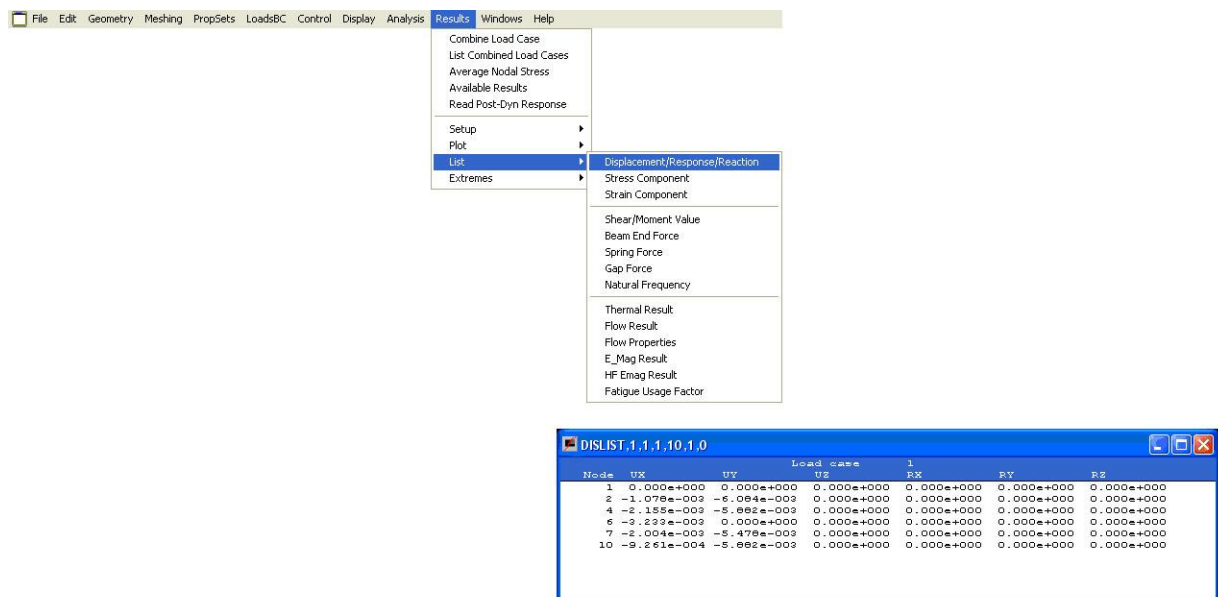


Figure 4.19 Fig. Stress component list

The displacements of nodes are interpreted in the global coordinate system (see Figure 4.20).



4.20. Fig. The displacements of nodes

#### 4.4. Remarks

During the solution, we have not dealt with buckling of the compressed bars. If this is a real problem, it should have to verify with solution a finite element problem, or with any analytic method.

During the solutions the tare weight (~81.59 kN) was neglected because this order of magnitude smaller than the external load.

Both problems are explained in later chapters which deal with BEAM elements.

Furthermore, the structural joint was not examined. The other specialized areas of structural design deal with this problems.

## 5. TWO-DIMENSIONAL BENT BARS VARIATION PROBLEM, STIFFNESS EQUATIONS AND SOLVING THEM BY FINITE ELEMENT METHOD

### 5.1. Two-dimensional bent beam element variation study

Examine the two-dimensional, straight beam shown in figure 5.1. The loads are  $q(x)$  distributed load,  $F$  concentrated force and  $M$  concentrated moment. During the solution we use the Euler-Bernoulli's beam theory. According to this theory the cross-section of the beam remains normal to the beam neutral axis, so we do not account for the shear deformation. Thus, the total potential can be written as a functional read on  $v(x)$  displacement function.

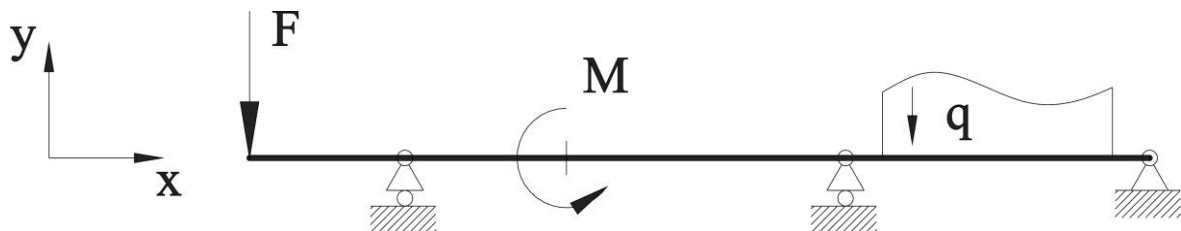


Figure 5.1 The tested beam

The displacement function of the bent beam known as differential equation of the elastic curve:

$$v'' = -\frac{M_h(x)}{I_z E} \quad (5.1)$$

Also known as the bent beam strain energy:

$$U = \frac{1}{2E} \int_L \frac{M_h^2(x)}{I_z(x)} dx. \quad (5.2)$$

Solving the differential equation of the elastic curve for  $M_h(x)$  and substituting this in the equation

$$U(v(x)) = \frac{1}{2} E \int_L I_z(x) (v''(x))^2 dx \quad (5.3)$$

Define the total potential energy needed the work of external forces, which consists of three members;

Work of the concentrated forces are perpendicular to the beam:

$$\sum F_i v(x_i) \quad (5.4)$$

work of the concentrated bending moments:

$$\sum M_j v'(x_j) \quad (5.5)$$

work of the distributed loads perpendicular to the beam:

$$\int_{x_a}^{x_b} v(x) q(x) dx \quad (5.6)$$

So, the total potential:

$$\Pi(v) = \frac{1}{2} E \int_L I_z(x) (v''(x))^2 dx - \int_{x_a}^{x_b} v(x) q(x) dx - \sum F_i v(x_i) - \sum M_j v'(x_j). \quad (5.7)$$

The  $\delta\Pi = 0$  criterion of first variation of (5.7) potential leads to the basic equation and to the natural boundary conditions. The approximate solution of the task is the direct minimization of the total potential energy.

So, find the minimum of the potential  $\Pi(v)$ , and the corresponding  $v(x)$  function. This minimization problem is solved by using the Ritz method, when the unknown  $v(x)$  function is looking as the following form:

$$v(x) = \omega(x) \sum_{k=0}^n a_k x^k \quad (5.8)$$

where  $\omega(x)$  the shape function, which satisfies the kinematical boundary conditions, i.e. the displacements at the supports are  $\omega(x) = 0$  and the angular displacements at the restrain are  $\omega'(x) = 0$ . With this substitution the potential  $\Pi(v)$  became a multivariable function for  $a_1, a_2, \dots, a_n$ . This function has a minimum when:

$$\frac{\partial \Pi}{\partial a_k} = 0. \quad (5.9)$$

Since the Ritz-method is an approximation procedure, the solution accuracy depends on how many members of the shape functions. For simple task enough a single tag, so the above equation depends on the  $a_0$  only, i.e., univariate.

Matrix formulation and solution of the equation system leads to the base equation of the finite element method:

$$\underline{\underline{K}} \underline{u} = \underline{F}. \quad (5.10)$$

## 5.2. Solving the problem using finite element method

The problem shown in Figure 5.2, is a two-dimensional rod structure. The structure is overloaded by two concentrated force lies in plane with the cantilever beam. Compression and

bending generated in the beam 1 of the structure and only bending stress generated in the beam 2, so this problem can not be solved by using TRUSS elements presented in the chapter 3.

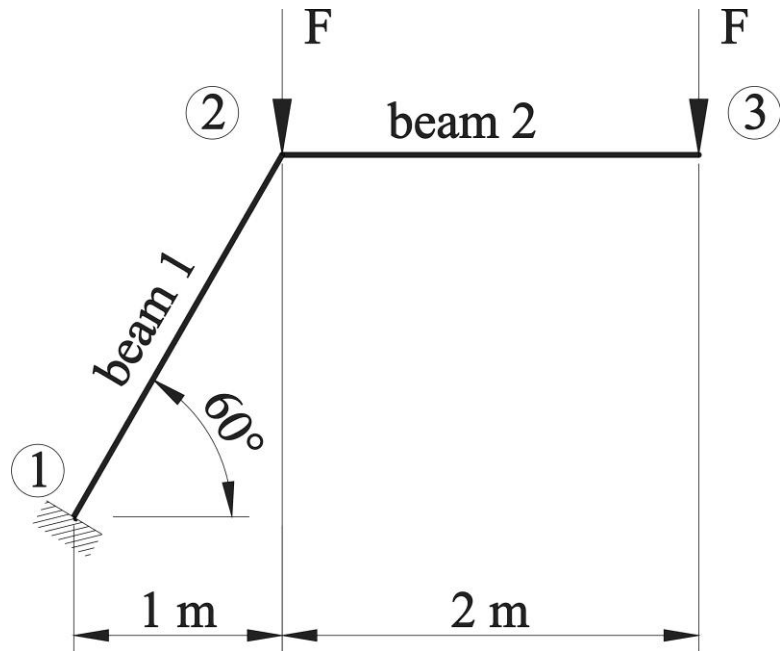


Figure 5.2 A two-dimensional rod structure

Both beam of the structure are 60x40x4 box section. The properties of cross-sections are steel standards:

$$A = 8.69 \text{ cm}^2$$

$$I_z = 44.8 \text{ cm}^4$$

The two forces are 200 N each.

During the solution we use bent beam elements according to Euler- Bernoulli's beam theory.

We have seen that the finite element solution means the solution of an equations system:

$$\underline{\underline{K}}\underline{u} = \underline{F} \quad (5.11)$$

First we have to develop the element stiffness matrix, then assembly the stiffness matrix of total structure.

### 5.2.1. The element stiffness matrix

The previous equations system written to single element:

$$\begin{bmatrix} k_{11} & k_{12} & k_{13} & k_{14} & k_{15} & k_{16} \\ k_{21} & \cdot & \cdot & \cdot & \cdot & \cdot \\ k_{31} & \cdot & \cdot & \cdot & \cdot & \cdot \\ k_{41} & \cdot & \cdot & \cdot & \cdot & \cdot \\ k_{51} & \cdot & \cdot & \cdot & \cdot & \cdot \\ k_{61} & \cdot & \cdot & \cdot & \cdot & k_{66} \end{bmatrix} \begin{bmatrix} u_1 \\ v_1 \\ \phi_1 \\ u_2 \\ v_2 \\ \phi_2 \end{bmatrix} = \begin{bmatrix} F_{1x} \\ F_{1y} \\ M_1 \\ F_{2x} \\ F_{2y} \\ M_2 \end{bmatrix} \quad (5.12)$$

The physical interpretation of columns of stiffness matrix is forces and moment necessary to ensure the one unit displacement and the boundary conditions. Using this, we can easily produce the stiffness matrix in case of using beam elements. Let one member of the  $\mathbf{u}$  vector one unit and all other is zero. In this case the  $k_{11}$  element of stiffness matrix belongs to  $u_1=1$  and according to the general procedure:

$$\begin{bmatrix} k_{11} & k_{12} & k_{13} & k_{14} & k_{15} & k_{16} \\ k_{21} & \cdot & \cdot & \cdot & \cdot & \cdot \\ k_{31} & \cdot & \cdot & \cdot & \cdot & \cdot \\ k_{41} & \cdot & \cdot & \cdot & \cdot & \cdot \\ k_{51} & \cdot & \cdot & \cdot & \cdot & \cdot \\ k_{61} & \cdot & \cdot & \cdot & \cdot & k_{66} \end{bmatrix} \begin{bmatrix} 1 \\ 0 \\ 0 \\ 0 \\ 0 \\ 0 \end{bmatrix} = \begin{bmatrix} F_{1x} \\ F_{1y} \\ M_1 \\ F_{2x} \\ F_{2y} \\ M_2 \end{bmatrix} \quad (5.13)$$

Solution of the equation system:

$$\begin{aligned} F_{1x} &= k_{11} \\ F_{1y} &= k_{21} \\ M_1 &= k_{31} \\ F_{2x} &= k_{41} \\ F_{2y} &= k_{51} \\ M_2 &= k_{61} \end{aligned} \quad (5.14)$$

The physical content of this case is illustrated in Figure 5.3.

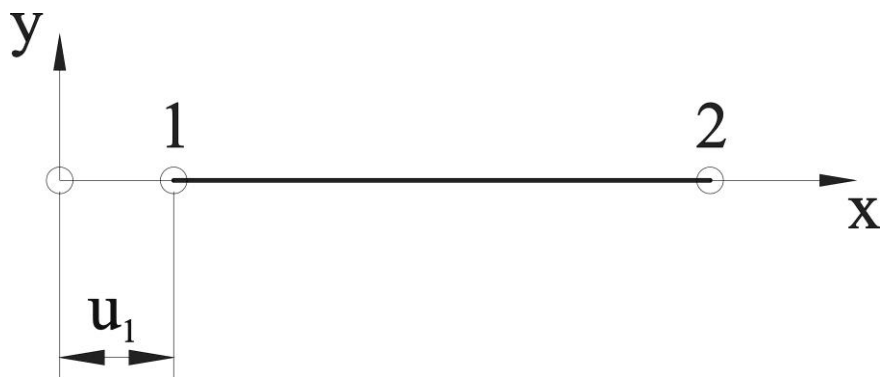


Figure 5.3 The physical interpretation of the first column of the stiffness matrix

Based on the figure, the individual beam stressed by pure compression, so using the Hook's law:

$$k_{11} = \frac{F_{1x}}{A} = E\varepsilon = E \frac{\Delta l}{L} \quad (5.15)$$

The value of  $\Delta l$  is one unit, so that after rearrangement:

$$k_{11} = F_{1x} = \frac{AE}{L} \quad (5.16)$$

To satisfy the boundary conditions still necessary that:

$$F_{1x} = -F_{2x} \quad (5.17)$$

i.e.:

$$k_{11} = -k_{41} \quad (5.18)$$

The other members of the first column of the stiffness matrix are zero.

We may act similarly with the second column of the stiffness matrix. In this case the equation system:

$$\begin{bmatrix} k_{11} & k_{12} & k_{13} & k_{14} & k_{15} & k_{16} \\ k_{21} & \cdot & \cdot & \cdot & \cdot & \cdot \\ k_{31} & \cdot & \cdot & \cdot & \cdot & \cdot \\ k_{41} & \cdot & \cdot & \cdot & \cdot & \cdot \\ k_{51} & \cdot & \cdot & \cdot & \cdot & \cdot \\ k_{61} & \cdot & \cdot & \cdot & \cdot & k_{66} \end{bmatrix} \begin{bmatrix} 0 \\ 1 \\ 0 \\ 0 \\ 0 \\ 0 \end{bmatrix} = \begin{bmatrix} F_{1x} \\ F_{1y} \\ M_1 \\ F_{2x} \\ F_{2y} \\ M_2 \end{bmatrix} \quad (5.19)$$

Solution of the equation system:

$$\begin{aligned} F_{1x} &= k_{12} \\ F_{1y} &= k_{22} \\ M_1 &= k_{32} \\ F_{2x} &= k_{42} \\ F_{2y} &= k_{52} \\ M_2 &= k_{62} \end{aligned} \quad (5.20)$$

The physical content of this case is illustrated in figure 5.4. This state is produced superposition of cantilever beams. In the first case (see Figure 5.4 b) the end of the beam is loaded by concentrated force and in the other case (see Figure 5.4 c) loaded by concentrated bending moment.

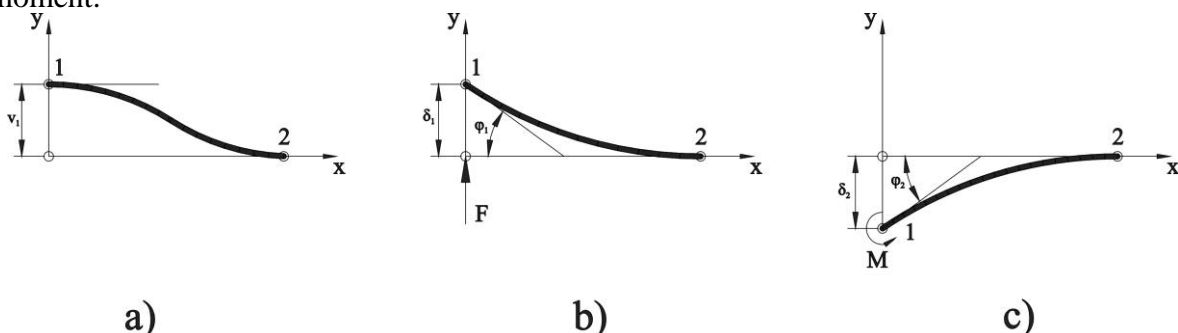


Figure 5.4 The physical interpretation of the second column of the stiffness matrix

These cases are well known in the strength of materials, so we can write it using equations which from solution of the differential equation of the elastic curve:

$$v_1 = 1 = \delta_1 + \delta_2 = \frac{F_{1y}L^3}{3IE} - \frac{M_1L^2}{2IE} \quad (5.21)$$

and the angular displacements:

$$\Phi = 0 = \varphi_1 + \varphi_2 = -\frac{F_{1y}L^2}{2IE} + \frac{M_1L}{IE} \quad (5.22)$$

The solution of the multivariable equation system:

$$F_{1y} = \frac{12IE}{L^3} = k_{22} \quad (5.23)$$

$$M_1 = \frac{6IE}{L^2} = k_{32} \quad (5.24)$$

Furthermore, ensuring the equilibrium conditions:

$$\Sigma F_y = 0 = F_{1y} + F_{2y} \rightarrow F_{2y} = -F_{1y} = k_{52} \quad (5.25)$$

and moments to the 2nd point:

$$\Sigma M = 0 = M_2 + M_1 - F_{1y}L = M_2 + \frac{6IE}{L^2} - \frac{12IE}{L^3}L \rightarrow M_2 = \frac{6IE}{L^2} = K_{62} \quad (5.26)$$

The first and fourth members in the second column of the stiffness matrix are zero.

Elements in the third column of the stiffness matrix is determined similarly, so that the  $\phi_1$  in  $v(x)$  vector is one unit, and all other member 0.

$$\begin{bmatrix} k_{11} & k_{12} & k_{13} & k_{14} & k_{15} & k_{16} \\ k_{21} & \cdot & \cdot & \cdot & \cdot & \cdot \\ k_{31} & \cdot & \cdot & \cdot & \cdot & \cdot \\ k_{41} & \cdot & \cdot & \cdot & \cdot & \cdot \\ k_{51} & \cdot & \cdot & \cdot & \cdot & \cdot \\ k_{61} & \cdot & \cdot & \cdot & \cdot & k_{66} \end{bmatrix} \begin{bmatrix} 0 \\ 0 \\ 1 \\ 0 \\ 0 \\ 0 \end{bmatrix} = \begin{bmatrix} F_{1x} \\ F_{1y} \\ M_1 \\ F_{2x} \\ F_{2y} \\ M_2 \end{bmatrix}. \quad (5.27)$$

The solution of the equation system is:

$$\begin{aligned}
 F_{1x} &= k_{13} \\
 F_{1y} &= k_{23} \\
 M_1 &= k_{33} \\
 F_{2x} &= k_{43} \\
 F_{2y} &= k_{53} \\
 M_2 &= k_{63}
 \end{aligned} \tag{5.28}$$

The physical content of this case is illustrated in figure 5.5.

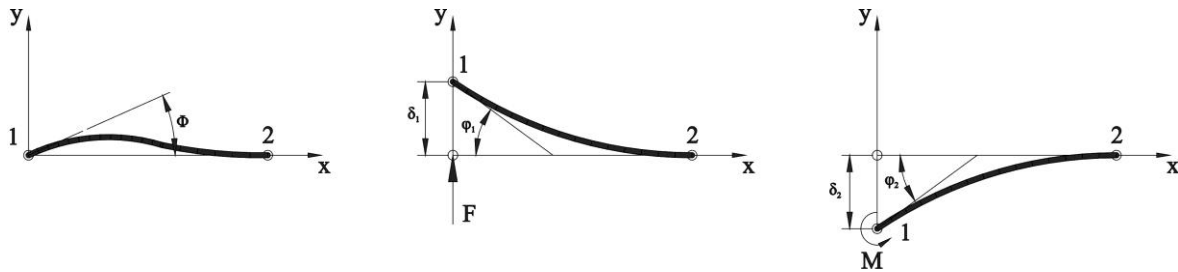


Figure 5.5 The physical interpretation of the third column of the stiffness matrix

The displacements presented in figure 5.5 is produced superposition of two displacements in this case too, so:

$$v_1 = 0 = \delta_1 + \delta_2 = \frac{F_{1y}L^3}{3IE} - \frac{M_1L^2}{2IE} \tag{5.29}$$

and the angular displacements:

$$\Phi = 1 = \varphi_1 + \varphi_2 = -\frac{F_{1y}L^2}{2IE} + \frac{M_1L}{IE} \tag{5.30}$$

The solution of the multivariable equation system is:

$$F_{1y} = \frac{6IE}{L^2} = k_{23} \tag{5.31}$$

$$M_1 = \frac{4IE}{L} = k_{33}. \tag{5.32}$$

Furthermore, ensuring the equilibrium conditions:

$$\Sigma F_y = 0 = F_{1y} + F_{2y} \rightarrow F_{2y} = -F_{1y} = k_{53} \tag{5.33}$$

and moments to the 2<sup>nd</sup> point:

$$\Sigma M = 0 = M_2 + M_1 - F_{1y}L = M_2 + \frac{4IE}{L} - \frac{6IE}{L^2}L \rightarrow M_2 = \frac{2IE}{L} = K_{63}. \tag{5.34}$$

The first and fourth members in the third column of the stiffness matrix is zero.

The members in 4<sup>th</sup>-6<sup>th</sup> column of stiffness matrix are defined similarly. Eventually the entire element stiffness matrix:

$$k_{ie} = \begin{bmatrix} \frac{A_i E_i}{L_i} & 0 & 0 & -\frac{A_i E_i}{L_i} & 0 & 0 \\ 0 & \frac{12I_i E_i}{L_i^3} & \frac{6I_i E_i}{L_i^2} & 0 & -\frac{12I_i E_i}{L_i^3} & \frac{6I_i E_i}{L_i^2} \\ 0 & \frac{6I_i E_i}{L_i^2} & \frac{4I_i E_i}{L_i} & 0 & -\frac{6I_i E_i}{L_i^2} & \frac{2I_i E_i}{L_i} \\ -\frac{A_i E_i}{L_i} & 0 & 0 & \frac{A_i E_i}{L_i} & 0 & 0 \\ 0 & -\frac{12I_i E_i}{L_i^3} & -\frac{6I_i E_i}{L_i^2} & 0 & \frac{12I_i E_i}{L_i^3} & -\frac{6I_i E_i}{L_i^2} \\ 0 & \frac{6I_i E_i}{L_i^2} & \frac{2I_i E_i}{L_i} & 0 & -\frac{6I_i E_i}{L_i^2} & \frac{4I_i E_i}{L_i} \end{bmatrix} \quad (5.35)$$

It should be noted that in generally the element stiffness matrix are generated by:

$$\underline{\underline{K}}_e = \int_{V_e} \underline{\underline{B}}^T \underline{\underline{C}}^T \underline{\underline{B}} dV \quad (5.36)$$

equation, when  $\underline{\underline{C}}$  is the matrix of material properties and  $\underline{\underline{B}}$  is the matrix of deformation-strain. This solution found in third chapter. The above presented solution would be difficult in case of using more complex elements. It is only for understanding of the concept of stiffness matrix.

The stiffness properties of the element were determined only in the element local coordinate system. In the global coordinate system these stiffness values change depending on the position of elements. Elements properties in the global coordinate system are produced using the transformation matrix which was presented in chapter 3 (3.35 equation). However, in this case the transformation matrix is of order 6x6 according to degree of freedom of beam element.

$$T = \begin{bmatrix} \cos \alpha & \sin \alpha & 0 & 0 & 0 & 0 \\ -\sin \alpha & \cos \alpha & 0 & 0 & 0 & 0 \\ 0 & 0 & 1 & 0 & 0 & 0 \\ 0 & 0 & 0 & \cos \alpha & \sin \alpha & 0 \\ 0 & 0 & 0 & -\sin \alpha & \cos \alpha & 0 \\ 0 & 0 & 0 & 0 & 0 & 1 \end{bmatrix}. \quad (5.37)$$

The members of transformation matrix can be easily calculated by known element nodal coordinates:

$$\cos \alpha_i = \frac{x_{i2} - x_{i1}}{L_i} \quad (5.38)$$

$$\sin \alpha_i = \frac{y_{i2} - y_{i1}}{L_i} \quad (5.39)$$

$$L_i = \sqrt{(x_{i2} - x_{i1})^2 + (y_{i2} - y_{i1})^2} \quad (5.40)$$

So the stiffness matrix of 1<sup>st</sup> element in global coordinate system:

$$k_1 = \begin{vmatrix} k_{11} \cdot \cos(\alpha)^2 + k_{22} \cdot \sin(\alpha)^2 & \cos(\alpha) \cdot \sin(\alpha) \cdot k_{22} - \cos(\alpha) \cdot \sin(\alpha) \cdot k_{11} & \sin(\alpha) \cdot k_{23} & k_{14} \cdot \cos(\alpha)^2 + k_{25} \cdot \sin(\alpha)^2 & \cos(\alpha) \cdot \sin(\alpha) \cdot k_{25} - \cos(\alpha) \cdot \sin(\alpha) \cdot k_{14} & \sin(\alpha) \cdot k_{26} \\ \cos(\alpha) \cdot \sin(\alpha) \cdot k_{22} - \cos(\alpha) \cdot \sin(\alpha) \cdot k_{11} & k_{22} \cdot \cos(\alpha)^2 + k_{11} \cdot \sin(\alpha)^2 & \cos(\alpha) \cdot k_{23} & \cos(\alpha) \cdot \sin(\alpha) \cdot k_{25} - \cos(\alpha) \cdot \sin(\alpha) \cdot k_{14} & k_{25} \cdot \cos(\alpha)^2 + k_{14} \cdot \sin(\alpha)^2 & \cos(\alpha) \cdot k_{26} \\ \sin(\alpha) \cdot k_{32} & \cos(\alpha) \cdot k_{32} & k_{33} & \sin(\alpha) \cdot k_{35} & \cos(\alpha) \cdot k_{35} & k_{36} \\ k_{41} \cdot \cos(\alpha)^2 + k_{52} \cdot \sin(\alpha)^2 & \cos(\alpha) \cdot \sin(\alpha) \cdot k_{52} - \cos(\alpha) \cdot \sin(\alpha) \cdot k_{41} & \sin(\alpha) \cdot k_{53} & k_{44} \cdot \cos(\alpha)^2 + k_{55} \cdot \sin(\alpha)^2 & \cos(\alpha) \cdot \sin(\alpha) \cdot k_{55} - \cos(\alpha) \cdot \sin(\alpha) \cdot k_{44} & \sin(\alpha) \cdot k_{56} \\ \cos(\alpha) \cdot \sin(\alpha) \cdot k_{52} - \cos(\alpha) \cdot \sin(\alpha) \cdot k_{41} & k_{52} \cdot \cos(\alpha)^2 + k_{41} \cdot \sin(\alpha)^2 & \cos(\alpha) \cdot k_{53} & \cos(\alpha) \cdot \sin(\alpha) \cdot k_{55} - \cos(\alpha) \cdot \sin(\alpha) \cdot k_{44} & k_{55} \cdot \cos(\alpha)^2 + k_{44} \cdot \sin(\alpha)^2 & \cos(\alpha) \cdot k_{56} \\ \sin(\alpha) \cdot k_{62} & \cos(\alpha) \cdot k_{62} & k_{63} & \sin(\alpha) \cdot k_{65} & \cos(\alpha) \cdot k_{65} & k_{66} \end{vmatrix}$$

### 5.2.2. The entire structure stiffness matrix

The size of the stiffness matrix of entire structure is equal to the number of degrees of freedom of the whole structure. So now the stiffness matrix of entire system is of order 9x9, because the system composed of two elements with 3 nodes, each with 3 degrees of freedom. In the whole stiffness matrix the elementary stiffness of the common nodes are added together, so:

$$K = \begin{bmatrix} k_{11}^1 & k_{12}^1 & k_{13}^1 & k_{14}^1 & k_{15}^1 & k_{16}^1 & 0 & 0 & 0 \\ k_{21}^1 & k_{22}^1 & k_{23}^1 & k_{24}^1 & k_{25}^1 & k_{26}^1 & 0 & 0 & 0 \\ k_{31}^1 & k_{32}^1 & k_{33}^1 & k_{34}^1 & k_{35}^1 & k_{36}^1 & 0 & 0 & 0 \\ k_{41}^1 & k_{42}^1 & k_{43}^1 & k_{44}^1 + k_{11}^2 & k_{45}^1 + k_{12}^2 & k_{46}^1 + k_{13}^2 & k_{14}^2 & k_{15}^2 & k_{16}^2 \\ k_{51}^1 & k_{52}^1 & k_{53}^1 & k_{54}^1 + k_{21}^2 & k_{55}^1 + k_{22}^2 & k_{56}^1 + k_{23}^2 & k_{24}^2 & k_{25}^2 & k_{26}^2 \\ k_{61}^1 & k_{62}^1 & k_{63}^1 & k_{64}^1 + k_{31}^2 & k_{65}^1 + k_{32}^2 & k_{66}^1 + k_{33}^2 & k_{34}^2 & k_{35}^2 & k_{36}^2 \\ 0 & 0 & 0 & k_{41}^2 & k_{42}^2 & k_{43}^2 & k_{44}^2 & k_{45}^2 & k_{46}^2 \\ 0 & 0 & 0 & k_{51}^2 & k_{52}^2 & k_{53}^2 & k_{54}^2 & k_{55}^2 & k_{56}^2 \\ 0 & 0 & 0 & k_{61}^2 & k_{62}^2 & k_{63}^2 & k_{64}^2 & k_{65}^2 & k_{66}^2 \end{bmatrix} \quad (5.42)$$

## 5.2.3. The complete equations system and the solution

$$\begin{bmatrix} k_{11}^1 & k_{12}^1 & k_{13}^1 & k_{14}^1 & k_{15}^1 & k_{16}^1 & 0 & 0 & 0 \\ k_{21}^1 & k_{22}^1 & k_{23}^1 & k_{24}^1 & k_{25}^1 & k_{26}^1 & 0 & 0 & 0 \\ k_{31}^1 & k_{32}^1 & k_{33}^1 & k_{34}^1 & k_{35}^1 & k_{36}^1 & 0 & 0 & 0 \\ k_{41}^1 & k_{42}^1 & k_{43}^1 & k_{44}^1 + k_{11}^2 & k_{45}^1 + k_{12}^2 & k_{46}^1 + k_{13}^2 & k_{14}^2 & k_{15}^2 & k_{16}^2 \\ k_{51}^1 & k_{52}^1 & k_{53}^1 & k_{54}^1 + k_{21}^2 & k_{55}^1 + k_{22}^2 & k_{56}^1 + k_{23}^2 & k_{24}^2 & k_{25}^2 & k_{26}^2 \\ k_{61}^1 & k_{62}^1 & k_{63}^1 & k_{64}^1 + k_{31}^2 & k_{65}^1 + k_{32}^2 & k_{66}^1 + k_{33}^2 & k_{34}^2 & k_{35}^2 & k_{36}^2 \\ 0 & 0 & 0 & k_{41}^2 & k_{42}^2 & k_{43}^2 & k_{44}^2 & k_{45}^2 & k_{46}^2 \\ 0 & 0 & 0 & k_{51}^2 & k_{52}^2 & k_{53}^2 & k_{54}^2 & k_{55}^2 & k_{56}^2 \\ 0 & 0 & 0 & k_{61}^2 & k_{62}^2 & k_{63}^2 & k_{64}^2 & k_{65}^2 & k_{66}^2 \end{bmatrix} \cdot \begin{bmatrix} u_2 \\ v_2 \\ \varphi_2 \\ u_3 \\ v_3 \\ \varphi_3 \end{bmatrix} = \begin{bmatrix} F_{Rx} \\ F_{Ry} \\ M_R \\ 0 \\ 0 \\ 0 \end{bmatrix}. \quad (5.43)$$

During the solution the displacement 0 locations (at the supports) are skipped. So we can delete rows and columns of the stiffness matrix in these places. In our case, this is the first three rows and columns. Thus we get the condensed stiffness matrix and the equation system to solve:

$$\begin{bmatrix} k_{44}^1 + k_{11}^2 & k_{45}^1 + k_{12}^2 & k_{46}^1 + k_{13}^2 & k_{14}^2 & k_{14}^2 & k_{14}^2 \\ k_{54}^1 + k_{21}^2 & k_{55}^1 + k_{22}^2 & k_{56}^1 + k_{23}^2 & k_{24}^2 & k_{25}^2 & k_{26}^2 \\ k_{64}^1 + k_{31}^2 & k_{65}^1 + k_{32}^2 & k_{66}^1 + k_{33}^2 & k_{34}^2 & k_{35}^2 & k_{36}^2 \\ k_{41}^2 & k_{42}^2 & k_{43}^2 & k_{44}^2 & k_{45}^2 & k_{46}^2 \\ k_{51}^2 & k_{52}^2 & k_{53}^2 & k_{54}^2 & k_{55}^2 & k_{56}^2 \\ k_{61}^2 & k_{62}^2 & k_{63}^2 & k_{64}^2 & k_{65}^2 & k_{66}^2 \end{bmatrix} \cdot \begin{bmatrix} u_2 \\ v_2 \\ \varphi_2 \\ u_3 \\ v_3 \\ \varphi_3 \end{bmatrix} = \begin{bmatrix} 0 \\ F_1 \\ 0 \\ 0 \\ F_2 \\ 0 \end{bmatrix}. \quad (5.44)$$

Substituting the data, solving the equations we obtain:

$$U = \begin{bmatrix} u_2 \\ v_2 \\ \varphi_2 \\ u_3 \\ v_3 \\ \varphi_3 \end{bmatrix} = \begin{bmatrix} 0,01227 \\ -0,00709 \\ -0,01276 \\ 0,01227 \\ -0,03827 \\ -0,01701 \end{bmatrix} \text{ m rad} \quad (5.45)$$

The reaction forces can be calculated by the known results. From the equations of entire system, in this case, these are the first three lines:

$$F_{Rx} = k_{14}^1 \cdot u_2 + k_{15}^1 \cdot v_2 + k_{16}^1 \cdot \varphi_2 = 0 \text{ N} \quad (5.46)$$

$$F_{Ry} = k_{24}^1 \cdot u_2 + k_{25}^1 \cdot v_2 + k_{26}^1 \cdot \varphi_2 = 400 \text{ N}$$

$$M_R = k_{34}^1 \cdot u_2 + k_{35}^1 \cdot v_2 + k_{36}^1 \cdot \varphi_2 = 800 \text{ Nm}$$

### 5.3. Remarks

The program systems based on finite element method can handle not only Euler-Bernoulli's beams. In such a case the shear factor of the section must be determined. It should be noted, this shear factor can only be reliably used in the case of linear static analysis.

## **6. ANALYSIS OF TWO-DIMENSIONAL BENT BARS USING FINITE ELEMENT METHOD BASED PROGRAM SYSTEM**

### **6.1. Planar beam structures**

As discussed in chapter 4, two-dimensional trusses are only a part of the bar structures which we have to analyze. In most cases the bending generated in beams can not be neglected. This situation arises when the bars of the beam structure are loaded not only by axial forces but even by bending moments.

Such cases usually are:

- A simply and multi-supported beams, cantilever beams,
- Curved bars,
- If the tare weight of the beam structure can not be neglected,
- A two-dimensional frame structure, etc..

This chapter deals with these beam structures. The chapters 7-8 deal with three-dimensional, bent and twisted beams and the chapters 9-10 deal with buckling of the compressed bars.

Other than as described in chapter 4, there are some more questions to be answered:

- The magnitude and direction of the forces and moments generated in supports,
- Magnitude and direction of the axial and shear forces, bending and torque moments in each bar,
- The  $\sigma_x, \sigma_y$  and  $\tau_{xy}$  stresses which characterized of the planar-stressed state,
- Displacements of each point of the structure, and deformation of each beam.

These structures may be tested for the stability of the structure and dynamic behavior (the critical forces of compressed bars and natural frequencies). We deal with these problems in the chapters 5-10.

The previous chapter has mentioned the externally and internally determination and indeterminacy structures. We will see that it is irrelevant in this case too.

### **6.2. The used finite elements in modeling**

The chapter 4 clarified that program system based on the finite element method use two types of element for modeling beam structures. The TRUSS element for modeling structure loaded axial forces only and the BEAM element for modeling loaded axial and shear forces, bending and torque moments. In both cases, the finite elements are planar, so that is characterized by a single straight line.

The properties of the TRUSS elements have already been described in the previous chapters.

#### **6.2.1. Properties of the BEAM element**

The BEAM elements can be divided into two groups. The BEAM2D elements for models characterized by planar-stressed state, such as generally the planar structures, with symmetrical cross-section bars, loaded the plane of the structure only. The BEAM3D elements are used for three-dimensional modeling. These are usually the three-dimensional constructions, or

two-dimensional constructions loaded perpendicular to own plane, or two-dimensional construction consisting of asymmetrical cross-section bars.

The chapters 7-8. will deal with BEAM3D elements.

The BEAM2D elements are two-node uniaxial elements, have three degree of freedom in both nodes (two displacement and a rotational degrees of freedom). The local coordinate system of the element is shown in figure 6.1. The coordinate system x-axis pointing from the first to the second node, the y-axis parallel to the global coordinate system XY plane and perpendicular to x-axis, the z axis is perpendicular to x and y axis and create a right-handed Cartesian coordinate system.

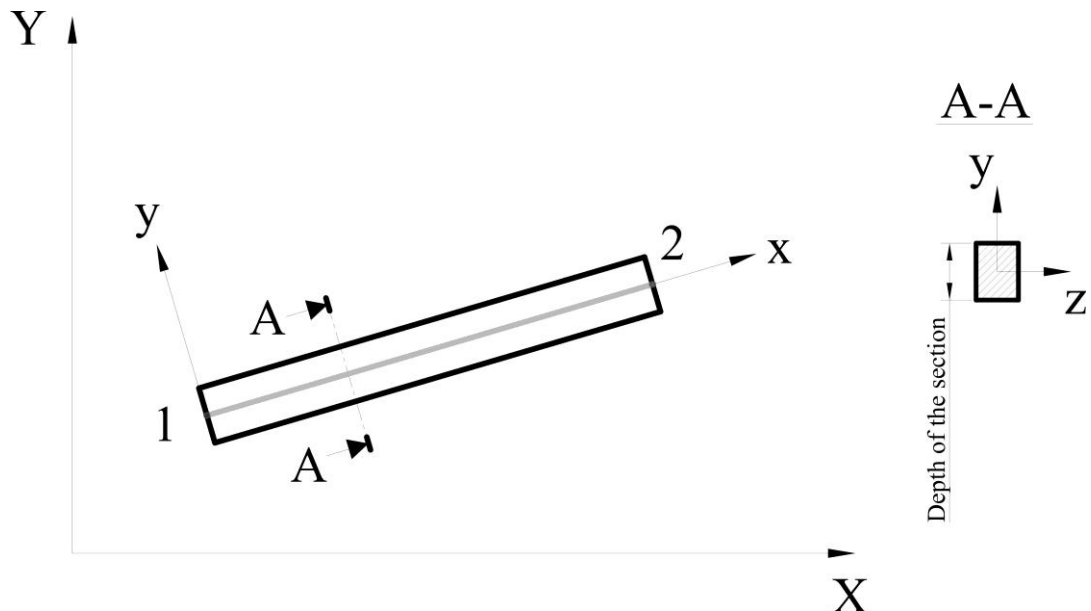


Figure 6.1 The BEAM2D element

The linear static analysis are required the real constants of BEAM2D elements. In this case it means cross-sectional area, the moment of inertia, depth of the section and shear factor. The value of shear factor depends on the shape of the section.

We will also need the material properties of the bar. In this case, the elastic modulus and the Poisson's ratio determination is sufficient because there are planar-stressed state in all points of the BEAM2D elements. If the tare weight of the structure must be considered as a load, the material density determination is needed.

The BEAM2D elements are suitable buckling and thermodynamic analysis. This requires additional real constants and material properties.

### 6.2.2. The shear deformation

The shear deformation is usually neglected. It is possible simply to take this into account using finite element model for more accurate results.

The shear deformation is deduced from work of internal forces. The work of shear forces of the two-dimensional beam:

$$W_{int} = \int \frac{V^2 S^2}{GI^2 b^2} dx dy dz$$

Sort of the equation the shear (shape) factor is:

$$f_s = \frac{A}{I^2} \int_A \left( \frac{S^2}{b^2} \right) dA$$

The work of the shear forces in constant cross-section beam:

$$W_{int} = f_s \int_l \frac{V^2}{GA} dx$$

This is the shape factor, and this inverse using in the finite element solution as shear factor. The shear factor values of some often used cross section shown in figure 6.2.

| The cross section | $f_s$       | The Shear factor |
|-------------------|-------------|------------------|
| Rectangle         | $6/5=1,2$   | $5/6=0,833$      |
| Circle            | $10/9=1,11$ | $9/10=0,9$       |
| Thin walled pipe  | 2           | 0,5              |

Figure 6.2 Shear factor of sections

In the technical practice we often use section where the tensioned chords and the sheared web are separable (see Figure 6.3). In this case, the approximate value of shear factor:

| The cross section | $f_s$              | The Shear factor   |
|-------------------|--------------------|--------------------|
| Web<br>Chords     | $A/A_{\text{Web}}$ | $A_{\text{Web}}/A$ |

Figure 6.3 The simplified definition of shear factor

### 6.3. The study solution

The solution of the finite element studies we follow the following procedure:

- Analysis of the problem,
- Creation of the geometry model,
- Define the properties of finite elements (element types, real constants, material properties),
- Define the boundary conditions and loads,
- Run the analysis,
- Evaluation of the results.

The open frame is shown in figure 6.4, loaded 10 kN on marked point. The force lies in plane of the structure. The bars are 100x100x4 cold bended box sections.

We have to determine the reaction forces, the stress generated in the bars, the deflections, and the bending-, torque moments and shear force diagrams.

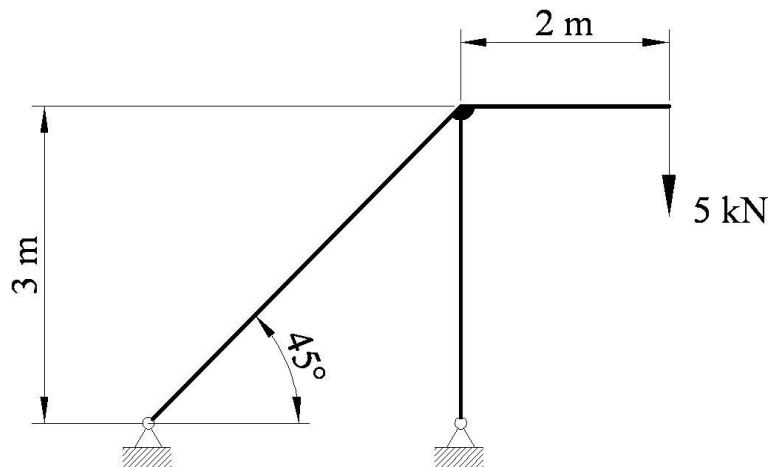


Figure 6.4 The cross section

The finite element programs usually contain built-in 3D geometric modeling, graphics pre- and postprocessor. Thus, we can prepare the geometric model in its (see Figure 6.5)

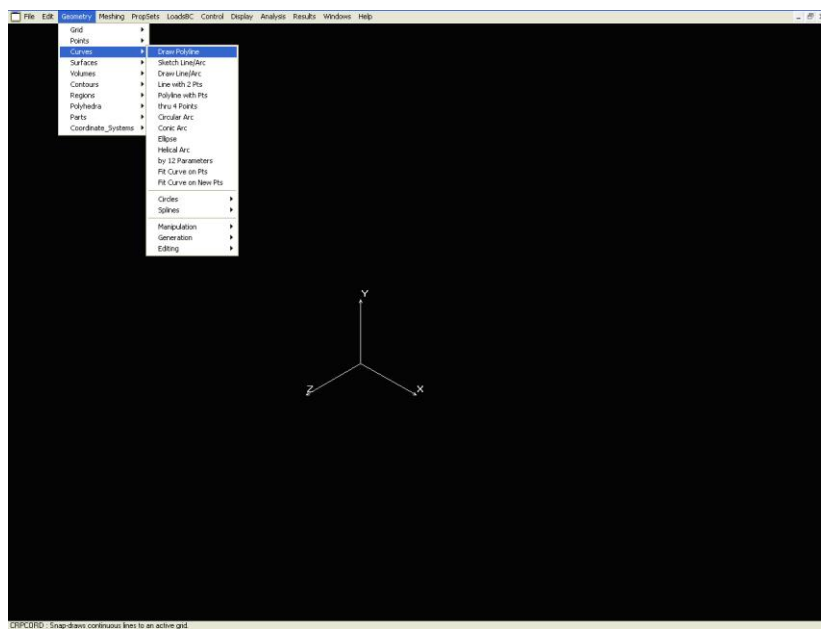
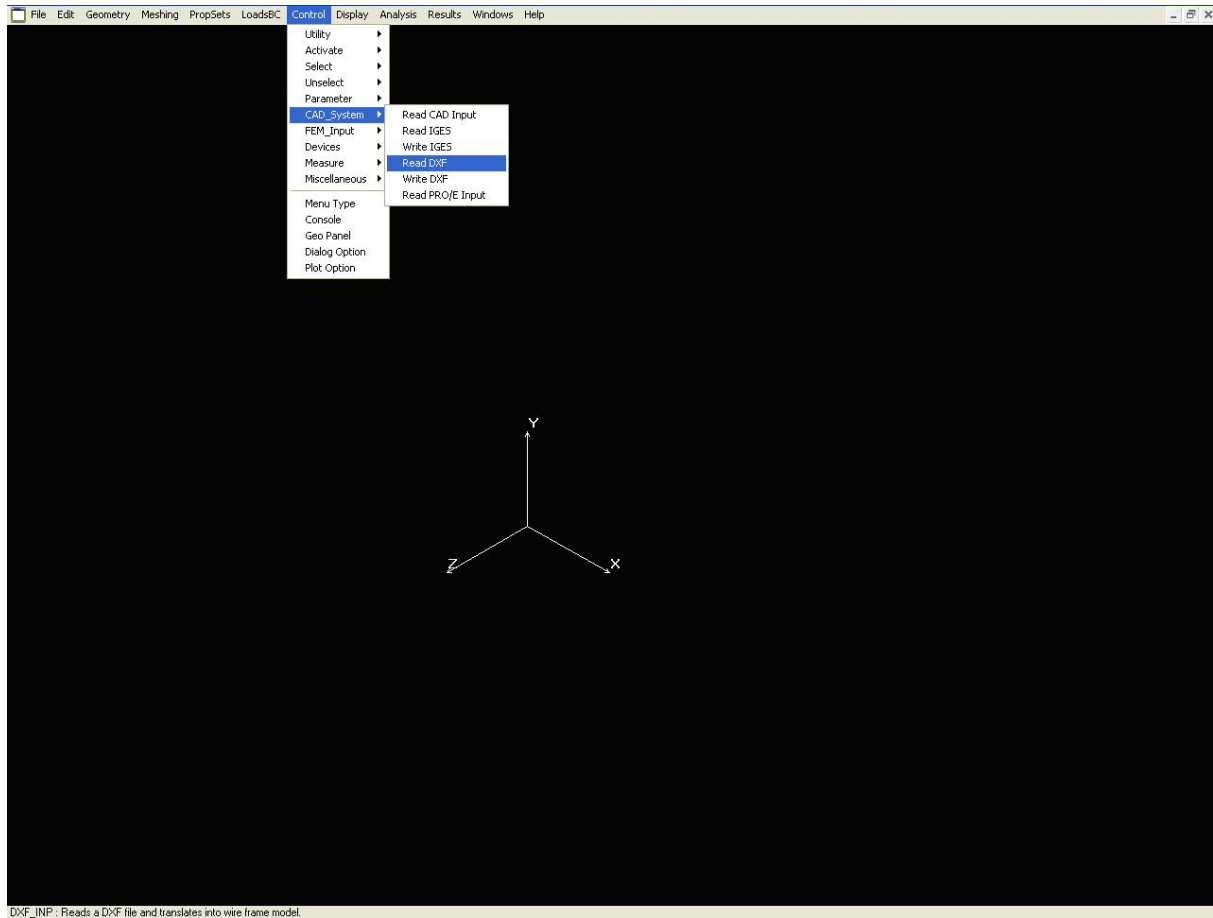


Figure 6.5 Geometric modeler in the finite element program

These built-in geometric modelers do not always offer you the convenience of modern CAD systems. Often we have to analyze existing models. In this case, the data exchange procedure can be convenient and efficient with other CAD systems by any available standard file format such as SAT, IGS, DXF, etc.. (see figure 6.6).



*Figure 6.6 Import geometric model from another geometric modeler*

Do not forget, in this case the geometric model only helps to create a finite element mesh. It does not comply with the rules of technical drawing, and has no relevance to real shape of the structure. It is true in this exercise, because the 100 mm box sections appears only lines (see Figure 6.7). Thus, we have to transform (simplify and extend) the technical documentation before finite element analysis. This is shown in Figure 6.7, which shows the imported geometric model.

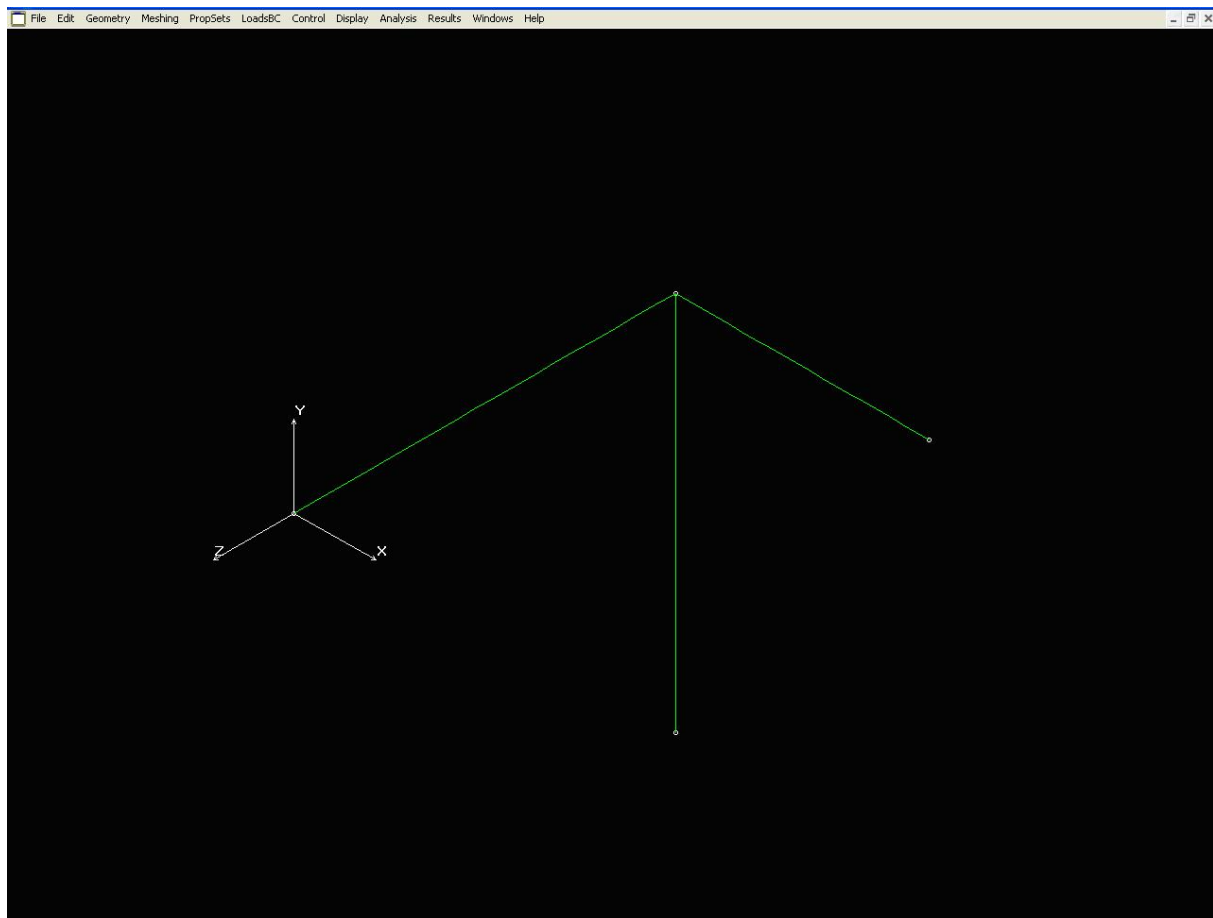


Figure 6.7 The imported geometric model

It is also shown that the elements lie in the XY plane.

The next step is to determine element group (see Figure 6.8).

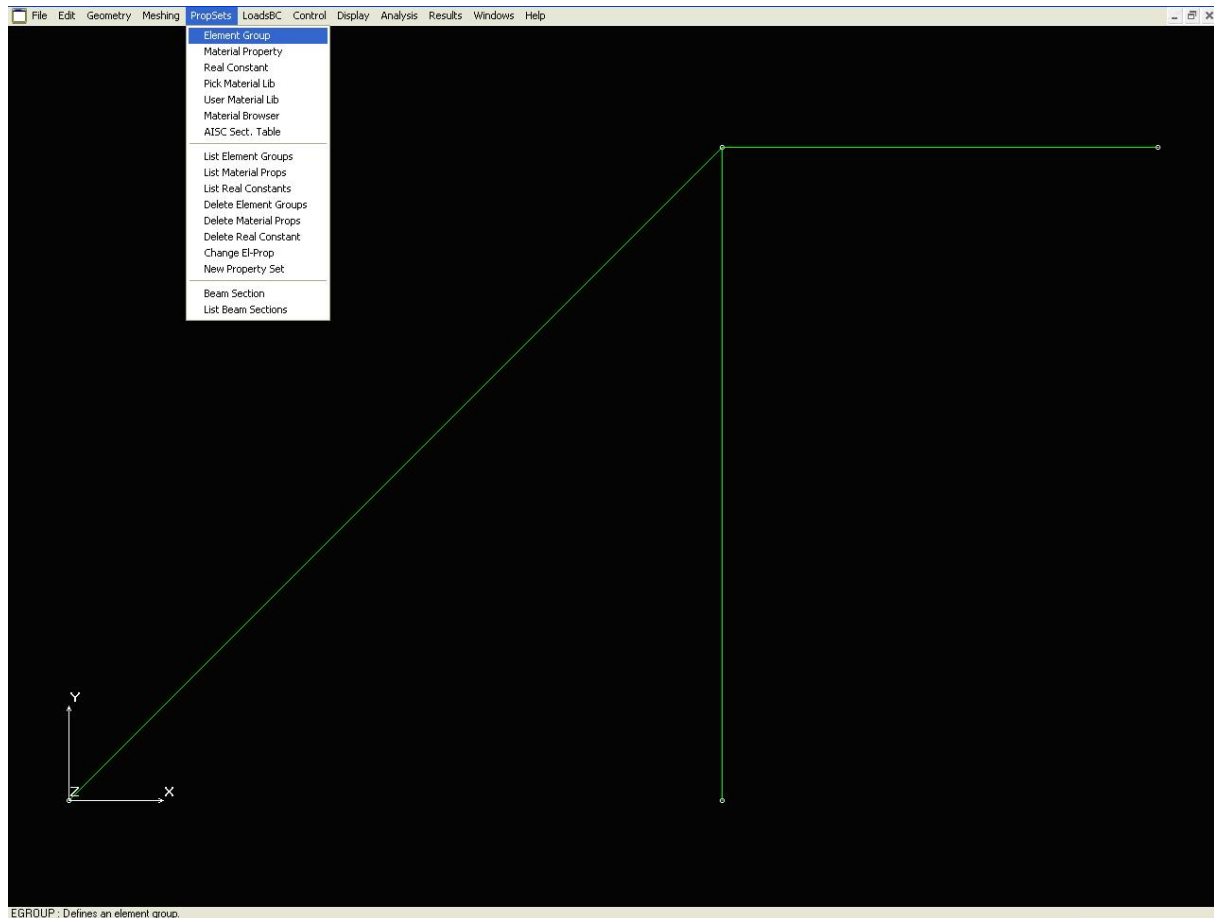


Figure 6.8 Determination of element group

We have clarified that we use linear behavior, BAEM2D elements (see Figure 6.9).

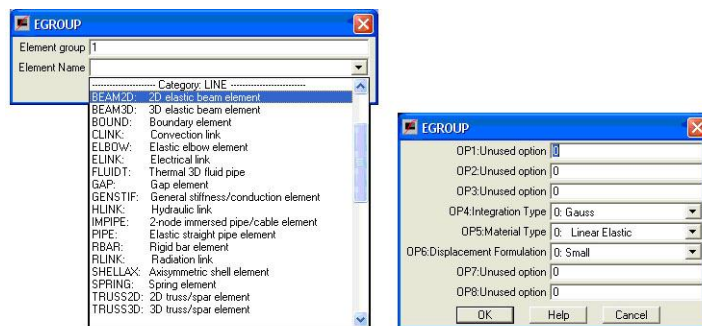


Figure 6.9 Select the BEAM2D elements and determination of these properties

Next task is to determine the real constants of elements (see Figure 6.10).



Figure 6.10 Real constants definition

As previously described we have to define real constants of BEAM2D elements, the cross-sectional area of the bars, the inertial moment ( $I_z$ ), deep of the section, and the shear factor (see Figure 6.11). Making sure use the selected unit system what is in this case the SI system.

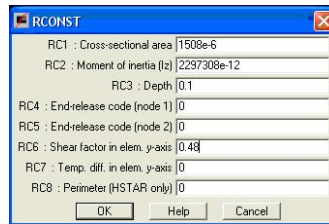


Figure 6.11 Real constants definition

Needs to be explained in the fourth and fifth real constants (End-release code). The end-release code for each end is specified by a six digit number with combinations of 0 and 1. The six digit code corresponds in order to the six degrees of freedom at each end of the beam elements. For example, end release code 000001 for a BEAM2D element represent a condition in which the moment about z axis is zero and forces in x- and y direction are to be calculated. The degree of freedom refers to the element local coordinate system (see Figure 6.1).

The seventh and eighth real constants use only in thermal analysis, so we do not deal with them now.

Still, the definition of material properties (see Figure 6.12).



Figure 6.12 Definition of material properties

It is sufficient to specify the value of the modulus of elasticity and Poisson's coefficient for the beam elements, as shown in figure 6.13 and figure 6.14.

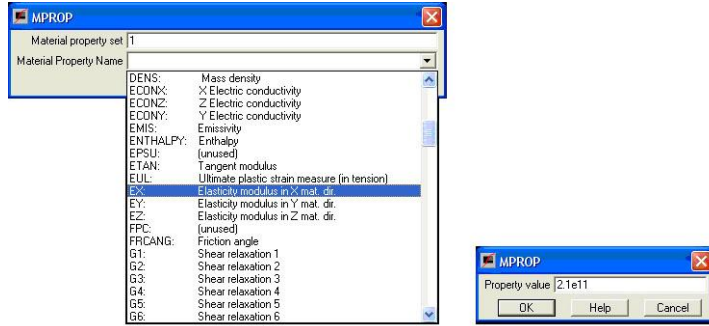


Figure 6.13 Definition of the elastic modulus

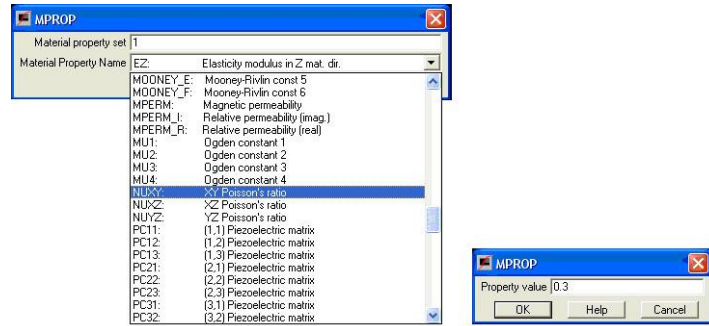


Figure 6.14 Definition of the Poisson's coefficient

If necessary, we can define more material properties.

After defining properties of the finite element mesh, may follow the finite element mesh generation. The FEM programs offer several methods for this, now we select the automatic mesh (see figure 6.15).

The size of the elements is determined by required precision of the results, the available capabilities of the computer and the available time. Now we choose 0,1 m average element size.

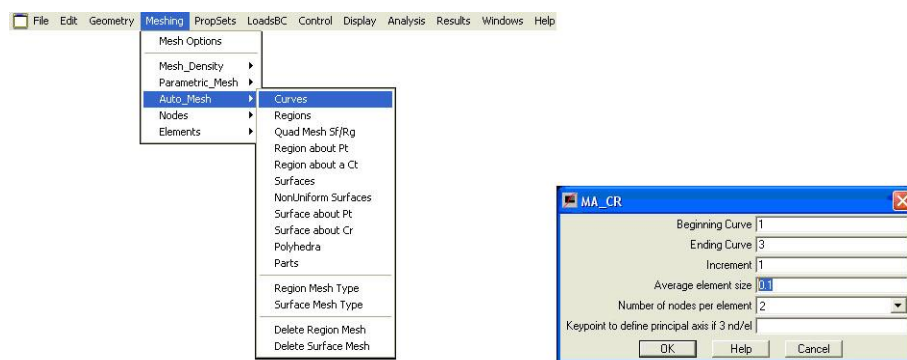


Figure 6.15 Automatic mesh generation

The finite element mesh and the numbered nodes shown in the Figure 6.16.

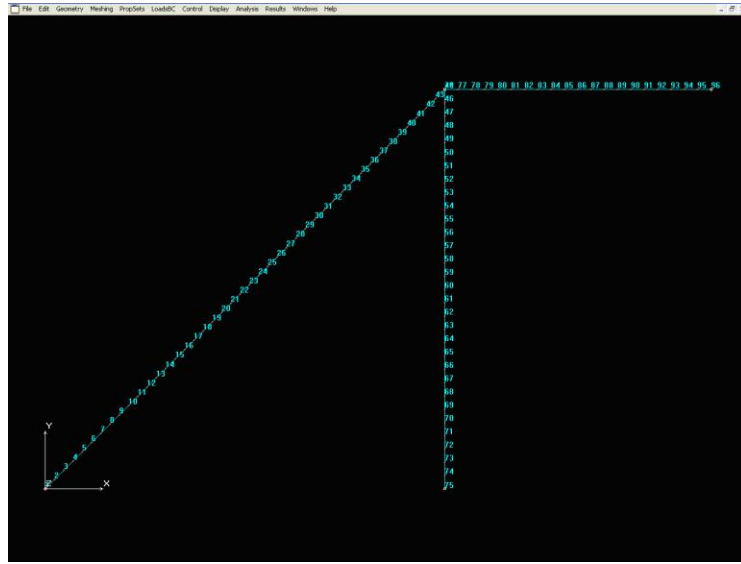


Figure 6.16 The finite element mesh

It is visible in the figure that created an independent node at each three endpoint of the beam elements. Because, the finite element mesh created each geometry object separately, it is necessary to merge the nodes in each end of the bars (see Figure 6.17).

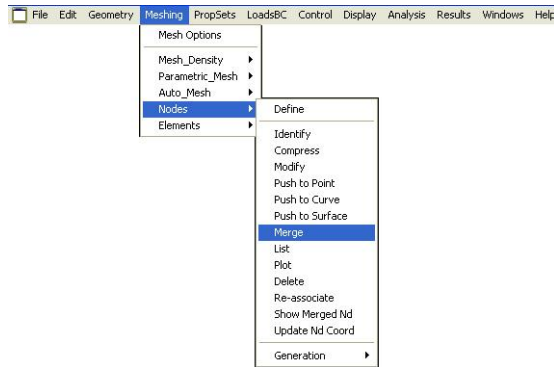


Figure 6.17 Merge of the end of bars

In the next step the boundary conditions should be given. In this case, these are two size 0 displacements on the supports.

We fix two degrees of freedom of the structure, in x and y directions at the both support (see figure 6.18).

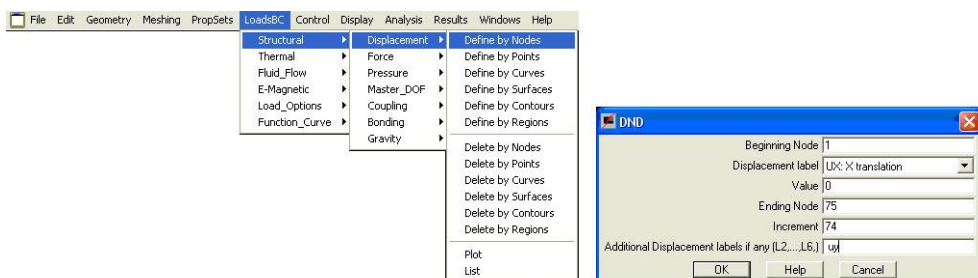


Figure 6.18 Displacement constraints

Finally, it should be given the loads the 5 kN concentrated force (see Figure 6.19). The direction of forces must be given in the global coordinate system, so the downward forces are negative sign.

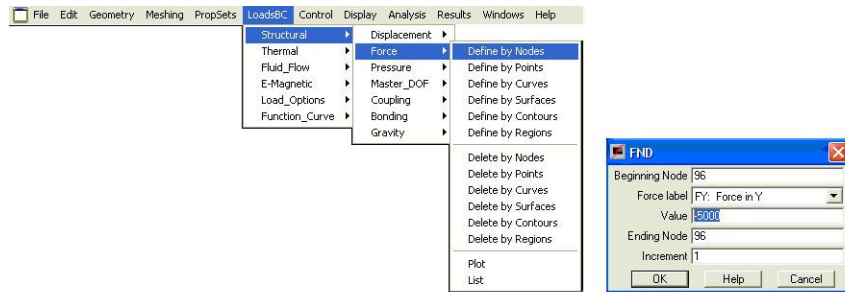


Figure 6.19 Defining the load

The completed finite element model is presented in Figure 6.20.

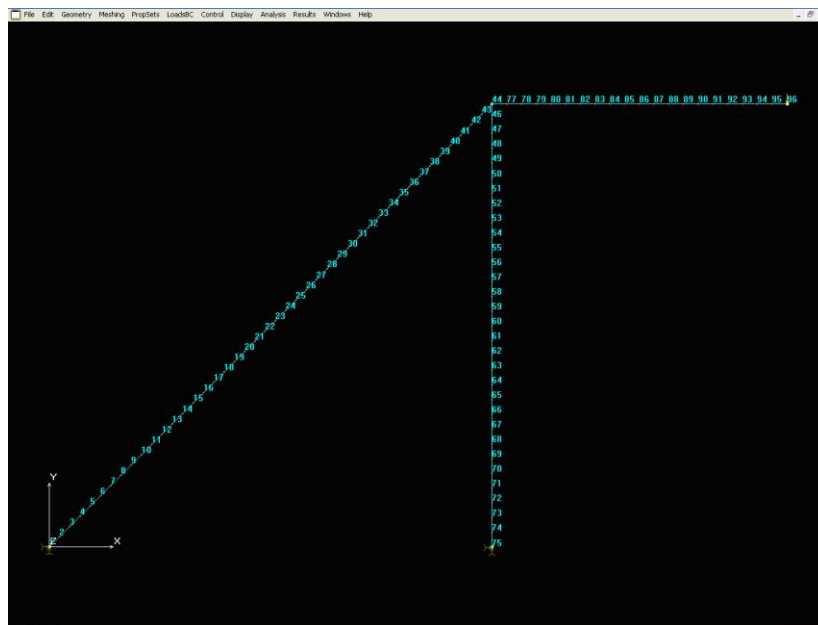


Figure 6.20 The completed finite element model

Follows, the running linear static analysis (see Figure 6.21).

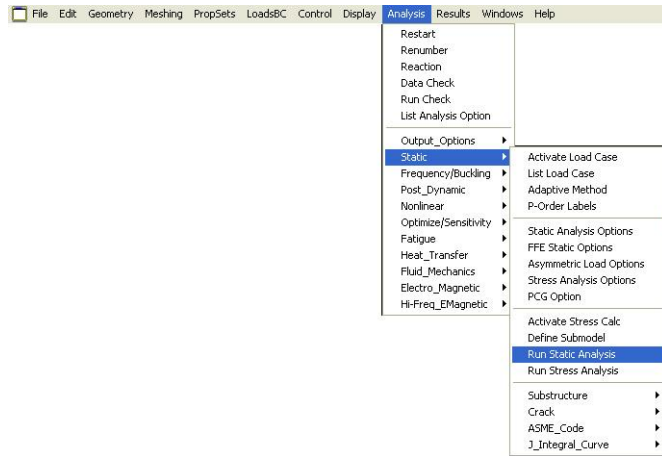


Figure 6.21 Run linear static analyses

After the successful solving, follows the display and evaluation of results.

The displaying stresses generated in bars (see Figure 6.22) can be done in several ways.

The stresses are interpreted on the element and in the element coordinate system like case of the TRUSS elements.



Figure 6.22 Display stresses

The results are shown in Figure 6.23. The deformation is not real, of course, the program generates a specific scale factor, so that data can be evaluated.

Notice, that the bars are bent, due to bending moments.

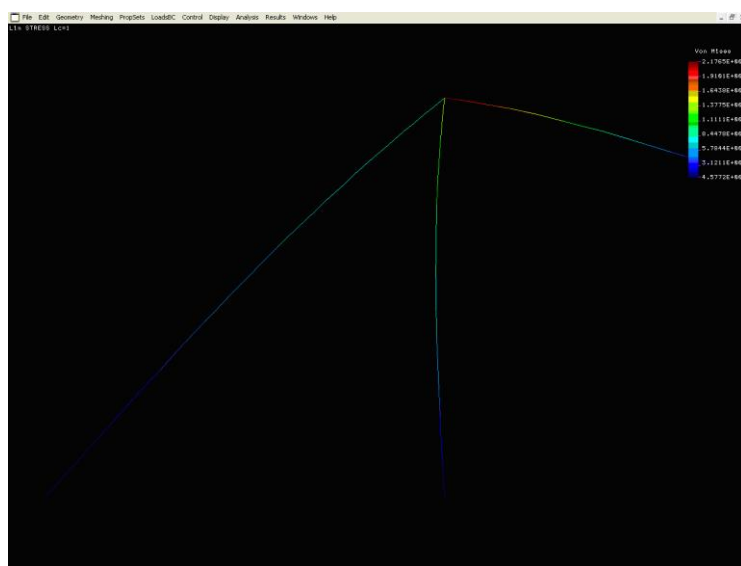


Figure 6.23 Stresses on deformed shape

It is possible to display stress components (see Figure 6.24). The negative sign of the stress indicate compressive stress.

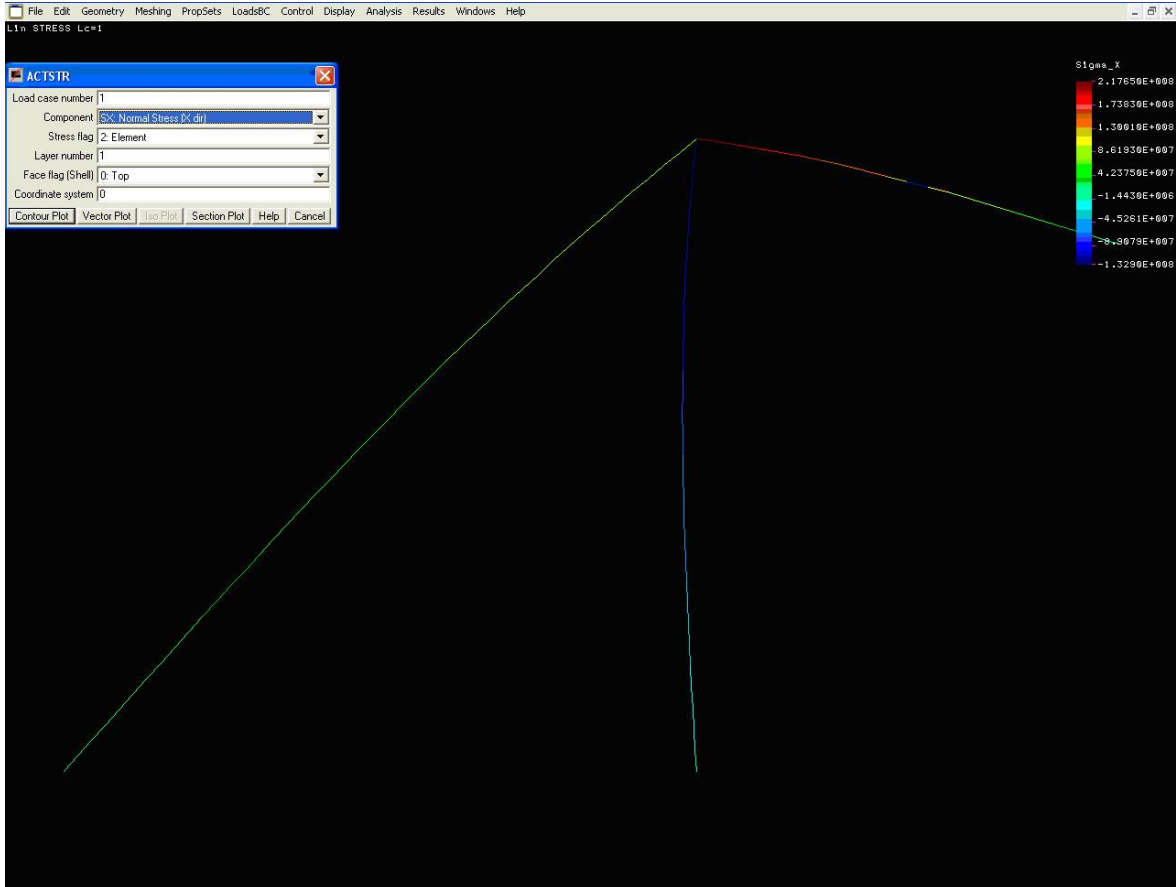


Figure 6.24 Display stress components

We examine the deflections i.e., y direction displacements in next step, (see Figure 6.25).

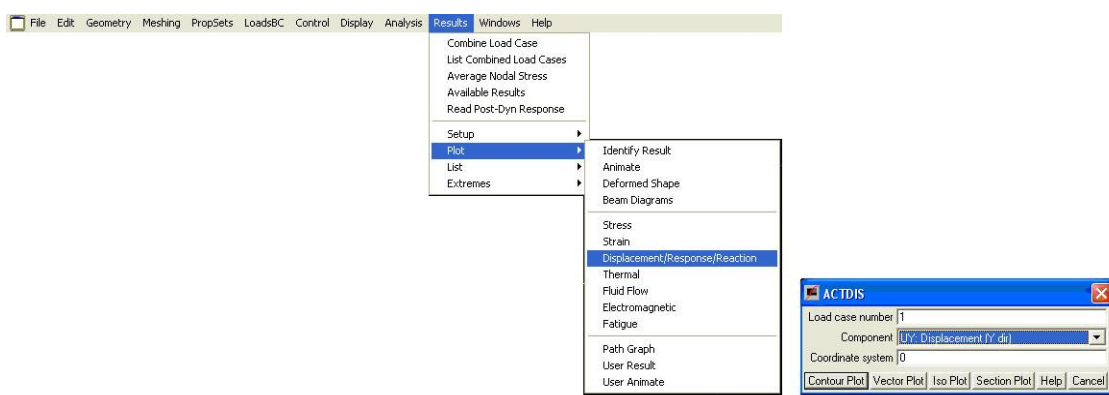


Figure 6.25 Display the deflection

The Figure 6.26 shows the results. The negative signs indicate downward displacements.

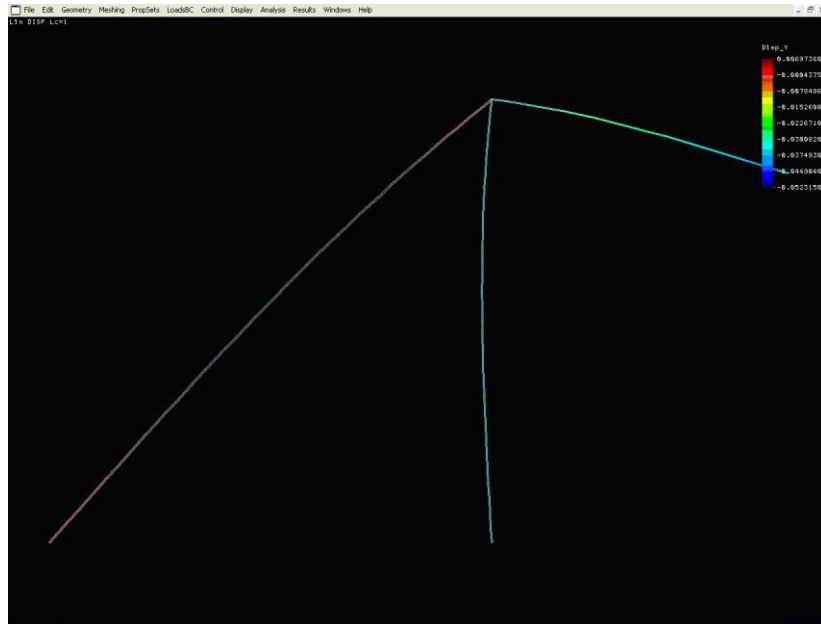


Figure 6.26 The deflections

We can display the moment and shear force diagrams in beam elements (see Figure 6.27).

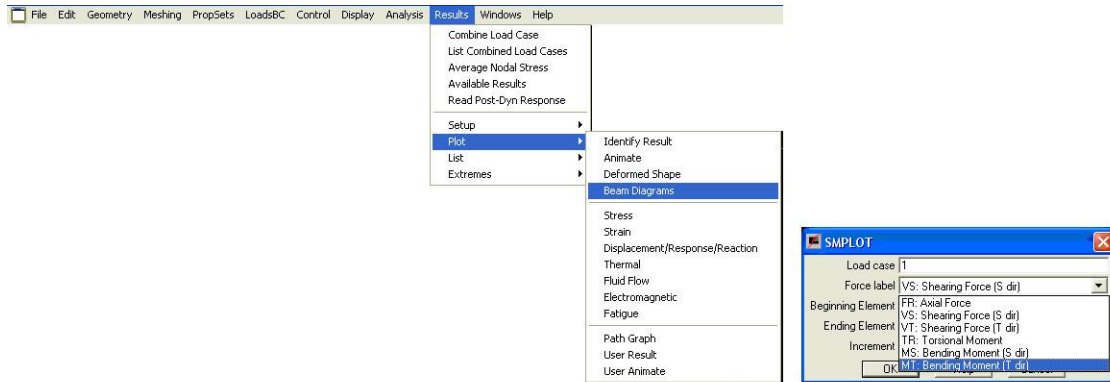


Figure 6.27 Display the bending moment diagram

The bending moment diagram shown in figure 6.28. There is not numerical value in diagram, even so useful because it helps to determine the minimal stressed locations.

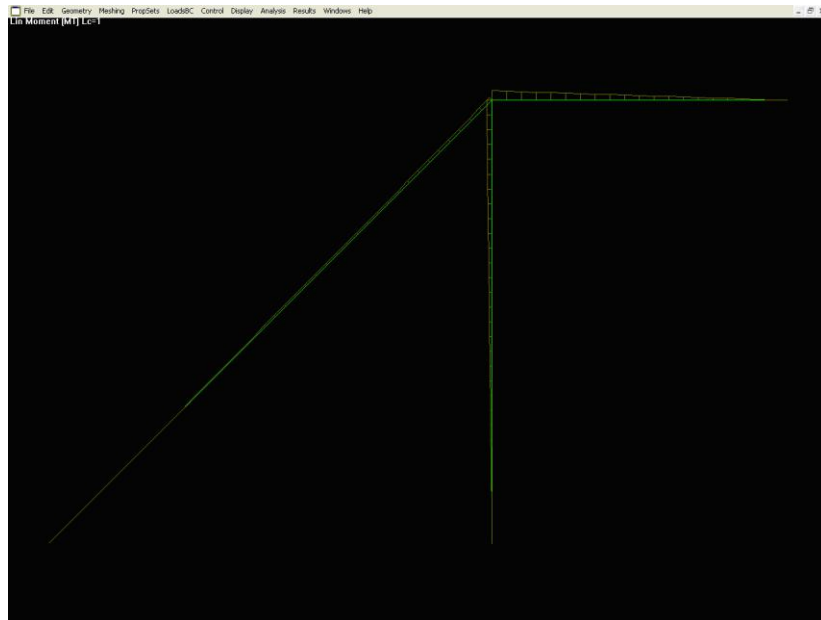


Figure 6.28 Bending moment diagram

It is possible to display the reaction forces and moments generated in supports (see Figure 6.29).

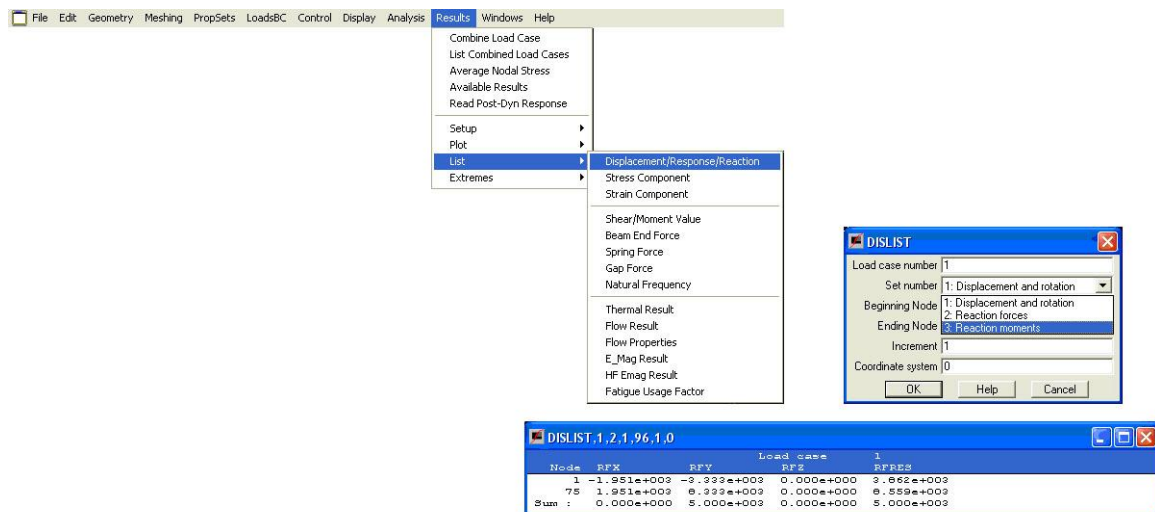
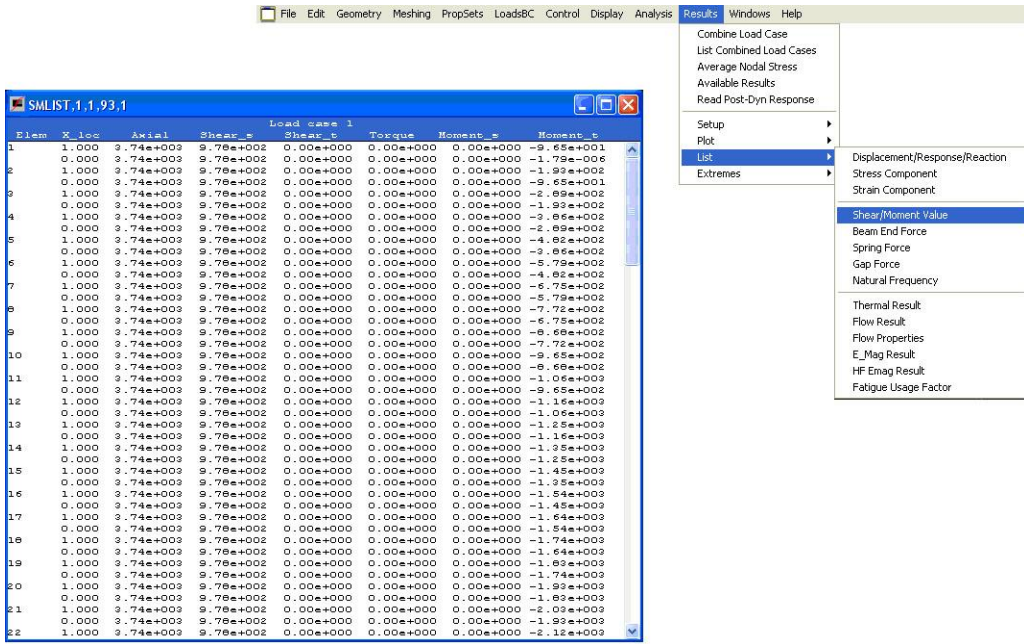


Figure 6.29 Display the reactions forces

It is possible to list the force and moments components generated in elements (see Figure 6.30).

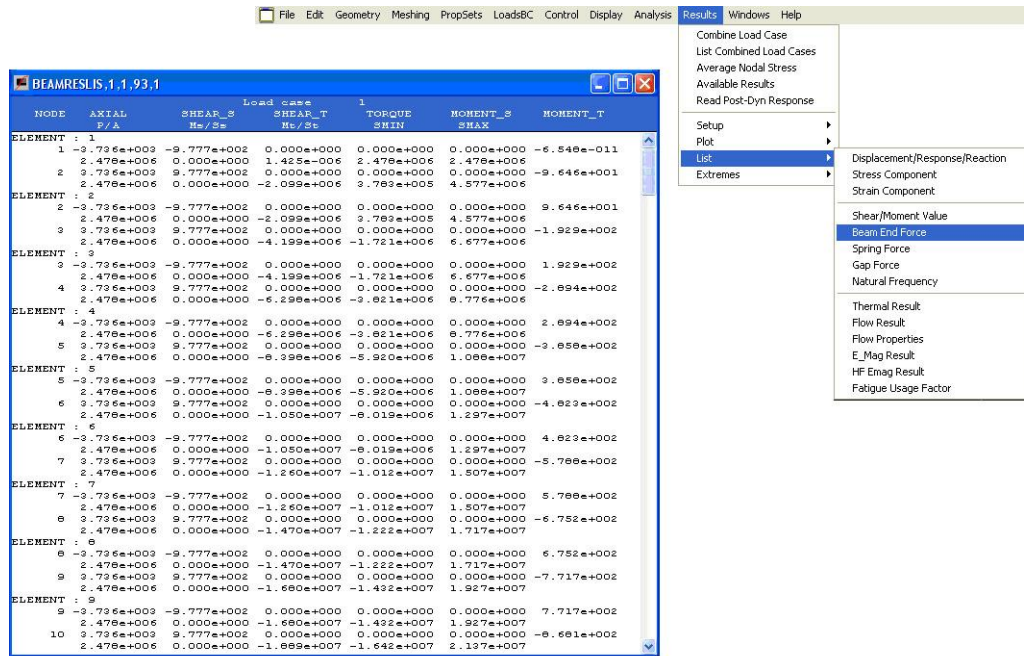


The screenshot shows the SMLIST software interface. The main window displays a table titled "Load case 1" with columns for Element, X\_loc, Axial, Shear\_s, Shear\_t, Torque, Moment\_s, and Moment\_t. The data in the table consists of 22 rows of numerical values. The software has a standard Windows-style menu bar at the top. On the right side, there is a "Results" menu with various options like "Combine Load Case", "List Combined Load Cases", "Average Nodal Stress", etc. A context menu is open over the table, with "List" highlighted under the "Setup" section.

| Element | X_loc | Axial     | Shear_s   | Shear_t   | Torque    | Moment_s   | Moment_t   |
|---------|-------|-----------|-----------|-----------|-----------|------------|------------|
| 1       | 1.000 | 9.74e+003 | 9.76e+002 | 0.00e+000 | 0.00e+000 | -9.65e+001 | -9.65e+001 |
| 0       | 0.000 | 9.74e+003 | 9.76e+002 | 0.00e+000 | 0.00e+000 | -1.92e+002 | -1.92e+002 |
| 1       | 0.000 | 9.74e+003 | 9.76e+002 | 0.00e+000 | 0.00e+000 | -1.92e+002 | -1.92e+002 |
| 2       | 0.000 | 3.74e+003 | 9.76e+002 | 0.00e+000 | 0.00e+000 | -9.65e+001 | -9.65e+001 |
| 3       | 1.000 | 3.74e+003 | 9.76e+002 | 0.00e+000 | 0.00e+000 | -2.89e+002 | -2.89e+002 |
| 0       | 0.000 | 3.74e+003 | 9.76e+002 | 0.00e+000 | 0.00e+000 | -1.92e+002 | -1.92e+002 |
| 4       | 1.000 | 3.74e+003 | 9.76e+002 | 0.00e+000 | 0.00e+000 | -3.86e+002 | -3.86e+002 |
| 1       | 0.000 | 3.74e+003 | 9.76e+002 | 0.00e+000 | 0.00e+000 | -1.92e+002 | -1.92e+002 |
| 5       | 1.000 | 3.74e+003 | 9.76e+002 | 0.00e+000 | 0.00e+000 | -4.82e+002 | -4.82e+002 |
| 0       | 0.000 | 3.74e+003 | 9.76e+002 | 0.00e+000 | 0.00e+000 | -2.86e+002 | -2.86e+002 |
| 6       | 1.000 | 3.74e+003 | 9.76e+002 | 0.00e+000 | 0.00e+000 | -4.82e+002 | -4.82e+002 |
| 0       | 0.000 | 3.74e+003 | 9.76e+002 | 0.00e+000 | 0.00e+000 | -4.82e+002 | -4.82e+002 |
| 7       | 1.000 | 3.74e+003 | 9.76e+002 | 0.00e+000 | 0.00e+000 | -7.72e+002 | -7.72e+002 |
| 0       | 0.000 | 3.74e+003 | 9.76e+002 | 0.00e+000 | 0.00e+000 | -5.75e+002 | -5.75e+002 |
| 8       | 1.000 | 3.74e+003 | 9.76e+002 | 0.00e+000 | 0.00e+000 | -7.72e+002 | -7.72e+002 |
| 0       | 0.000 | 3.74e+003 | 9.76e+002 | 0.00e+000 | 0.00e+000 | -6.75e+002 | -6.75e+002 |
| 9       | 1.000 | 3.74e+003 | 9.76e+002 | 0.00e+000 | 0.00e+000 | -6.75e+002 | -6.75e+002 |
| 1       | 0.000 | 3.74e+003 | 9.76e+002 | 0.00e+000 | 0.00e+000 | -6.75e+002 | -6.75e+002 |
| 10      | 1.000 | 3.74e+003 | 9.76e+002 | 0.00e+000 | 0.00e+000 | -7.72e+002 | -7.72e+002 |
| 0       | 0.000 | 3.74e+003 | 9.76e+002 | 0.00e+000 | 0.00e+000 | -8.69e+002 | -8.69e+002 |
| 11      | 1.000 | 3.74e+003 | 9.76e+002 | 0.00e+000 | 0.00e+000 | -1.06e+003 | -1.06e+003 |
| 0       | 0.000 | 3.74e+003 | 9.76e+002 | 0.00e+000 | 0.00e+000 | -9.65e+002 | -9.65e+002 |
| 12      | 1.000 | 3.74e+003 | 9.76e+002 | 0.00e+000 | 0.00e+000 | -1.16e+003 | -1.16e+003 |
| 0       | 0.000 | 3.74e+003 | 9.76e+002 | 0.00e+000 | 0.00e+000 | -1.16e+003 | -1.16e+003 |
| 13      | 1.000 | 3.74e+003 | 9.76e+002 | 0.00e+000 | 0.00e+000 | -1.16e+003 | -1.16e+003 |
| 0       | 0.000 | 3.74e+003 | 9.76e+002 | 0.00e+000 | 0.00e+000 | -1.16e+003 | -1.16e+003 |
| 14      | 1.000 | 3.74e+003 | 9.76e+002 | 0.00e+000 | 0.00e+000 | -1.16e+003 | -1.16e+003 |
| 0       | 0.000 | 3.74e+003 | 9.76e+002 | 0.00e+000 | 0.00e+000 | -1.25e+003 | -1.25e+003 |
| 15      | 1.000 | 3.74e+003 | 9.76e+002 | 0.00e+000 | 0.00e+000 | -1.45e+003 | -1.45e+003 |
| 0       | 0.000 | 3.74e+003 | 9.76e+002 | 0.00e+000 | 0.00e+000 | -1.39e+003 | -1.39e+003 |
| 16      | 1.000 | 3.74e+003 | 9.76e+002 | 0.00e+000 | 0.00e+000 | -1.45e+003 | -1.45e+003 |
| 0       | 0.000 | 3.74e+003 | 9.76e+002 | 0.00e+000 | 0.00e+000 | -1.45e+003 | -1.45e+003 |
| 17      | 1.000 | 3.74e+003 | 9.76e+002 | 0.00e+000 | 0.00e+000 | -1.54e+003 | -1.54e+003 |
| 0       | 0.000 | 3.74e+003 | 9.76e+002 | 0.00e+000 | 0.00e+000 | -1.54e+003 | -1.54e+003 |
| 18      | 1.000 | 3.74e+003 | 9.76e+002 | 0.00e+000 | 0.00e+000 | -1.74e+003 | -1.74e+003 |
| 0       | 0.000 | 3.74e+003 | 9.76e+002 | 0.00e+000 | 0.00e+000 | -1.92e+003 | -1.92e+003 |
| 19      | 1.000 | 3.74e+003 | 9.76e+002 | 0.00e+000 | 0.00e+000 | -1.82e+003 | -1.82e+003 |
| 0       | 0.000 | 3.74e+003 | 9.76e+002 | 0.00e+000 | 0.00e+000 | -1.74e+003 | -1.74e+003 |
| 20      | 1.000 | 3.74e+003 | 9.76e+002 | 0.00e+000 | 0.00e+000 | -1.92e+003 | -1.92e+003 |
| 0       | 0.000 | 3.74e+003 | 9.76e+002 | 0.00e+000 | 0.00e+000 | -1.82e+003 | -1.82e+003 |
| 21      | 1.000 | 3.74e+003 | 9.76e+002 | 0.00e+000 | 0.00e+000 | -2.02e+003 | -2.02e+003 |
| 0       | 0.000 | 3.74e+003 | 9.76e+002 | 0.00e+000 | 0.00e+000 | -1.92e+003 | -1.92e+003 |
| 22      | 1.000 | 3.74e+003 | 9.76e+002 | 0.00e+000 | 0.00e+000 | -2.12e+003 | -2.12e+003 |

Figure 6.30 List the force and moments components

The listing of the nodal forces and moments are shown in the figure 6.31.



The screenshot shows the BEAMRESL software interface. The main window displays a table titled "Load case 1" with columns for NODE, ELEMENT, AXIAL, SHEAR\_S, SHEAR\_T, TORQUE, MOMENT\_S, and MOMENT\_T. The data in the table consists of 10 rows of numerical values. The software has a standard Windows-style menu bar at the top. On the right side, there is a "Results" menu with various options like "Combine Load Case", "List Combined Load Cases", "Average Nodal Stress", etc. A context menu is open over the table, with "List" highlighted under the "Setup" section.

| Element      | Node | Axial       | Shear_s     | Shear_t     | Torque      | Moment_s   | Moment_t    |
|--------------|------|-------------|-------------|-------------|-------------|------------|-------------|
| ELEMENT : 1  | 1    | -9.736e+003 | -9.777e+002 | 0.000e+000  | 0.000e+000  | 0.000e+000 | -6.546e-011 |
|              | 2    | 2.476e+006  | 0.000e+000  | 1.425e-006  | 2.478e+006  | 0.000e+000 |             |
|              | 2    | 3.736e+003  | 9.777e+002  | 0.000e+000  | 0.000e+000  | 0.000e+000 | -9.646e+001 |
| ELEMENT : 2  | 2    | -9.736e+003 | -9.777e+002 | 0.000e+000  | 0.000e+000  | 0.000e+000 | 9.646e+001  |
|              | 2    | 2.476e+006  | 0.000e+000  | -2.099e+006 | 3.782e+005  | 4.577e+005 |             |
|              | 3    | 3.736e+003  | 9.777e+002  | 0.000e+000  | 0.000e+000  | 0.000e+000 | -1.929e+002 |
| ELEMENT : 3  | 3    | -9.736e+003 | -9.777e+002 | 0.000e+000  | 0.000e+000  | 0.000e+000 | 1.929e+002  |
|              | 2    | 2.476e+006  | 0.000e+000  | -4.199e+006 | -1.721e+006 | 6.677e+005 |             |
|              | 4    | 3.736e+003  | 9.777e+002  | 0.000e+000  | 0.000e+000  | 0.000e+000 | -2.694e+002 |
| ELEMENT : 4  | 4    | -9.736e+003 | -9.777e+002 | 0.000e+000  | 0.000e+000  | 0.000e+000 | 2.694e+002  |
|              | 2    | 2.476e+006  | 0.000e+000  | -6.298e+006 | -3.621e+005 | 6.776e+005 |             |
|              | 5    | 3.736e+003  | 9.777e+002  | 0.000e+000  | 0.000e+000  | 0.000e+000 | -3.656e+002 |
| ELEMENT : 5  | 5    | -9.736e+003 | -9.777e+002 | 0.000e+000  | 0.000e+000  | 0.000e+000 | 3.656e+002  |
|              | 2    | 2.476e+006  | 0.000e+000  | -8.398e+006 | -5.920e+006 | 1.088e+007 |             |
|              | 6    | 3.736e+003  | 9.777e+002  | 0.000e+000  | 0.000e+000  | 0.000e+000 | -4.623e+002 |
| ELEMENT : 6  | 6    | -9.736e+003 | -9.777e+002 | 0.000e+000  | 0.000e+000  | 0.000e+000 | 4.623e+002  |
|              | 2    | 2.476e+006  | 0.000e+000  | -1.050e+007 | -8.019e+006 | 1.297e+007 |             |
|              | 7    | 3.736e+003  | 9.777e+002  | 0.000e+000  | 0.000e+000  | 0.000e+000 | -5.766e+002 |
| ELEMENT : 7  | 7    | -9.736e+003 | -9.777e+002 | 0.000e+000  | 0.000e+000  | 0.000e+000 | 5.766e+002  |
|              | 2    | 2.476e+006  | 0.000e+000  | -1.150e+007 | -9.019e+006 | 1.307e+007 |             |
|              | 8    | 3.736e+003  | 9.777e+002  | 0.000e+000  | 0.000e+000  | 0.000e+000 | -5.766e+002 |
| ELEMENT : 8  | 8    | -9.736e+003 | -9.777e+002 | 0.000e+000  | 0.000e+000  | 0.000e+000 | 5.766e+002  |
|              | 2    | 2.476e+006  | 0.000e+000  | -1.250e+007 | -1.012e+007 | 1.507e+007 |             |
|              | 9    | 3.736e+003  | 9.777e+002  | 0.000e+000  | 0.000e+000  | 0.000e+000 | -5.722e+002 |
| ELEMENT : 9  | 9    | -9.736e+003 | -9.777e+002 | 0.000e+000  | 0.000e+000  | 0.000e+000 | 5.722e+002  |
|              | 2    | 2.476e+006  | 0.000e+000  | -1.350e+007 | -1.172e+007 | 1.717e+007 |             |
|              | 10   | 3.736e+003  | 9.777e+002  | 0.000e+000  | 0.000e+000  | 0.000e+000 | -5.717e+002 |
| ELEMENT : 10 | 10   | -9.736e+003 | -9.777e+002 | 0.000e+000  | 0.000e+000  | 0.000e+000 | 5.717e+002  |
|              | 2    | 2.476e+006  | 0.000e+000  | -1.450e+007 | -1.342e+007 | 1.927e+007 |             |

Figure 6.31 The nodal forces and moments

The listing of the stress component shows figure 6.32.

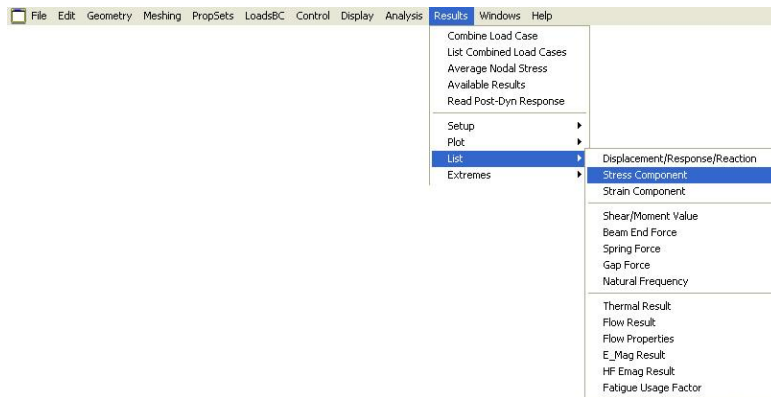


Figure 6.32 The stress component list

The numerical results tables can appear incomplete, some component is 0. As explained by the BEAM2D elements. The shear forces perpendicular to plane of structure, bending moments in this plane and torque does not exist in this case.

#### 6.4. Remarks

During the solutions we do not deal with buckling of the compressed bars. If this is a real problem, one should be to verify with solution a finite element problem, or with any analytic method.

During the solutions the tare weight was neglected.

Both problems are explained in later chapters.

Furthermore, the structural joint was not tested. The other specialized areas of structural design deal with this problems.

## 7. APPLICATION THE PRINCIPLE OF THE MINIMUM POTENTIAL ENERGY IN FIELD OF THREE-DIMENSIONAL BENT BAR ELEMENTS, RITZ METHOD AND FINITE ELEMENT METHOD

### 7.1. Three-dimensional bent bars variational problem

The chapter 5 deals with the analysis of two-dimensional bent bars. Nodes of these elements have three degrees of freedom, two displacements and a rotation.

In this section we analyze three-dimensional beam elements, extension of the previous chapters. The position of the element in the local element coordinate system and the used notations are shown in Figure 7.1.

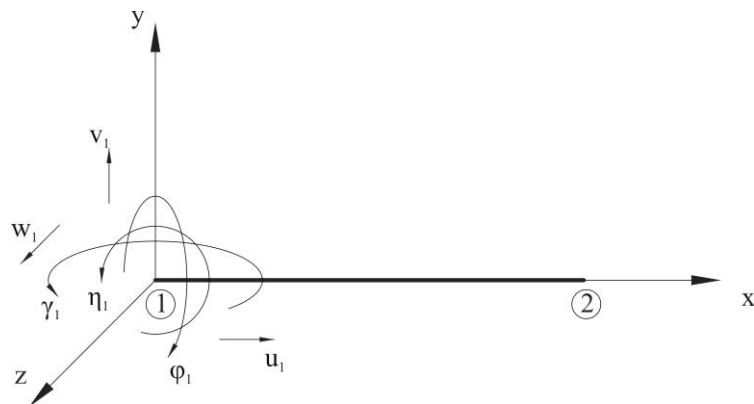


Figure 7.1 Element position in the local element coordinate system

The figure also shows that degrees of freedom of nodes are extended with displacement in the x-z plane, rotation in the x-z plane and rotation around x-axis (i.e. torsion).

In addition, as previously described, between the angle displacement (twist) of the beam and the torque is a linear connection, so the work of the torque:

$$W = \frac{1}{2} M_t \rho \quad (7.1)$$

$$\rho = \frac{M_t L}{I_p G} \quad (7.2)$$

thus:

$$W = \frac{1}{2G} \frac{M_t^2 L}{I_p} \quad (7.3)$$

In the previous chapter we saw that the basic formula of the finite element method is the following linear equation:

$$\underline{\underline{K}}\underline{u} = \underline{F} \quad (7.4)$$

which in this case, for the two nodes, 12 degree of freedom elements:

$$\begin{bmatrix} k_{1,1} & k_{1,2} & \cdot & k_{1,12} \\ k_{2,1} & \cdot \\ \cdot & \cdot \\ \cdot & \cdot \\ \cdot & \cdot \\ \cdot & \cdot \\ \cdot & \cdot \\ \cdot & \cdot \\ \cdot & \cdot \\ \cdot & \cdot \\ \cdot & \cdot \\ k_{12,1} & \cdot & k_{12,12} \end{bmatrix} \begin{bmatrix} u_1 \\ v_1 \\ w_1 \\ \varphi_1 \\ \gamma_1 \\ \eta_1 \\ u_2 \\ v_2 \\ w_2 \\ \varphi_2 \\ \gamma_2 \\ \eta_2 \end{bmatrix} = \begin{bmatrix} F_{N1} \\ F_{T1} \\ F_{S1} \\ M_{Z1} \\ M_{Y1} \\ M_{X1} \\ F_{N2} \\ F_{T2} \\ F_{S2} \\ M_{Z2} \\ M_{Y2} \\ M_{X2} \end{bmatrix} \quad (7.5)$$

We can describe the deformation of the element by interpolation polynomials, like that seen in chapter 3. This way, displacement of a point:

$$u_x(x) = \sum_1^{12} \psi_{xk}(x) u_k \quad (7.6)$$

$$u_y(x) = \sum_1^{12} \psi_{yk}(x) u_k \quad (7.7)$$

$$u_z(x) = \sum_1^{12} \psi_{zk}(x) u_k \quad (7.8)$$

The  $\psi_{xk}$ ,  $\psi_{yk}$ ,  $\psi_{zk}$  interpolation functions satisfy the boundary conditions and differentiable. According to the Euler-Bernoulli's beam theory, we approximate the displacement in x direction and rotation around x axis with linear interpolation functions:

$$\psi_{x1} = \psi_{x4} = 1 - \frac{x}{L} \quad (7.9)$$

$$\psi_{x7} = \psi_{x10} = \frac{x}{L} \quad (7.10)$$

$$\psi_{x2} = \psi_{x3} = \psi_{x4} = \psi_{x5} = \psi_{x6} = \psi_{x8} = \psi_{x9} = \psi_{x11} = \psi_{x12} = 0 \quad (7.11)$$

The bending of the element is approximated with cubic functions:

$$\psi_{y2} = \psi_{z3} = 1 - 3\left(\frac{x}{L}\right)^2 + 2\left(\frac{x}{L}\right)^3 \quad (7.12)$$

$$\psi_{y6} = \psi_{z5} = \left( \frac{x}{l} - 3\left(\frac{x}{L}\right)^2 + \left(\frac{x}{L}\right)^3 \right) L \quad (7.13)$$

$$\psi_{y8} = \psi_{z9} = 3\left(\frac{x}{L}\right)^2 - 2\left(\frac{x}{L}\right)^3 \quad (7.14)$$

$$\psi_{y12} = \psi_{z11} = \left( -\left(\frac{x}{L}\right)^2 + \left(\frac{x}{L}\right)^3 \right) L \quad (7.15)$$

$$\psi_{y1} = \psi_{y4} = \psi_{y5} = \psi_{y7} = \psi_{y9} = \psi_{y10} = \psi_{y11} = \psi_{z1} = \psi_{y2} = \psi_{y4} = \psi_{y6} = \psi_{y7} = \psi_{y8} = \psi_{y10} = \psi_{y12} = 0 \quad (7.16)$$

These functions can be obtained analytic solving the differential equation of the elastic curve of the bent beam. The total potential energy (the difference between strain energy and the work of external forces), is minimal in the equilibrium position of the rigid body, i.e. the first variation is zero  $\delta\Pi = \delta(U - L) = 0$ . The application of this theorem is based on the examination of the strain energy changes, so the strain energy belongs to each load cases have to be prescribed.

The axial displacements belong to elongations:

$$\varepsilon_x = \frac{\partial u_x}{\partial x} = \sum_{k=1}^{12} \frac{\partial}{\partial x} \psi'_{xk}(x) \cdot u_k = \sum_{k=1}^{12} \psi'_{xk}(x) \cdot u_k \quad (7.17)$$

Thus, the potential energy for constant cross-sectional bar:

$$U = \frac{1}{2} \int_{x=0}^L EA \varepsilon_x^2 dx = \frac{1}{2} \int_{x=0}^L EA \left( \sum_{k=1}^{12} \psi'_{xk}(x) \cdot u_k \right)^2 dx \quad (7.18)$$

The ij-th member of element stiffness matrix in case k=1 and k=7:

$$k_{ij} = \frac{\partial}{\partial u_i} \frac{\partial}{\partial u_j} \frac{1}{2} \int_{x=0}^L EA \left( \sum_{k=1}^{12} \psi'_{xk}(x) \cdot u_k \right)^2 dx = \int_{x=0}^L EA \psi'_{xi}(x) \psi'_{xj}(x) dx \quad (7.19)$$

Deformation in case torsion around x-axis:

$$\gamma_x = \frac{\partial u_x}{\partial x} = \sum_{k=1}^{12} \frac{\partial}{\partial x} \psi'_{xk}(x) \cdot u_k = \sum_{k=1}^{12} \psi'_{xk}(x) \cdot u_k \quad (7.20)$$

Thus, the potential energy for constant cross-sectional bar:

$$U = \frac{1}{2} \int_{x=0}^L G I_p \gamma_x^2 dx = \frac{1}{2} \int_{x=0}^L G I_p \left( \sum_{k=1}^{12} \psi'_{xk}(x) \cdot u_k \right)^2 dx \quad (7.21)$$

The  $ij^{\text{th}}$  member of element stiffness matrix in case  $k=4$  and  $k=10$ :

$$k_{ij} = \frac{\partial}{\partial u_i} \frac{\partial}{\partial u_j} \frac{1}{2} \int_{x=0}^L G I_p \left( \sum_{k=1}^{12} \psi'_{xk}(x) \cdot u_k \right)^2 dx = \int_{x=0}^L G I_p \psi'_{xi}(x) \psi'_{xj}(x) dx \quad (7.22)$$

The potential energy of bent beam is the function of the rotation (the shear deformation is neglected according to Euler-Bernoulli's theory). In case bending in the xy plane:

$$\phi_z = \frac{\partial^2 u_y}{\partial x^2} = \sum_{k=1}^{12} \frac{\partial^2}{\partial x^2} \psi_{yk}(x) \cdot u_k = \sum_{k=1}^{12} \psi''_{yk}(x) \cdot u_k \quad (7.23)$$

Thus, the potential energy for constant cross-sectional bar:

$$U = \frac{1}{2} \int_{x=0}^L E I_z \phi_z^2 dx = \frac{1}{2} \int_{x=0}^L E I_z \left( \sum_{k=1}^{12} \psi''_{yk}(x) \cdot u_k \right)^2 dx \quad (7.24)$$

The  $ij^{\text{th}}$  member of element stiffness matrix in case  $k=2, k=6, k=8$  and  $k=12$ :

$$k_{ij} = \frac{\partial}{\partial u_i} \frac{\partial}{\partial u_j} \frac{1}{2} \int_{x=0}^L E I_z \left( \sum_{k=1}^{12} \psi''_{yk}(x) \cdot u_k \right)^2 dx = \int_{x=0}^L E I_z \psi''_{yi}(x) \psi''_{yj}(x) dx \quad (7.25)$$

Easy to see that, in case bending in the xz plane,  $I_y$  must be used instead of  $I_z$ .

Thus, the  $ij^{\text{th}}$  member of element stiffness matrix in case  $k=3, k=5, k=9$  and  $k=11$ :

$$k_{ij} = \frac{\partial}{\partial u_i} \frac{\partial}{\partial u_j} \frac{1}{2} \int_{x=0}^L E I_y \left( \sum_{k=1}^{12} \psi''_{zk}(x) \cdot u_k \right)^2 dx = \int_{x=0}^L E I_y \psi''_{zi}(x) \psi''_{zj}(x) dx \quad (7.26)$$

Thus the element stiffness matrix:

$$K_e = \begin{bmatrix} \frac{AE}{L} & 0 & 0 & 0 & 0 & -\frac{AE}{L} & 0 & 0 & 0 & 0 & 0 \\ 0 & \frac{12EI_z}{L^3} & 0 & 0 & 0 & \frac{6EI_z}{L^2} & 0 & -\frac{12EI_z}{L^3} & 0 & 0 & \frac{6EI_z}{L^2} \\ 0 & 0 & \frac{12EI_y}{L^3} & 0 & -\frac{6EI_y}{L^2} & 0 & 0 & 0 & -\frac{12EI_y}{L^3} & 0 & -\frac{6EI_y}{L^2} \\ 0 & 0 & 0 & \frac{GI_p}{L} & 0 & 0 & 0 & 0 & 0 & -\frac{GI_p}{L} & 0 \\ 0 & 0 & -\frac{6EI_y}{L^2} & 0 & \frac{4EI_y}{L} & 0 & 0 & 0 & \frac{6EI_y}{L^2} & 0 & \frac{2EI_y}{L} \\ 0 & \frac{6EI_z}{L^2} & 0 & 0 & 0 & \frac{4EI_z}{L} & 0 & -\frac{6EI_z}{L^2} & 0 & 0 & \frac{2EI_z}{L} \\ -\frac{AE}{L} & 0 & 0 & 0 & 0 & 0 & \frac{AE}{L} & 0 & 0 & 0 & 0 \\ 0 & -\frac{12EI_z}{L^3} & 0 & 0 & 0 & -\frac{6EI_z}{L^2} & 0 & \frac{12EI_z}{L^3} & 0 & 0 & -\frac{6EI_z}{L^2} \\ 0 & 0 & -\frac{12EI_y}{L^3} & 0 & \frac{6EI_y}{L^2} & 0 & 0 & 0 & \frac{12EI_y}{L^3} & 0 & \frac{6EI_y}{L^2} \\ 0 & 0 & 0 & -\frac{GI_p}{L} & 0 & 0 & 0 & 0 & 0 & \frac{GI_p}{L} & 0 \\ 0 & 0 & -\frac{6EI_y}{L^2} & 0 & \frac{2EI_y}{L} & 0 & 0 & 0 & \frac{6EI_y}{L^2} & 0 & \frac{4EI_y}{L} \\ 0 & \frac{6EI_z}{L^2} & 0 & 0 & 0 & \frac{2EI_z}{L} & 0 & -\frac{6EI_z}{L^2} & 0 & 0 & \frac{4EI_z}{L} \end{bmatrix}$$

The element stiffness matrix in global coordinate system can be produced using transformation matrix as well as described in chapter 5. In this case, the transformation matrix is of order 12x12. The notations are shown in figure 7.2:

$$T = \begin{bmatrix} c\alpha c\beta & c\alpha s\beta & s\alpha & 0 & 0 & 0 & 0 & 0 & 0 & 0 & 0 & 0 \\ -s\beta & c\beta & 0 & 0 & 0 & 0 & 0 & 0 & 0 & 0 & 0 & 0 \\ -s\alpha c\beta & -s\alpha s\beta & c\alpha & 0 & 0 & 0 & 0 & 0 & 0 & 0 & 0 & 0 \\ 0 & 0 & 0 & c\alpha c\beta & -c\alpha s\beta & s\alpha & 0 & 0 & 0 & 0 & 0 & 0 \\ 0 & 0 & 0 & s\beta & c\beta & 0 & 0 & 0 & 0 & 0 & 0 & 0 \\ 0 & 0 & 0 & -s\alpha c\beta & s\alpha s\beta & c\alpha & 0 & 0 & 0 & 0 & 0 & 0 \\ 0 & 0 & 0 & 0 & 0 & 0 & c\alpha c\beta & c\alpha s\beta & s\alpha & 0 & 0 & 0 \\ 0 & 0 & 0 & 0 & 0 & 0 & -s\beta & c\beta & 0 & 0 & 0 & 0 \\ 0 & 0 & 0 & 0 & 0 & 0 & -s\alpha c\beta & -s\alpha s\beta & c\alpha & 0 & 0 & 0 \\ 0 & 0 & 0 & 0 & 0 & 0 & 0 & 0 & 0 & c\alpha c\beta & -c\alpha s\beta & s\alpha \\ 0 & 0 & 0 & 0 & 0 & 0 & 0 & 0 & 0 & s\beta & c\beta & 0 \\ 0 & 0 & 0 & 0 & 0 & 0 & 0 & 0 & 0 & -s\alpha c\beta & s\alpha s\beta & c\alpha \end{bmatrix}$$

where:  
 $c = \cos$   
 $s = \sin$

The element stiffness matrix in global coordinate system:

$$\underline{\underline{K}}_e^* = \underline{\underline{T}}^T \underline{\underline{K}}_e \underline{\underline{T}} \quad (7.27)$$

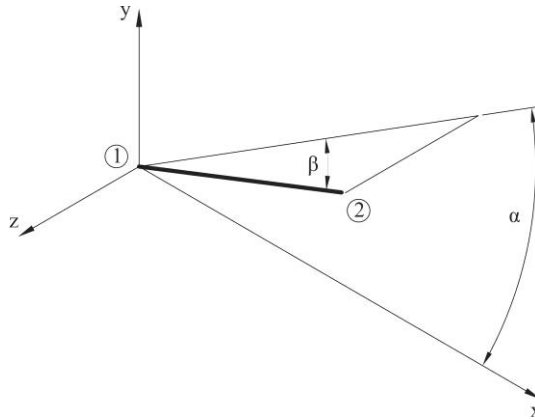


Figure 7.2 The element position in global coordinate system

## 7.2. Solving the problem using finite element method

An outdoor information board is placed on a holder (see Figure 7.3.). The board weight is 50 kg. A 300 N force acting on the board perpendicular to its plane (e.g. wind pressure).

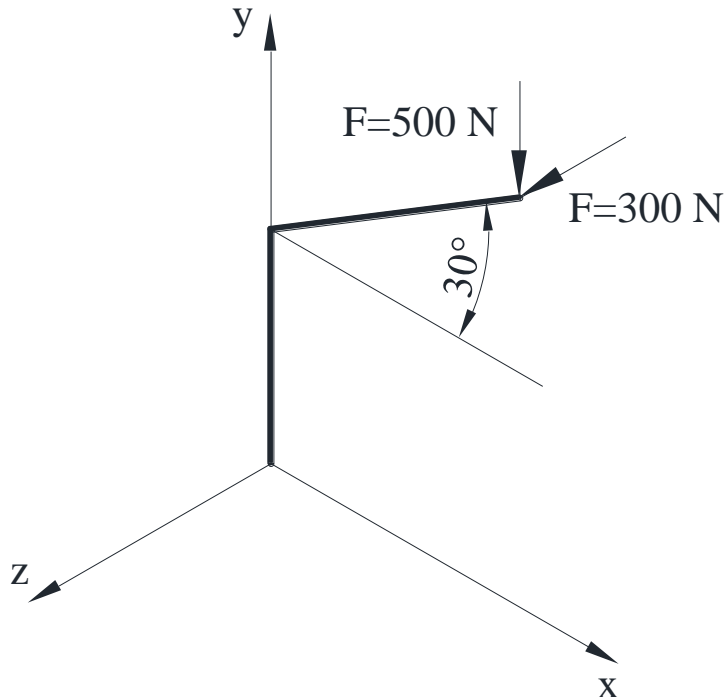


Figure 7.3 The holder

We place the finite element model in x-y plane (see figure 7.4), so we have to develop the transformed stiffness matrix of the beam 2 only.

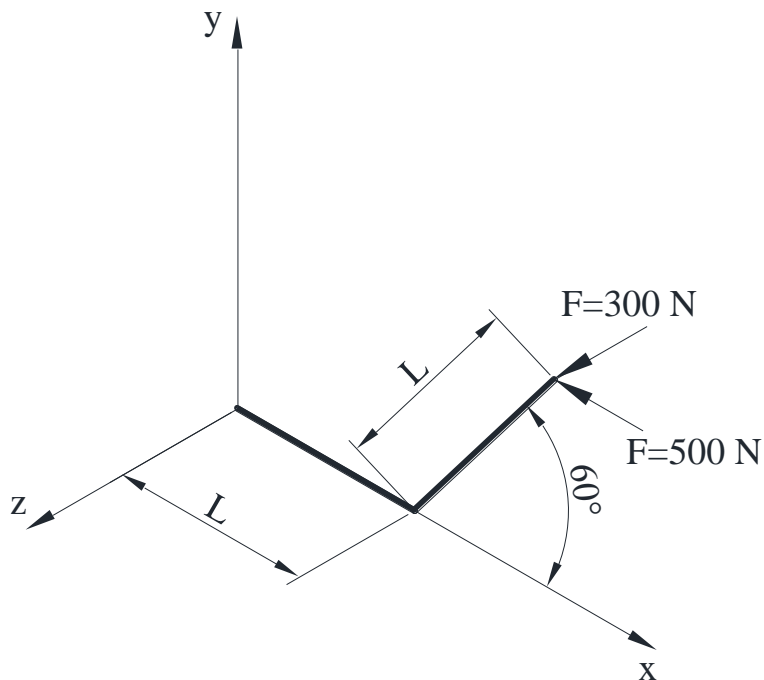


Figure 7.4 The placed holder in the global coordinate system

The element 2 stiffness matrix by the following notation:

$$\underline{\underline{k}}_2 = \begin{pmatrix} k_{11} & 0 & 0 & 0 & 0 & 0 & k_{17} & 0 & 0 & 0 & 0 & 0 \\ 0 & k_{22} & 0 & 0 & 0 & k_{26} & 0 & k_{28} & 0 & 0 & 0 & k_{212} \\ 0 & 0 & k_{33} & 0 & k_{35} & 0 & 0 & 0 & k_{39} & 0 & k_{311} & 0 \\ 0 & 0 & 0 & k_{44} & 0 & 0 & 0 & 0 & 0 & k_{410} & 0 & 0 \\ 0 & 0 & k_{53} & 0 & k_{55} & 0 & 0 & 0 & k_{59} & 0 & k_{511} & 0 \\ 0 & k_{62} & 0 & 0 & 0 & k_{66} & 0 & k_{68} & 0 & 0 & 0 & k_{612} \\ k_{71} & 0 & 0 & 0 & 0 & 0 & k_{77} & 0 & 0 & 0 & 0 & 0 \\ 0 & k_{82} & 0 & 0 & 0 & k_{86} & 0 & k_{88} & 0 & 0 & 0 & k_{812} \\ 0 & 0 & k_{93} & 0 & k_{95} & 0 & 0 & 0 & k_{99} & 0 & k_{911} & 0 \\ 0 & 0 & 0 & k_{104} & 0 & 0 & 0 & 0 & 0 & k_{1010} & 0 & 0 \\ 0 & 0 & k_{113} & 0 & k_{115} & 0 & 0 & 0 & k_{119} & 0 & k_{1111} & 0 \\ e & 0 & k_{122} & 0 & 0 & k_{126} & 0 & k_{128} & 0 & 0 & 0 & k_{1212} \end{pmatrix} \emptyset$$

the stiffness matrix of this element in global coordinate system:

|   |                              |   |   |                             |   |   |                               |   |   |                             |   |
|---|------------------------------|---|---|-----------------------------|---|---|-------------------------------|---|---|-----------------------------|---|
| $\frac{k_{11}}{4} + \frac{3k_{33}}{4}$                | 0                            | $\frac{\sqrt{3}k_{11} - \sqrt{3}k_{33}}{4}$ | 0   | $\frac{\sqrt{3}k_{35}}{2}$  | 0   | $\frac{k_{17}}{4} + \frac{3k_{39}}{4}$      | 0                             | $\frac{\sqrt{3}k_{17} - \sqrt{3}k_{39}}{4}$ | 0   | $\frac{\sqrt{3}k_{11}}{2}$  | 0   |
| 0   | k22                          | 0   | $\frac{\sqrt{3}k_{26}}{2}$                    | 0                           | $\frac{k_{26}}{2}$                            | 0   | k28                           | 0   | $\frac{\sqrt{3}k_{212}}{2}$                     | 0                           | $\frac{k_{212}}{2}$                             |
| $\frac{\sqrt{3}k_{11}}{4} - \frac{\sqrt{3}k_{33}}{4}$ | 0                            | $\frac{3k_{11} + k_{33}}{4}$                | 0   | $\frac{k_{35}}{2}$          | 0   | $\frac{\sqrt{3}k_{17} - \sqrt{3}k_{39}}{4}$ | 0                             | $\frac{3k_{17} + k_{39}}{4}$                | 0   | $\frac{k_{311}}{2}$         | 0   |
| 0   | $\frac{-\sqrt{3}k_{62}}{2}$  | 0   | $\frac{k_{44} + \frac{3k_{66}}{4}}{4}$        | 0                           | $\frac{\sqrt{3}k_{44} - \sqrt{3}k_{66}}{4}$   | 0   | $\frac{\sqrt{3}k_{68}}{2}$    | 0   | $\frac{k_{410} + \frac{3k_{612}}{4}}{4}$        | 0                           | $\frac{\sqrt{3}k_{410} - \sqrt{3}k_{612}}{4}$   |
| $\frac{-\sqrt{3}k_{53}}{2}$                           | 0                            | $\frac{k_{53}}{2}$                          | 0   | k55                         | 0   | $\frac{\sqrt{3}k_{59}}{2}$                  | 0                             | $\frac{k_{59}}{2}$                          | 0   | k511                        | 0   |
| 0   | $\frac{k_{62}}{2}$           | 0   | $\frac{\sqrt{3}k_{44} - \sqrt{3}k_{66}}{4}$   | 0                           | $\frac{3k_{44} + k_{66}}{4}$                  | 0   | $\frac{k_{68}}{2}$            | 0   | $\frac{\sqrt{3}k_{410} - \sqrt{3}k_{612}}{4}$   | 0                           | $\frac{3k_{410} + k_{612}}{4}$                  |
| $\frac{k_{71}}{4} + \frac{3k_{93}}{4}$                | 0                            | $\frac{\sqrt{3}k_{71} - \sqrt{3}k_{93}}{4}$ | 0   | $\frac{-\sqrt{3}k_{95}}{2}$ | 0   | $\frac{k_{77} + \frac{3k_{99}}{4}}{4}$      | 0                             | $\frac{\sqrt{3}k_{77} - \sqrt{3}k_{99}}{4}$ | 0   | $\frac{\sqrt{3}k_{911}}{2}$ | 0   |
| 0   | k82                          | 0   | $\frac{\sqrt{3}k_{86}}{2}$                    | 0                           | $\frac{k_{86}}{2}$                            | 0   | k88                           | 0   | $\frac{\sqrt{3}k_{812}}{2}$                     | 0                           | $\frac{k_{812}}{2}$                             |
| $\frac{\sqrt{3}k_{71} - \sqrt{3}k_{93}}{4}$           | 0                            | $\frac{3k_{71} + k_{93}}{4}$                | 0   | $\frac{k_{95}}{2}$          | 0   | $\frac{\sqrt{3}k_{77} - \sqrt{3}k_{99}}{4}$ | 0                             | $\frac{3k_{77} + k_{99}}{4}$                | 0   | $\frac{k_{911}}{2}$         | 0   |
| 0   | $\frac{-\sqrt{3}k_{122}}{2}$ | 0   | $\frac{k_{104} + \frac{3k_{126}}{4}}{4}$      | 0                           | $\frac{\sqrt{3}k_{104} - \sqrt{3}k_{126}}{4}$ | 0   | $\frac{\sqrt{3}k_{48128}}{2}$ | 0   | $\frac{k_{1010} + \frac{3k_{1212}}{4}}{4}$      | 0                           | $\frac{\sqrt{3}k_{1010} - \sqrt{3}k_{1212}}{4}$ |
| $\frac{-\sqrt{3}k_{113}}{2}$                          | 0                            | $\frac{k_{113}}{2}$                         | 0   | k115                        | 0   | $\frac{-\sqrt{3}k_{119}}{2}$                | 0                             | $\frac{k_{119}}{2}$                         | 0   | k1111                       | 0   |
| 0   | $\frac{k_{122}}{2}$          | 0   | $\frac{\sqrt{3}k_{104} - \sqrt{3}k_{126}}{4}$ | 0                           | $\frac{3k_{104} + k_{126}}{4}$                | 0   | $\frac{k_{8128}}{2}$          | 0   | $\frac{\sqrt{3}k_{1010} - \sqrt{3}k_{1212}}{4}$ | 0                           | $\frac{3k_{1010} + k_{1212}}{4}$                |

Combine the stiffness matrix of the two elements so that in the common nodes, the stiffness does add up. Thus, the system describing equations:

$$\begin{array}{l}
\left[ \begin{array}{ccccccccc} k_{11}^1 & k_{12}^1 & k_{13}^1 & k_{14}^1 & k_{15}^1 & k_{16}^1 & k_{17}^1 & k_{18}^1 & k_{19}^1 \\ k_{21}^1 & k_{22}^1 & k_{23}^1 & k_{24}^1 & k_{25}^1 & k_{26}^1 & k_{27}^1 & k_{28}^1 & k_{29}^1 \\ k_{31}^1 & k_{32}^1 & k_{33}^1 & k_{34}^1 & k_{35}^1 & k_{36}^1 & k_{37}^1 & k_{38}^1 & k_{39}^1 \\ k_{41}^1 & k_{42}^1 & k_{43}^1 & k_{44}^1 & k_{45}^1 & k_{46}^1 & k_{47}^1 & k_{48}^1 & k_{49}^1 \\ k_{51}^1 & k_{52}^1 & k_{53}^1 & k_{54}^1 & k_{55}^1 & k_{56}^1 & k_{57}^1 & k_{58}^1 & k_{59}^1 \\ k_{61}^1 & k_{62}^1 & k_{63}^1 & k_{64}^1 & k_{65}^1 & k_{66}^1 & k_{67}^1 & k_{68}^1 & k_{69}^1 \\ k_{71}^1 & k_{72}^1 & k_{73}^1 & k_{74}^1 & k_{75}^1 & k_{76}^1 & k_{77}^1 + k_{11}^1 & k_{78}^1 + k_{12}^1 & k_{79}^1 + k_{13}^1 \\ k_{81}^1 & k_{32}^1 & k_{93}^1 & k_{104}^1 & k_{85}^1 & k_{36}^1 & k_{87}^1 + k_{21}^1 & k_{88}^1 + k_{22}^1 & k_{89}^1 + k_{23}^1 \\ k_{91}^1 & k_{92}^1 & k_{93}^1 & k_{94}^1 & k_{95}^1 & k_{96}^1 & k_{97}^1 + k_{31}^1 & k_{98}^1 + k_{32}^1 & k_{99}^1 + k_{33}^1 \\ k_{101}^1 & k_{102}^1 & k_{103}^1 & k_{104}^1 & k_{105}^1 & k_{106}^1 & k_{107}^1 + k_{41}^1 & k_{108}^1 + k_{42}^1 & k_{109}^1 + k_{43}^1 \\ k_{111}^1 & k_{112}^1 & k_{113}^1 & k_{114}^1 & k_{115}^1 & k_{116}^1 & k_{117}^1 + k_{51}^1 & k_{118}^1 + k_{52}^1 & k_{119}^1 + k_{53}^1 \\ k_{121}^1 & k_{122}^1 & k_{123}^1 & k_{124}^1 & k_{125}^1 & k_{126}^1 & k_{127}^1 + k_{61}^1 & k_{128}^1 + k_{62}^1 & k_{129}^1 + k_{63}^1 \end{array} \right] \left[ \begin{array}{ccccccccc} k_{111}^1 & k_{112}^1 & 0 & 0 & 0 & 0 & 0 & 0 & 0 \\ k_{211}^1 & k_{212}^1 & 0 & 0 & 0 & 0 & 0 & 0 & 0 \\ k_{311}^1 & k_{312}^1 & 0 & 0 & 0 & 0 & 0 & 0 & 0 \\ k_{411}^1 & k_{412}^1 & 0 & 0 & 0 & 0 & 0 & 0 & 0 \\ k_{511}^1 & k_{512}^1 & 0 & 0 & 0 & 0 & 0 & 0 & 0 \\ k_{611}^1 & k_{612}^1 & 0 & 0 & 0 & 0 & 0 & 0 & 0 \\ k_{711}^1 & k_{712}^1 & u_2 & 0 & 0 & 0 & 0 & 0 & 0 \\ k_{811}^1 & k_{812}^1 & v_2 & 0 & 0 & 0 & 0 & 0 & 0 \\ k_{911}^1 & k_{912}^1 & w_2 & 0 & 0 & 0 & 0 & 0 & 0 \\ k_{1011}^1 & k_{1012}^1 & \varphi_2 & 0 & 0 & 0 & 0 & 0 & 0 \\ k_{1111}^1 & k_{1112}^1 & \gamma_2 & 0 & 0 & 0 & 0 & 0 & 0 \\ k_{1211}^1 & k_{1212}^1 & \eta_2 & 0 & 0 & 0 & 0 & 0 & 0 \end{array} \right] = \boxed{(7.28)} \\
\left[ \begin{array}{ccccccccc} 0 & 0 & 0 & 0 & 0 & 0 & k_{71}^2 & k_{72}^2 & k_{73}^2 \\ 0 & 0 & 0 & 0 & 0 & 0 & k_{81}^2 & k_{82}^2 & k_{83}^2 \\ 0 & 0 & 0 & 0 & 0 & 0 & k_{91}^2 & k_{92}^2 & k_{93}^2 \\ 0 & 0 & 0 & 0 & 0 & 0 & k_{101}^2 & k_{102}^2 & k_{103}^2 \\ 0 & 0 & 0 & 0 & 0 & 0 & k_{111}^2 & k_{112}^2 & k_{113}^2 \\ 0 & 0 & 0 & 0 & 0 & 0 & k_{121}^2 & k_{122}^2 & k_{123}^2 \end{array} \right] \left[ \begin{array}{ccccccccc} k_{75}^2 & k_{76}^2 & k_{77}^2 & k_{78}^2 & k_{79}^2 & k_{710}^2 & k_{711}^2 & k_{712}^2 & -500 \\ k_{85}^2 & k_{86}^2 & k_{87}^2 & k_{88}^2 & k_{89}^2 & k_{810}^2 & k_{811}^2 & k_{812}^2 & 0 \\ k_{95}^2 & k_{96}^2 & k_{97}^2 & k_{98}^2 & k_{99}^2 & k_{910}^2 & k_{911}^2 & k_{912}^2 & -300 \\ k_{104}^2 & k_{105}^2 & k_{106}^2 & k_{107}^2 & k_{108}^2 & k_{109}^2 & k_{110}^2 & k_{111}^2 & \Phi_3 \\ k_{119}^2 & k_{120}^2 & k_{121}^2 & k_{122}^2 & k_{123}^2 & k_{124}^2 & k_{125}^2 & k_{126}^2 & 0 \\ k_{127}^2 & k_{128}^2 & k_{129}^2 & k_{1210}^2 & k_{1211}^2 & k_{1212}^2 & k_{1213}^2 & k_{1214}^2 & \eta_3 \end{array} \right] = 0 \end{array}$$

During the solution the displacement 0 locations (at the supports) are skip. So we can delete rows and columns of the stiffness matrix in these places. In our case, this is the first six rows and columns. Thus we get the condensed stiffness matrix and the equation system to solve.

Substituting the data and solving the equations system obtained the displacements:

$$U = \begin{bmatrix} u_2 \\ v_2 \\ w_2 \\ \varphi_2 \\ \gamma_2 \\ \eta_2 \\ u_3 \\ v_3 \\ w_3 \\ \varphi_3 \\ \gamma_3 \\ \eta_3 \end{bmatrix} = \begin{bmatrix} -0.0000040933278755628325829 \\ 0.0069897483690587138863 \\ 0.008647570933808134537 \\ -0.0045399747402492706319 \\ -0.0057650472892054230247 \\ 0.003994141925176407935 \\ -0.019975826285726493216 \\ 0.028770303554786313407 \\ 0.020175893049255852386 \\ -0.0062694889270108975393 \\ -0.008647570933808134537 \\ 0.0049926774064705099188 \end{bmatrix} m \quad (7.29)$$

The reaction forces can be calculated by the known results. From the equations of entire system, which are in this case the first six lines:

$$F_{Rv} = k_{28}^1 \cdot v_2 + k_{212}^1 \cdot \eta_2 = 1.5301999986150468986847 \text{e-17 N} \quad (7.31)$$

$$M_{R_y} = k_{A110}^1 \cdot \varphi_2 = 779.42286340599478208459 \text{ Nm} \quad (7.33)$$

$$M_{R_y} = k_{59}^1 \cdot w_2 + k_{511}^1 \cdot \gamma_2 = 1299.0381056766579701327 \text{ Nm} \quad (7.34)$$

$$M_{p_2} = k_{68}^1 \cdot v_2 + k_{612}^1 \cdot \eta_2 = -1350.00000000000000013 \text{ Nm} \quad (7.35)$$

### 7.3. Remarks

We did not deal with not circle or ring cross sections. The properties of these cross-sections can be determined only by approximation methods (i.e. the Bredt's formula for thin closed section, Weber's formula for thin-wall open cross-section).

Also did not deal with asymmetric sections, i.e. cold bended or rolled U sections. The shear center and center of gravity of those sections does not coincide, so the bending combines with torsion usually.

The shear deformation was neglected, because we used Euler-Bernoulli beam theory.

## **8. ANALYSIS OF THREE-DIMENSIONAL BENT BARS USING FINITE ELEMENT METHOD BASED PROGRAM SYSTEM**

### **8.1. Three-dimensional beam structures**

In case of two-dimensional bent bar structures discussed in chapter 6, the deflections may be generated in plane of structure. In engineering practice, using three-dimensional models are required many of the cases.

Such cases usually are:

- Two dimensional construction, with asymmetrical cross section beams,
- Two dimensional construction, with loads perpendicular to plane of structure,
- The general three-dimensional beam structures.

This chapter deals with these structures. The chapter 9-10. deals with buckling of the compressed bars.

Because the buckling of the compression chords and the shear buckling of the web sheets require different calculations, so we do not deal with this.

Questions to be answered

- The magnitude and direction of the reaction forces and moments generated in supports,
- Magnitude and direction of the axial and shear forces, bending and torque moments in each bar,
- The  $\sigma$  and  $\tau$  stresses which characterized of the stressed state,
- Displacements of each point of the structure, and deformation of each beam.

These structures may be testing for the stability of the structure and dynamic behavior (the critical forces of compressed bars and natural frequencies). We deal with these problems later.

The previous chapter has mentioned the externally and internally determination and indeterminacy structures. We will see that it is irrelevant in this case too.

### **8.2. The used finite elements in modeling**

The chapter 4 clarified that program system based on the finite element method use two types of element for modeling beam structures. The TRUSS element for modeling structure loaded axial forces only and BEAM element for modeling loaded axial and shear forces, bending and torque moments. Both TRUSS and BEAM elements can be two- or three-dimensional.

In all cases, the finite elements are characterized by a single straight line.

The properties of the TRUSS and BEAM2D elements already described in the previously chapters.

#### **8.2.1. The properties of the BEAM3D elements**

The properties of the BEAM2D elements have already written in chapter 6.

The BEAM3D characterized by three dimensional stressed state, and it is general three-dimensional bar structures or displaced perpendicular to the own plane under the loads.

The BEAM3D elements are two or three-node, uniaxial element, have six degrees of freedom (three translations and three rotations) per each end node. The third node points towards

y-axis in the element local coordinate system. It or an orientation angle (as real constant) is required only for determine the element orientation.

The element coordinate system shown in figure 8.1. The coordinate system x-axis pointing from the first to the second node, the y-axis perpendicular to x axis and central principal axes of cross section, z axis perpendicular to x-y plane and create a right-handed Cartesian coordinate system.

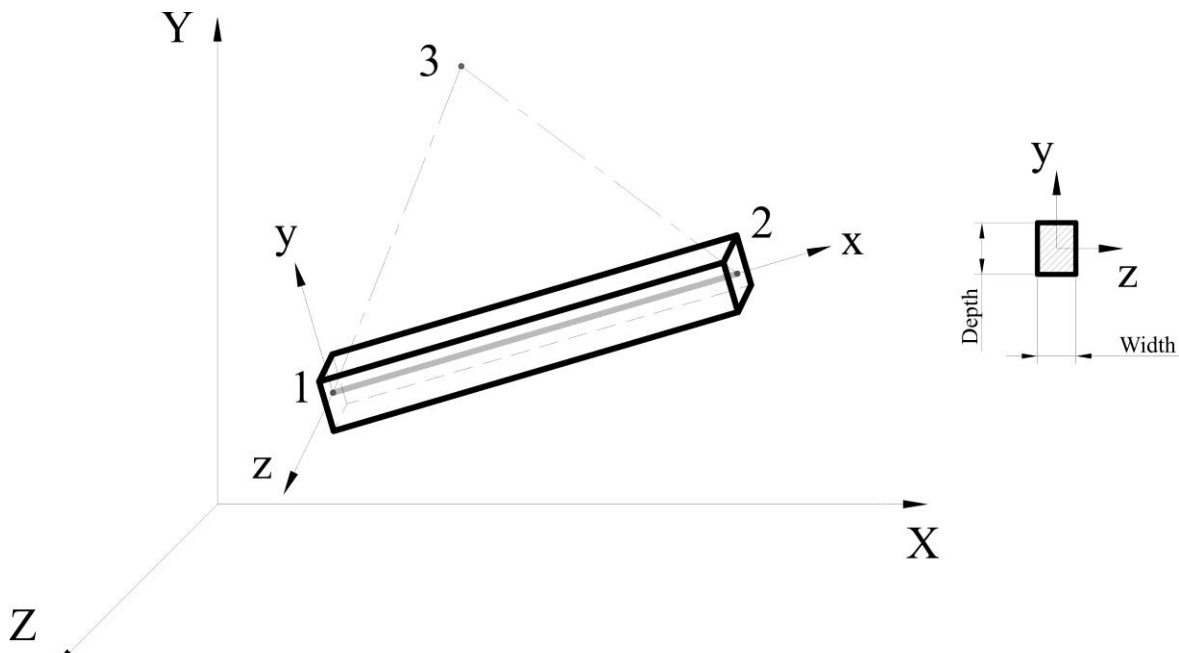


Figure 8.1 BEAMD3D element local coordinate system

The linear static analysis requires some real constant (marking as shown Figure 8.2):

- The cross-sectional area,
- Moment of inertia about the element Y axis,
- Moment of inertia about the element Z axis,
- Depth of the beam,
- Width of the beam,
- Relationship between the ends of the connected elements (end release code, two sets of data),
- Torsional constant J (see also 8.2.2),
- Shear factor in the element y axis (see also 8.2.2),
- Shear factor in the element z axis (see also 8.2.2),
- Orientation angle of the cross section (only if the orientation does not define by the third node),
- Constant for maximum shear stress calculation (see also 8.2.2),
- x, y, z distance of the section centroid relative to the nodal point in each node of the beam (total six data),
- y, z distance of the shear center relative to the section centroid at each node of the beam (total four data),
- y, z distance of the point where stresses are to be calculated at each node of the beam (total four data),
- Centroidal product of inertia of the element cross section

Usually there can be defined tapered beam properties and more real constant for thermal analysis also. These properties are not dealt in this chapter.

In usually, we can specify often used cross-sections in engineering practice, such as rectangular, a square hole, circle, ring, I, L, T sections, by geometrical dimensions. In this case the other sectional properties will be calculated by the program.

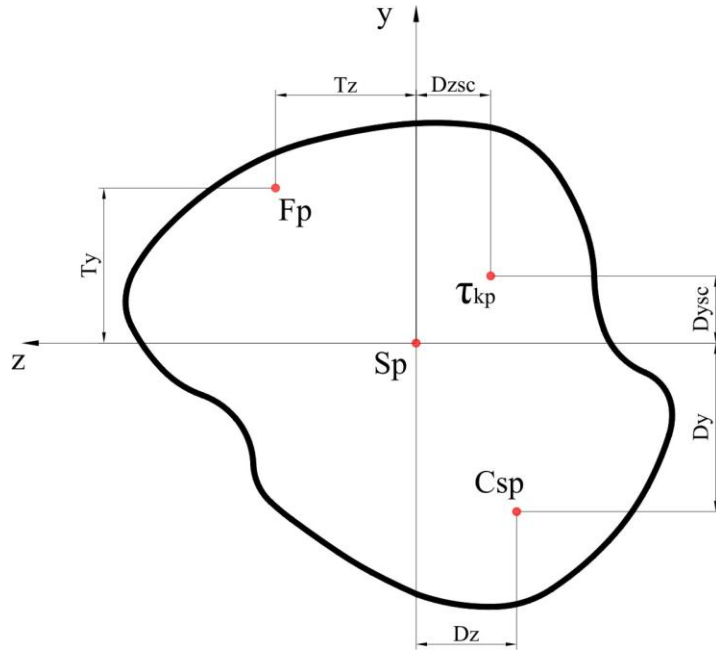


Figure 8.2 BEAM3D elements properties

We also need the material properties of the elements. In this case, is sufficient to specify the value of the modulus of elasticity, Poisson's coefficient and density of the beam elements.

If necessary, we can define more material properties for the buckling or heat transfer analysis.

The interpretation of the bending moments and shear forces shown in Figure 8.3.

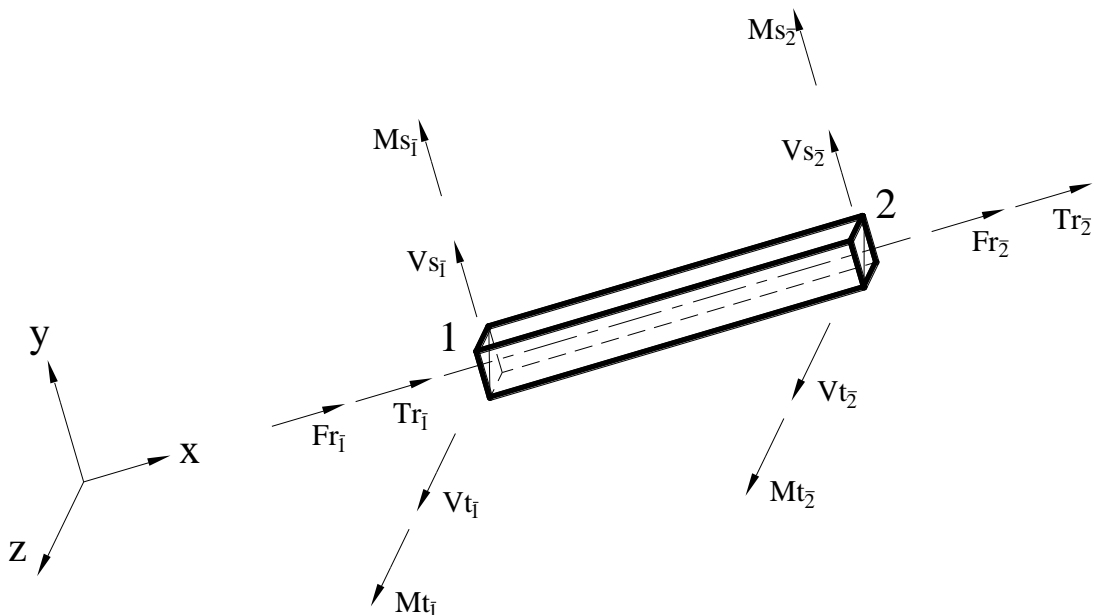


Figure 8.3 Forces and moments in BEAM3D elements

### 8.2.2. The special properties of BEAM3D elements

The shear deformation is usually neglected. The chapter 6.2.2 has shown that how this can be taken into account. Also in this chapter we have properties of several common used sections.

We have dealt with the simplified definition of the shear factor (see Figure 8.4). This concept will also be used in this chapter.

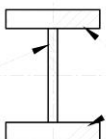
| The cross section  | $f_s$              | The Shear factor   |
|--|--------------------|--------------------|
| Web<br><br>Chords | $A/A_{\text{Web}}$ | $A_{\text{Web}}/A$ |

Figure 8.4 The simplified definition of Shear factor

The calculations will be needed to determine a shape factor ( $C_{\text{tor}}$ ) for calculate the maximum stress  $\tau$  comes from torsion.

In case of circular and thin-walled ring section, the maximum stress  $\tau$  generated on perimeter of the circle, so:

$$\tau_{\max} = \frac{T}{I_p} r$$

In case of non-circular cross section, the maximum stress  $\tau$  depends on the section shape. In such cases we can use only approximate procedures, such as Constantin Weber approximate method:

$$\tau_{\max} = \frac{T}{I_w} C_{\text{tor}} = \frac{T}{K_w}$$

where:  $I_w$ : Weber's centroidal product of inertia,

$K_w$ : Weber's polar section modulus,

$C_{\text{tor}}$ : the shape factor.

Circular cross section, of course,  $I_w=I_p$ ,  $K_w=K_p$  and  $C_{\text{tor}}=r$ .

An open cross-section (see figure 8.5), where  $h \gg v$ , we can apply the splitting, and so:

$$I_w = \eta \frac{\sum_i (v_i^3 h_i)}{3},$$

$$K_w = \frac{I_w}{v_{\max}}$$

$$C_{\text{tor}} = v_{\max}$$

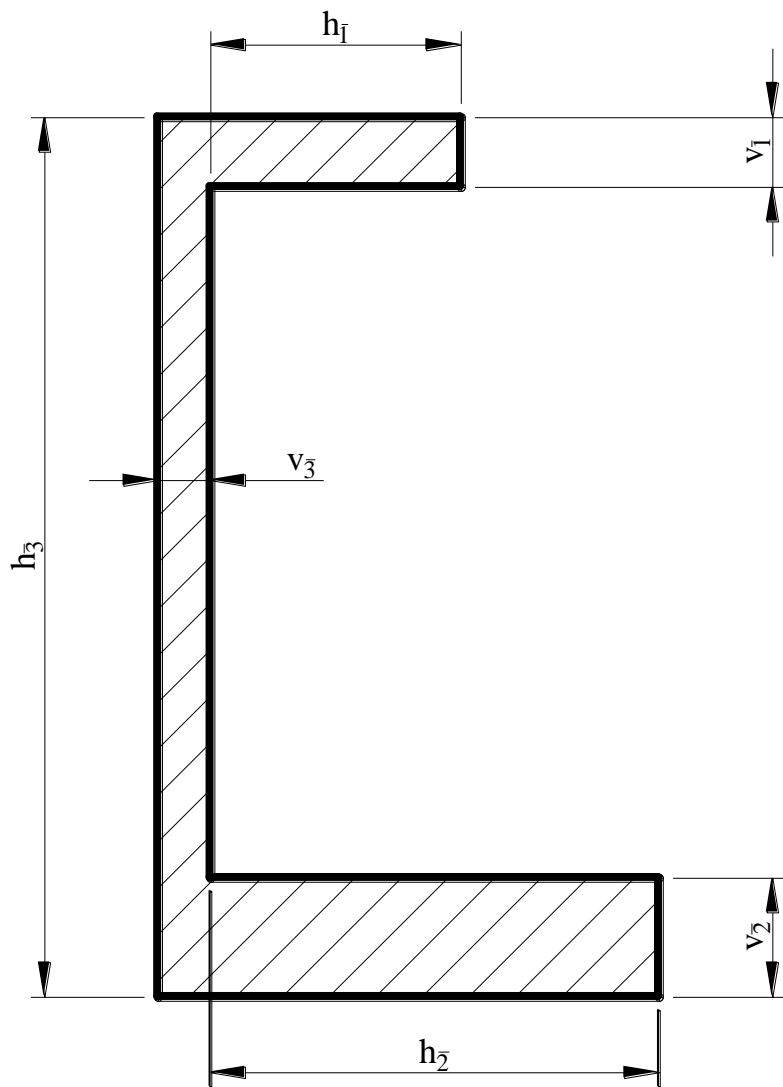


Figure 8.5 Splitting of open cross-sections

The  $\eta$  is a factor to correction error of splitting.

|               |      |      |      |      |      |      |
|---------------|------|------|------|------|------|------|
| Section shape | L    | T    | L    | +    | C    | I    |
| $\eta$        | 0,99 | 1,15 | 1,15 | 1,17 | 1,20 | 1,31 |

Figure 8.6 The  $\eta$  factor of some cross-section

### 8.3. The study solution

The study is a frame (see Figure 8.7), assembled by U120 standard steel. The actual live load is 5000 N, distributed forces. The horizontal load is the 6% of the live load, what is generated from movement on live load. The supports are from each end 100 to 100 mm.

Have to determine the reaction forces, stresses generated in beams, the deflections and bending moment diagrams.

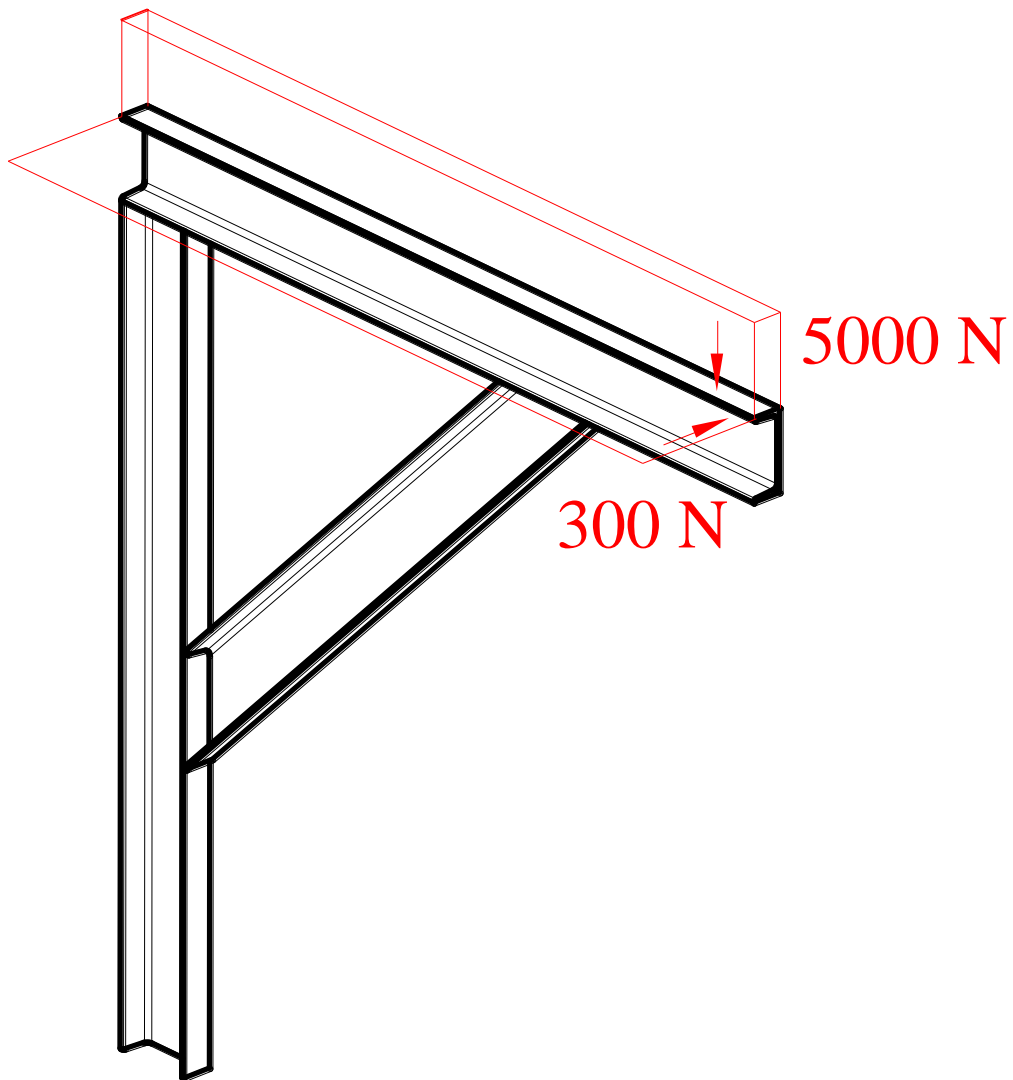


Figure 8.7 The tested frame

The followed procedure:

- Study analysis,
- Create a geometry model,
- Define the properties of finite elements (element type, real constant, material properties),
- Define boundary conditions, and loads,
- Run the analysis,
- Evaluation of the results.

The cross-sectional properties of the used rolled bars U120 and geometric dimensions shown in Figure 8.8. These technical data are available in standards and design aids tables.

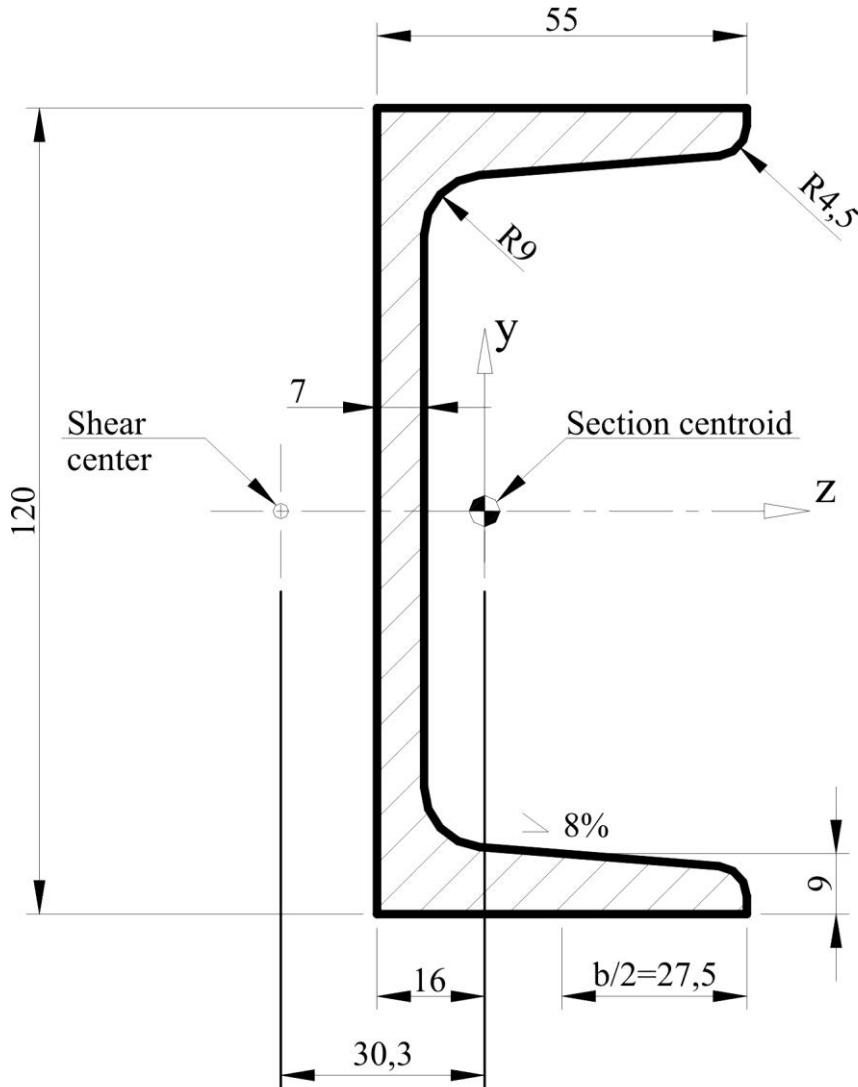


Figure 8.8 The used U120 section

We need some data what are not included in tables.

First we have to define the shear factor in element y and z axis. We use the simplified calculation shown in Figure 8.4. Using the Zuravsky's theorem, the shear stress in a point of the cross section is:

$$\tau = \frac{F_T S_x'}{s I_x}$$

where: F<sub>T</sub> :shear force,

S<sub>x</sub>: statical moment of an area outside a point about section x axis

I<sub>x</sub>: Moment of inertia about the element x

s: width of the section at the point.

Of course, the stress distribution depends on the relative position of the section and shear force, so that it should be determined about the element z and y axis separately. The used U120 cross section properties known and shown in the Figure 8.9.

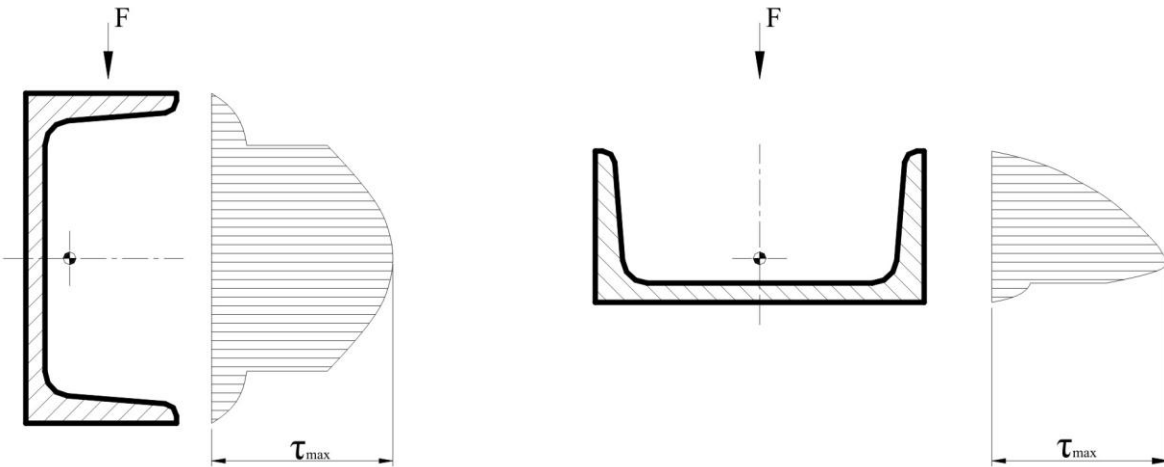


Figure 8.9 Shear stress distribution in the cross section

The exposed area of the shear can be determined by graphic editing, so the shear shape factor can be calculated:

$$S_{fz} = \frac{A_{nyírt-z}}{A} = \frac{6,69}{17} = 0,39$$

$$S_{fy} = \frac{A_{nyírt-y}}{A} = \frac{8,59}{17} = 0,51$$

In addition, we need the cross-sectional modulus of torsion, which can be determined by Weber's method (see Figure 8.5):

$$I_w = \eta \frac{\sum_i (v_i^3 h_i)}{3} = 1,2 \frac{0,7^3 \cdot 12 + 2 \cdot 0,9^3 \cdot 4,8}{3} = 3,09 \text{ cm}^4$$

For the determination the largest shear stress  $\tau$  caused by torsion:

$$C_{tor} = v_{max} = 0,9 \text{ cm}$$

After determining the necessary data we can begin the computer-aided analysis.

The geometrical model is very simple, so we can create it in the own graphics editor of finite element program. The structural model is created in the XY plane, but the loads and the deformations will be three-dimensional. In the figure 8.10, the drew lines represent the neutral axis of beams.

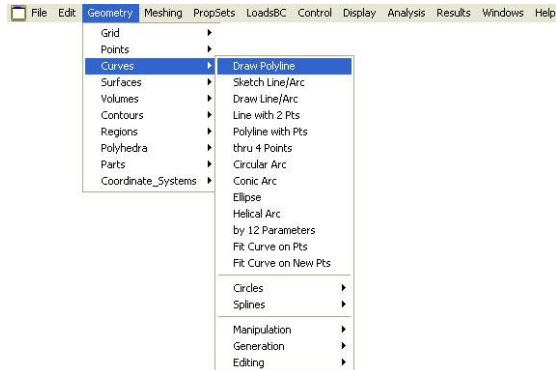


Figure 8.10. Draw line in the finite element program

The orientation of BEAM3D element can be defined by the third node. We also need a geometric point (key point). Since the lines represent the neutral axis of beams, so the third node must lie in XY plane too. It is sufficient to take only one point because the neutral axis of all bars lies in a common plane. The definition a geometric point is shown in the Figure 8.11.



Figure 8.11 Place a geometric point (key point)

The completed geometric model shown in Figure 8.12.

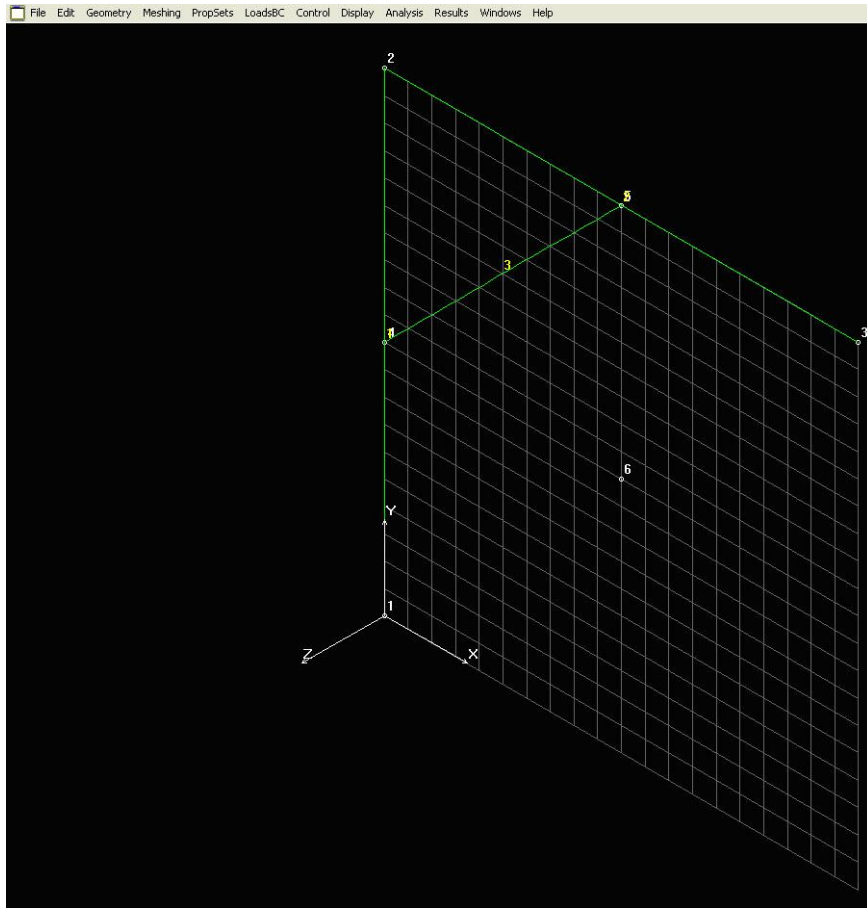


Figure 8.12 The geometric model

In the next step we determine the element group. We have clarified that we are use linear behavior, BAEM3D elements (see Figure 8.13).

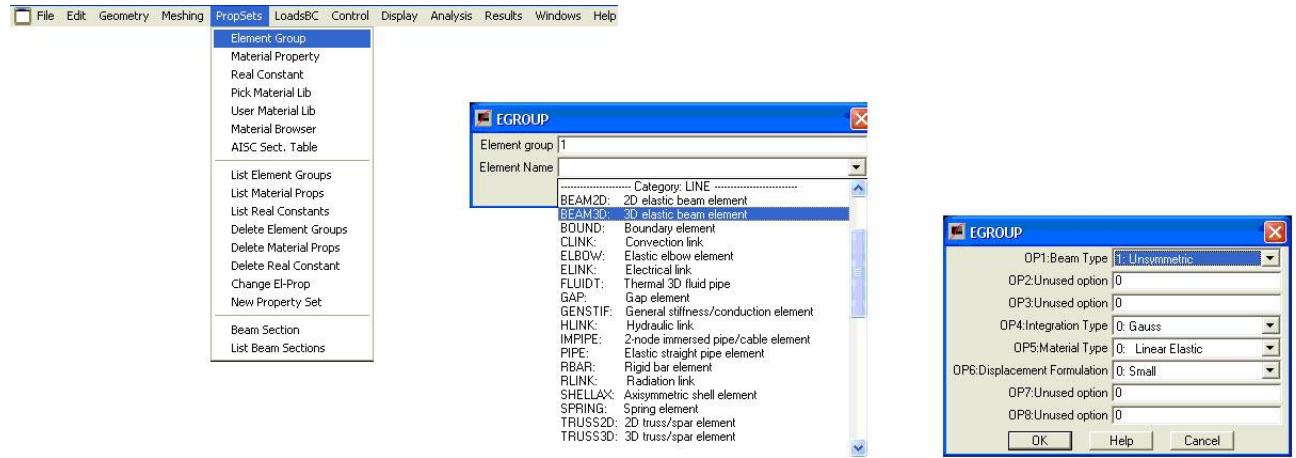


Figure 8.13 Determination of element group

During the determination the real constant (see figure 8.14) we use the SI unit system, i.e., the linear dimension must be defined in m, and the weight must be in kg.

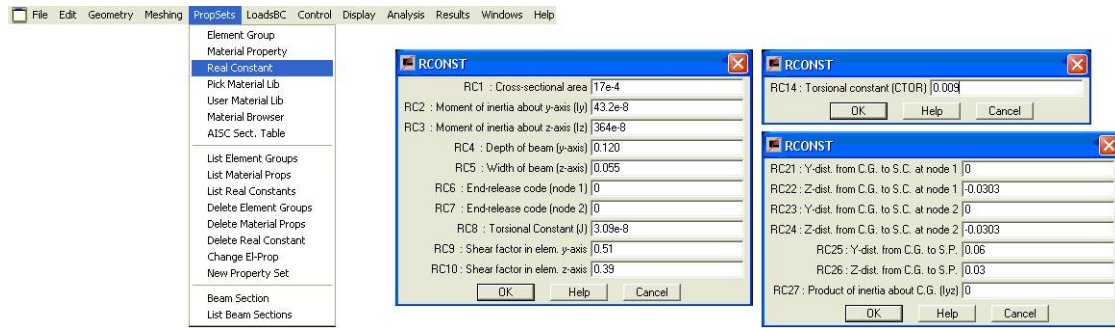


Figure 8.14 The real constant definition

It's also necessary to specify the material properties (see Figure 8.15). In this case it is sufficient to enter the values of the modulus of elasticity and Poisson's coefficient. If necessary, we can define more material properties e.g. the density to calculate tare weight of the structure.

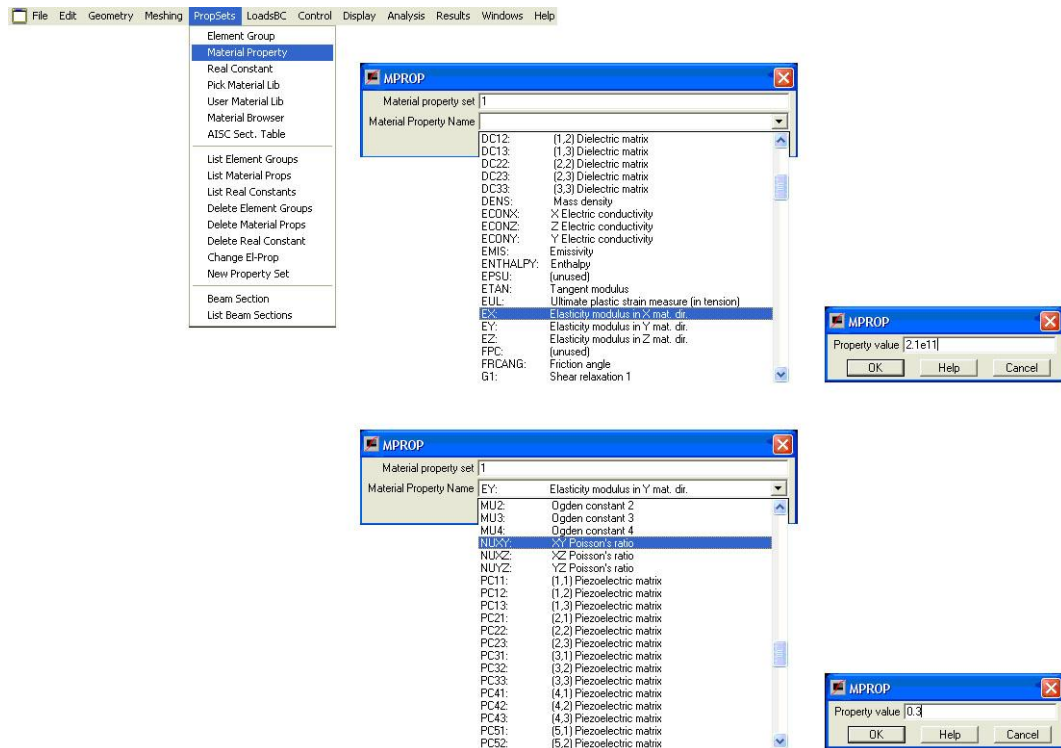


Figure 8.15 Specify the material properties

During the finite element mesh generation, same size but different number of elements can be created on each bar (see Figure 8.16).

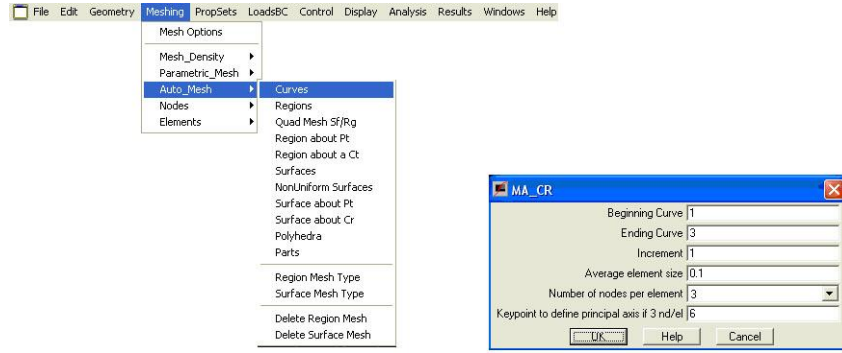


Figure 8.16 The finite element mesh generation

Because, the finite element mesh created each geometry object separately, the ends of the beams are not in connection (see Figure 8.17)

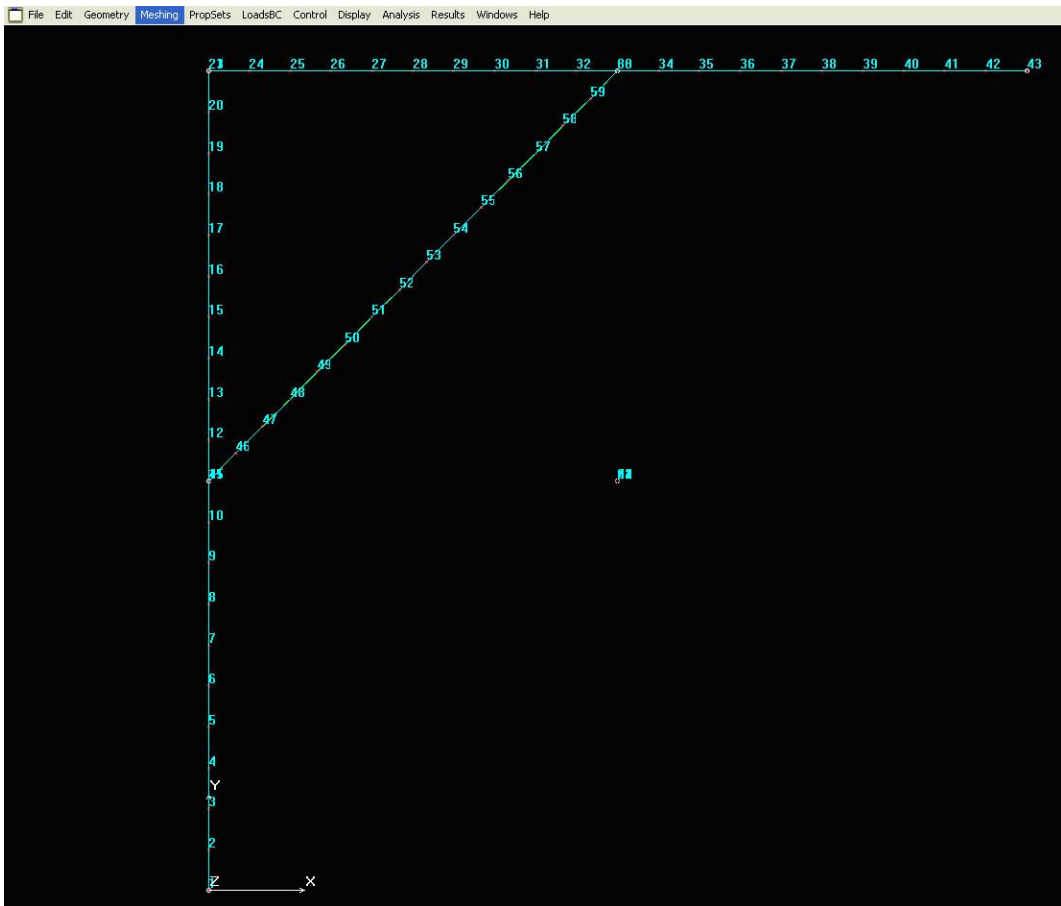
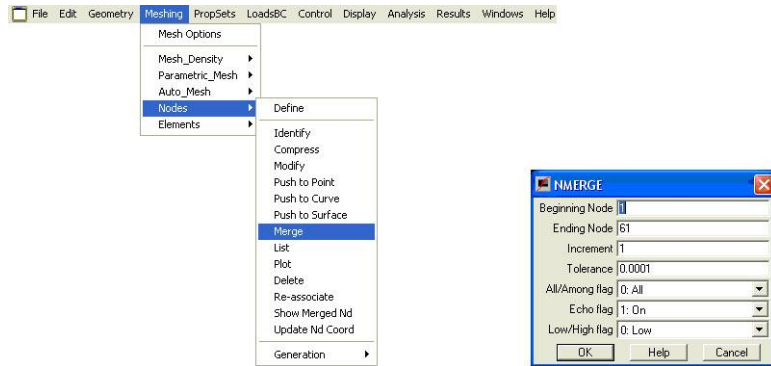


Figure 8.17 The finite element mesh

To create connection between bars, necessary to merge the nodes in each end of the bars. (see Figure 8.18).



8.18. Fig. Merge nodes on the end of the bar

The completed finite element mesh shown in Figure 8.19.

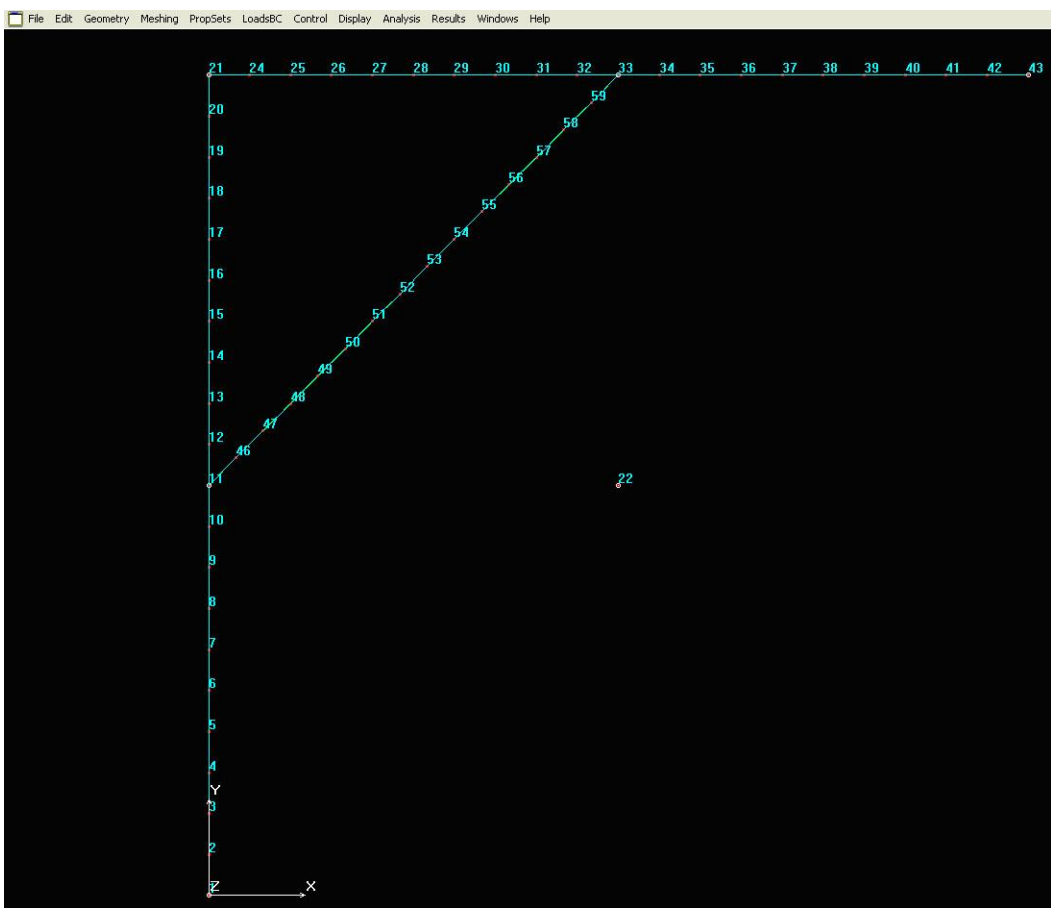


Figure 8.19 The final finite element mesh

The displacement constraints are placed on the finite element mesh. The constraints assumed rigid but the bar can deformed freely between the two supports. An example of place displacement constrains shown in Figure 8.20.

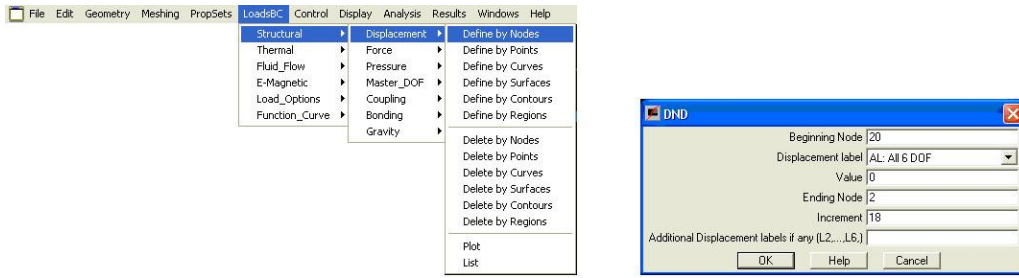


Figure 8.20 Specify the displacement constraints

Next step, define the distributed load on the horizontal bar which shown in the Figure 8.7. In our case, the specified force effect in all nodes of the element. The definition loads shown in Figure 8.21.

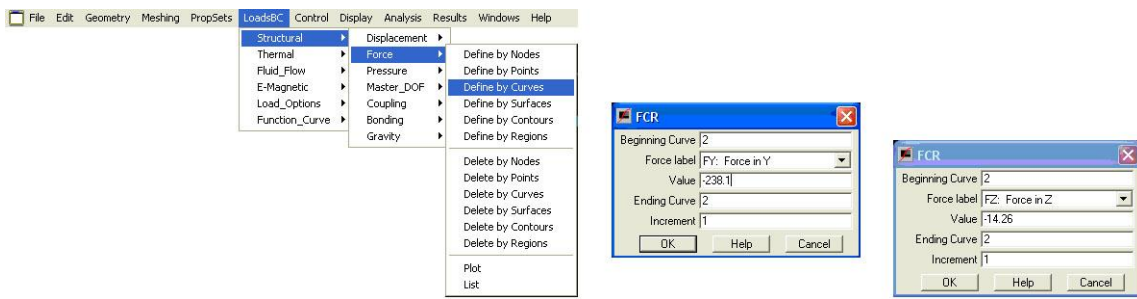


Figure 8.21 Definition the distributed loads

It is advisable to check what forces have been created. We can use listing commands for this (see Figure 8.22).

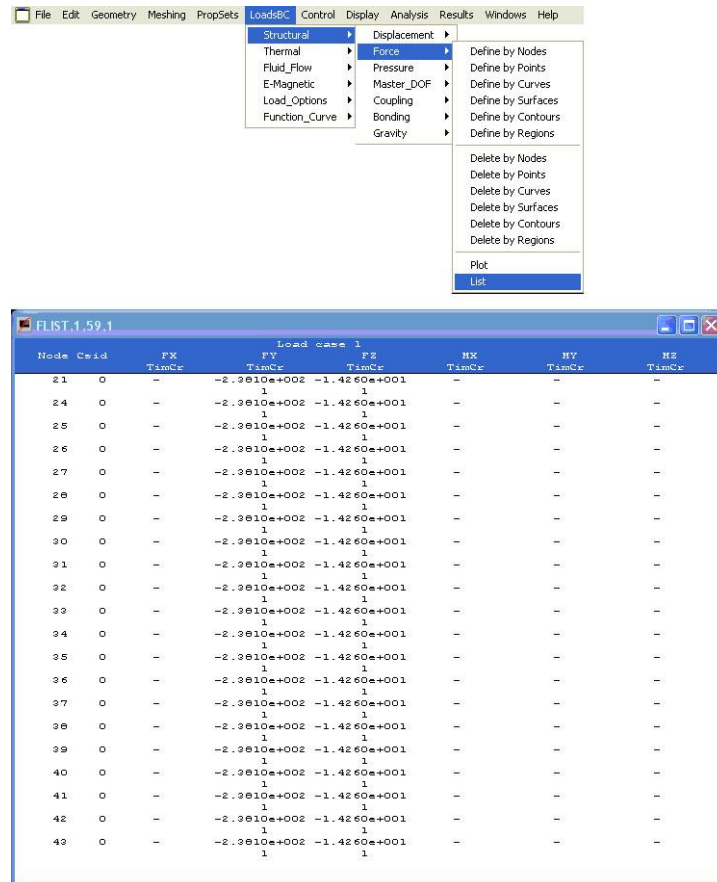


Figure 8.22 List forces

The completed finite element model is presented in figure 8.23.

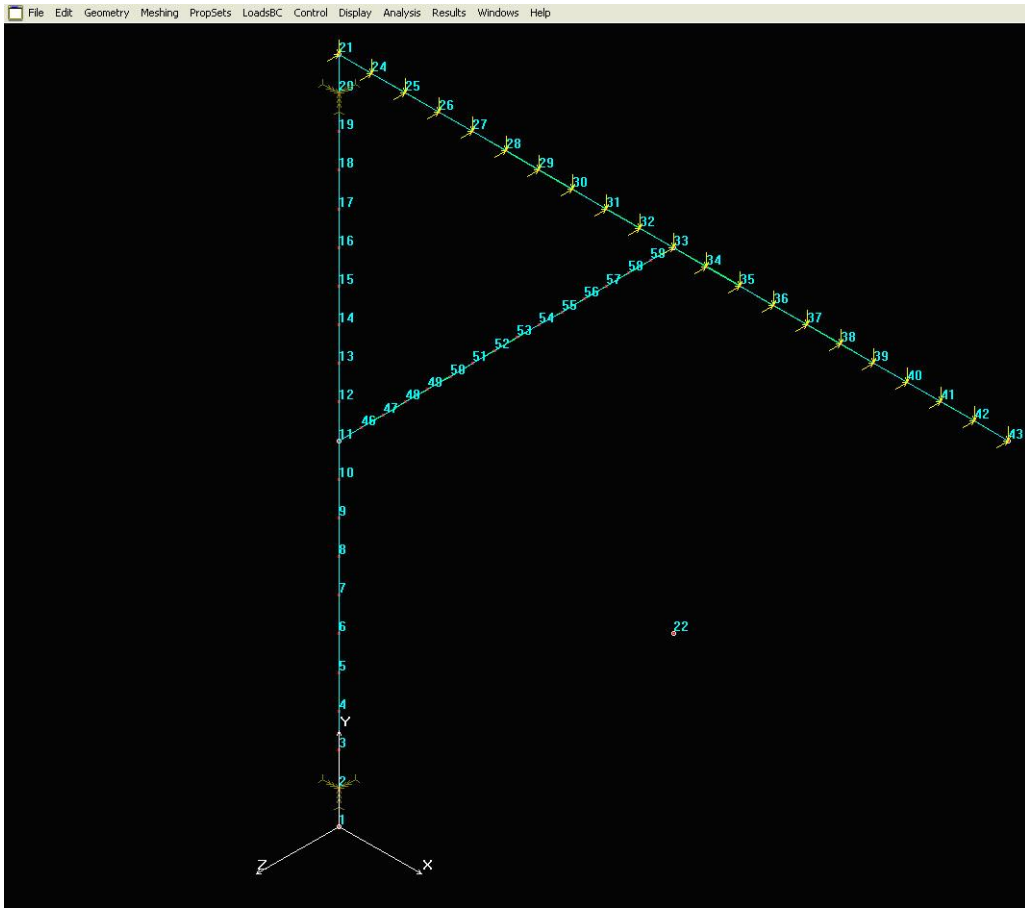


Figure 8.23 The completed finite element model

The running linear static analysis follows (see Figure 8.24).

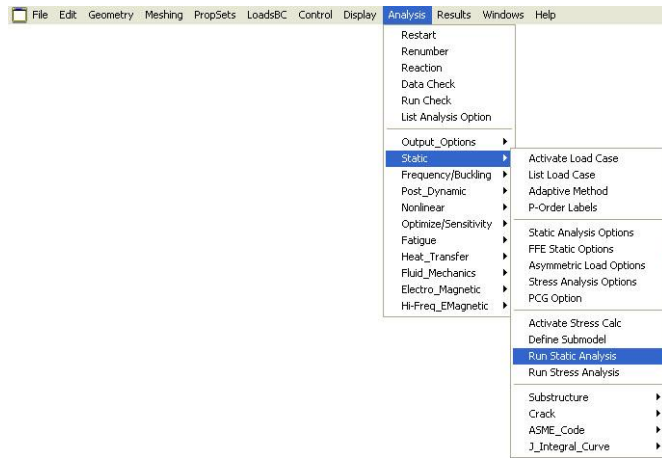


Figure 8.24. Run linear static analysis

The generated stress results can be displayed on deformed shape (see Figure 8.25).

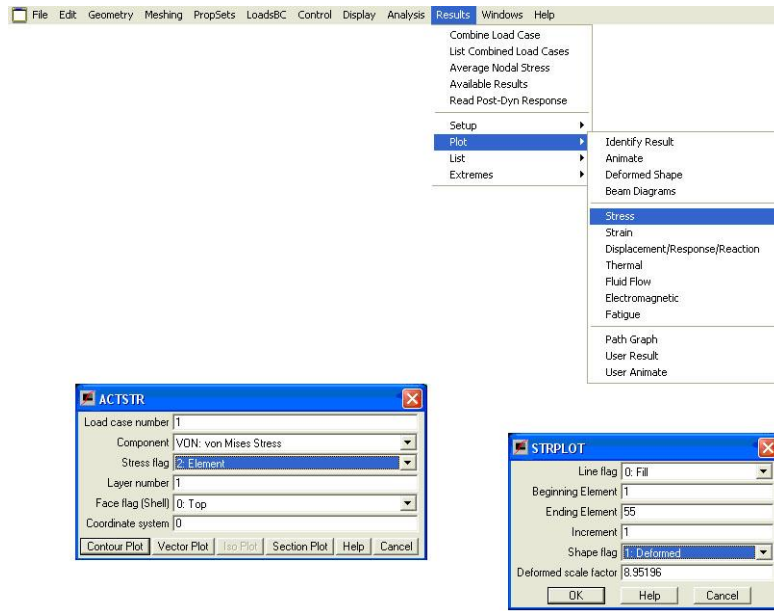


Figure 8.25 Display stress results

The results are shown in Figure 8.26.

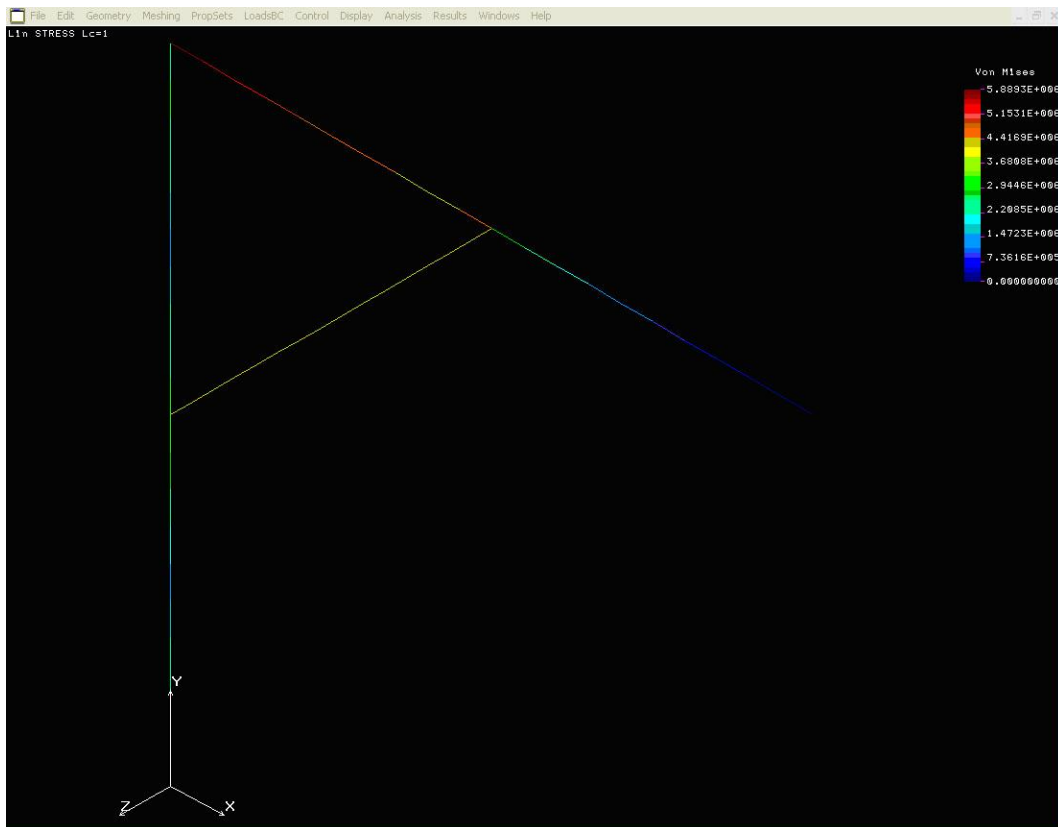


Figure 8.26 The equivalent stresses

We can use listing commands to display numerical results (see Figure 8.27).

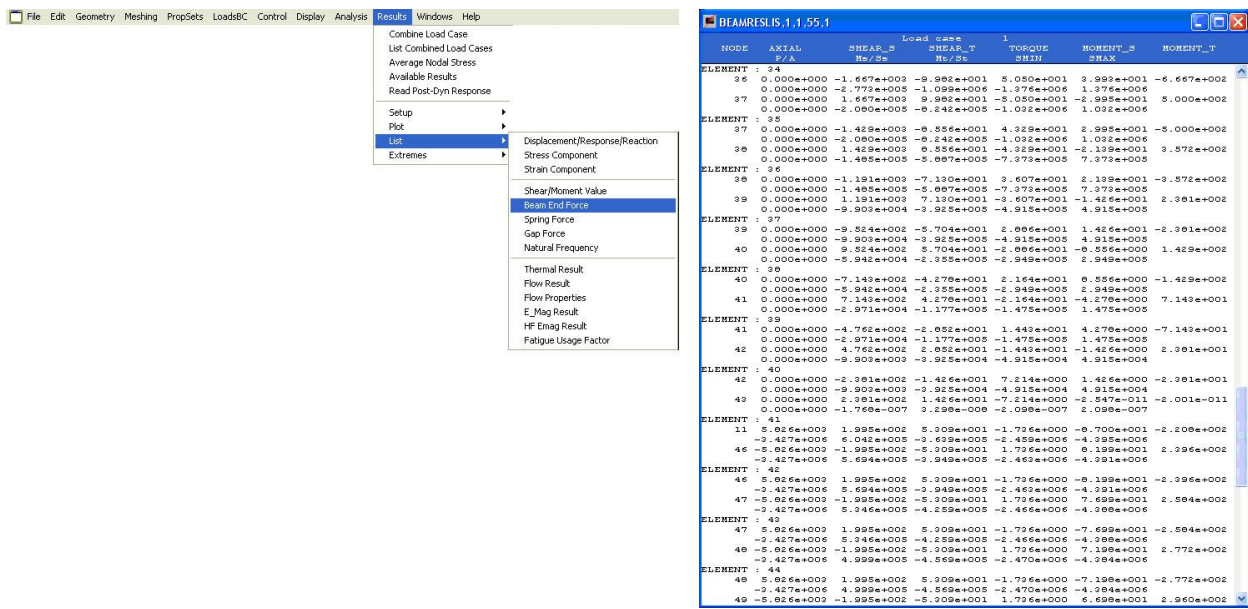


Figure 8.27 Display stress components

Examine the bending moment generated in the structure (see Figure 8.28).

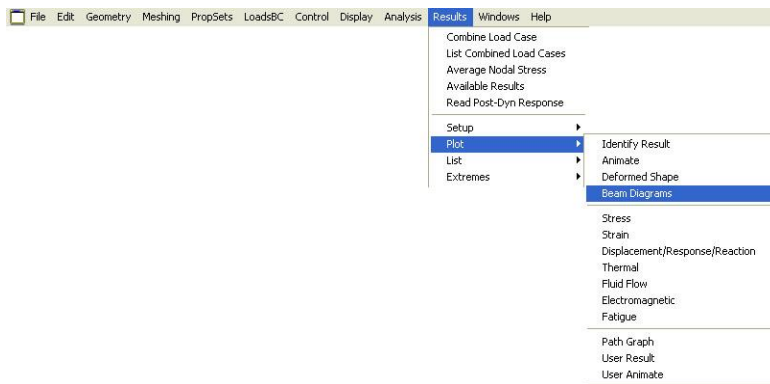


Figure 8.28 Display the moment diagrams for beams

Since the bars are curved in two directions, so we examine bending moments caused by vertical and horizontal loads separately (see Figure 8.29).

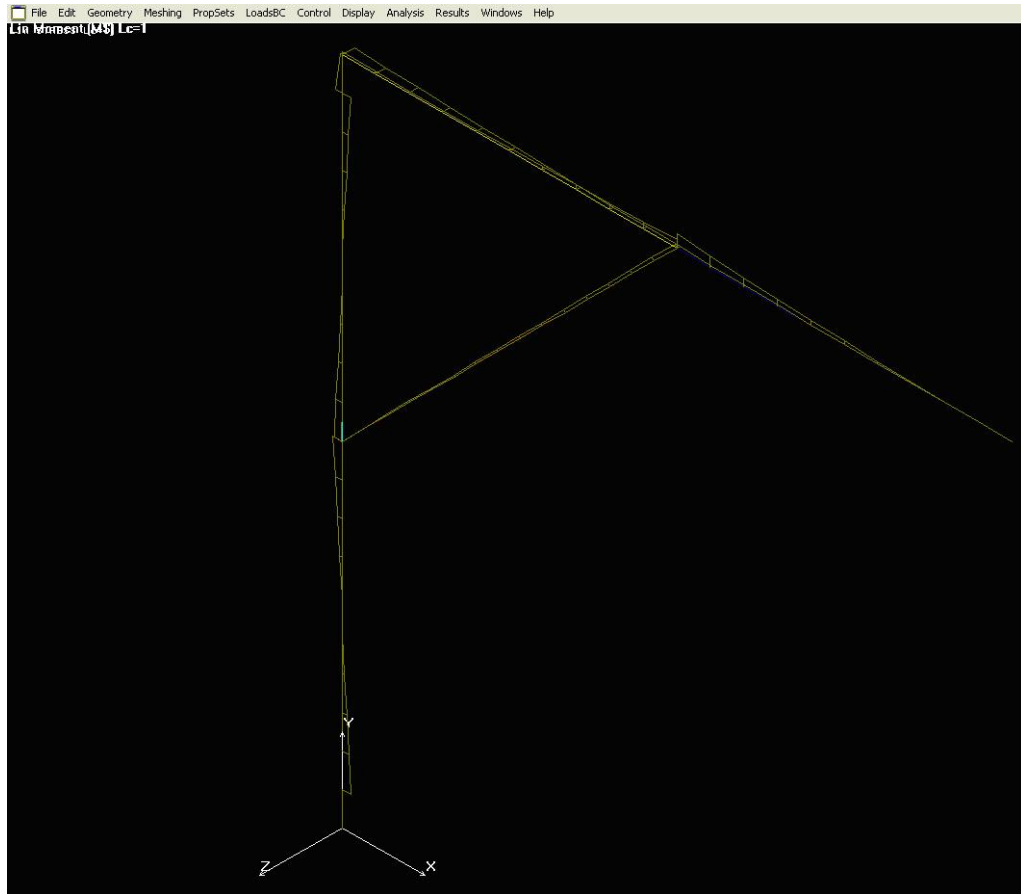


Figure 8.29  $M_s$  and  $M_t$  bending moment diagrams

Examine the deflections, i.e. the displacements in Y direction (see Figure 8.30)

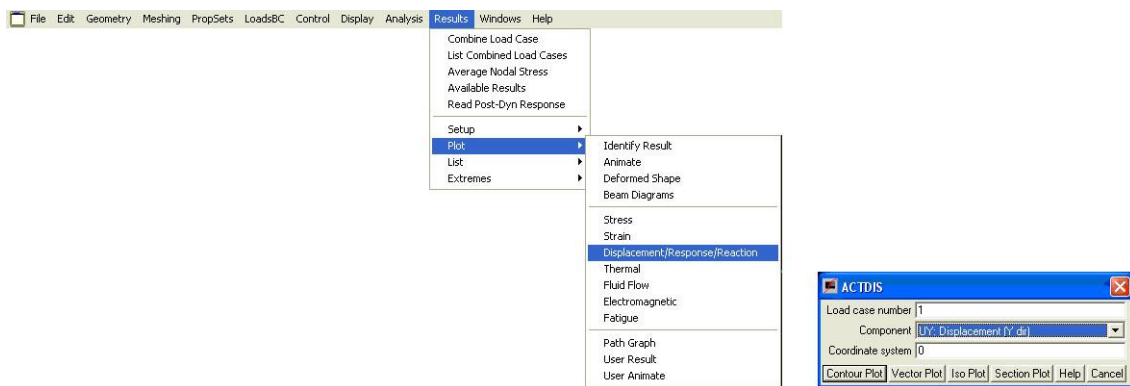


Figure 8.30 Display the deflections

The results shown in Figure 8.31.

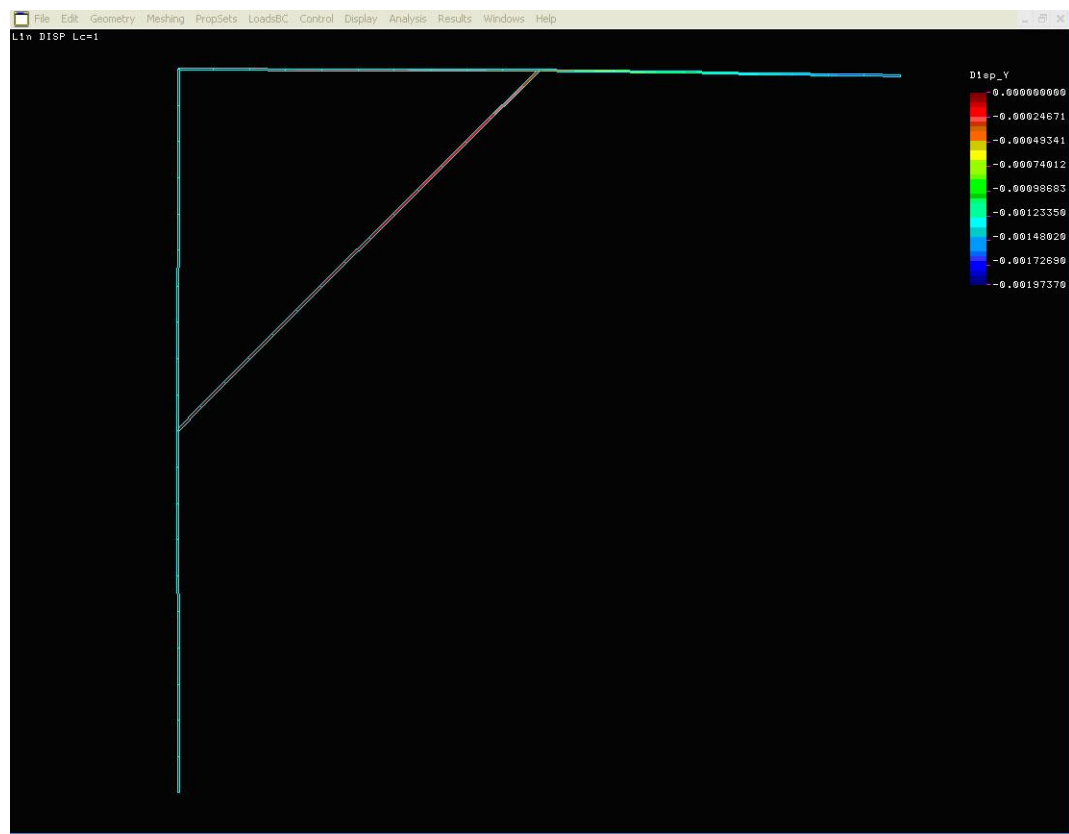


Figure 8.31 The deflections

Display the numerical displacements result also possible (see Figure 8:32).

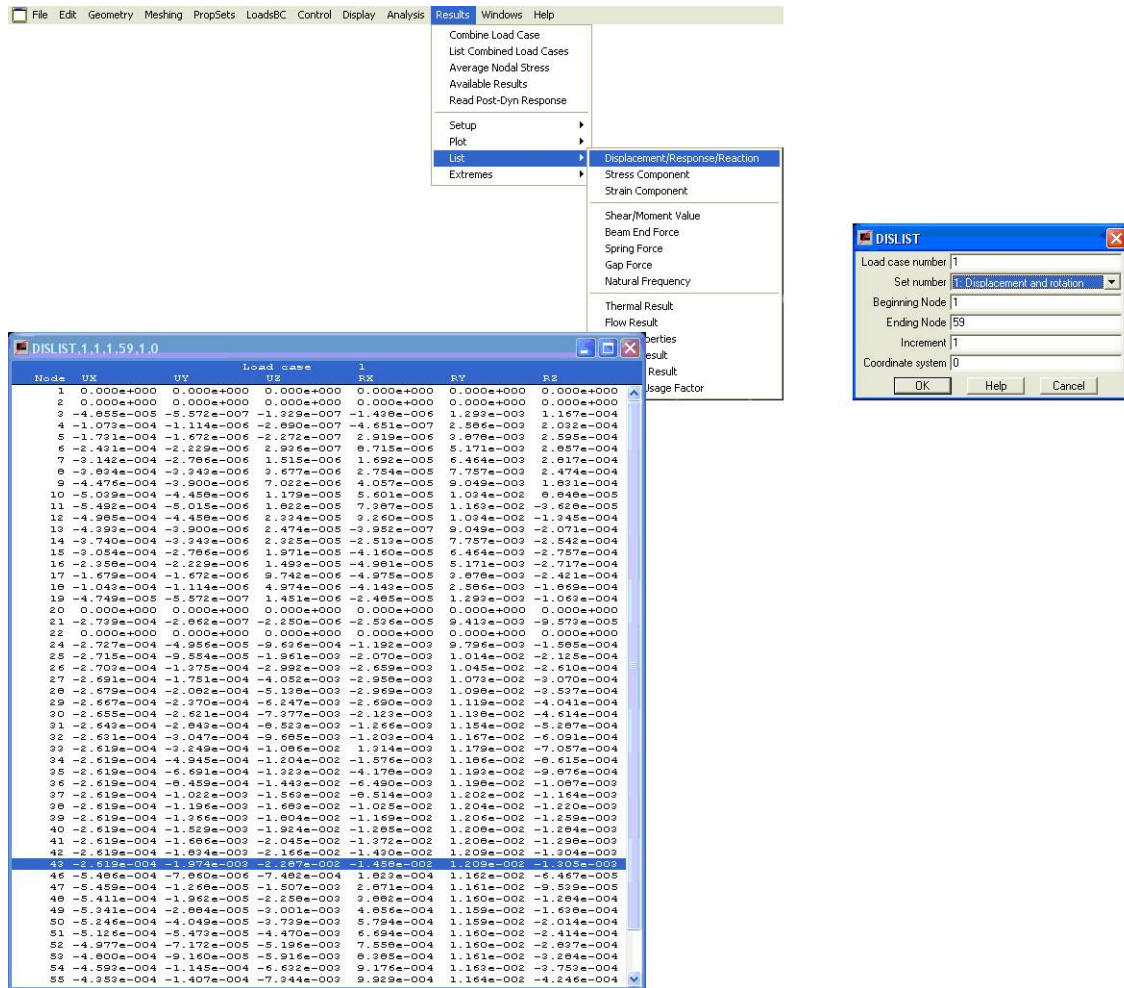


Figure 8:32 List of displacements components

## 8.4. Remarks

During the solutions are not dealt with buckling of the compressed bars. If this is a real problem, we should have to verify with solution a finite element problem, or with any analytic calculation.

During the solutions the tare weight was neglected.

Both problems are explained in later chapters.

Furthermore, the structural joint was not tested. The other specialized areas of structural design deal with this problems.

## **9. DYNAMICS OF BEAM STRUCTURES, MASS MATRIX, NATURAL FREQUENCY ANALYSIS**

### **9.1. Extending of the finite element method**

Such as the historical survey also showed, the finite element method "invention" does not associate to a date. It should not speak about invention, rather to talk about progress or development. This development is begun in 1940-50s, and still continues today. After the first successful solution in field of theory of elasticity, raised the possibility that, other physical problems can be solved using the finite element method. Thus, today we can get finite element solutions in fields of heat transfer, electromagnetic radiation, fluid flow, fatigue and oscillating systems analysis. The mathematical solutions are used in these areas slightly differ from those described at theory of elasticity.

The development of the finite element solution of the structure-dynamics analysis began in the 1960s, when the element mass matrix has been determined.

### **9.2. Finite element formulation of the elastic bodies' natural oscillation**

The previous chapters dealt with elastic bodies in balance. We used the full potential is prescribed as a function of the displacement  $\underline{u}$ :

$$\Pi(\underline{u}) = \frac{1}{2} \int_V \underline{\underline{\sigma}} : \underline{\underline{\epsilon}} dV - \int_V \underline{u} \cdot \underline{q} dV - \int_A \underline{u} \cdot \underline{p} dA \quad (9.1)$$

The potential represents the equality of the elastic strain energy and the work of external forces i.e. the static equilibrium.

D 'Alambert, rearranging the Newton 2<sup>nd</sup> law and wrote the following form:

$$F - m \cdot a = 0$$

so the "ma" is no longer momentum, it is the force of inertia. According to the d'Alambert's principle, the external forces and the force of inertia act on the body are balanced. This is called the kinetic equilibrium.

Following the principle, we complement the above potential with the work of force of inertia and so we get the potential, which describes the system of kinetic equilibrium state:

$$\Pi(\underline{v}) = \frac{1}{2} \int_V \underline{\underline{\sigma}} : \underline{\underline{\epsilon}} dV - \int_V \underline{u} \cdot \underline{q} dV - \int_A \underline{u} \cdot \underline{p} dA + \int_V \underline{u} \cdot \ddot{\underline{u}} \rho dV \quad (9.2)$$

where:

- $\ddot{\underline{u}}$ -the time of the second derivative of the displacement vector (i.e. acceleration)
- $\rho$ -Density of the material.

During the finite element solution we follow the method which is presented in a previous chapter with the addition that, the three coordinates of the function describing the motion of the body, are supplemented by the fourth coordinate which is the time:

$$\underline{u} = u(x, y, z, t) \quad (9.3)$$

We interpolate this function by the previously presented shape functions:

$$u(x, y, z, t) = \underline{\underline{N}}(x, y, z)\underline{u}_e(t) \quad (9.4)$$

Thus, the acceleration:

$$\ddot{u}(x, y, z, t) = \underline{\underline{N}}(x, y, z)\ddot{u}_e(t) \quad (9.5)$$

With this supplementing the potential, work of the inertial forces on an element:

$$\int_{V_e} \underline{u} \cdot \dot{\underline{u}} \rho dV = \int_{V_e} \underline{u}_e^T \cdot \dot{\underline{u}}_e \rho dV = \underline{u}_e^T \left( \int_{V_e} \underline{\underline{N}}^T \underline{\underline{N}} \rho dV \right) \dot{\underline{u}}_e = \underline{u}_e^T \underline{\underline{M}}_e \dot{\underline{u}}_e \quad (9.6)$$

The  $\underline{\underline{M}}_e$  is the consistent mass matrix of the element which contains the inertial properties.

The full potential can be written in a matrix form:

$$\Pi = \frac{1}{2} \underline{U}^T \underline{\underline{K}} \underline{U} - \underline{U}^T \underline{F} + \underline{U}^T \underline{\underline{M}} \ddot{\underline{U}} \quad (9.7)$$

The equation which is satisfactory of the  $\Pi = \min$  condition

$$\underline{\underline{M}} \ddot{\underline{U}} + \underline{\underline{K}} \underline{U} = \underline{F}(t) \quad (9.8)$$

a linear differential equation system.

The right side of the equation contains constant and time variable forces (i.e. pre-loading and exciting forces). The engineering practice there is very much study when external forces do not act. Think of the most common engineering practice oscillation problem, determining of the critical angular velocity of rotating shafts. The critical angular velocity approximately equal to the smallest angular natural frequency of the shaft. Thus, the equation system of an undamped vibration system without external forces becomes simpler:

$$\underline{\underline{M}} \ddot{\underline{U}} + \underline{\underline{K}} \underline{U} = 0 \quad (9.9)$$

The body does harmonic oscillation, so the solution of differentialequations:

$$\underline{U} = A \sin(\omega t + \phi) \quad (9.10)$$

where:

- $\underline{A}$  the amplitude vector of the nodes,
- $\alpha$  the natural frequency,
- $\varepsilon$  phase angle.

substitute  $\underline{U}$ , and the time of the second derivative of the  $\underline{U}$  in the basic equation:

$$(-\alpha^2 \underline{\underline{M}} + \underline{\underline{K}}) \underline{A} = 0 \quad (9.11)$$

we obtain a homogeneous algebraic equations system. Search the eigenvalues of  $\underline{A}$  and the associated natural frequency  $\alpha$ .

The above equations have solution different the trivial solution, if the determinant of the coefficient matrix is zero, i.e.:

$$\det(-\alpha^2 \underline{\underline{M}} + \underline{\underline{K}}) = 0 \quad (9.12)$$

Since the  $\underline{\underline{M}}$  and  $\underline{\underline{K}}$  matrices in the equation system according to degrees of freedom of finite element model, the matrices are of order  $n \times n$ , so the equations have  $n$  roots for  $\alpha^2$ . The degrees of freedom of finite element models used in practice can be few hundred to several million. It need not determine so many eigenvalue and natural frequency, the first few value have relevance in the practice.

### 9.3. Natural frequency calculation of two-dimensional bar structures using finite element method

See a shaft bearings at the two ends, with a fast pulley at an intermediate point shown in Figure 9.1. Determined the shaft critical angular speed.

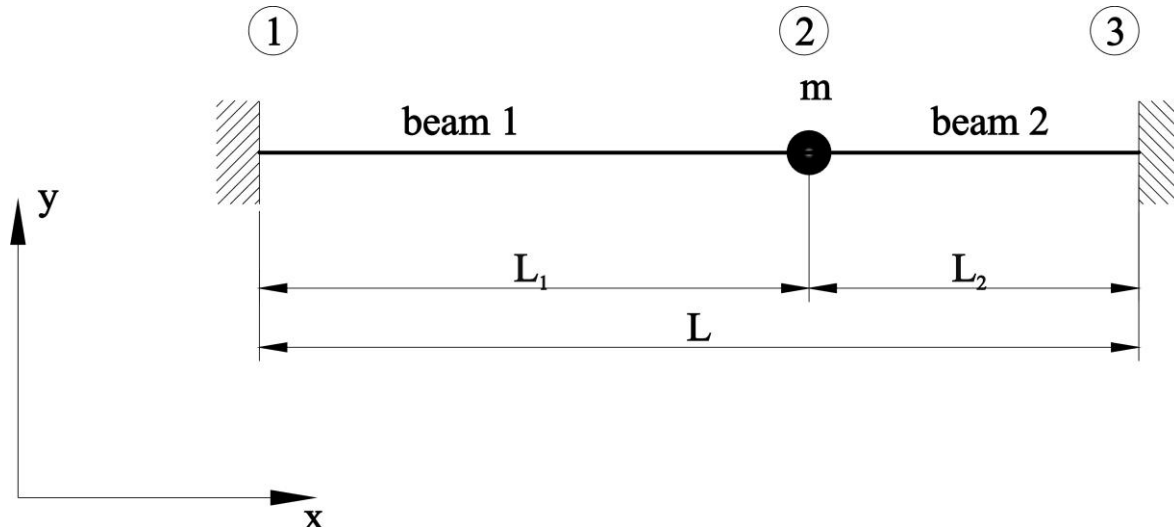


Figure 9.1 The shaft

The diameter of the shaft is 30 mm, made of solid steel. The pulley weighs 1 kg. The shaft length 400 mm,  $L_1 = 250$  mm and  $L_2 = 150$  mm.

We have to determine the  $\underline{\underline{M}}$  mass matrix and the  $\underline{\underline{K}}$  stiffness matrix for solution the  $(-\alpha^2 \underline{\underline{M}} + \underline{\underline{K}}) \underline{\underline{A}} = \underline{\underline{0}}$  equation.

### 9.3.1. Determination of the element mass matrix

As we have seen, for determination of the element mass matrix, the  $N(x, y, z)$  interpolation functions are used.

First, place the element in an "s" coordinate system, which is independent of the length and coincides with the element axis. The element location in the global coordinate system is shown in figure 9.2 a, and the element location in the local "s" coordinate system shown in figure 9.2 b.

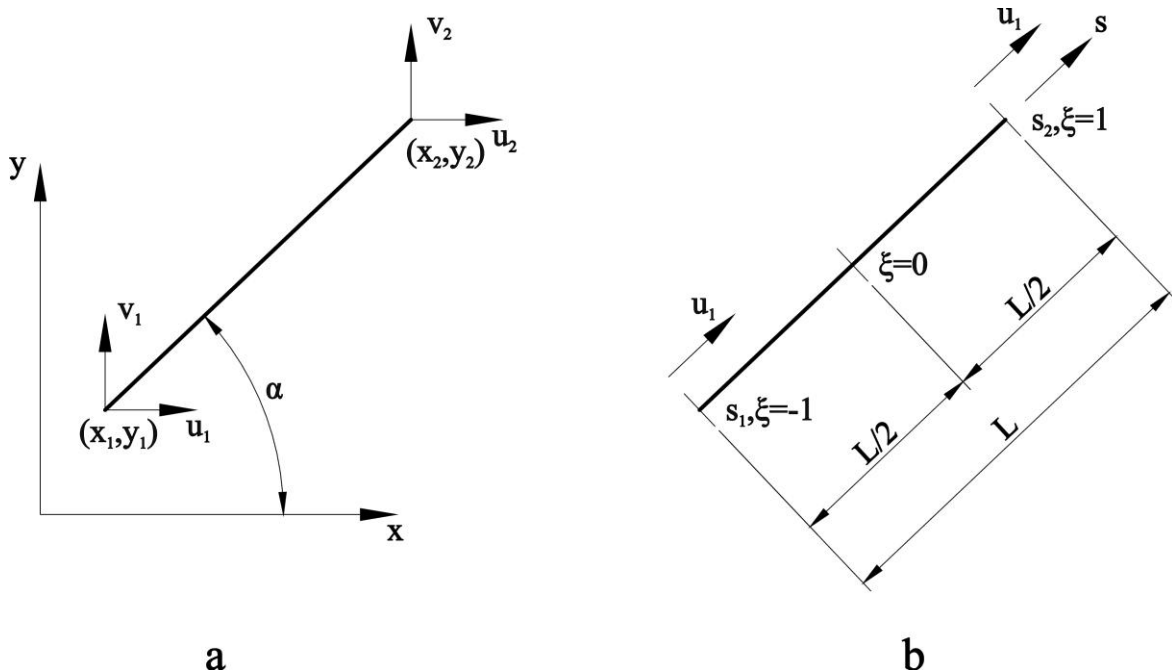


Figure 9.2 The element local coordinate system

The element mass matrix can be determined based on the following:

$$\underline{\underline{M}}_e = \int_{-1}^1 \underline{N} \underline{N}^T \rho A L d\xi \quad (9.13)$$

The axial displacements are interpolated:

$$\begin{aligned} N_1 &= (1 - \xi)/2, \\ N_4 &= (1 + \xi)/2 \end{aligned} \quad (9.14)$$

with shape functions linearly,  
the displacements perpendicular to beam are interpolated:

$$\begin{aligned}
 N_2 &= (2 - 3\xi + \xi^3)/4, \\
 N_3 &= (1 - \xi - \xi^2 + \xi^3)\frac{L}{8}, \\
 N_5 &= (2 + 3\xi - \xi^3)/4, \\
 N_6 &= -(1 + \xi - \xi^2 - \xi^3)\frac{L}{8}
 \end{aligned} \tag{9.15}$$

with shape functions cubical.

For the linear members:

$$\underline{N}_{\text{lin}} = \begin{bmatrix} N_1 \\ N_4 \end{bmatrix} \tag{9.16}$$

If the cross-section of the beam element and density is constant, then the associated mass matrix is:

$$\underline{\underline{M}}_{e \text{ lin}} = \rho AL \frac{1}{2} \int_{-1}^1 \underline{N}_{\text{lin}} \underline{N}_{\text{lin}}^T d\xi = \rho AL \frac{1}{6} \begin{bmatrix} 2 & 1 \\ 1 & 2 \end{bmatrix} \tag{9.17}$$

For the cubical members:

$$\underline{N}_{\text{köb}} = \begin{bmatrix} N_2 \\ N_3 \\ N_5 \\ N_6 \end{bmatrix} \tag{9.18}$$

and the associated mass matrix:

$$\underline{\underline{M}}_{e \text{ köb}} = \rho AL \frac{1}{2} \int_{-1}^1 \underline{N}_{\text{köb}} \underline{N}_{\text{köb}}^T d\xi = \rho AL \frac{1}{420} \begin{bmatrix} 156 & 22L & 54 & -13L \\ 22L & 4L^2 & 13L & -3L^2 \\ 51 & 13L & 156 & -22L \\ -13L & -3L^2 & -22L & 4L^2 \end{bmatrix} \tag{9.19}$$

This matrix is expanded, with the matrix associated linear members thus we get the total element mass matrix:

$$\underline{\underline{M}}_e = \rho A L \frac{1}{420} \begin{bmatrix} 140 & 0 & 0 & 70 & 0 & 0 \\ 0 & 156 & 22L & 0 & 54 & -13L \\ 0 & 22L & 4L^2 & 0 & 13L & -3L^2 \\ 70 & 0 & 0 & 140 & 0 & 0 \\ 0 & 54 & 13L & 0 & 156 & -22L \\ 0 & -13L & -3L^2 & 0 & -22L & 4L^2 \end{bmatrix} \quad (9.20)$$

### 9.3.2. Element stiffness matrix

The stiffness matrix of beam element is also derived from the above interpolation functions. The axial relative elongation of the element:

$$\varepsilon_s = \frac{du_e}{ds} = \frac{du_e}{d\xi} \frac{d\xi}{ds} \quad (9.21)$$

The axial displacements of the element mark by  $J = \frac{ds}{d\xi}$ , the strain-displacement vector:

$$\underline{B}_{lin} = J^{-1} \begin{bmatrix} N_1' \\ N_4' \end{bmatrix} = \frac{2}{L} \begin{bmatrix} -0.5 \\ 0.5 \end{bmatrix} = \begin{bmatrix} -1/L \\ 1/L \end{bmatrix} \quad (9.22)$$

and the element stiffness matrix is:

$$\underline{\underline{K}}_{e\text{lin}} = \int_L \underline{B} E \underline{B}^T A ds = \int_{-1}^1 \underline{B} E \underline{B}^T A J d\xi = \frac{AE}{L} \begin{bmatrix} 1 & -1 \\ -1 & 1 \end{bmatrix} \quad (9.23)$$

Similarly, the displacements and angular displacements perpendicular to element axis are approximated cubic interpolation:

$$\underline{B}_{k\ddot{o}b} = \frac{1}{J^2} \begin{bmatrix} N_2' \\ N_3'' \\ N_5' \\ N_6'' \end{bmatrix} = \frac{4}{L^2} \begin{bmatrix} 1,5\xi \\ -0,5+1,5\xi \\ -1\xi,5 \\ -0,5-1,5\xi \end{bmatrix} \quad (9.24)$$

and the stiffness matrix:

$$\underline{\underline{K}}_{e\text{k}\ddot{o}b} = \int_L \underline{B} I_z E \underline{B}^T ds = \int_{-1}^1 \underline{B} I_z E \underline{B}^T J d\xi = \frac{I_z E}{L^3} \begin{bmatrix} 12 & 6L & -12 & 6L \\ 6L & 4L^2 & -6L & 2L^2 \\ -12 & -6L & 12 & -6L \\ 6L & 2L^2 & -6L & 4L^2 \end{bmatrix} \quad (9.25)$$

The element stiffness matrix can be obtained by the combination of the two stiffness matrix:

$$\underline{\underline{K}}_e = \begin{bmatrix} \frac{AE}{L} & 0 & 0 & -\frac{AE}{L} & 0 & 0 \\ 0 & \frac{12I_zE}{L^3} & \frac{6I_zE}{L^2} & 0 & -\frac{12I_zE}{L^3} & \frac{6I_zE}{L^2} \\ 0 & \frac{6I_zE}{L^2} & -\frac{4I_zE}{L} & 0 & -\frac{6I_zE}{L^2} & \frac{2I_zE}{L} \\ -\frac{AE}{L} & 0 & 0 & \frac{AE}{L} & 0 & 0 \\ 0 & -\frac{12I_zE}{L^3} & -\frac{6I_zE}{L^2} & 0 & -\frac{12I_zE}{L^3} & -\frac{6I_zE}{L^2} \\ 0 & \frac{6I_zE}{L^2} & \frac{2I_zE}{L} & 0 & -\frac{6I_zE}{L^2} & \frac{4I_zE}{L} \end{bmatrix}$$

### 9.3.3. The system total mass and stiffness matrix

The mass point shown in Figure 9.1 has not mass matrix, we take into account the mass in the mass matrix of the entire system as an inertia on a node.

The mass matrix of the entire system shown in Figure 9.1:

$$\underline{\underline{M}} = \frac{\rho A}{420} \begin{bmatrix} 140L_1 & 0 & 0 & 70L_1 & 0 & 0 & 0 & 0 & 0 \\ 0 & 156L_1 & 22L_1^2 & 0 & 54L_1 & -13L_1^2 & 0 & 0 & 0 \\ 0 & 22L_1^2 & 4L_1^3 & 0 & 13L_1^2 & -3L_1^3 & 0 & 0 & 0 \\ 70 & 0 & 0 & 140(L_1 + L_2) & 0 & 0 & 0 & 54L_2 & -13L_2^2 \\ 0 & 54L_2 & 13L_2^2 & 0 & 156(L_1 + L_2) & 22(L_2^2 - L_1^2) & 0 & 13L_2^2 & -3L_2^3 \\ 0 & -13L_1^2 & -3L_1^3 & 0 & 22(L_2^2 - L_1^2) & 4(L_1^3 + L_2^3) & 0 & 0 & 0 \\ 0 & 0 & 0 & 70L_2 & 0 & 0 & 140L_2 & 0 & 0 \\ 0 & 0 & 0 & 0 & 54L_2 & 13L_2^2 & 0 & 156L_2 & -22L_2^2 \\ 0 & 0 & 0 & 0 & -13L_2^2 & -3L_2^3 & 0 & -22L_2^2 & 4L_2^3 \end{bmatrix}$$

and stiffness matrix of the entire system:

$$\underline{\underline{K}} = \begin{bmatrix} \frac{AE}{L_1} & 0 & 0 & -\frac{AE}{L_1} & 0 & 0 & 0 & 0 & 0 \\ 0 & \frac{12I_zE}{L_1^3} & \frac{6I_zE}{L_1^2} & 0 & -\frac{12I_zE}{L_1^3} & \frac{6I_zE}{L_1^2} & 0 & 0 & 0 \\ 0 & \frac{6I_zE}{L_1^2} & -\frac{4I_zE}{L_1} & 0 & -\frac{6I_zE}{L_1^2} & \frac{2I_zE}{L_1} & 0 & 0 & 0 \\ -\frac{AE}{L_1} & 0 & 0 & \frac{AE}{L_1} + \frac{AE}{L_2} & 0 & 0 & -\frac{AE}{L_2} & 0 & 0 \\ 0 & -\frac{12I_zE}{L_1^3} & -\frac{6I_zE}{L_1^2} & 0 & \frac{12I_zE}{L_2^3} - \frac{12I_zE}{L_1^3} & \frac{6I_zE}{L_2^2} - \frac{6I_zE}{L_1^2} & 0 & -\frac{12I_zE}{L_2^3} & \frac{6I_zE}{L_2^2} \\ 0 & \frac{6I_zE}{L_1^2} & \frac{2I_zE}{L_1} & 0 & \frac{6I_zE}{L_2^2} - \frac{6I_zE}{L_1^2} & \frac{4I_zE}{L_1} - \frac{4I_zE}{L_2} & 0 & -\frac{6I_zE}{L_2^2} & \frac{2I_zE}{L_2} \\ 0 & 0 & 0 & -\frac{AE}{L_2} & 0 & 0 & \frac{AE}{L_2} & 0 & 0 \\ 0 & 0 & 0 & 0 & -\frac{12I_zE}{L_2^3} & -\frac{6I_zE}{L_2^2} & 0 & -\frac{12I_zE}{L_2^3} & -\frac{6I_zE}{L_2^2} \\ 0 & 0 & 0 & 0 & \frac{6I_zE}{L_2^2} & \frac{2I_zE}{L_2} & 0 & -\frac{6I_zE}{L_2^2} & \frac{4I_zE}{L_2} \end{bmatrix}$$

If the axis of the element is not parallel to the global coordinate system X axis, then the stiffness and mass matrices of the element must be transformed first, using the transformation matrix described in previous chapters.

The equations can now be simplified so that the displacements and angular displacements at locations (at the bearings) are skipped. So we can delete rows and columns of the equation system in these places. In our case, this is the 1-3. and 7-9. rows and columns. Thus, the matrices in the system of equations:

$$\underline{\underline{M}}^* = \begin{bmatrix} \frac{140}{420} \rho A(L_1 + L_2) + m & 0 & 0 \\ 0 & \frac{156}{420} \rho A(L_1 + L_2) + m & \frac{22}{420} \rho A(L_2^2 - L_1^2) \\ 0 & \frac{22}{420} \rho A(L_2^2 - L_1^2) & \frac{4}{420} \rho A(L_1^3 + L_2^3) \end{bmatrix}$$

$$\underline{\underline{K}}^* = \begin{bmatrix} \frac{AE}{L_1} + \frac{AE}{L_2} & 0 & 0 \\ 0 & \frac{12I_zE}{L_2^3} - \frac{12I_zE}{L_1^3} & \frac{6I_zE}{L_2^2} - \frac{6I_zE}{L_1^2} \\ 0 & \frac{6I_zE}{L_2^2} - \frac{6I_zE}{L_1^2} & \frac{4I_zE}{L_1} - \frac{4I_zE}{L_2} \end{bmatrix}$$

The problem to be solved:

$$\det(-\alpha^2 \underline{\underline{M}}^* + \underline{\underline{K}}^*) = 0$$

equations, which from we get the:

$$\alpha^2 = \begin{bmatrix} 4,1074 \cdot 10^8 \\ 9,1253 \cdot 10^8 \\ 1,5681 \cdot 10^7 \end{bmatrix}$$

solution. Real roots of  $\alpha$ :

$$\alpha = \begin{bmatrix} 20266,82 \\ 30208,13 \\ 3959,96 \end{bmatrix}$$

#### 9.4. Remarks

In practice, we can use the simplified mass matrix:

$$\underline{\underline{M}}_e = \frac{\rho A L}{2} \begin{bmatrix} 1 & 0 & 0 & 0 & 0 & 0 \\ 0 & 1 & 0 & 0 & 0 & 0 \\ 0 & 0 & 0 & 0 & 0 & 0 \\ 0 & 0 & 0 & 1 & 0 & 0 \\ 0 & 0 & 0 & 0 & 1 & 0 \\ 0 & 0 & 0 & 0 & 0 & 0 \end{bmatrix}$$

which expresses that the mass of the element are divided into two equal parts, and place this to the two ends of the element. This corresponds to the analytical calculation when we reduce the mass of the bar to its endpoint. In the case of finite element solutions, sufficiently accurate results can be obtained using this procedure if the bar is divided sufficiently many finite elements.

## **10. DYNAMIC ANALYSIS OF THREE-DIMENSIONAL BARS, DETERMINATION OF NATURAL FREQUENCY USING PROGRAM SYSTEM BASED ON FINITE ELEMENT METHOD**

### **10.1. Introduction**

The engineering works are all oscillating systems. Buildings, structures, vehicles, machine parts, vibrations carry out each. These are neglected usually, due to their high frequency and small amplitude. These do not disturb the functionality of the machine.

However, there are many cases in which these vibrations can not or should not be ignored. Everyone knows disaster of the Tacoma Bridge. The oscillation of the bridge was forced by the wind. But in our daily lives we can find examples of the importance of oscillating systems. The wheels of our cars are balanced. The unbalanced wheels cause uncomfortable driving, and malfunction in bearings, shafts and tires. But the state of shock absorbers, are regularly checked not only because of the convenience, but also because it is related to safety. In field of manufacturing process there are several examples to the vibration of machines and machinery parts can not be ignored.

But there are some engineering applications, where the vibrations should not be damped or avoided, but on the contrary, should strengthen them. Consider, for example vibration feeders and screens machines are used in the field of materials handling, or vibration compaction machines are used in the field of building industry.

### **10.2. Properties of the used finite elements**

The properties of BEAM3D elements used for three-dimensional modeling are described in chapters 8.

However, we will use a new element. The finite element modeling programs use a 0-dimensional MASS element (mass, or inertia). This element has only one node, in this node of the element accumulates the total mass and moment of inertia. The MASS element has mass (inertia) in X, Y and Z direction, and the moment of inertia is interpreted around the three-axis. This interpretation allows me that in the case of 2D problems ignore some effects.

### **10.3. The study description**

In the mechanical engineering practice, the most common tasks are the examination the bending and torsional vibration of the rotating shaft. In this study we analyze a rotating shaft with two flanges shown in Figure 10.1.

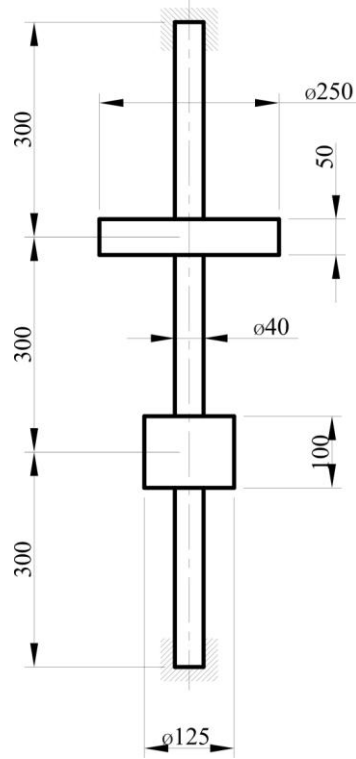


Figure 10.1 Tested shaft

This problem has been also discussed in the subjects of mechanical engineering studies, in machine design, shafts and couplings, in mechanics dynamics.

These subjects showed that the bending and torsional vibrations are generated in shafts. It also clarified that these vibrations can be dangerous, if the rotation angular velocity of the shaft equal to the first angular natural frequency of the system.

The angular natural frequencies of bending vibrations in the structure shown in Figure 10.1 are calculated by Dunkerley's simplified formula:

$$\frac{1}{\alpha^2} = m_1 \eta_1 + m_2 \eta_2 \quad (10.1)$$

where:  $\alpha$  - the angular frequency (10.1)

$\eta$  - deflection of the shaft caused by a unit radial force.

According to the known formulas:

$$\frac{1}{\alpha^2} = m_1 \frac{8}{18} \frac{a^3}{IE} + m_2 \frac{8}{18} \frac{a^3}{IE} \quad (10.2)$$

Thus, the angular natural frequency of the shaft is:  
 $\alpha=276.76 \text{ 1/s}$ , which is equal to  $n=2642.86 \text{ rpm}$ .

The torsional vibrations from the characteristic equations of multi-degree-of-freedom system are:

$$\alpha_0 = \sqrt{\frac{\Theta_1 + \Theta_2}{\Theta_1 \Theta_2 c_0}} \quad (10.3)$$

where:  
 -  $\Theta$  the moment of inertia of the disks around Y axis  
 -  $c_0$  the torsional spring constant,:  
 On this basis, the torsional natural frequency is:

$$c_0 = \frac{a}{I_p G} \quad (10.4)$$

where:  
 -  $I_p$  polar moment of inertia  
 -  $G$  - modulus of rigidity

$\omega_0 = 1503.87 \text{ rad/s}$  i.e.  $n=14360.9 \text{ rpm}$ .

#### 10.4. The finite element solution of the task

Structure shown in Figure 10.1 is a very simple geometric model, shaft can be characterized by a single line. We draw it as three separated line to help generating of the finite element mesh. So we can place the MASS elements on the end of the sections, on geometrical (key-) points. The drawn sections shown in Figure 10.2.

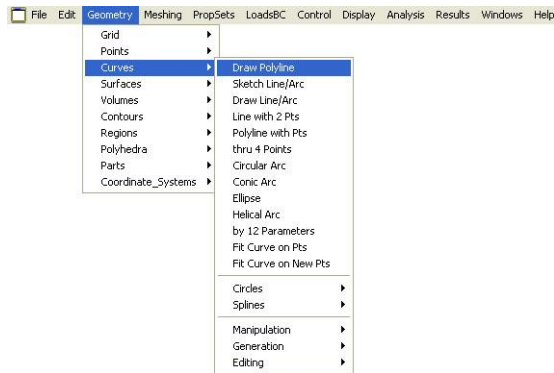


Figure 10.2. Creating a geometric model

After the creation of the geometric model, follows the describing the properties of finite element mesh. First we select the needed element type (element group) (see Figure 10.3), which is in our case the BEAM3D element.

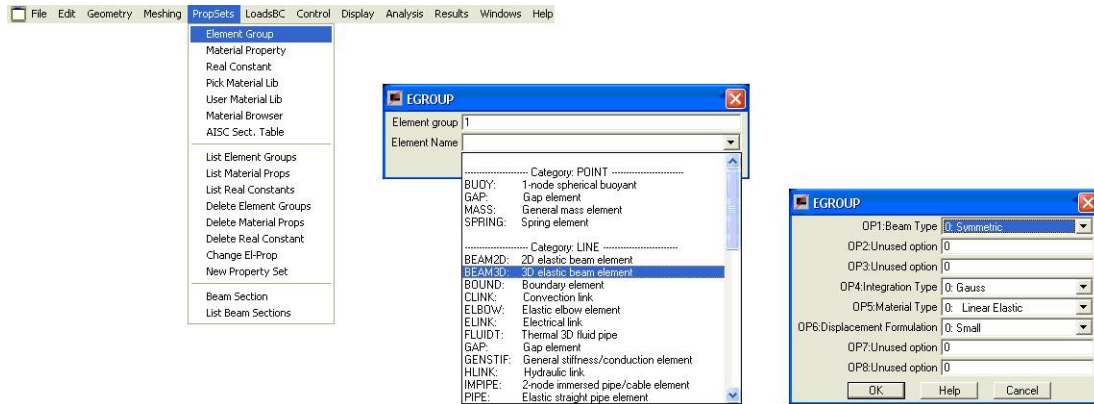


Figure 10.3 Select the element type

In the next step we define the required material properties, the elastic modulus and the modulus of rigidity (see Figure 10.4).

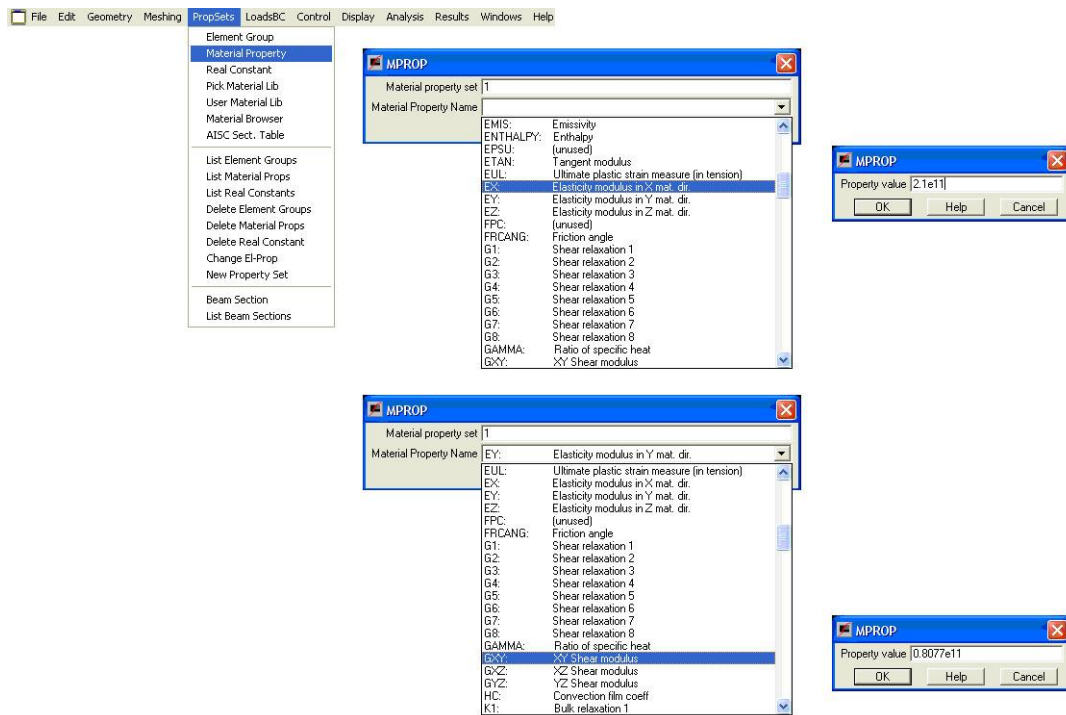


Figure 10.4 Define the material properties

Finally, the real constants are defined. The Figure 10.5 shows an example of simplified procedures for definition the real constant by geometrical dimensions. The "2" sign indicate that the cross-section is circular.

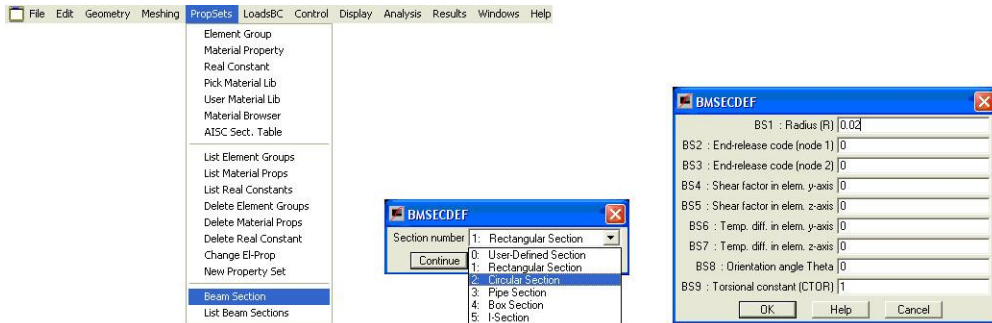


Figure 10.5 Definition the real constant

If we have defined all properties of the finite elements, then we can create the finite element mesh (see Figure 10.6.). We create 10-10 element in each section. The section of BEAM3D elements is a circle, thus definition of the third node is not required.

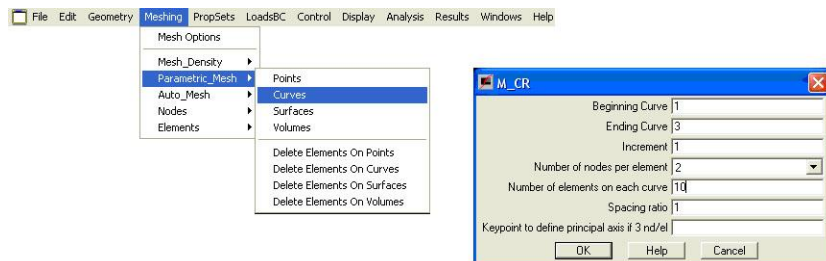


Figure 10.6 Create the finite element mesh

We have to define the properties of the two disks. To this end, we define a new element group already described above, the MASS (inertial) element (see Figure 10.7).

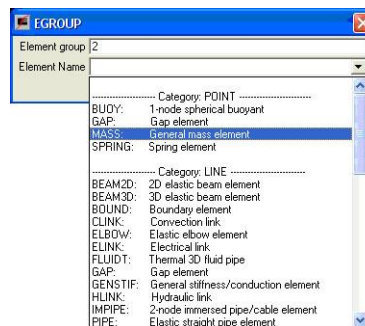


Figure 10.7 Define the MASS element

To this element type does not belong to any material property, such as sufficient for definition the real constant. These constant of the first disc shown in Figure 10.8. The moments of inertia of the disk around X and Z axis can be ignored, so their values shall be 0.

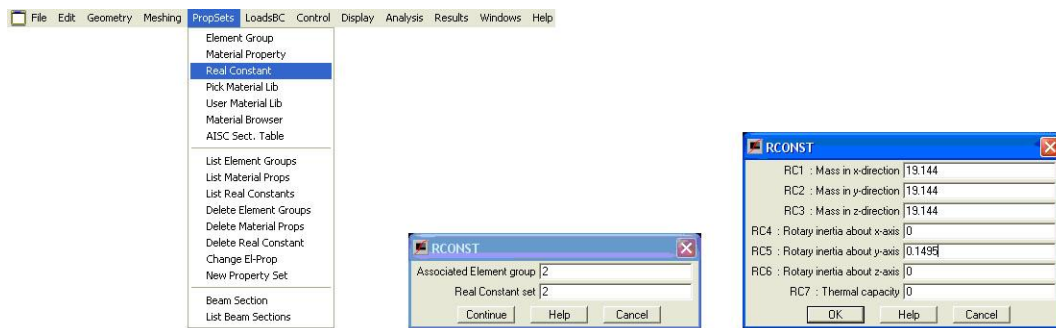


Figure 10.8 Real constant of first disk

The MASS element is placed on a single node in the finite element mesh. The creation of the MASS element shown in Figure 10.9.

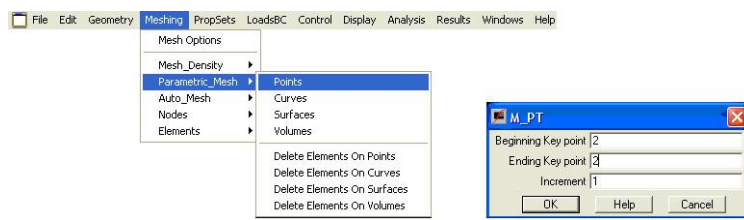


Figure 10.9 Create a disc as finite element

We have to define the real constant of the second disc (see Figure 10.10).

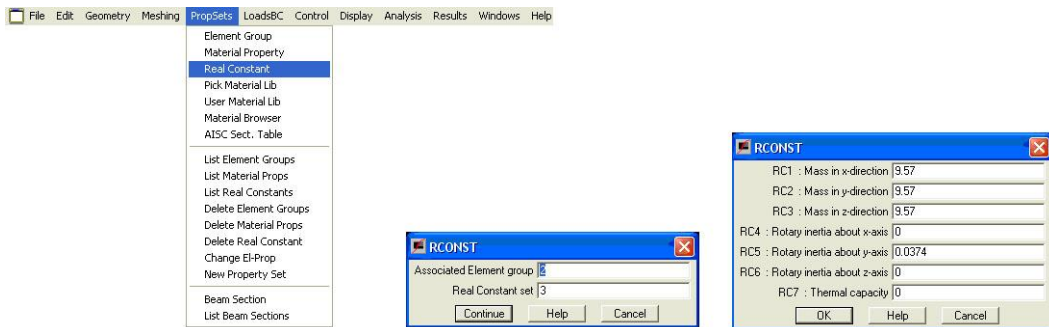


Figure 10.10 Real constant of second disk

The creation of the second disc is similar to the previous one, just on another point of the geometric model.

The finite element mesh has five independent parts (the three shaft section and the two mass). We have to merge the common nodes to join these independent parts (see Figure 10.11).

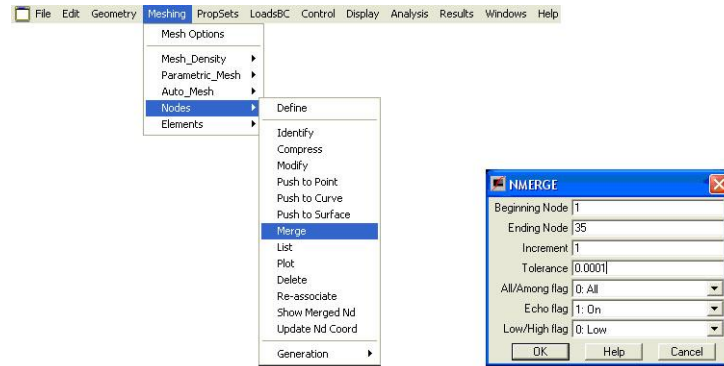


Figure 10.11 Merge the common nodes

In the next step we determine the boundary conditions, shown in Figure 10.1 as bearings. This is similar to the previous examples, it can be defined fixing the three displacement degree of freedom at both ends of the shaft (see Figure 10.12.).

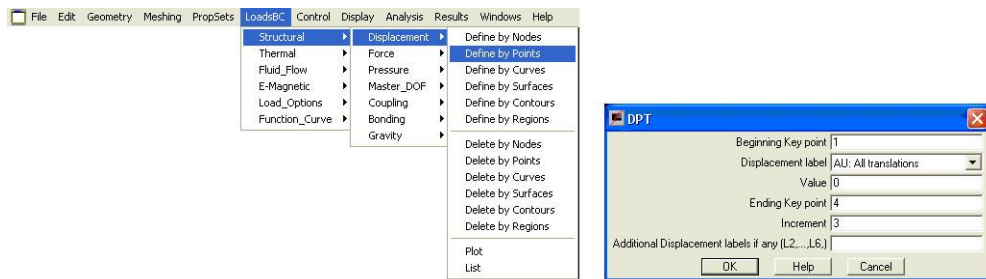


Figure 10.12 Define displacement constrains

Thus the created finite element model shown in Figure 13.10.

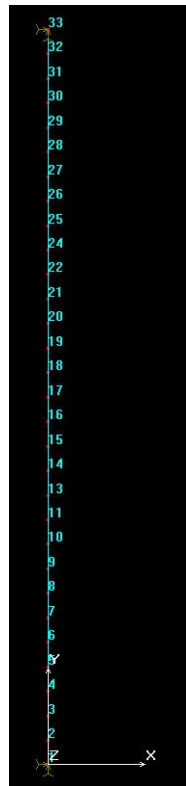


Figure 10.13 The complete finite element model with the node numbering

Before the solving it is possible to set number of the calculated natural frequency (see Figure 14.10). It is appropriate to set calculate more harmonious, because we expect two-way bending and torsional vibrations. In this study we will calculate the first 10 natural frequencies.

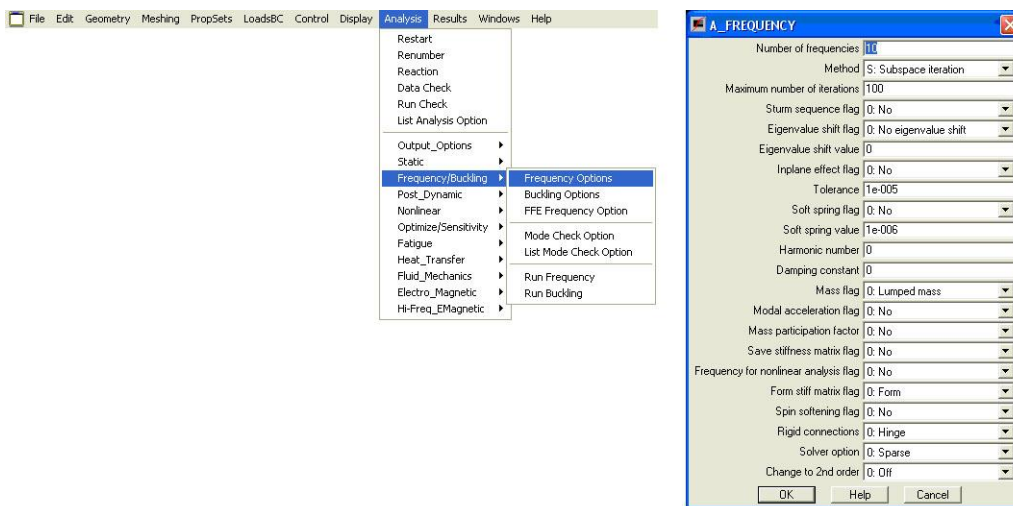


Figure 10.14 The natural frequency analysis settings

After the setting follows the solution (see Figure 10.15)

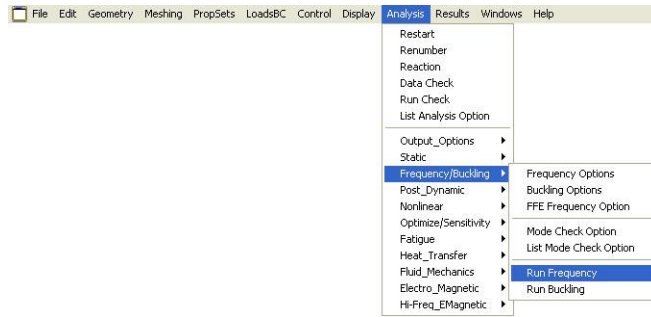


Figure 10.15 Run frequency analysis

After a successful run the results can be displayed. The calculated first eight natural angular frequencies are shown in Figure 10.16.

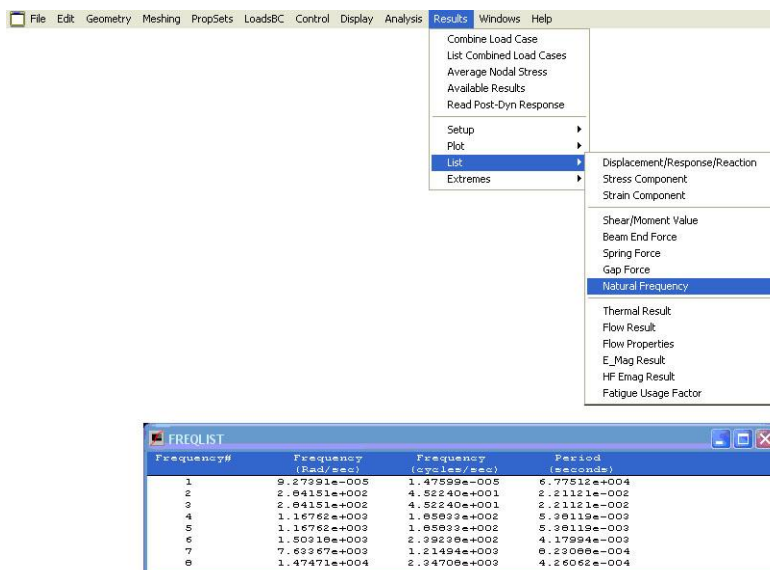


Figure 10.16 The calculated natural angular frequencies

In the list, the first natural angular frequency is  $10^{-5}$  1/s , which is negligibly small in the engineering practice. This is consistent with the learned in mechanics. The first natural frequency of the multi-degree-of-freedom systems is zero. We observe that the 2-3. and 4-5. natural frequencies are the same. Later we will see that these two oscillation generated in X and Z directions. The 6. natural frequency has not pair. This is the torsional oscillation of the shaft between the two disks.

The finite element programs can display graphically the mode shapes as the deformed shape of the shaft (see Figure 17.10).

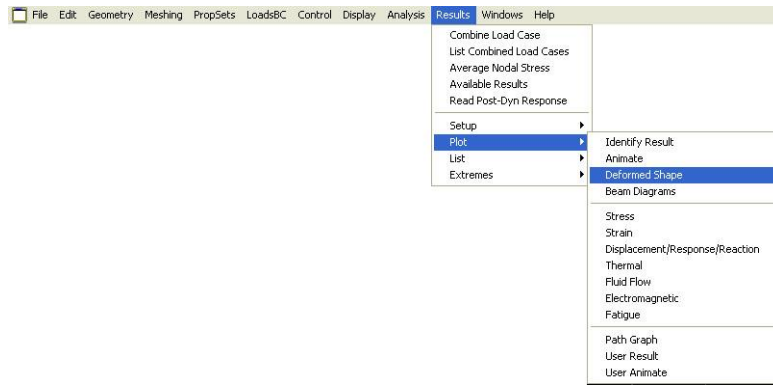


Figure 10.17 Display the mode shapes

The finite-element programs offer a scale factor to display the deformed shape. We override this scale factor and use 0,5 to do comparable mode shapes (see Figure 10.18)

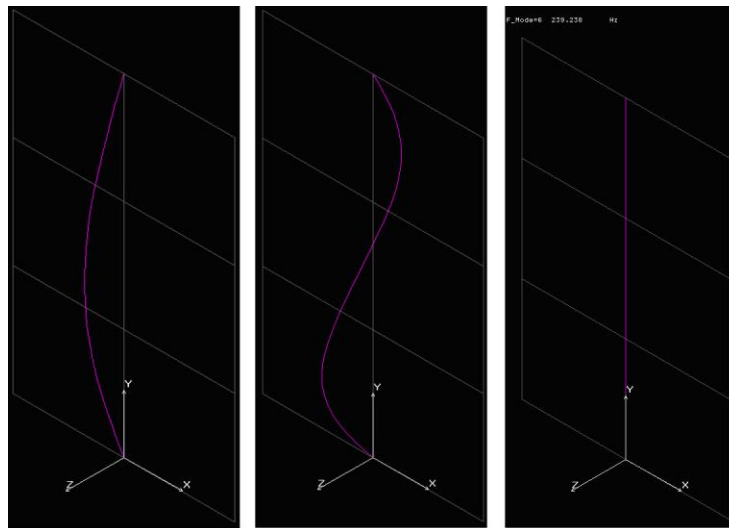


Figure 10.18 The 2 4. and 6 mode shapes

In the figure, we observe that only one node belongs to the first mode shape. Also observed that in case 6 mode shape there is not visible deformation because the twisting around the Y axis is not visible in this representation

The displacements belong to 2. and 3. mode shapes are shown in Figure 10.19.

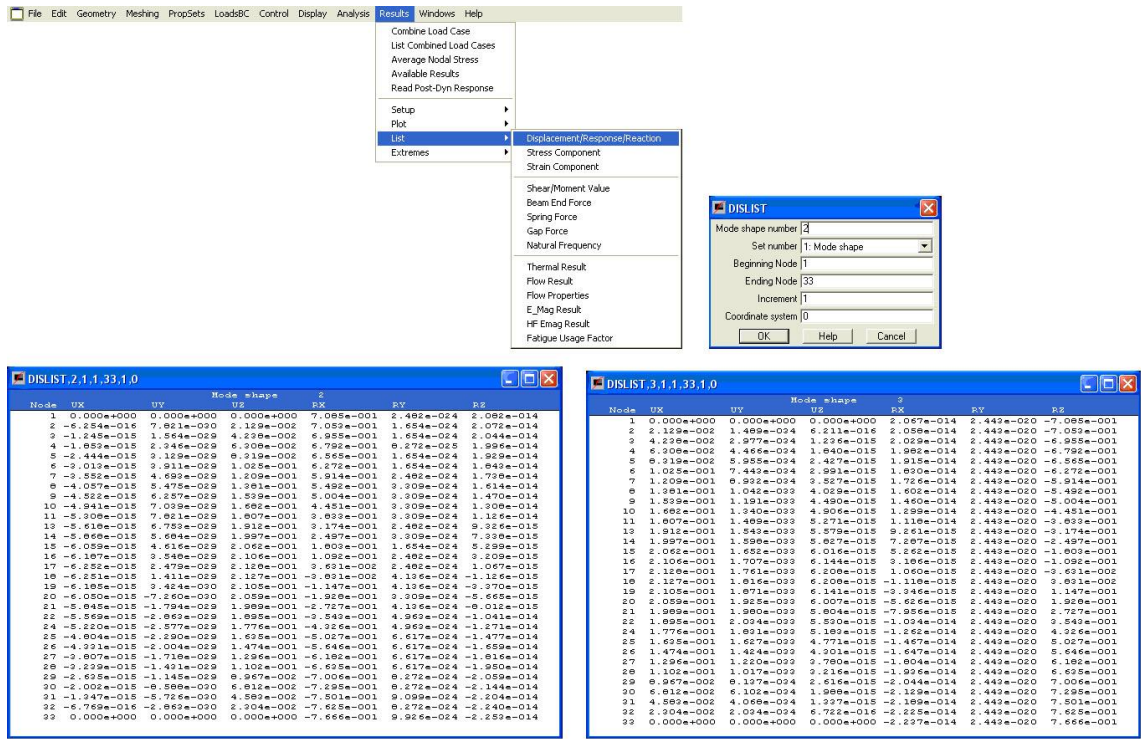


Figure 10.19 Values of 2 and 3 mode shape

The table contains very small magnitude displacements. These are not real values, only generated during the solve as calculation errors.

The mode shape 6th is shown in Figure 10.20.

| Node | UX         | UY          | UZ          | EX           | EY          | EZ          |
|------|------------|-------------|-------------|--------------|-------------|-------------|
| 1    | 0.000e+000 | 0.000e+000  | 0.000e+000  | 1.341e-014   | 4.624e+000  | -1.165e-020 |
| 2    | 9.559e-022 | -7.080e-030 | 4.040e-016  | 1.324e-014   | 4.624e+000  | -1.179e-020 |
| 3    | 7.085e-022 | -1.416e-022 | 7.974e-016  | 1.270e-014   | 4.624e+000  | -1.163e-020 |
| 4    | 1.055e-021 | -1.242e-022 | 1.169e-015  | 1.162e-014   | 4.624e+000  | -1.136e-020 |
| 5    | 1.412e-021 | -1.068e-022 | 1.566e-015  | 1.054e-014   | 4.624e+000  | -1.109e-020 |
| 6    | 1.714e-021 | -9.540e-023 | 1.067e-015  | 9.978e-015   | 4.624e+000  | -1.049e-020 |
| 7    | 2.021e-021 | -8.145e-023 | 2.052e-015  | 9.702e-015   | 4.623e+000  | -9.989e-021 |
| 8    | 2.308e-021 | -6.956e-023 | 2.322e-015  | 9.421e-015   | 4.623e+000  | -9.162e-021 |
| 9    | 2.579e-021 | -5.664e-023 | 2.938e-015  | 2.051e-015   | 4.622e+000  | -8.366e-021 |
| 10   | 2.811e-021 | -6.372e-023 | 2.359e-015  | 9.845e-015   | 4.621e+000  | -7.575e-021 |
| 11   | 3.053e-021 | -5.080e-023 | 1.644e-015  | 4.624e-015   | 4.620e+000  | -6.410e-021 |
| 12   | 3.219e-021 | -6.112e-023 | 2.096e-015  | 7.540e-015   | 4.044e+000  | -5.308e-021 |
| 13   | 3.917e-021 | -5.145e-023 | 1.026e-015  | -1.009e-014  | 3.466e+000  | -4.177e-021 |
| 14   | 9.339e-021 | -4.176e-023 | 1.826e-015  | 1.406e-015   | 2.066e+000  | -3.017e-021 |
| 15   | 2.946e-021 | -4.176e-023 | 1.406e-015  | 1.199e-014   | 2.066e+000  | -1.827e-021 |
| 16   | 9.521e-021 | -3.811e-023 | 1.100e-015  | -1.322e-014  | 2.310e+000  | -1.608e-021 |
| 17   | 9.505e-021 | -3.811e-023 | 6.816e-016  | -1.322e-014  | 1.782e+000  | -1.576e-021 |
| 18   | 9.489e-021 | -3.787e-023 | 6.629e-016  | 1.193e-014   | 1.899e+000  | -1.555e-021 |
| 19   | 9.519e-021 | -3.096e-023 | -1.407e-016 | -1.2344e-014 | 5.764e-001  | 1.916e-021  |
| 20   | 9.449e-021 | 6.575e-023  | -5.157e-016 | 1.152e-014   | -1.507e-003 | 9.223e-021  |
| 21   | 9.326e-021 | 1.625e-023  | -8.389e-016 | -9.446e-015  | -8.794e-001 | 4.558e-021  |
| 22   | 9.169e-021 | 2.592e-023  | -1.099e-016 | -6.706e-015  | -1.157e+000 | 5.923e-021  |
| 23   | 9.204e-021 | 2.592e-023  | -1.079e-016 | -9.395e-015  | -1.157e+000 | 5.923e-021  |
| 24   | 2.074e-021 | 6.076e-023  | -1.913e-016 | 1.158e-015   | 0.405e-021  | 0.405e-021  |
| 25   | 2.624e-021 | 1.814e-021  | -1.310e-015 | 1.124e-015   | -1.156e+000 | 9.440e-021  |
| 26   | 2.166e-021 | 1.555e-021  | -1.243e-015 | 4.810e-015   | -1.158e+000 | 1.034e-020  |
| 27   | 2.166e-021 | 1.296e-021  | -1.120e-015 | 4.810e-015   | -1.158e+000 | 1.110e-020  |
| 28   | 1.643e-021 | 1.027e-021  | -8.546e-016 | 4.810e-015   | -1.158e+000 | 1.175e-020  |
| 29   | 1.398e-021 | 7.609e-020  | -7.485e-016 | 7.266e-015   | 1.158e+000  | 2.203e-020  |
| 30   | 7.562e-022 | 5.184e-020  | -5.125e-016 | 8.024e-015   | 1.158e+000  | 2.254e-020  |
| 31   | 9.652e-022 | 2.592e-020  | -2.609e-016 | 8.495e-015   | -1.158e+000 | 1.275e-020  |
| 32   | 9.652e-022 | 2.592e-020  | -2.609e-016 | 8.495e-015   | -1.158e+000 | 1.262e-020  |
| 33   | 0.000e+000 | 0.000e+000  | 0.000e+000  | 8.648e-015   | -1.158e+000 | 1.262e-020  |

Figure 10.20. The 6. mode shape

The table contains only rotation results around the Y axis. It is also shown that the torsional oscillation can only be between the two disks.

## 10.5. Remarks

In engineering practice the torsional vibration analysis usually are used only a long, flexible shafts, flexible couplings.

The bending oscillation of rotating shaft with circle or pipe cross section may also be examined using BEAM2D elements.

## 11. INTRODUCTION TO PLANE PROBLEMS SUBJECT. APPLICATION OF PLANE STRESS, PLANE STRAIN AND REVOLUTION SYMMETRIC (AXISYMMETRIC) MODELS

### 11.1. Basic types of plane problems

In the case of plane problems we have two-dimensional or two-variable problems; the basic equations of elasticity can be significantly simplified compared to spatial problems. There are two major categories of plane problems [1]:

- plane stress – a thin structure with constant thickness under in-plane loading, (Fig.11.1a),
- plane strain – a long structure with constant cross section under constant loads along the length (Fig.11.1b).

We note that the generalized plane stress state belongs also to the two-variable problems, if we relate the mechanical quantities to their average values.

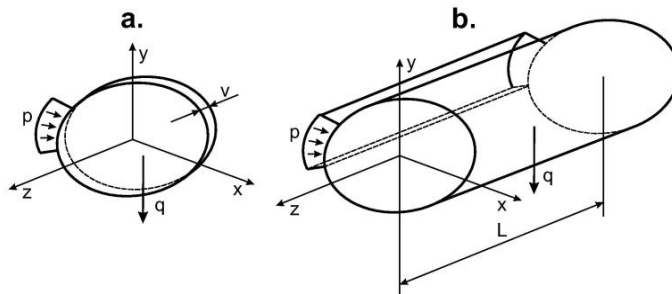


Fig.11.1. Demonstration of plane stress (a) and plane strain (b) states.

For plane problems the displacement vector field is the function of  $x$  and  $y$  only:

$$\underline{u} = \underline{u}(x, y) = \begin{bmatrix} u(x, y) \\ v(x, y) \end{bmatrix} \quad (11.1)$$

Consequently, even the strain and stress fields depend upon  $x$  and  $y$ :

$$\underline{\underline{\varepsilon}} = \underline{\underline{\varepsilon}}(x, y), \quad \underline{\underline{\sigma}} = \underline{\underline{\sigma}}(x, y). \quad (11.2)$$

In the followings we develop the relationship among the former mechanical quantities.

### 11.2. Equilibrium equation, displacement and deformation

The equilibrium equation represents the internal equilibrium of a differential plane element. Based on Fig.11.2 it is possible to express the equilibrium of the forces in directions  $x$  and  $y$  as [1,2]:

$$(\sigma_x + d\sigma_x)dy - \sigma_x dy + (\tau_{yx} + d\tau_{yx})dx - d\tau_{yx} dx + q_x dxdy = 0, \quad (11.3)$$

$$(\sigma_y + d\sigma_y)dx - \sigma_y dx + (\tau_{xy} + d\tau_{xy})dy - d\tau_{xy} dy + q_y dxdy = 0,$$

where  $\sigma$  is the normal,  $\tau$  is the shear stress,  $q_x$  and  $q_y$  are the components of density vector of volume forces. The simplification of Eq.(11.3) leads to the following equations:

$$\frac{\partial \sigma_x}{\partial x} + \frac{\partial \tau_{xy}}{\partial y} + q_x = 0, \quad \frac{\partial \tau_{xy}}{\partial x} + \frac{\partial \sigma_y}{\partial y} + q_y = 0. \quad (11.4)$$

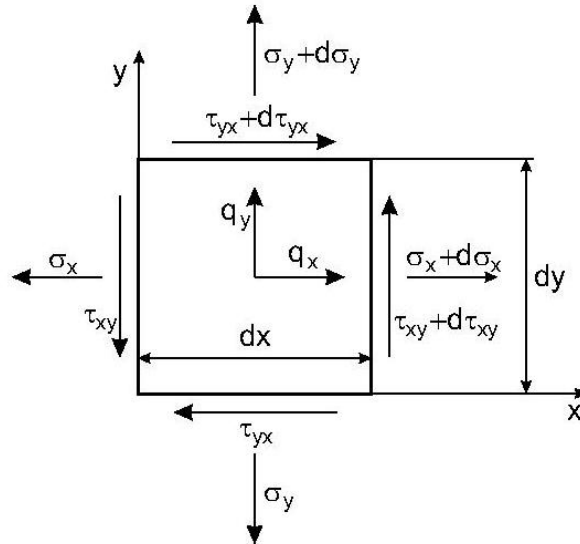


Fig.11.2. Equilibrium of a differential plane element.

The equilibrium equation can be formulated also in vector form [1,2]:

$$\underline{\underline{\sigma}} \cdot \nabla + \underline{q} = \underline{0}, \quad (11.5)$$

where  $\underline{q} = \underline{q}(x,y)$  is the density vector of volume forces,  $\nabla$  is the Hamiltonian differential operator (vector operator) in two dimensions:

$$\nabla = \frac{\partial}{\partial x} \underline{i} + \frac{\partial}{\partial y} \underline{j}. \quad (11.6)$$

In order to establish the relationship between the strain and displacement fields we investigate the displacement and deformation of some points of the differential plane element depicted in Fig.11.3. The normal and shear strains in direction  $x$  of distance AB, and in direction  $y$  of distance AD of the element are:

$$\varepsilon_x = \frac{A'B' - AB}{AB} = \frac{A'B' - dx}{dx}, \quad \varepsilon_y = \frac{A'D' - AD}{AD} = \frac{A'D' - dy}{dy}, \quad \gamma_{yx} = \frac{\pi}{2} - \beta = \theta + \lambda. \quad (11.7)$$

By the help of the figure we can write the following:

$$(A'B')^2 = [dx(1 + \varepsilon_x)]^2 = (dx + \frac{\partial u}{\partial x} dx)^2 + (\frac{\partial v}{\partial x} dx)^2, \quad (11.8)$$

from which we obtain:

$$1 + 2\varepsilon_x + \varepsilon_x^2 = 1 + 2\frac{\partial u}{\partial x} + \left(\frac{\partial u}{\partial x}\right)^2 + \left(\frac{\partial v}{\partial x}\right)^2. \quad (11.9)$$

The expression above is applicable to calculate the normal strain in direction  $x$  in the case of the so-called large displacement. After all, within the scope of elasticity, in most of the cases we obtain reasonably accurate results by the linearization of the expression above. The normal strain in direction  $y$  is derived similarly. Neglecting the higher order terms we obtain the linearized formulae:

$$\varepsilon_x = \frac{\partial u}{\partial x}, \quad \varepsilon_y = \frac{\partial v}{\partial y}. \quad (11.10)$$

Utilizing Fig.11. 3 we calculate the angle denoted by  $\theta$ :

$$\theta = \frac{(\partial v / \partial x) dx}{dx + (\partial u / \partial x) dx}. \quad (11.11)$$

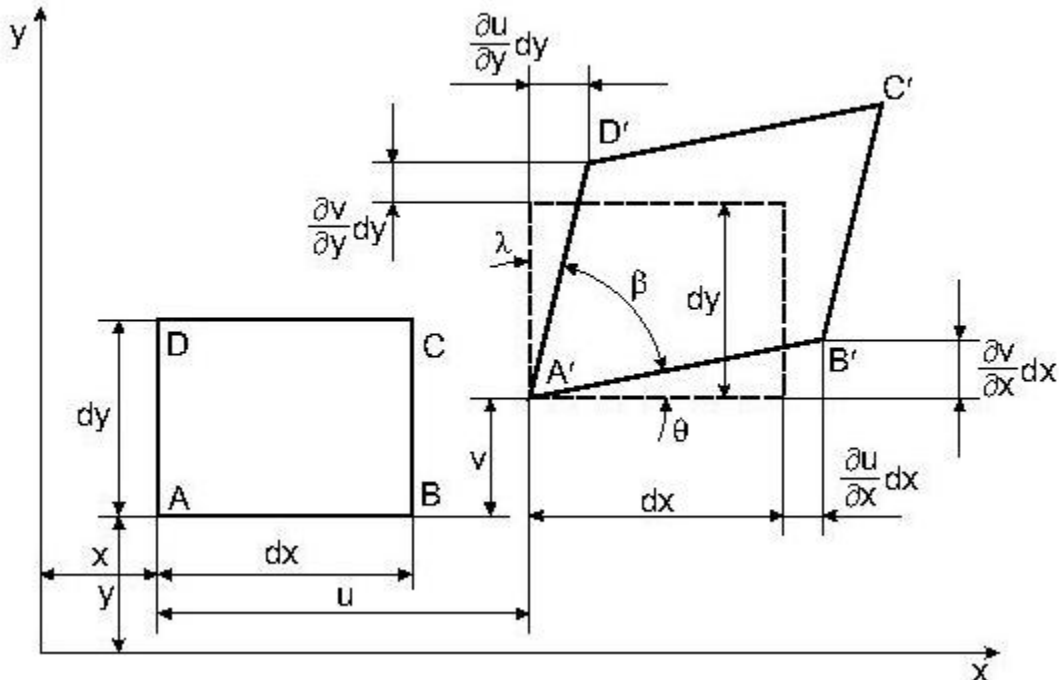


Fig.11.3. Displacement and deformation of a differential plane element.

Assuming that there are only small angles, we can write:

$$\theta = \frac{\partial v}{\partial x}, \lambda = \frac{\partial u}{\partial y}. \quad (11.12)$$

Based on Eq.(11.7) we obtain:

$$\gamma_{xy} = \frac{\partial u}{\partial y} + \frac{\partial v}{\partial x}. \quad (11.13)$$

We obtain the so-called strain-displacement equation by summarizing Eqs.(11.10) and (11.13) in tensorial form. The strain-displacement equation is valid also for spatial problems [1,2]:

$$\underline{\underline{\varepsilon}} = \frac{1}{2} (\underline{u} \circ \nabla + \nabla \circ \underline{u}), \quad (11.14)$$

where the circle means dyadic product.

### 11.3. Constitutive equations

The material behavior, in other words the stress-strain relationship of a homogeneous, linear elastic, isotropic body is given by Hooke's law [3]:

$$\underline{\underline{\varepsilon}} = \frac{1}{2G} \left[ \underline{\underline{\sigma}} - \frac{\nu}{1+\nu} \underline{\underline{\sigma}}_I \underline{\underline{E}} \right], \quad \underline{\underline{\sigma}} = 2G \left[ \underline{\underline{\varepsilon}} + \frac{\nu}{1-2\nu} \underline{\underline{\varepsilon}}_I \underline{\underline{E}} \right], \quad (11.15)$$

where  $\nu$  is Poisson's ratio,  $E$  is the modulus of elasticity,  $G = E/(2(1+\nu))$  is the shear modulus,  $\underline{\underline{E}}$  is the identity tensor,  $\underline{\underline{\sigma}}_I$  and  $\underline{\underline{\varepsilon}}_I$  are the first scalar invariants, respectively.

#### 11.3.1. Plane stress state

The stress components under plane stress state are:

$$\sigma_x = \sigma_x(x, y), \sigma_y = \sigma_y(x, y), \tau_{xy} = \tau_{xy}(x, y) \text{ and } \tau_{xz} = \tau_{yz} = \sigma_z = 0, \quad (11.16)$$

i.e. the normal stress perpendicular to the  $x$ - $y$  plane and the shear stresses acting on the plane with outward normal in direction  $z$  are zero. The stress and strain tensors have the following forms:

$$\underline{\underline{\sigma}} = \begin{bmatrix} \sigma_x & \tau_{xy} & 0 \\ \tau_{xy} & \sigma_y & 0 \\ 0 & 0 & 0 \end{bmatrix}, \quad \underline{\underline{\varepsilon}} = \begin{bmatrix} \varepsilon_x & 1/2 \cdot \gamma_{xy} & 0 \\ 1/2 \cdot \gamma_{xy} & \sigma_y & 0 \\ 0 & 0 & \varepsilon_z \end{bmatrix}. \quad (11.17)$$

From the first of Eq.(11.15) we obtain:

$$\varepsilon_x = \frac{1+\nu}{E} \left[ \sigma_x - \frac{\nu}{1+\nu} (\sigma_x + \sigma_y) \right] = \frac{1}{E} (\sigma_x - \nu \sigma_y), \quad (11.18)$$

$$\varepsilon_y = \frac{1+\nu}{E} \left[ \sigma_y - \frac{\nu}{1+\nu} (\sigma_x + \sigma_y) \right] = \frac{1}{E} (\sigma_y - \nu \sigma_x), \quad \gamma_{xy} = \frac{2(1+\nu)}{E} \tau_{xy}.$$

The normal strain in direction  $z$  is:

$$\varepsilon_z = \frac{1+\nu}{E} \left[ -\frac{\nu}{1+\nu} (\sigma_x + \sigma_y) \right] = -\frac{\nu}{E} (\sigma_x + \sigma_y) = -\frac{\nu}{1-\nu} (\varepsilon_x + \varepsilon_y). \quad (11.19)$$

We note, that although  $\varepsilon_z$  is not included in the equations, it can always be calculated by using the strains in the other two directions. Using the former equations we can express even the stresses:

$$\sigma_x = \frac{E}{1-\nu^2} [\varepsilon_x + \nu \varepsilon_y], \quad \sigma_y = \frac{E}{1-\nu^2} [\varepsilon_y + \nu \varepsilon_x], \quad \tau_{xy} = \frac{E}{2(1+\nu)} \gamma_{xy}. \quad (11.20)$$

An alternative formulation of the stress-strain relationship is that we collect the components in vectors:

$$\underline{\varepsilon}^T = [\varepsilon_x, \varepsilon_y, \gamma_{xy}], \quad \underline{\sigma}^T = [\sigma_x, \sigma_y, \tau_{xy}]. \quad (11.21)$$

As a result, the relationship is established through a matrix:

$$\underline{\sigma} = \underline{\underline{C}} \underline{\varepsilon}. \quad (11.22)$$

where  $\underline{\underline{C}}$  is the constitutive matrix. On the base of Eqs.(11.20)-(11.22) under plane stress state matrix  $\underline{\underline{C}}$  becomes:

$$\underline{\underline{C}}^{str} = \frac{E}{1-\nu^2} \begin{bmatrix} 1 & \nu & 0 \\ \nu & 1 & 0 \\ 0 & 0 & \frac{1-\nu}{2} \end{bmatrix}. \quad (11.23)$$

The inverse and the determinant of the matrix is:

$$\underline{\underline{C}}^{str} = \frac{1}{E} \begin{bmatrix} 1 & -\nu & 0 \\ -\nu & 1 & 0 \\ 0 & 0 & 2(1+\nu) \end{bmatrix}, \det \underline{\underline{C}}^{str} = \frac{E^3}{2(1-\nu)(1+\nu)^2}. \quad (11.24)$$

The latter form of the stress-strain relationship is applied in finite element calculations.

### 11.3.2. Plane strain state

Under plane strain state the condition is:  $\varepsilon_z = 0$ , i.e. the normal strain perpendicular to the  $x$ - $y$  plane is zero. In this case the stress and strain tensors are:

$$\underline{\underline{\sigma}} = \begin{bmatrix} \sigma_x & \tau_{xy} & 0 \\ \tau_{xy} & \sigma_y & 0 \\ 0 & 0 & \sigma_z \end{bmatrix}, \underline{\underline{\varepsilon}} = \begin{bmatrix} \varepsilon_x & 1/2 \cdot \gamma_{xy} & 0 \\ 1/2 \cdot \gamma_{xy} & \varepsilon_y & 0 \\ 0 & 0 & 0 \end{bmatrix}. \quad (11.25)$$

According to Hooke's law we obtain:

$$\sigma_x = \frac{E}{1+\nu} \left[ \varepsilon_x + \frac{\nu}{1-2\nu} (\varepsilon_x + \varepsilon_y) \right], \sigma_y = \frac{E}{1+\nu} \left[ \varepsilon_y + \frac{\nu}{1-2\nu} (\varepsilon_x + \varepsilon_y) \right],$$

$$\tau_{xy} = \frac{E}{2(1+\nu)} \gamma_{xy}, \sigma_z = \nu(\sigma_x + \sigma_y).$$

Developing the stress-strain relationship from  $\underline{\underline{\sigma}} = \underline{\underline{C}} \underline{\underline{\varepsilon}}$  we get:

$$\underline{\underline{C}}^{stn} = \frac{E}{(1+\nu)(1-2\nu)} \begin{bmatrix} 1-\nu & \nu & 0 \\ \nu & 1-\nu & 0 \\ 0 & 0 & \frac{1-2\nu}{2} \end{bmatrix}, \quad (11.27)$$

and:

$$(\underline{\underline{C}}^{stn})^{-1} = \frac{1-\nu^2}{E} \begin{bmatrix} 1 & -\frac{\nu}{1-\nu} & 0 \\ -\frac{\nu}{1-\nu} & 1 & 0 \\ 0 & 0 & \frac{2}{1-\nu} \end{bmatrix}, \det \underline{\underline{C}}^{stn} = \frac{E^3}{2(1-2\nu)(1+\nu)^3}. \quad (11.28)$$

## 11.4. Basic equations of plane elasticity

The number of unknowns in case of plane problems is always eight:  $\sigma_x$ ,  $\sigma_y$ ,  $\tau_{xy}$ ,  $\varepsilon_x$ ,  $\varepsilon_y$ ,  $\gamma_{xy}$ ,  $u$  and  $v$ . Under plane stress  $\varepsilon_z$ , under plane strain  $\sigma_z$  component can always be calculated by the help of the components in directions  $x$  and  $y$ .

### 11.4.1. Compatibility equation

The combination of Eqs.(11.10) and (11.13) leads to the so-called compatibility equation [1,2]:

$$\frac{\partial^2 \varepsilon_x}{\partial y^2} + \frac{\partial^2 \varepsilon_y}{\partial x^2} = \frac{\partial^2 \gamma_{yx}}{\partial x \partial y}. \quad (11.29)$$

The equation above is equally true for plane stress and plane strain states. It is possible to formulate the compatibility equation in terms of stresses. Let us express Eq.(11.29) in terms of stresses for plane stress state by utilizing Eq.(11.19):

$$\frac{1}{E} \left( \frac{\partial^2 \sigma_x}{\partial y^2} - \nu \frac{\partial^2 \sigma_y}{\partial y^2} + \frac{\partial^2 \sigma_y}{\partial x^2} - \nu \frac{\partial^2 \sigma_x}{\partial x^2} \right) = \frac{1}{G} \frac{\partial^2 \tau_{yx}}{\partial x \partial y}. \quad (11.30)$$

We express the mixed derivative of the shear stress from Eq.(11.4):

$$\frac{\partial^2 \tau_{xy}}{\partial x \partial y} = -\frac{1}{2} \left( \frac{\partial q_x}{\partial x} + \frac{\partial q_y}{\partial y} + \frac{\partial^2 \sigma_x}{\partial x^2} + \frac{\partial^2 \sigma_y}{\partial y^2} \right). \quad (11.31)$$

The combination of the two former equations results in:

$$\nabla^2(\sigma_x + \sigma_y) = -(1 + \nu) \left( \frac{\partial q_x}{\partial x} + \frac{\partial q_y}{\partial y} \right), \quad (11.32)$$

where:

$$\nabla^2 = \frac{\partial^2}{\partial x^2} + \frac{\partial^2}{\partial y^2}. \quad (11.33)$$

In a similar way we can develop the following equation for plane strain state:

$$\nabla^2(\sigma_x + \sigma_y) = -\frac{1}{1-\nu} \left( \frac{\partial q_x}{\partial x} + \frac{\partial q_y}{\partial y} \right). \quad (11.34)$$

It can be seen, that if there is no volume force, then the compatibility equation has the same form under plane stress as that under plane strain. In that case, when the force field is

conservative, then a potential function,  $U$  exists, of which gradient gives the components of the density vector of volume force, i.e.:

$$q_x = \frac{\partial U}{\partial x} \text{ and } q_y = \frac{\partial U}{\partial y}. \quad (11.35)$$

#### 11.4.2. Airy's stress function

The equilibrium and the compatibility equations can be reduced to one equation by introducing the Airy's stress function. Let  $\chi = \chi(x,y)$  be the Airy's stress function, which is defined in the following way [1,2]:

$$\sigma_x + U = \frac{\partial^2 \chi}{\partial y^2}, \quad \sigma_y + U = \frac{\partial^2 \chi}{\partial x^2}, \quad \tau_{xy} = -\frac{\partial^2 \chi}{\partial x \partial y}. \quad (11.36)$$

Taking them back into the equilibrium equations given by Eq.(11.4), it is seen that the equations are identically satisfied. The stress function can be derived for every stress field, which satisfies the equilibrium equations and the body force field is conservative. In terms of the stresses the compatibility equation given by Eq.(11.34) becomes:

$$\nabla^4 \chi = (1-\nu) \nabla^2 U, \quad (11.37)$$

where:

$$\nabla^4 = \nabla^2(\nabla^2) = \frac{\partial^4}{\partial x^4} + 2 \frac{\partial^4}{\partial x^2 \partial y^2} + \frac{\partial^4}{\partial y^4} \quad (11.38)$$

is called the biharmonic operator. Eq.(11.37) is the governing field equation for plane stress problems in which the body forces are conservative. If a function  $\chi = \chi(x,y)$  is found such that it satisfies Eq.(11.37) and the proper prescribed boundary conditions, then it represents the solution of the problem. The corresponding stresses and strains may be determined from Eqs.(11.36) and (11.19), respectively. If the body forces are constant, or if  $U$  is a harmonic function, then the governing equation is:

$$\nabla^4 \chi = 0, \quad (11.39)$$

which is a partial differential equation called biharmonic equation.

#### 11.4.3. Navier's equation

Now let us formulate the governing equations in terms of displacement field for plane stress state! The combination of Eqs.(11.10), (11.13) and (11.19) provides the followings [1,2]:

$$\frac{\partial u}{\partial x} = \frac{1}{E} (\sigma_x - \nu \sigma_y), \quad \frac{\partial v}{\partial y} = \frac{1}{E} (\sigma_y - \nu \sigma_x), \quad \frac{\partial u}{\partial y} + \frac{\partial v}{\partial x} = \frac{1}{G} \tau_{xy}. \quad (11.40)$$

After a simple rearrangement we obtain:

$$\sigma_x = \frac{E}{1-\nu^2} \left[ \frac{\partial u}{\partial x} + \nu \frac{\partial v}{\partial y} \right], \quad \sigma_y = \frac{E}{1-\nu^2} \left[ \frac{\partial v}{\partial y} + \nu \frac{\partial u}{\partial x} \right], \quad \tau_{xy} = \frac{E}{2(1+\nu)} \left[ \frac{\partial u}{\partial y} + \frac{\partial v}{\partial x} \right]. \quad (11.41)$$

Substitution of the above stresses into the equilibrium equation given by Eq.(11.4) gives the Navier's equation:

$$G\nabla^2 u + \frac{E}{2(1-\nu)} \frac{\partial}{\partial x} \left( \frac{\partial u}{\partial x} + \frac{\partial v}{\partial y} \right) + q_x = 0, \quad (11.42)$$

$$G\nabla^2 v + \frac{E}{2(1-\nu)} \frac{\partial}{\partial y} \left( \frac{\partial u}{\partial x} + \frac{\partial v}{\partial y} \right) + q_y = 0.$$

We can develop Navier's equation for plane strain state in a similar way, the result is:

$$G\nabla^2 u + \frac{E}{2(1+\nu)(1-2\nu)} \frac{\partial}{\partial x} \left( \frac{\partial u}{\partial x} + \frac{\partial v}{\partial y} \right) + q_x = 0, \quad (11.43)$$

$$G\nabla^2 v + \frac{E}{2(1+\nu)(1-2\nu)} \frac{\partial}{\partial y} \left( \frac{\partial u}{\partial x} + \frac{\partial v}{\partial y} \right) + q_y = 0.$$

Under plane stress state the first scalar invariant of the stress tensor is:

$$\sigma_I = \sigma_x + \sigma_y = \nabla^2 \chi. \quad (11.44)$$

#### 11.4.4. Boundary value problems

It can be shown that for plates under symmetrically distributed external forces with respect to the plane  $z = 0$ , the exact solution satisfying all of the equilibrium and compatibility equations is [2]:

$$\chi = \chi_0 - \frac{1}{2} \frac{\nu}{1+\nu} (\nabla^2 \chi_0) z^2, \quad (11.45)$$

where:

$$\chi_0 = \chi_0(x, y), \quad (11.46)$$

which satisfies

$$\nabla^4 \chi_0 = 0. \quad (11.47)$$

The second term in Eq.(11.45), however, depends on  $z$  and may be neglected for thin plates, in which case we have:

$$\nabla^4 \chi \equiv \nabla^4 \chi_0 = 0. \quad (11.48)$$

That is, for thin plates, solutions by Eq.(11.48) very closely approximate the stress distributions by Eq.(11.45).

Let us summarize what kind of requirements should be met of plane stress state! The actual elastic body must be a thin plate, the two  $z$  surfaces of the plate must be free from load, the external forces can have only  $x$  and  $y$  components, the external forces should be distributed symmetrically with respect to the  $x$  and  $y$  axes.

The governing equation system of plane problems is a system of partial differential equations (equilibrium equation, strain-displacement equation and material law) with corresponding boundary conditions. The dynamic boundary condition is the relationship between the stress tensor and the vector of external load at certain points of the lateral boundary curve:

$$\underline{\sigma} \underline{n} = \underline{p}, \quad (11.49)$$

where  $\underline{p}$  is traction vector of the corresponding boundary surface,  $\underline{n}$  is the outward normal of the boundary surface or the outward normal of a certain part of it, which is parallel to the  $x$ - $y$  plane. The kinematic boundary condition represents the imposed displacement of a point (or certain points):

$$\underline{u}(x_0, y_0) = \underline{u}_b, \quad (11.50)$$

where  $\underline{u}_b$  is the imposed displacements vector,  $x_0$  and  $y_0$  are the coordinates of the actual point. The system of governing partial differential equations together with relevant dynamic and kinematic boundary conditions built a boundary value problem.

We note that closed form solutions of the governing partial differential equations of plane problems with prescribed boundary conditions which occur in elasticity problems are very difficult to obtain directly, and they are frequently impossible to achieve. Because of this fact the inverse and semi-inverse methods may be attempted in the solution of certain problems [1]. In the inverse method we select a specific solution which satisfies the governing equations, and then search for the boundary conditions which can be satisfied by this solution, i.e., we have the solution first and then ask what problem it can solve. In the semi-inverse method, we assume a partial solution to a given problem. A partial solution consists of an assumed form for each dependent variable in terms of known and unknown functions. The assumed partial solution is then substituted into the original set of governing equations. As a result, these equations will be reduced to a set of simplified differential equations, which govern the remaining unknown functions. This simplified set of equations, together with proper boundary conditions, is then solved by direct methods.

## 11.5. Examples for plane stress

### 11.5.1. Determination of the traction on the boundaries of a square shape plate

For the square shape plate shown in Fig.11.4 we know the Airy's stress function in the  $x$ - $y$  coordinate system [3]:

$$\chi(x, y) = \frac{P_0}{a^2} \left( \frac{1}{2} x^2 y^2 - \frac{1}{6} y^4 \right). \quad (11.51)$$

where  $p_0$  is the intensity of the distributed line load. The body force is negligible; we assume that the plate is in plane stress state.

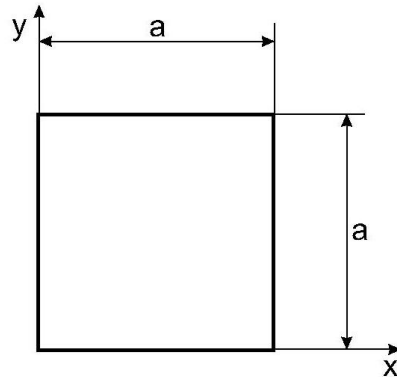


Fig.11.4. Square shape plate under plane stress.

What kind of system of forces loads the boundary curves of the plate?

First, we produce the stress field:

$$\sigma_x = \frac{\partial^2 \chi}{\partial y^2} = \frac{p_0}{a^2} (x^2 - 2y^2), \quad \sigma_y = \frac{\partial^2 \chi}{\partial x^2} = \frac{p_0}{a^2} y^2, \quad (11.52)$$

$$\tau_{xy} = \tau_{yx} = -\frac{\partial^2 \chi}{\partial x \partial y} = -\frac{p_0}{a^2} 2xy, \quad \sigma_z = 0.$$

The traction vectors can be calculated by the help of the definition of dynamic boundary condition and the localization of it into the boundary curves. Therefore, we need the outward normal of each boundary curve:

| boundary curve | constant coordinate | outward normal ( $n$ ) |
|----------------|---------------------|------------------------|
| 1              | $x = 0$             | $-i$                   |
| 2              | $x = a$             | $i$                    |
| 3              | $y = 0$             | $-j$                   |
| 4              | $y = a$             | $j$                    |

Furthermore, we need Eqs.(11.49) and (11.52). We obtain the traction vectors by applying the former equations:

$$\underline{p}_1 = -\underline{\underline{\sigma}}\underline{i} = \begin{bmatrix} \sigma_x(0, y) & \tau_{xy}(0, y) & 0 \\ \tau_{xy}(0, y) & \sigma_y(0, y) & 0 \\ 0 & 0 & 0 \end{bmatrix} \begin{bmatrix} -1 \\ 0 \\ 0 \end{bmatrix} = \begin{bmatrix} -\sigma_x(0, y) \\ 0 \\ 0 \end{bmatrix} = \begin{bmatrix} \frac{p_0}{a^2} 2y^2 \\ 0 \\ 0 \end{bmatrix}, \quad (11.53)$$

$$\underline{p}_2 = \underline{\underline{\sigma}}\underline{i} = \begin{bmatrix} \sigma_x(a, y) & \tau_{xy}(a, y) & 0 \\ \tau_{xy}(a, y) & \sigma_y(a, y) & 0 \\ 0 & 0 & 0 \end{bmatrix} \begin{bmatrix} 1 \\ 0 \\ 0 \end{bmatrix} = \begin{bmatrix} \sigma_x(a, y) \\ \tau_{xy}(a, y) \\ 0 \end{bmatrix} = \begin{bmatrix} \frac{p_0}{a^2} (a^2 - 2y^2) \\ -\frac{p_0}{a} 2y \\ 0 \end{bmatrix},$$

$$\underline{p}_3 = -\underline{\underline{\sigma}}\underline{j} = \begin{bmatrix} \sigma_x(x, 0) & \tau_{xy}(x, 0) & 0 \\ \tau_{xy}(x, 0) & \sigma_y(x, 0) & 0 \\ 0 & 0 & 0 \end{bmatrix} \begin{bmatrix} 0 \\ -1 \\ 0 \end{bmatrix} = \begin{bmatrix} -\tau_{xy}(x, 0) \\ -\sigma_y(x, 0) \\ 0 \end{bmatrix} = \begin{bmatrix} 0 \\ 0 \\ 0 \end{bmatrix},$$

$$\underline{p}_4 = \underline{\underline{\sigma}}\underline{j} = \begin{bmatrix} \sigma_x(x, a) & \tau_{xy}(x, a) & 0 \\ \tau_{xy}(x, a) & \sigma_y(x, a) & 0 \\ 0 & 0 & 0 \end{bmatrix} \begin{bmatrix} 0 \\ 1 \\ 0 \end{bmatrix} = \begin{bmatrix} \tau_{xy}(x, a) \\ \sigma_y(x, a) \\ 0 \end{bmatrix} = \begin{bmatrix} -\frac{p_0}{a} 2x \\ p_0 \\ 0 \end{bmatrix}.$$

The system of forces acting on the boundary curves can be obtained by plotting the components of the vectors above along the corresponding boundary curve. Fig.11.5 demonstrates the function plots, where Fig.11.5a depicts the loads in the normal direction (perpendicularly to the boundary curve), Fig.11.5b represents the tangential (with respect to the boundary curve) stress distributions.

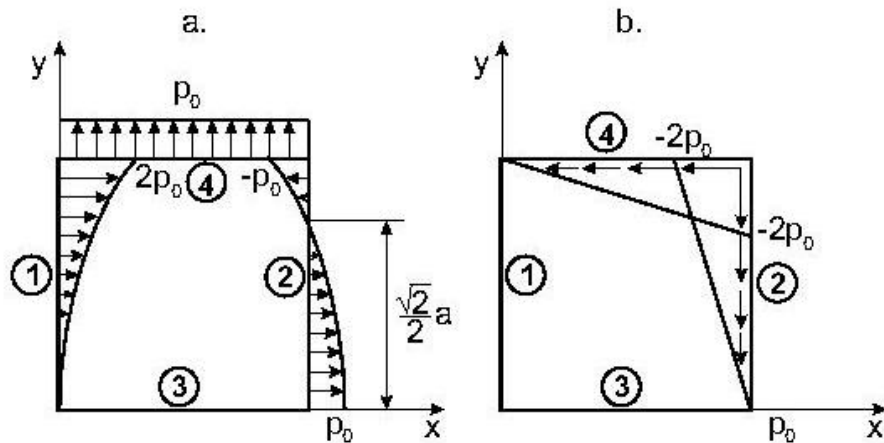


Fig.11.5. Normal (a) and tangential (b) loads on the boundary curves of a square plate under plane stress state.

### 11.5.2. Analysis of a tangentially loaded plate

For the plate shown in Fig.11.6 with dimensions of  $2h \cdot L$  the body force is negligible, we can assume plane stress state. The form of the Airy's stress function for the load shown in Fig. 11.6 is [3]:

$$\chi(x, y) = \frac{p_t}{4} \left( xy - \frac{xy^2}{h} - \frac{xy^3}{h^2} + \frac{Ly^2}{h} + \frac{Ly^3}{h^2} \right). \quad (11.54)$$

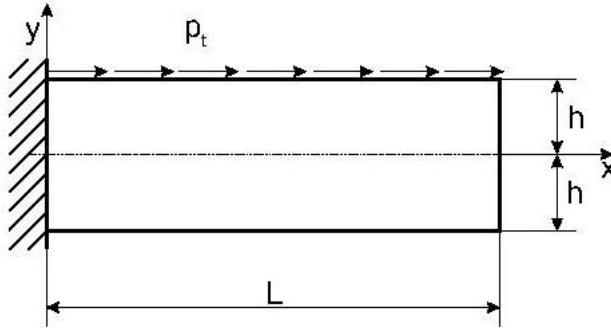


Fig.11.6. Thin plate loaded by tangentially distributed force under plane stress state.

Is the given  $\chi(x,y)$  function an exact solution of the problem above?

A function,  $\chi(x,y)$  is the exact solution of the problem if it satisfies the governing partial differential equation of plane problems and the dynamic boundary conditions. Based on the given  $\chi(x,y)$  function it is seen that Eq.(11.39) is satisfied in this case, since the governing equation is a fourth order partial differential equation, while the functions contains to a maximum the third power of  $y$ . Let us investigate the dynamic boundary conditions! Similarly to the former example we calculate the stress field first:

$$\sigma_x = \frac{\partial^2 \chi}{\partial y^2} = \frac{1}{2} p_t \left( \frac{L-x}{h} + \frac{3(L-x)}{h^2} y \right), \quad \sigma_y = \frac{\partial^2 \chi}{\partial x^2} = 0, \quad (11.55)$$

$$\tau_{xy} = \tau_{yx} = -\frac{\partial^2 \chi}{\partial x \partial y} = -\frac{1}{4} p_t \left( 1 - \frac{2y}{h} - \frac{3y^2}{h^2} \right), \quad \sigma_z = 0.$$

Based on the stresses, the loads on the boundary curves are:

$$x = L: \quad \sigma_x = 0, \quad \tau_{xy} = -\frac{1}{4} p_t \left( 1 - \frac{2y}{h} - \frac{3y^2}{h^2} \right), \quad (11.56)$$

$$y = h: \quad \sigma_y = 0, \quad \tau_{xy} = p_t,$$

$$y = -h: \quad \sigma_y = 0, \quad \tau_{xy} = 0.$$

Finally, independently of Eq.(11.56) we formulate the dynamic boundary conditions by the help of Fig. 11.6. In accordance with the dynamic boundary condition definition the stress components acting on the actual boundary curve should be equal to the corresponding (normal or tangential) components of the traction vector. That means:

$$x = L: \sigma_x = 0, \tau_{yx} = 0, \quad (11.57)$$

$$y = h: \sigma_y = 0, \tau_{xy} = p_t,$$

$$y = -h: \sigma_y = 0, \tau_{xy} = 0.$$

Comparing the boundary conditions to the boundary loads it is seen, that one condition is not satisfied, namely the shear stress,  $\tau_{yx}$  on the boundary at  $x = L$  is not zero, i.e. one of the conditions is violated. Nevertheless, there are two points, where in accordance with the formula:

$$-\frac{1}{4} p_t \left( 1 - \frac{2y}{h} - \frac{3y^2}{h^2} \right) = 0 \Rightarrow 1 - \frac{2y}{h} - \frac{3y^2}{h^2} = 0 \Rightarrow 3y^2 + 2yh - h^2 = 0, \quad (11.58)$$

with solutions of  $y_1 = 1/3 \cdot h$  and  $y_2 = -h$ , i.e. at two points the dynamic boundary condition is satisfied. As a final word, the given  $\chi(x,y)$  function is not the exact solution of the problem in Fig.11.6, because one of the dynamic boundary conditions is violated. After all, it is acceptable, since together with Eq.(11.39) the given function satisfies eight from the total ten conditions. It should be highlighted, that the boundary at  $x = 0$  is a fixed boundary, which involves kinematic boundary condition, that is why we did not investigated this boundary curve in the example.

## 11.6. The governing equation of plane problems using polar coordinates

The solutions of many elasticity problems are conveniently formulated in terms of cylindrical coordinates. On the base of Fig.11.7 we have the functional relations [1]:

$$x = r \cos \vartheta, y = r \sin \vartheta, \quad (11.59)$$

$$\vartheta = \arctan \frac{y}{x}, \quad r^2 = x^2 + y^2.$$

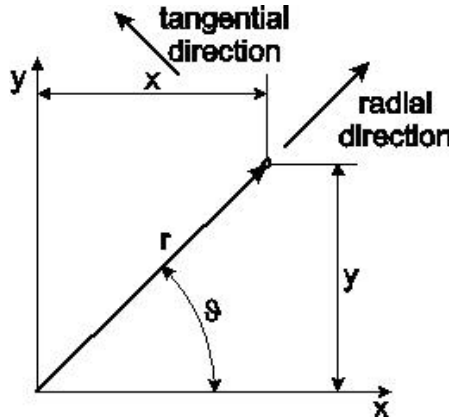


Fig.11.7. Parameters of a polar coordinate system.

The derivatives of the polar coordinates with respect to  $x$  and  $y$  using the last of Eq.(11.59) are:

$$\frac{\partial r}{\partial x} = \frac{x}{r} = \cos \vartheta, \quad \frac{\partial r}{\partial y} = \frac{y}{r} = \sin \vartheta, \quad (11.60)$$

$$\frac{\partial \vartheta}{\partial x} = -\frac{y}{r^2} = -\frac{\sin \vartheta}{r}, \quad \frac{\partial \vartheta}{\partial y} = \frac{x}{r^2} = \frac{\cos \vartheta}{r}.$$

Again, the derivatives with respect to  $x$  and  $y$  can be formulated based on the chain rule:

$$\frac{\partial}{\partial x} = \frac{\partial r}{\partial x} \frac{\partial}{\partial r} + \frac{\partial \vartheta}{\partial x} \frac{\partial}{\partial \vartheta} = \cos \vartheta \frac{\partial}{\partial r} - \frac{\sin \vartheta}{r} \frac{\partial}{\partial \vartheta}, \quad (11.61)$$

$$\frac{\partial}{\partial y} = \frac{\partial r}{\partial y} \frac{\partial}{\partial r} + \frac{\partial \vartheta}{\partial y} \frac{\partial}{\partial \vartheta} = \sin \vartheta \frac{\partial}{\partial r} + \frac{\cos \vartheta}{r} \frac{\partial}{\partial \vartheta}$$

To derive the governing equations in terms of polar coordinates we incorporate the stress transformation expressions [1]. The normal and shear stresses are transformed to a coordinate system given by rotation about axis  $z$  by an angle  $\vartheta$ :

$$\underline{\sigma}_n = \underline{n}^T \underline{\underline{\sigma}} \underline{n}, \quad \underline{\tau}_{mn} = \underline{m}^T \underline{\underline{\sigma}} \underline{n}, \quad (11.62)$$

where:

$$\underline{n}^T = [\cos \vartheta \quad \sin \vartheta \quad 0], \quad \underline{m}^T = [-\sin \vartheta \quad \cos \vartheta \quad 0], \quad (11.63)$$

which leads to:

$$\sigma_x = \sigma_r \cos^2 \vartheta + \sigma_\vartheta \sin^2 \vartheta + \tau_{r\vartheta} \sin 2\vartheta, \quad (11.64)$$

$$\sigma_y = \sigma_r \sin^2 \vartheta + \sigma_\vartheta \cos^2 \vartheta - \tau_{r\vartheta} \sin 2\vartheta,$$

$$\tau_{xy} = (\sigma_\vartheta - \sigma_r) \sin \vartheta \cos \vartheta + \tau_{r\vartheta} (\cos^2 \vartheta - \sin^2 \vartheta),$$

The strain components ( $\varepsilon_x$ ,  $\varepsilon_y$ ,  $\gamma_{xy}$ ) can be transformed similarly. Taking Eq.(11.64) back into the equilibrium equations given by Eq.(11.4), moreover by assuming that there are also body forces, we have [1,2]:

$$\frac{\partial \sigma_r}{\partial r} + \frac{1}{r} \frac{\partial \tau_{r\vartheta}}{\partial \vartheta} + \frac{\sigma_r - \sigma_\vartheta}{r} + q_r = 0, \quad (11.65)$$

$$\frac{1}{r} \frac{\partial \sigma_\vartheta}{\partial \vartheta} + \frac{\partial \tau_{r\vartheta}}{\partial r} + \frac{2\tau_{r\vartheta}}{r} + q_\vartheta = 0,$$

where the former is the equation in the radial, the latter is the equation in the tangential direction. By a similar technique, the strain-displacement equations may be transformed into:

$$\varepsilon_r = \frac{\partial u_r}{\partial r}, \quad \varepsilon_\vartheta = \frac{u_r}{r} + \frac{1}{r} \frac{\partial u_\vartheta}{\partial \vartheta}, \quad \gamma_{r\vartheta} = \frac{1}{r} \frac{\partial u_r}{\partial \vartheta} + \frac{\partial u_\vartheta}{\partial r} - \frac{u_\vartheta}{r}, \quad (11.66)$$

where  $u_r$  and  $u_\vartheta$  are the radial and tangential displacements. Eliminating the displacement components we obtain the compatibility equation:

$$\frac{\partial^2 \varepsilon_\vartheta}{\partial r^2} + \frac{1}{r^2} \frac{\partial^2 \varepsilon_r}{\partial \vartheta^2} + \frac{2}{r} \frac{\partial \varepsilon_\vartheta}{\partial r} - \frac{1}{r} \frac{\partial \varepsilon_r}{\partial \vartheta} = \frac{1}{r} \frac{\partial^2 \gamma_{r\vartheta}}{\partial r \partial \vartheta} + \frac{1}{r^2} \frac{\partial \gamma_{r\vartheta}}{\partial \vartheta}. \quad (11.67)$$

In the case of Hooke's law there is no need to perform the transformation, due to the fact that the polar coordinate system is an orthogonal system. Therefore, e.g. in Eq.(11.20) referring to plane stress state, we have to substitute  $x$  by  $r$ , and  $y$  by  $\vartheta$ :

$$\varepsilon_r = \frac{1}{E} (\sigma_r - \nu \sigma_\vartheta), \quad \varepsilon_\vartheta = \frac{1}{E} (\sigma_\vartheta - \nu \sigma_r), \quad \gamma_{r\vartheta} = \frac{2(1+\nu)}{E} \tau_{r\vartheta}, \quad (11.68)$$

$$\sigma_r = \frac{E}{1-\nu^2} [\varepsilon_r + \nu \varepsilon_\vartheta], \quad \sigma_\vartheta = \frac{E}{1-\nu^2} [\varepsilon_\vartheta + \nu \varepsilon_r], \quad \tau_{r\vartheta} = \frac{E}{2(1+\nu)} \gamma_{r\vartheta}.$$

The formulation incorporating plane strain state based on Eq.(11.26) leads to:

$$\varepsilon_r = \frac{1-\nu^2}{E} (\sigma_r - \frac{\nu}{1-\nu} \sigma_\vartheta), \quad \varepsilon_\vartheta = \frac{1-\nu^2}{E} (\sigma_\vartheta - \frac{\nu}{1-\nu} \sigma_r), \quad \gamma_{r\vartheta} = \frac{2(1+\nu)}{E} \tau_{r\vartheta}, \quad (11.69)$$

$$\sigma_r = \frac{E}{1+\nu} \left[ \varepsilon_r + \frac{\nu}{1-2\nu} (\varepsilon_r + \varepsilon_\vartheta) \right], \quad \sigma_\vartheta = \frac{E}{1+\nu} \left[ \varepsilon_\vartheta + \frac{\nu}{1-2\nu} (\varepsilon_r + \varepsilon_\vartheta) \right], \quad \tau_{r\vartheta} = \frac{E}{2(1+\nu)} \gamma_{r\vartheta}.$$

The first scalar invariant of the strain tensor (plane dilatation) under plane strain state is:

$$\varepsilon_I = \varepsilon_r + \varepsilon_\vartheta = \frac{1}{r} \frac{\partial(ru_r)}{\partial r} + \frac{1}{r} \frac{\partial u_\vartheta}{\partial \vartheta}. \quad (11.70)$$

Substituting the stress and strain components into the equilibrium equation given by Eq.(11.65) (plane strain) and incorporating the first scalar invariant we obtain the Navier's equation in terms of polar coordinates [1,2]:

$$(\lambda + 2G) \frac{\partial \varepsilon_I}{\partial r} - \frac{2G}{r} \frac{\partial \omega}{\partial \vartheta} + q_r = 0, \quad (11.71)$$

$$(\lambda + 2G) \frac{1}{r} \frac{\partial \varepsilon_I}{\partial \vartheta} + 2G \frac{\partial \omega}{\partial r} + q_\vartheta = 0,$$

where

$$\omega = \frac{1}{2r} \left( \frac{\partial(ru_\vartheta)}{\partial r} - \frac{\partial u_r}{\partial \vartheta} \right) \quad (11.72)$$

is the rotation about axis  $z$ ,  $\lambda$  is the Lamé-constant:

$$\lambda = \frac{\nu E}{(1+\nu)(1-2\nu)}. \quad (11.73)$$

The governing equation of plane problems in terms of polar coordinates can be formulated by using the Hamilton operator. Based on Eqs.(11.48) and (11.61) we get:

$$\nabla^4 \chi = \nabla^2 \nabla^2 \chi = \left( \frac{\partial^2}{\partial r^2} + \frac{1}{r} \frac{\partial}{\partial r} + \frac{1}{r^2} \frac{\partial^2}{\partial \vartheta^2} \right) \left( \frac{\partial^2}{\partial r^2} + \frac{1}{r} \frac{\partial}{\partial r} + \frac{1}{r^2} \frac{\partial^2}{\partial \vartheta^2} \right) \chi = 0. \quad (11.74)$$

The stresses may be obtained by using the differential quotients given by Eq.(11.61) and the transformation expressions given by Eq.(11.64):

$$\sigma_r = \frac{1}{r} \frac{\partial \chi}{\partial r} + \frac{1}{r^2} \frac{\partial^2 \chi}{\partial \vartheta^2}, \quad \sigma_\vartheta = \frac{\partial^2 \chi}{\partial r^2}, \quad \tau_{r\vartheta} = -\frac{\partial}{\partial r} \left( \frac{1}{r} \frac{\partial \chi}{\partial \vartheta} \right). \quad (11.75)$$

The last three formulae are equally valid under plane stress and plane strain states. The equilibrium equations, strain-displacement relationship can also be formulated by using infinitesimal elements in polar coordinate system [1].

### 11.7. Axisymmetric plane problems

The use of polar coordinates is particularly convenient in the solution of revolution symmetric or in other words axisymmetric problems. In this case displacement field, stresses are independent of the angle coordinate ( $\vartheta$ ), consequently the derivates with respect to  $\vartheta$  vanish everywhere. In accordance with Eq.(11.74) the governing equation of plane problems becomes:

$$\left( \frac{d^4}{dr^4} + \frac{2}{r} \frac{d^3}{dr^3} - \frac{1}{r^2} \frac{d^2}{dr^2} + \frac{1}{r^3} \frac{d}{dr} \right) \chi = 0. \quad (11.76)$$

By introducing a new independent variable,  $\xi$ , this equation can be reduced to a differential equation with constant coefficients:

$$r = e^\xi. \quad (11.77)$$

As a result, Eq.(11.76) becomes:

$$\left( \frac{d^4}{d\xi^4} - 4 \frac{d^3}{d\xi^3} + 4 \frac{d^2}{d\xi^2} \right) \chi = 0, \quad (11.78)$$

for which the general solution is:

$$\chi = A\xi e^{2\xi} + B\xi e^{-2\xi} + C\xi + D. \quad (11.79)$$

Taking back  $e^\xi$  we have:

$$\chi = Ar^2 \ln r + Br^2 + C \ln r + D, \quad (11.80)$$

where  $A, B, C$  and  $D$  are constants. The stresses based on Eq.(11.75) are:

$$\sigma_r = \frac{1}{r} \frac{\partial \chi}{\partial r}, \sigma_\vartheta = \frac{\partial^2 \chi}{\partial r^2}, \tau_{r\vartheta} = 0. \quad (11.81)$$

Taking the solution function back we see that:

$$\sigma_r = 2A \ln r + \frac{C}{r^2} + A + 2B, \sigma_\vartheta = 2A \ln r - \frac{C}{r^2} + 3A + 2B, \tau_{r\vartheta} = 0. \quad (11.82)$$

#### 11.7.1. Solid circular cylinder and thick-walled tube

Let us see some examples for the application of the equations and formulae above [1]! For a solid circular cylinder the stresses at  $r = 0$  can not be infinitely high, therefore:

$$A = C = 0. \quad (11.83)$$

The stresses in a solid circular cylinder are:

$$\sigma_r = \sigma_\theta = 2B, \tau_{r\theta} = 0. \quad (11.84)$$

This is the solution of a circular cylinder loaded by external pressure with magnitude of  $2B$  on the outer surface. In the case of a hollow circular cylinder or a thick-walled tube (Fig.11.8a) it is not sufficient to investigate only the dynamic boundary conditions, we need to impose also kinematic boundary conditions.

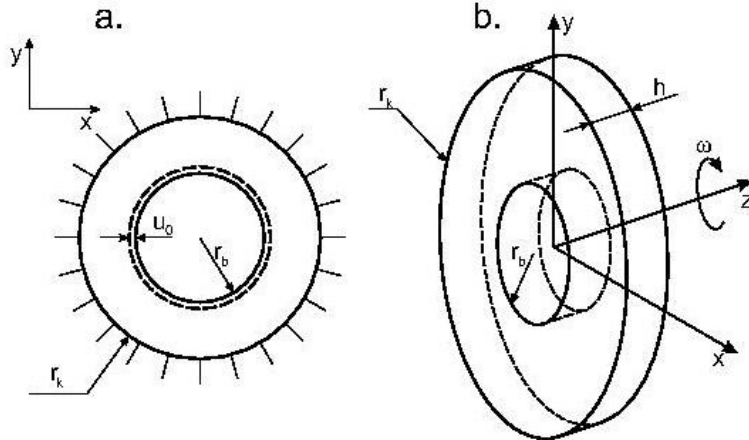


Fig.11.8. Hollow circular cylinder with imposed displacement at the inner boundary (a), thick-walled rotating disk (b).

The strain components by using Eq.(11.66) become:

$$\varepsilon_r = \frac{du_r}{dr}, \varepsilon_\theta = \frac{u_r}{r}, \gamma_{r\theta} = 0. \quad (11.85)$$

Using the stress-strain relationship given by Eq.(11.68) we obtain the equations below:

$$\frac{du_r}{dr} = K_1(\sigma_r - K_2\sigma_\theta), \frac{u_r}{r} = K_1(\sigma_\theta - K_2\sigma_r), \quad (11.86)$$

where:

$$K_1 = \frac{1}{E}, \quad K_2 = \frac{\nu}{1-\nu}, \quad (11.87)$$

for plane stress, and

$$K_1 = \frac{1-\nu^2}{E}, \quad K_2 = \nu, \quad (11.88)$$

for plane strain. Next, we express the strain components:

$$\frac{du_r}{dr} = K_1(2A \ln r + \frac{C}{r^2} + A + 2B - K_2(2A \ln r - \frac{C}{r^2} + 3A + 2B)), \quad (11.89)$$

$$\frac{u_r}{r} = K_1(2A \ln r - \frac{C}{r^2} + 3A + 2B - K_2(2A \ln r + \frac{C}{r^2} + A + 2B)).$$

Integrating the former equation we get:

$$u_r = K_1(2Ar \ln r - Ar + 2Br - \frac{C}{r}) - K_2(2Ar \ln r + Ar + 2Br + \frac{C}{r}) + H, \quad (11.90)$$

where  $H$  is an integration constant. Dividing the formulae above by  $r$  and equating it to the second of Eq.(11.89) gives the following:

$$4Ar - H = 0. \quad (11.91)$$

Since the equation must be satisfied for all values of  $r$  in the region, we must consider the trivial solution:

$$A = H = 0. \quad (11.92)$$

The remaining constants,  $B$  and  $C$ , are to be determined from the boundary conditions imposed on the inner and outer boundary surfaces. Therefore, the general solution is:

$$u_r(r) = K_1(2Br(1 - K_2)) - \frac{C}{r}(1 + K_2). \quad (11.93)$$

The problem of hollow circular cylinder can also be solved by Navier's equation. If the displacement field is independent of coordinate  $\vartheta$ , then  $\omega = 0$ , i.e. from Eqs.(11.70)-(11.71) we obtain:

$$\frac{d^2 u_r}{dr^2} + \frac{1}{r} \frac{du_r}{dr} - \frac{u_r}{r^2} = 0, \quad (11.94)$$

for which the general solution is:

$$u_r(r) = c_1 r + \frac{c_2}{r}. \quad (11.95)$$

It is seen that it is mathematically identical to (11.93). For a circular cylinder with fixed outer surface and with internal pressure the kinematic boundary conditions are:

$$u_r(r_b) = u_0, \quad u_r(r_k) = 0. \quad (11.96)$$

Based on the solution function the constants are:

$$c_1 = \frac{r_b}{r_b^2 - r_k^2} u_0, \quad c_2 = \frac{-r_b r_k^2}{r_b^2 - r_k^2} u_0, \quad (11.97)$$

and the solution is:

$$u_r(r) = \frac{r_b u_0}{r_b^2 - r_k^2} \left( r - \frac{r_k^2}{r} \right). \quad (11.98)$$

The strain components are to be determined by Eq.(11.85), the stresses by Eq.(11.68).

### 11.7.2. Rotating disks

If the thickness of the circular cylinder is small, then it is said to be a disk (Fig.11.8b). If the disk rotates, then there is a body force in the reference coordinate system. The equilibrium equation in the radial direction (see Eq.(11.65)) becomes [2]:

$$\frac{d\sigma_r}{dr} + \frac{\sigma_r - \sigma_g}{r} + q_r = 0 \text{ and } q_r = \rho r \omega^2, \quad (11.99)$$

where  $\omega$  is the angular velocity of the disk,  $\rho$  is the density of the disk material. Rearranging the equation we obtain:

$$\frac{d}{dr}(r\sigma_r) - \sigma_g + \rho r^2 \omega^2 = 0. \quad (11.100)$$

This equation can be satisfied by introducing the stress function,  $F$ , in accordance with the following:

$$r\sigma_r = F, \quad \sigma_g = \frac{dF}{dr} + \rho r^2 \omega^2. \quad (11.101)$$

The strain components have already been derived for a hollow circular cylinder, eliminating  $u_r$  from Eq.(11.85) we obtain:

$$\varepsilon_g - \varepsilon_r + r \frac{d\varepsilon_g}{dr} = 0. \quad (11.102)$$

Assuming plane stress state and utilizing Eq.(11.68) we have:

$$\varepsilon_r = \frac{1}{E}(\sigma_r - \nu \sigma_g) = \frac{1}{E} \left( \frac{F}{r} - \nu \left( \frac{dF}{dr} + \rho r^2 \omega^2 \right) \right), \quad (11.103)$$

$$\varepsilon_g = \frac{1}{E}(\sigma_g - \nu \sigma_r) = \frac{1}{E} \left( \frac{dF}{dr} + \rho r^2 \omega^2 - \nu \frac{F}{r} \right).$$

Taking it back into Eq.(11.101) yields the following:

$$r^2 \frac{d^2 F}{dr^2} + r \frac{dF}{dr} - F + (3+\nu)\rho r^3 \omega^2 = 0, \quad (11.104)$$

i.e. we have a second order differential equation for the stress function, which involves the following solution:

$$F = Ar + B \frac{1}{r} - \frac{3+\nu}{8} \rho r^3 \omega^2. \quad (11.105)$$

The stress components based on Eq.(11.101) are:

$$\sigma_r(r) = A + B \frac{1}{r^2} - \frac{3+\nu}{8} \rho r^2 \omega^2, \quad \sigma_\theta(r) = A - B \frac{1}{r^2} - \frac{1+3\nu}{8} \rho r^2 \omega^2, \quad (11.106)$$

where  $A$  and  $B$  are integration constants, which can be determined by the boundary conditions. To calculate the displacement field we incorporate Eq.(11.85), from which we have:

$$\frac{du_r}{dr} = A \frac{(1-\nu)}{E} + B \frac{(1+\nu)}{Er^2} - \frac{3(1-\nu^2)}{8E} \rho r^2 \omega^2, \quad (11.107)$$

and the integration of it yields:

$$u_r(r) = A \frac{(1-\nu)}{E} r - B \frac{(1+\nu)}{Er} - \frac{(1-\nu^2)}{8E} \rho r^3 \omega^2 \quad (11.108)$$

The basic equations of the rotating disk are then:

$$\sigma_r(r) = A + B \frac{1}{r^2} + C_1 r^2, \quad (11.109)$$

$$\sigma_\theta(r) = A - B \frac{1}{r^2} + C_2 r^2,$$

$$u_r(r) = ar - b \frac{1}{r} + cr^3,$$

where:

$$C_1 = -\frac{3+\nu}{8} \rho \omega^2, \quad C_2 = -\frac{1+3\nu}{8} \rho \omega^2, \quad (11.110)$$

$$a = A \frac{(1-\nu)}{E}, b = B \frac{(1+\nu)}{E}, c = -\frac{(1-\nu^2)}{8E} \rho \omega^2. \quad (11.111)$$

Let us solve an example using the equations above! The elastic disk shown in Fig.11.9 is fixed to the shaft with an overlap of  $\delta$  [3].

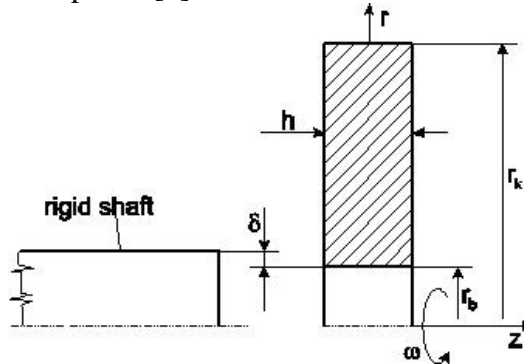


Fig.11.9. Rotating disk on a rigid shaft.

*Given:*

$$r_b = 0,02 \text{ m}, r_k = 0,2 \text{ m}, h = 0,04 \text{ m}, \delta = 0,02 \cdot 10^{-3} \text{ m}, \rho = 7800 \text{ kg/m}^3, E = 200 \text{ GPa}, \nu = 0,3.$$

- a. How large can be the maximum angular velocity if we want the disk not to get loose?
- b. Calculate the contact pressure between the shaft and disk, when the structure does not rotate!

For point a. first we formulate the boundary conditions. A kinematic boundary condition is, that the radial displacement on the inner surface of the disk must be equal to the value of overlap:

$$u_r(r_b) = \delta \Rightarrow ar_b - b \frac{1}{r_b} + cr_b^3 = \delta. \quad (11.112)$$

The outer surface of the disk is free to load, therefore in accordance with the dynamic boundary condition, the radial stress perpendicular to the outer surface is zero:

$$\sigma_r(r_k) = 0 \Rightarrow A + B \frac{1}{r_k^2} + C_1 r_k^2 = 0. \quad (11.113)$$

If the disk gets loose, then a free surface is created, that is why the radial stress should be equal to zero, i.e.:

$$\sigma_r(r_b) = 0 \Rightarrow A + B \frac{1}{r_b^2} + C_1 r_b^2 = 0. \quad (11.114)$$

The system of equations contains three unknowns:  $A$ ,  $B$  and  $\omega$ , since  $a$  and  $b$  are not independent of  $A$  and  $B$ . We now subtract Eq.(11.113) from Eq.(11.114) and we obtain:

$$B\left(\frac{1}{r_k^2} - \frac{1}{r_b^2}\right) + C_1(r_k^2 - r_b^2) = 0 \Rightarrow B = C_1 r_b^2 r_k^2. \quad (11.115)$$

The back substitution into Eq.(11.114) gives:

$$A = -C_1(r_b^2 + r_k^2), \quad (11.116)$$

consequently:

$$a = -\frac{(1-\nu)}{E} C_1(r_b^2 + r_k^2), \quad b = \frac{(1+\nu)}{E} C_1 r_b^2 r_k^2. \quad (11.117)$$

Taking the constants back into the kinematic boundary condition equation yields:

$$-\frac{(1-\nu)}{E} C_1(r_b^2 + r_k^2) r_b - \frac{(1+\nu)}{E} C_1 r_b^2 r_k^2 \frac{1}{r_b} - \frac{(1-\nu^2)}{8E} \rho \omega^2 r_b^3 = \delta. \quad (11.118)$$

Incorporating the constant  $C_1$ , and rearranging the resulting equation the maximum angular velocity becomes:

$$\omega = 880,5 \text{ rad/s} = \omega_{\max}. \quad (11.119)$$

In terms of the angular velocity the constants can be determined:

$$A = 1,008 \cdot 10^8 \text{ Pa}, \quad B = -39915 \text{ N}, \quad C_1 = -2,495 \cdot 10^9 \text{ N/m}^4, \quad (11.120)$$

$$C_2 = -1,436 \cdot 10^9 \text{ N/m}^4, \quad a = 3,53 \cdot 10^{-4}, \quad b = 2,59 \cdot 10^{-7} \text{ m}^2, \quad c = -3,439 \cdot 10^{-3} \text{ 1/m}^2.$$

For point  $b$ . we find out that if the disk does not rotate then  $\omega = 0$  and this way:  $C_1 = C_2 = c = 0$ . Under these circumstances the radial displacement on the inner surface must be equal to the value of overlap:

$$u_r(r_b) = \delta \Rightarrow ar_b - b \frac{1}{r_b} + cr_b^3 = \delta. \quad (11.121)$$

The outer surface of the disk is still free to load, i.e.:

$$\sigma_r(r_k) = 0 \Rightarrow A + B \frac{1}{r_k^2} + C_1 r_k^2 = 0. \quad (11.122)$$

The solution is:

$$A = 1,530 \cdot 10^6 \text{ Pa}, \quad B = -61208,9 \text{ N}, \quad (11.123)$$

$$a = 5,356 \cdot 10^{-6}, b = 3,978 \cdot 10^{-7} \text{ m}^2.$$

The distribution of the radial and tangential stresses under two different conditions are demonstrated in Fig.11.10.

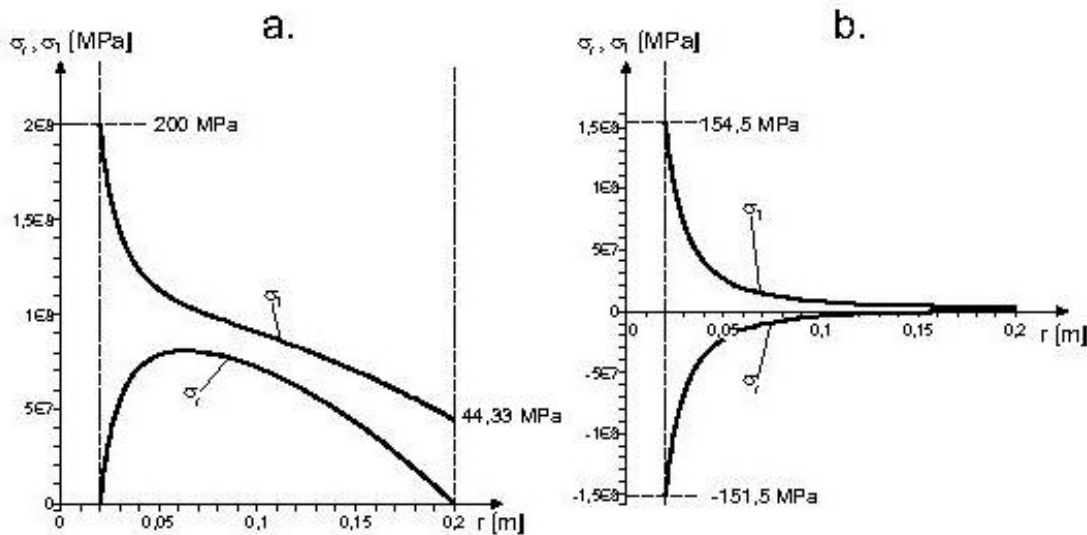


Fig.11.10. Distribution of the radial and tangential stresses in the disk structure when the structure rotates (a) and when there is no rotation (b).

## 11.8. Bibliography

- [1] Pei Chi Chou, Nicholas J. Pagano, *Elasticity – Tensor, dyadic and engineering approaches*, D. Van Nostrand Company, Inc., 1967, Princeton, New Jersey, Toronto, London.
- [2] S. Timoshenko, J. N. Godier. *Theory of elasticity*. McGraw-Hill Book Company, Inc., 1951, New York, Toronto, London.
- [3] József Uj, *Lectures and practices of the subject Elasticity and FEM*, Budapest University of Technology and Economics, Faculty of Mechanical Engineering, Department of Applied Mechanics, 1998/1999 autumn semester, Budapest (in Hungarian).

## 12. MODELING OF PLANE STRESS STATE USING FEM SOFTWARE SYSTEMS. MODELING, ANALYSIS OF PROBLEM EVALUATION

### 12.1. Finite element solution of plane problems

In the application of the finite element method we divide the plane domain of the whole structure into discrete elements as it is illustrated in Fig.12.1 [1].

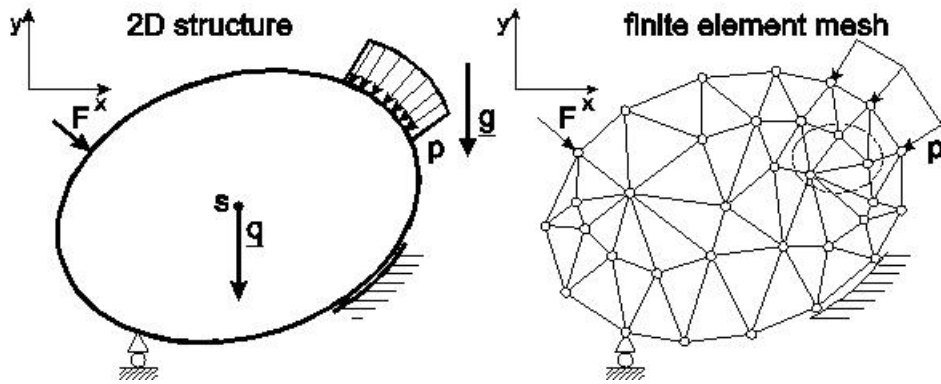


Fig.12.1. The basic concept of the finite element method in the case of plane elements.

In the FE method we apply the minimum principle of the total potential energy to develop the finite element equilibrium equations. For a single plane element the total potential energy is [2]:

$$\Pi_e = U - W = \frac{1}{2} \int_{V_e} \underline{\sigma}^T \underline{\varepsilon} dV - \int_{A_{pe}} \underline{u}^T \underline{p} dA - \int_{V_e} \underline{u}^T \underline{q} dV - \sum_{i=1}^n \underline{u}^T (x_i, y_i) \underline{F}_i, \quad (12.1)$$

where  $\underline{\sigma}$  is the vector of stress components,  $\underline{\varepsilon}$  is the vector strain components, respectively:

$$\underline{\varepsilon}^T = [\varepsilon_x, \varepsilon_y, \gamma_{xy}], \quad (12.2)$$

$$\underline{\sigma}^T = [\sigma_x, \sigma_y, \tau_{xy}],$$

moreover  $\underline{u} = u \cdot \underline{i} + v \cdot \underline{j}$  is the displacement vector field,  $\underline{p}$  is the density vector of surface forces,  $\underline{q}$  is the density vector of volume (or body) forces,  $\underline{F}_i$  is the vector of concentrated forces acting on the plane element with coordinates of point of action,  $x_i$  and  $y_i$ ,  $A_{pe}$  is that part of the boundary curves, which is loaded by surfaces forces,  $V_e$  is the volume of the element, respectively. We provide the displacement vector field by interpolation:

$$\underline{u}(x, y) = \underline{\underline{N}}(x, y) \underline{u}_e, \quad (12.3)$$

where  $\underline{\underline{N}}$  is the matrix of interpolation functions, its dimension depends on the degrees of freedom of the plane element,  $\underline{u}_e$  is vector of nodal displacements. Referring to the basic equations of elasticity, the relationship between the strain and displacement fields in matrix form is:

$$\underline{\varepsilon} = \underline{\underline{\partial}} \underline{u}, \quad (12.4)$$

where  $\underline{\underline{\partial}}$  is the matrix of differential operators, it can be obtained by Eqs.(11.10) and (11.13):

$$\underline{\underline{\partial}} = \begin{bmatrix} \frac{\partial}{\partial x} & 0 \\ 0 & \frac{\partial}{\partial y} \\ \frac{\partial}{\partial y} & \frac{\partial}{\partial x} \end{bmatrix}. \quad (12.5)$$

The combination of the latter relations gives:

$$\underline{\varepsilon} = \underline{\underline{\partial}} \underline{u} = \underline{\underline{\underline{N}}} \underline{u}_e = \underline{\underline{\underline{B}}} \underline{u}_e, \quad (12.6)$$

where  $\underline{\underline{\underline{B}}}$  is the strain-displacement matrix. The stress field can be obtained by:

$$\underline{\sigma} = \underline{\underline{C}} \underline{\varepsilon}, \quad \underline{\sigma} = \underline{\underline{\underline{C}}} \underline{u}_e, \quad (12.7)$$

where  $\underline{\underline{C}}$  is the constitutive matrix – its calculation has already been made in section 11 for plane stress and plane strain states. The strain energy for a single finite element is:

$$U_e = \frac{1}{2} \int_{V_e} \underline{\sigma}^T \underline{\varepsilon} dV = \frac{1}{2} \int \int \underline{u}_e^T \underline{\underline{\underline{B}}}^T \underline{\underline{C}}^T \underline{\underline{\underline{B}}} \underline{u}_e v dx dy = \frac{1}{2} \underline{u}_e^T \underline{\underline{\underline{K}}}_e \underline{u}_e, \quad (12.8)$$

where  $\underline{\underline{\underline{K}}}_e$  is the element stiffness matrix,

$$\underline{\underline{\underline{K}}}_e = \int_{V_e} \underline{\underline{\underline{B}}}^T \underline{\underline{C}}^T \underline{\underline{\underline{B}}} dV = \int \int \underline{\underline{\underline{B}}}^T \underline{\underline{C}}^T \underline{\underline{\underline{B}}} v dx dy, \quad (12.9)$$

its dimension depends on the degrees of freedom of the element. For plane elements the differential volume is written in the form of:  $dV = v dA = v dx dy$ , where  $v$  is the thickness of element. The work of external forces acting on the element by the help of Eq.(12.3) becomes:

$$W_e = \int_{A_{pe}} \underline{u}^T \underline{p} dA + \int_{V_e} \underline{u}^T \underline{q} dV + \sum_{i=1}^n \underline{u}^T (x_i, y_i) \underline{F}_i = \underline{u}_e^T \int_{A_{pe}} \underline{\underline{\underline{N}}}^T \underline{p} dA + \underline{u}_e^T \int_{V_e} \underline{\underline{\underline{N}}}^T \underline{q} dV + \underline{u}_e^T \underline{F}_{ec}, \quad (12.10)$$

where  $\underline{F}_{ec}$  is the vector of concentrated forces acting in the nodes of element. Thus, the total potential energy can be written as:

$$\Pi_e = \frac{1}{2} \underline{u}_e^T \underline{\underline{K}}_e \underline{u}_e - \underline{u}_e^T \underline{F}_e, \quad (12.11)$$

where:

$$\underline{F}_e = \int_{A_{pe}} \underline{\underline{N}}^T \underline{p} dA + \int_{V_e} \underline{\underline{N}}^T \underline{q} dV + \underline{F}_{ec} = \underline{F}_{eb} + \underline{F}_{ep} + \underline{F}_{ec}, \quad (12.12)$$

is the vector forces acting on the element. We can formulate the equilibrium equation in the element level by means of the minimum principle of the total potential energy:

$$\underline{\underline{K}}_e \underline{u}_e - \underline{F}_e = 0. \quad (12.13)$$

The assembly of element stiffness matrices, vector of nodal displacements and forces leads to the structural equilibrium equation:

$$\underline{\underline{K}} \underline{U} - \underline{F} = 0, \quad (12.14)$$

where  $\underline{\underline{K}}$  is structural stiffness matrix,  $\underline{U}$  is the structural vector of nodal displacements,  $\underline{F}$  is the structural vector of nodal forces, respectively. That is, the finite element equilibrium equation is a system of algebraic equations for which the solutions are the values of nodal displacements. In terms of the nodal displacements we can calculate the nodal forces and stresses.

For the solution of plane problems there exist many types of plane elements. In the sequel we review the simplest element types.

## 12.2. Linear three node triangle element

The linear triangle element (Turner triangle) [1,3], which is often called the triangle membrane element or constant strain triangle (CST) element is depicted in Fig.12.2. At each node there are two degrees of freedom. Consequently the degrees of freedom are equal to six for the whole element. The arrow in the center point of the element refers to the orientation of the element, i.e. for each element we have a direction, which means how the nodes are followed by each other.

### 12.2.1. Interpolation of the displacement field

We collect the nodal  $x, y$  coordinates and displacement components in vectors:

$$\underline{x}_e^T = [x_1 \quad y_1 \quad x_2 \quad y_2 \quad x_3 \quad y_3], \quad (12.15)$$

$$\underline{u}_e^T = [u_1 \quad v_1 \quad u_2 \quad v_2 \quad u_3 \quad v_3].$$

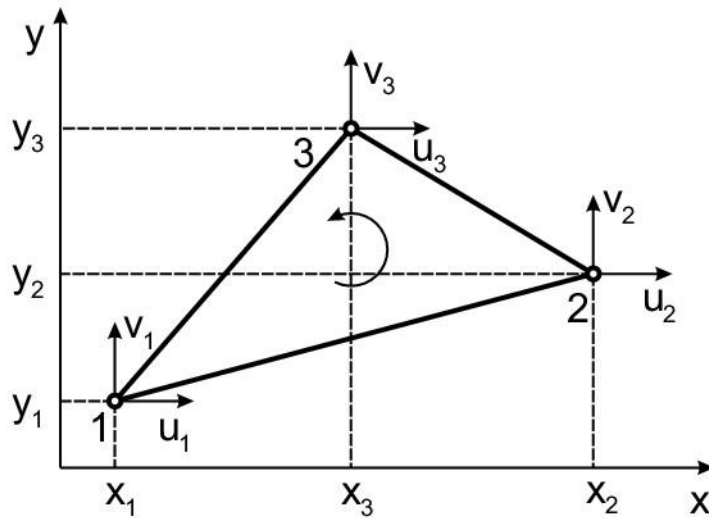


Fig.12.2. Linear triangle element. Nodal coordinates and displacements.

The triangle area can be expressed as a determinant:

$$2A_e = \begin{vmatrix} 1 & x_1 & y_1 \\ 1 & x_2 & y_2 \\ 1 & x_3 & y_3 \end{vmatrix} = (x_2 y_3 - x_3 y_2) + (x_3 y_1 - x_1 y_3) + (x_1 y_2 - x_2 y_1) = \alpha_1 + \alpha_2 + \alpha_3. \quad (12.16)$$

The  $u$  and  $v$  components of the displacement field are formulated as the linear function of  $x$  and  $y$ :

$$u(x, y) = a_0 + a_1 x + a_2 y, \quad (12.17)$$

$$v(x, y) = b_0 + b_1 x + b_2 y,$$

where  $a_0, a_1, a_2, b_0, b_1$  and  $b_2$  are unknown constants. The vector of strain components is:

$$\underline{\varepsilon}^T = [\varepsilon_x, \varepsilon_y, \gamma_{xy}], \quad (12.18)$$

where using Eqs.(11.10) and (11.13) we have:

$$\varepsilon_x = \frac{\partial u}{\partial x} = a_1, \quad \varepsilon_y = \frac{\partial v}{\partial y} = b_2, \quad \gamma_{xy} = \frac{\partial u}{\partial y} + \frac{\partial v}{\partial x} = a_2 + b_1. \quad (12.19)$$

The nodal displacements must be obtained if we take back the nodal coordinates into the  $u(x,y)$  and  $v(x,y)$  functions given by Eq.(12.17), i.e.:

$$u_1 = a_0 + a_1 x_1 + a_2 y_1, \quad v_1 = b_0 + b_1 x_1 + b_2 y_1, \quad (12.20)$$

$$u_2 = a_0 + a_1 x_2 + a_2 y_2, \quad v_2 = b_0 + b_1 x_2 + b_2 y_2,$$

$$u_3 = a_0 + a_1 x_3 + a_2 y_3, \quad v_3 = b_0 + b_1 x_3 + b_2 y_3.$$

The solution of the system of equations above results in:

$$\begin{aligned} a_0 &= \frac{\alpha_1 u_1 + \alpha_2 u_2 + \alpha_3 u_3}{2A_e}, \quad a_1 = \frac{\beta_1 u_1 + \beta_2 u_2 + \beta_3 u_3}{2A_e}, \quad a_2 = \frac{\gamma_1 u_1 + \gamma_2 u_2 + \gamma_3 u_3}{2A_e}, \\ b_0 &= \frac{\alpha_1 v_1 + \alpha_2 v_2 + \alpha_3 v_3}{2A_e}, \quad b_1 = \frac{\beta_1 v_1 + \beta_2 v_2 + \beta_3 v_3}{2A_e}, \quad b_2 = \frac{\gamma_1 v_1 + \gamma_2 v_2 + \gamma_3 v_3}{2A_e}, \end{aligned} \quad (12.21)$$

where:

$$\alpha_1 = x_2 y_3 - x_3 y_2, \quad \beta_1 = y_2 - y_3, \quad \gamma_1 = x_3 - x_2, \quad (12.22)$$

$$\alpha_2 = x_3 y_1 - x_1 y_3, \quad \beta_2 = y_3 - y_1, \quad \gamma_2 = x_1 - x_3,$$

$$\alpha_3 = x_1 y_2 - x_2 y_1, \quad \beta_3 = y_1 - y_2, \quad \gamma_3 = x_2 - x_1.$$

Substituting the solution above back into the components of displacement field (Eq.(12.17)) we obtain:

$$u(x, y) = \frac{1}{2A_e} [(\alpha_1 + \beta_1 x + \gamma_1 y) u_1 + (\alpha_2 + \beta_2 x + \gamma_2 y) u_2 + (\alpha_3 + \beta_3 x + \gamma_3 y) u_3], \quad (12.23)$$

$$v(x, y) = \frac{1}{2A_e} [(\alpha_1 + \beta_1 x + \gamma_1 y) v_1 + (\alpha_2 + \beta_2 x + \gamma_2 y) v_2 + (\alpha_3 + \beta_3 x + \gamma_3 y) v_3].$$

Considering the fact that for the triangle element we have three interpolation functions (see. Eq.(12.3)), we can write that:

$$u(x, y) = N_1 u_1 + N_2 u_2 + N_3 u_3 = \sum_{i=1}^3 N_i(x, y) u_i, \quad (12.24)$$

$$v(x, y) = N_1 v_1 + N_2 v_2 + N_3 v_3 = \sum_{i=1}^3 N_i(x, y) v_i.$$

In accordance with Eq.(12.21) the interpolation functions can be derived in the following form:

$$N_i(x, y) = \frac{\alpha_i + \beta_i x + \gamma_i y}{2A_e}, \quad i = 1, 2, 3. \quad (12.25)$$

Based on the relation of  $\underline{u}(x, y) = \underline{\underline{N}}(x, y)\underline{u}_e$  the matrix of interpolation functions becomes:

$$\underline{\underline{N}} = \begin{bmatrix} N_1 & 0 & N_2 & 0 & N_3 & 0 \\ 0 & N_1 & 0 & N_2 & 0 & N_3 \end{bmatrix}. \quad (12.26)$$

The parameter lines of the interpolation function are shown in Fig.12.3, which implies the following properties:

- at the nodes ( $N_1, N_2, N_3$ ): (1,0,0), (0,1,0), (0,0,1),
- at the midpoints of the triangle sides ( $N_1, N_2, N_3$ ): (1/2,1/2,0), (1/2,0,1/2), (0,1/2,1/2),
- at the centroid ( $N_1, N_2, N_3$ ): (1/3,1/3,1/3),
- i.e., it is seen that at every point:  $N_1 + N_2 + N_3 = 1$ ,
- finally:

$$\int_{A_e} N_1^i N_2^j N_3^k dA = \frac{i! j! k!}{(i+j+k+2)!} 2A_e. \quad (12.27)$$

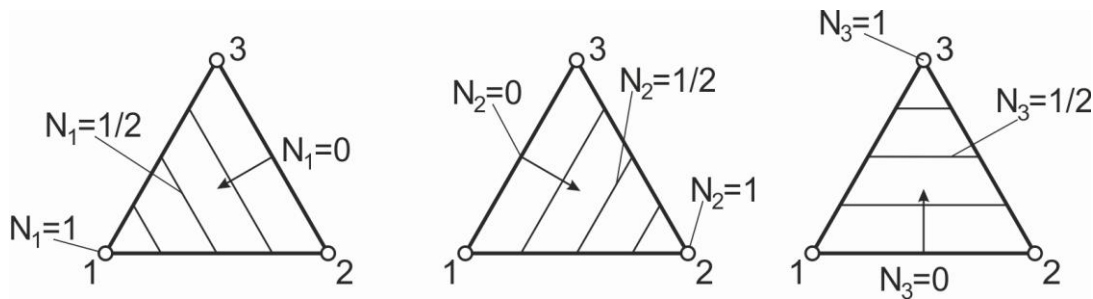


Fig.12.3. Parameter lines of the interpolation functions of linear triangle element.

### 12.2.2. Calculation of the stiffness matrix

According to Eq.(12.9) the definition of the element stiffness matrix is:

$$\underline{\underline{K}}_e = \iint \underline{\underline{B}}^T \underline{\underline{C}} \underline{\underline{B}} v dx dy, \quad (12.28)$$

where the previously mentioned strain-displacement matrix using Eqs.(12.5) and (12.26) becomes:

$$\underline{\underline{B}} = \underline{\underline{\partial N}} = \begin{bmatrix} \frac{\partial}{\partial x} & 0 \\ 0 & \frac{\partial}{\partial y} \\ \frac{\partial}{\partial y} & \frac{\partial}{\partial x} \end{bmatrix} \begin{bmatrix} N_1 & 0 & N_2 & 0 & N_3 & 0 \\ 0 & N_1 & 0 & N_2 & 0 & N_3 \end{bmatrix} =$$

$$= \begin{bmatrix} \frac{\partial N_1}{\partial x} & 0 & \frac{\partial N_2}{\partial x} & 0 & \frac{\partial N_3}{\partial x} & 0 \\ 0 & \frac{\partial N_1}{\partial y} & 0 & \frac{\partial N_2}{\partial y} & 0 & \frac{\partial N_3}{\partial y} \\ \frac{\partial N_1}{\partial y} & \frac{\partial N_1}{\partial x} & \frac{\partial N_2}{\partial y} & \frac{\partial N_2}{\partial x} & \frac{\partial N_3}{\partial y} & \frac{\partial N_3}{\partial x} \end{bmatrix} = \frac{1}{2A_e} \begin{bmatrix} \beta_1 & 0 & \beta_2 & 0 & \beta_3 & 0 \\ 0 & \gamma_1 & 0 & \gamma_2 & 0 & \gamma_3 \\ \gamma_1 & \beta_1 & \gamma_2 & \beta_2 & \gamma_3 & \beta_3 \end{bmatrix}. \quad (12.29)$$

This formulation implies that the elements of matrix  $\underline{\underline{B}}$  are independent of the  $x$  and  $y$  variables, they depend only on the nodal coordinates. Therefore, the stiffness matrix can be written as:

$$\underline{\underline{K}}_e = \underline{\underline{B}}^T \underline{\underline{C}}^T \underline{\underline{B}} v A_e = \underline{\underline{B}}^T \underline{\underline{C}}^T \underline{\underline{B}} V_e, \quad (12.30)$$

where  $A_e$  is the element area,  $V_e = A_e v$  is the element volume, respectively. As a consequence, the stiffness matrix of the linear triangle element can be computed in a relatively simple way and in closed form.

### 12.2.3. Definition of the loads

*Body force or volume force.* Let the vector of body forces be equal to:

$$\underline{q} = \begin{bmatrix} q_x \\ q_y \end{bmatrix}, \quad (12.31)$$

from which we have:

$$\underline{F}_{eb} = \iint_{A_e} \underline{\underline{N}}^T \underline{q} v dx dy = \int_{A_e} \begin{bmatrix} N_1 & 0 \\ 0 & N_1 \\ N_2 & 0 \\ 0 & N_2 \\ N_3 & 0 \\ 0 & N_3 \end{bmatrix} \begin{bmatrix} q_x \\ q_y \end{bmatrix} v dA = \int_{A_e} \begin{bmatrix} N_1 q_x \\ N_1 q_y \\ N_2 q_x \\ N_2 q_y \\ N_3 q_x \\ N_3 q_y \end{bmatrix} v dA. \quad (12.32)$$

Utilizing the special properties of the interpolation functions given by Eq.(12.27), e.g. if  $i = 1, j = 0$  and  $k = 0$ , we have:

$$\int_{A_e} N_1 dA = \frac{1}{3} A_e . \quad (12.33)$$

Consequently we have:

$$\underline{F}_{eb}^T = \frac{1}{3} A_e v [q_x \quad q_y \quad q_x \quad q_y \quad q_x \quad q_y]. \quad (12.34)$$

As an explanation, the body force acting on the element (e.g. the whole weight and the resulting resultant force) is divided into three equal parts and put into the nodes. The body force can be originated from gravitation or acceleration (inertia force).

*Distributed force along element edges.* For the calculation of force vectors as a result of line loads along element edges we should take the 1-2 edge of the element shown in Fig.12.4 into consideration. We define a dimensionless parameter,  $\xi$  along the element edge. The arc length along the element edge is then:

$$s = l_{12} \xi \text{ and } ds = l_{12} d\xi . \quad (12.35)$$

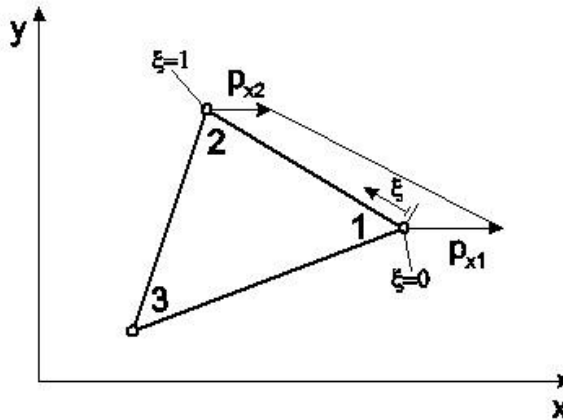


Fig.12.4. Linear triangle element with line load in direction  $x$  along element edge 1-2.

The linearly distributed load in direction  $x$  can be described by the following function:

$$p_x(\xi) = p_{x1}(1 - \xi) + p_{x2}\xi . \quad (12.36)$$

Similarly, the displacement function in direction  $x$  along element edge 1-2 can be written as:

$$u(\xi) = u_1(1 - \xi) + u_2\xi . \quad (12.37)$$

The work of the distributed load is generally the integration of the load function multiplied by displacement function between the corresponding nodes:

$$\begin{aligned}
W_p &= \underline{u}_e^T \underline{F}_{ep} = \int_{l_{12}} \underline{u}_e^T \underline{p}_l v ds = \int_0^1 p_x(\xi) u(\xi) l_{12} v d\xi = \\
&= \int_0^1 u_1 \left\{ p_{x1}(1-\xi)^2 + p_{x2}(1-\xi)\xi \right\} l_{12} v d\xi + \int_0^1 u_2 \left\{ p_{x1}(1-\xi)\xi + p_{x2}\xi^2 \right\} l_{12} v d\xi = \\
&= \frac{l_{12}v}{3} \left\{ u_1 \left( p_{x1} + \frac{1}{2} p_{x2} \right) + u_2 \left( \frac{1}{2} p_{x1} + p_{x2} \right) \right\}.
\end{aligned} \tag{12.38}$$

That is, the force vector from a linearly distributed line load becomes:

$$\underline{F}_{ep}^T = \frac{l_{12}v}{3} \begin{bmatrix} p_{x1} + \frac{1}{2} p_{x2} & 0 & \frac{1}{2} p_{x1} + p_{x2} & 0 & 0 & 0 \end{bmatrix}. \tag{12.39}$$

If the line load is constant along the element edge, then  $p_{x1} = p_{x2} = p_x$  which implies:

$$\underline{F}_{ep}^T = \frac{l_{12}v}{2} \begin{bmatrix} p_x & 0 & p_x & 0 & 0 & 0 \end{bmatrix}. \tag{12.40}$$

The form of the vector of forces in the finite element equation is similar in the case of a linearly distributed load in direction y.

*Concentrated forces.* Concentrated forces can act only at nodes. The force vector can be simply formulated based on the nodes:

$$\underline{F}_{ec}^T = [F_{x1} \ F_{y1} \ F_{x2} \ F_{y2} \ F_{x3} \ F_{y3}]. \tag{12.41}$$

The total force vector is the sum of the vectors detailed in the previous points, i.e.:

$$\underline{F}_e = \underline{F}_{eb} + \underline{F}_{ep} + \underline{F}_{ec}. \tag{12.42}$$

We demonstrate the solution of the finite element equation and the construction of the stiffness matrix and force vector through an example.

### 12.3. Example for the linear triangle element – plane stress state

The model shown in Fig.12.5a is loaded by distributed forces. Calculate the nodal displacements and forces in that case when we built-up the plate using two linear triangle elements! Calculate the strain and stress components [4]!

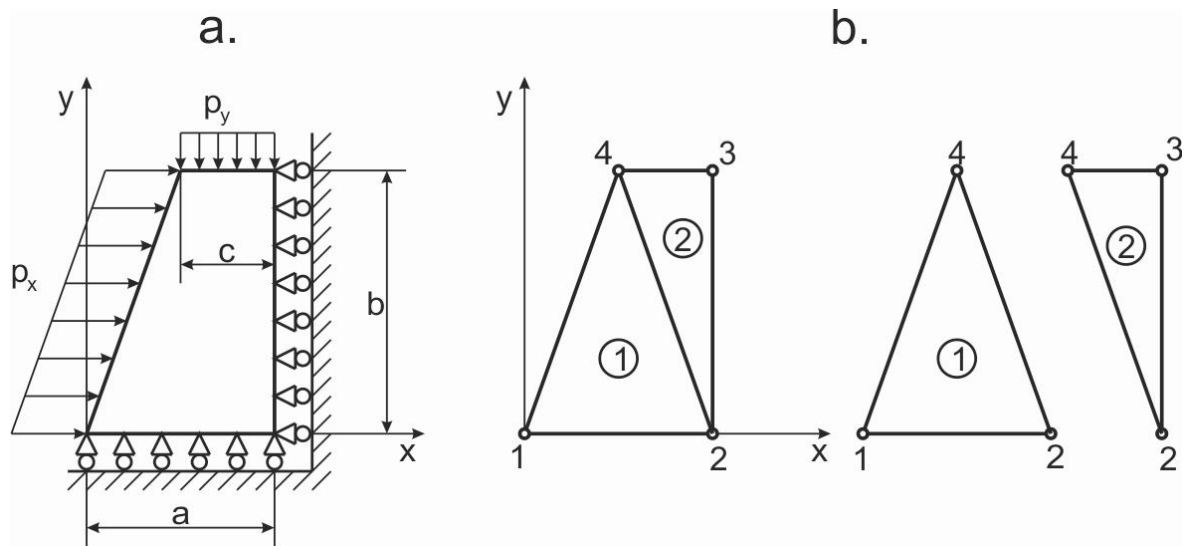


Fig.12.5. Plane model loaded by distributed forces (a), finite element model made by two linear triangle elements (b).

Given:

$p_x = 0,12 \text{ MPa}$ ,  $E = 150 \text{ GPa}$ ,  $a = 20 \text{ mm}$ ,  $c = 10 \text{ mm}$ ,  $p_y = 0,06 \text{ MPa}$ ,  $\nu = 0,25$ ,  $b = 30 \text{ mm}$ ,  $\nu = 5 \text{ mm}$

In the course of the computation we calculate the distances in [mm] and the force in [N]. Following Fig.12.5b, we see that the model is constructed by two triangle elements. The nodal coordinates are:

| node | x [mm] | y [mm] |
|------|--------|--------|
| 1    | 0      | 0      |
| 2    | 20     | 0      |
| 3    | 20     | 30     |
| 4    | 10     | 30     |

The so-called element-node table is:

| element | nodes |   |   |
|---------|-------|---|---|
|         | 1     | 2 | 4 |
| 2       | 2     | 3 | 4 |

The finite element equilibrium equation to be solved is:

$$\underline{\underline{K}} \underline{U} = \underline{F}, \quad (12.43)$$

where:

$$\underline{U}^T = [u_1 \quad v_1 \quad u_2 \quad v_2 \quad u_3 \quad v_3 \quad u_4 \quad v_4], \quad (12.44)$$

is the structural vector of nodal displacements. Because of the boundary conditions ( $v_1 = v_2 = u_2 = u_3 = 0$ ) we have:

$$\underline{U}^T = [u_1 \ 0 \ 0 \ 0 \ v_3 \ u_4 \ v_4]. \quad (12.45)$$

In order to calculate the stiffness matrix we need the constitutive matrix for plane stress state (see section 11.23):

$$\underline{\underline{C}} = \underline{\underline{C}}^{str} = \frac{E}{1-\nu^2} \begin{bmatrix} 1 & \nu & 0 \\ \nu & 1 & 0 \\ 0 & 0 & \frac{1-\nu}{2} \end{bmatrix} = \begin{bmatrix} 1,6 & 0,4 & 0 \\ 0,4 & 1,6 & 0 \\ 0 & 0 & 0,6 \end{bmatrix} \cdot 10^5 \text{ MPa.} \quad (12.46)$$

The coefficients of the interpolation functions for the first element are:

$$\beta_1 = y_2 - y_4 = -30 \text{ mm}, \gamma_1 = x_4 - x_2 = -10 \text{ mm}, \quad (12.47)$$

$$\beta_2 = y_4 - y_1 = 30 \text{ mm}, \gamma_2 = x_1 - x_4 = -10 \text{ mm},$$

$$\beta_3 = y_1 - y_2 = 0 \text{ mm}, \gamma_3 = x_2 - x_1 = 20 \text{ mm},$$

and for the second element, respectively:

$$\beta_1 = y_3 - y_4 = 0 \text{ mm}, \gamma_1 = x_4 - x_3 = -10 \text{ mm}, \quad (12.48)$$

$$\beta_2 = y_4 - y_2 = 30 \text{ mm}, \gamma_2 = x_2 - x_4 = 10 \text{ mm},$$

$$\beta_3 = y_2 - y_3 = -30 \text{ mm}, \gamma_3 = x_3 - x_2 = 0 \text{ mm}.$$

The triangle areas are:

$$A_{e1} = \frac{1}{2} 20 \cdot 30 = 300 \text{ mm}^2, A_{e2} = \frac{1}{2} 10 \cdot 30 = 150 \text{ mm}^2. \quad (12.49)$$

Matrix  $\underline{\underline{B}}$  for the first element is:

$$\underline{\underline{B}}_1 = \frac{1}{2A_{e1}} \begin{bmatrix} \beta_1 & 0 & \beta_2 & 0 & \beta_3 & 0 \\ 0 & \gamma_1 & 0 & \gamma_2 & 0 & \gamma_3 \\ \gamma_1 & \beta_1 & \gamma_2 & \beta_2 & \gamma_3 & \beta_3 \end{bmatrix} = \frac{1}{20} \begin{bmatrix} -1 & 0 & 1 & 0 & 0 & 0 \\ 0 & -\frac{1}{3} & 0 & -\frac{1}{3} & 0 & \frac{2}{3} \\ -\frac{1}{3} & -1 & -\frac{1}{3} & 1 & \frac{2}{3} & 0 \end{bmatrix} \frac{1}{\text{mm}}, \quad (12.50)$$

For the second element it is:

$$\underline{\underline{B}}_2 = \frac{1}{2A_{e2}} \begin{bmatrix} \beta_1 & 0 & \beta_2 & 0 & \beta_3 & 0 \\ 0 & \gamma_1 & 0 & \gamma_2 & 0 & \gamma_3 \\ \gamma_1 & \beta_1 & \gamma_2 & \beta_2 & \gamma_3 & \beta_3 \end{bmatrix} = \frac{1}{10} \begin{bmatrix} 0 & 0 & 1 & 0 & -1 & 0 \\ 0 & -\frac{1}{3} & 0 & \frac{1}{3} & 0 & 0 \\ -\frac{1}{3} & 0 & \frac{1}{3} & 1 & 0 & -1 \end{bmatrix} \frac{1}{\text{mm}} . \quad (12.51)$$

Based on Eq.(12.30) the element stiffness matrices are:

$$\underline{\underline{K}}_{e1} = \underline{\underline{B}}_1^T \underline{\underline{C}}^T \underline{\underline{B}}_1 V_{e1} = \begin{bmatrix} 6,25 & 1,25 & -5,75 & -0,25 & -0,5 & -1 \\ 1,25 & 35/12 & 0,25 & -57/36 & -1,5 & -4/3 \\ -5,75 & 0,25 & 6,25 & -1,25 & -0,5 & 1 \\ -0,25 & -57/36 & -1,25 & 35/12 & 1,5 & -4/3 \\ -0,5 & -1,5 & -0,5 & 1,5 & 1 & 0 \\ -1 & -4/3 & 1 & -4/3 & 0 & 8/3 \end{bmatrix} \cdot 10^5 \frac{\text{N}}{\text{mm}}, \quad (12.52)$$

$$\underline{\underline{K}}_{e2} = \underline{\underline{B}}_2^T \underline{\underline{C}}^T \underline{\underline{B}}_2 V_{e2} = \begin{bmatrix} 0,5 & 0 & -0,5 & -1,5 & 0 & 1,5 \\ 0 & 4/3 & -1 & -4/3 & 1 & 0 \\ -0,5 & -1 & 12,5 & 2,5 & -12 & -1,5 \\ -1,5 & -4/3 & 2,5 & 35/6 & -1 & -4,5 \\ 0 & 1 & -12 & -1 & 12 & 0 \\ 1,5 & 0 & -1,5 & -4,5 & 0 & 4,5 \end{bmatrix} \cdot 10^5 \frac{\text{N}}{\text{mm}},$$

where  $V_{e1} = A_{e1} \cdot v = 300 \cdot 5 = 1500 \text{ mm}^3$  and  $V_{e2} = A_{e2} \cdot v = 150 \cdot 5 = 750 \text{ mm}^3$  are the element volumes. For the construction of the structural stiffness matrix we complete the element matrices with empty rows and columns corresponding to the missing degrees of freedom. On the base of Fig.12.5 and the element-node table, it is seen, that the first element includes only nodes 1, 2 and 4. Consequently those rows and columns, which belong to node 3, should be filled up with zeros:

$$\underline{\underline{K}}_1 = \begin{bmatrix} k_{e11}^1 & k_{e12}^1 & k_{e13}^1 & k_{e14}^1 & 0 & 0 & k_{e15}^1 & k_{e16}^1 \\ k_{e21}^1 & k_{e22}^1 & k_{e23}^1 & k_{e24}^1 & 0 & 0 & k_{e25}^1 & k_{e26}^1 \\ k_{e31}^1 & k_{e32}^1 & k_{e33}^1 & k_{e34}^1 & 0 & 0 & k_{e35}^1 & k_{e36}^1 \\ k_{e41}^1 & k_{e42}^1 & k_{e43}^1 & k_{e44}^1 & 0 & 0 & k_{e45}^1 & k_{e46}^1 \\ 0 & 0 & 0 & 0 & 0 & 0 & 0 & 0 \\ 0 & 0 & 0 & 0 & 0 & 0 & 0 & 0 \\ k_{e51}^1 & k_{e52}^1 & k_{e53}^1 & k_{e54}^1 & 0 & 0 & k_{e55}^1 & k_{e56}^1 \\ k_{e61}^1 & k_{e62}^1 & k_{e63}^1 & k_{e64}^1 & 0 & 0 & k_{e65}^1 & k_{e66}^1 \end{bmatrix} . \quad (12.53)$$

In contrast, for the second element the rows and columns corresponding with the first node must be completed by the placement of zeros:

$$\underline{\underline{K}}_2 = \begin{bmatrix} 0 & 0 & 0 & 0 & 0 & 0 & 0 & 0 \\ 0 & 0 & 0 & 0 & 0 & 0 & 0 & 0 \\ 0 & 0 & k_{e11}^2 & k_{e12}^2 & k_{e13}^2 & k_{e14}^2 & k_{e15}^2 & k_{e16}^2 \\ 0 & 0 & k_{e21}^2 & k_{e22}^2 & k_{e23}^2 & k_{e24}^2 & k_{e25}^2 & k_{e26}^2 \\ 0 & 0 & k_{e31}^2 & k_{e32}^2 & k_{e33}^2 & k_{e34}^2 & k_{e35}^2 & k_{e36}^2 \\ 0 & 0 & k_{e41}^2 & k_{e42}^2 & k_{e43}^2 & k_{e44}^2 & k_{e45}^2 & k_{e46}^2 \\ 0 & 0 & k_{e51}^2 & k_{e52}^2 & k_{e53}^2 & k_{e54}^2 & k_{e55}^2 & k_{e56}^2 \\ 0 & 0 & k_{e61}^2 & k_{e62}^2 & k_{e63}^2 & k_{e64}^2 & k_{e65}^2 & k_{e66}^2 \end{bmatrix}. \quad (12.54)$$

The structural stiffness matrix is calculated as the sum of the two former matrices:

$$\underline{\underline{K}} = \underline{\underline{K}}_1 + \underline{\underline{K}}_2 = \begin{bmatrix} k_{e11}^1 & k_{e12}^1 & k_{e13}^1 & k_{e14}^1 & 0 & 0 & k_{e15}^1 & k_{e16}^1 \\ k_{e21}^1 & k_{e22}^1 & k_{e23}^1 & k_{e24}^1 & 0 & 0 & k_{e25}^1 & k_{e26}^1 \\ k_{e31}^1 & k_{e32}^1 & k_{e33}^1 + k_{e11}^2 & k_{e34}^1 + k_{e12}^2 & k_{e13}^2 & k_{e14}^2 & k_{e35}^1 + k_{e15}^2 & k_{e36}^1 + k_{e16}^2 \\ k_{e41}^1 & k_{e42}^1 & k_{e43}^1 + k_{e21}^2 & k_{e44}^1 + k_{e22}^2 & k_{e23}^2 & k_{e24}^2 & k_{e45}^1 + k_{e25}^2 & k_{e46}^1 + k_{e26}^2 \\ 0 & 0 & k_{e31}^2 & k_{e32}^2 & k_{e33}^2 & k_{e34}^2 & k_{e35}^2 & k_{e36}^2 \\ 0 & 0 & k_{e41}^2 & k_{e42}^2 & k_{e43}^2 & k_{e44}^2 & k_{e45}^2 & k_{e46}^2 \\ k_{e51}^1 & k_{e52}^1 & k_{e53}^1 + k_{e51}^2 & k_{e54}^1 + k_{e52}^2 & k_{e53}^2 & k_{e54}^2 & k_{e55}^1 + k_{e56}^2 & k_{e56}^1 + k_{e56}^2 \\ k_{e61}^1 & k_{e62}^1 & k_{e63}^1 + k_{e61}^2 & k_{e64}^1 + k_{e62}^2 & k_{e63}^2 & k_{e64}^2 & k_{e65}^1 + k_{e65}^2 & k_{e66}^1 + k_{e66}^2 \end{bmatrix}. \quad (12.55)$$

The force vector related to the distributed load is calculated by Eq.(12.39):

$$\underline{F}_{ep1}^T = \frac{l_{14}v}{2} [p_x \ 0 \ 0 \ 0 \ p_x \ 0], \quad (12.56)$$

$$\underline{F}_{ep2}^T = \frac{l_{34}v}{2} [0 \ 0 \ 0 \ p_y \ 0 \ p_y],$$

where  $l_{14} = \sqrt{10^2 + 30^2} = \sqrt{1000}$  m and  $l_{34} = 10$  mm are the element edge lengths between the nodes indicated in the subscript. By completing the element vectors with zeros at the positions of the proper degrees of freedom, we get the structural force vectors:

$$\underline{F}_{l1}^T = \frac{l_{14}v}{2} [p_x \ 0 \ 0 \ 0 \ 0 \ p_x \ 0] = [3\sqrt{10} \ 0 \ 0 \ 0 \ 0 \ 0 \ 3\sqrt{10} \ 0] \text{N}, \quad (12.57)$$

$$\underline{F}_{l2}^T = \frac{l_{34}v}{2} [0 \ 0 \ 0 \ 0 \ 0 \ p_y \ 0 \ p_y] = [0 \ 0 \ 0 \ 0 \ 0 \ -1.5 \ 0 \ -1.5] \text{N}.$$

We consider the reaction forces as concentrated forces at the constrained nodes:

$$\underline{F}_c^T = [F_{x1} \quad F_{y1} \quad F_{x2} \quad F_{y2} \quad F_{x3} \quad F_{y3} \quad F_{x4} \quad F_{y4}]. \quad (12.58)$$

Taking it into account, that at node 4 there is no external force and that the surfaces are frictionless, i.e.:  $F_{x1} = F_{y3} = 0$ , we have:

$$\underline{F}_c^T = [0 \quad F_{y1} \quad F_{x2} \quad F_{y2} \quad F_{x3} \quad 0 \quad 0 \quad 0]. \quad (12.59)$$

The structural force vector is:

$$\underline{F} = \underline{F}_{p1} + \underline{F}_{p2} + \underline{F}_c. \quad (12.60)$$

The finite element equilibrium equation is  $\underline{\underline{K}}\underline{U} = \underline{F}$ , i.e. we have:

$$\begin{bmatrix} 6,25 & 1,25 & 5,75 & -0,25 & 0 & 0 & -0,5 & -1 \\ 1,25 & 35/12 & 0,25 & -57/36 & 0 & 0 & -1,25 & -4/3 \\ -5,75 & 0,25 & 6,25 & -1,25 & -0,5 & -1,5 & -0,5 & 2,5 \\ -0,25 & -57/36 & -1,25 & 4,25 & -1 & -4/3 & 2,5 & -4/3 \\ 0 & 0 & -0,5 & -1 & 12,5 & 2,5 & -12 & -1,5 \\ 0 & 0 & -1,5 & -4/3 & 2,5 & 35/6 & -1 & -4,5 \\ -0,5 & -1,5 & -0,5 & 2,5 & -12 & -1 & 13 & 0 \\ -1 & -4/3 & 2,5 & -4/3 & -1,5 & -4,5 & 0 & 43/6 \end{bmatrix} \cdot 10^5 = \begin{bmatrix} u_1 \\ 0 \\ 0 \\ 0 \\ v_3 \\ u_4 \\ 3\sqrt{10} \\ F_{y1} \\ F_{x2} \\ F_{y2} \\ F_{x3} \\ -1,5 \\ 3\sqrt{10} \\ -1,5 \end{bmatrix}. \quad (12.61)$$

The nodal displacements can be determined from the system of equations constructed by the 1<sup>st</sup>, 6<sup>th</sup>, 7<sup>th</sup> and 8<sup>th</sup> component equations of the matrix equation:

$$6,25u_1 - 0,5u_4 - v_4 = 3\sqrt{10}, \quad (12.62)$$

$$35/6v_3 - u_4 - 4,5v_4 = -1,5,$$

$$-0,5u_1 - v_3 + 13u_4 = 3\sqrt{10},$$

$$-u_1 - 4,5v_3 + 43/6v_4 = -1,5.$$

The equations above, in fact were obtained by the condensation of Eq.(12.61). When we perform the matrix condensation only those component equations remain, which contain unknowns with respect to the displacements only. On the right hand side, in the force vector there are no unknowns. The solutions are:

$$u_1 = 1,557 \cdot 10^{-5} \text{ mm}, v_3 = -0,22997 \cdot 10^{-5} \text{ mm}, \quad (12.63)$$

$$u_4 = 0,771983 \cdot 10^{-5} \text{ mm}, v_4 = -0,13633 \cdot 10^{-5} \text{ mm}.$$

Taking the nodal displacements back into the 2<sup>nd</sup>, 3<sup>rd</sup>, 4<sup>th</sup> and 5<sup>th</sup> rows of the matrix equation, we can determine the nodal forces:

$$1,25u_1 - 1,25u_4 - 4/3v_4 = F_{y1}, \quad (12.64)$$

$$-5,75u_1 - 1,5v_3 - 0,5u_4 + 2,5v_4 = F_{x2},$$

$$-0,25u_1 - 4/3v_3 + 2,5u_4 - 4/3v_4 = F_{y2},$$

$$2,5v_3 - 12u_4 - 1,5v_4 = F_{y3}$$

The solutions are:

$$F_{y1} = 0,971095 \text{ N}, F_{x2} = -9,339434 \text{ N}, \quad (12.65)$$

$$F_{y2} = 2,0289 \text{ N}, F_{x3} = -9,63423 \text{ N}.$$

Using Eq.(12.19) we calculate now the strain components:

$$\varepsilon_x = \frac{\partial u}{\partial x} = a_1, \quad \varepsilon_y = \frac{\partial v}{\partial y} = b_2, \quad \gamma_{xy} = \frac{\partial u}{\partial y} + \frac{\partial v}{\partial x} = a_2 + b_1. \quad (12.66)$$

For the first element we obtain:

$$a_1 = \frac{\beta_1 u_1 + \beta_2 u_2 + \beta_3 u_4}{2A_{e1}} = \frac{-30u_1}{2 \cdot 300} = -7,7892 \cdot 10^{-7} \quad (12.67)$$

$$b_1 = \frac{\beta_1 v_1 + \beta_2 v_2 + \beta_3 v_4}{2A_{e1}} = 0,$$

$$a_2 = \frac{\gamma_1 u_1 + \gamma_2 u_2 + \gamma_3 u_4}{2A_{e1}} = \frac{-10u_1 + 20u_4}{2 \cdot 300} = -2,3121 \cdot 10^{-9},$$

$$b_2 = \frac{\gamma_1 v_1 + \gamma_2 v_2 + \gamma_3 v_4}{2A_{e1}} = \frac{20v_4}{2 \cdot 300} = -4,54435 \cdot 10^{-8}.$$

The vector of strain components fro the first element is:

$$\underline{\varepsilon}_1 = \begin{bmatrix} \varepsilon_{x1} \\ \varepsilon_{y1} \\ \gamma_{xy1} \end{bmatrix} = \begin{bmatrix} -778,92 \\ -45,4435 \\ -2,3121 \end{bmatrix} \cdot 10^{-9} \quad (12.68)$$

For the second element we can write:

$$a_1 = \frac{\beta_1 u_2 + \beta_2 u_3 + \beta_3 u_4}{2A_{e2}} = \frac{30u_4}{2 \cdot 150} = -7,7198 \cdot 10^{-7}, \quad (12.69)$$

$$b_1 = \frac{\beta_1 v_2 + \beta_2 v_3 + \beta_3 v_4}{2A_{e2}} = \frac{30v_3 - 30v_4}{2 \cdot 150} = -9,36416 \cdot 10^{-8},$$

$$a_2 = \frac{\gamma_1 u_2 + \gamma_2 u_3 + \gamma_3 u_4}{2A_{e2}} = 0,$$

$$b_2 = \frac{\gamma_1 v_2 + \gamma_2 v_3 + \gamma_3 v_4}{2A_{e1}} = \frac{10v_3}{2 \cdot 150} = -7,6657 \cdot 10^{-8},$$

from which we have:

$$\underline{\varepsilon}_2 = \begin{bmatrix} \varepsilon_{x2} \\ \varepsilon_{y2} \\ \gamma_{xy2} \end{bmatrix} = \begin{bmatrix} -771,98 \\ -76,657 \\ -93,6416 \end{bmatrix} \cdot 10^{-9}. \quad (12.70)$$

Since the plate is under plane stress state we can write based on Eq.(11.19) that:

$$\varepsilon_{z1} = -\frac{\nu}{1-\nu}(\varepsilon_{x1} + \varepsilon_{y1}) = 274,787 \cdot 10^{-9}, \quad (12.71)$$

$$\varepsilon_{z2} = -\frac{\nu}{1-\nu}(\varepsilon_{x2} + \varepsilon_{y2}) = 282,88 \cdot 10^{-9}.$$

The normal and shear strains are, accordingly constants within the individual elements, we referred to this fact in the introduction of the triangle element. Incorporating the constitutive matrix we can determine the stress components too based on Eq.(12.46):

$$\underline{\sigma} = \underline{\underline{C}}^{str} \underline{\varepsilon}. \quad (12.72)$$

This equation gives the stresses of the elements, which is in general referred to as „element stress” in the commercial finite element packages. For the first element we have:

$$\sigma_{x1} = (1,6\varepsilon_{x1} + 0,4\varepsilon_{y1}) \cdot 10^5 = -0,12644 \text{ MPa}, \quad (12.73)$$

$$\sigma_{y1} = (0,4\varepsilon_{x1} + 1,6\varepsilon_{y1}) \cdot 10^5 = -0,038428 \text{ MPa},$$

$$\tau_{xy1} = 0,6\gamma_{xy1} \cdot 10^5 = -0,13873 \cdot 10^{-3} \text{ MPa.}$$

Similarly, for the second element the stresses are:

$$\sigma_{x2} = (1,6\varepsilon_{x2} + 0,4\varepsilon_{y2}) \cdot 10^5 = -0,12658 \text{ MPa,} \quad (12.74)$$

$$\sigma_{y2} = (0,4\varepsilon_{x2} + 1,6\varepsilon_{y2}) \cdot 10^5 = -0,043145 \text{ MPa,}$$

$$\tau_{xy2} = 0,6\gamma_{xy2} \cdot 10^5 = -0,56185 \cdot 10^{-2} \text{ MPa.}$$

Considering the stresses it is possible to produce nodal stress solution. By computing the average stresses in the mutual nodes we obtain the so-called „nodal stress” or „average stress” solution:

Node 1:  $\sigma_x = -0,12644 \text{ MPa,}$

$$\sigma_y = -0,038428 \text{ MPa,}$$

$$\tau_{xy} = -0,13873 \cdot 10^{-3} \text{ MPa,} \quad (12.75)$$

Node 2:  $\sigma_x = \frac{1}{2}(\sigma_{x1} + \sigma_{x2}) = -0,12651 \text{ MPa,}$

$$\sigma_y = \frac{1}{2}(\sigma_{y1} + \sigma_{y2}) = -0,0407865 \text{ MPa,}$$

$$\tau_{xy} = \frac{1}{2}(\tau_{xy1} + \tau_{xy2}) = -0,28786 \cdot 10^{-2} \text{ MPa.}$$

Node 3:  $\sigma_x = -0,12658 \text{ MPa,}$

$$\sigma_y = -0,043145 \text{ MPa,}$$

$$\tau_{xy} = -0,56185 \cdot 10^{-3} \text{ MPa.}$$

Node 4:  $\sigma_x = \frac{1}{2}(\sigma_{x1} + \sigma_{x2}) = -0,12651 \text{ MPa,}$

$$\sigma_y = \frac{1}{2}(\sigma_{y1} + \sigma_{y2}) = -0,0407865 \text{ MPa,}$$

$$\tau_{xy} = \frac{1}{2}(\tau_{xy1} + \tau_{xy2}) = -0,28786 \cdot 10^{-2} \text{ MPa.}$$

The problem presented in section 12.3 was verified by the finite element code ANSYS 12, resulting in the same results. The solution with the above applied low mesh resolution is naturally very inaccurate.

#### 12.4. Quadratic six node triangle element

The more advanced version of the linear triangle element is the six node quadratic triangle element, in which there are additional nodes in the midpoints of the element sides [2,5]. Because of the additional nodes we need displacement functions including six unknowns, which are:

$$u(x, y) = a_0 + a_1x + a_2y + a_3xy + a_4x^2 + a_5y^2, \quad (12.76)$$

$$v(x, y) = b_0 + b_1x + b_2y + b_3xy + b_4x^2 + b_5y^2.$$

The calculation of the stiffness matrix and force vector can be performed in the same fashion as it was done in the linear triangle element. Within the individual elements the strain and stress components vary linearly. As a consequence, using identical mesh resolution, the quadratic triangle element provides a better approximation of the problem than the linear one.

#### 12.5. Isoparametric four node quadrilateral

The isoparametric quadrilateral (see Fig.12.6a) is one of the most important finite element type for plane problems [2,4,5]. An element is called isoparametric if we formulate the local geometry and displacement field by the same set of functions.

##### 12.5.1. Interpolation of the geometry

For the sake of simplicity we map the quadrilateral element to a regular square into the  $\xi$ - $\eta$  natural coordinate system, as it is shown in Fig 12.6b. We give the functions of the  $x$  and  $y$  coordinates of element edges in the following form:

$$x(\xi, \eta) = N_1(\xi, \eta)x_1 + N_2(\xi, \eta)x_2 + N_3(\xi, \eta)x_3 + N_4(\xi, \eta)x_4 = \underline{N}^T(\xi, \eta)\underline{x}, \quad (12.77)$$

$$y(\xi, \eta) = N_1(\xi, \eta)y_1 + N_2(\xi, \eta)y_2 + N_3(\xi, \eta)y_3 + N_4(\xi, \eta)y_4 = \underline{N}^T(\xi, \eta)\underline{y},$$

where:

$$\underline{x}^T = [x_1 \quad x_2 \quad x_3 \quad x_4], \quad \underline{y}^T = [y_1 \quad y_2 \quad y_3 \quad y_4]. \quad (12.78)$$

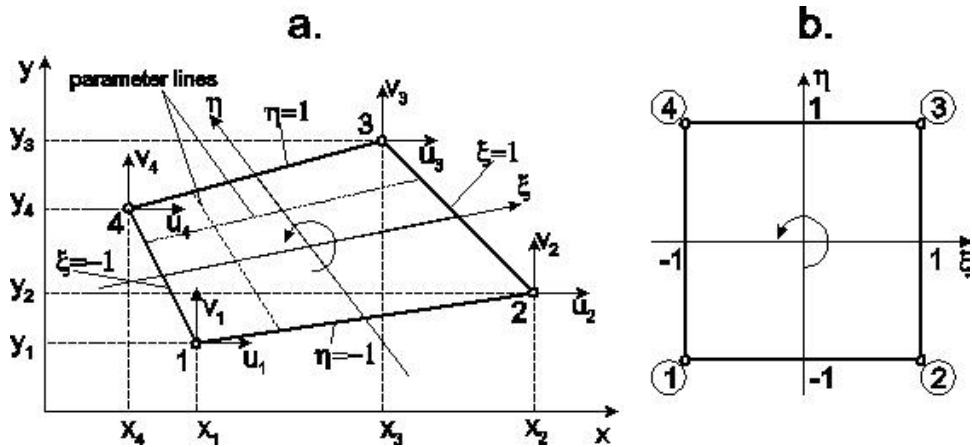


Fig.12.6. Isoparametric quadrilateral in the global (a) and natural (b) coordinate systems.

Due to the fact that we have four nodes, the interpolation function may contain to a maximum four unknowns:

$$x(\xi, \eta) = a_0 + a_1\xi + a_2\eta + a_3\xi\eta = \underline{P}^T \underline{A}, \quad (12.79)$$

where  $\underline{A}$  is the vector of coefficients,  $\underline{P}$  is the vector of basis polynomials, respectively:

$$\underline{A}^T = [a_0 \quad a_1 \quad a_2 \quad a_3], \quad \underline{P}^T = [1 \quad \xi \quad \eta \quad \xi\eta]. \quad (12.80)$$

The function given by Eq.(12.79) must satisfy the following conditions:

$$x(-1, -1) = a_0 - a_1 - a_2 + a_3 = x_1, \quad (12.81)$$

$$x(1, -1) = a_0 + a_1 - a_2 - a_3 = x_2,$$

$$x(1, 1) = a_0 + a_1 + a_2 + a_3 = x_3,$$

$$x(-1, 1) = a_0 - a_1 + a_2 - a_3 = x_4.$$

In matrix form it is:

$$\underline{\underline{M}} \underline{A} = \underline{x}, \quad (12.82)$$

where:

$$\underline{\underline{M}} = \begin{bmatrix} 1 & -1 & -1 & 1 \\ 1 & 1 & -1 & -1 \\ 1 & 1 & 1 & 1 \\ 1 & -1 & 1 & -1 \end{bmatrix}. \quad (12.83)$$

Then the coefficients can be determined by using Eq.(12.82):

$$\underline{A} = \underline{\underline{M}}^{-1} \underline{x} \text{ and: } x(\xi, \eta) = \underline{P}^T \underline{A} = \underline{P}^T \underline{\underline{M}}^{-1} \underline{x}. \quad (12.84)$$

The solutions for the coefficients are:

$$a_0 = \frac{1}{4}(x_1 + x_2 + x_3 + x_4), \quad a_1 = \frac{1}{4}(-x_1 + x_2 + x_3 - x_4), \quad (12.85)$$

$$a_2 = \frac{1}{4}(-x_1 - x_2 + x_3 + x_4), \quad a_3 = \frac{1}{4}(x_1 - x_2 + x_3 - x_4).$$

Taking them back into Eq.(12.79) we get:

$$\begin{aligned} x(\xi, \eta) = & \frac{1}{4}(x_1 + x_2 + x_3 + x_4) + \frac{1}{4}(-x_1 + x_2 + x_3 - x_4)\xi + \\ & + \frac{1}{4}(-x_1 - x_2 + x_3 + x_4)\eta + \frac{1}{4}(x_1 - x_2 + x_3 - x_4)\xi\eta = \\ & \frac{1}{4}(1 - \xi - \eta + \xi\eta)x_1 + \frac{1}{4}(1 + \xi - \eta - \xi\eta)x_2 + \frac{1}{4}(1 + \xi + \eta + \xi\eta)x_3 + \frac{1}{4}(1 - \xi + \eta - \xi\eta)x_4. \end{aligned} \quad (12.86)$$

The interpolation polynomials on the base of Eq.(12.86) are:

$$N_1(\xi, \eta) = \frac{1}{4}(1 - \xi)(1 - \eta), \quad N_2(\xi, \eta) = \frac{1}{4}(1 + \xi)(1 - \eta), \quad (12.87)$$

$$N_3(\xi, \eta) = \frac{1}{4}(1 + \xi)(1 + \eta), \quad N_4(\xi, \eta) = \frac{1}{4}(1 - \xi)(1 + \eta).$$

Performing the same computation for coordinate  $y$  we obtain the same interpolation functions. The three dimensional plot of the  $N_i(\xi, \eta)$  interpolation functions represents line surfaces, of which value in the location of the  $i^{\text{th}}$  node is equal to unity, while in the location of the other nodes it is equal to zero, as it is demonstrated in Fig.12.7.

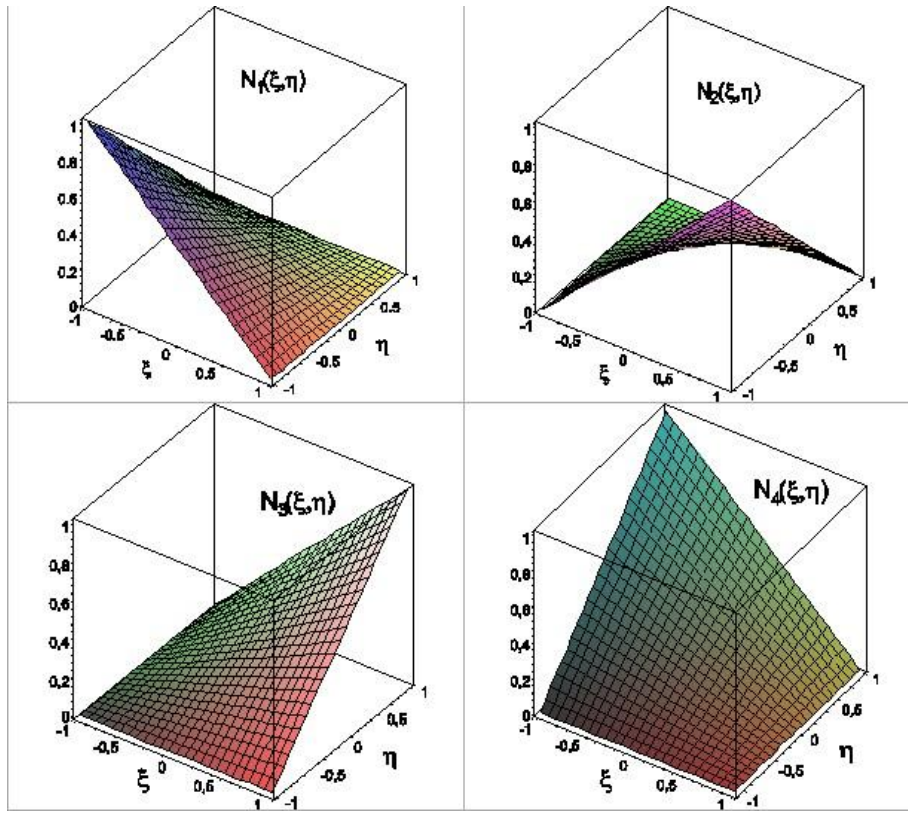


Fig.12.7. Interpolation functions of the isoparametric quadrilateral element.

The summary of the geometry is given by the formulae below:

$$\begin{bmatrix} x(\xi, \eta) \\ y(\xi, \eta) \end{bmatrix} = \underline{\underline{N}}(\xi, \eta) \underline{R}_e, \quad (12.88)$$

where:

$$\underline{R}_e^T = [x_1 \quad y_1 \quad x_2 \quad y_2 \quad x_3 \quad y_3 \quad x_4 \quad y_4], \quad (12.89)$$

is the vector of nodal coordinates, and:

$$\underline{\underline{N}}(\xi, \eta) = \begin{bmatrix} N_1 & 0 & N_2 & 0 & N_3 & 0 & N_4 & 0 \\ 0 & N_1 & 0 & N_2 & 0 & N_3 & 0 & N_4 \end{bmatrix}.$$

The compact form of the interpolation functions is:

$$N_i(\xi, \eta) = \frac{1}{4}(1 + \xi\xi_i)(1 + \eta\eta_i), \quad (12.90)$$

where  $\xi_i$  and  $\eta_i$  are the corner node coordinates according to Fig.12.6b.

### 12.5.2. Interpolation of the displacement field

The displacement vector field of the isoparametric quadrilateral element can be written as:

$$\underline{u}(\xi, \eta) = \begin{bmatrix} u(\xi, \eta) \\ v(\xi, \eta) \end{bmatrix} = \underline{\underline{N}}(\xi, \eta) \underline{u}_e, \quad (12.91)$$

where:

$$u(\xi, \eta) = N_1(\xi, \eta)u_1 + N_2(\xi, \eta)u_2 + N_3(\xi, \eta)u_3 + N_4(\xi, \eta)u_4, \quad (12.92)$$

$$v(\xi, \eta) = N_1(\xi, \eta)v_1 + N_2(\xi, \eta)v_2 + N_3(\xi, \eta)v_3 + N_4(\xi, \eta)v_4,$$

moreover, the matrix of interpolation functions and the vector of nodal displacements are:

$$\underline{\underline{N}}(\xi, \eta) = \begin{bmatrix} N_1 & 0 & N_2 & 0 & N_3 & 0 & N_4 & 0 \\ 0 & N_1 & 0 & N_2 & 0 & N_3 & 0 & N_4 \end{bmatrix}, \quad (12.93)$$

$$\underline{u}_e^T = [u_1 \ v_1 \ u_2 \ v_2 \ u_3 \ v_3 \ u_4 \ v_4].$$

The displacement field must result in the nodal displacements if we substitute the coordinates of the proper nodes back, i.e. it must satisfy the following conditions:

$$u(-1, -1) = u_1, u(1, -1) = u_2, u(1, 1) = u_3, u(-1, 1) = u_4 \quad (12.94)$$

Mathematically this is the same set of conditions for the displacements as that formulated in the case of the geometrical parameters. Consequently the computation leads to the same interpolation functions as those given by Eq.(12.87). The quadrilateral element is called isoparametric element because of the fact, that the same interpolation functions are applied for the displacement field and local geometry.

### 12.5.3. Calculation of strain components, Jacobi matrix and Jacobi determinant

The vector of strain components using Eq.(12.2) is the following:

$$\underline{\varepsilon} = \begin{bmatrix} \varepsilon_x \\ \varepsilon_y \\ \gamma_{xy} \end{bmatrix} = \begin{bmatrix} u_{,x} \\ v_{,y} \\ u_{,y} + v_{,x} \end{bmatrix} = \underline{\partial} \underline{u} = \underline{\underline{N}} \underline{u}_e = \underline{\underline{B}} \underline{u}_e, \quad (12.95)$$

where  $u_{,x}$  is the partial derivative of  $u$  with respect to  $x$ ,  $v_{,y}$  is the partial derivative of  $v$  with respect to  $y$ . Moreover:

$$\underline{\underline{B}} = \underline{\underline{\partial N}} = \begin{bmatrix} \frac{\partial}{\partial x} & 0 \\ 0 & \frac{\partial}{\partial y} \\ \frac{\partial}{\partial y} & \frac{\partial}{\partial x} \end{bmatrix} \begin{bmatrix} N_1 & 0 & N_2 & 0 & N_3 & 0 & N_4 & 0 \\ 0 & N_1 & 0 & N_2 & 0 & N_3 & 0 & N_4 \end{bmatrix} =$$

$$= \begin{bmatrix} \frac{\partial N_1}{\partial x} & 0 & \frac{\partial N_2}{\partial x} & 0 & \frac{\partial N_3}{\partial x} & 0 & \frac{\partial N_4}{\partial x} & 0 \\ 0 & \frac{\partial N_1}{\partial y} & 0 & \frac{\partial N_2}{\partial y} & 0 & \frac{\partial N_3}{\partial y} & 0 & \frac{\partial N_4}{\partial y} \\ \frac{\partial N_1}{\partial y} & \frac{\partial N_1}{\partial x} & \frac{\partial N_2}{\partial y} & \frac{\partial N_2}{\partial x} & \frac{\partial N_3}{\partial y} & \frac{\partial N_3}{\partial x} & \frac{\partial N_4}{\partial y} & \frac{\partial N_4}{\partial x} \end{bmatrix}. \quad (12.96)$$

Apparently, matrix  $\underline{\underline{B}}$  contains the first derivatives of the interpolation functions with respect to  $x$  and  $y$ . it can be elaborated based on Eq.(12.87) that the  $N_i$  interpolation functions are known in terms of  $\xi$  and  $\eta$ . We refer to the chain rule of differentiation:

$$\frac{\partial}{\partial x} = \frac{\partial}{\partial \xi} \frac{\partial \xi}{\partial x} + \frac{\partial}{\partial \eta} \frac{\partial \eta}{\partial x}, \quad \frac{\partial}{\partial y} = \frac{\partial}{\partial \xi} \frac{\partial \xi}{\partial y} + \frac{\partial}{\partial \eta} \frac{\partial \eta}{\partial y}, \quad (12.97)$$

$$\frac{\partial}{\partial \xi} = \frac{\partial}{\partial x} \frac{\partial x}{\partial \xi} + \frac{\partial}{\partial y} \frac{\partial y}{\partial \xi}, \quad \frac{\partial}{\partial \eta} = \frac{\partial}{\partial x} \frac{\partial x}{\partial \eta} + \frac{\partial}{\partial y} \frac{\partial y}{\partial \eta}.$$

Utilizing Eq.(12.77) the local geometry and the first derivative of the functions with respect to  $\xi$  and  $\eta$  are:

$$x(\xi, \eta) = \sum_{i=1}^4 N_i(\xi, \eta) x_i, \quad \frac{\partial x}{\partial \xi} = \sum_{i=1}^4 \frac{\partial N_i}{\partial \xi} x_i, \quad \frac{\partial x}{\partial \eta} = \sum_{i=1}^4 \frac{\partial N_i}{\partial \eta} x_i, \quad (12.98)$$

$$y(\xi, \eta) = \sum_{i=1}^4 N_i(\xi, \eta) y_i, \quad \frac{\partial y}{\partial \xi} = \sum_{i=1}^4 \frac{\partial N_i}{\partial \xi} y_i, \quad \frac{\partial y}{\partial \eta} = \sum_{i=1}^4 \frac{\partial N_i}{\partial \eta} y_i.$$

Writing it in matrix form we have:

$$\begin{bmatrix} \frac{\partial}{\partial \xi} \\ \frac{\partial}{\partial \eta} \end{bmatrix} = \begin{bmatrix} \frac{\partial x}{\partial \xi} & \frac{\partial y}{\partial \xi} \\ \frac{\partial x}{\partial \eta} & \frac{\partial y}{\partial \eta} \end{bmatrix} \begin{bmatrix} \frac{\partial}{\partial x} \\ \frac{\partial}{\partial y} \end{bmatrix} = \underline{\underline{J}} \begin{bmatrix} \frac{\partial}{\partial x} \\ \frac{\partial}{\partial y} \end{bmatrix}, \quad (12.99)$$

where  $\underline{\underline{J}}$  is the so-called Jacobi matrix:

$$\underline{\underline{J}} = \begin{bmatrix} \frac{\partial x}{\partial \xi} & \frac{\partial y}{\partial \xi} \\ \frac{\partial x}{\partial \eta} & \frac{\partial y}{\partial \eta} \end{bmatrix} = \begin{bmatrix} J_{11} & J_{12} \\ J_{21} & J_{22} \end{bmatrix}. \quad (12.100)$$

The Jacobi determinant is:

$$J = J_{11}J_{22} - J_{12}J_{21} = \frac{\partial x}{\partial \xi} \frac{\partial y}{\partial \eta} - \frac{\partial y}{\partial \xi} \frac{\partial x}{\partial \eta}. \quad (12.101)$$

The derivatives with respect to  $x$  and  $y$  are provided by the help of the inverse Jacobi matrix:

$$\underline{\underline{J}}^{-1} = \frac{1}{J} \begin{bmatrix} \frac{\partial y}{\partial \eta} & -\frac{\partial y}{\partial \xi} \\ -\frac{\partial x}{\partial \eta} & \frac{\partial x}{\partial \xi} \end{bmatrix} = \frac{1}{J} \begin{bmatrix} J_{22} & -J_{12} \\ -J_{21} & J_{11} \end{bmatrix}, \quad (12.102)$$

furthermore:

$$\begin{bmatrix} \frac{\partial}{\partial x} \\ \frac{\partial}{\partial y} \end{bmatrix} = \underline{\underline{J}}^{-1} \begin{bmatrix} \frac{\partial}{\partial \xi} \\ \frac{\partial}{\partial \eta} \end{bmatrix}, \quad (12.103)$$

From which we obtain the followings:

$$\frac{\partial}{\partial x} = \frac{1}{J} (J_{22} \frac{\partial}{\partial \xi} - J_{12} \frac{\partial}{\partial \eta}), \quad (12.104)$$

$$\frac{\partial}{\partial y} = \frac{1}{J} (-J_{21} \frac{\partial}{\partial \xi} + J_{11} \frac{\partial}{\partial \eta}).$$

With the aid of the former matrix  $\underline{\underline{B}}$  becomes:

$$\underline{\underline{B}} = \frac{1}{J} \begin{bmatrix} J_{22}N_{1,\xi} - J_{12}N_{1,\eta} & 0 & J_{22}N_{2,\xi} - J_{12}N_{2,\eta} & 0 & \dots \\ 0 & -J_{21}N_{1,\xi} + J_{11}N_{1,\eta} & 0 & J_{21}N_{2,\xi} - J_{11}N_{2,\eta} & \dots \\ -J_{21}N_{1,\xi} + J_{11}N_{1,\eta} & J_{22}N_{1,\xi} - J_{12}N_{1,\eta} & J_{21}N_{2,\xi} - J_{11}N_{2,\eta} & J_{22}N_{2,\xi} - J_{12}N_{2,\eta} & \dots \\ \dots & J_{22}N_{3,\xi} - J_{12}N_{3,\eta} & 0 & J_{22}N_{4,\xi} - J_{12}N_{4,\eta} & 0 \\ \dots & 0 & -J_{21}N_{3,\xi} + J_{11}N_{3,\eta} & 0 & -J_{21}N_{4,\xi} + J_{11}N_{4,\eta} \\ \dots & -J_{21}N_{3,\xi} + J_{11}N_{3,\eta} & J_{22}N_{3,\xi} - J_{12}N_{3,\eta} & -J_{21}N_{4,\xi} + J_{11}N_{4,\eta} & J_{22}N_{4,\xi} - J_{12}N_{4,\eta} \end{bmatrix} \quad (12.105)$$

$$\begin{bmatrix} J_{22}N_{1,\xi} - J_{12}N_{1,\eta} & 0 & J_{22}N_{2,\xi} - J_{12}N_{2,\eta} & 0 & \dots \\ 0 & -J_{21}N_{1,\xi} + J_{11}N_{1,\eta} & 0 & J_{21}N_{2,\xi} - J_{11}N_{2,\eta} & \dots \\ -J_{21}N_{1,\xi} + J_{11}N_{1,\eta} & J_{22}N_{1,\xi} - J_{12}N_{1,\eta} & J_{21}N_{2,\xi} - J_{11}N_{2,\eta} & J_{22}N_{2,\xi} - J_{12}N_{2,\eta} & \dots \\ \dots & J_{22}N_{3,\xi} - J_{12}N_{3,\eta} & 0 & J_{22}N_{4,\xi} - J_{12}N_{4,\eta} & 0 \\ \dots & 0 & -J_{21}N_{3,\xi} + J_{11}N_{3,\eta} & 0 & -J_{21}N_{4,\xi} + J_{11}N_{4,\eta} \\ \dots & -J_{21}N_{3,\xi} + J_{11}N_{3,\eta} & J_{22}N_{3,\xi} - J_{12}N_{3,\eta} & -J_{21}N_{4,\xi} + J_{11}N_{4,\eta} & J_{22}N_{4,\xi} - J_{12}N_{4,\eta} \end{bmatrix}$$

We need the derivatives of the interpolations functions and the elements of the Jacobi matrix, which are:

$$\frac{\partial N_1}{\partial \xi} = -\frac{1}{4}(1-\eta), \quad \frac{\partial N_2}{\partial \xi} = \frac{1}{4}(1-\eta), \quad \frac{\partial N_3}{\partial \xi} = \frac{1}{4}(1+\eta), \quad \frac{\partial N_4}{\partial \xi} = -\frac{1}{4}(1+\eta), \quad (12.106)$$

$$\frac{\partial N_1}{\partial \eta} = -\frac{1}{4}(1-\xi), \quad \frac{\partial N_2}{\partial \eta} = -\frac{1}{4}(1+\xi), \quad \frac{\partial N_3}{\partial \eta} = \frac{1}{4}(1+\xi), \quad \frac{\partial N_4}{\partial \eta} = \frac{1}{4}(1-\xi),$$

respectively, and:

$$J_{11} = \frac{\partial x}{\partial \xi} = \sum_{i=1}^4 \frac{\partial N_i}{\partial \xi} x_i = \frac{1}{4} \{ -(1-\eta)x_1 + (1-\eta)x_2 + (1+\eta)x_3 - (1+\eta)x_4 \}, \quad (12.107)$$

$$J_{12} = \frac{\partial y}{\partial \xi} = \sum_{i=1}^4 \frac{\partial N_i}{\partial \xi} y_i = \frac{1}{4} \{ -(1-\eta)y_1 + (1-\eta)y_2 + (1+\eta)y_3 - (1+\eta)y_4 \},$$

$$J_{21} = \frac{\partial x}{\partial \eta} = \sum_{i=1}^4 \frac{\partial N_i}{\partial \eta} x_i = \frac{1}{4} \{ -(1-\xi)x_1 - (1+\xi)x_2 + (1+\xi)x_3 + (1-\xi)x_4 \},$$

$$J_{22} = \frac{\partial y}{\partial \eta} = \sum_{i=1}^4 \frac{\partial N_i}{\partial \eta} y_i = \frac{1}{4} \{ -(1-\xi)y_1 - (1+\xi)y_2 + (1+\xi)y_3 + (1-\xi)y_4 \}.$$

Based on the former equations we can formulate the Jacobi matrix either in the following form:

$$J = \begin{bmatrix} J_{11} & J_{12} \\ J_{21} & J_{22} \end{bmatrix} = \begin{bmatrix} N_{1,\xi} & N_{2,\xi} & N_{3,\xi} & N_{4,\xi} \\ N_{1,\eta} & N_{2,\eta} & N_{3,\eta} & N_{4,\eta} \end{bmatrix} \begin{bmatrix} x_1 & y_1 \\ x_2 & y_2 \\ x_3 & y_3 \\ x_4 & y_4 \end{bmatrix}. \quad (12.108)$$

#### 12.5.4. The importance of the Jacobi determinant, example

Calculate the elements of the Jacobi matrix for the quadrilateral shown in Fig.12.8! The nodal coordinates are:

$$x_1 = 0, \quad y_1 = 0, \quad x_2 = a, \quad y_2 = 0, \quad x_3 = a, \quad y_3 = a, \quad x_4 = \frac{2}{3}a, \quad y_4 = \frac{1}{3}a. \quad (12.109)$$

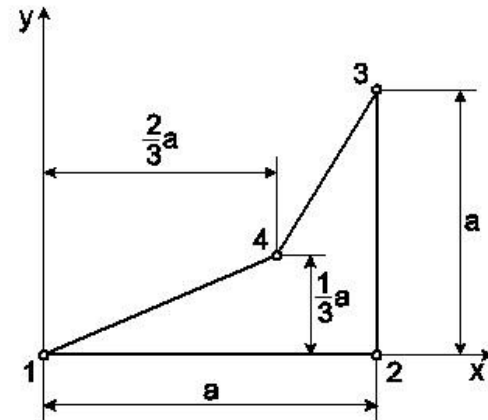


Fig.12.8. Isoparametric quadrilateral element with excessive distortion.

The elements of the Jacobi matrix based on Eq.(12.107) are:

$$J_{11} = \frac{1}{4} \left\{ -(1-\eta)0 + (1-\eta)a + (1+\eta)a - (1+\eta)\frac{2}{3}a \right\} = \frac{1}{3}a - \frac{1}{6}a\eta, \quad (12.110)$$

$$J_{12} = \frac{1}{4} \left\{ -(1-\eta)0 + (1-\eta)0 + (1+\eta)a - (1+\eta)\frac{1}{3}a \right\} = \frac{1}{6}a + \frac{1}{6}a\eta,$$

$$J_{21} = \frac{1}{4} \left\{ -(1-\xi)0 - (1+\xi)a + (1+\xi)a + (1-\xi)\frac{2}{3}a \right\} = \frac{1}{6}a - \frac{1}{6}a\xi,$$

$$J_{22} = \frac{1}{4} \left\{ -(1-\xi)0 - (1+\xi)0 + (1+\xi)a + (1-\xi)\frac{1}{3}a \right\} = \frac{1}{3}a + \frac{1}{6}a\xi,$$

from which the Jacobi determinant is:

$$J = J_{11}J_{22} - J_{12}J_{21} = \frac{1}{12}a^2(1+\xi-\eta). \quad (12.111)$$

The Jacobi determinant is 0, if e.g.  $\xi = -1$  and  $\eta = 0$ , or  $\xi = 0$  and  $\eta = -1$ . This case is said to be excessive distortion, it means that we have degenerate element. If  $J = 0$ , then the inverse Jacobi matrix does not exist at the point under consideration. Moreover, the parameter lines intersect each other outside the domain of the quadrilateral. That is why the sum of the inner angles of quadrilateral must be less than  $180^\circ$ , in other words the quadrilateral can not be concave.

#### 12.5.5. Calculation of the stress field

The vector of stress components can be obtained from Eq.(12.7):

$$\underline{\sigma} = \underline{\underline{C}} \underline{\varepsilon} = \underline{\underline{C}} \underline{\underline{B}} \underline{u}_e , \quad (12.112)$$

where  $\underline{\underline{C}} = \underline{\underline{C}}^{str}$  for plane stress and  $\underline{\underline{C}} = \underline{\underline{C}}^{sm}$  for plane strain (see section 11.)

### 12.5.6. Calculation of the stiffness matrix

The stiffness matrix for plane problems is calculated by Eq.(12.9):

$$\underline{\underline{K}}_e = \iint \underline{\underline{B}}^T \underline{\underline{C}}^T \underline{\underline{B}} v dx dy . \quad (12.113)$$

In the case of the isoparametric quadrilateral the elements of matrix  $\underline{\underline{B}}$  contains the derivatives of the interpolation functions. Consequently, for the stiffness matrix calculation the transformation of surface integrals must be performed. The vectors and parameters, which are required for the analysis, are shown in Fig.12.9. The ranges of parameters  $c_1$  and  $c_2$  are:

$$-1 \leq c_1 \leq 1, -1 \leq c_2 \leq 1. \quad (12.114)$$

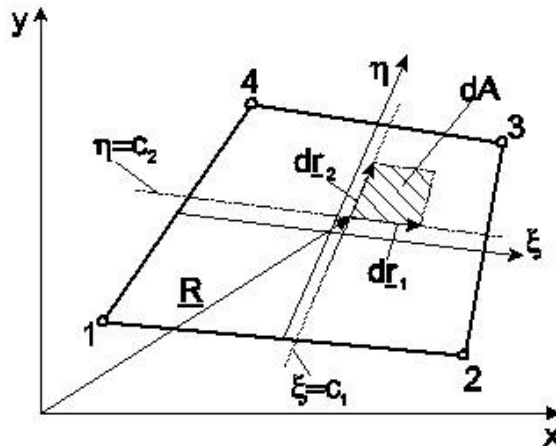


Fig.12.9. Transformation of surface integral in the isoparametric quadrilateral.

The differential vectors written by lowercase letters, can be formulated by utilizing Eq. (12.100):

$$d\underline{r}_1 = \begin{bmatrix} dx \\ dy \end{bmatrix}_{\eta=konst} = \begin{bmatrix} \frac{\partial x}{\partial \xi} d\xi + \frac{\partial x}{\partial \eta} d\eta \\ \frac{\partial y}{\partial \xi} d\xi + \frac{\partial y}{\partial \eta} d\eta \end{bmatrix}_{\eta=konst} = \begin{bmatrix} \frac{\partial x}{\partial \xi} d\xi \\ \frac{\partial x}{\partial \eta} d\xi \end{bmatrix} = \begin{bmatrix} J_{11} \\ J_{12} \end{bmatrix} d\xi , \quad (12.115)$$

and similarly:

$$d\underline{r}_2 = \begin{bmatrix} dx \\ dy \end{bmatrix}_{\xi=konst} = \begin{bmatrix} \frac{\partial x}{\partial \eta} d\eta \\ \frac{\partial y}{\partial \eta} d\eta \end{bmatrix} = \begin{bmatrix} J_{21} \\ J_{22} \end{bmatrix} d\eta. \quad (12.116)$$

The definition of the elementary area is:

$$dA = |d\underline{r}_1 \times d\underline{r}_2| = \text{abs} \left( \begin{vmatrix} i & j & k \\ J_{11}d\xi & J_{12}d\xi & 0 \\ J_{21}d\eta & J_{22}d\eta & 0 \end{vmatrix} \right) = (J_{11}J_{22} - J_{12}J_{21})d\xi d\eta = dx dy, \quad (12.117)$$

this yields:

$$dA = dx dy = J d\xi d\eta \text{ and: } \int_A dx dy = \int_{-1}^1 \int_{-1}^1 J d\xi d\eta. \quad (12.118)$$

The stiffness matrix becomes:

$$\underline{\underline{K}}_e = \int_A \underline{\underline{B}}^T \underline{\underline{C}}^T \underline{\underline{B}} v dx dy = \int_{-1}^1 \int_{-1}^1 \underline{\underline{B}}^T \underline{\underline{C}}^T \underline{\underline{B}} v J d\xi d\eta, \quad (12.119)$$

i.e., the stiffness matrix can be computed by the help of an area integral. For the calculation we can apply analytical or numerical method. The commercial finite element packages, in general, implement the Gaussian quadrature to perform the integration. This method will be presented in section 12.6.

#### 12.5.7. Calculation of the force vector

*Distributed load along the element edge.* The force vector resulting from the distributed load along element edge 1-2 shown in Fig.12.10 can be defined as:

$$\underline{F}_{ep} = v \int \underline{\underline{N}}^T \underline{p}_{12} ds, \quad (12.120)$$

where:

$$s = \frac{1}{2} l_{12} \xi \text{ and } ds = \frac{1}{2} l_{12} d\xi, \quad (12.121)$$

where  $l_{12}$  is the element edge length between nodes 1 and 2.

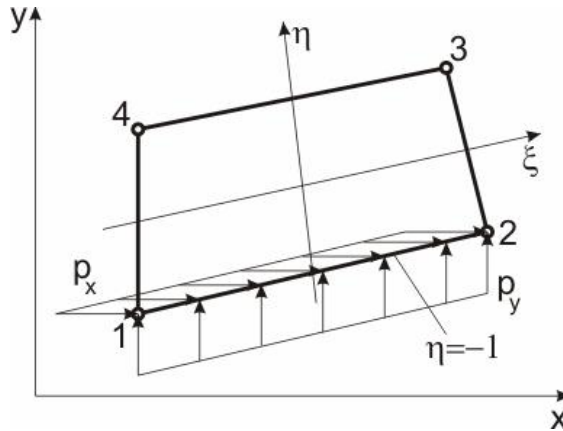


Fig.12.10. Distributed load along the element edge of an isoparametric quadrilateral element.

Moreover, we know that along edge 1-2  $\eta = -1$  and  $-1 \leq \xi \leq 1$  (see. Fig.12.6). We can write after all, that:

$$F_{ep} = v \int_{l_{12}} \underline{N}^T \underline{p}_{12} ds \Big|_{\eta=-1} = \frac{1}{2} v \int_{-1}^1 \begin{bmatrix} N_1 & 0 \\ 0 & N_1 \\ N_2 & 0 \\ 0 & N_2 \\ N_3 & 0 \\ 0 & N_3 \\ N_4 & 0 \\ 0 & N_4 \end{bmatrix} \begin{bmatrix} p_x \\ p_y \end{bmatrix} l_{12} d\xi \Big|_{\eta=-1} = \frac{1}{2} v l_{12} \int_{-1}^1 \begin{bmatrix} p_x N_1 \\ p_y N_1 \\ p_x N_2 \\ p_x N_2 \\ p_y N_3 \\ p_x N_3 \\ p_y N_3 \\ p_x N_4 \\ p_y N_4 \end{bmatrix} d\xi \Big|_{\eta=-1}. \quad (12.122)$$

For further calculation we must evaluate the interpolation functions along the parameter line, for which  $\eta = -1$ :

$$N_1 \Big|_{\eta=-1} = \frac{1}{4}(1-\xi)(1-\eta) \Big|_{\eta=-1} = \frac{1}{2}(1-\xi), \quad (12.123)$$

$$N_2 \Big|_{\eta=-1} = \frac{1}{4}(1+\xi)(1-\eta) \Big|_{\eta=-1} = \frac{1}{2}(1+\xi),$$

$$N_3 \Big|_{\eta=-1} = \frac{1}{4}(1+\xi)(1+\eta) \Big|_{\eta=-1} = 0,$$

$$N_4 \Big|_{\eta=-1} = \frac{1}{4}(1-\xi)(1+\eta) \Big|_{\eta=-1} = 0.$$

This yields:

$$\int_{-1}^1 p_x N_1 \Big|_{\eta=-1} d\xi = \frac{1}{2} p_x \int_{-1}^1 (1-\xi) d\xi = \frac{1}{2} p_x \left[ \xi - \frac{\xi^2}{2} \right]_{-1}^1 = \frac{1}{2} p_x \left[ 1 - \frac{1}{2} - (-1 - \frac{1}{2}) \right] = p_x, \quad (12.124)$$

$$\int_{-1}^1 p_y N_2 \Big|_{\eta=-1} d\xi = \frac{1}{2} p_y \int_{-1}^1 (1+\xi) d\xi = \frac{1}{2} p_y \left[ \xi + \frac{\xi^2}{2} \right]_{-1}^1 = \frac{1}{2} p_y \left[ 1 + \frac{1}{2} - (-1 + \frac{1}{2}) \right] = p_y.$$

By taking the results back into the force vector we obtain:

$$\underline{F}_{ep}^T = \frac{1}{2} v l_{12} [p_x \quad p_y \quad p_x \quad p_y \quad 0 \quad 0 \quad 0 \quad 0]. \quad (12.125)$$

The resultant of the uniformly distributed load is divided into two parts and (similarly to the beam and linear triangle elements) put into the nodes of element edge. The calculation can be made also in the case of linearly distributed load; naturally it results in a different force vector.

*Body force.* The force vector calculated from the body force is:

$$\underline{F}_{eb} = v \int_{-1}^1 \int_{-1}^1 \underline{\underline{N}}^T \underline{q} J d\xi d\eta, \quad (12.126)$$

for which we need again the evaluation of surface integral. Similarly to the stiffness matrix, the Gaussian quadrature will be applied to evaluate the integral.

*Concentrated loads.* For plane problems there are concentrated forces acting in the nodes and there are no moments. The  $x$  and  $y$  components of the concentrated forces are collected in a vector:

$$\underline{F}_{ec}^T = [F_{x1} \quad F_{y1} \quad F_{x2} \quad F_{y2} \quad F_{x3} \quad F_{y3} \quad F_{x4} \quad F_{y4}]. \quad (12.127)$$

The total vector of forces is the sum of vectors presented in the last three points:

$$\underline{F}_e = \underline{F}_{ep} + \underline{F}_{eb} + \underline{F}_{ec}. \quad (12.128)$$

## 12.6. Numerical integration, the Gauss rule

For the calculation of the element stiffness matrix and the body force vector of isoparametric quadrilaterals there are numerical integration schemes implemented in the finite element packages. Commonly, the Gauss rule is applied because it uses minimal number of sample points and it is relatively accurate [1,2,6].

### 12.6.1. One dimensional Gauss rule

The main aim is the approximate but relatively accurate calculation of the area under the curve shown by Fig.12.11 using the one dimensional rule.

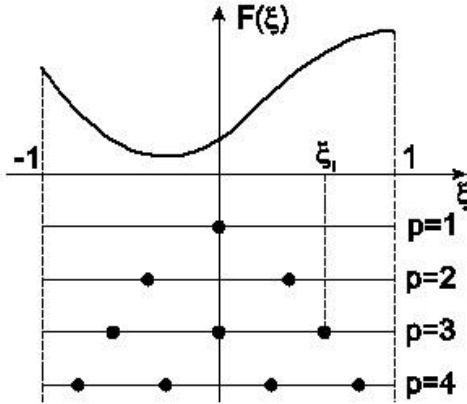


Fig.12.11. Sample points of the one dimensional Gauss rule.

The approximate area under the curve is calculated by:

$$\int_{-1}^1 F(\xi) d\xi \approx \sum_{i=1}^p w_i F(\xi_i). \quad (12.129)$$

The sample (or integration) point coordinates,  $\xi_i$  and the integration weights,  $w_i$  are listed in table 12.1. The one dimensional rule provides the exact solution for a polynomial up to the order of  $2p-1$ .

| <b>p</b> | <b><math>\xi_i</math></b>   | <b><math>w_i</math></b> |
|----------|-----------------------------|-------------------------|
| 1        | 0                           | 2                       |
| 2        | $-1/\sqrt{3}$               | 1                       |
|          | $1/\sqrt{3}$                | 1                       |
| 3        | $-\sqrt{3}/5$               | $5/9$                   |
|          | 0                           | $8/9$                   |
|          | $\sqrt{3}/5$                | $5/9$                   |
| 4        | $-\sqrt{(3-2\sqrt{6}/5)/7}$ | $1/2 - (\sqrt{5}/6)/6$  |
|          | $-\sqrt{(3+2\sqrt{6}/5)/7}$ | $1/2 + (\sqrt{5}/6)/6$  |
|          | $\xi_3 = -\xi_2$            | $w_3 = w_2$             |
|          | $\xi_4 = -\xi_1$            | $w_4 = w_1$             |

Table 12.1. Parameters of the one dimensional Gauss rule.

Let us solve an example for the application of the Gauss rule! Calculate the exact value of the integral:

$$I = \int_1^3 \frac{1}{x} dx \quad (12.130)$$

as well as its approximate value using one, two and three integration points!

*Exact solution:*

$$I = [\ln x]_1^3 = \ln 3 - \ln 1 = 1,098612. \quad (12.131)$$

*Gauss rule, p = 1.* Let  $\xi = x-2$ . If  $x = 3$ , then  $\xi = 1$ , on the other hand if  $x = 1$ , then  $\xi = -1$ , consequently:

$$I = \int_1^3 \frac{1}{x} dx = \int_{-1}^1 \frac{1}{\xi+2} d\xi, \text{ and: } F(\xi) = \frac{1}{\xi+2}. \quad (12.132)$$

The approximate value of the integral is:

$$I_1 \equiv w_1 F(0) = 2 \frac{1}{2} = 1. \quad (12.133)$$

That means an error of 9,9% compared to the exact solution.

*Gauss rule, p = 2.* In this case:

$$I_2 \equiv w_1 F(-\frac{1}{\sqrt{3}}) + w_2 F(\frac{1}{\sqrt{3}}) = 1 \frac{1}{-\frac{1}{\sqrt{3}+2}} + 1 \frac{1}{\frac{1}{\sqrt{3}+2}} = 1,090909. \quad (12.134)$$

The value of the integral differs with 0,7 % from the exact solution.

*Gauss rule, p = 3.*

$$I_3 \equiv w_1 F(-\sqrt{\frac{3}{5}}) + w_2 F(0) + w_3 F(\sqrt{\frac{3}{5}}) = \frac{5}{9} \frac{1}{-\sqrt{\frac{3}{5}+2}} + \frac{8}{9} \frac{1}{2} + \frac{5}{9} \frac{1}{\sqrt{\frac{3}{5}+2}} = 1,0980387. \quad (12.135)$$

The error of approximation is only 0,052%.

### 12.6.2. Two dimensional Gauss rule

The two dimensional Gauss rule makes it possible to evaluate the approximate value of surface integrals. The integral is approximated by the expression below:

$$\iint_a^b f(x, y) dx dy = \int_{-1}^1 \int_{-1}^1 f(\xi, \eta) J d\xi d\eta \cong \sum_{j=1}^n \sum_{i=1}^n w_i w_j f(\xi_i, \eta_j) |J(\xi_i, \eta_j)|, \quad (12.136)$$

where  $w_i$  and  $w_j$  are the integration weights,  $\xi_i$  and  $\eta_j$  are the integration point coordinates, moreover, the ranges are  $-1 \leq \xi_i \leq 1$ ,  $-1 \leq \eta_j \leq 1$ , respectively. Depending on the number of integration points we can define different Gaussian quadratures, as it is demonstrated in Fig.12.12.

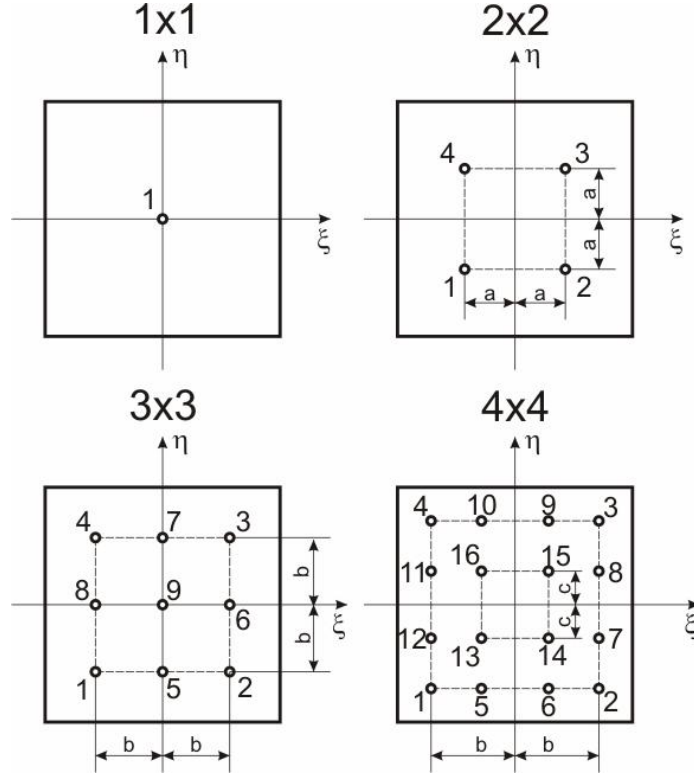


Fig.12.12. Integration points of the 1x1, 2x2, 3x3 and 4x4 Gaussian quadratures.

For the 1x1 quadrature there is only a single integration point, for the 2x2 we have 4, etc. The parameters of the 1x1, 2x2 and 3x3 Gaussian quadratures are summarized in Table 12.2.

| 1x1          | 2x2              |               | 3x3              |               |       |
|--------------|------------------|---------------|------------------|---------------|-------|
|              | $a = 1/\sqrt{3}$ |               | $b = \sqrt{3}/5$ |               |       |
| $\xi_1 = 0$  | $\xi_1 = -a$     | $\eta_1 = -a$ | $\xi_1 = -b$     | $\eta_1 = -b$ | $w_i$ |
| $\eta_1 = 0$ | $\xi_2 = a$      | $\eta_2 = -a$ | $\xi_2 = b$      | $\eta_2 = -b$ | $w_j$ |
| $w_1 = 2$    | $\xi_3 = a$      | $\eta_3 = a$  | $\xi_3 = b$      | $\eta_3 = b$  |       |
|              | $\xi_4 = -a$     | $\eta_4 = a$  | $\xi_4 = -b$     | $\eta_4 = b$  |       |
|              |                  |               | $\xi_5 = 0$      | $\eta_5 = -b$ | $5/9$ |
|              | $w_1 = 1$        | $w_2 = 1$     | $\xi_6 = b$      | $\eta_6 = 0$  | $5/9$ |
|              | $w_3 = 1$        | $w_4 = 1$     | $\xi_7 = 0$      | $\eta_7 = b$  | $5/9$ |
|              |                  |               | $\xi_8 = -b$     | $\eta_8 = 0$  | $5/9$ |
|              |                  |               | $\xi_9 = 0$      | $\eta_9 = 0$  | $8/9$ |

Table 12.2. Parameters of the Gaussian quadratures.

*Example for the application of Gaussian quadrature.* Calculate the approximate value of the integral:

$$I = \int_A xy dA \quad (12.137)$$

using the 2x2 Gauss quadrature for the domain of parallelogram depicted in Fig.12.13! Compare the result to that of the exact integration [4]!

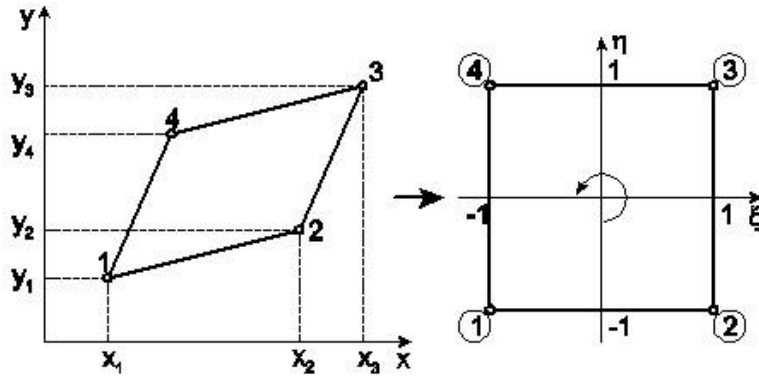


Fig.12.13. Example for the application of Gaussian quadrature.

The nodal coordinates are:

$$x_1 = 1, x_2 = 3, x_3 = 4, x_4 = 2, y_1 = 1, y_2 = 2, y_3 = 4, y_4 = 3. \quad (12.138)$$

Based on the approximate expression of the 2x2 Gaussian quadrature we can write:

$$I = \int_A xy dA \cong \sum_{i=1}^2 \sum_{j=1}^2 w_i w_j f(\xi_i, \eta_j) |J(\xi_i, \eta_j)|. \quad (12.139)$$

The calculation requires the elements of the Jacobi matrix. We need the nodal coordinates and also the derivatives of the interpolation functions (see Eq.(12.110)):

$$J_{11} = \frac{1}{4} \{ -(1-\eta)1 + (1-\eta)3 + (1+\eta)4 - (1+\eta)2 \} = 1, \quad (12.140)$$

$$J_{12} = \frac{1}{4} \{ -(1-\eta)1 + (1-\eta)2 + (1+\eta)4 - (1+\eta)3 \} = \frac{1}{2},$$

$$J_{21} = \frac{1}{4} \{ -(1-\xi)1 - (1+\xi)3 + (1+\xi)4 + (1-\xi)2 \} = \frac{1}{2},$$

$$J_{22} = \frac{1}{4} \{ -(1-\xi)1 - (1+\xi)2 + (1+\xi)4 + (1-\xi)3 \} = 1.$$

The Jacobi matrix is:

$$\underline{\underline{J}} = \begin{bmatrix} J_{11} & J_{12} \\ J_{21} & J_{22} \end{bmatrix} = \begin{bmatrix} 1 & \frac{1}{2} \\ \frac{1}{2} & 1 \end{bmatrix}, \quad (12.141)$$

and the Jacobi determinant is:

$$J = 1 \cdot 1 - \frac{1}{2} \cdot \frac{1}{2} = \frac{3}{4} = \text{const.} \quad (12.142)$$

The  $x$  and  $y$  parameters utilizing the interpolated form given by Eq.(12.77) are:

$$x(\xi, \eta) = \sum_{i=1}^4 N_i x_i = \frac{1}{4} \left\{ (1-\xi)(1-\eta)1 + (1+\xi)(1-\eta)3 + (1+\xi)(1+\eta)4 + (1-\xi)(1+\eta)2 \right\}, \quad (12.143)$$

$$y(\xi, \eta) = \sum_{i=1}^4 N_i y_i = \frac{1}{4} \left\{ (1-\xi)(1-\eta)1 + (1+\xi)(1-\eta)2 + (1+\xi)(1+\eta)4 + (1-\xi)(1+\eta)3 \right\}.$$

The function,  $f(\xi, \eta)$  is:

$$f(\xi, \eta) = xy = \frac{1}{4} \left\{ (5+2\xi+\eta) \cdot (5+\xi+2\eta) \right\}. \quad (12.144)$$

We can calculate the approximate value of the integral based on the figure and table above:

$$I = [f(-a, -a) + f(-a, a) + f(a, -a) + f(a, a)] \frac{3}{4} = 19,75. \quad (12.145)$$

The exact value of the integral is:

$$I = \int_{-1}^1 \int_{-1}^1 f(\xi, \eta) d\xi d\eta = xy = \int_{-1}^1 \int_{-1}^1 \frac{1}{4} \left\{ (5+2\xi+\eta) \cdot (5+\xi+2\eta) \right\} \frac{3}{4} d\xi d\eta = \frac{79}{4} = 19,75. \quad (12.146)$$

It is shown apparently, that the Gaussian quadrature provides the exact value in this case. Most of the commercial finite element packages implements 2x2 quadrature.

## 12.7. Example for the isoparametric quadrilateral

Solve the example presented in section 12.3 using one isoparametric quadrilateral element! The data are the same as those given in the linear triangle element. Apply a single finite element by following Fig.12.14 [4]. Determine the nodal displacements and the reactions!

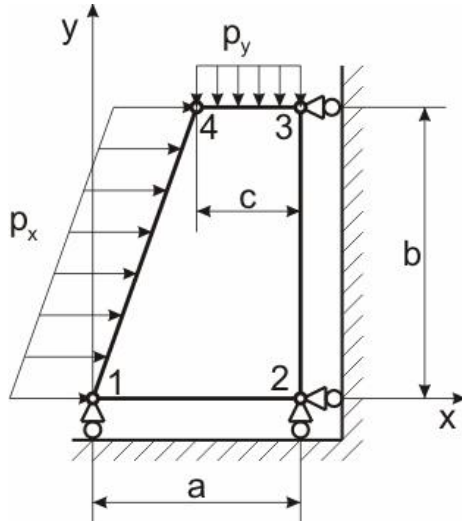


Fig.12.14. Example for the application of the isoparametric quadrilateral element.

The finite element equilibrium equation to be solved is:

$$\underline{\underline{K}}\underline{U} = \underline{F}. \quad (12.147)$$

Since we have only a single element, in this case Eq.(12.147) corresponds to the equilibrium equation in the element level:

$$\underline{\underline{K}}_e \underline{u}_e = \underline{F}_e, \quad (12.148)$$

where:

$$\underline{U}^T = [u_1 \ v_1 \ u_2 \ v_2 \ u_3 \ v_3 \ u_4 \ v_4] \quad (12.149)$$

is the vector of nodal displacements. Due to the boundary conditions ( $v_1 = v_2 = u_2 = u_3 = 0$ ) we have:

$$\underline{U}^T = [u_1 \ 0 \ 0 \ 0 \ 0 \ v_3 \ u_4 \ v_4]. \quad (12.150)$$

Similarly to the linear triangle element, we have a system of equations including four unknowns. The element stiffness matrix is calculated by the Gaussian quadrature, i.e. we can write, that:

$$\underline{\underline{K}}_e = \int_{-1}^1 \int_{-1}^1 \underline{\underline{B}}^T \underline{\underline{C}}^T \underline{\underline{B}} v J d\xi d\eta \cong v \sum_{i=1}^p \sum_{j=1}^p w_i w_j \underline{\underline{B}}^T(\xi_i, \eta_j) \underline{\underline{C}}^T \underline{\underline{B}}(\xi_i, \eta_j) |J(\xi_i, \eta_j)|. \quad (12.151)$$

The elements of the Jacobi matrix are equally required:

$$\begin{aligned} J_{11} &= \frac{\partial x}{\partial \xi} = \sum_{i=1}^4 \frac{\partial N_i}{\partial \xi} x_i = \frac{1}{4} \left\{ -(1-\eta)x_1 + (1-\eta)x_2 + (1+\eta)x_3 - (1+\eta)x_4 \right\} = \\ &= \frac{1}{4} \left\{ -(1-\eta)0 + (1-\eta)20 + (1+\eta)20 - (1+\eta)10 \right\} = \frac{15}{2} - \frac{5}{2}\eta, \end{aligned} \quad (12.152)$$

$$\begin{aligned} J_{12} &= \frac{\partial y}{\partial \xi} = \sum_{i=1}^4 \frac{\partial N_i}{\partial \xi} y_i = \frac{1}{4} \left\{ -(1-\eta)y_1 + (1-\eta)y_2 + (1+\eta)y_3 - (1+\eta)y_4 \right\} = \\ &= \frac{1}{4} \left\{ -(1-\eta)0 + (1-\eta)0 + (1+\eta)30 - (1+\eta)30 \right\} = 0, \end{aligned}$$

$$\begin{aligned} J_{21} &= \frac{\partial x}{\partial \eta} = \sum_{i=1}^4 \frac{\partial N_i}{\partial \eta} x_i = \frac{1}{4} \left\{ -(1-\xi)x_1 - (1+\xi)x_2 + (1+\xi)x_3 + (1-\xi)x_4 \right\} = \\ &= \frac{1}{4} \left\{ -(1-\xi)0 - (1+\xi)20 + (1+\xi)20 + (1-\xi)10 \right\} = \frac{5}{2} - \frac{5}{2}\xi, \end{aligned}$$

$$\begin{aligned} J_{22} &= \frac{\partial y}{\partial \eta} = \sum_{i=1}^4 \frac{\partial N_i}{\partial \eta} y_i = \frac{1}{4} \left\{ -(1-\xi)y_1 - (1+\xi)y_2 + (1+\xi)y_3 + (1-\xi)y_4 \right\} = \\ &= \frac{1}{4} \left\{ -(1-\xi)0 - (1+\xi)0 + (1+\xi)30 + (1-\xi)30 \right\} = 15. \end{aligned}$$

Constructing the Jacobi matrix we have:

$$\underline{\underline{J}} = \begin{bmatrix} J_{11} & J_{12} \\ J_{21} & J_{22} \end{bmatrix} = \begin{bmatrix} \frac{15}{2} - \frac{5}{2}\eta & 0 \\ \frac{5}{2} - \frac{5}{2}\eta & 15 \end{bmatrix}, \quad (12.153)$$

and the Jacobi determinant is:

$$J = \frac{225}{2} - \frac{75}{2}\eta. \quad (12.154)$$

It can be seen, that if  $-1 \leq \eta \leq 1$ , then  $J > 0$  for each case, consequently the element is not degenerate, which is obviously seen based on Fig.12.5. The inverse Jacobi matrix is:

$$\underline{\underline{J}}^{-1} = \frac{1}{J} \begin{bmatrix} J_{22} & -J_{12} \\ -J_{21} & J_{11} \end{bmatrix} = \begin{bmatrix} \frac{2}{5(-3+\eta)} & 0 \\ \frac{1-\xi}{15(\eta-3)} & \frac{1}{15} \end{bmatrix}. \quad (12.155)$$

As a next step, we calculate matrix  $\underline{\underline{B}}$  (see Eq.(12.96)), where referring to Eq.(12.105) we have:

$$\frac{\partial N_1}{\partial x} = \frac{1}{J} (J_{22}N_{1,\xi} - J_{12}N_{1,\eta}) = -\frac{1-\eta}{10(3-\eta)}, \quad (12.156)$$

$$\frac{\partial N_1}{\partial y} = \frac{1}{J} (-J_{21}N_{1,\xi} + J_{11}N_{1,\eta}) = -\frac{1-\xi}{30(3-\eta)},$$

$$\frac{\partial N_2}{\partial x} = \frac{1}{J} (J_{22}N_{2,\xi} - J_{12}N_{2,\eta}) = -\frac{1-\eta}{10(3-\eta)}, \quad \frac{\partial N_2}{\partial y} = \frac{1}{J} (-J_{21}N_{2,\xi} + J_{11}N_{2,\eta}) = -\frac{2+\xi-\eta}{30(3-\eta)},$$

$$\frac{\partial N_3}{\partial x} = \frac{1}{J} (J_{22}N_{3,\xi} - J_{12}N_{3,\eta}) = \frac{1+\eta}{10(3-\eta)}, \quad \frac{\partial N_3}{\partial y} = \frac{1}{J} (-J_{21}N_{3,\xi} + J_{11}N_{3,\eta}) = \frac{1+2\xi-\eta}{30(3-\eta)},$$

$$\frac{\partial N_4}{\partial x} = \frac{1}{J} (J_{22}N_{4,\xi} - J_{12}N_{4,\eta}) = -\frac{1+\eta}{10(3-\eta)}, \quad \frac{\partial N_4}{\partial y} = \frac{1}{J} (-J_{21}N_{4,\xi} + J_{11}N_{4,\eta}) = \frac{1-\xi}{15(3-\eta)}.$$

Matrix  $\underline{\underline{B}}$  becomes:

$$\underline{\underline{B}} = \begin{bmatrix} -\frac{1-\eta}{10(3-\eta)} & 0 & -\frac{1-\eta}{10(3-\eta)} & 0 & \dots \\ 0 & -\frac{1-\xi}{30(3-\eta)} & 0 & -\frac{2+\xi-\eta}{30(3-\eta)} & \dots \\ -\frac{1-\xi}{30(3-\eta)} & -\frac{1-\eta}{10(3-\eta)} & -\frac{2+\xi-\eta}{30(3-\eta)} & -\frac{1-\eta}{10(3-\eta)} & \dots \\ \dots & \frac{1+\eta}{10(3-\eta)} & 0 & -\frac{1+\eta}{10(3-\eta)} & 0 \\ \dots & 0 & \frac{1+2\xi-\eta}{30(3-\eta)} & 0 & \frac{1-\xi}{15(3-\eta)} \\ \dots & \frac{1+2\xi-\eta}{30(3-\eta)} & \frac{1+\eta}{10(3-\eta)} & \frac{1-\xi}{15(3-\eta)} & -\frac{1+\eta}{10(3-\eta)} \end{bmatrix}. \quad (12.157)$$

We calculate the element [1,1] of the stiffness matrix by the Gaussian quadrature. For that, let us calculate the following:

$$[\underline{\underline{B}}^T \underline{\underline{C}}^T \underline{\underline{B}}]_{1,1} = \frac{1600(1-\eta)^2}{(3-\eta)^2} + \frac{200(1-\xi)^2}{3(3-\xi)^2}, \quad (12.158)$$

and:

$$\begin{aligned} [\underline{\underline{K}}_e]_{1,1} &= v \int_{-1}^1 \int_{-1}^1 [\underline{\underline{B}}^T \underline{\underline{C}}^T \underline{\underline{B}}]_{1,1} J d\xi d\eta = \\ &= v \int_{-1}^1 \int_{-1}^1 \left[ \frac{1600(1-\eta)^2}{(3-\eta)^2} + \frac{200(1-\xi)^2}{3(3-\xi)^2} \right] \left[ \frac{225}{2} - \frac{75}{2}\eta \right] d\xi d\eta = v \int_{-1}^1 \int_{-1}^1 f(\xi, \eta) J(\xi, \eta) d\xi d\eta, \end{aligned} \quad (12.159)$$

where  $v = 5$  mm is the thickness of the plate. We carry out the calculation in three ways, by using the 2x2, 3x3 Gaussian quadratures and the exact integration, respectively.

*I. 2x2 Gaussian quadrature:*

$$\begin{aligned} [\underline{\underline{K}}_e]_{:,1} &\equiv v \cdot \{f(-a, -a)|J(-a, -a)| + f(a, -a)|J(a, -a)| + f(a, a)|J(a, a)|f(-a, a)|J(-a, a)|\} = \\ &= (2.1734 + 2.0927 + 0.2304 + 0.3496) \cdot 10^5 = 4,8462 \cdot 10^5 \frac{\text{N}}{\text{mm}}. \end{aligned} \quad (12.160)$$

*II. 3x3 Gaussian quadrature:*

$$\begin{aligned} [\underline{\underline{K}}_e]_{:,1} &\equiv v \cdot \{f(-b, -b)|J(-b, -b)| + f(b, -b)|J(b, -b)| + f(b, b)|J(b, b)|f(-b, b)|J(-b, b)|\} \frac{5}{9} \frac{5}{9} + \\ &+ v \cdot \{f(0, -b)|J(0, -b)| + f(b, 0)|J(b, 0)| + f(0, b)|J(0, b)|f(-b, 0)|J(-b, 0)|\} \frac{8}{9} \frac{8}{9} + \\ &+ v \cdot f(0, 0)|J(0, 0)| \frac{8}{9} \frac{8}{9} = (2.6072 + 2.5046 + 0.07134 + 0.2454) \frac{25}{81} \cdot 10^5 + \\ &+ (2.5360 + 1.0021 + 0.1247 + 1.1312) \frac{40}{81} \cdot 10^5 + 1.0417 \frac{64}{81} \cdot 10^5 = 4,8660 \cdot 10^5 \frac{\text{N}}{\text{mm}}. \end{aligned} \quad (12.161)$$

*III. Exact integration:*

$$[\underline{\underline{K}}_e]_{:,1} = 4,8666 \cdot 10^5 \frac{\text{N}}{\text{mm}}. \quad (12.162)$$

Calculating all of the components of the element stiffness matrix we obtain:

$$\underline{\underline{K}}_e = \begin{bmatrix} 4,8666 & 0,76713 & -4,3666 & 0,23287 & -2,7668 & -0,9657 & 2,2668 & -0,03426 \\ . & 2,3545 & 0,7329 & -1,0211 & -0,9657 & -1,1244 & -0,5343 & -0,20891 \\ . & . & 5,3666 & -1,7329 & 2,2668 & -0,53426 & -3,2668 & 1,5343 \\ . & . & . & 3,6878 & -0,03426 & -0,20891 & 1,5343 & -2,4578 \\ . & . & . & . & 6,9663 & 0,5685 & -6,4663 & 0,43147 \\ . & . & . & . & . & 3,5845 & 0,93147 & -2,2512 \\ . & . & . & . & . & . & 7,4663 & -1,9315 \\ . & . & . & . & . & . & . & 4,9178 \end{bmatrix} \cdot 10^5 \frac{\text{N}}{\text{mm}}. \quad (12.163)$$

The vector of forces can be constructed in a similar way to that shown in the triangle element:

$$\underline{F}_{p1}^T = \frac{l_{14}v}{2} [p_x \ 0 \ 0 \ 0 \ 0 \ p_x \ 0] = [3\sqrt{10} \ 0 \ 0 \ 0 \ 0 \ 0 \ 3\sqrt{10} \ 0] \text{N}, \quad (12.164)$$

$$\underline{F}_{p2}^T = \frac{l_{34}v}{2} [0 \ 0 \ 0 \ 0 \ 0 \ p_y \ 0 \ p_y] = [0 \ 0 \ 0 \ 0 \ 0 \ -1,5 \ 0 \ -1,5] \text{N}.$$

We consider the reactions as concentrated forces in the kinematically constrained nodes:

$$\underline{F}_c^T = [F_{x1} \quad F_{y1} \quad F_{x2} \quad F_{y2} \quad F_{x3} \quad F_{y3} \quad F_{x4} \quad F_{y4}]. \quad (12.165)$$

Considering the fact that the surfaces are frictionless and that at node 4 there is no external force, we have  $F_{x1} = F_{y3} = F_{x4} = F_{y4} = 0$ , which leads to:

$$\underline{F}_c^T = [0 \quad F_{y1} \quad F_{x2} \quad F_{y2} \quad F_{x3} \quad 0 \quad 0 \quad 0]. \quad (12.166)$$

The structural force vector becomes:

$$\underline{F} = \underline{F}_{p1} + \underline{F}_{p2} + \underline{F}_c. \quad (12.167)$$

The construction of the finite element equilibrium equation results in:

$$\begin{bmatrix} 4,8666 & 0,76713 & -4,3666 & 0,23287 & -2,7668 & -0,9657 & 2,2668 & -0,03426 \\ . & 2,3545 & 0,7329 & -1,0211 & -0,9657 & -1,1244 & -0,5343 & -0,20891 \\ . & . & 5,3666 & -1,7329 & 2,2668 & -0,53426 & -3,2668 & 1,5343 \\ . & . & . & 3,6878 & -0,03426 & -0,20891 & 1,5343 & -2,4578 \\ . & . & . & . & 6,9663 & 0,5685 & -6,4663 & 0,43147 \\ . & . & . & . & . & 3,5845 & 0,93147 & -2,2512 \\ . & . & . & . & . & . & 7,4663 & -1,9315 \\ . & . & . & . & . & . & . & 4,9178 \end{bmatrix} \cdot 10^5 = \begin{bmatrix} u_1 \\ v_1 \\ F_{y1} \\ F_{x2} \\ F_{y2} \\ F_{x3} \\ -1,5 \\ 3\sqrt{10} \end{bmatrix}. \quad (12.168)$$

In the stiffness matrix we eliminate those rows and columns, for which the corresponding displacement component is a prescribed (here constrained) value. This way we obtain the so-called condensed stiffness matrix, which is used to expand the system of equations, of which solutions are the nodal displacements:

$$\begin{bmatrix} 4,8666 & -0,9657 & 2,2668 & -0,03426 \\ . & 3,5845 & 0,93147 & -2,2512 \\ . & . & 7,4663 & -1,9315 \\ . & . & . & 4,9178 \end{bmatrix} \cdot 10^5 \begin{bmatrix} u_1 \\ v_3 \\ u_4 \\ v_4 \end{bmatrix} = \begin{bmatrix} 3\sqrt{10} \\ -1,5 \\ 3\sqrt{10} \\ -1,5 \end{bmatrix}. \quad (12.169)$$

The solutions are:

$$u_1 = 1,5078 \cdot 10^{-5} \text{ mm}, v_3 = -0,29199 \cdot 10^{-5} \text{ mm}, \quad (12.170)$$

$$u_4 = 0,822016 \cdot 10^{-5} \text{ mm}, v_4 = -0,10532 \cdot 10^{-5} \text{ mm}.$$

Then, the reactions are calculated by the 2<sup>nd</sup>, 3<sup>rd</sup>, 4<sup>th</sup> and 5<sup>th</sup> component equations of Eq. (12.168). The solutions are:

$$F_{y1} = 1,0678 \text{ N}, F_{x2} = -9,27494 \text{ N}, \quad (12.171)$$

$$F_{y2} = 1,93216 \text{ N}, F_{x3} = -9,6987 \text{ N}.$$

The strain and stress components of the element can be expressed in parametric form (as the function of  $\xi$  and  $\eta$ ) from Eqs.(12.95) and (12.105). Taking the coordinates of the corresponding node back, the strain and stress components can be calculated. The example above was verified by the finite element code ANSYS 12.

## 12.8. Quadratic isoparametric quadrilateral

The advanced version of the linear quadrilateral is the quadratic quadrilateral, in which the curves of the element sides as well as the displacements are approximated by a second order function of the  $\xi$  and  $\eta$  coordinates [2,7]. On each element edge we provide a midside node, as it is shown in Fig.12.15, implying 8 nodes and 8 unknown coefficients in the approximate function of e.g. the  $x$  coordinate:

$$x(\xi, \eta) = a_0 + a_1\xi + a_2\eta + a_3\xi\eta + a_4\xi^2 + a_5\eta^2 + a_6\xi^2\eta + a_7\xi\eta^2. \quad (12.172)$$

Using the nodal conditions we can derive the interpolation functions of the quadratic element in a similar way to that shown in the four node quadrilateral. The interpolation functions become:

$$N_1(\xi, \eta) = -\frac{1}{4}(1-\xi)(1-\eta)(1+\xi+\eta), \quad N_2(\xi, \eta) = \frac{1}{2}(1-\xi^2)(1-\eta), \quad (12.173)$$

$$N_3(\xi, \eta) = -\frac{1}{4}(1+\xi)(1-\eta)(1-\xi+\eta), \quad N_4(\xi, \eta) = \frac{1}{2}(1+\xi)(1-\eta^2),$$

$$N_5(\xi, \eta) = -\frac{1}{4}(1+\xi)(1+\eta)(1-\eta-\xi), \quad N_6(\xi, \eta) = \frac{1}{2}(1-\xi^2)(1+\eta),$$

$$N_7(\xi, \eta) = -\frac{1}{4}(1-\xi)(1+\eta)(1+\xi-\eta), \quad N_8(\xi, \eta) = \frac{1}{2}(1-\xi)(1-\eta^2).$$

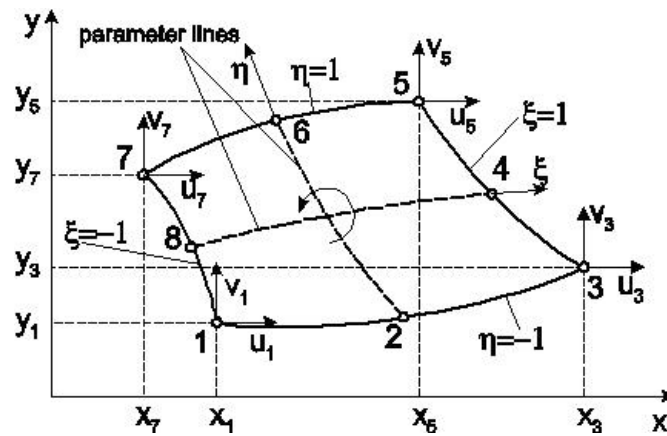


Fig.12.15. Quadratic isoparametric quadrilateral.

The interpolation functions can be formulated also in compact form:

$$N_i = \frac{1}{4}(1 + \xi\xi_i)(1 + \eta\eta_i)(\xi\xi_i + \eta\eta_i - 1), i = 1, 3, 5, 7, \quad (12.174)$$

$$N_i = \frac{1}{2}\xi_i^2(1 + \xi\xi_i)(1 - \eta^2) + \frac{1}{2}\eta_i^2(1 + \eta\eta_i)(1 - \xi^2), i = 2, 4, 6, 8.$$

where  $\xi_i$  and  $\eta_i$  are the coordinates of the nodes. Fig.12.16 shows the function plot of the interpolation functions  $N_5$  and  $N_8$ .

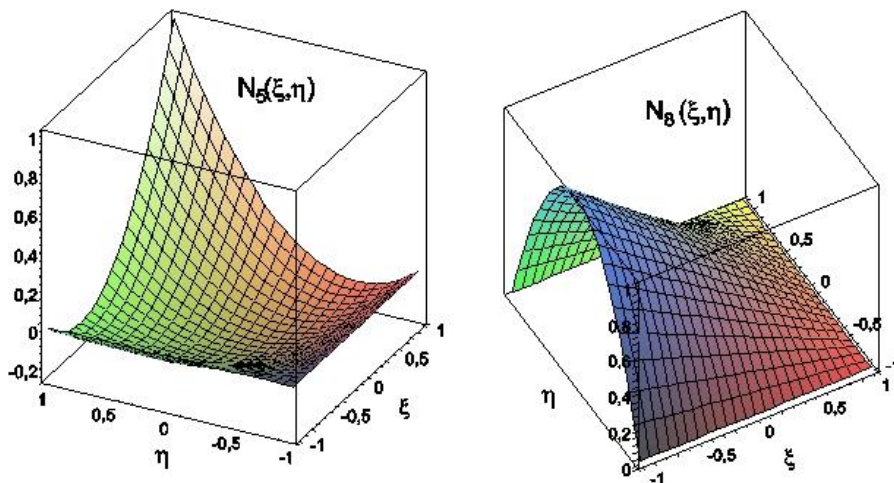


Fig.12.16. Interpolation functions of the quadratic isoparametric quadrilateral.

The value of  $N_i$  corresponding to the  $i^{\text{th}}$  node is equal to unity, in the other nodes it is zero. The calculation of the stiffness matrix and the vector of forces can be made in the same way as that shown in the quadrilateral with straight edges. The Jacobi determinant and the Gaussian quadrature is equally required.

## 12.9. Bibliography

- [1] Gábor Vörös, *Finite element analysis*, Mechanical Engineering Modeling MSc formation, Budapest University of Technology and Economics, Faculty of Mechanical Engineering, Department of Applied Mechanics, lecture note, 2008/2009 autumn semester.
- [2] József Uj, *Lectures and practices of the subject Numerical methods in mechanics*, PhD formation, Budapest University of Technology and Economics, Faculty of Mechanical Engineering, Department of Applied Mechanics, 2002/2003 spring semester (in Hungarian).
- [3] Singiresu S. Rao, *The finite element method in engineering – fourth edition*. 2004, Elsevier Science & Technology Books.
- [4] Erdogan Madenci, Ibrahim Guven, *The finite element method and applications in engineering using ANSYS*. Springer Science+Business Media Inc., 2006, New York, USA.
- [5] Imre Bojtár, György Molnár, Tamás Nagy, *Application of the finite element method to plane problems*. Technical Book Publisher, 1988, Budapest (in Hungarian)

- [6] Ádám Kovács, József Uj, *Fundamentals of finite element method*, University Press, 2007, Budapest (in Hungarian).
- [7] Klaus-Jürgen Bathe, *Finite element procedures*. Prentice Hall, Upper Saddle River, 1996, New Jersey 17458.

## 13. MODELING OF AXISYMMETRIC STATE BY FEM SOFTWARE SYSTEMS. MODELING, ANALYSIS OF PROBLEM EVALUATION

### 13.1. Finite element solution of axisymmetric problems

For axisymmetric problems both the geometry and the load are independent of the angle coordinate,  $\vartheta$ . An example is shown in Fig.13.1.

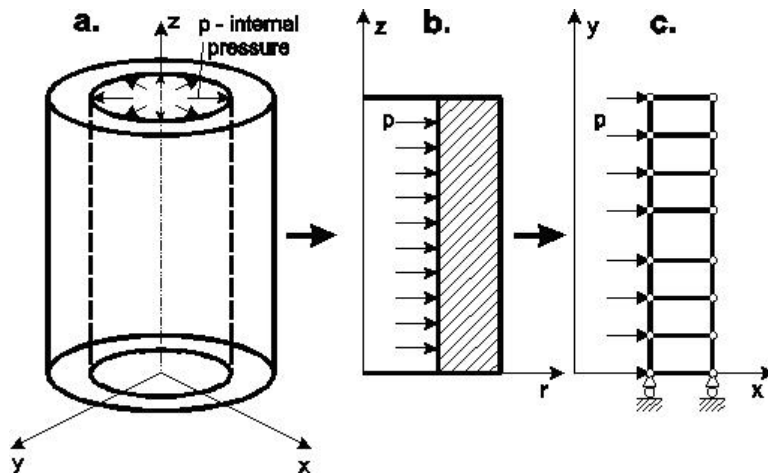


Fig.13.1. Thick-walled tube under internal pressure (a), axisymmetric model of the tube (b), and the simplified finite element problem (c).

Plane problems are defined in plane as the meridian section of an actual body; mathematically they can be solved as two-variable problems. The element types of axisymmetric problems are actually ring shape elements. That is why there is no concentrated force in such problems, except for the case when the force coincides with the axis of symmetry. A line load with constant intensity on the outer surface of the model defined by a radius of  $r$ , looks as a concentrated force. For axisymmetric problems the displacement field has the following form [1]:

$$\underline{u} = u(r, z)\underline{e}_r + w(r, z)\underline{e}_z. \quad (13.1)$$

The strain-displacement equation is:

$$\underline{\varepsilon} = \frac{1}{2}(\underline{u} \circ \nabla + \nabla \circ \underline{u}), \quad (13.2)$$

where  $\nabla$  is the Hamilton operator in cylindrical coordinate system (CCS). It can be derived by the help of Eq.(11.61). Based on Fig.11.7 the radial and tangential unit basis vectors become [1]:

$$\underline{e}_r = \cos \vartheta \underline{i} + \sin \vartheta \underline{j}, \quad \underline{e}_t = -\sin \vartheta \underline{i} + \cos \vartheta \underline{j}. \quad (13.3)$$

Operator nabla in the  $x$ - $y$ - $z$  coordinate system is:

$$\nabla = \frac{\partial}{\partial x} \underline{i} + \frac{\partial}{\partial y} \underline{j} + \frac{\partial}{\partial z} \underline{k}. \quad (13.4)$$

Utilizing Eq.(11.61) and substituting it into Eq.(13.4) leads to:

$$\nabla = \frac{\partial}{\partial r} \underline{e}_r + \frac{1}{r} \frac{\partial}{\partial \varphi} \underline{e}_t + \frac{\partial}{\partial z} \underline{e}_z. \quad (13.5)$$

The strain components in CCS can be written as [2,3] (see Eq.(11.66)):

$$\underline{\varepsilon}_r = \frac{\partial u}{\partial r}, \underline{\varepsilon}_t = \frac{u}{r}, \underline{\varepsilon}_z = \frac{\partial w}{\partial z}, \underline{\gamma}_{rz} = \frac{\partial u}{\partial z} + \frac{\partial w}{\partial r}. \quad (13.6)$$

In vector form:

$$\underline{\varepsilon}^T = [\underline{\varepsilon}_r \quad \underline{\varepsilon}_t \quad \underline{\varepsilon}_z \quad \underline{\gamma}_{rz}]. \quad (13.7)$$

The vector of strain components is written in the following form:

$$\underline{\varepsilon} = \underline{\underline{\varepsilon}} u, \quad (13.8)$$

where, based on Eq.(13.6) the matrix of differential operators is completed with an additional element compared to the plane stress or plane strain states:

$$\underline{\underline{\varepsilon}} = \begin{bmatrix} \frac{\partial}{\partial r} & 0 \\ \frac{1}{r} & 0 \\ 0 & \frac{\partial}{\partial z} \\ \frac{\partial}{\partial z} & \frac{\partial}{\partial r} \end{bmatrix}. \quad (13.9)$$

The vector of stress components is:

$$\underline{\sigma}^T = [\sigma_r \quad \sigma_t \quad \sigma_z \quad \tau_{rz}]. \quad (13.10)$$

Independently of the coordinate system we have Hooke's law in the form below:

$$\underline{\underline{\sigma}} = 2G \left[ \underline{\underline{\varepsilon}} + \frac{\nu}{1-2\nu} \underline{\underline{\varepsilon}} E \right], \quad (13.11)$$

$$\underline{\underline{\sigma}} = \begin{bmatrix} \sigma_r & 0 & \tau_{rz} \\ 0 & \sigma_t & 0 \\ \tau_{rz} & 0 & \sigma_z \end{bmatrix}, \underline{\underline{\varepsilon}} = \begin{bmatrix} \varepsilon_r & 0 & 1/2 \cdot \gamma_{rz} \\ 0 & \varepsilon_t & 0 \\ 1/2 \cdot \gamma_{rz} & 0 & \varepsilon_z \end{bmatrix}, \quad (13.12)$$

from which we have:

$$\sigma_r = \frac{E}{1+\nu} \left[ \varepsilon_r + \frac{\nu}{1-2\nu} (\varepsilon_r + \varepsilon_t + \varepsilon_z) \right] = \frac{E}{(1+\nu)(1-2\nu)} [\varepsilon_r(1-\nu) + \varepsilon_t\nu + \varepsilon_z\nu], \quad (13.13)$$

$$\sigma_t = \frac{E}{1+\nu} \left[ \varepsilon_t + \frac{\nu}{1-2\nu} (\varepsilon_r + \varepsilon_t + \varepsilon_z) \right] = \frac{E}{(1+\nu)(1-2\nu)} [\varepsilon_r\nu + \varepsilon_t(1-\nu) + \varepsilon_z\nu],$$

$$\sigma_z = \frac{E}{1+\nu} \left[ \varepsilon_z + \frac{\nu}{1-2\nu} (\varepsilon_r + \varepsilon_t + \varepsilon_z) \right] = \frac{E}{(1+\nu)(1-2\nu)} [\varepsilon_r\nu + \varepsilon_t\nu + \varepsilon_z(1-\nu)],$$

$$\tau_{rz} = \frac{E}{1+\nu} \gamma_{rz}.$$

Accordingly, the constitutive matrix based on  $\underline{\underline{\sigma}} = \underline{\underline{C}} \underline{\underline{\varepsilon}}$  is [2,3]:

$$\underline{\underline{C}} = \frac{E}{(1+\nu)(1-2\nu)} \begin{bmatrix} 1-\nu & \nu & \nu & 0 \\ \nu & 1-\nu & \nu & 0 \\ \nu & \nu & 1-\nu & 0 \\ 0 & 0 & 0 & \frac{1-2\nu}{2} \end{bmatrix}. \quad (13.14)$$

The calculation of the element stiffness matrix is possible through the following definition [4]:

$$\underline{\underline{K}}_e = \int_{V_e} \underline{\underline{B}}^T \underline{\underline{C}} \underline{\underline{B}} dV, \quad (13.15)$$

where the dimension of matrix  $\underline{\underline{B}}$  depends on the degrees of freedom of the element. The vector of forces can be determined in the same way as it was shown for plane problems.

The domain of axisymmetric bodies can be meshed by ring shape elements. Elements can be defined in the meridian section, i.e. in plane. In the finite element softwares the same element types are available as those for plane problems; however the axisymmetric behavior should be set. In the course of the finite element analysis the same interpolation functions are applied as those presented for plane stress and plane strain states. In most of the finite element codes the plane model should be prepared in the  $x$ - $y$  plane, where  $y$  is the axis of revolution (see Fig.13.1c). In the sequel we review the application of the linear triangle and the isoparametric quadrilateral elements.

### 13.2. Axisymmetric linear triangle element

The steps of the finite element discretization using linear triangle element have already been presented in section 12.2. Some modification is required considering the axisymmetric application of the triangle element. In the displacement field we change the  $x$  and  $y$  parameters to  $r$  and  $z$ , respectively [1]:

$$\underline{u}(r, z) = \begin{bmatrix} u(r, z) \\ w(r, z) \end{bmatrix} = \underline{\underline{N}}(r, z) \underline{u}_e, \quad (13.16)$$

where the displacement components can be provided by changing the coordinate  $x$  to  $r$  and coordinate  $y$  to  $z$  in Eq.(12.24), respectively:

$$u(r, z) = N_1(r, z)u_1 + N_2(r, z)u_2 + N_3(r, z)u_3, \quad (13.17)$$

$$w(r, z) = N_1(r, z)w_1 + N_2(r, z)w_2 + N_3(r, z)w_3,$$

moreover, the matrix of interpolation functions and the vector of nodal displacements become:

$$\begin{aligned} \underline{\underline{N}}(r, z) &= \begin{bmatrix} N_1 & 0 & N_2 & 0 & N_3 & 0 \\ 0 & N_1 & 0 & N_2 & 0 & N_3 \end{bmatrix}, \\ \underline{u}_e^T &= [u_1 \quad w_1 \quad u_2 \quad w_2 \quad u_3 \quad w_3]. \end{aligned} \quad (13.18)$$

The calculation of the strain components is made in a similar fashion to that presented in plane problems:

$$\underline{\underline{\varepsilon}} = \underline{\underline{\partial u}} = \underline{\underline{\partial N}} \underline{u}_e = \underline{\underline{B}} \underline{u}_e, \quad (13.19)$$

where the strain-displacement matrix using Eqs.(13.9) and (13.18) is:

$$\underline{\underline{B}} = \underline{\underline{\partial N}} = \begin{bmatrix} \frac{\partial}{\partial r} & 0 \\ \frac{1}{r} & 0 \\ 0 & \frac{\partial}{\partial z} \\ \frac{\partial}{\partial z} & \frac{\partial}{\partial r} \end{bmatrix} \begin{bmatrix} N_1 & 0 & N_2 & 0 & N_3 & 0 \\ 0 & N_1 & 0 & N_2 & 0 & N_3 \end{bmatrix} =$$

$$= \begin{bmatrix} \frac{\partial N_1}{\partial r} & 0 & \frac{\partial N_2}{\partial r} & 0 & \frac{\partial N_3}{\partial r} & 0 \\ \frac{N_1}{r} & 0 & \frac{N_2}{r} & 0 & \frac{N_3}{r} & 0 \\ 0 & \frac{\partial N_1}{\partial z} & 0 & \frac{\partial N_2}{\partial z} & 0 & \frac{\partial N_3}{\partial z} \\ \frac{\partial N_1}{\partial z} & \frac{\partial N_1}{\partial r} & \frac{\partial N_2}{\partial z} & \frac{\partial N_2}{\partial r} & \frac{\partial N_3}{\partial z} & \frac{\partial N_3}{\partial r} \end{bmatrix}, \quad (13.20)$$

where in the second row the term  $N_i/r$  appears. Considering the axisymmetric nature of the problem we can write that:

$$\underline{\underline{K}}_e = 2\pi \int_{A_e} \underline{\underline{B}}^T \underline{\underline{C}}^T \underline{\underline{B}} dA = 2\pi \int \int \underline{\underline{B}}^T \underline{\underline{C}}^T \underline{\underline{B}} dr dz. \quad (13.21)$$

The vector of forces consists of three different terms even in axisymmetric problems. For a distributed load the formula is:

$$\underline{F}_{ep} = 2\pi \int \underline{\underline{N}}^T \underline{p} r ds, \quad (13.22)$$

where  $\underline{p}$  is the vector of pressures in the radial and axial directions:

$$\underline{p} = \begin{bmatrix} p_r \\ p_z \end{bmatrix}. \quad (13.23)$$

In the case of body force the force vector becomes:

$$\underline{F}_{eb} = 2\pi \int \int \underline{\underline{N}}^T \underline{q} r dr dz, \quad (13.24)$$

where:

$$\underline{q} = \begin{bmatrix} q_r \\ q_z \end{bmatrix} \quad (13.25)$$

is the density vector of volume forces. Finally, the vector of concentrated forces is:

$$\underline{F}_{ec}^T = [F_{1r} \quad F_{1z} \quad F_{2r} \quad F_{2z} \quad F_{3r} \quad F_{3z}]. \quad (13.26)$$

The total force vector is the sum the following three vectors:

$$\underline{F}_e = \underline{F}_{ep} + \underline{F}_{eb} + \underline{F}_{ec}. \quad (13.27)$$

The problem solution involves the composition of the element and structural stiffness matrices. We calculate first the nodal displacements from the structural equation, then the reactions and strain and stress components, respectively. Let us see an example for the application of the element.

### 13.3. Example for the application of axisymmetric triangle element

Fig.13.2 shows a hollow disk with triangular cross section under internal pressure. The angular velocity of the disk is  $\omega = 5 \text{ rad/s}$ . Consider also the own weight of the disk! Calculate the nodal displacements and reactions!

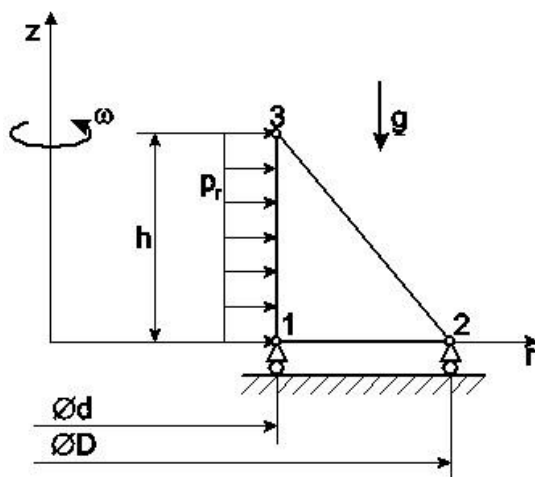


Fig.13.2. Finite element model of a hollow disk with triangular cross section.

Given:

$$p_r = 20 \text{ KPa}, E = 200 \text{ GPa}, d = 6 \text{ m}, D = 8 \text{ m}, g = 9,81 \text{ m/s}^2, \nu = 0,3, h = 1 \text{ m}$$

Solve the problem using a single axisymmetric triangular element [1]! The distances are given in [m], the force is given in [N]. The nodal coordinates are:

| node | r [m] | z [m] |
|------|-------|-------|
| 1    | 3     | 0     |
| 2    | 4     | 0     |
| 3    | 3     | 1     |

Since we have only a single element, the element equilibrium equation is the same as the structural equation:

$$\underline{\underline{K}}_e \underline{u}_e = \underline{F}_e, \quad (13.28)$$

where:

$$\underline{u}_e^T = [u_1 \quad w_1 \quad u_2 \quad w_2 \quad u_3 \quad w_3]. \quad (13.29)$$

Because of the boundary conditions only four unknowns remain, i.e.:

$$\underline{u}_e^T = [u_1 \quad 0 \quad u_2 \quad 0 \quad u_3 \quad w_3]. \quad (13.30)$$

The constitutive matrix based on Eq.(13.14) is:

$$\begin{aligned} \underline{\underline{C}} &= \frac{E}{(1+\nu)(1-2\nu)} \begin{bmatrix} 1-\nu & \nu & \nu & 0 \\ \nu & 1-\nu & \nu & 0 \\ \nu & \nu & 1-\nu & 0 \\ 0 & 0 & 0 & \frac{1-2\nu}{2} \end{bmatrix} = \\ &= \begin{bmatrix} 269,2 & 115,38 & 115,38 & 0 \\ 115,38 & 269,2 & 115,38 & 0 \\ 115,38 & 115,38 & 269,2 & 0 \\ 0 & 0 & 0 & 76,9 \end{bmatrix} \cdot 10^9 \text{ Pa} \end{aligned} \quad (13.31)$$

The coefficients of the interpolation functions using Eq.(12.22) and Fig.13.2 are:

$$\alpha_1 = r_2 z_3 - r_3 z_2 = 4 \text{ m}^2, \quad \alpha_2 = r_3 z_1 - r_1 z_3 = -3 \text{ m}^2, \quad \alpha_3 = r_1 z_2 - r_2 z_1 = 0, \quad (13.32)$$

$$\beta_1 = z_2 - z_3 = -1 \text{ m}, \quad \beta_2 = z_3 - z_1 = 1 \text{ m}, \quad \beta_3 = z_1 - z_2 = 0,$$

$$\gamma_1 = r_3 - r_2 = -1 \text{ m}, \quad \gamma_2 = r_1 - r_3 = 0, \quad \gamma_3 = r_2 - r_1 = 1 \text{ m}.$$

The area of the triangle is:

$$A_e = \frac{1}{2}(\alpha_1 + \alpha_2 + \alpha_3) = \frac{1}{2}(4 - 3 + 0) = \frac{1}{2} \text{ m}^2. \quad (13.33)$$

The interpolation functions can be calculated as:

$$N_i(r, z) = \frac{\alpha_i + \beta_i r + \gamma_i z}{2A_e}, \quad (13.34)$$

which yields:

$$N_1(r, z) = 4 - r - z, \quad N_2(r, z) = -3 + r, \quad N_3(r, z) = z. \quad (13.35)$$

Matrix  $\underline{\underline{N}}$  becomes:

$$\underline{\underline{N}}(r, z) = \begin{bmatrix} N_1 & 0 & N_2 & 0 & N_3 & 0 \\ 0 & N_1 & 0 & N_2 & 0 & N_3 \end{bmatrix} = \begin{bmatrix} 4-r-z & 0 & -3+r & 0 & z & 0 \\ 0 & 4-r-z & 0 & -3+r & 0 & z \end{bmatrix}. \quad (13.36)$$

Accordingly, the strain-displacement matrix  $\underline{\underline{B}}$  is:

$$\underline{\underline{B}} = \frac{\partial \underline{\underline{N}}}{\partial \underline{\underline{r}}} = \begin{bmatrix} \frac{\partial N_1}{\partial r} & 0 & \frac{\partial N_2}{\partial r} & 0 & \frac{\partial N_3}{\partial r} & 0 \\ \frac{N_1}{r} & 0 & \frac{N_2}{r} & 0 & \frac{N_3}{r} & 0 \\ 0 & \frac{\partial N_1}{\partial z} & 0 & \frac{\partial N_2}{\partial z} & 0 & \frac{\partial N_3}{\partial z} \\ \frac{\partial N_1}{\partial z} & \frac{\partial N_1}{\partial r} & \frac{\partial N_2}{\partial z} & \frac{\partial N_2}{\partial r} & \frac{\partial N_3}{\partial z} & \frac{\partial N_3}{\partial r} \end{bmatrix} = \begin{bmatrix} -1 & 0 & 1 & 0 & 0 & 0 \\ \frac{4-r-z}{r} & 0 & \frac{-3+r}{r} & 0 & \frac{z}{r} & 0 \\ 0 & -1 & 0 & 0 & 0 & 1 \\ -1 & -1 & 0 & 1 & 1 & 0 \end{bmatrix}. \quad (13.37)$$

The stiffness matrix is given by:

$$\underline{\underline{K}}_e = 2\pi \int_0^{4-r} \int_3^4 \underline{\underline{B}}^T \underline{\underline{C}}^T \underline{\underline{B}} dr dz = \begin{bmatrix} 3,43 & 1,89 & -2,79 & -0,81 & -0,90 & -1,09 \\ 1,89 & 3,64 & -1,33 & -0,81 & -0,93 & -2,82 \\ -2,80 & -1,33 & 3,10 & 0 & 0,14 & 1,33 \\ -0,81 & -0,81 & 0 & 0,81 & 0,81 & 0 \\ -0,90 & -0,93 & 0,14 & 0,81 & 0,85 & 0,12 \\ -1,09 & -2,82 & 1,33 & 0 & 0,12 & 2,82 \end{bmatrix} \cdot 10^{12} \frac{\text{N}}{\text{m}}, \quad (13.38)$$

where all of the elements were calculated by exact integration (using the code Maple). The upper range of the first integration is the equation of the hypotenuse of the triangle:  $z = 4-r$ . The vector of forces is constructed as the sum of three vectors. The first one is related to distributed load along element edge 1-3, based on Eq.(13.21) it is:

$$\underline{F}_{ep} = 2\pi \int \underline{\underline{N}}^T \underline{p} r ds, \quad \underline{p} = \begin{bmatrix} p_r \\ p_z \end{bmatrix} = \begin{bmatrix} 20 \\ 0 \end{bmatrix} \text{ KPa}. \quad (13.39)$$

Obviously, the radius is  $r = 3$  m constant along element edge 1-3, furthermore the coordinate of integration is  $z$ , leading to:

$$\underline{F}_{ep} = 2\pi \cdot 3 \int_0^1 \underline{\underline{N}}^T \underline{p} dz = 2\pi \cdot 3 \int_0^1 \begin{bmatrix} 1-z & 0 \\ 0 & 1-z \\ 0 & 0 \\ 0 & 0 \\ z & 0 \\ 0 & z \end{bmatrix} \begin{bmatrix} 20000 \\ 0 \end{bmatrix} dz = \begin{bmatrix} 6\pi \\ 0 \\ 0 \\ 0 \\ 6\pi \\ 0 \end{bmatrix} \cdot 10^4 \text{ N}. \quad (13.40)$$

The force vectors related to the revolution and own weight requires vector  $\underline{q}$ , which is calculated using  $g$  and  $\omega$ :

$$\underline{q} = \begin{bmatrix} q_r \\ q_z \end{bmatrix} = \begin{bmatrix} \rho r \omega^2 \\ -\rho g \end{bmatrix}. \quad (13.41)$$

After this, we calculate  $\underline{F}_{eb}$  using Eq.(13.23):

$$\underline{F}_{eb} = 2\pi \int_0^{4-r} \int_3^4 \underline{\underline{N}}^T \underline{q} r dr dz = 2\pi \int_0^{4-r} \int_3^4 \begin{bmatrix} 4-r-z & 0 \\ 0 & 4-r-z \\ -3+r & 0 \\ 0 & -3+r \\ z & 0 \\ 0 & z \end{bmatrix} \begin{bmatrix} \rho r \omega^2 \\ -\rho g \end{bmatrix} r dr dz, \quad (13.42)$$

i.e., we have:

$$\underline{F}_{eb}^T = [6,89 \quad -0,829 \quad 7,995 \quad -0,893 \quad 6,89 \quad -0,829] \pi \cdot 10^5 \text{ N}. \quad (13.43)$$

Finally, the unknown reactions are collected in vector  $\underline{F}_{ec}$ . Considering the boundary conditions we obtain:

$$\underline{F}_{ec}^T = [0 \quad F_{1z} \quad 0 \quad F_{2z} \quad 0 \quad 0]. \quad (13.44)$$

Thus, the finite element equilibrium equation becomes:

$$\begin{bmatrix} 3,43 & 1,89 & -2,79 & -0,81 & -0,90 & -1,09 \\ 1,89 & 3,64 & -1,33 & -0,81 & -0,93 & -2,82 \\ -2,80 & -1,33 & 3,10 & 0 & 0,14 & 1,33 \\ -0,81 & -0,81 & 0 & 0,81 & 0,81 & 0 \\ -0,90 & -0,93 & 0,14 & 0,81 & 0,85 & 0,12 \\ -1,09 & -2,82 & 1,33 & 0 & 0,12 & 2,82 \end{bmatrix} \cdot 10^{12} \begin{bmatrix} u_1 \\ u_2 \\ u_3 \\ w_3 \end{bmatrix} = \begin{bmatrix} 7,49\pi \cdot 10^5 \\ -0,829\pi \cdot 10^5 + F_{1z} \\ 7,995\pi \cdot 10^5 \\ -0,893 \cdot 10^5 + F_{2z} \\ 7,49\pi \cdot 10^5 \\ -0,829\pi \cdot 10^5 \end{bmatrix}. \quad (13.45)$$

The solution can be obtained by the 1<sup>st</sup>, 3<sup>rd</sup>, 5<sup>th</sup> and 6<sup>th</sup> component equations. The other possibility is the application of the matrix equation using the condensed stiffness matrix, which has already been presented in section 12. The solutions are:

$$u_1 = 3,701 \cdot 10^{-5} \text{ m}, u_2 = 3,400 \cdot 10^{-5} \text{ m}, u_3 = 3,675 \cdot 10^{-5} \text{ m}, w_4 = -0,3424 \cdot 10^{-5} \text{ m}. \quad (13.46)$$

The reactions utilizing the 2<sup>nd</sup> and 4<sup>th</sup> component equations of the finite element equilibrium equation are:

$$F_{1z} = 7,272 \cdot 10^5 \text{ N}, F_{2z} = 74144 \text{ N}. \quad (13.47)$$

The example was verified by the finite element code ANSYS 12. We note that similarly to the examples of section 12 we considered the reactions in the vector of external forces.

The term  $N_i/r$  appearing in the second row of matrix  $\underline{\underline{B}}$  can cause trouble in the course of integration if one of the element edges lies on the axis of revolution (where  $r = 0$ ). To avoid this problem a local coordinate system is introduced for each element, or the integration is made by approaching  $r$  to zero by constructing a hole with very small diameter [1].

### 13.4. Axisymmetric isoparametric quadrilateral element

The isoparametric quadrilateral element for plane problems has been presented in section 12. The element is applicable to solve axisymmetric problems too. The functions of the local  $r$  and  $z$  coordinates of element edges are [4]:

$$r(\xi, \eta) = N_1(\xi, \eta)r_1 + N_2(\xi, \eta)r_2 + N_3(\xi, \eta)r_3 + N_4(\xi, \eta)r_4 = \underline{\underline{N}}^T(\xi, \eta)\underline{r}, \quad (13.48)$$

$$z(\xi, \eta) = N_1(\xi, \eta)z_1 + N_2(\xi, \eta)z_2 + N_3(\xi, \eta)z_3 + N_4(\xi, \eta)z_4 = \underline{\underline{N}}^T(\xi, \eta)\underline{z},$$

where in Eq.(12.77) coordinate  $x$  was changed to  $r$ , coordinate  $y$  was changed to  $z$ . Consequently the same interpolation functions can be used:

$$N_1(\xi, \eta) = \frac{1}{4}(1-\xi)(1-\eta), \quad N_2(\xi, \eta) = \frac{1}{4}(1+\xi)(1-\eta), \quad (13.49)$$

$$N_3(\xi, \eta) = \frac{1}{4}(1+\xi)(1+\eta), \quad N_4(\xi, \eta) = \frac{1}{4}(1-\xi)(1+\eta).$$

The displacement is formulated in the usual way:

$$\underline{u}(\xi, \eta) = \begin{bmatrix} u(\xi, \eta) \\ w(\xi, \eta) \end{bmatrix} = \underline{\underline{N}}(\xi, \eta)\underline{u}_e, \quad (13.50)$$

where:

$$u(\xi, \eta) = N_1(\xi, \eta)u_1 + N_2(\xi, \eta)u_2 + N_3(\xi, \eta)u_3 + N_4(\xi, \eta)u_4, \quad (13.51)$$

$$w(\xi, \eta) = N_1(\xi, \eta)w_1 + N_2(\xi, \eta)w_2 + N_3(\xi, \eta)w_3 + N_4(\xi, \eta)w_4,$$

with that the matrix of interpolation functions and the vector of nodal displacements are, respectively:

$$\underline{\underline{N}}(\xi, \eta) = \begin{bmatrix} N_1 & 0 & N_2 & 0 & N_3 & 0 & N_4 & 0 \\ 0 & N_1 & 0 & N_2 & 0 & N_3 & 0 & N_4 \end{bmatrix}, \quad (13.52)$$

$$\underline{\underline{u}}_e^T = [u_1 \quad w_1 \quad u_2 \quad w_2 \quad u_3 \quad w_3 \quad u_4 \quad w_4]. \quad (13.53)$$

The well-known strain-displacement matrix is used to calculate the strain components as:

$$\underline{\underline{\varepsilon}} = \underline{\underline{\partial u}} = \underline{\underline{\partial N}} \underline{\underline{u}}_e = \underline{\underline{B}} \underline{\underline{u}}_e, \quad (13.54)$$

where:

$$\begin{aligned} \underline{\underline{B}} = \underline{\underline{\partial N}} &= \begin{bmatrix} \frac{\partial}{\partial r} & 0 \\ \frac{1}{r} & 0 \\ 0 & \frac{\partial}{\partial z} \\ \frac{\partial}{\partial z} & \frac{\partial}{\partial r} \end{bmatrix} \begin{bmatrix} N_1 & 0 & N_2 & 0 & N_3 & 0 & N_4 & 0 \\ 0 & N_1 & 0 & N_2 & 0 & N_3 & 0 & N_4 \end{bmatrix} = \\ &= \begin{bmatrix} \frac{\partial N_1}{\partial r} & 0 & \frac{\partial N_2}{\partial r} & 0 & \frac{\partial N_3}{\partial r} & 0 & \frac{\partial N_4}{\partial r} & 0 \\ \frac{N_1}{r} & 0 & \frac{N_2}{r} & 0 & \frac{N_3}{r} & 0 & \frac{N_4}{r} & 0 \\ 0 & \frac{\partial N_1}{\partial z} & 0 & \frac{\partial N_2}{\partial z} & 0 & \frac{\partial N_3}{\partial z} & 0 & \frac{\partial N_4}{\partial z} \\ \frac{\partial N_1}{\partial z} & \frac{\partial N_1}{\partial r} & \frac{\partial N_2}{\partial z} & \frac{\partial N_2}{\partial r} & \frac{\partial N_3}{\partial z} & \frac{\partial N_3}{\partial r} & \frac{\partial N_4}{\partial z} & \frac{\partial N_4}{\partial r} \end{bmatrix}. \end{aligned} \quad (13.55)$$

As it is shown, we need the derivatives of the interpolation functions with respect to  $r$  and  $z$ . Due to the fact that the functions  $N_i$  are known in terms of the natural coordinates  $\xi$  and  $\eta$ , we need again the Jacobi matrix and its determinant, referring to Eq.(12.104) we have [4]:

$$\frac{\partial}{\partial r} = \frac{1}{J} (J_{22} \frac{\partial}{\partial \xi} - J_{12} \frac{\partial}{\partial \eta}), \quad (13.56)$$

$$\frac{\partial}{\partial z} = \frac{1}{J} (-J_{21} \frac{\partial}{\partial \xi} + J_{11} \frac{\partial}{\partial \eta}),$$

where:

$$J_{11} = \frac{\partial r}{\partial \xi} = \sum_{i=1}^4 \frac{\partial N_i}{\partial \xi} r_i = \frac{1}{4} \{ -(1-\eta)r_1 + (1-\eta)r_2 + (1+\eta)r_3 - (1+\eta)r_4 \}, \quad (13.57)$$

$$J_{12} = \frac{\partial z}{\partial \xi} = \sum_{i=1}^4 \frac{\partial N_i}{\partial \xi} z_i = \frac{1}{4} \{ -(1-\eta)z_1 + (1-\eta)z_2 + (1+\eta)z_3 - (1+\eta)z_4 \},$$

$$J_{21} = \frac{\partial r}{\partial \eta} = \sum_{i=1}^4 \frac{\partial N_i}{\partial \eta} r_i = \frac{1}{4} \{ -(1-\xi)r_1 - (1+\xi)r_2 + (1+\xi)r_3 + (1-\xi)r_4 \},$$

$$J_{22} = \frac{\partial z}{\partial \eta} = \sum_{i=1}^4 \frac{\partial N_i}{\partial \eta} z_i = \frac{1}{4} \{ -(1-\xi)z_1 - (1+\xi)z_2 + (1+\xi)z_3 + (1-\xi)z_4 \}.$$

Matrix  $\underline{\underline{B}}$  can be produced in a similar way as it was shown by Eq.(12.105), except for the fact that we must consider the term  $N_i/r$  appearing in the second row of the matrix. The calculation of the new terms is possible incorporating Eqs.(13.48)-(13.49). Coordinate  $r$  in terms of  $\xi$  and  $\eta$  parameters is given by Eq.(13.48). The formula of the stiffness matrix is:

$$\underline{\underline{K}}_e = 2\pi \int_{-1}^1 \int_{-1}^1 \underline{\underline{B}}^T \underline{\underline{C}}^T \underline{\underline{B}} r J d\xi d\eta. \quad (13.58)$$

To provide the vector of forces we need three vectors, the first one is:

$$\underline{F}_{ep} = 2\pi \int_{-1}^1 \underline{\underline{N}}^T \underline{p} r J d\xi, \quad \underline{F}_{ep} = 2\pi \int_{-1}^1 \underline{\underline{N}}^T \underline{p} r J d\eta, \quad (13.59)$$

depending on the fact that which one of the element edges is loaded by the line load, moreover the second and third vectors are:

$$\underline{F}_{eb} = 2\pi \int_{-1}^1 \int_{-1}^1 \underline{\underline{N}}^T \underline{q} r J d\xi d\eta, \quad (13.60)$$

$$\underline{F}_{ec}^T = [F_{r1} \quad F_{z1} \quad F_{r2} \quad F_{z2} \quad F_{r3} \quad F_{z3} \quad F_{r4} \quad F_{z4}]. \quad (13.61)$$

Finally the total force vector is:

$$\underline{F}_e = \underline{F}_{ep} + \underline{F}_{eb} + \underline{F}_{ec}. \quad (13.62)$$

In the sequel we present an example for the application of the element.

### 13.5. Example for the application of axisymmetric isoparametric quadrilateral element

Solve the problem of the rotating disk of which analytical solution has been presented in section 11.6.2 using two isoparametric quadrilateral elements! The finite element model of the disk is shown in Fig.13.3.

- The angular velocity of the disk is  $\omega = 880,5 \text{ rad/s}$ , verify if the disk gets loose!
- Calculate the stresses in that case when there is no revolution, i.e.:  $\omega = 0$ , but there is an overlap of  $\delta = 0,02 \cdot 10^{-3} \text{ m}$ !

Given:

$$r_b = 0,02 \text{ m}, r_k = 0,2 \text{ m}, h = 0,04 \text{ m}, \rho = 7800 \text{ kg/m}^3, E = 200 \text{ GPa}, \nu = 0,3.$$

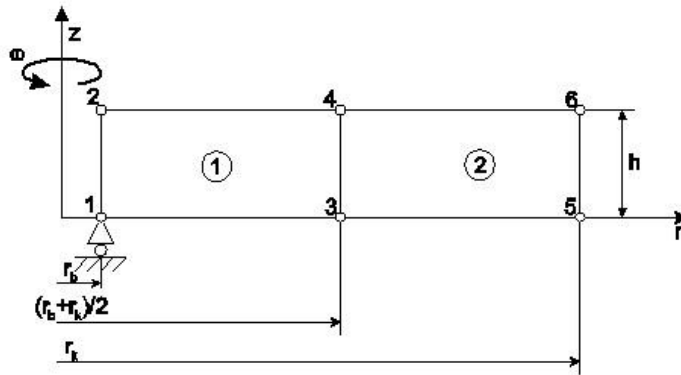


Fig.13.3. A simple finite element model of a rotating disk.

We give the distances in [m] and the force in [N]. The nodal coordinates are:

| node | r [m] | z [m] | node | r [m] | z [m] |
|------|-------|-------|------|-------|-------|
| 1    | 0,02  | 0     | 4    | 0,11  | 0,04  |
| 2    | 0,02  | 0,04  | 5    | 0,2   | 0     |
| 3    | 0,11  | 0     | 6    | 0,2   | 0,04  |

The element-node table becomes:

| element | node |   |   |   |  |
|---------|------|---|---|---|--|
|         | 1    | 3 | 4 | 2 |  |
| 2       | 3    | 5 | 6 | 4 |  |

In the knowledge of the boundary conditions the structural vector of nodal displacements is:

$$\underline{U}^T = [u_1 \quad 0 \quad u_2 \quad w_2 \quad u_3 \quad w_3 \quad u_4 \quad w_4 \quad u_5 \quad w_5 \quad u_6 \quad w_6]. \quad (13.63)$$

The constitutive matrix using Eq.(13.14) is:

$$\underline{C} = \begin{bmatrix} 269,2 & 115,38 & 115,38 & 0 \\ 115,38 & 269,2 & 115,38 & 0 \\ 115,38 & 115,38 & 269,2 & 0 \\ 0 & 0 & 0 & 76,9 \end{bmatrix} \cdot 10^9 \text{ Pa.} \quad (13.64)$$

The elements of the Jacobi matrix must be produced for both elements based on Eq.(13.57):

$$J_{11}^{(1)} = \frac{1}{4} \{ -(1-\eta)r_1 + (1-\eta)r_3 + (1+\eta)r_4 - (1+\eta)r_2 \} = 0,045, \quad (13.65)$$

$$J_{12}^{(1)} = \frac{1}{4} \{ -(1-\eta)z_1 + (1-\eta)z_3 + (1+\eta)z_4 - (1+\eta)z_2 \} = 0,$$

$$J_{21}^{(1)} = \frac{1}{4} \{ -(1-\xi)r_1 - (1+\xi)r_3 + (1+\xi)r_4 + (1-\xi)r_2 \} = 0,$$

$$J_{22}^{(1)} = \frac{1}{4} \{ -(1-\xi)z_1 - (1+\xi)z_3 + (1+\xi)z_4 + (1-\xi)z_2 \} = 0,02.$$

and:

$$J_{11}^{(2)} = \frac{1}{4} \{ -(1-\eta)r_3 + (1-\eta)r_5 + (1+\eta)r_6 - (1+\eta)r_4 \} = 0,045, \quad (13.66)$$

$$J_{12}^{(2)} = \frac{1}{4} \{ -(1-\eta)z_3 + (1-\eta)z_5 + (1+\eta)z_6 - (1+\eta)z_4 \} = 0,$$

$$J_{21}^{(2)} = \frac{1}{4} \{ -(1-\xi)r_3 - (1+\xi)r_5 + (1+\xi)r_6 + (1-\xi)r_4 \} = 0,$$

$$J_{22}^{(2)} = \frac{1}{4} \{ -(1-\xi)z_3 - (1+\xi)z_5 + (1+\xi)z_6 + (1-\xi)z_4 \} = 0,02.$$

The elements of the Jacobi matrix, and so the determinant is constant and identical for both elements:

$$J^{(1)} = J^{(2)} = J = 0,0009. \quad (13.67)$$

Continuing the calculation we compute the derivatives of interpolation functions with respect to  $r$  and  $z$  in accordance with Eq.(13.56). Due to the identical Jacobi determinants of the elements, the derivatives of the interpolation functions will be identical too. Therefore, we can omit the superscripts of the elements of Jacobi matrix:

$$\frac{\partial N_1}{\partial r}^{(1)} = \frac{\partial N_1}{\partial r}^{(2)} = \frac{1}{J} (J_{22} \frac{\partial N_1}{\partial \xi} - J_{12} \frac{\partial N_1}{\partial \eta}) = -5,55555 + 5,55555 \eta, \quad (13.68)$$

$$\frac{\partial N_2}{\partial r}^{(1)} = \frac{\partial N_2}{\partial r}^{(2)} = \frac{1}{J} (J_{22} \frac{\partial N_2}{\partial \xi} - J_{12} \frac{\partial N_2}{\partial \eta}) = 5,55555 - 5,55555 \eta,$$

$$\frac{\partial N_3}{\partial r}^{(1)} = \frac{\partial N_3}{\partial r}^{(2)} = \frac{1}{J} (J_{22} \frac{\partial N_3}{\partial \xi} - J_{12} \frac{\partial N_3}{\partial \eta}) = 5,55555 + 5,55555 \eta,$$

$$\frac{\partial N_4}{\partial r}^{(1)} = \frac{\partial N_4}{\partial r}^{(2)} = \frac{1}{J} (J_{22} \frac{\partial N_4}{\partial \xi} - J_{12} \frac{\partial N_4}{\partial \eta}) = -5,55555 - 5,55555 \eta,$$

$$\frac{\partial N_1}{\partial z}^{(1)} = \frac{\partial N_1}{\partial z}^{(2)} = \frac{1}{J} (-J_{21} \frac{\partial N_1}{\partial \xi} + J_{11} \frac{\partial N_1}{\partial \eta}) = -12,5 + 12,5 \xi, \quad (13.69)$$

$$\frac{\partial N_2}{\partial z}^{(1)} = \frac{\partial N_2}{\partial z}^{(2)} = \frac{1}{J} (-J_{21} \frac{\partial N_2}{\partial \xi} + J_{11} \frac{\partial N_2}{\partial \eta}) = -12,5 - 12,5 \xi,$$

$$\frac{\partial N_3}{\partial z}^{(1)} = \frac{\partial N_3}{\partial z}^{(2)} = \frac{1}{J} (-J_{21} \frac{\partial N_3}{\partial \xi} + J_{11} \frac{\partial N_3}{\partial \eta}) = 12,5 + 12,5 \xi,$$

$$\frac{\partial N_4}{\partial z}^{(1)} = \frac{\partial N_4}{\partial z}^{(2)} = \frac{1}{J} (-J_{21} \frac{\partial N_4}{\partial \xi} + J_{11} \frac{\partial N_4}{\partial \eta}) = 12,5 - 12,5 \xi,$$

Coordinate  $r$  should be given for both elements separately based on Eq.(13.48):

$$\begin{aligned} r^{(1)} &= N_1 r_1 + N_2 r_3 + N_3 r_4 + N_4 r_2 = \\ &= 0,005(1-\eta)(1-\xi) + 0,0275(1-\eta)(1+\xi) + 0,0275(1+\eta)(1+\xi) + 0,005(1+\eta)(1-\xi), \end{aligned} \quad (13.70)$$

$$\begin{aligned} r^{(2)} &= N_1 r_3 + N_2 r_5 + N_3 r_6 + N_4 r_4 = \\ &= 0,0275(1-\eta)(1-\xi) + 0,005(1-\eta)(1+\xi) + 0,005(1+\eta)(1+\xi) + 0,0275(1+\eta)(1-\xi), \end{aligned}$$

where we considered also the element orientation (the local numbering of the nodes of element). As a next step, we provide the strain-displacement matrix for each element using Eq.(13.55). The elements of matrices are the functions of  $\xi$  and  $\eta$ , which are extremely complicated, therefore we do not give them here. The element stiffness matrices can be calculated using the  $\underline{B}$  matrices:

$$\begin{aligned}
\underline{\underline{K}}_{e1} &= 2\pi \int_{-1}^1 \int_{-1}^1 \underline{\underline{B}}^{(1)T} \underline{\underline{C}}^T \underline{\underline{B}}^{(1)} J d\xi d\eta = \\
&= \begin{bmatrix} 40,62 & 4,23 & 1,34 & 3,02 & -17,00 & -15,10 & -2,80 & 7,85 \\ . & 58,57 & -4,83 & 36,58 & -24,17 & -43,56 & -7,85 & -51,59 \\ . & . & 65,83 & -35,04 & -14,66 & 15,71 & -17,00 & 24,17 \\ . & . & . & 115,67 & -15,71 & -108,69 & 15,10 & -43,56 \\ . & . & . & . & 65,84 & 35,04 & 1,34 & 4,83 \\ . & . & . & . & . & 115,67 & -3,02 & 36,58 \\ . & . & . & . & . & . & 40,62 & -4,23 \\ . & . & . & . & . & . & . & 58,57 \end{bmatrix} \cdot 10^9 \frac{\text{N}}{\text{m}}, \quad (13.71) \\
\underline{\underline{K}}_{e2} &= 2\pi \int_{-1}^1 \int_{-1}^1 \underline{\underline{B}}^{(2)T} \underline{\underline{C}}^T \underline{\underline{B}}^{(2)} J d\xi d\eta = \\
&= \begin{bmatrix} 82,40 & 31,42 & -8,53 & 8,46 & -46,41 & -42,29 & -30,85 & 2,42 \\ . & 179,20 & -10,27 & 87,23 & -51,35 & -103,87 & -2,42 & -162,56 \\ . & . & 116,71 & -62,23 & -38,16 & 21,15 & -46,40 & 51,35 \\ . & . & . & 236,30 & -21,15 & -219,65 & 42,29 & -103,88 \\ . & . & . & . & 116,71 & 62,23 & -8,53 & 10,23 \\ . & . & . & . & . & 236,30 & -8,46 & 87,23 \\ . & . & . & . & . & . & 82,40 & -31,42 \\ . & . & . & . & . & . & . & 179,20 \end{bmatrix} \cdot 10^9 \frac{\text{N}}{\text{m}}
\end{aligned}$$

As the node numbering does not correspond to the element orientations we need to rearrange the element stiffness matrices in accordance with the numerals of degrees of freedom. Let the vector of nodal displacements be equal to:

$$\underline{u}_{e1}^T = [u_1 \quad w_1 \quad u_2 \quad w_2 \quad u_3 \quad w_3 \quad u_4 \quad w_4], \quad (13.72)$$

$$\underline{u}_{e2}^T = [u_3 \quad w_3 \quad u_4 \quad w_4 \quad u_5 \quad w_5 \quad u_6 \quad w_6].$$

Corresponding to the former, the original element stiffness matrices are rearranged as:

$$\underline{\underline{K}}_{e1} = \begin{bmatrix} k_{e11}^1 & k_{e12}^1 & k_{e17}^1 & k_{e18}^1 & k_{e13}^1 & k_{e14}^1 & k_{e15}^1 & k_{e16}^1 \\ k_{e21}^1 & k_{e22}^1 & k_{e27}^1 & k_{e28}^1 & k_{e23}^1 & k_{e24}^1 & k_{e25}^1 & k_{e26}^1 \\ k_{e71}^1 & k_{e72}^1 & k_{e77}^1 & k_{e78}^1 & k_{e73}^1 & k_{e74}^1 & k_{e75}^1 & k_{e76}^1 \\ k_{e81}^1 & k_{e82}^1 & k_{e87}^1 & k_{e88}^1 & k_{e83}^1 & k_{e84}^1 & k_{e85}^1 & k_{e86}^1 \\ k_{e31}^1 & k_{e32}^1 & k_{e37}^1 & k_{e38}^1 & k_{e33}^1 & k_{e34}^1 & k_{e35}^1 & k_{e36}^1 \\ k_{e41}^1 & k_{e42}^1 & k_{e47}^1 & k_{e48}^1 & k_{e43}^1 & k_{e44}^1 & k_{e45}^1 & k_{e46}^1 \\ k_{e51}^1 & k_{e52}^1 & k_{e57}^1 & k_{e58}^1 & k_{e53}^1 & k_{e54}^1 & k_{e55}^1 & k_{e56}^1 \\ k_{e61}^1 & k_{e62}^1 & k_{e67}^1 & k_{e68}^1 & k_{e63}^1 & k_{e64}^1 & k_{e65}^1 & k_{e66}^1 \end{bmatrix}. \quad (13.73)$$

Based on the nodes of the second element the rearrangement is made as:

$$\underline{\underline{K}}_{e2} = \begin{bmatrix} k_{e11}^2 & k_{e12}^2 & k_{e17}^2 & k_{e18}^2 & k_{e13}^2 & k_{e14}^2 & k_{e15}^2 & k_{e16}^2 \\ k_{e21}^2 & k_{e22}^2 & k_{e27}^2 & k_{e28}^2 & k_{e23}^2 & k_{e24}^2 & k_{e25}^2 & k_{e26}^2 \\ k_{e71}^2 & k_{e72}^2 & k_{e77}^2 & k_{e78}^2 & k_{e73}^2 & k_{e74}^2 & k_{e75}^2 & k_{e76}^2 \\ k_{e81}^2 & k_{e82}^2 & k_{e87}^2 & k_{e88}^2 & k_{e83}^2 & k_{e84}^2 & k_{e85}^2 & k_{e86}^2 \\ k_{e31}^2 & k_{e32}^2 & k_{e37}^2 & k_{e38}^2 & k_{e33}^2 & k_{e34}^2 & k_{e35}^2 & k_{e36}^2 \\ k_{e41}^2 & k_{e42}^2 & k_{e47}^2 & k_{e48}^2 & k_{e43}^2 & k_{e44}^2 & k_{e45}^2 & k_{e46}^2 \\ k_{e51}^2 & k_{e52}^2 & k_{e57}^2 & k_{e58}^2 & k_{e53}^2 & k_{e54}^2 & k_{e55}^2 & k_{e56}^2 \\ k_{e61}^2 & k_{e62}^2 & k_{e67}^2 & k_{e68}^2 & k_{e63}^2 & k_{e64}^2 & k_{e65}^2 & k_{e66}^2 \end{bmatrix}. \quad (13.74)$$

Now, we can construct the structural stiffness matrix. The mutual nodes are the third and fourth ones. Accordingly, the combination of the two matrices results in:

$$\underline{\underline{K}} = \begin{bmatrix} k_{e11}^1 & k_{e12}^1 & k_{e17}^1 & k_{e18}^1 & k_{e13}^1 & k_{e14}^1 & k_{e15}^1 & k_{e16}^1 & 0 & 0 & 0 & 0 \\ k_{e21}^1 & k_{e22}^1 & k_{e27}^1 & k_{e28}^1 & k_{e23}^1 & k_{e24}^1 & k_{e25}^1 & k_{e26}^1 & 0 & 0 & 0 & 0 \\ k_{e71}^1 & k_{e72}^1 & k_{e77}^1 & k_{e78}^1 & k_{e73}^1 & k_{e74}^1 & k_{e75}^1 & k_{e76}^1 & 0 & 0 & 0 & 0 \\ k_{e81}^1 & k_{e82}^1 & k_{e87}^1 & k_{e88}^1 & k_{e83}^1 & k_{e84}^1 & k_{e85}^1 & k_{e86}^1 & 0 & 0 & 0 & 0 \\ k_{e31}^1 & k_{e32}^1 & k_{e37}^1 & k_{e38}^1 & k_{e33}^1 + k_{e11}^1 & k_{e34}^1 + k_{e12}^1 & k_{e35}^1 + k_{e17}^1 & k_{e36}^1 + k_{e18}^1 & k_{e13}^1 & k_{e14}^1 & k_{e15}^1 & k_{e16}^1 \\ k_{e41}^1 & k_{e42}^1 & k_{e47}^1 & k_{e48}^1 & k_{e43}^1 + k_{e21}^1 & k_{e44}^1 + k_{e22}^1 & k_{e45}^1 + k_{e27}^1 & k_{e46}^1 + k_{e28}^1 & k_{e23}^1 & k_{e24}^1 & k_{e25}^1 & k_{e26}^1 \\ k_{e51}^1 & k_{e52}^1 & k_{e57}^1 & k_{e58}^1 & k_{e53}^1 + k_{e71}^1 & k_{e54}^1 + k_{e72}^1 & k_{e55}^1 + k_{e77}^1 & k_{e56}^1 + k_{e78}^1 & k_{e73}^1 & k_{e74}^1 & k_{e75}^1 & k_{e76}^1 \\ k_{e61}^1 & k_{e62}^1 & k_{e67}^1 & k_{e68}^1 & k_{e63}^1 + k_{e81}^1 & k_{e64}^1 + k_{e82}^1 & k_{e65}^1 + k_{e87}^1 & k_{e66}^1 + k_{e88}^1 & k_{e83}^1 & k_{e84}^1 & k_{e85}^1 & k_{e86}^1 \\ 0 & 0 & 0 & 0 & k_{e31}^2 & k_{e32}^2 & k_{e37}^2 & k_{e38}^2 & k_{e33}^2 & k_{e34}^2 & k_{e35}^2 & k_{e36}^2 \\ 0 & 0 & 0 & 0 & k_{e41}^2 & k_{e42}^2 & k_{e47}^2 & k_{e48}^2 & k_{e43}^2 & k_{e44}^2 & k_{e45}^2 & k_{e46}^2 \\ 0 & 0 & 0 & 0 & k_{e51}^2 & k_{e52}^2 & k_{e57}^2 & k_{e58}^2 & k_{e53}^2 & k_{e54}^2 & k_{e55}^2 & k_{e56}^2 \\ 0 & 0 & 0 & 0 & k_{e61}^2 & k_{e62}^2 & k_{e67}^2 & k_{e68}^2 & k_{e63}^2 & k_{e64}^2 & k_{e65}^2 & k_{e66}^2 \end{bmatrix}. \quad (13.75)$$

We note that the finite element codes provide the structural stiffness matrix using the element-node table. The numerical values can be obtained using Eq.(13.71). The force vector consists of the vectors of body and concentrated forces. The density vector of the body force is:

$$\underline{q} = \begin{bmatrix} q_r \\ 0 \end{bmatrix} = \begin{bmatrix} \rho r \omega^2 \\ 0 \end{bmatrix}, \text{ and: } \underline{q}^{(1)} = \begin{bmatrix} \rho r^{(1)} \omega^2 \\ 0 \end{bmatrix}, \underline{q}^{(2)} = \begin{bmatrix} \rho r^{(2)} \omega^2 \\ 0 \end{bmatrix}, \quad (13.76)$$

from which we have:

$$\underline{F}_{eb}^{(1)} = 2\pi \int_{-1}^1 \int_{-1}^1 \underline{\underline{N}}^T \underline{q}^{(1)} \underline{r}^{(1)} J d\xi d\eta = [1,01 \ 0 \ 2,34 \ 0 \ 2,34 \ 0 \ 1,01 \ 0]^T \cdot 10^5 \text{ N}, \quad (13.77)$$

$$\underline{F}_{eb}^{(2)} = 2\pi \int_{-1}^1 \int_{-1}^1 \underline{\underline{N}}^T \underline{q}^{(2)} \underline{r}^{(2)} J d\xi d\eta = [6,86 \ 0 \ 10,04 \ 0 \ 10,04 \ 0 \ 6,86 \ 0]^T \cdot 10^5 \text{ N}.$$

Similarly to the stiffness matrices, the rearrangement is required also in the force vectors according to the local node numbering:

$$\underline{F}_{eb}^{(1)} = \begin{bmatrix} F_{eb1}^{(1)} \\ F_{eb2}^{(1)} \\ F_{eb7}^{(1)} \\ F_{eb8}^{(1)} \\ F_{eb3}^{(1)} \\ F_{eb4}^{(1)} \\ F_{eb5}^{(1)} \\ F_{eb6}^{(1)} \end{bmatrix} = \begin{bmatrix} 1,01 \\ 0 \\ 1,01 \\ 0 \\ 2,34 \\ 0 \\ 2,34 \\ 0 \end{bmatrix} \cdot 10^5 \text{ N} \text{ and } \underline{F}_{eb}^{(2)} = \begin{bmatrix} F_{eb1}^{(2)} \\ F_{eb2}^{(2)} \\ F_{eb7}^{(2)} \\ F_{eb8}^{(2)} \\ F_{eb3}^{(2)} \\ F_{eb4}^{(2)} \\ F_{eb5}^{(2)} \\ F_{eb6}^{(2)} \end{bmatrix} = \begin{bmatrix} 6,86 \\ 0 \\ 6,86 \\ 0 \\ 10,04 \\ 0 \\ 10,04 \\ 0 \end{bmatrix} \cdot 10^5 \text{ N}. \quad (13.78)$$

The structural force vector is calculated as the sum the two former vectors:

$$\begin{aligned} \underline{F}_b^T &= \begin{bmatrix} F_{eb1}^{(1)} & F_{eb2}^{(1)} & F_{eb7}^{(1)} & F_{eb8}^{(1)} & F_{eb3}^{(1)} + F_{eb4}^{(1)} + F_{eb5}^{(1)} + F_{eb6}^{(1)} & F_{eb3}^{(2)} & F_{eb4}^{(2)} & F_{eb5}^{(2)} & F_{eb6}^{(2)} \end{bmatrix} = \\ &= [1,01 \ 0 \ 1,01 \ 0 \ 9,20 \ 0 \ 9,20 \ 0 \ 10,04 \ 0 \ 10,04 \ 0] \cdot 10^5 \text{ N}. \end{aligned} \quad (13.79)$$

The vector containing the reaction is:

$$\underline{F}_c^T = [0 \ F_{1z} \ 0 \ 0 \ 0 \ 0 \ 0 \ 0 \ 0 \ 0 \ 0 \ 0]. \quad (13.80)$$

The structural force vector is:

$$\underline{F} = \underline{F}_b + \underline{F}_c. \quad (13.81)$$

Finally, the structural equation is:

$$\underline{\underline{K}} \underline{U} = \underline{F}. \quad (13.82)$$

The system of equations consists of twelve equations. From the 1<sup>st</sup> and 3<sup>rd</sup>-12<sup>th</sup> equations we determine the nodal displacements. The solutions are:

$$u_1 = u_2 = 0,0168 \cdot 10^{-3} \text{ m}, w_1 = 0, w_2 = -0,0149 \cdot 10^{-3} \text{ m} \quad (13.83)$$

$$u_3 = u_4 = 0,0368 \cdot 10^{-3} \text{ m}, w_3 = -0,00365 \cdot 10^{-3} \text{ m}, w_4 = -0,0113 \cdot 10^{-3} \text{ m},$$

$$u_5 = u_6 = 0,0440 \cdot 10^{-3} \text{ m}, w_5 = -0,0051 \cdot 10^{-3} \text{ m}, w_6 = -0,0098 \cdot 10^{-3} \text{ m},$$

It is seen that if the disk rotates with maximal angular velocity, then in accordance with the finite element model we do not reach the overlap value of  $0,02 \cdot 10^{-3}$  m calculated from the analytical model, i.e. the disk will not get loose. This disagreement can be explained by the coarse mesh of the finite element model, which consists of only two elements. The deformed shape of the structure compared to the original state is shown in Fig.13.4. Based on the displacement solutions we construct the nodal displacement vectors of the elements:

$$\underline{u}_{e1}^T = [u_1 \ 0 \ u_3 \ w_3 \ u_4 \ w_4 \ u_2 \ w_2], \quad (13.84)$$

$$\underline{u}_{e2}^T = [u_3 \ w_3 \ u_5 \ w_5 \ u_6 \ w_6 \ u_4 \ w_4].$$

In the former two vectors we followed the original order of the local node numbering, because matrix  $\underline{\underline{B}}$  was constructed in accordance with this fact. The vectors of strain components for both elements are calculated using matrix  $\underline{\underline{\varepsilon}}$ :

$$\underline{\varepsilon}^{(1)} = \underline{\underline{B}}^{(1)} \underline{u}_{e1}, \underline{\varepsilon}^{(2)} = \underline{\underline{B}}^{(2)} \underline{u}_{e2}. \quad (13.85)$$

The vector of stress components are:

$$\underline{\sigma}^{(1)} = \underline{\underline{C}} \underline{\varepsilon}^{(1)}, \underline{\sigma}^{(2)} = \underline{\underline{C}} \underline{\varepsilon}^{(2)}. \quad (13.86)$$

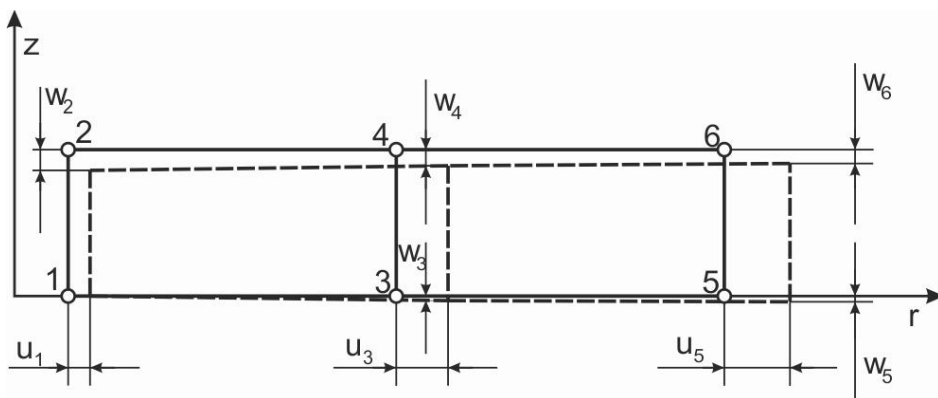


Fig.13.4. Deformed shape of the finite element model of rotating disk.

The results are summarized in Tables 13.1 and 13.2. In the tables we listed the nodal solutions. Element solutions are possible to calculate only at mutual nodes 3 and 4 by averaging the nodal solution. According to Table 13.2 it is seen that the dynamic boundary conditions are violated, concretely speaking the radial stress at nodes 1, 2, 5 and 6 is not zero. The reason for that is the low resolution of the mesh and the linear interpolation. On the contrary, the tangential stress agrees quite well at the inner and outer boundaries with the results presented in Fig.11.10a. The example was verified by the code ANSYS 12.

| element | node | $\varepsilon_r [\cdot 10^{-3}]$ | $\varepsilon_t [\cdot 10^{-3}]$ | $\varepsilon_z [\cdot 10^{-3}]$ | $\gamma_{rz} [\cdot 10^{-3}]$ |
|---------|------|---------------------------------|---------------------------------|---------------------------------|-------------------------------|
| 1       | 1    | 0,222                           | 0,840                           | -0,373                          | -0,041                        |
|         | 2    | 0,222                           | 0,840                           | -0,373                          | 0,041                         |
|         | 3    | 0,222                           | 0,335                           | -0,191                          | -0,041                        |
|         | 4    | 0,222                           | 0,335                           | -0,191                          | 0,041                         |
| 2       | 3    | 0,080                           | 0,335                           | -0,191                          | -0,016                        |
|         | 4    | 0,080                           | 0,335                           | -0,191                          | 0,016                         |
|         | 5    | 0,080                           | 0,220                           | -0,118                          | -0,016                        |
|         | 6    | 0,080                           | 0,220                           | -0,118                          | 0,016                         |

Table 13.1. Strain components in the rotating disk in the case of  $\omega = 880,5 \text{ rad/s}$ .

| element | node | $\sigma_r [\text{MPa}]$ | $\sigma_t [\text{MPa}]$ | $\sigma_z [\text{MPa}]$ | $\tau_{rz} [\text{MPa}]$ |
|---------|------|-------------------------|-------------------------|-------------------------|--------------------------|
| 1       | 1    | 113,7                   | 208,7                   | 22,1                    | -3,1                     |
|         | 2    | 113,7                   | 208,7                   | 22,1                    | 3,1                      |
|         | 3    | 76,4                    | 93,7                    | 12,9                    | -3,1                     |
|         | 4    | 76,4                    | 93,7                    | 12,9                    | 3,1                      |
| 2       | 3    | 38,1                    | 77,3                    | -3,5                    | -1,25                    |
|         | 4    | 38,1                    | 77,3                    | -3,53                   | 1,25                     |
|         | 5    | 33,4                    | 54,9                    | 2,97                    | -1,25                    |
|         | 6    | 33,4                    | 54,9                    | 2,97                    | 1,25                     |

Table 13.2. Stresses in the rotating disk in the case of  $\omega = 880,5 \text{ rad/s}$ .

In that case, when there is no rotation the structural vector of nodal displacements becomes:

$$\underline{U}^T = [\delta \quad 0 \quad \delta \quad w_2 \quad u_3 \quad w_3 \quad u_4 \quad w_4 \quad u_5 \quad w_5 \quad u_6 \quad w_6]. \quad (13.87)$$

The stiffness matrix remains the same, the vector of forces is:

$$\underline{F}_c^T = [F_{1r} \quad F_{1z} \quad F_{2r} \quad 0 \quad 0 \quad 0 \quad 0 \quad 0 \quad 0 \quad 0]. \quad (13.88)$$

The solutions are:

$$u_1 = u_2 = 0,02 \cdot 10^{-3} \text{ m}, w_1 = 0, w_2 = -0,0049 \cdot 10^{-3} \text{ m}, \quad (13.89)$$

$$u_3 = u_4 = 0,0055 \cdot 10^{-3} \text{ m}, w_3 = 0,0056 \cdot 10^{-3} \text{ m}, w_4 = -0,0020 \cdot 10^{-3} \text{ m},$$

$$u_5 = u_6 = 0,0038 \cdot 10^{-3} \text{ m}, w_5 = -0,0022 \cdot 10^{-3} \text{ m}, w_6 = -0,0027 \cdot 10^{-3} \text{ m}.$$

Table 13.3 contains the stresses in the disk when there is no rotation. Compared to the results of the analytical solution the differences are quite large, which can be explained again by the low resolution finite element mesh and the linear interpolation.

| element | node | $\sigma_r$ [MPa] | $\sigma_t$ [MPa] | $\sigma_z$ [MPa] | $\tau_{rz}$ [MPa] |
|---------|------|------------------|------------------|------------------|-------------------|
| 1       | 1    | 58,1             | 236,6            | 63,9             | -2,5              |
|         | 2    | 58,1             | 236,6            | 63,9             | 2,5               |
|         | 3    | -34,8            | -2,3             | -6,7             | -2,5              |
|         | 4    | -34,8            | -2,3             | 6,7              | 2,5               |
| 2       | 3    | 3,2              | 13,9             | 9,6              | 0,6               |
|         | 4    | 3,2              | 13,9             | 9,6              | -0,6              |
|         | 5    | -4,5             | 1,4              | -3,6             | 0,6               |
|         | 6    | -4,5             | 1,4              | -3,6             | -0,6              |

Table 13.3. Stresses in the disk in the case of  $\omega = 0$ .

### 13.6. Bibliography

- [1] József Uj, *Lectures and practices of the subject Numerical methods in mechanics*, PhD formation, Budapest University of Technology and Economics, Faculty of Mechanical Engineering, Department of Applied Mechanics, 2002/2003 spring semester (in Hungarian).
- [2] David V. Hutton, *Fundamentals of finite element analysis*, 1st edition. McGraw-Hill, 2004, New York.
- [3] O.C. Zienkiewicz, R.L. Taylor, *The finite element method – fifth edition, Volume 1: The basis*. Butterworth-Heinemann, 2000, Oxford, Auckland, Boston, Johannesburg, Melbourne, New Delhi.
- [4] Erdogan Madenci, Ibrahim Guven, *The finite element method and applications in engineering using ANSYS*. Springer Science+Business Media Inc., 2006, New York, USA.

## 14. MODELING OF THIN-WALLED SHELLS AND PLATES. INTRODUCTION TO THE THEORY OF SHELL FINITE ELEMENT MODELS

### 14.1. Plate and shell theories

Plane structures are called plates if the thickness of structure is significantly less than the other dimensions, moreover if the structure is loaded perpendicularly to its plane. The plate can be bounded along its sides by an optional geometrical object; the kinematic boundary conditions can be various (point-supported, rigidly or elastically supported along the sides, simply supported, etc.) [1]. The plate can be considered as the extension of a beam in two dimensions, because both implies the dominance of the bending load and most commonly the load is introduced transversely. Nevertheless, there are significant differences too, since e.g. the flexure of the beam can be either straight or curved, on the other hand the midplane of a plate is always flat. If the midplane of the plate is curved then it is no longer plate but a shell [2]. In the sequel we overview the most important details of the theory of plates and shells.

### 14.2. The basic equations of Kirchhoff plate theory

The Kirchhoff plate theory is often called the theory of thin plates. We note that if the plate is relatively thick then the transverse shear deformation can be considered too. The relevant plate solution is provided by the Mindlin plate theory [1].

#### 14.2.1. Displacement field

Based on Fig.14.1 we investigate the displacement of a point of the midplane of an elastic flat plate [2,3]. The displacement field can be captured by three components: the transverse displacement along  $z$  and the rotations about  $x$  and  $y$ , i.e.:

$$u = \begin{bmatrix} \beta z \\ -\alpha z \\ w \end{bmatrix}, \quad (14.1)$$

where  $\alpha = \alpha(x,y)$  is the rotation about axis  $x$ ,  $\beta = \beta(x,y)$  is the rotation about axis  $y$  and  $w = w(x,y)$  is the transverse displacement.

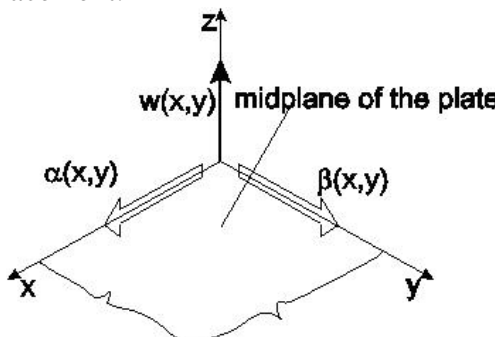


Fig.14.1. Displacement of a point in the midplane of a flat plate.

### 14.2.2. Strain components

Assuming small strains we can calculate the strain components by using the strain-displacement equation defined in section 11 by Eq.(11.14) [1,4]:

$$\varepsilon_x = \frac{\partial u}{\partial x} = \beta_{,x} z, \quad \varepsilon_y = \frac{\partial v}{\partial y} = -\alpha_{,y} z, \quad \varepsilon_z = 0, \quad (14.2)$$

$$\gamma_{xy} = \frac{\partial u}{\partial y} + \frac{\partial v}{\partial x} = (\beta_{,y} - \alpha_{,x})z, \quad \gamma_{xz} = \frac{\partial u}{\partial z} + \frac{\partial w}{\partial x} = \beta + w_{,x}, \quad \gamma_{yz} = \frac{\partial v}{\partial z} + \frac{\partial w}{\partial y} = -\alpha + w_{,y},$$

where – for the sake of simplicity - the derivatives with respect to  $x$  and  $y$  are indicated in the subscript. In the sequel we assume that the cross section planes remain flat and the outward normal of each cross section is perpendicular to the cross section plane after the deformation. This assumption is called Kirchhoff-Love hypothesis [1]. From the latter it follows that in the planes perpendicular to the midplane of the plate the shear strains are equal to zero:

$$\gamma_{xz} = \gamma_{yz} = 0 \Rightarrow \beta = -w_{,x} \text{ and } \alpha = w_{,y}. \quad (14.3)$$

Utilizing the former we obtain from Eq.(14.1) that:

$$\underline{u} = \begin{bmatrix} -w_{,x} \cdot z \\ -w_{,y} \cdot z \\ w \end{bmatrix}. \quad (14.4)$$

The strain components become:

$$\varepsilon_x = -w_{,xx} \cdot z, \quad \varepsilon_y = -w_{,yy} \cdot z, \quad \gamma_{xy} = -2w_{,xy} \cdot z. \quad (14.5)$$

Consequently in the midplane points  $\varepsilon_z = 0$ . According to the Kirchhoff plate theory under the assumption of small strains the components of the displacement and strain field can be defined by  $w(x,y)$ .

### 14.2.3. Stress field, forces and moments in the midplane

Assuming plane stress state we express the stress components by Eqs.(11.18) and (14.5):

$$\sigma_x = \frac{E}{1-\nu^2} [\varepsilon_x + \nu \varepsilon_y] = -E_l (w_{,xx} + \nu \cdot w_{,yy}) \cdot z = A \cdot z, \quad (14.6)$$

$$\sigma_y = \frac{E}{1-\nu^2} [\varepsilon_y + \nu \varepsilon_x] = -E_l (w_{,yy} + \nu \cdot w_{,xx}) \cdot z = B \cdot z,$$

$$\tau_{xy} = \frac{E}{2(1+\nu)} \gamma_{xy} = -E_1(1-\nu)w_{,xy} \cdot z = C \cdot z,$$

where  $E_1 = E/(1-\nu^2)$ ,  $A$ ,  $B$  and  $C$  are constants. Similarly to the theory of beams subjected to bending the stress distributions are given by linear functions along the thickness direction, as it is shown by Fig.14.2.

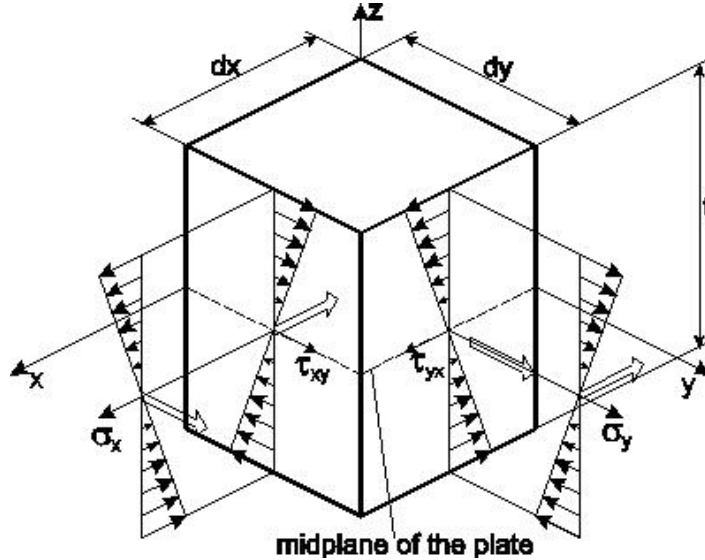


Fig.14.2. Distribution of the stresses along the thickness direction of a differential plate element.

The stress couples in the midplane of the plate are calculated by integrating the stresses over the thickness [3]:

$$M_x = \int_{-t/2}^{t/2} \sigma_x z dz = \int_{-t/2}^{t/2} Az^2 dz = -I_1 E_1 (w_{,xx} + \nu \cdot w_{,yy}), \quad (14.7)$$

$$M_y = \int_{-t/2}^{t/2} \sigma_y z dz = \int_{-t/2}^{t/2} Bz^2 dz = -I_1 E_1 (w_{,yy} + \nu \cdot w_{,xx}),$$

$$M_{xy} = - \int_{-t/2}^{t/2} \tau_{xy} z dz = - \int_{-t/2}^{t/2} Cz^2 dz = I_1 E_1 (1-\nu) w_{,xy},$$

$$M_{yx} = \int_{-t/2}^{t/2} \tau_{yx} z dz = \int_{-t/2}^{t/2} Cz^2 dz = -I_1 E_1 (1-\nu) w_{,xy},$$

where  $M_x$  is the bending moment along axis  $x$ ,  $M_y$  is the bending moment along axis  $y$ ,  $M_{xy}$  and  $M_{yx}$  are the twisting moments. Moreover:

$$I_1 = \frac{t^3}{12}, \quad (14.8)$$

which is – similarly to beams – the second order moment of inertia of the cross section. The stress couples in the midplane of the plate are demonstrated in Fig.14.3a. The relationships between stresses and stress couples (bending and twisting moments) based on Eqs.(14.6) and (14.7) are:

$$\sigma_x = \frac{M_x}{I_1} z, \sigma_y = \frac{M_y}{I_1} z, \tau_{xy} = \frac{M_{xy}}{I_1} z. \quad (14.9)$$

For the equilibrium of a differential plate element transverse shear forces are required. Transverse shear forces are shown by Fig.14.3b and they can be calculated using the following formulae [1,3]:

$$Q_x = \int_{-t/2}^{t/2} \tau_{xz} dz, Q_y = \int_{-t/2}^{t/2} \tau_{yz} dz. \quad (14.10)$$

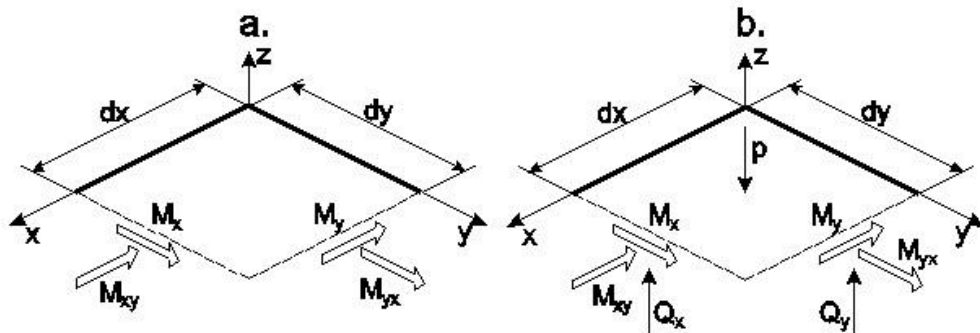


Fig.14.3. Stress couples in the midplane of a thin differential plate element (a) and its equilibrium in the case of transverse shear forces and distributed load (b).

#### 14.2.4. The equilibrium and governing equation of thin plates

The homogeneous equilibrium equation with respect to the stress field has already been introduced in section 11. [4]:

$$\underline{\underline{\sigma}} \cdot \nabla = \underline{0}, \quad (14.11)$$

of which first component equation is:

$$\frac{\partial \sigma_x}{\partial x} + \frac{\partial \tau_{xy}}{\partial y} + \frac{\partial \tau_{xz}}{\partial z} = 0. \quad (14.12)$$

Integrating the equation with respect to  $z$  yields:

$$\int \frac{\partial}{\partial x} A_z dz + \int \frac{\partial}{\partial y} C_z dz + \tau_{xz} - \tau_{xz}^0 = 0, \quad (14.13)$$

and:

$$\frac{\partial}{\partial x} \left( \frac{1}{2} A z^2 \right) + \frac{\partial}{\partial y} \left( \frac{1}{2} C z^2 \right) = \tau_{xz}^0 - \tau_{xz}, \quad (14.14)$$

finally:

$$\frac{\partial}{\partial x} \left( \frac{1}{2} \sigma_x z \right) + \frac{\partial}{\partial y} \left( \frac{1}{2} \tau_{xy} z \right) = \tau_{xz}^0 - \tau_{xz}. \quad (14.15)$$

Next, we integrate Eq.(14.15) within the ranges of  $-t/2$  and  $t/2$ :

$$\frac{\partial}{\partial x} \left( \int_{-t/2}^{t/2} \sigma_x z dz \right) + \frac{\partial}{\partial y} \left( \int_{-t/2}^{t/2} \tau_{xy} z dz \right) = 2 \int_{-t/2}^{t/2} (\tau_{xz}^0 - \tau_{xz}(z)) dz, \quad (14.16)$$

where  $\tau_{xz}^0$  is an integration constant. A possible solution for  $\tau_{xz}$ , which satisfies even the dynamic boundary conditions is [3]:

$$\tau_{xz} = \tau_{xz}^0 \left( 1 - \frac{4z^2}{t^2} \right). \quad (14.17)$$

In fact Eq.(14.17) gives the difference between the area under a rectangle and a parabola, which is  $1/3$  of the total area. Accordingly, if it is multiplied by two, then mathematically we obtain the area under the parabola, that is, from Eq.(14.16) we have:

$$2 \int_{-t/2}^{t/2} (\tau_{xz}^0 - \tau_{xz}(z)) dz = \int_{-t/2}^{t/2} \tau_{xz} z dz = Q_x, \quad (14.18)$$

which is not else than the shear force along axis  $x$  given by Eq.(14.10). Taking Eqs.(14.6), (14.9) and (14.18) back into the equilibrium equation we obtain:

$$\frac{\partial M_x}{\partial x} - \frac{\partial M_{xy}}{\partial y} - Q_x = 0. \quad (14.19)$$

The second component equation and the corresponding equilibrium equation in terms of the stress couples and transverse shear force are:

$$\frac{\partial \tau_{xy}}{\partial x} + \frac{\partial \sigma_y}{\partial y} + \frac{\partial \tau_{yz}}{\partial z} = 0, \quad (14.20)$$

$$\frac{\partial M_{yx}}{\partial x} + \frac{\partial M_y}{\partial y} - Q_y = 0,$$

and:

$$M_{xy} = -M_{yx}. \quad (14.21)$$

From the third component equation of Eq.(14.11) we obtain the following:

$$\frac{\partial \tau_{xz}}{\partial x} + \frac{\partial \tau_{yz}}{\partial y} + \frac{\partial \sigma_z}{\partial z} = 0. \quad (14.22)$$

We integrate Eq.(14.22) within the ranges of  $-t/2$  and  $t/2$  with respect to  $z$ :

$$\int_{-t/2}^{t/2} \frac{\partial \tau_{xz}}{\partial x} dz + \int_{-t/2}^{t/2} \frac{\partial \tau_{yz}}{\partial y} dz + \int_{-t/2}^{t/2} \frac{\partial \sigma_z}{\partial z} dz = 0, \quad (14.23)$$

and:

$$\frac{\partial}{\partial x} \int_{-t/2}^{t/2} \tau_{xz} dz + \frac{\partial}{\partial y} \int_{-t/2}^{t/2} \tau_{yz} dz + \int_{-t/2}^{t/2} d\sigma_z = 0. \quad (14.24)$$

Based on Eq.(14.10) the first two terms are the shear forces  $Q_x$  and  $Q_y$ , the third one is – in accordance with the dynamic boundary condition – the intensity of the distributed load,  $p$ , perpendicularly to the midplane, i.e.:

$$\frac{\partial Q_x}{\partial x} + \frac{\partial Q_y}{\partial y} + p = 0. \quad (14.25)$$

Summarizing the equilibrium equations we have:

$$M_{x,x} - M_{xy,y} - Q_x = 0, \quad (14.26)$$

$$M_{y,y} + M_{yx,x} - Q_y = 0,$$

$$Q_{x,x} + Q_{y,y} + p = 0.$$

To derive the plate equation we rearrange the first two equations:

$$Q_{x,x} = M_{x,xx} - M_{xy,yx}, \quad (14.27)$$

$$Q_{y,y} = M_{y,yy} + M_{yx,xy}.$$

Taking them back into the third of Eq.(14.26) we obtain the following:

$$M_{x,xx} - 2M_{xy,xy} + M_{y,yy} + p = 0. \quad (14.28)$$

By the help of Eq.(14.7) we have:

$$-I_1 E_1 (w_{,xxxx} + \nu \cdot w_{,yyxx} + w_{,yyyy} + \nu \cdot w_{,xxyy} + 2(1-\nu)w_{,xyxy}) = -p, \quad (14.29)$$

which, after a simple rearrangement have the form of [5]:

$$\frac{\partial^4 w}{\partial x^4} + 2 \frac{\partial^4 w}{\partial x^2 \partial y^2} + \frac{\partial^4 w}{\partial y^4} = \frac{p}{I_1 E_1}, \quad (14.30)$$

or:

$$\nabla^2 \nabla^2 w(x, y) = \frac{p}{I_1 E_1}. \quad (14.31)$$

Consequently the governing equation is a fourth order partial differential equation with the proper kinematic and dynamic boundary conditions. That means that the problem of plates subjected to bending is a boundary value problem.

### 14.3. Finite element equations of thin plates

For the finite element solution of the problem of thin plates subjected to bending we collect the strain and stress field components into vectors and we assume plane stress state [1,6]:

$$\underline{\varepsilon}^T = [\varepsilon_x, \varepsilon_y, \gamma_{xy}], \quad (14.32)$$

$$\underline{\sigma}^T = [\sigma_x, \sigma_y, \tau_{xy}].$$

Based on Eq.(14.5) the strain components can be written as:

$$\underline{\varepsilon}^T = -z \underline{\kappa}, \quad (14.33)$$

where  $\underline{\kappa}$  is the vector of curvatures:

$$\underline{\kappa} = \begin{bmatrix} \kappa_x \\ \kappa_y \\ \kappa_{xy} \end{bmatrix} = \begin{bmatrix} w_{,xx} \\ w_{,yy} \\ 2w_{,xy} \end{bmatrix}. \quad (14.34)$$

Incorporating the material law we formulate the vector of stress components as:

$$\underline{\sigma} = \underline{\underline{C}}^{str} \underline{\varepsilon}. \quad (14.35)$$

The strain components can be obtained by a two-variable function  $w(x,y)$ , the finite element interpolation of the  $w(x,y)$  function depends on the element type and the chosen degrees of freedom, but it can always be formulated in the form below:

$$w(x, y) = \underline{A}^T \underline{\lambda}, \quad (14.36)$$

where  $\underline{A}$  is the vector of unknown coefficients,  $\underline{\lambda}$  is the vector of basis polynomials. The vector of nodal displacements is:

$$\underline{u}_e = \underline{\underline{M}} \underline{A}, \quad (14.37)$$

which, for example in the case of a triangle element with three nodes becomes:

$$\underline{u}_e^T = [w_1 \quad \alpha_1 \quad \beta_1 \quad w_2 \quad \alpha_2 \quad \beta_2 \quad w_3 \quad \alpha_3 \quad \beta_3]. \quad (14.38)$$

In Eq.(14.37) matrix  $\underline{\underline{M}}$  can be calculated based on the approximate  $w(x,y)$  function and Eq.(14.1). The  $\alpha_i$  and  $\beta_i$  parameters are the rotations about the axes  $x$  and  $y$  in the corresponding nodes, where  $i = 1, 2, 3$ . From Eq.(14.37) we have:

$$\underline{A} = \underline{\underline{M}}^{-1} \underline{u}_e. \quad (14.39)$$

Generally speaking, the vector of strain components can be determined using the strain-displacement matrix:

$$\underline{\varepsilon} = \underline{\underline{B}} \underline{u}_e, \quad (14.40)$$

where Eq.(14.40) can be reformulated utilizing Eqs.(14.5), (14.37) and (14.39) as follows:

$$\underline{\varepsilon} = \underline{\underline{R}} \underline{A} = \underline{\underline{\underline{M}}}^{-1} \underline{u}_e, \quad (14.41)$$

where matrix  $\underline{\underline{R}}$  establishes the relationship between the vector of strain components and the vector of unknown coefficients, its dimension is element dependent. Consequently we have:

$$\underline{\underline{B}} = \underline{\underline{\underline{M}}}^{-1}. \quad (14.42)$$

Following the definition by Eq.(12.9) we formulate the element stiffness matrix as:

$$\underline{\underline{\underline{K}}}_e = \int_{V_e} \underline{\underline{B}}^T \underline{\underline{C}}^{str} \underline{\underline{B}} dV. \quad (14.43)$$

The dimension of the element stiffness matrix depends on the number of nodes and the number of nodal degrees of freedom. Similarly to the plane membrane element, the vector of forces is composed as the sum of several terms. The most common is the distributed (surface) load and concentrated force. By formulating the work of external forces we derive the force vector related to the distributed load:

$$W_e = \int_{A_{pe}} p \cdot w(x, y) dA = \underline{u}_e^T \underline{F}_{ep}, \quad (14.44)$$

where  $p$  is the intensity of the distributed load perpendicularly to the midplane of the plate,  $w(x, y)$  is the approximate function of the deflection surface according to Eq.(14.36). The vector  $\underline{F}_{ep}$  can be determined based on the vector of nodal displacements. In the case of concentrated loads, considering e.g. a triangular shape plate element with three nodes, at each node there can be a force perpendicularly to the plate surface and even concentrated moments acting about the  $x$  and  $y$  axes, respectively:

$$\underline{F}_{ec}^T = [F_{z1} \quad M_{x1} \quad M_{y1} \quad F_{z2} \quad M_{x2} \quad M_{y2} \quad F_{z3} \quad M_{x3} \quad M_{y3}]. \quad (14.45)$$

Thus, the vector of forces becomes:

$$\underline{F}_e = \underline{F}_{ep} + \underline{F}_{ec}. \quad (14.46)$$

Eventually, the finite element equilibrium equation for a single element and for the whole structure is:

$$\underline{\underline{K}}_e \underline{u}_e = \underline{F}_e, \quad \underline{\underline{K}} \underline{U} = \underline{F}. \quad (14.47)$$

Similarly to the plane membrane elements there is large number of plate bending elements. These elements will be reviewed in section 15.

#### 14.4. Basic equations of the technical theory of thin shells

In that case when the midplane of a thin-walled structure is not flat but curved, then we talk about shells. The analytical investigation of shells requires considerably complicated mathematical computations. Therefore in the sequel only the most important equations will be presented.

##### 14.4.1. Geometrical equations

Due to the fact that the midsurface of shells is curved, we need to introduce curvilinear coordinate systems, as it is shown by Fig.14.4.

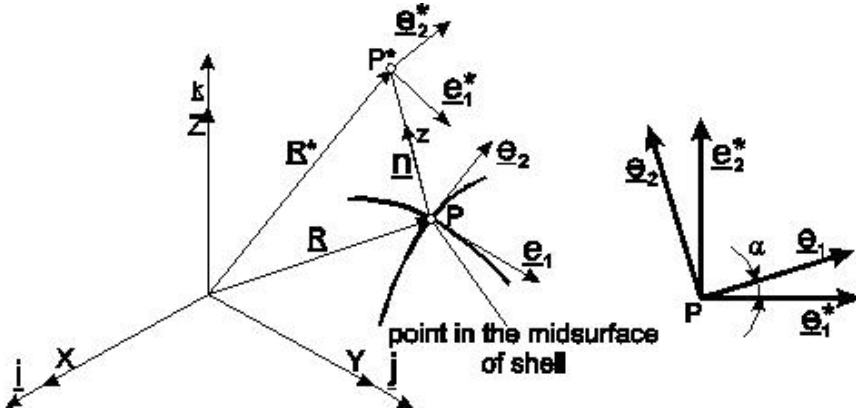


Fig.14.4. Coordinate lines and unit basis vectors of the midsurface of a shell.

The two-parameter representation of the midsurface of shells can be formulated in the form of a vector equation [1,4]:

$$\underline{R} = \underline{R}(q_1, q_2), \quad (14.48)$$

where:

$$X = X(q_1, q_2), \quad Y = Y(q_1, q_2), \quad Z = Z(q_1, q_2), \quad (14.49)$$

are the global coordinates,  $\underline{R}$  is the position vector of a point in the,  $q_1$  and  $q_2$  are the general or curvilinear coordinates of the surface (see Fig.14.4). If the parameters take on the values  $q_1 = \text{constant}$  and  $q_2 = \text{constant}$ , we obtain the  $q_1$  and  $q_2$  coordinate lines. The tangent unit vectors  $\underline{e}_i$  and the arc lengths  $dS_i$  of the coordinate lines are:

$$\underline{e}_i = \frac{1}{H_i} \frac{\partial \underline{R}}{\partial q_i} = \frac{1}{H_i} \underline{R}_i, \quad dS_i = H_i dq_i, \quad (14.50)$$

where:

$$H_i = |\underline{R}_{,i}|, \quad i = 1, 2, \quad (14.51)$$

are the so-called Lamé parameters [1] or metric coefficients [4]. In the followings we assume that the local coordinate axes are mutually perpendicular at each point, and the curvilinear system is orthogonal, i.e.  $\underline{e}_1 \cdot \underline{e}_2 = 0$ . The outward unit normal vector of the midsurface becomes:

$$\underline{n} = \underline{e}_1 \times \underline{e}_2. \quad (14.52)$$

The triad of unit orthogonal vectors  $[\underline{e}_1, \underline{e}_2, \underline{n}]$  determines an orthogonal curvilinear coordinate system at an actual point  $P$ . The curvature and the torsion of coordinate lines are given by the Frenet formulae [1,7]:

$$\frac{1}{R_i} = -\underline{n} \cdot \frac{\partial^2 \underline{R}}{\partial S_i^2} = -\underline{n} \cdot \frac{1}{H_i^2} \frac{\partial^2 \underline{R}}{\partial q_i^2} = -\frac{1}{H_i^2} \underline{n} \cdot \underline{R}_{,ii}, \quad i = 1, 2, \quad (14.53)$$

$$\frac{1}{R_{12}} = -\underline{n} \cdot \frac{\partial^2 \underline{R}}{\partial S_1 \partial S_2} = -\underline{n} \cdot \frac{1}{H_1 H_2} \underline{R}_{,12},$$

where  $R_1$  and  $R_2$  are the radii of curvature. If  $R_{12} = 0$ , then the  $q_1$  and  $q_2$  lines are the lines of principal curvatures on the midsurface, moreover the directions of the unit basis vectors  $\underline{e}_1$  and  $\underline{e}_2$  are the principal directions. The curvature of the midsurface is a tensor quantity. If the directions of vectors  $\underline{e}_1$  and  $\underline{e}_2$  are not the principal directions, then the angle, which determines the principal directions can be obtained by:

$$\operatorname{tg} 2\alpha = \frac{2/R_{12}'}{1/R_1' + 1/R_2'}. \quad (14.54)$$

The values of the principal curvatures are [1,7]:

$$\frac{1}{R_1} = \frac{\cos^2 \alpha}{R_1'} + \frac{\sin^2 \alpha}{R_2'} + \frac{\sin 2\alpha}{R_{12}'}, \quad (14.55)$$

$$\frac{1}{R_2} = \frac{\sin^2 \alpha}{R_1'} + \frac{\cos^2 \alpha}{R_2'} - \frac{\sin 2\alpha}{R_{12}'}, \quad \frac{1}{R_{12}} = 0.$$

In the followings we investigate the special case, when the directions of unit basis vectors coincide with the principal directions. The derivatives of the unit basis vectors of the coordinate system on the midsurface are [1,4]:

$$\underline{e}_{i,i} = -\frac{H_{i,j}}{H_j} \underline{e}_j - \frac{H_i}{R_i} \underline{n}, \quad \underline{e}_{i,j} = -\frac{H_{j,i}}{H_i} \underline{e}_j, \quad \underline{n}_{,j} = \frac{H_j}{R_j} \underline{e}_j, \quad i \neq j, \quad i, j = 1, 2. \quad (14.56)$$

Point  $P^*$  is located on a surface parallel to the midsurface and the distance of point  $P^*$  from point  $P$  is given by coordinate  $z$  measured along the normal vector  $\underline{n}$ . Based on Fig.14.4 the position vector of point  $P^*$  is:

$$\underline{R}^* = \underline{R} + z \underline{n}. \quad (14.57)$$

The unit vectors are independent of coordinate  $z$ , viz.:

$$\underline{e}_i^* = \underline{e}_i. \quad (14.58)$$

The derivative of the position vector of point  $P^*$  can be written as:

$$\underline{R}_i^* = \underline{R}_{,i} + z\underline{n}_{,i} = H_i(1 + \frac{z}{R_i})\underline{e}_i. \quad (14.59)$$

Consider the followings:

$$H_i^* = H_i(1 + \frac{z}{R_i}) \text{ and } dS_i^* = dS_i(1 + \frac{z}{R_i}), i = 1, 2. \quad (14.60)$$

which are the Lamé parameters and arc lengths with respect to point  $P^*$ .

#### 14.4.2. Stress resultants and couples, equilibrium equations

Fig.14.5 shows the stresses on the boundary planes of a differential shell element, while Fig.14.6 presents the stress resultants and couples (internal forces and moments) on the mid-surface of the differential shell element with dimensions of  $dS_1 \times dS_2$ .

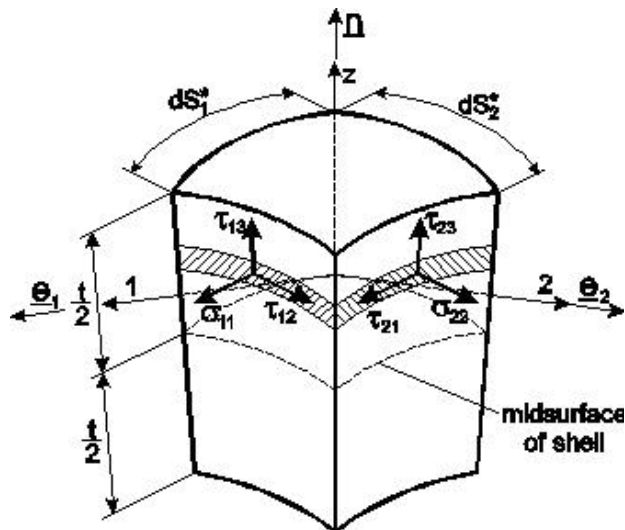


Fig.14.5. Stress components on the boundary planes of a differential shell element.

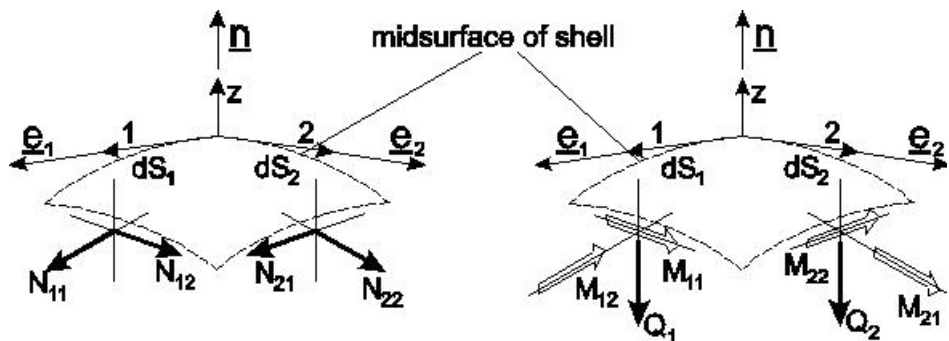


Fig.14.6. Internal forces and moments in the midsurface of a differential shell element.

We must consider the relationship between the arc lengths  $dS_i$  and  $dS_i^*$  given by Eq.(14.60) when we establish the relationship between the stresses acting on the differential shell element

with thickness  $t$  and the internal forces, moments on the midsurface of the shell element. The stress resultants and stress couples acting on the curve with outward normal  $\underline{e}_1$  are:

$$\begin{aligned} N_{11} &= \int_{-t/2}^{t/2} \sigma_{11}(1 + \frac{z}{R_2}) dz, \quad N_{12} = \int_{-t/2}^{t/2} \tau_{12}(1 + \frac{z}{R_2}) dz \neq N_{21}, \quad Q_1 = - \int_{-t/2}^{t/2} \tau_{13}(1 + \frac{z}{R_2}) dz, \\ M_{11} &= \int_{-t/2}^{t/2} \sigma_{11}z(1 + \frac{z}{R_2}) dz, \quad M_{12} = \int_{-t/2}^{t/2} \tau_{12}z(1 + \frac{z}{R_2}) dz \neq M_{21}, \end{aligned} \quad (14.61)$$

where  $N_{11}$  is the in-plane normal force,  $N_{12}$  and  $N_{21}$  are the in-plane shear forces,  $Q_1$  is the transverse shear force,  $M_{11}$  is the bending moment,  $M_{12}$  and  $M_{21}$  are the twisting moments, respectively. It must be taken into consideration that although the reciprocity law of shear stresses implies  $\tau_{12} = \tau_{21}$ , in the equations above  $N_{12} \neq N_{21}$  and  $M_{12} \neq M_{21}$ , which can be explained by the fact that the radii of curvatures are in general not equal to each other, i.e.:  $R_1 \neq R_2$ . The development of equilibrium equations establishing the equilibrium between external loads and internal forces and moments in the shell structure is also very complicated. Therefore we present only the resulting equations. The equilibrium equations in the case of stress resultants are [1,7]:

$$\begin{aligned} (H_2 N_{11})_{,1} + (H_1 N_{21})_{,2} + N_{12} H_{1,2} - N_{22} H_{2,1} - H_1 H_2 \left( \frac{Q_1}{R_1} + p_1 \right) &= 0, \\ (H_2 N_{12})_{,1} + (H_1 N_{22})_{,2} + N_{21} H_{2,1} - N_{11} H_{1,2} - H_1 H_2 \left( \frac{Q_2}{R_2} + p_2 \right) &= 0, \\ (H_2 Q_1)_{,1} + (H_1 Q_2)_{,2} + H_1 H_2 \left( \frac{N_{11}}{R_1} + \frac{N_{22}}{R_2} - p_3 \right) &= 0, \end{aligned} \quad (14.62)$$

where  $p_1$  and  $p_2$  are the tangentially distributed loads along directions 1 and 2,  $p_3$  is the distributed load perpendicularly to the shell midsurface. The equilibrium equations in the case of stress couples and moment of stress resultants are:

$$(H_2 M_{12})_{,1} + (H_1 M_{22})_{,2} + M_{21} H_{2,1} - M_{11} H_{1,2} - H_1 H_2 Q_2 = 0, \quad (14.63)$$

$$(H_2 M_{11})_{,1} + (H_1 M_{21})_{,2} + M_{12} H_{1,2} - M_{22} H_{2,1} + H_1 H_2 Q_1 = 0,$$

$$\frac{M_{12}}{R_1} - \frac{M_{21}}{R_2} + N_{12} - N_{21} = 0, \quad (14.64)$$

where in the subscript the comma and the number refer to the differentiation with respect to the corresponding coordinate.

### 14.4.3. Displacement field, strain components

Based on Fig.14.7 the vector of displacements and rotations in a point  $P$  on the shell midsurface can be written as:

$$\underline{u} = u \underline{e}_1 + v \underline{e}_2 + w \underline{n}, \quad \underline{\beta} = \beta_1 \underline{e}_1 - \beta_2 \underline{e}_2 + \beta_3 \underline{n}. \quad (14.65)$$

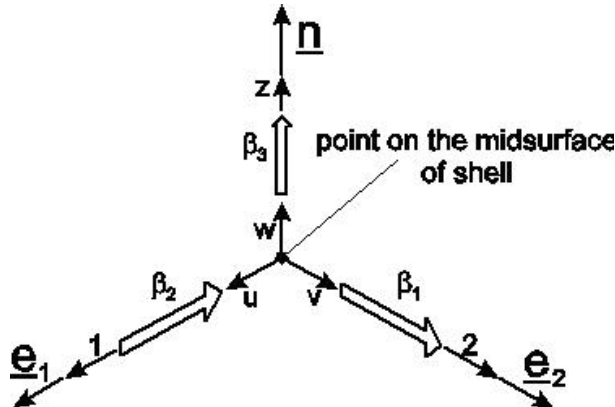


Fig.14.7. Displacement of a point on the midsurface of a thin shell.

In accordance with the kinematic hypothesis of the shell theory the components of vector  $\underline{u}$  in a point  $P^*$  out of the midsurface are [1,7]:

$$u^* = u + \beta_1 z, \quad v^* = v + \beta_2 z, \quad w^* = w, \quad (14.66)$$

i.e. the line of material points, which is perpendicular to the shell midsurface remains perpendicular during the deformation. The equations describing the in-plane strains and changes in curvature are [1,7]:

$$\varepsilon_{11} = \frac{1}{H_1} u_{,1} + \frac{H_{1,2}}{H_1 H_2} v + \frac{1}{R_1} w, \quad (14.67)$$

$$\varepsilon_{22} = \frac{1}{H_2} v_{,2} + \frac{H_{2,1}}{H_1 H_2} u + \frac{1}{R_2} w,$$

$$2\gamma_{12} = \frac{H_1}{H_2} \left( \frac{u}{H_1} \right)_{,2} + \frac{H_2}{H_1} \left( \frac{v}{H_2} \right)_{,1},$$

$$\kappa_{11} = \frac{1}{H_1} \beta_{1,1} + \frac{H_{1,2}}{H_1 H_2} \beta_2,$$

$$\kappa_{22} = \frac{1}{H_2} \beta_{2,2} + \frac{H_{2,1}}{H_1 H_2} \beta_1,$$

$$2\kappa_{12} = \frac{H_1}{H_2} \left( \frac{\beta_1}{H_2} \right)_{,2} + \frac{H_2}{H_1} \left( \frac{\beta_2}{H_1} \right)_{,1} + \left( \frac{1}{R_2} - \frac{1}{R_1} \right) \beta_3,$$

where  $\varepsilon_1$  and  $\varepsilon_2$  are the in-plane strains in the directions of  $q_1$  and  $q_2$  coordinate lines,  $\gamma_{12}$  is the shear strain related to the change of angle between unit vectors  $\underline{e}_1$  and  $\underline{e}_2$  during the deformation,  $\kappa_{11}$  and  $\kappa_{22}$  are the changes in curvatures in the directions of  $q_1$  and  $q_2$  parameters,  $\kappa_{12}$  is the twisting curvature. The shear strains related to the unit normal and unit vectors  $\underline{e}_1$ ,  $\underline{e}_2$  are [1,7]:

$$\gamma_{13} = -\frac{u}{R_1} + \frac{1}{H_1} w_{,1} + \beta_1, \quad \gamma_{23} = -\frac{v}{R_2} + \frac{1}{H_2} w_{,2} + \beta_2. \quad (14.68)$$

We assume that during the deformation of shell an actual line of material points remain perpendicular to the curved shape of shell midsurface, accordingly the shear strains given by (14.68) are equal to zero. The kinematic hypothesis of shell theory together with the one mentioned before is called the Kirchhoff–Love hypothesis. Under these assumptions we have:

$$\beta_1 = \frac{u}{R_1} - \frac{1}{H_1} w_{,1}, \quad \beta_2 = \frac{v}{R_2} - \frac{1}{H_2} w_{,2}. \quad (14.69)$$

In other words the additional transverse shear deformation is neglected (similarly to Kirchhoff's theory of thin plates). The rotation about axis  $z$  can be formulated by the following expression [1,7]:

$$\beta_3 = \frac{1}{2H_1 H_2} [(H_2 v)_{,1} - (H_1 u)_{,2}]. \quad (14.70)$$

Nevertheless, in most of the cases the rotation about  $z$  is negligible; therefore it is not considered in the equations.

#### 14.4.4. Approximations within the technical theory of thin shells

The shell is considered to be thin if the thickness is relatively small compared to the smaller radius of curvature, viz. [1]:

$$\frac{z}{R_2} \ll 1. \quad (14.71)$$

Consequently, the Lamé parameters and the arc lengths on the midsurface and out of the midsurface are approximately equal, which leads to:

$$H_i^* \cong H_i \text{ and: } dS_i^* \cong dS_i, \quad i = 1, 2. \quad (14.72)$$

Accordingly, Eq.(14.61) can be simplified significantly:

$$\begin{aligned} N_{11} &= \int_{-t/2}^{t/2} \sigma_{11} dz, \quad N_{12} = \int_{-t/2}^{t/2} \tau_{12} dz = N_{21}, \quad Q_1 = - \int_{-t/2}^{t/2} \tau_{13} dz, \\ M_{11} &= \int_{-t/2}^{t/2} \sigma_{11} z dz, \quad M_{12} = \int_{-t/2}^{t/2} \tau_{12} z dz = M_{21}. \end{aligned} \quad (14.73)$$

It is seen that in this case the transverse shear forces and torsional moments are equal to each other, which violates the equilibrium equations given by Eq. (14.64). This approximation is permitted within the technical theory of thin shells.

#### 14.5. Major steps in the finite element modeling of shells

In the course of the finite element discretization of shells – similarly to the plane and plate problems – we proceed the interpolation of the geometry and the displacement field [1,7]. The vector of displacement and rotation components in a point located on the shell midsurface is:

$$\underline{u}^T = [u \quad v \quad w], \quad (14.74)$$

$$\underline{\beta}^T = [\beta_1 \quad \beta_2 \quad \beta_3].$$

The components of these vectors are not independent of each other. From Eq.(14.67) we calculate the in-plane strains and the changes in curvature:

$$\underline{\varepsilon}^T = [\varepsilon_{11} \quad \varepsilon_{22} \quad 2\gamma_{12}], \quad (14.75)$$

$$\underline{\kappa}^T = [\kappa_{11} \quad \kappa_{22} \quad 2\kappa_{12}].$$

We collect the in-plane forces and moments into a vector:

$$\underline{N}^T = [N_{11} \quad N_{22} \quad N_{12}], \quad (14.76)$$

$$\underline{M}^T = [M_{11} \quad M_{22} \quad M_{12}].$$

Transverse shear forces  $Q_1, Q_2$  are not considered in the calculation of the deformation. Finally the vectors of the surface loads and concentrated forces and moments are:

$$\underline{p}^T = [p_1 \quad p_1 \quad p_3], \quad (14.77)$$

$$\underline{\rho}_N^T = [N_1 \quad N_2 \quad -Q],$$

$$\underline{\rho}_M^T = [M_1 \quad M_2 \quad 0],$$

where  $\underline{p}$  contains the distributed loads in the directions of coordinate lines  $q_1$  and  $q_2$  and also the distributed load perpendicularly to the shell midsurface,  $\underline{\rho}_N$  and  $\underline{\rho}_M$  contain the concentrated forces and moments acting in the nodes. Using the vectors given by Eqs.(14.75)-(14.77) the total potential energy is formulated as:

$$\Pi_e = \frac{1}{2} \int_A (\underline{\varepsilon}^T \underline{N} + \underline{\kappa}^T \underline{M}) H_1 H_2 dq_1 dq_2 - \int_A \underline{u}^T \underline{p} H_1 H_2 dq_1 dq_2 - \int_S (\underline{u}^T \underline{\rho}_N + \underline{\beta}^T \underline{\rho}_M) dS. \quad (14.78)$$

We assume that the material of the thin shell is linear elastic, homogeneous and isotropic. Then, the vector of in-plane forces and vector of moments can be calculated as follows:

$$\underline{N} = t \underline{\underline{C}}^{str} \underline{\varepsilon}, \quad \underline{M} = \frac{t^3}{12} \underline{\underline{C}}^{str} \underline{\kappa}, \quad (14.79)$$

where the constitutive matrix assuming plane stress state is:

$$\underline{\underline{C}}^{str} = \frac{E}{1-\nu^2} \begin{bmatrix} 1 & \nu & 0 \\ \nu & 1 & 0 \\ 0 & 0 & \frac{1-\nu}{2} \end{bmatrix}. \quad (14.80)$$

Accordingly, Eq.(14.78) becomes:

$$\begin{aligned} \Pi_e = & \frac{1}{2} \int_A (t \underline{\varepsilon}^T \underline{\underline{C}}^{str} \underline{\varepsilon} + \frac{t^2}{12} \underline{\kappa}^T \underline{\underline{C}}^{str} \underline{\kappa}) H_1 H_2 dq_1 dq_2 + \\ & - \int_A \underline{u}^T \underline{p} H_1 H_2 dq_1 dq_2 - \int_S (\underline{u}^T \underline{\rho}_N + \underline{\beta}^T \underline{\rho}_M) dS, \end{aligned} \quad (14.81)$$

Utilizing the definition of the element stiffness matrix and the vector of nodal forces we can derive the expression below:

$$\Pi_e = \frac{1}{2} \underline{u}_e^T \underline{\underline{K}}_e \underline{u}_e - \underline{u}_e^T \underline{F}_e, \quad (14.82)$$

from which the finite element equilibrium equation for a single element (the first of Eq.(14.47)) can be derived. As a next step we summarize the potential energy of each element:

$$\Pi = \sum \Pi_e = \frac{1}{2} \underline{U}^T \underline{\underline{K}} \underline{U} - \underline{U}^T \underline{F}, \quad (14.83)$$

and finally applying the minimum principle of the total potential energy we obtain the structural equilibrium equation:

$$\underline{\underline{K}}\underline{\underline{U}} = \underline{\underline{F}} . \quad (14.84)$$

For the finite element modeling of shells there is very large number of element types. Not only the flat shell elements, which give more accurate result under high mesh resolution, but also the curved (e.g. cylindrical shell element) and doubly-curved shell element types are available, which approximate better both the geometry and the displacement field using the same element number. The different plate and shell elements are discussed in sections 15-17.

#### 14.6. Bibliography

- [1] Imre Bojtár, Gábor Vörös, *Application of the finite element method to plate and shell structures*. Technical Book Publisher, 1986, Budapest (in Hungarian).
- [2] Robert D. Cook, *Finite element modeling for stress analysis*. John Wiley and sons, Inc., 1995, New York, Chichester, Brisbane, Toronto, Singapore.
- [3] Gábor Vörös, *Lectures and practices of the subject Elasticity and finite element method, manuscript*, Applied Mechanics Module, Budapest University of Technology and Economics, Faculty of Mechanical Engineering, Department of Applied Mechanics, 2002, Budapest (in Hungarian).
- [4] Pei Chi Chou, Nicholas J. Pagano. *Elasticity – Tensor, dyadic and engineering approaches*. D. Van Nostrand Company, Inc., 1967, Princeton, New Jersey, Toronto, London.
- [5] S. Timoshenko, S. Woinowsky-Krieger. *Theory of plates and shells*. Technical Book Publisher, 1966, Budapest (in hungarian).
- [6] Singiresu S. Rao. *The finite element method in engineering – fourth edition*. Elsevier Science & Technology Books, 2004.
- [7] Eduard Ventsel, Theodor Krauthammer. *Thin plates and shells – Theory, analysis and applications*. Marcel Dekker Inc., 2001, New York, Basel.

## 15. MODELING OF IN-PLANE THIN-WALLED SHELLS UNDER IN-PLANE AND TRANSVERSE LOAD BY FINITE ELEMENT METHOD BASED SOFTWARE SYSTEMS

### 15.1. Plate elements subjected to bending

Flat plate elements are suitable to determine the internal forces, stress resultants and stress couples in plate shape structures. The plate element is the extension of beam elements so that bending, shear and torsion take place in two orthogonal planes involving some interactions. Similarly to the plane membrane elements, the triangle and quadrilateral shape elements are available for the modeling of shells. The application of general triangle shape elements is reasonable when the shape of the structure is irregular, triangular or similar to the triangle. In this section we overview primarily the plate elements subjected to transverse load. In that case when the plate is loaded in-plane and also transversely we can solve the problem by combining the plane membrane and plate bending elements. We have already seen by Eq.(14.3) that due to neglecting the transverse shear forces the rotations in an actual point of the plate are:

$$\beta = -w_{,x} \text{ and } \alpha = w_{,y}. \quad (15.1)$$

The curvatures related to the bending deformation are:

$$\underline{\kappa} = -\begin{bmatrix} w_{,xx} \\ w_{,yy} \\ 2w_{,xy} \end{bmatrix}, \text{ and } \underline{\varepsilon} = -z \cdot \underline{\kappa}. \quad (15.2)$$

For thin plates we assume plane stress state, i.e.:

$$\underline{\varepsilon}^T = [\varepsilon_x, \varepsilon_y, \gamma_{xy}]. \quad (15.3)$$

In the course of the introduction of Kirchhoff plate theory we have observed that the deflection surface is given by a two-variable  $w(x,y)$  function, with that both the curvatures and strain components can be calculated. For plate bending problems this  $w(x,y)$  function must be produced by interpolation polynomials, and then we can provide the element stiffness matrix and force vector. In the followings we give the details of few element types for plate bending.

### 15.2. Triangular plate bending element or Tocher triangle element

In the course of the finite element discretization of plate shape structures we approximate the transverse deflection by a third order polynomial in terms of the  $x$  and  $y$  coordinates [1,2]:

$$w(x, y) = a_0 + a_1x + a_2y + a_3x^2 + a_4xy + a_5y^2 + a_6x^3 + a_7(x^2y + xy^2) + a_8y^3. \quad (15.4)$$

This approximation was one of the first triangular finite elements, which was published by Tocher [1]. The element is shown in Fig.15.1. The deflection surface in vector form is:

$$w(x, y) = \underline{A}^T \underline{\lambda}, \quad (15.5)$$

where  $\underline{A}$  is the vector unknown coefficients,  $\underline{\lambda}$  is the vector of basis polynomials, respectively:

$$\underline{A}^T = [a_0 \ a_1 \ a_2 \ a_3 \ a_4 \ a_5 \ a_6 \ a_7 \ a_8], \quad (15.6)$$

$$\underline{\lambda}^T = [1 \ x \ y \ x^2 \ xy \ y^2 \ x^3 \ (x^2y + xy^2) \ y^3].$$

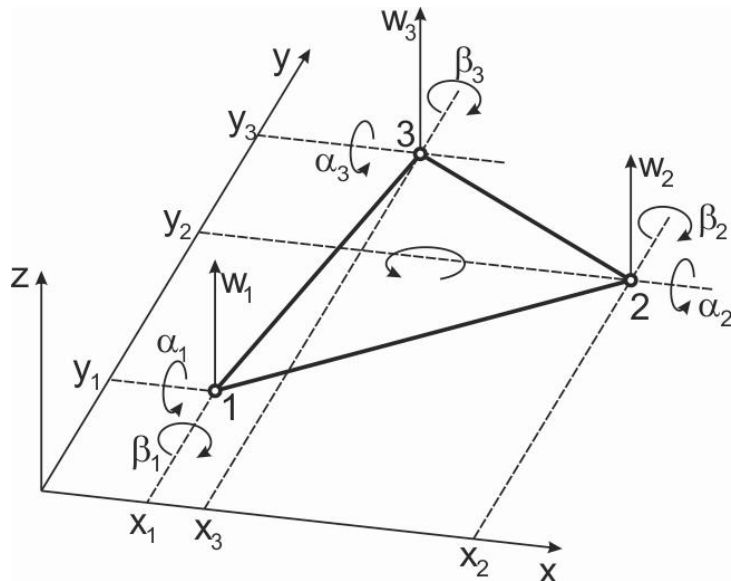


Fig.15.1. The nine degrees of freedom Tocher triangular plate element.

The unknown coefficients can be calculated based on the nodal conditions. Namely, the displacement function must give back the actual nodal displacement if we substitute the nodal coordinates of the same node. Therefore, in Eq.(15.4) the number of terms is always equal to the number of degrees of freedom. For the Tocher triangle element the eighth term contains the sum of  $x^2y$  and  $xy^2$ . Actually, in vector  $\underline{A}$  there is nine unknown coefficients. Following Fig.15.1 the vector of nodal degrees of freedom for a single element is:

$$\underline{u}_e^T = [w_1 \ \alpha_1 \ \beta_1 \ w_2 \ \alpha_2 \ \beta_2 \ w_3 \ \alpha_3 \ \beta_3], \quad (15.7)$$

where  $w_i$  is the transverse displacement perpendicularly to the midplane,  $\alpha_i$  and  $\beta_i$  are the rotations about axes  $x$  and  $y$ , respectively. Accordingly, the Tocher plate element has nine degrees of freedom. The nodal conditions for the calculation of the coefficients are [1,2]:

$$w(x_1, y_1) = w_1, \frac{\partial w}{\partial y}(x_1, y_1) = \alpha_1, -\frac{\partial w}{\partial x}(x_1, y_1) = \beta_1, \quad (15.8)$$

$$w(x_2, y_2) = w_2, \frac{\partial w}{\partial y}(x_2, y_2) = \alpha_2, -\frac{\partial w}{\partial x}(x_2, y_2) = \beta_2,$$

$$w(x_3, y_3) = w_3, \frac{\partial w}{\partial y}(x_3, y_3) = \alpha_3, -\frac{\partial w}{\partial x}(x_3, y_3) = \beta_3.$$

We need the derivatives of the  $w(x,y)$  function with respect to  $x$  and  $y$  to calculate both the coefficients and the strain components, i.e we can write using Eq. (15.4):

$$\frac{\partial w}{\partial x} = a_1 + 2a_3x + a_4y + 3a_6x^2 + a_7(2xy + y^2), \quad (15.9)$$

$$\frac{\partial w}{\partial y} = a_2 + a_4x + 2a_5y + a_7(x^2 + 2xy) + 3a_8y^2,$$

$$\frac{\partial^2 w}{\partial x^2} = 2a_3 + 6a_6x + 2a_7y,$$

$$\frac{\partial^2 w}{\partial y^2} = 2a_5 + 2a_7x + 6a_8y,$$

$$\frac{\partial^2 w}{\partial x \partial y} = a_4 + 2a_7(x + y).$$

The substitution of the derivatives above into Eq.(15.7) leads to the following system of equation reduced to matrix form [1]:

$$\underline{u}_e = \underline{\underline{M}} \underline{A}, \quad (15.10)$$

where:

$$\underline{\underline{M}} = \begin{bmatrix} 1 & x_1 & y_1 & x_1^2 & x_1y_1 & y_1^2 & x_1^3 & (x_1^2y_1 + x_1y_1^2) & y_1^3 \\ 0 & 0 & 1 & 0 & x_1 & 2y_1 & 0 & (x_1^2 + 2x_1y_1) & 3y_1^2 \\ 0 & -1 & 0 & -2x_1 & -y_1 & 0 & -3x_1^2 & -(2x_1y_1 + y_1^2) & 0 \\ 1 & x_2 & y_2 & x_2^2 & x_2y_2 & y_2^2 & x_2^3 & (x_2^2y_2 + x_2y_2^2) & y_2^3 \\ 0 & 0 & 1 & 0 & x_2 & 2y_2 & 0 & (x_2^2 + 2x_2y_2) & 3y_2^2 \\ 0 & -1 & 0 & -2x_2 & -y_2 & 0 & -3x_2^2 & -(2x_2y_2 + y_2^2) & 0 \\ 1 & x_3 & y_3 & x_3^2 & x_3y_3 & y_3^2 & x_3^3 & (x_3^2y_3 + x_3y_3^2) & y_3^3 \\ 0 & 0 & 1 & 0 & x_3 & 2y_3 & 0 & (x_3^2 + 2x_3y_3) & 3y_3^2 \\ 0 & -1 & 0 & -2x_3 & -y_2 & 0 & -3x_3^2 & -(2x_3y_3 + y_3^2) & 0 \end{bmatrix}. \quad (15.11)$$

The coefficients of the interpolation function are the solutions of the system of equation given by Eq.(15.10):

$$\underline{A} = \underline{\underline{M}}^{-1} \underline{u}_e . \quad (15.12)$$

The expressions of the coefficients are extremely complicated; hence they are not detailed here. The vector of strain components based on Eqs.(14.5) and (15.5) are:

$$\underline{\varepsilon} = \begin{bmatrix} \varepsilon_x \\ \varepsilon_y \\ \gamma_{xy} \end{bmatrix} = -z \begin{bmatrix} w_{,xx} \\ w_{,yy} \\ 2 \cdot w_{,xy} \end{bmatrix} = \underline{\underline{R}} \underline{A}, \quad (15.13)$$

where matrix  $\underline{\underline{R}}$  is:

$$\underline{\underline{R}} = -z \cdot \begin{bmatrix} 0 & 0 & 0 & 2 & 0 & 0 & 6x & 2y & 0 \\ 0 & 0 & 0 & 0 & 0 & 2 & 0 & 2x & 6y \\ 0 & 0 & 0 & 0 & 2 & 0 & 0 & 4(x+y) & 0 \end{bmatrix}. \quad (15.14)$$

Taking back Eq.(15.12) into Eq.(15.13) the strain-displacement matrix can be derived:

$$\underline{\varepsilon} = \underline{\underline{R}} \underline{A} = \underline{\underline{\underline{M}}}^{-1} \underline{u}_e = \underline{\underline{B}} \underline{u}_e . \quad (15.15)$$

For thin plates we assume plane stress state, consequently we can write:

$$\underline{\sigma} = \underline{\underline{C}}^{str} \underline{\varepsilon}, \quad \underline{\sigma} = \underline{\underline{C}}^{str} \underline{\underline{B}} \underline{u}_e , \quad (15.16)$$

where matrix  $\underline{\underline{C}}^{str}$  refers to plane stress state. According to Eq.(14.43) the definition of the element stiffness matrix is:

$$\underline{\underline{K}}_e = \int_{V_e} \underline{\underline{B}}^T \underline{\underline{C}}^{strT} \underline{\underline{B}} dV . \quad (15.17)$$

Incorporating Eq.(15.15) we obtain:

$$\underline{\underline{K}}_e = (\underline{\underline{M}}^{-1})^T \int_{A_e} \left\{ \int_{-t/2}^{t/2} \underline{\underline{R}}^T \underline{\underline{C}}^{strT} \underline{\underline{R}} dz \right\} dA (\underline{\underline{M}}^{-1}) . \quad (15.18)$$

The middle term in the expression above is [1]:

$$\begin{aligned}
& \int_{A_e} \left\{ \int_{-t/2}^{t/2} \underline{\underline{R}}^T \underline{\underline{C}}^{g^T} \underline{\underline{R}} dz \right\} dA = \\
&= \int_{A_e} I_1 E_1 \begin{bmatrix} 0 & 0 & 0 & 0 & 0 & 0 & 0 & 0 \\ 0 & 0 & 0 & 0 & 0 & 0 & 0 & 0 \\ 0 & 0 & 0 & 0 & 0 & 0 & 0 & 0 \\ 0 & 0 & 0 & 4 & 0 & 4\nu & 12x & 4(\nu x + y) \\ 0 & 0 & 0 & 0 & 2(1-\nu) & 0 & 0 & 4(1-\nu)(x+y) \\ 0 & 0 & 0 & 4\nu & 0 & 4 & 12\nu x & 4(x+\nu y) \\ 0 & 0 & 0 & 12x & 0 & 12\nu x & 36x^2 & 12x(\nu x + y) \\ 0 & 0 & 0 & 4(\nu x + y) & 4(1-\nu)(x+y) & 4(x+\nu y) & 12x(\nu x + y) & \{(12-8\nu)(x+y)^2 + \\ & & & & & & -8(1-\nu)xy\} & 12y(x+\nu y) \\ 0 & 0 & 0 & 12\nu xy & 0 & 12y & 36\nu xy & 12y(x+\nu y) & 36y^2 \end{bmatrix} dA. \tag{15.19}
\end{aligned}$$

where  $I_1 = t^3/12$  and  $E_1 = E/(1-\nu^2)$ . To calculate the stiffness matrix the inverse of matrix  $\underline{\underline{M}}$  is required. Since it is very complicated, it is not detailed here. In Eq.(15.19) it is possible to simplify the components by the surface integral transformations given below [1]:

$$\int_{A_e} dA = \iint_{A_e} dx dy = A_e = \frac{1}{2}[(x_2 y_3 - x_3 y_2) + (x_3 y_1 - x_1 y_3) + (x_1 y_2 - x_2 y_1)], \tag{15.20}$$

$$\int_{A_e} x dA = \iint_{A_e} x dx dy = \frac{A_e}{3}(x_1 + x_2 + x_3),$$

$$\int_{A_e} y dA = \iint_{A_e} y dx dy = \frac{A_e}{3}(y_1 + y_2 + y_3),$$

$$\int_{A_e} x^2 dA = \iint_{A_e} x^2 dx dy = \frac{A_e}{6}(x_1^2 + x_2^3 + x_3^2 + x_1 x_2 + x_2 x_3 + x_3 x_1),$$

$$\int_{A_e} y^2 dA = \iint_{A_e} y^2 dx dy = \frac{A_e}{6}(y_1^2 + y_2^3 + y_3^2 + y_1 y_2 + y_2 y_3 + y_3 y_1),$$

$$\int_{A_e} xy dA = \iint_{A_e} xy dx dy = \frac{A_e}{12}(y_1(2x_1 + x_2 + x_3) + y_2(x_1 + 2x_2 + x_3) + y_3(x_1 + x_2 + 2x_3)),$$

$$\begin{aligned}
\int_{A_e} x^2 y dA = \iint_{A_e} x^2 y dx dy = & \frac{A_e}{60}(y_1(3x_1^2 + x_2^2 + x_3^2 + 2x_1(x_2 + x_3) + x_2 x_3) + \\
& + y_2(x_1^2 + 3x_2^2 + x_3^2 + 2x_2(x_1 + x_3) + x_1 x_3) + y_3(x_1^2 + x_2^2 + 3x_3^2 + 2x_3(x_1 + x_2) + x_1 x_2)),
\end{aligned}$$

$$\int_{A_e} xy^2 dA = \iint_{A_e} xy^2 dx dy = \frac{A_e}{60} (x_1(3y_1^2 + y_2^2 + y_3^2 + 2y_1(y_2 + y_3) + y_2y_3) + \\ + x_2(y_1^2 + 3y_2^2 + y_3^2 + 2y_2(y_1 + y_3) + y_1y_3) + x_3(y_1^2 + y_2^2 + 3y_3^2 + 2y_3(y_1 + y_2) + y_1y_2)),$$

$$\int_{A_e} x^3 dA = \iint_{A_e} x^3 dx dy = \frac{A_e}{20} (x_1^3 + x_2^3 + x_3^2 + x_1x_2^2 + x_1^2x_2 + x_2x_3^2 + x_2^2x_3 + x_1x_3^2 + x_1^2x_3 + x_1x_2x_3),$$

$$\int_{A_e} y^3 dA = \iint_{A_e} y^3 dx dy = \frac{A_e}{20} (y_1^3 + y_2^3 + y_3^2 + y_1y_2^2 + y_1^2y_2 + y_2y_3^2 + y_2^2y_3 + y_1y_3^2 + y_1^2y_3 + y_1y_2y_3),$$

here  $A_e$  is the triangle area,  $x_i$  and  $y_i$ ,  $i = 1, 2, 3$  are the nodal coordinates, respectively. In most of the cases the force vector is composed by two terms. The force vector related to the distributed force can be derived by expressing the work of external force:

$$W_e = \int_{A_{pe}} pw(x, y) dA = \underline{u}_e^T \underline{F}_{ep}. \quad (15.21)$$

The calculation of  $\underline{F}_{ep}$  is difficult, we need the inverse of matrix  $\underline{\underline{M}}$  and the simplification of surface integrals, respectively. The concentrated forces and moments are collected in a vector in accordance with the nodal degrees of freedom:

$$\underline{F}_{ec}^T = [F_{z1} \quad M_{x1} \quad M_{y1} \quad F_{z2} \quad M_{x2} \quad M_{y2} \quad F_{z3} \quad M_{x3} \quad M_{y3}], \quad (15.22)$$

where  $F_{zi}$  is the concentrated force perpendicularly to the midplane of plate,  $M_{xi}$  and  $M_{yi}$  are the concentrated moments acting in the  $x$  and  $y$  directions. In the sequel we present a detailed example.

### 15.3. Example for the application of the Tocher triangle plate element

Determine the displacement and the reactions of the built-in plate depicted in Fig.15.2 [1]!

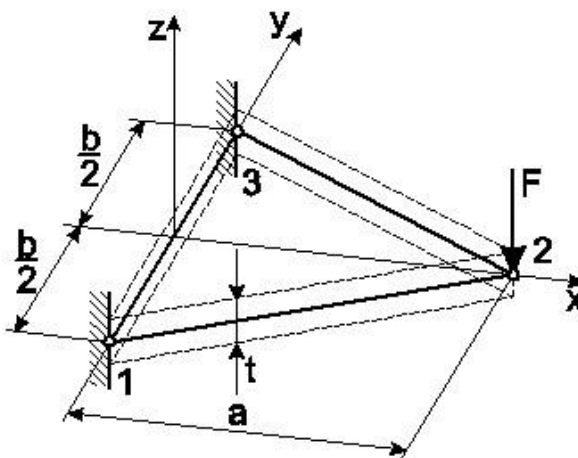


Fig.15.2. Triangle shape built-in plate loaded by concentrated force.

*Given:*

$E = 200 \text{ GPa}$ ,  $\nu = 0,3$ ,  $t = 5 \text{ mm}$ ,  $F = 1 \text{ kN}$ ,  $a = 200 \text{ mm}$ ,  $b = 75 \text{ mm}$ .

The nodal coordinates are:

| node | x | y    |
|------|---|------|
| 1    | 0 | -b/2 |
| 2    | a | 0    |
| 3    | 0 | b/2  |

In the sequel the distances are calculated in [mm], the force is given in [N]. Because of the kinematic constraints (built-in nodes) the vector of nodal displacements becomes:

$$\underline{u}_e^T = [0 \ 0 \ 0 \ w_2 \ \alpha_2 \ \beta_2 \ 0 \ 0 \ 0]. \quad (15.23)$$

For the calculation of stiffness matrix we need the constitutive matrix, which is:

$$\underline{\underline{C}} = \underline{\underline{C}}^{str} = \frac{E}{1-\nu^2} \begin{bmatrix} 1 & \nu & 0 \\ \nu & 1 & 0 \\ 0 & 0 & \frac{1-\nu}{2} \end{bmatrix} = \begin{bmatrix} 219,78 & 65,93 & 0 \\ 65,93 & 219,78 & 0 \\ 0 & 0 & 76,92 \end{bmatrix} \text{GPa}. \quad (15.24)$$

Utilizing the nodal coordinates we calculate matrix  $\underline{\underline{M}}$  based on Eq.(15.11):

$$\underline{\underline{M}} = \begin{bmatrix} 1 & 0 & -75 & 0 & 0 & 5625 & 0 & 0 & -421875 \\ 0 & 0 & 1 & 0 & 0 & -150 & 0 & 0 & 16875 \\ 0 & -1 & 0 & 0 & 75 & 0 & 0 & -5625 & 0 \\ 1 & 200 & 0 & 40000 & 0 & 0 & 8000000 & 0 & 0 \\ 0 & 0 & 1 & 0 & 200 & 0 & 0 & 40000 & 0 \\ 0 & -1 & 0 & -400 & 0 & 0 & -120000 & 0 & 0 \\ 1 & 0 & 75 & 0 & 0 & 5625 & 0 & 0 & 421875 \\ 0 & 0 & 1 & 0 & 0 & 150 & 0 & 0 & 16875 \\ 0 & -1 & 0 & 0 & -75 & 0 & 0 & -5625 & 0 \end{bmatrix}. \quad (15.25)$$

The determinant of matrix  $\underline{\underline{M}}$  is  $-4,86 \cdot 10^{12}$ , i.e. the matrix is not singular, its inverse exists. The stiffness matrix is obtained by calculating matrix  $\underline{\underline{R}}$  (see Eq.(15.14)) and computing the surface integrals:

$$\underline{\underline{K}}_e = (\underline{\underline{M}}^{-1})^T \int_{A_e}^t \left\{ \int_{-t/2}^{t/2} \underline{\underline{R}}^T \underline{\underline{C}}^{str T} \underline{\underline{R}} dz \right\} dA (\underline{\underline{M}}^{-1}) =$$

$$= \begin{bmatrix} 629,1 & 30559,9 & -15383,6 & -80,5 & 16472,0 & -7887,6 & -548,7 & 41301,7 & 7174,0 \\ . & 3731523,2 & 236741,0 & -7055,9 & -392240,8 & -304505,1 & -23503,9 & 715499,7 & -1343422,4 \\ . & . & 2433109,2 & 10731,5 & -772851,1 & 765510,5 & 4652,2 & -966573,2 & -1052328,6 \\ . & . & . & 257,6 & 4829,2 & 17170,3 & -177,1 & 9470,5 & 23609,2 \\ . & . & . & . & 1716949,1 & 69754,5 & -21301,1 & 1508270,3 & 1668927,7 \\ . & . & . & . & . & 1717032,9 & -9282,7 & 339382,2 & 951522,4 \\ . & . & . & . & . & . & 725,71 & -50772,2 & -30783,3 \\ . & . & . & . & . & . & . & 4681778,8 & 2521292,8 \\ . & . & . & . & . & . & . & . & 4822646,8 \end{bmatrix} \frac{\text{N}}{\text{mm}}, \quad (15.26)$$

In Eq.(15.26) only the independent components are indicated, the reason for that is the stiffness matrix is always symmetric. The force vector based on the concentrated loads is:

$$\underline{F}_{ec}^T = [F_{z1} \quad M_{x1} \quad M_{y1} \quad -F \quad 0 \quad 0 \quad F_{z3} \quad M_{x3} \quad M_{y3}]. \quad (15.27)$$

The condensed stiffness matrix and the resulting matrix equation for the calculation of nodal displacements is the following:

$$\begin{bmatrix} 257,6 & 4869,2 & 17170,3 \\ 4829,2 & 1716949,1 & 69754,5 \\ 17170,3 & 69754,5 & 1717033,0 \end{bmatrix} \begin{bmatrix} w_2 \\ \alpha_2 \\ \beta_2 \end{bmatrix} = \begin{bmatrix} -1000 \\ 0 \\ 0 \end{bmatrix}. \quad (15.28)$$

The nodal solutions are:

$$w_2 = -13,1764 \text{ mm}, \alpha_2 = 0,03176 \text{ rad}, \beta_2 = 0,130477 \text{ rad}. \quad (15.29)$$

It is seen that although the problem is symmetric with respect to axis  $x$  for both the geometry and load, the deformation of the triangle element is not symmetric. Taking the nodal displacements back to original equation we can determine the reactions:

$$F_{z1} = 554,5 \text{ N}, M_{x1} = 40784,5 \text{ Nmm}, M_{y1} = -66068,6 \text{ Nmm}. \quad (15.30)$$

Using Eq.(15.15) the vectors of strain and stress components are:

$$\underline{\varepsilon} = \begin{bmatrix} \varepsilon_x \\ \varepsilon_y \\ \gamma_{xy} \end{bmatrix} = \underline{\underline{R}} \underline{\underline{M}}^{-1} \underline{u}_e = \begin{bmatrix} 5,824 \cdot 10^{-4} z + 4,764 \cdot 10^{-7} zx - 1,5879 \cdot 10^{-6} zy \\ -1,5879 \cdot 10^{-6} zx \\ -7,9399 \cdot 10^{-7} z(4x + 4y) \end{bmatrix}, \quad (15.31)$$

$$\underline{\sigma} = \begin{bmatrix} \sigma_x \\ \sigma_y \\ \tau_{xy} \end{bmatrix} = \underline{\underline{C}}^{str} \underline{\varepsilon} = \begin{bmatrix} 128,0z + 2,0 \cdot 10^{-10} zx - 0,349 zy \\ 38,4z - 0,3176zx - 0,1047zy \\ -0,06107z(4x + 4y) \end{bmatrix}.$$

The strain and stress components can be obtained at any point of the triangle element by taking back the coordinates in [mm]. The example above was verified by a finite element

code developed in Matlab [3] and we obtained the same results. In general the accuracy of the Tocher plate element is not satisfactory and even the convergence of the results is bad. To reduce the deficiencies of the Tocher triangle the so-called reduced triangle element was developed, where area coordinates are introduced [4]. Apart from the Tocher triangular plate element there are several more element types, e.g.: Adini or Cowper triangle element, Adini-Clough-Melosh, Bogner-Fox-Schmit rectangle element, etc [1]. In the sequel we present some rectangle shape plate elements.

#### 15.4. Incompatible rectangular shape plate element

Fig.15.3 presents one of the first rectangle shape elements in a global, local and natural coordinate system.

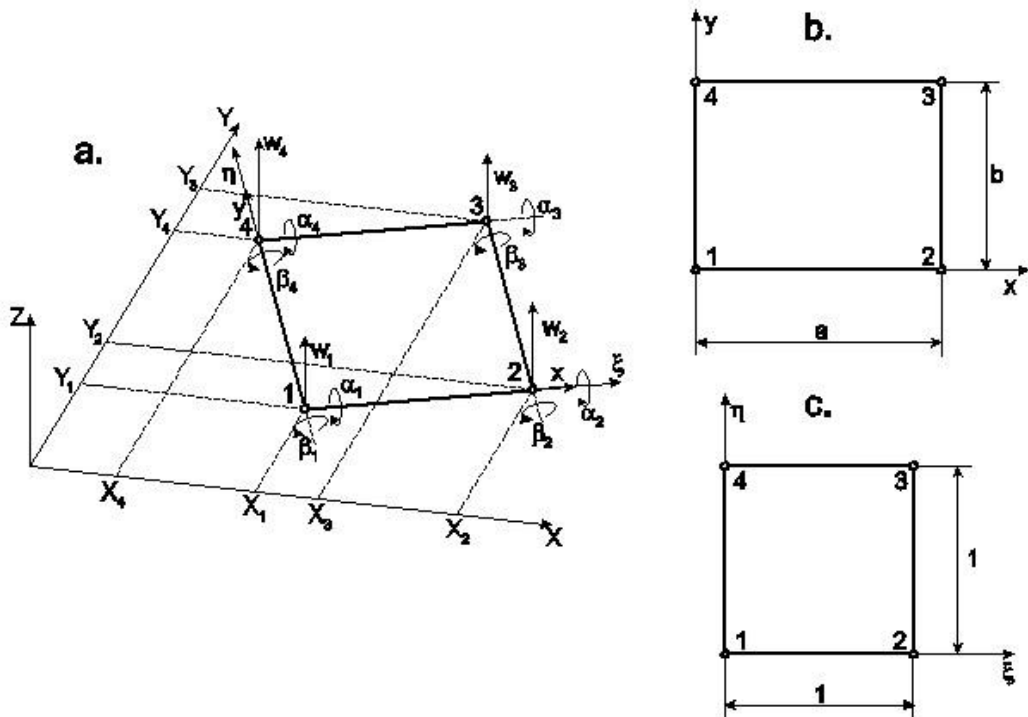


Fig.15.3. Incompatible rectangle shape plate element in a global (a), local (b) and natural (c) coordinate system.

The dimensionless local  $\xi$  and  $\eta$  coordinates are:

$$\xi = \frac{x}{a}, \quad \eta = \frac{y}{b}, \text{ and: } d\xi = \frac{1}{a} dx, \quad d\eta = \frac{1}{b} dy. \quad (15.32)$$

The following differential quotients are also required:

$$\frac{d}{dx} = \frac{1}{a} \frac{d}{d\xi}, \quad \frac{d}{dy} = \frac{1}{b} \frac{d}{d\eta}. \quad (15.33)$$

According to Fig.15.3b we consider three degrees of freedom in the local coordinate system at each node, which are the displacement  $w$  perpendicularly to the midplane of plate and the rotations about the  $x$  and  $y$  axes, respectively. The vector of nodal displacements for a single element is:

$$\underline{u}_e^T = [w_1 \quad \alpha_1 \quad \beta_1 \quad w_2 \quad \alpha_2 \quad \beta_2 \quad w_3 \quad \alpha_3 \quad \beta_3 \quad w_4 \quad \alpha_4 \quad \beta_4], \quad (15.34)$$

i.e. totally the element has 12 degrees of freedom, where the rotations can be determined by means of Eq.(15.1) and the Kirchhoff-Love hypothesis. The displacement in direction  $z$  and the rotations are not independent of each other and there can only be a maximum of 12 unknown parameters in the interpolation function. Along the element edges the expression of  $w$  should be a third order function, and accordingly the derivative in the normal direction should vary linearly [2]. A complete third order function contains 10 terms, but in accordance with the number of nodal parameters we need two additional terms in the interpolated function. We can choose from the three possibilities below:

$$\xi^3\eta \text{ and } \xi\eta^3, \text{ or: } \xi^3\eta^2 \text{ and } \xi^2\eta^3, \text{ or: } \xi^2\eta^2 \text{ and } \xi^3\eta^3. \quad (15.35)$$

Any of the above possibilities is chosen, we obtain a cubic change in the derivatives in the normal direction instead of the expected linear one [1,2]. Therefore this element is not compatible, in other words it is incompatible. Choosing the first alternative we have:

$$w(\xi, \eta) = a_0 + a_1\xi + a_2\eta + a_3\xi^2 + a_4\xi\eta + a_5\eta^2 + a_6\xi^3 + \\ + a_7\xi^2\eta + a_8\xi\eta^2 + a_9\eta^3 + a_{10}\xi^3\eta + a_{11}\xi\eta^3. \quad (15.36)$$

The nodal conditions for the determination of the unknown coefficients are:

$$w(0,0) = w_1, \frac{1}{b} \frac{\partial w}{\partial \eta}(0,0) = \alpha_1, -\frac{1}{a} \frac{\partial w}{\partial \xi}(0,0) = \beta_1, \quad (15.37)$$

$$w(1,0) = w_2, \frac{1}{b} \frac{\partial w}{\partial \eta}(1,0) = \alpha_2, -\frac{1}{a} \frac{\partial w}{\partial \xi}(1,0) = \beta_2,$$

$$w(1,1) = w_3, \frac{1}{b} \frac{\partial w}{\partial \eta}(1,1) = \alpha_3, -\frac{1}{a} \frac{\partial w}{\partial \xi}(1,1) = \beta_3,$$

$$w(0,1) = w_4, \frac{1}{b} \frac{\partial w}{\partial \eta}(0,1) = \alpha_4, -\frac{1}{a} \frac{\partial w}{\partial \xi}(0,1) = \beta_4.$$

Taking back the coefficients into the function given by Eq.(15.36), moreover by utilizing the fact that the displacement function can be formulated as the product of interpolation functions and nodal parameters it is possible to obtain:

$$w(\xi, \eta) = N_1 w_1 + N_2 \alpha_1 + N_3 \beta_1 + N_4 w_2 + N_5 \alpha_2 + N_6 \beta_2 + \\ + N_7 w_3 + N_8 \alpha_3 + N_9 \beta_3 + N_{10} w_4 + N_{11} \alpha_4 + N_{12} \beta_4, \quad (15.38)$$

from which we obtain the mathematical form of the interpolation functions:

$$N_1 = 2(\eta - 1)(\xi - 1) \left( \frac{1}{2}(1 + \xi + \eta) - \xi^2 - \eta^2 \right), \quad (15.39)$$

$$N_2 = -b\eta(\eta - 1)^2(\xi - 1),$$

$$N_3 = a\xi(\eta - 1)(\xi - 1)^2,$$

$$N_4 = 2(\eta - 1)\xi \left( \xi^2 + \eta^2 - \frac{3}{2}\xi - \frac{1}{2}\eta \right),$$

$$N_5 = b\xi\eta(\eta - 1)^2,$$

$$N_6 = a\xi^2(\eta - 1)(\xi - 1),$$

$$N_7 = 2\eta\xi \left( -\xi^2 - \eta^2 - \frac{1}{2} + \frac{3}{2}(\xi + \eta) \right),$$

$$N_8 = b\xi\eta^2(\eta - 1),$$

$$N_9 = -a\xi^2\eta(\xi - 1),$$

$$N_{10} = 2\eta(\xi - 1) \left( \xi^2 + \eta^2 - \frac{1}{2}\xi - \frac{3}{2}\eta \right),$$

$$N_{11} = -b\eta^2(\eta - 1)(\xi - 1),$$

$$N_{12} = -a\xi\eta(\xi - 1)^2,$$

and:

$$w(\xi, \eta) = \underline{N}^T \underline{u}_e, \quad (15.40)$$

where:

$$\underline{N}^T = [N_1 \ N_2 \ N_3 \ N_4 \ N_5 \ N_6 \ N_7 \ N_8 \ N_9 \ N_{10} \ N_{11} \ N_{12}], \quad (15.41)$$

is the vector of interpolation polynomials. As a next step we express the vector of strain components using Eq.(14.5):

$$\underline{\varepsilon} = \begin{bmatrix} \varepsilon_x \\ \varepsilon_y \\ \gamma_{xy} \end{bmatrix} = -z \begin{bmatrix} w_{,xx} \\ w_{,yy} \\ 2 \cdot w_{,xy} \end{bmatrix} = -z \underline{\kappa}, \quad (15.42)$$

where:

$$\underline{\kappa} = \begin{bmatrix} \underline{N}_{,xx}^T \\ \underline{N}_{,yy}^T \\ 2 \cdot \underline{N}_{,xy}^T \end{bmatrix} \underline{u}_e = \underline{\underline{C}} \underline{u}_e. \quad (15.43)$$

where  $\underline{N}_{,xx}$ ,  $\underline{N}_{,yy}$  and  $\underline{N}_{,xy}$  are vectors containing the second order derivatives of the interpolation functions by Eq.(15.40) with respect to the corresponding subscript. Hence, the vector of strain components and the vector of stress components become:

$$\underline{\varepsilon} = -z \underline{\underline{C}} \underline{u}_e, \quad (15.44)$$

$$\underline{\sigma} = \underline{\underline{C}}^{\text{str}} \underline{\varepsilon} = -z \underline{\underline{C}}^{\text{str}} \underline{\underline{C}} \underline{u}_e.$$

The vector of bending and twisting moments can be given in vector form; they are calculated based on Eqs.(14.7) and (15.43):

$$\underline{M} = \begin{bmatrix} M_x \\ M_y \\ M_{xy} \end{bmatrix} = -I_1 E_1 \begin{bmatrix} \underline{N}_{,xx}^T + \nu \underline{N}_{,yy}^T \\ \underline{N}_{,yy}^T + \nu \underline{N}_{,xx}^T \\ (1-\nu) \underline{N}_{,xy}^T \end{bmatrix} \underline{u}_e. \quad (15.45)$$

Taking the previously calculated vectors back into the total potential energy we obtain:

$$\Pi_e = \frac{1}{2} \int_{V_e} \underline{\sigma}^T \underline{\varepsilon} dV - \int_{A_{pe}} \underline{u}^T p dA = \frac{1}{2} \underline{u}_e^T \int_{V_e} z^2 \underline{\kappa}^T \underline{\underline{C}}^{\text{str}T} \underline{\kappa} dV \underline{u}_e - \int_{A_{pe}} p w(\xi, \eta) dA. \quad (15.46)$$

We transform the volume integral over the element by integration with respect to the parameters  $x$ ,  $y$  and  $z$ . Moreover, we assume that in the second term the intensity of the distributed load is constant. Consequently we can write:

$$\Pi_e = \frac{1}{2} \underline{u}_e^T \left\{ \int_0^1 \int_0^1 \frac{t^3}{12} ab \cdot \underline{\kappa}^T \underline{\underline{C}}^{\text{str}T} \underline{\kappa} d\eta d\xi \right\} \underline{u}_e - \underline{u}_e^T \int_0^1 \int_0^1 p \cdot ab \underline{N} d\eta d\xi = \frac{1}{2} \underline{u}_e^T \underline{\underline{K}}_e \underline{u}_e - \underline{u}_e^T \underline{\underline{F}}_{ep}, \quad (15.47)$$

where the element stiffness matrix is:

$$\underline{\underline{K}}_e = \int_0^1 \int_0^1 \frac{t^3}{12} ab \cdot \underline{\underline{\kappa}}^T \underline{\underline{C}}^{strT} \underline{\underline{\kappa}} d\eta d\xi, \quad (15.48)$$

and the force vector from the uniformly distributed load is:

$$\begin{aligned} \underline{F}_{ep} &= \int_0^1 \int_0^1 p \cdot ab \underline{N} d\eta d\xi = \\ &= \frac{pab}{4} \begin{bmatrix} 1 & \frac{b}{6} & -\frac{a}{6} & 1 & \frac{b}{6} & \frac{a}{6} & 1 & -\frac{b}{6} & \frac{a}{6} & 1 & -\frac{b}{6} & -\frac{a}{6} \end{bmatrix}^T, \end{aligned} \quad (15.49)$$

that is, similarly to the beam element subjected to bending the distributed load is represented by concentrated forces and moments at the nodes referring to the discretization procedure. It is also necessary to consider that there can be concentrated loads in the nodes, viz.:

$$\underline{F}_{ec}^T = [F_{z1} \ M_{x1} \ M_{y1} \ F_{z2} \ M_{x2} \ M_{y2} \ F_{z3} \ M_{x3} \ M_{y3} \ F_{z4} \ M_{x4} \ M_{y4}], \quad (15.50)$$

and:

$$\underline{F}_e = \underline{F}_{ec} + \underline{F}_{ep}. \quad (15.51)$$

The application of the minimum principle yields the element equilibrium equation:

$$\underline{\underline{K}}_e \underline{u}_e = \underline{F}_e, \quad (15.52)$$

which can be used only if the structure consists of a single element. For multi-element structures we obtain the structural equation by summing the potential energies of the elements:

$$\underline{\underline{K}} \underline{U} = \underline{F}. \quad (15.53)$$

Let us solve an example for the incompatible rectangle shape element!

## 15.5. Example for the application of the incompatible rectangle shape element

Calculate the nodal displacements and the reactions of the built-in plate shown in Fig.15.4!

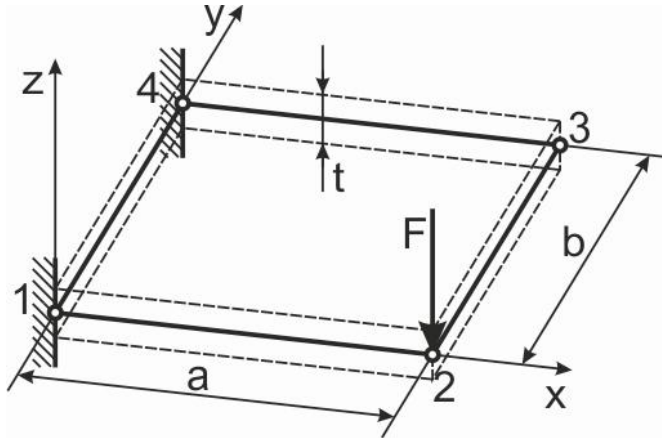


Fig.15.4. Example for the application of incompatible plate element.

Given:

$$E = 200 \text{ GPa}, \nu = 0.3, t = 1 \text{ mm}, F = 5 \text{ N}, a = 600 \text{ mm}, \quad b = 400 \text{ mm}.$$

In the sequel the distances are substituted in [m], the force is given in [N]. The nodal coordinates are:

| node | x | y |
|------|---|---|
| 1    | 0 | 0 |
| 2    | a | 0 |
| 3    | a | b |
| 4    | 0 | b |

Considering the kinematic constraints in the construction of the vector of nodal displacement we obtain:

$$\underline{u}_e^T = [0 \ 0 \ 0 \ w_2 \ \alpha_2 \ \beta_2 \ w_3 \ \alpha_3 \ \beta_3 \ 0 \ 0 \ 0]. \quad (15.54)$$

The force vector considering the external force and the reactions is:

$$\underline{F}_{ec}^T = [F_{z1} \ M_{x1} \ M_{y1} \ -F \ 0 \ 0 \ 0 \ 0 \ F_{z4} \ M_{x1} \ M_{y4}]. \quad (15.55)$$

For plane stress state the constitutive matrix is:

$$\underline{\underline{C}}^{str} = \frac{E}{1-\nu^2} \begin{bmatrix} 1 & \nu & 0 \\ \nu & 1 & 0 \\ 0 & 0 & \frac{1-\nu}{2} \end{bmatrix} = \begin{bmatrix} 200 & 60 & 0 \\ 60 & 200 & 0 \\ 0 & 0 & 70 \end{bmatrix} \text{ GPa.} \quad (15.56)$$

Next we calculate matrix  $\underline{\underline{\kappa}}$  which is required for the stiffness matrix:

$$\underline{\underline{K}}^T = \begin{bmatrix} -\frac{50}{3}(\eta-1)(2\xi-1) & -\frac{75}{2}(2\eta-1)(\xi-1) & -50(\xi^2 + \eta^2 - \xi - \eta + \frac{1}{6}) \\ 0 & -5(3\eta-2)(\xi-1) & -\frac{10}{3}(3\eta-1)(\eta-1) \\ \frac{10}{3}(\eta-1)(3\xi-2) & 0 & 5(3\xi-1)(\xi-1) \\ \frac{50}{3}(\eta-1)(2\xi-1) & \frac{75}{2}\xi(2\eta-1) & 50(\xi^2 + \eta^2 - \xi - \eta + \frac{1}{6}) \\ 0 & 5\xi(3\eta-2) & \frac{10}{3}(3\eta-1)(\eta-1) \\ \frac{10}{3}(\eta-1)(3\xi-1) & 0 & 5\xi(3\xi-2) \\ -\frac{50}{3}\eta(2\xi-1) & -\frac{75}{2}\xi(2\eta-1) & -50(\xi^2 + \eta^2 - \xi - \eta + \frac{1}{6}) \\ 0 & 5\xi(3\eta-2) & \frac{10}{3}\eta(3\eta-2) \\ -\frac{10}{3}\eta(3\xi-1) & 0 & -5\xi(3\xi-2) \\ \frac{50}{3}\eta(2\xi-1) & \frac{75}{2}(2\eta-1)(\xi-1) & 50(\xi^2 + \eta^2 - \xi - \eta + \frac{1}{6}) \\ 0 & -5(3\eta-1)(\xi-1) & -\frac{10}{3}\eta(3\eta-2) \\ -\frac{10}{3}\eta(3\xi-2) & 0 & -5(3\xi-1)(\xi-1) \end{bmatrix}. \quad (15.57)$$

The dimension of the stiffness matrix is 12x12; therefore it is not detailed here. Instead of the stiffness matrix we give the resulting finite element equilibrium equation system from Eq.(15.52):

$$11,27w_2 + 50,28\alpha_2 - 42,87\beta_2 - 196,45w_3 + 58,61\alpha_3 - 12,69\beta_3 = F_{z1}, \quad (15.58)$$

$$50,28w_2 + 14,59\alpha_2 - 58,61w_3 + 8,85\alpha_3 = M_{x1},$$

$$42,87w_2 + 6,24\beta_2 + 12,69w_3 + 4,87\beta_3 = M_{y1},$$

$$926,23w_2 + 137,22\alpha_2 + 55,37\beta_2 - 741,05w_3 + 128,89\alpha_3 + 0,19\beta_3 = -5,$$

$$137,22w_2 + 35,41\alpha_2 + 5,00\beta_2 - 128,89w_3 + 16,15\alpha_3 = 0,$$

$$55,37w_2 + 5,00\alpha_2 + 19,48\beta_2 + 0,19w_3 + 2,74\beta_3 = 0,$$

$$- 741,05w_2 - 128,89\alpha_2 + 0,19\beta_2 + 926,23w_3 - 137,22\alpha_3 + 55,37\beta_3 = 0,$$

$$128,89w_2 + 16,15\alpha_2 - 137,22w_3 + 35,41\alpha_3 - 5,0\beta_3 = 0,$$

$$0,19w_2 + 2,74\beta_2 + 55,37w_3 - 5,00\alpha_3 + 19,48\beta_3 = 0,$$

$$-196,45w_2 - 58,61\alpha_2 - 12,69\beta_2 + 11,27w_3 - 50,28\alpha_3 - 42,87\beta_3 = F_{z4},$$

$$58,61w_2 + 8,85\alpha_2 - 50,28w_3 + 14,59\alpha_3 = M_{x4},$$

$$12,69w_2 + 4,87\beta_2 + 42,87w_3 + 6,24\beta_3 = M_{y4}.$$

Calculating the nodal displacements from the 4<sup>th</sup>, 5<sup>th</sup>, 6<sup>th</sup>, 7<sup>th</sup>, 8<sup>th</sup> and 9<sup>th</sup> equations of Eq.(15.56) we have:

$$w_2 = -0,0655 \text{ m}, \alpha_2 = 0,039 \text{ rad}, \beta_2 = 0,159 \text{ rad}, \quad (15.59)$$

$$w_3 = -0,0448 \text{ m}, \alpha_3 = 0,0645 \text{ rad}, \beta_3 = 0,122 \text{ rad}.$$

From the 1<sup>st</sup>, 2<sup>nd</sup>, 3<sup>rd</sup> and 10<sup>th</sup>, 11<sup>th</sup>, 12<sup>th</sup> equations of Eq.(15.56) we can determine the reactions:

$$F_{1z} = 5,42 \text{ N}, M_{x1} = 0,47 \text{ Nm}, M_{y1} = -1,79 \text{ Nm}, \quad (15.60)$$

$$F_{z4} = -0,42 \text{ N}, M_{x4} = -0,30 \text{ Nm}, M_{y4} = -1,21 \text{ Nm}.$$

The bending and twisting moments can be obtained from Eq.(15.45), the stresses can be determined from Eq.(15.44) by taking back the nodal coordinates. Example 15.5 was verified by the finite element code ANSYS 12 and we obtained the same results.

## 15.6. Compatible rectangular shape plate element

In that case when we want to develop a compatible plate element the interpolation function given by Eq.(15.36) has to be modified in accordance with the followings [2]:

$$w(\xi, \eta) = a_0 + a_1\xi + a_2\eta + a_3\xi^2 + a_4\xi\eta + a_5\eta^2 + a_6\xi^3 + a_7\xi^2\eta + a_8\xi\eta^2 + a_9\eta^3 + a_{10}\xi^3\eta + a_{11}\xi\eta^3 + a_{12}\xi^2\eta^2 + a_{13}\xi^3\eta^2 + a_{14}\xi^2\eta^3 + a_{15}\xi^3\eta^3. \quad (15.61)$$

However, this formulation implies 16 unknown nodal parameters. That is, at each node we must consider the mixed derivative  $w_{,xy}$ . The vector of nodal displacement becomes:

$$\underline{u}_e^T = [w_1 \quad \alpha_1 \quad \beta_1 \quad w_{,xy1} \quad w_2 \quad \alpha_2 \quad \beta_2 \quad w_{,xy2} \quad w_3 \quad \alpha_3 \quad \beta_3 \quad w_{,xy3} \quad w_4 \quad \alpha_4 \quad \beta_4 \quad w_{,xy4}] \quad (15.62)$$

The conditions for the determination of the unknown parameters are:

$$w(0,0) = w_1, \frac{1}{b} \frac{\partial w}{\partial \eta}(0,0) = \alpha_1, -\frac{1}{a} \frac{\partial w}{\partial \xi}(0,0) = \beta_1, \frac{1}{ab} \frac{\partial^2 w}{\partial \xi \partial \eta}(0,0) = w_{,xy1}, \quad (15.63)$$

$$w(1,0) = w_2, \frac{1}{b} \frac{\partial w}{\partial \eta}(1,0) = \alpha_2, -\frac{1}{a} \frac{\partial w}{\partial \xi}(1,0) = \beta_2, \quad \frac{1}{ab} \frac{\partial^2 w}{\partial \xi \partial \eta}(1,0) = w_{,xy2},$$

$$w(1,1) = w_3, \frac{1}{b} \frac{\partial w}{\partial \eta}(1,1) = \alpha_3, -\frac{1}{a} \frac{\partial w}{\partial \xi}(1,1) = \beta_3, \quad \frac{1}{ab} \frac{\partial^2 w}{\partial \xi \partial \eta}(1,1) = w_{,xy3},$$

$$w(0,1) = w_4, \frac{1}{b} \frac{\partial w}{\partial \eta}(0,1) = \alpha_4, -\frac{1}{a} \frac{\partial w}{\partial \xi}(0,1) = \beta_4, \quad \frac{1}{ab} \frac{\partial^2 w}{\partial \xi \partial \eta}(0,1) = w_{,xy4}.$$

The deflection surface is approximated by using 16 interpolation functions:

$$\begin{aligned} w(\xi, \eta) = & N_1 w_1 + N_2 \alpha_1 + N_3 \beta_1 + N_4 w_{,xy1} + N_5 w_2 + N_6 \alpha_2 + N_7 \beta_2 + N_8 w_{,xy2} \\ & + N_9 w_3 + N_{10} \alpha_3 + N_{11} \beta_3 + N_{12} w_{,xy3} + N_{13} w_4 + N_{14} \alpha_4 + N_{15} \beta_4 + N_{16} w_{,xy4}. \end{aligned} \quad (15.64)$$

The interpolation functions can be written by the help of the Hermitian polynomials, which are presented in the beam finite elements (see Fig.15.5) [2]:

$$f_1(\lambda) = 2\lambda^3 - 3\lambda^2 + 1, f_2(\lambda) = -2\lambda^3 + 3\lambda^2, \quad (15.65)$$

$$f_3(\lambda) = \lambda^3 - 2\lambda^2 + \lambda, f_4(\lambda) = \lambda^3 - \lambda^2,$$

with that the 16 interpolation functions become:

$$N_1 = f_1(\xi) \cdot f_1(\eta), N_9 = f_2(\xi) \cdot f_2(\eta), \quad (15.66)$$

$$N_2 = b \cdot f_1(\xi) \cdot f_3(\eta), N_{10} = b \cdot f_2(\xi) \cdot f_4(\eta),$$

$$N_3 = -a \cdot f_3(\xi) \cdot f_1(\eta), N_{11} = -a \cdot f_4(\xi) \cdot f_2(\eta),$$

$$N_4 = a \cdot b \cdot f_3(\xi) \cdot f_3(\eta), N_{12} = a \cdot b \cdot f_4(\xi) \cdot f_4(\eta),$$

$$N_5 = f_2(\xi) \cdot f_1(\eta), N_{13} = f_1(\xi) \cdot f_2(\eta),$$

$$N_6 = b \cdot f_2(\xi) \cdot f_3(\eta), N_{14} = b \cdot f_1(\xi) \cdot f_4(\eta),$$

$$N_7 = -a \cdot f_4(\xi) \cdot f_1(\eta), N_{15} = -a \cdot f_3(\xi) \cdot f_2(\eta),$$

$$N_8 = a \cdot b \cdot f_4(\xi) \cdot f_3(\eta), N_{16} = a \cdot b \cdot f_3(\xi) \cdot f_4(\eta).$$

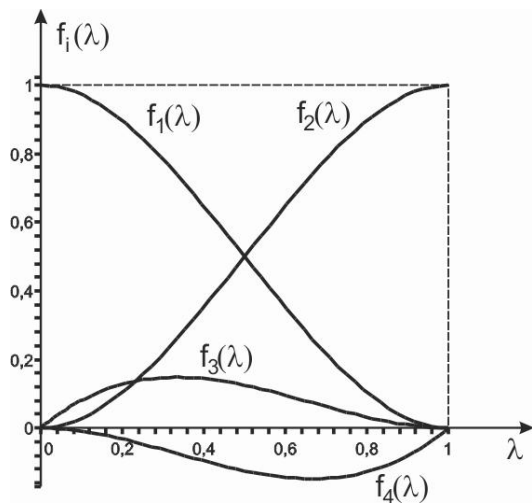


*Fig.15.5. Function plot of the Hermitian interpolation polynomials.*

By using the interpolation polynomials the stiffness matrix can be built-up by the same methodology as that presented in the incompatible plate element. The only difference is that we obtain a matrix with dimension of 16x16. Assuming a constant distributed force, the relevant term in the force vector is:

$$\underline{F}_{ep} = \int_0^1 \int_0^1 p \cdot ab \underline{N} d\eta d\xi = \\ = \frac{pab}{4} \left[ 1 \quad \frac{b}{6} \quad -\frac{a}{6} \quad \frac{ab}{36} \quad 1 \quad \frac{b}{6} \quad \frac{a}{6} \quad -\frac{ab}{36} \quad 1 \quad -\frac{b}{6} \quad \frac{a}{6} \quad \frac{ab}{36} \quad 1 \quad -\frac{b}{6} \quad -\frac{a}{6} \quad -\frac{ab}{36} \right]^T, \quad (15.67)$$

i.e., similarly to the plane beam element subjected to bending the distributed load is represented by concentrated forces and moments in the nodes. As usual, we have to consider the case of concentrated loads, the relevant vector term is:

$$\underline{F}_{ec}^T = \begin{bmatrix} F_{z1} & M_{x1} & M_{y1} & M_{xy1} & F_{z2} & M_{x2} & M_{y2} & M_{xy2} & \dots \\ \dots & F_{z3} & M_{x3} & M_{y3} & M_{xy3} & F_{z4} & M_{x4} & M_{y4} & M_{xy4} \end{bmatrix} \quad (15.68)$$

Example 15.5 was solved by using the compatible plate element too. In this case the nodal displacements are:

$$w_2 = -0,0658 \text{ m}, \alpha_2 = 0,062 \text{ rad}, \beta_2 = 0,165 \text{ rad}, w_{xy2} = 0,2414 \frac{\text{rad}}{\text{m}}, \quad (15.69)$$

$$w_3 = -0,0450 \text{ m}, \alpha_3 = 0,043 \text{ rad}, \beta_3 = 0,128 \text{ rad}, w_{xy2} = -0,0415 \frac{\text{rad}}{\text{m}}.$$

The reactions are given below:

$$F_{z1} = 5,512 \text{ N}, M_{x1} = 0,676 \text{ Nm}, M_{y1} = -1,84 \text{ Nm}, M_{xy1} = 0,138 \text{ Nm}^2. \quad (15.70)$$

$$F_{z4} = -0,512 \text{ N}, M_{x4} = -0,471 \text{ Nm}, M_{y4} = -1,155 \text{ Nm}, M_{xy4} = 0,115 \text{ Nm}^2.$$

It is seen, that the difference between the results of the two solutions is not significant.

### 15.7. Plates under in-plane and transverse load

If the plate is loaded by in-plane and transverse forces simultaneously, then we have to produce an element by having both in-plane and bending load-carrying capability, i.e. it means the superposition of plane membrane and plate bending elements. This problem can be solved based on sections 12 and 15 in a relatively simple way. First we collect the corresponding nodal displacements into a vector. Second, we create the stiffness matrix of the combined element by placing the stiffness matrix components corresponding to the membrane and bending deformation into the right positions. The vector of forces is obtained by a similar combination of the element vectors. This technique is suitable to model in-plane plate structures too. However, if we connect the elements by containing an angle differing from  $180^\circ$  among the surfaces, then it is possible to approximate curved surfaces. In other words the combined membrane-plate element is suitable to model spatial shells and shell structures too. Since in the modeling of plane and spatial shells similar steps are required, these issues will be detailed in section 16.

### 15.8. Bibliography

- [1] Singiresu S. Rao, *The finite element method in engineering – fourth edition*. Elsevier Science & Technology Books, 2004.
- [2] Imre Bojtár, Gábor Vörös, *Application of the finite element method to plate and shell structures*. Technical Book Publisher, 1986, Budapest (in Hungarian).
- [3] Ali Ozgul. *Edge Nodes of Triangular Kirchhoff Bending Thin Plate F.E.M. (Adini, Tocher, BCIZ)*, 31 Aug 2006 (Updated 15 Sep 2006).  
<http://www.mathworks.com/matlabcentral/fileexchange/12113-edge-nodes-of-triangular-kirchoff-bending-thin-plate-f-e-m-adinitocherbciz>
- [4] O.C. Zienkiewicz, R.L. Taylor, *The finite element method – fifth edition, Volume 1: The basis*. Butterworth-Heinemann, 2000, Oxford, Auckland, Boston, Johannesburg, Melbourne, New Delhi.

## 16. MODELING OF SPATIAL THIN-WALLED SHELLS BY FINITE ELEMENT METHOD-BASED SOFTWARE SYSTEMS

### 16.1. Simple flat shell elements

The stiffness matrix of flat shell elements are easily calculated using the stiffness matrices of the membrane and plate bending elements. Accordingly, it is possible to derive the different version of flat shell finite elements by combining the available triangle and rectangle shape elements [1,2]. The approximation of a curved surface by flat shell elements is shown by Fig.16.1. This kind of approximation is another source of error apart from the displacement field interpolation. By increasing the number of elements we can decrease the geometrical inaccuracies. The application of flat shell elements is justified, when the advantage of the higher order elements – namely the larger element size – can not be exploited. In the sequel we demonstrate the combination of the linear (membrane) triangle and the Tocher plate (bending) elements.

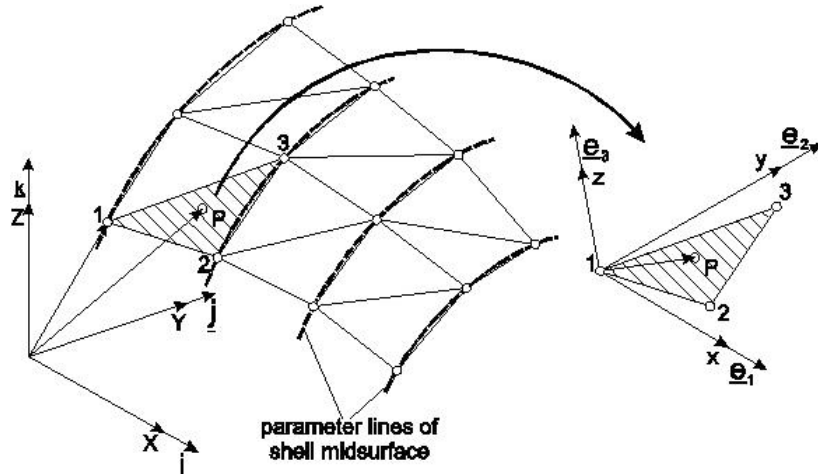


Fig.16.1. Triangular shape flat shell element in the global and local coordinate systems.

### 16.2. Superposition of the linear triangle and Tocher bending plate elements

The element mentioned above is not conform because of the discontinuity of displacements at the element boundaries [1,2]. However, due to its simplicity we use this combination to demonstrate the application of flat shell elements. The linear triangular membrane element (see Fig.12.2) has two degrees of freedom at each node, the stiffness matrix in the local element coordinate system is:

$$\tilde{\underline{\underline{K}}}^m_{\frac{6 \times 6}{6 \times 6}} = \begin{bmatrix} \left\{ \tilde{k}_{11}^m \right\} & \left\{ \tilde{k}_{12}^m \right\} & \left\{ \tilde{k}_{13}^m \right\} \\ \left\{ 2 \times 2 \right\} & \left\{ 2 \times 2 \right\} & \left\{ 2 \times 2 \right\} \\ \left\{ \tilde{k}_{21}^m \right\} & \left\{ \tilde{k}_{22}^m \right\} & \left\{ \tilde{k}_{23}^m \right\} \\ \left\{ 2 \times 2 \right\} & \left\{ 2 \times 2 \right\} & \left\{ 2 \times 2 \right\} \\ \left\{ \tilde{k}_{31}^m \right\} & \left\{ \tilde{k}_{32}^m \right\} & \left\{ \tilde{k}_{33}^m \right\} \\ \left\{ 2 \times 2 \right\} & \left\{ 2 \times 2 \right\} & \left\{ 2 \times 2 \right\} \end{bmatrix}, \quad (16.1)$$

where the submatrices ( $\tilde{k}_{ij}^m$ ) correspond to the stiffness matrix components associated with nodes  $i$  and  $j$ . The tilde over the matrix indicates the local coordinate system; the superscript ( $m$ ) refers to the membrane action. The finite element equation is:

$$\tilde{\underline{\underline{K}}}^m_{\frac{6 \times 6}{6 \times 1}} \tilde{\underline{u}}^m_{e \frac{6 \times 1}{6 \times 1}} = \tilde{\underline{F}}^m_{e \frac{6 \times 1}{6 \times 1}}, \quad (16.2)$$

where the vector of nodal displacements and concentrated forces of the membrane element are:

$$\tilde{\underline{u}}^m_{e \frac{6 \times 1}{6 \times 1}} = [\tilde{u}_1 \quad \tilde{v}_1 \quad \tilde{u}_2 \quad \tilde{v}_2 \quad \tilde{u}_3 \quad \tilde{v}_3]^T, \quad (16.3)$$

$$\tilde{\underline{F}}^m_{e \frac{6 \times 1}{6 \times 1}} = [F_{x1} \quad F_{y1} \quad F_{x2} \quad F_{y2} \quad F_{x3} \quad F_{y3}]^T,$$

where  $u$  is the displacement in the local  $x$ ,  $v$  is the displacement in the local  $y$  direction. In the displacement vector we refer to the local parameters by using the tilde. In the force vector we identify the local parameters by lowercase  $x$ ,  $y$  and  $z$  in the subscript of components. A distinction like that was not necessary until now, which can be explained by the fact that in all of the previous examples the local and global coordinate systems coincided.

At each node of the Tocher triangular plate element (see Fig.15.1) there are three degrees of freedom; therefore the stiffness matrix has nine rows and nine columns:

$$\tilde{\underline{\underline{K}}}^b_{\frac{6 \times 6}{6 \times 6}} = \begin{bmatrix} \left\{ \tilde{k}_{11}^b \right\} & \left\{ \tilde{k}_{12}^b \right\} & \left\{ \tilde{k}_{13}^b \right\} \\ \left\{ 3 \times 3 \right\} & \left\{ 3 \times 3 \right\} & \left\{ 3 \times 3 \right\} \\ \left\{ \tilde{k}_{21}^b \right\} & \left\{ \tilde{k}_{22}^b \right\} & \left\{ \tilde{k}_{23}^b \right\} \\ \left\{ 3 \times 3 \right\} & \left\{ 3 \times 3 \right\} & \left\{ 3 \times 3 \right\} \\ \left\{ \tilde{k}_{31}^b \right\} & \left\{ \tilde{k}_{32}^b \right\} & \left\{ \tilde{k}_{33}^b \right\} \\ \left\{ 3 \times 3 \right\} & \left\{ 3 \times 3 \right\} & \left\{ 3 \times 3 \right\} \end{bmatrix}, \quad (16.4)$$

where the superscript  $b$  indicates bending action. In the local coordinate system the displacement and concentrated force vectors of the Tocher triangular plate element are:

$$\tilde{\underline{u}}_e^{h^T} = \begin{bmatrix} \tilde{w}_1 & \tilde{\alpha}_1 & \tilde{\beta}_1 & \tilde{w}_2 & \tilde{\alpha}_2 & \tilde{\beta}_2 & \tilde{w}_3 & \tilde{\alpha}_3 & \tilde{\beta}_3 \end{bmatrix}_{9 \times 1}, \quad (16.5)$$

$$\tilde{\underline{F}}_{ec}^{h^T} = \begin{bmatrix} F_{z1} & M_{x1} & M_{y1} & F_{z2} & M_{x2} & M_{y2} & F_{z3} & M_{x3} & M_{y3} \end{bmatrix}_{9 \times 1}.$$

The degrees of freedom of the combined element are shown by Fig.16.2. The membrane and bending stiffness matrices have to be combined in accordance with the following observations [2]:

- a. for small displacement  $s$  the membrane and bending stiffnesses are uncoupled (independent),
- b. the in-plane rotation  $\psi$  in the local  $x$ - $y$  plane is not necessary for a single element, however,  $\psi$  and its conjugate moment  $M_z$  have to be considered in the analysis by including the appropriate number of zeros to obtain the element stiffness matrix for the purpose of assembling several elements or assembling the flat shell element with different type of elements.

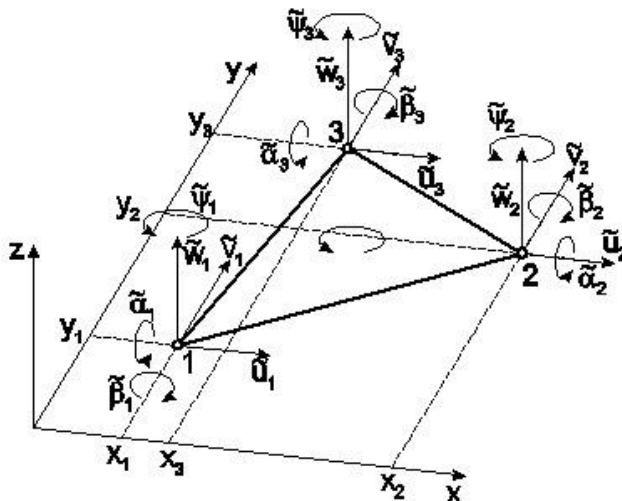


Fig.16.2. Combination of the linear membrane triangle element and the Tocher triangular plate bending element.

The nodal displacement vector of the combined element in the local coordinate system is:

$$\tilde{\underline{u}}_e^{m+b^T} = \begin{bmatrix} \tilde{u}_1 & \tilde{v}_1 & \tilde{w}_1 & \tilde{\alpha}_1 & \tilde{\beta}_1 & \tilde{\psi}_1 & \tilde{u}_2 & \tilde{v}_2 & \tilde{w}_2 & \dots \\ \dots & \dots \\ \tilde{\alpha}_2 & \tilde{\beta}_2 & \tilde{\psi}_2 & \tilde{u}_3 & \tilde{v}_3 & \tilde{w}_3 & \tilde{\alpha}_3 & \tilde{\beta}_3 & \tilde{\psi}_3 & \end{bmatrix}_{18 \times 1} \quad (16.6)$$

The vector of concentrated forces becomes:

$$\tilde{\underline{F}}_{ec}^{m+b^T} = \begin{bmatrix} F_{x1} & F_{y1} & F_{z1} & M_{x1} & M_{y1} & M_{z1} & F_{x2} & F_{y2} & F_{z2} & \dots \\ \dots & \dots \\ M_{x2} & M_{y2} & M_{z2} & F_{x3} & F_{y3} & F_{z3} & M_{x3} & M_{y3} & M_{z3} & \end{bmatrix}_{18 \times 1} \quad (16.7)$$

Accordingly, the stiffness matrix is shown below [1,2]:

$$\underline{\underline{K}}_e^{m+b} = \begin{bmatrix} \left\{ \begin{array}{c} \tilde{k}_{11}^m \\ 2 \times 2 \end{array} \right\} & \begin{array}{|c|c|c|c|} \hline 0 & 0 & 0 & 0 \\ 0 & 0 & 0 & 0 \\ \hline \end{array} & \left\{ \begin{array}{c} \tilde{k}_{12}^m \\ 2 \times 2 \end{array} \right\} & \begin{array}{|c|c|c|c|} \hline 0 & 0 & 0 & 0 \\ 0 & 0 & 0 & 0 \\ \hline \end{array} & \left\{ \begin{array}{c} \tilde{k}_{13}^m \\ 2 \times 2 \end{array} \right\} & \begin{array}{|c|c|c|c|} \hline 0 & 0 & 0 & 0 \\ 0 & 0 & 0 & 0 \\ \hline \end{array} \\ \hline 0 & 0 & \left\{ \begin{array}{c} \tilde{k}_{11}^b \\ 3 \times 3 \end{array} \right\} & \begin{array}{|c|c|c|c|} \hline 0 & 0 & 0 & 0 \\ 0 & 0 & 0 & 0 \\ 0 & 0 & 0 & 0 \\ \hline \end{array} & \left\{ \begin{array}{c} \tilde{k}_{12}^b \\ 3 \times 3 \end{array} \right\} & \begin{array}{|c|c|c|c|} \hline 0 & 0 & 0 & 0 \\ 0 & 0 & 0 & 0 \\ 0 & 0 & 0 & 0 \\ \hline \end{array} & \left\{ \begin{array}{c} \tilde{k}_{13}^b \\ 3 \times 3 \end{array} \right\} & \begin{array}{|c|c|c|c|} \hline 0 & 0 & 0 & 0 \\ 0 & 0 & 0 & 0 \\ 0 & 0 & 0 & 0 \\ \hline \end{array} \\ \hline 0 & 0 & 0 & 0 & 0 & 0 & 0 & 0 & 0 \\ \hline \left\{ \begin{array}{c} \tilde{k}_{21}^m \\ 2 \times 2 \end{array} \right\} & \begin{array}{|c|c|c|c|} \hline 0 & 0 & 0 & 0 \\ 0 & 0 & 0 & 0 \\ \hline \end{array} & \left\{ \begin{array}{c} \tilde{k}_{22}^m \\ 2 \times 2 \end{array} \right\} & \begin{array}{|c|c|c|c|} \hline 0 & 0 & 0 & 0 \\ 0 & 0 & 0 & 0 \\ \hline \end{array} & \left\{ \begin{array}{c} \tilde{k}_{23}^m \\ 2 \times 2 \end{array} \right\} & \begin{array}{|c|c|c|c|} \hline 0 & 0 & 0 & 0 \\ 0 & 0 & 0 & 0 \\ \hline \end{array} \\ \hline 0 & 0 & \left\{ \begin{array}{c} \tilde{k}_{21}^b \\ 3 \times 3 \end{array} \right\} & \begin{array}{|c|c|c|c|} \hline 0 & 0 & 0 & 0 \\ 0 & 0 & 0 & 0 \\ 0 & 0 & 0 & 0 \\ \hline \end{array} & \left\{ \begin{array}{c} \tilde{k}_{22}^b \\ 3 \times 3 \end{array} \right\} & \begin{array}{|c|c|c|c|} \hline 0 & 0 & 0 & 0 \\ 0 & 0 & 0 & 0 \\ 0 & 0 & 0 & 0 \\ \hline \end{array} & \left\{ \begin{array}{c} \tilde{k}_{23}^b \\ 3 \times 3 \end{array} \right\} & \begin{array}{|c|c|c|c|} \hline 0 & 0 & 0 & 0 \\ 0 & 0 & 0 & 0 \\ 0 & 0 & 0 & 0 \\ \hline \end{array} \\ \hline 0 & 0 & 0 & 0 & 0 & 0 & 0 & 0 & 0 \\ \hline \left\{ \begin{array}{c} \tilde{k}_{31}^m \\ 2 \times 2 \end{array} \right\} & \begin{array}{|c|c|c|c|} \hline 0 & 0 & 0 & 0 \\ 0 & 0 & 0 & 0 \\ \hline \end{array} & \left\{ \begin{array}{c} \tilde{k}_{32}^m \\ 2 \times 2 \end{array} \right\} & \begin{array}{|c|c|c|c|} \hline 0 & 0 & 0 & 0 \\ 0 & 0 & 0 & 0 \\ \hline \end{array} & \left\{ \begin{array}{c} \tilde{k}_{33}^m \\ 2 \times 2 \end{array} \right\} & \begin{array}{|c|c|c|c|} \hline 0 & 0 & 0 & 0 \\ 0 & 0 & 0 & 0 \\ \hline \end{array} \\ \hline 0 & 0 & \left\{ \begin{array}{c} \tilde{k}_{31}^b \\ 3 \times 3 \end{array} \right\} & \begin{array}{|c|c|c|c|} \hline 0 & 0 & 0 & 0 \\ 0 & 0 & 0 & 0 \\ 0 & 0 & 0 & 0 \\ \hline \end{array} & \left\{ \begin{array}{c} \tilde{k}_{32}^b \\ 3 \times 3 \end{array} \right\} & \begin{array}{|c|c|c|c|} \hline 0 & 0 & 0 & 0 \\ 0 & 0 & 0 & 0 \\ 0 & 0 & 0 & 0 \\ \hline \end{array} & \left\{ \begin{array}{c} \tilde{k}_{33}^b \\ 3 \times 3 \end{array} \right\} & \begin{array}{|c|c|c|c|} \hline 0 & 0 & 0 & 0 \\ 0 & 0 & 0 & 0 \\ 0 & 0 & 0 & 0 \\ \hline \end{array} \\ \hline 0 & 0 & 0 & 0 & 0 & 0 & 0 & 0 & 0 \\ \hline \end{bmatrix} \quad (16.8)$$

The stiffness matrix above is valid in the local coordinate system. We highlight again, that the tilde over the matrices and vectors refers to the local system. In the analysis of three-dimensional structures in which different finite elements have different orientations, it is necessary to transform the local stiffness matrices to a common set of global coordinates. In the quantities of global coordinate system there is no tilde indicated. The transformation of the element stiffness matrix is given by the expression below:

$$\underline{\underline{K}}_e^{m+b} = \underline{\lambda}^T \underline{\underline{K}}_e^{m+b} \underline{\lambda}, \quad (16.9)$$

where  $\underline{\lambda}$  is the transformation matrix with dimension of 18 x 18:

$$\underline{\underline{\lambda}} = \begin{bmatrix} \underline{\underline{L}} & \underline{\underline{0}} & \underline{\underline{0}} \\ \underline{\underline{0}} & \underline{\underline{L}} & \underline{\underline{0}} \\ \underline{\underline{0}} & \underline{\underline{0}} & \underline{\underline{L}} \end{bmatrix}, \quad (16.10)$$

and:

$$\underline{\underline{0}} = \begin{bmatrix} 0 & 0 & 0 \\ 0 & 0 & 0 \\ 0 & 0 & 0 \end{bmatrix}. \quad (16.11)$$

Matrix  $\underline{\underline{L}}$  contains the unit basis vectors of the local coordinate system,  $e_1$ ,  $e_2$  and  $e_3$ , (see Fig.16.1) in the form of column vectors formulated in the global coordinate system:

$$\underline{\underline{L}} = \begin{bmatrix} e_{1X} & e_{2X} & e_{3X} \\ e_{1Y} & e_{2Y} & e_{3Y} \\ e_{1Z} & e_{2Z} & e_{3Z} \end{bmatrix}. \quad (16.12)$$

Eventually matrix  $\underline{\underline{L}}$  contains the direction cosines of the angles between the local and global axes. The definition of the direction cosines for an optional  $\underline{A}$  vector based on Fig.16.3 is [4]:

$$l = \cos \alpha = \frac{A_x}{\sqrt{A_x^2 + A_y^2 + A_z^2}}, \quad (16.13)$$

$$m = \cos \beta = \frac{A_y}{\sqrt{A_x^2 + A_y^2 + A_z^2}},$$

$$n = \cos \gamma = \frac{A_z}{\sqrt{A_x^2 + A_y^2 + A_z^2}}.$$

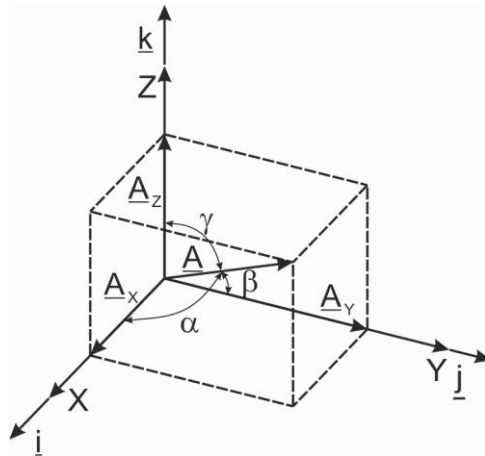


Fig.16.3. Direction cosines of vector  $\underline{A}$ .

Since the basis vectors  $\underline{e}_1$ ,  $\underline{e}_2$  and  $\underline{e}_3$  are unit vectors it is not easy to see, that their components are eventually the direction cosines. To construct the structural stiffness matrix the local quantities have to be transformed into the global system. The vector of nodal displacement and vector of forces in the global system are:

$$\underline{u}_e^{m+b} = \underline{\underline{\lambda}}^T \tilde{\underline{u}}_e^{m+b}, \quad (16.14)$$

$$\underline{F}_e^{m+b} = \underline{\underline{\lambda}}^T \tilde{\underline{F}}_e^{m+b}.$$

For shell structures the most common load type is the constant pressure perpendicularly to the shell surface, i.e. in direction of the local  $z$  axis. It is a reasonable assumption, that there is membrane stress state, under these assumptions the force vector is: [2]:

$$\tilde{\underline{F}}_{ep}^{m+b} = p \frac{A_e}{3} [0 \ 0 \ 1 \ 0 \ 0 \ 0 \ 0 \ 1 \ 0 \ 0 \ 0 \ 1 \ 0 \ 0 \ 0], \quad (16.15)$$

where  $A_e$  is the triangular area. If the pressure on the shell surface is not constant, but its change over the element area is insignificant, then we can still use the vector above, but we use the pressure averaged by the nodal loads instead of  $p$ :

$$p = \frac{1}{3}(p_1 + p_2 + p_3). \quad (16.16)$$

Finally we summarize the finite element equations. In the local  $x, y, z$  system the quantities indicated by the tilde are used, i.e.:

$$\tilde{\underline{\underline{K}}}_e^{m+b} \tilde{\underline{u}}_e^{m+b} = \tilde{\underline{F}}_e^{m+b}. \quad (16.17)$$

Transforming Eq.(16.17) into the global  $X, Y, Z$  system by using the transformation matrix, we have:

$$\underline{\underline{K}}_e^{m+b} \underline{u}_e^{m+b} = \underline{\underline{F}}_e^{m+b}, \quad (16.18)$$

where the quantities in the global coordinate system are calculated based on Eqs.(16.9) and (16.14). For the whole structure the finite element equation is:

$$\underline{\underline{K}}^{m+b} \underline{U}^{m+b} = \underline{\underline{F}}^{m+b}, \quad (16.19)$$

of which solutions are the components of vector  $\underline{U}^{m+b}$ , which are the nodal displacements in the global coordinate system. From that we can calculate the global element displacement vectors,  $\underline{u}_e^{m+b}$ , and then we can transform them into the local system by the following expression:

$$\tilde{\underline{u}}_e^{m+b} = \underline{\underline{\lambda}}^{T^{-1}} \underline{u}_e^{m+b}. \quad (16.20)$$

The transformation matrix is orthogonal, therefore we can write that:  $\underline{\underline{\lambda}}^{-1} = \underline{\underline{\lambda}}^T$  and  $\underline{\underline{\lambda}}^{T^{-1}} \underline{\underline{\lambda}}^T = \underline{\underline{E}}$ , viz.:

$$\tilde{\underline{u}}_e^{m+b} = \underline{\underline{\lambda}} \underline{u}_e^{m+b}. \quad (16.21)$$

Using the local displacements in the nodes we can calculate the membrane and bending stresses.

A significant advantage of the flat shell elements is a novel software can be easily constructed by combining the softwares of the existing membrane and plate elements, which can be used for engineering calculations [2,3]. This computation requires only the knowledge of matrix  $\underline{\underline{L}}$ . The accuracy of the results depends on the element size. Higher mesh resolution is necessary, where the curvature of the surface is larger, or the change in stresses is expected to be more significant. The expected error of the calculation is higher in the vicinity of the sides, notches and the connection of different surfaces. Let us solve an example to understand the application of the method!

### 16.3. Example for the combination of the linear triangle and Tocher triangle elements

Solve the shell problem given in Fig.16.4! Calculate the nodal displacements, reactions in the local coordinate system, and transform the results into the global coordinate system!

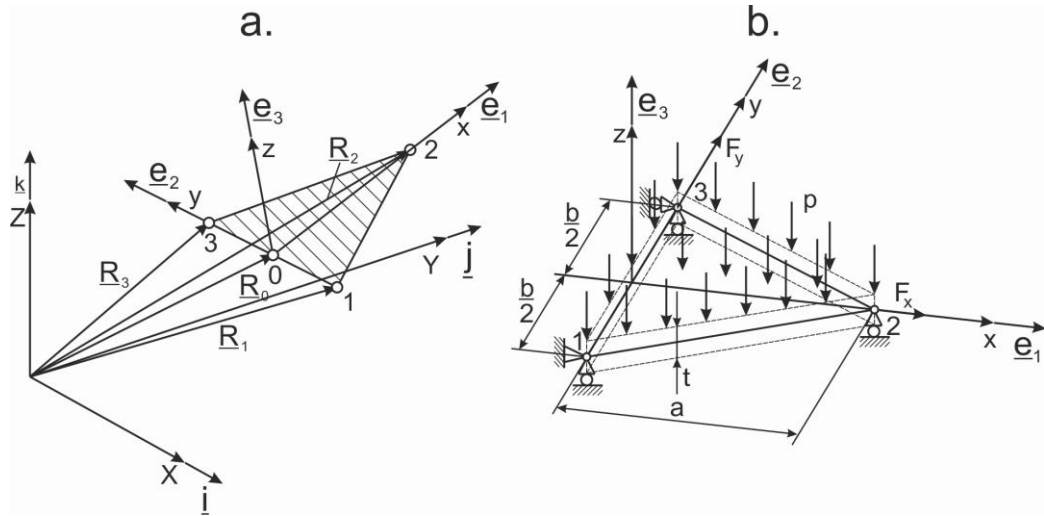


Fig.16.4. Flat triangular shell element in the local and global coordinate systems (a), application example for the flat shell element (b).

Given:

$$a = 0,8 \text{ m}, b = 0,5 \text{ m}, t = 3 \text{ mm}, E = 200 \text{ GPa}, \nu = 0,3, F_x = 6000 \text{ kN}, F_y = 8000 \text{ kN}, p = 1200 \text{ N/m}^2$$

The distances are substituted in [m], the force is interpreted in [N]. The nodal coordinates in the local coordinate system are:

| node | x | y    | z |
|------|---|------|---|
| 1    | 0 | -b/2 | 0 |
| 2    | a | 0    | 0 |
| 3    | 0 | b/2  | 0 |

We give the nodal coordinates also in the global coordinate system. We note that the global coordinates depend on how the element is built-in the actual structure.

| node | X [m]  | Y [m] | Z [m] |
|------|--------|-------|-------|
| 1    | 0,6795 | 0,57  | 0,2   |
| 2    | 0,4    | 1,225 | 0,5   |
| 3    | 0,5004 | 0,6   | 0,4   |

The vectors of nodal displacements and concentrated forces in the local coordinate system are:

$$\tilde{\underline{u}}_e^{m+b}{}^T = \begin{bmatrix} 0 & 0 & 0 & \tilde{\alpha}_1 & \tilde{\beta}_2 & \tilde{\psi}_1 & \tilde{u}_2 & \tilde{v}_2 & 0 & \tilde{\alpha}_2 & \tilde{\beta}_2 & \tilde{\psi}_2 & 0 & \tilde{v}_3 & 0 & \tilde{\alpha}_3 & \tilde{\beta}_3 & \tilde{\psi}_3 \end{bmatrix}_{18 \times 1}, \quad (16.22)$$

$$\tilde{\underline{F}}_{ec}^{m+b}{}^T = \begin{bmatrix} F_{x1} & F_{y1} & F_{z1} & 0 & 0 & 0 & F_x & 0 & 0 & 0 & 0 & F_{x3} & F_y & F_{z3} & 0 & 0 & 0 \end{bmatrix}_{18 \times 1}.$$

The terms in. the force vector related to the distributed load can be calculated based on the integral transformation formulae presented in section 15. We can construct the force vector of the Tocher triangle from distributed load by formulating the work of the distributed load:

$$W_e = \int_{A_{pe}} pw(x, y)dA = \tilde{\underline{u}}_e^T \tilde{\underline{F}}_{ep}. \quad (16.23)$$

Based on Eq.(16.23) and the integral transformation expressions given by Eq.(15.20) we have:

$$\tilde{\underline{F}}_{ep}^b = p \begin{bmatrix} 7/40ba - 1/80b^2 \\ 1/120ab^2 - 1/40ba^2 \\ 1/30ab^3 - 1/480b^3 \\ 3/20ba \\ 1/30ba^2 \\ -1/120b^3 \\ 7/40ba + 1/80b^2 \\ -1/120ab^2 - 1/40ba^2 \\ -1/30ab^2 - 1/480b^3 \end{bmatrix}_{9 \times 1} = p \begin{bmatrix} 0,0669 \\ -0,0063 \\ 0,0064 \\ 0,060 \\ 0,0107 \\ -0,0010 \\ 0,0731 \\ -0,0097 \\ -0,0069 \end{bmatrix}. \quad (16.24)$$

We note that in the Tocher triangle the distributed load is divided into three parts and put into the nodes; however the division is made in unequal degree, as it is seen in the vector of forces. On the other hand, by summing the forces in direction  $z$  and the moments about  $x$  and  $y$  we obtain:

$$\left[ \begin{bmatrix} \tilde{\underline{F}}_{ep}^b \end{bmatrix}_1 + \begin{bmatrix} \tilde{\underline{F}}_{ep}^b \end{bmatrix}_4 + \begin{bmatrix} \tilde{\underline{F}}_{ep}^b \end{bmatrix}_7 \right] = pA_e = \frac{1}{2}pab, \quad (16.25)$$

$$\left[ \begin{bmatrix} \tilde{\underline{F}}_{ep}^b \end{bmatrix}_2 + \begin{bmatrix} \tilde{\underline{F}}_{ep}^b \end{bmatrix}_5 + \begin{bmatrix} \tilde{\underline{F}}_{ep}^b \end{bmatrix}_8 \right] = -\frac{pa}{30}A_e = -\frac{pa^2b}{15},$$

$$\left[ \begin{bmatrix} \tilde{\underline{F}}_{ep}^b \end{bmatrix}_3 + \begin{bmatrix} \tilde{\underline{F}}_{ep}^b \end{bmatrix}_6 + \begin{bmatrix} \tilde{\underline{F}}_{ep}^b \end{bmatrix}_9 \right] = -\frac{pb^2}{40a}A_e = -\frac{pab^2}{20},$$

which are the resultant forces in direction  $z$  and the resultant moments about axes  $x$  and  $y$ . The force vector of the 18 degrees of freedom flat shell element in the local coordinate system is:

$$\tilde{F}_{e_{18 \times 1}}^{m+b^T} = \tilde{F}_{e_{18 \times 1}}^{m+b^T} + \tilde{F}_{e_{18 \times 1}}^{m+b^T} = \begin{bmatrix} F_{x1} \\ F_{y1} \\ F_{z1} \\ 0 \\ 0 \\ 0 \\ F_x \\ 0 \\ 0 \\ F_{z2} \\ -p \\ 0 \\ 0 \\ 0 \\ 0 \\ F_{x3} \\ F_y \\ F_{z3} \\ 0 \\ 0 \\ 0 \end{bmatrix} = \begin{bmatrix} 0 \\ 0 \\ 0,0069 \\ -0,0063 \\ 0,0064 \\ 0 \\ 0 \\ 0 \\ 0 \\ 0,0600 \\ 0,0107 \\ -0,0010 \\ 0 \\ 0 \\ 0 \\ 0 \\ 0 \\ 0,0731 \\ -0,0097 \\ -0,0069 \\ 0 \end{bmatrix} = \begin{bmatrix} F_{x1} \\ F_{y1} \\ F_{z1} - 80,25 \\ 7,6 \\ -7,6875 \\ 0 \\ 6000000 \\ 0 \\ 0 \\ F_{z2} - 72,0 \\ -12,8 \\ 1,25 \\ 0 \\ F_{x3} \\ 8000000 \\ F_{z3} - 87,75 \\ 11,6 \\ 8,3125 \\ 0 \end{bmatrix}. \quad (16.26)$$

The stiffness matrix of the linear (membrane) triangle element based on the calculations of section 15 is:

$$\tilde{K}_e^m = \begin{bmatrix} 2,48 & 1,44 & -1,26 & -1,15 & -1,22 & -0,29 \\ . & 6,64 & -1,73 & -0,36 & 0,29 & -6,28 \\ . & . & 2,52 & 0 & -1,26 & 1,73 \\ . & . & . & 0,72 & 1,15 & -0,36 \\ . & . & . & . & 2,48 & -1,44 \\ . & . & . & . & . & 6,64 \end{bmatrix} \cdot 10^8 \frac{\text{N}}{\text{m}}, \quad (16.27)$$

where due to symmetry of the matrix only the independent components are indicated. The stiffness matrix of the Tocher triangular element in the local coordinate system is:

$$\tilde{K}_e^b = \begin{bmatrix} 12,90 & 2,28 & -0,91 & -0,99 & 0,88 & -3,88 & -11,90 & 3,05 & 0,51 \\ . & 0,96 & 0,10 & -0,33 & -0,09 & -0,05 & -1,95 & 0,19 & -0,32 \\ . & . & 0,59 & 0,53 & -0,17 & 0,16 & 0,38 & -0,26 & -0,32 \\ . & . & . & 2,90 & 0,15 & 0,77 & -1,90 & 0,40 & 1,01 \\ . & . & . & . & 0,29 & -0,0007 & -1,03 & 0,28 & 0,29 \\ . & . & . & . & . & 0,31 & -0,38 & 0,05 & 0,15 \\ . & . & . & . & . & . & 13,80 & -3,45 & -1,52 \\ . & . & . & . & . & . & . & 1,15 & 0,53 \\ . & . & . & . & . & . & . & . & 0,97 \end{bmatrix} \cdot 10^3. \quad (16.28)$$

The combination of the membrane and bending stiffness matrices based on Eq.(16.8) lead s to:

$$\tilde{K}_e^{m+b} =$$

| 2,48  | 1,44 |                 |       |       |              | -1,26             | -1,   |       |              |       |  |
|-------|------|-----------------|-------|-------|--------------|-------------------|-------|-------|--------------|-------|--|
| 1,44  | 6,64 |                 | 0 0 0 |       |              | -1,73             | -0    | 0 0 0 |              |       |  |
|       |      | $\cdot 10^8$    |       |       |              | $\cdot 10^8$      |       |       |              |       |  |
| 0 0   | 0 0  | 12,9 2,28 -0,9  |       | 0 0   |              | -0,99 0,88 -3,88  |       |       |              |       |  |
| 0 0   | 0 0  | 2,28 0,96 0,10  |       | 0 0   |              | -0,33 -0,09 -0,05 |       | 0 0   |              |       |  |
| 0 0   | 0 0  | -0,91 0,10 0,59 |       | 0 0   |              | 0,52 -0,17 0,16   |       | 0 0   |              |       |  |
|       |      | $\cdot 10^3$    |       |       |              | $\cdot 10^3$      |       |       |              |       |  |
| 0 0   | 0 0  | 0 0 0           |       | 0 0   |              | 0 0 0             |       | 0 0   |              | 0 0 0 |  |
| -1,26 | -1,  |                 |       | 2,52  | 0            |                   |       |       | -1,26        | 1,    |  |
| -1,15 | -0,  |                 | 0 0 0 |       | 0 0,72       |                   | 0 0 0 |       | 1,15         | -0,   |  |
|       |      | $\cdot 10^8$    |       |       | $\cdot 10^8$ |                   |       |       | $\cdot 10^8$ |       |  |
| 0 0   | 0 0  | -0,99 -0,33 0,  |       | 0 0   |              | 2,90 0,15 0,71    |       |       |              |       |  |
| 0 0   | 0 0  | 0,88 -0,09 -0   |       | 0 0   |              | 0,15 0,29 -0,00   |       | 0 0   |              |       |  |
| 0 0   | 0 0  | -3,88 -0,05 0,  |       | 0 0   |              | 0,77 -0,0007 0,3  |       | 0 0   |              |       |  |
|       |      | $\cdot 10^3$    |       |       |              | $\cdot 10^3$      |       |       |              |       |  |
| 0 0   | 0 0  | 0 0 0           |       | 0 0   |              | 0 0 0             |       | 0 0   |              | 0 0 0 |  |
| -1,22 | 0,   |                 |       | -1,26 | 1,           |                   |       |       | 2,48         | -1,   |  |
| -0,29 | -6   |                 | 0 0 0 |       | 1,73 -0      |                   | 0 0 0 |       | -1,44        | 6,    |  |
|       |      | $\cdot 10^8$    |       |       | $\cdot 10^8$ |                   |       |       | $\cdot 10^8$ |       |  |
| 0 0   | 0 0  | -11,9 -1,95 0,3 |       | 0 0   |              | -1,90 -1,03 0,38  |       |       |              |       |  |
| 0 0   | 0 0  | 3,05 0,19 -0,   |       | 0 0   |              | 0,40 0,28 0,05    |       | 0 0   |              |       |  |
| 0 0   | 0 0  | 0,51 -0,32 -0,  |       | 0 0   |              | 1,01 0,29 0,15    |       | 0 0   |              |       |  |
|       |      | $\cdot 10^3$    |       |       |              | $\cdot 10^3$      |       |       |              |       |  |
| 0 0   | 0 0  | 0 0 0           |       | 0 0   |              | 0 0 0             |       | 0 0   |              | 0 0 0 |  |

(16.29)

The next step is the construction of the finite element equation using Eq.(16.17). The nodal displacements are calculated from the 4<sup>th</sup>, 5<sup>th</sup>, 7<sup>th</sup>, 8<sup>th</sup>, 10<sup>th</sup>, 11<sup>th</sup>, 14<sup>th</sup>, 16<sup>th</sup> and 17<sup>th</sup> equations of the system of equations. The solutions are:

$$\tilde{\alpha}_1 = 0,00406 \text{ rad}, \tilde{\beta}_1 = -0,02278 \text{ rad}, \quad (16.30)$$

$$\tilde{u}_2 = 0,0187 \text{ m}, \tilde{v}_2 = 0,00368 \text{ m}, \tilde{\alpha}_2 = -0,0948 \text{ rad}, \tilde{\beta}_2 = 0,00319 \text{ rad},$$

$$\tilde{v}_3 = 0,00737 \text{ m}, \tilde{\alpha}_3 = 0,01833 \text{ rad}, \tilde{\beta}_3 = 0,01994 \text{ rad}.$$

In the knowledge of the displacements we can determine the reactions utilizing the 1<sup>st</sup>, 2<sup>nd</sup>, 3<sup>rd</sup>, 9<sup>th</sup>, 13<sup>th</sup>, and 15<sup>th</sup> equations:

$$F_{x1} = -3000000 \text{ N}, F_{y1} = -8000000 \text{ N}, F_{z1} = 91,88 \text{ N}, \quad (16.31)$$

$$F_{z2} = 74,34 \text{ N}, F_{x3} = -3000000 \text{ N}, F_{z3} = 73,78 \text{ N}.$$

We note that the results by Eq.(16.31) are the components of the vector of concentrated forces, which is the first term in Eq.(16.26). Moreover the 6<sup>th</sup>, 12<sup>th</sup> and 18<sup>th</sup> component equations were not utilized here, which is explained by the fact that these equations are associated to the local rotations about axis  $z$ , and their values are zero in the local system. The total force vector by using Eq.(16.31) and Eq.(16.26) becomes:

$$\tilde{F}_{e \times 1}^{m+b^T} = \begin{bmatrix} -3000000 \\ 8000000 \\ 11,629 \\ 7,6 \\ -7,6876 \\ 0 \\ 6000000 \\ 0 \\ 2,344 \\ -12,8 \\ 1,25 \\ 0 \\ -3000000 \\ 8000000 \\ -13,973 \\ 11,6 \\ 8,3125 \\ 0 \end{bmatrix}. \quad (16.32)$$

In the sequel, we transform the results into the global  $X, Y, Z$  coordinate system. The global position vectors of the nodes based on the global coordinates are:

$$\underline{R}_1 = \begin{bmatrix} 0,6795 \\ 0,4 \\ 0,5004 \end{bmatrix} \text{m}, \underline{R}_2 = \begin{bmatrix} 0,57 \\ 1,225 \\ 0,6 \end{bmatrix} \text{m}, \underline{R}_3 = \begin{bmatrix} 0,2 \\ 0,5 \\ 0,4 \end{bmatrix} \text{m}. \quad (16.33)$$

The position vector of the origin of local coordinate system can be given in the global system as:

$$\underline{R}_0 = \frac{1}{2}(\underline{R}_1 + \underline{R}_3) = \begin{bmatrix} 0,43975 \\ 0,45 \\ 0,4502 \end{bmatrix} \text{m}. \quad (16.34)$$

We determine the unit basis vectors based on the position vectors in the global system using Fig.16.4:

$$\underline{e}_1 = \frac{\underline{R}_2 - \underline{R}_0}{|\underline{R}_2 - \underline{R}_0|} = \begin{bmatrix} 0,162825 \\ 0,96875 \\ 0,18725 \end{bmatrix}. \quad (16.35)$$

Similarly, the unit vectors  $\underline{e}_2$  and  $\underline{e}_3$  are

$$\underline{e}_2 = \frac{\underline{R}_3 - \underline{R}_0}{|\underline{R}_3 - \underline{R}_0|} = \begin{bmatrix} -0,959 \\ 0,2 \\ -0,2008 \end{bmatrix}, \quad (16.36)$$

$$\underline{e}_3 = \frac{\underline{R}_3 - \underline{R}_0}{|\underline{R}_3 - \underline{R}_0|} = \begin{bmatrix} -0,23197 \\ -0,14688 \\ 0,96159 \end{bmatrix}.$$

Based on the unit basis vectors and Eq.(16.12) matrix  $\underline{\underline{L}}$  becomes:

$$\underline{\underline{L}} = [\underline{e}_1 \quad \underline{e}_2 \quad \underline{e}_3] = \begin{bmatrix} 0,162825 & -0,959 & -0,23197 \\ 0,96875 & 0,2 & -0,14688 \\ 0,18725 & -0,2008 & 0,96159 \end{bmatrix}. \quad (16.37)$$

With that it is possible to construct matrix  $\underline{\lambda}$  with dimension of 18x18. Using Eqs.(16.10), (16.22) and (16.30) the nodal displacements in the global coordinate system are:

$$u_1 = 0, v_1 = 0, w_1 = 0, \quad (16.38)$$

$$\alpha_1 = -0,02141 \text{ rad}, \beta_1 = -0,00845 \text{ rad}, \psi_1 = 0,002405 \text{ rad},$$

$$u_2 = 0,00662 \text{ m}, v_2 = -0,017215 \text{ m}, w_2 = -0,004883 \text{ m},$$

$$\alpha_2 = -0,012352 \text{ rad}, \beta_2 = 0,091582 \text{ rad}, \psi_2 = 0,02153 \text{ rad},$$

$$u_3 = 0,0071365 \text{ m}, v_3 = 0,0014733 \text{ m}, w_3 = -0,001082 \text{ m},$$

$$\alpha_3 = 0,0223 \text{ rad}, \beta_3 = -0,013587 \text{ rad}, \psi_3 = -0,0071797 \text{ rad}.$$

It is seen that although in the local coordinate system the rotations about  $z$  are zero, in the global system as a result of the transformation even rotations about  $Z$  exist. The nodal forces are the followings:

$$F_{x1} = -8238600 \text{ N}, F_{y1} = 1277000 \text{ N}, F_{z1} = 1871000 \text{ N}, \quad (16.39)$$

$$M_{x1} = -6,21 \text{ Nm}, M_{y1} = -8,8259 \text{ Nm}, M_{z1} = -0,6338 \text{ Nm},$$

$$F_{x2} = 976920 \text{ N}, F_{y2} = -5754000 \text{ N}, F_{z2} = -1391800 \text{ N},$$

$$M_{x2} = -0,8732 \text{ Nm}, M_{y2} = 12,525 \text{ Nm}, M_{z2} = 2,7856 \text{ Nm},$$

$$F_{x3} = 7261500 \text{ N}, F_{y3} = 4477000 \text{ N}, F_{z3} = -479100 \text{ N},$$

$$M_{x3} = 9,9414 \text{ Nm}, M_{y3} = -9,4615 \text{ Nm}, M_{z3} = -3,9118 \text{ Nm}.$$

Accordingly, in the global system there are bending moments about axis  $Z$ , which are in fact the projections of the moments about local  $x$  and  $y$  axes with respect to  $Z$ . The solution method is applicable also for rectangle shape elements.

#### 16.4. Bibliography

- [1] Singiresu S. Rao, *The finite element method in engineering – fourth edition*. Elsevier Science & Technology Books, 2004.
- [2] Imre Bojtár, Gábor Vörös, *Application of the finite element method to plate and shell structures*. Technical Book Publisher, 1986, Budapest (in Hungarian).
- [3] Klaus-Jürgen Bathe, *Finite element procedures*. Prentice Hall, Upper Saddle River, 1996, New Jersey 17458.
- [4] Pei Chi Chou, Nicholas J. Pagano, *Elasticity – Tensor, dyadic and engineering approaches*. D. Van Nostrand Company, Inc., 1967, Princeton, New Jersey, Toronto, London.

## 17. MODELING OF CURVED AND DOUBLY-CURVED SHELLS BY FINITE ELEMENT METHOD BASED SOFTWARE SYSTEMS

### 17.1. Curved shell elements

Curved shell elements are suitable to model the midsurface geometry more accurately. In the case of certain surfaces – for example the cylindrical shell – it means the exact description of the original surface. For more complicated cases – similarly to the displacement field - the curvatures of the surface are approximated by interpolation functions. In this respect such elements belong to the parametric element types [1].

### 17.2. Thin-walled cylindrical shell element

The thin cylindrical shell element is presented in Fig.17.1. In accordance with the basic equations of the technical theory of thin shells the geometrical properties of the cylindrical shell are the followings [1,2]:

$$q_1 = x, H_1 = 1, R_1 = \infty, \quad (17.1)$$

$$q_2 = \varphi, H_2 = R, R_2 = R.$$

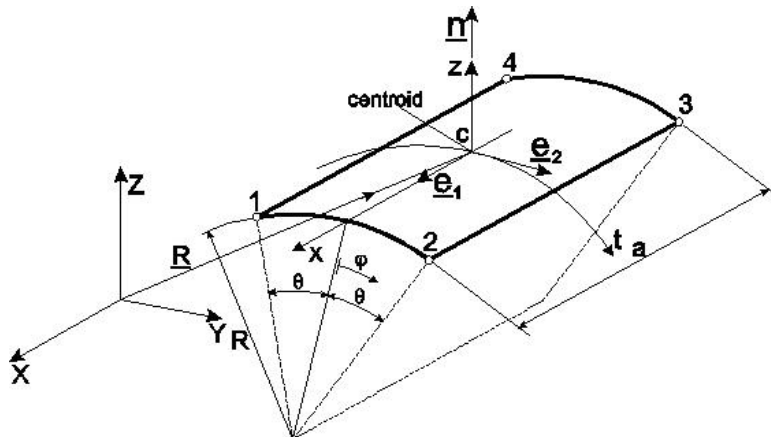


Fig.17.1. Parameters of the thin cylindrical shell element.

Apart from the displacement components  $u$ ,  $v$  and  $w$  we can derive the angle of rotations by applying the basic equations of the technical theory of thin shells based on Eqs.(14.69) and (14.70):

$$\beta_1 = \beta_x = \frac{u}{R_1} - \frac{1}{H_1} w_{,1} = -w_{,x}, \quad (17.2)$$

$$\beta_2 = \beta_\varphi = \frac{v}{R_2} - \frac{1}{H_2} w_{,2} = \frac{1}{R} (v - w_{,\varphi}),$$

$$\beta_3 = \frac{1}{2R} (R v_{,x} - u_{,\varphi}).$$

Next, we calculate the strain components using the parameters of the cylindrical shell surface (see Eq.(14.67)):

$$\varepsilon_{11} = \varepsilon_x = \frac{1}{H_1} u_{,1} + \frac{H_{1,2}}{H_1 H_2} v + \frac{1}{R_1} w = u_{,x}, \quad (17.3)$$

$$\varepsilon_{22} = \varepsilon_\varphi = \frac{1}{H_2} v_{,2} + \frac{H_{2,1}}{H_1 H_2} u + \frac{1}{R_2} w = \frac{1}{R} (u_{,\varphi} + w),$$

$$2\gamma_{12} = 2\gamma_{x\varphi} = \frac{H_1}{H_2} \left( \frac{u}{H_1} \right)_{,2} + \frac{H_2}{H_1} \left( \frac{v}{H_2} \right)_{,1} = \frac{1}{R} u_{,\varphi} + v_{,x},$$

$$\kappa_{11} = \kappa_x = \frac{1}{H_1} \beta_{1,1} + \frac{H_{1,2}}{H_1 H_2} \beta_2 = w_{,xx},$$

$$\kappa_{22} = \kappa_\varphi = \frac{1}{H_2} \beta_{2,2} + \frac{H_{2,1}}{H_1 H_2} \beta_1 = \frac{1}{R^2} (v_{,\varphi} - w_{,\varphi\varphi}),$$

$$2\kappa_{12} = 2\kappa_{x\varphi} = \frac{H_1}{H_2} \left( \frac{\beta_1}{H_1} \right)_{,2} + \frac{H_2}{H_1} \left( \frac{\beta_2}{H_2} \right)_{,1} + \left( \frac{1}{R_2} - \frac{1}{R_1} \right) \beta_3 = \frac{1}{R} (-2w_{,x\varphi} + v_{,x} + \beta_3).$$

The rigid body-like motion of the element involves six degrees of freedom, which are given by the displacement vector field given below [1]:

$$u_0 = a_1 + a_2 R (\cos \varphi - \cos \theta) - a_3 R \sin \varphi, \quad (17.4)$$

$$v_0 = -a_2 x \sin \varphi + a_3 x \cos \varphi + a_4 R (\cos \varphi \cos \theta - 1) - a_5 \sin \varphi + a_6 \cos \varphi,$$

$$w_0 = a_2 x \cos \varphi + a_3 x \sin \varphi + a_4 R \sin \varphi \cos \varphi + a_5 \cos \varphi + a_6 \sin \varphi.$$

In matrix form:

$$\underline{u}_0 = \underline{\Phi}_0 \underline{\alpha}_0, \quad (17.5)$$

where:

$$\underline{u}_0^T = [u_0 \quad v_0 \quad w_0], \quad (17.6)$$

$$\underline{\underline{\Phi}}_0 = \begin{bmatrix} 1 & R(\cos \varphi - \cos \theta) & -R \sin \varphi & 0 & 0 & 0 \\ 0 & -x \sin \varphi & x \cos \varphi & R(\cos \varphi \cos \theta - 1) & -\sin \varphi & \cos \varphi \\ 0 & x \cos \varphi & x \sin \varphi & R \sin \varphi \cos \varphi & \cos \varphi & \sin \varphi \end{bmatrix},$$

$$\underline{\alpha}_0^T = [a_1 \quad a_2 \quad a_3 \quad a_4 \quad a_5 \quad a_6].$$

where  $\underline{\underline{\Phi}}_0$  is the matrix of interpolation functions, which capture the rigid body-like motions,  $\underline{\alpha}_0$  is the vector of unknown coefficients. The displacement field of rigid body-like motion and that of the deformation together give the total displacement field, which is:

$$\underline{u} = \underline{u}_0 + \underline{u}_{01} = \begin{bmatrix} u \\ v \\ w \end{bmatrix}, \quad (17.7)$$

where:

$$\underline{u}_{01}^T = [u_{01} \quad v_{01} \quad w_{01}], \quad (17.8)$$

$$u_{01} = a_7 x + a_8 \varphi + a_9 x \varphi,$$

$$v_{01} = a_{10} \varphi + a_{11} x \varphi,$$

$$w_{01} = a_{12} x^2 + a_{13} x \varphi + a_{14} \varphi^2 + a_{15} x^3 + a_{16} x^2 \varphi + a_{17} x \varphi^2 + a_{18} \varphi^3 + a_{19} x^3 \varphi + a_{20} x^2 \varphi^2 + a_{21} x \varphi^3 + a_{22} x^3 \varphi^2 + a_{23} x^2 \varphi^3 + a_{24} x^3 \varphi^3.$$

In matrix form we have:

$$\underline{u} = \underline{u}_0 + \underline{u}_{01} = \underline{\underline{\Phi}}_0 \underline{\alpha}_0 + \underline{\underline{\Phi}}_1 \underline{\alpha}_1, \quad (17.9)$$

where  $\underline{\underline{\Phi}}_1$  is the interpolation functions matrix related to the deformation displacement field:

$$\underline{\underline{\Phi}}_1 = \begin{bmatrix} x & \varphi & x \varphi & 0 & 0 & 0 & 0 & 0 & 0 & 0 & 0 & 0 & 0 & 0 & 0 & 0 & 0 \\ 0 & 0 & 0 & \varphi & x \varphi & 0 & 0 & 0 & 0 & 0 & 0 & 0 & 0 & 0 & 0 & 0 & 0 \\ 0 & 0 & 0 & 0 & 0 & x^2 & x \varphi & \varphi^2 & x^3 & x^2 \varphi & x \varphi^2 & \varphi^3 & x^3 \varphi & x^2 \varphi^2 & x \varphi^3 & x^3 \varphi^2 & x^2 \varphi^3 & x^3 \varphi^3 \end{bmatrix}. \quad (17.10)$$

$\underline{\alpha}_1$  is the vector of unknown coefficients:

In the expression above there are 24 unknown coefficients. To determine all of them 24 displacement parameters are required, let us choose the followings:

$$\underline{\tilde{u}}_e^T = \left[ \begin{matrix} \tilde{u}_1 & \tilde{v}_1 & \tilde{w}_1 & \tilde{\beta}_{x1} & \tilde{\beta}_{\varphi 1} & \tilde{w}_{,x\varphi 1} & \tilde{u}_2 & \tilde{v}_2 & \tilde{w}_2 & \tilde{\beta}_{x2} & \tilde{\beta}_{\varphi 2} & \tilde{w}_{,x\varphi 2} \\ \dots & \dots & \dots & \tilde{u}_3 & \tilde{v}_3 & \tilde{w}_3 & \tilde{\beta}_{x3} & \tilde{\beta}_{\varphi 3} & \tilde{w}_{,x\varphi 3} & \tilde{u}_4 & \tilde{v}_4 & \tilde{w}_4 & \tilde{\beta}_{x4} & \tilde{\beta}_{\varphi 4} & \tilde{w}_{,x\varphi 4} \end{matrix} \right] \quad (17.12)$$

i.e. at each node there are displacements in the direction of the basis vectors, there are rotations about  $e_1$  and  $e_2$ , the sixth degrees of freedom is chosen to be the mixed derivative  $w_{,x\varphi}$ . The degrees of freedom for the cylindrical shell element based on Eqs.(17.2) and (17.7) are:

$$u = u_0 + u_{01}, v = v_0 + v_{01}, w = w_0 + w_{01}, \quad (17.13)$$

$$\begin{aligned}\beta_x = -w_{,x} = & -a_2 \cos \varphi - a_3 \sin \varphi - 2a_{12}x - a_{13}\varphi - 3a_{15}x^2 - 2a_{16}x\varphi - a_{17}\varphi^2 + \\ & - 3a_{19}x^2\varphi - 2a_{20}x\varphi^2 - a_{21}\varphi^3 - 3a_{22}x^2\varphi^2 - 2a_{23}x\varphi^3 - 3a_{24}x^2\varphi^3,\end{aligned}$$

$$\begin{aligned}\beta_\varphi = \frac{1}{R}(v - w_{,\varphi}) = & \frac{1}{R}(-a_4 R + a_{10}\varphi + a_{11}x\varphi - a_{13}x - 2a_{14}\varphi - a_{16}x^2 - 2a_{17}x\varphi - 3a_{18}\varphi^2 + \\ & - a_{19}x^3 - 2a_{20}x^2\varphi - 3a_{21}x\varphi^2 - 2a_{22}x^3\varphi - 3a_{23}x^2\varphi^2 - 3a_{24}x^3\varphi^2),\end{aligned}$$

$$w_{,x\varphi} = -a_2 \sin \varphi + a_3 \cos \varphi + a_{13} + 2a_{16}x + 2a_{17}\varphi + 3a_{19}x^2 + \\ + 4a_{20}x\varphi + 3a_{21}\varphi^2 + 6a_{22}x^2\varphi + 6a_{23}x\varphi^2 + 9a_{24}x^2\varphi^2.$$

The conditions for the determination of the parameters  $a_i$ ,  $i = 1 \dots 24$  are:

$$u(L/2, -\theta) = \tilde{u}_1, u(L/2, \theta) = \tilde{u}_2, \quad (17.14)$$

$$u(-L/2, \theta) = \tilde{u}_3, u(-L/2, -\theta) = \tilde{u}_4,$$

$$v(L/2, -\theta) = \tilde{v}_1, v(L/2, \theta) = \tilde{v}_2,$$

$$v(-L/2, \theta) = \tilde{v}_3, v(-L/2, -\theta) = \tilde{v}_4,$$

$$w(L/2, -\theta) = \tilde{w}_1, w(L/2, \theta) = \tilde{w}_2,$$

$$w(-L/2, \theta) = \tilde{w}_3, w(-L/2, -\theta) = \tilde{w}_4,$$

$$\beta(L/2, -\theta) = \tilde{\beta}_1, \beta(L/2, \theta) = \tilde{\beta}_2,$$

$$\beta_x(-L/2, \theta) = \tilde{\beta}_{x3}, \quad \beta_x(-L/2, -\theta) = \tilde{\beta}_{x4},$$

$$\beta_\varphi(L/2, -\theta) = \tilde{\beta}_{\varphi 1}, \beta_\varphi(L/2, \theta) = \tilde{\beta}_{\varphi 2},$$

$$\beta_\varphi(-L/2, \theta) = \tilde{\beta}_{\varphi^3}, \quad \beta_\varphi(-L/2, -\theta) = \tilde{\beta}_{\varphi^4},$$

$$w_{,x\varphi}(L/2,-\theta)=\tilde{w}_{,x\varphi 1}, w_{,x\varphi}(L/2,\theta)=\tilde{w}_{,x\varphi 2},$$

$$w_{,x\varphi}(-L/2,\theta) = \tilde{w}_{,x\varphi 3}, w_{,x\varphi}(-L/2,-\theta) = \tilde{w}_{,x\varphi 4}.$$

The vector of nodal displacements is formulated similarly to the plate element presented in section 15, viz. [3]:

$$\underline{\tilde{u}}_e = \underline{\underline{\underline{M}}}\underline{\underline{A}}, \quad (17.15)$$

where vector  $\underline{A}$  contains the elements of  $\underline{\alpha}_0$  and  $\underline{\alpha}_1$  in order, i.e.:

The coefficients of the interpolation polynomials are determined by the inversion of  $M$ :

$$\underline{\underline{A}} = \underline{\underline{M}}^{-1} \tilde{\underline{\underline{u}}}_e. \quad (17.17)$$

Due to their large length, the coefficients are not detailed here. Assuming that the angle rotation,  $\beta_3$  is approximately zero the strain components are formulated as follows:

$$\varepsilon_x = u_{,x}, \varepsilon_\varphi = \frac{1}{R}(u_{,\varphi} + w), 2\gamma_{x\varphi} = \frac{1}{R}u_{,\varphi} + v_{,x}, \quad (17.18)$$

$$K_x = w_{,xx}, K_\varphi = \frac{1}{R^2}(v_{,\varphi} - w_{,\varphi\varphi}), 2K_{x\varphi} = \frac{1}{R}(-2w_{,x\varphi} + v_{,x}).$$

The strain components can be classified into two parts: strains, shear strains and the curvatures, respectively. We can write that:

$$\underline{\varepsilon}_0 = \begin{bmatrix} \varepsilon_x \\ \varepsilon_y \\ 2\gamma_{xy} \end{bmatrix} = \underline{\underline{R}}_0 \underline{A}, \underline{\kappa} = \begin{bmatrix} \kappa_x \\ \kappa_y \\ 2\kappa_{xy} \end{bmatrix} = \underline{\underline{R}}_1 \underline{A}, \quad (17.19)$$

where matrices  $\underline{\underline{R}}_0$  and  $\underline{\underline{R}}_1$  are calculated based on the derivatives of the displacement functions:

$$\underline{\underline{R}}_0 = \begin{bmatrix} 0 & 0 & 0 & 0 & 0 & 0 & 1 & 0 & \varphi & 0 & 0 & 0 \\ 0 & \begin{cases} -\sin \varphi + \\ +\frac{x}{R} \cos \varphi \end{cases} & \begin{cases} 0 \\ -\cos \varphi + \\ +\frac{x}{R} \sin \varphi \end{cases} & \sin \varphi \cos \theta & \frac{\cos \varphi}{R} & \frac{\sin \varphi}{R} & 0 & \frac{1}{R} & \frac{x}{R} & 0 & 0 & \frac{x^2}{R} \\ 0 & -\frac{3}{2} \sin \varphi & \frac{1}{2} \cos \varphi & 0 & 0 & 0 & 0 & \frac{1}{2R} & \frac{x}{2R} & 0 & \varphi & 0 \\ \dots & \frac{x\varphi}{R} & \frac{\varphi^2}{R} & \frac{x^3}{R} & \frac{x^2\varphi}{R} & \frac{x\varphi^2}{R} & \frac{\varphi^3}{R} & \frac{x^3\varphi}{R} & \frac{x^2\varphi^2}{R} & \frac{x\varphi^3}{R} & \frac{x^3\varphi^2}{R} & \frac{x^3\varphi^3}{R} \\ 0 & 0 & 0 & 0 & 0 & 0 & 0 & 0 & 0 & 0 & 0 & 0 \end{bmatrix}, \quad (17.20)$$

$$\underline{\underline{R}}_1 = \begin{bmatrix} 0 & 0 & 0 & 0 & 0 & 0 & 0 & 0 & 0 & 2 & 0 & 0 & 6x & 2\varphi \\ 0 & 0 & 0 & 0 & 0 & 0 & 0 & 0 & \frac{1}{R^2} & \frac{x}{R^2} & 0 & 0 & -\frac{2}{R^2} & 0 & 0 \\ 0 & \frac{\sin \varphi}{2R} & -\frac{\cos \varphi}{2R} & 0 & 0 & 0 & 0 & 0 & 0 & \frac{\varphi}{2R} & 0 & -\frac{1}{R} & 0 & 0 & -\frac{2x}{R} \\ \dots & 0 & 0 & 6x\varphi & 2\varphi^2 & 0 & 6x\varphi^2 & 2\varphi^3 & 6x\varphi^3 & -\frac{2x}{R^2} & -\frac{6\varphi}{R^2} & -\frac{2x^3}{R^2} & -\frac{6x^2\varphi}{R^2} & -\frac{6x^3\varphi}{R^2} \\ -\frac{2x}{R^2} & -\frac{6\varphi}{R^2} & 0 & -\frac{2x^2}{R^2} & -\frac{6x\varphi}{R^2} & -\frac{2x^3}{R^2} & -\frac{6x^2\varphi}{R^2} & -\frac{6x^3\varphi}{R^2} & -\frac{6x^2\varphi^2}{R^2} & 0 & -\frac{3x^2}{R} & -\frac{4x\varphi}{R} & -\frac{3\varphi^2}{R} & -\frac{6x^2\varphi}{R} & -\frac{6x\varphi^2}{R} & -\frac{9x^2\varphi^2}{R} \end{bmatrix}. \quad (17.21)$$

For the calculation of the stiffness matrix and the force vector related to the distributed load we formulate the total potential energy of a single element. We note that the expression below contains only the strain energy and the work of the distributed load:

$$\Pi_e = \frac{1}{2} \int_{V_e} \underline{\sigma}^T \underline{\varepsilon} dV - \int_{A_{pe}} \underline{u}^T \underline{p} dA. \quad (17.22)$$

The constitutive law of the linear elastic material is:

$$\underline{\sigma} = \underline{\underline{C}} \underline{\varepsilon}, \quad (17.23)$$

where, similarly to the plates we assume plane stress state, i.e.  $\underline{\underline{C}} = \underline{\underline{C}}^{str}$ . Using Eqs.(17.17) and (17.19) we obtain:

$$\underline{\varepsilon}_0 = \underline{\underline{R}}_0 \underline{\underline{A}} = \underline{\underline{R}}_0 \underline{\underline{M}}^{-1} \tilde{\underline{u}}_e = \underline{\underline{B}}_0 \tilde{\underline{u}}_e, \quad (17.24)$$

$$\underline{\underline{B}}_0 = \underline{\underline{R}}_0 \underline{\underline{M}}^{-1}, \underline{\sigma}_0 = \underline{\underline{C}} \underline{\varepsilon}_0 = \underline{\underline{C}} \underline{\underline{B}}_0 \tilde{\underline{u}}_e,$$

furthermore:

$$\underline{\kappa} = \underline{\underline{R}}_1 \underline{A} = \underline{\underline{R}}_1 \underline{\underline{M}}^{-1} \underline{u}_e = \underline{\underline{B}}_1 \tilde{\underline{u}}_e, \quad (17.25)$$

$$\underline{\underline{B}}_1 = \underline{\underline{R}}_1 \underline{\underline{M}}^{-1}, \underline{\sigma}_1 = -z \underline{\kappa} \underline{\underline{C}} \underline{\kappa} = -z \underline{\underline{\underline{C}}} \underline{\underline{B}}_1 \tilde{\underline{u}}_e$$

Based on Eq.(17.7) the displacement field becomes:

$$\underline{u} = \underline{\lambda} \underline{A} = \underline{\lambda} \underline{\underline{M}}^{-1} \tilde{\underline{u}}_e, \quad (17.26)$$

where:

$$\underline{\lambda} = [\Phi_0 \quad \Phi_1]. \quad (17.27)$$

Eq.(17.24) is related to the stress resultants, while Eq.(17.25) is related to the stress couples. The total potential energy becomes:

$$\Pi_e = \frac{1}{2} \int_{V_e} \underline{\varepsilon}^T \underline{\underline{C}}^T \underline{\varepsilon} dV + \frac{1}{2} \int_{V_e} z^2 \underline{\kappa}^T \underline{\underline{C}}^T \underline{\kappa} dV - \tilde{\underline{u}}_e^T \int_{A_{pe}} \underline{\underline{M}}^{-1T} \underline{\lambda}^T \underline{p} dA, \quad (17.28)$$

which is written as:

$$\begin{aligned} \Pi_e = & \frac{1}{2} \tilde{\underline{u}}_e^T \left\{ \int_{-L/2-\theta}^{L/2} \int_0^\theta t \cdot \underline{\underline{B}}_0^T \underline{\underline{C}}^T \underline{\underline{B}}_0 R \cdot d\varphi \cdot dx \right\} \tilde{\underline{u}}_e + \frac{1}{2} \tilde{\underline{u}}_e^T \left\{ \int_{-L/2-\theta}^{L/2} \int_0^\theta \frac{t^3}{12} \underline{\underline{B}}_1^T \underline{\underline{C}}^T \underline{\underline{B}}_1 R \cdot d\varphi \cdot dx \right\} \tilde{\underline{u}}_e + \\ & - \tilde{\underline{u}}_e^T \int_{-L/2-\theta}^{L/2} \int_0^\theta \underline{\underline{M}}^{-1T} \underline{\lambda}^T \underline{p} \cdot R \cdot d\varphi \cdot dx. \end{aligned} \quad (17.29)$$

It is important to note that in Eq.(17.29) the term related to the concentrated loads is excluded, consequently the vector of concentrated loads should be produced additionally. This is an easy task based on the nodal degrees of freedom:

$$\begin{aligned} \tilde{\underline{F}}_{ec}^T = & [F_{x1} \quad F_{\varphi 1} \quad F_{z1} \quad M_{x1} \quad M_{\varphi 1} \quad M_{x\varphi 1} \quad F_{x2} \quad F_{\varphi 2} \quad F_{z2} \quad M_{x2} \quad M_{\varphi 2} \quad M_{x\varphi 2} \dots \dots \dots] \\ & \dots \dots \dots F_{x3} \quad F_{\varphi 3} \quad F_{z3} \quad M_{x3} \quad M_{\varphi 3} \quad M_{x\varphi 3} \quad F_{x4} \quad F_{\varphi 4} \quad F_{z4} \quad M_{x4} \quad M_{\varphi 4} \quad M_{x\varphi 4}] \end{aligned} \quad (17.30)$$

and the completed total potential energy becomes:

$$\Pi_e = \frac{1}{2} \tilde{\underline{u}}_e^T \tilde{\underline{\underline{K}}}_e \tilde{\underline{u}}_e - \tilde{\underline{u}}_e^T (\tilde{\underline{F}}_{ep} + \tilde{\underline{F}}_{ec}). \quad (17.31)$$

In Eq.(17.31)  $\tilde{\underline{\underline{K}}}_e$  is the element stiffness matrix in the local coordinate system

$$\tilde{\underline{\underline{K}}}_e = \int_{-L/2-\theta}^{L/2} \int_0^\theta \left( t \cdot \underline{\underline{B}}_0^T \underline{\underline{C}}^T \underline{\underline{B}}_0 + \frac{t^3}{12} \underline{\underline{B}}_1^T \underline{\underline{C}}^T \underline{\underline{B}}_1 \right) R \cdot d\varphi \cdot dx. \quad (17.32)$$

The force vector from the distributed load is:

$$\tilde{\underline{F}}_{ep} = \int_{-L/2-\theta}^{L/2} \int_0^\theta \underline{\underline{M}}^{-1T} \underline{\lambda}^T \underline{p} \cdot R \cdot d\varphi \cdot dx. \quad (17.33)$$

Finally the well-known finite element equilibrium equation in the local system is:

$$\tilde{\underline{\underline{K}}}_e \tilde{\underline{u}}_e = \tilde{\underline{F}}_e, \quad (17.34)$$

which is applicable only for a single element. The global equation of developed by a proper transformation. The structural equation is required when there are several elements connected to each other, which is mathematically the same as Eq. (14.86). The advantage of the thin cylindrical shell element is that the cylindrical surface is captured exactly; as a consequence it provides accurate result even if the number of elements is relatively low.

### 17.3. Axisymmetric shell problems – conical shell element

The midsurface of axisymmetric shells is produced by the rotation of the meridian curve about a straight axis [1]. An example is shown by Fig.17.2.

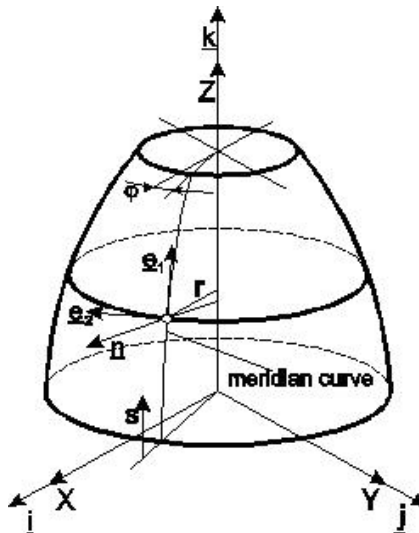


Fig.17.2. Axisymmetric shell.

The meridian curves and the circular curves perpendicularly to the meridian curves are principal curvature lines of the surface. If the load of the structure is axisymmetric, then in this kind of problem the displacement field is the function of arc length along the meridian curve only.

The meridian curve can be modeled by straight lines, and so we approximate the original shell structure by conical shell elements. Referring to the basic equations of the technical theory of thin shells, the parameters of the conical shell element shown in Fig.17.3 are:

$$q_1 = s, H_1 = 1, R_1 = \infty, \quad (17.35)$$

$$q_2 = \varphi, H_2 = r, R_2 = \frac{r}{\cos \theta},$$

where  $s$  is the arc length,  $\varphi$  is the angle coordinate,  $r$  is the radius for a point P,  $\theta$  is the half angle of inclination. To calculate the strain components we need to determine the  $r(s)$  relationship, based on Fig.17.3 we have:

$$r(s) = s \sin \theta + r_1 \text{ and } \frac{dr}{ds} = \sin \theta. \quad (17.36)$$

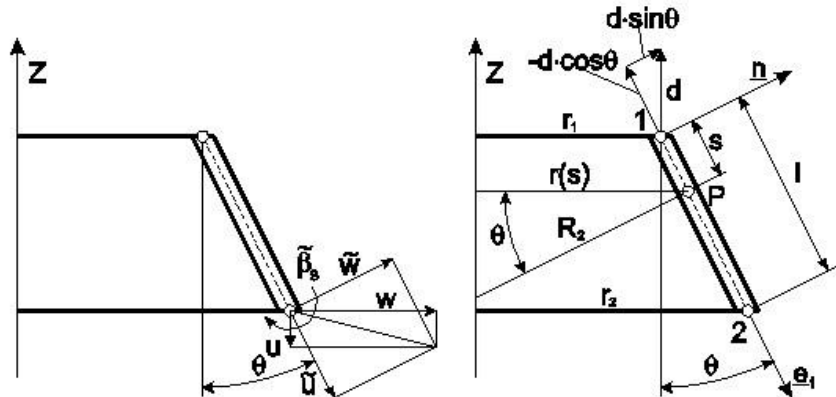


Fig.17.3. Axisymmetric conical shell element and its nodal parameters.

Using Eqs.(14.67), (14.69) and (14.70) of the technical theory of thin shells we can calculate the strain components as:

$$\beta_1 = \beta_s = -w_{,s}, \beta_2 = 0, \beta_3 = 0, \quad (17.37)$$

$$\varepsilon_{11} = \varepsilon_s = u_{,s}, \varepsilon_{22} = \varepsilon_\varphi = \frac{1}{r}(u \sin \theta + w \cos \theta), \gamma_{12} = 0,$$

$$\kappa_{11} = \kappa_s = -w_{,ss}, \kappa_{22} = \kappa_\varphi = -\frac{\sin \theta}{r} w_{,s}, \kappa_{12} = 0.$$

The displacement in the tangential direction at point P is  $v = 0$  due to the axisymmetry. The admissible rigid body-like motion of the element is a displacement given by  $d$  in direction Z, for which the displacement components are  $u = -d \cdot \cos \theta$  and  $w = d \cdot \sin \theta$  (see Fig.17.3). We consider three degrees of freedom at each node, these are:  $u$  (displacement along the meridian direction),  $w$  (displacement perpendicularly to the meridian curve) and  $\beta_s$  (angle of ro-

tation about the axis perpendicularly to the meridian curve in accordance with Fig.17.3), therefore the element has six degrees of freedom. The displacement in the meridian direction is interpolated by a linear function of the arc length. On the other hand we apply third order interpolation with respect to the displacement in the normal direction:

$$\begin{bmatrix} u \\ w \end{bmatrix} = \begin{bmatrix} 1 & s & 0 & 0 & 0 & 0 \\ 0 & 0 & 1 & s & s^2 & s^3 \end{bmatrix} \underline{\alpha} = \underline{\Phi} \underline{\alpha}, \quad (17.38)$$

where  $\underline{\alpha}$  is the vector of unknown coefficients:

$$\underline{\alpha}^T = [a_1 \ a_2 \ a_3 \ a_4 \ a_5 \ a_6]. \quad (17.39)$$

The vector of nodal displacements is:

$$\tilde{\underline{u}}_e^T = [\tilde{u}_1 \ \tilde{w}_1 \ \tilde{\beta}_{s1} \ \tilde{u}_2 \ \tilde{w}_2 \ \tilde{\beta}_{s2}]. \quad (17.40)$$

The conditions required for the determination of the coefficients are:

$$u(s_1) = a_1 + a_2 s_1 = \tilde{u}_1, \quad (17.41)$$

$$w(s_1) = a_3 + a_4 s_1 + a_5 s_1^2 + a_6 s_1^3 = \tilde{w}_1,$$

$$\beta_s(s_1) = a_4 + 2a_5 s_1 + 3a_6 s_1^2 = \tilde{\beta}_{s1},$$

$$u(s_2) = a_1 + a_2 s_2 = \tilde{u}_2,$$

$$w(s_2) = a_3 + a_4 s_2 + a_5 s_2^2 + a_6 s_2^3 = \tilde{w}_2,$$

$$\beta_s(s_2) = a_4 + 2a_5 s_2 + 3a_6 s_2^2 = \tilde{\beta}_{s2}.$$

The solutions for the coefficients are moderately complicated, therefore they are not included here. The displacement functions can be formulated also in the way presented below:

$$u(s) = N_1 \tilde{u}_1 + N_2 \tilde{u}_2, \quad (17.42)$$

$$w(s) = N_3 \tilde{w}_1 + N_4 \tilde{\beta}_{s1} + N_5 \tilde{w}_2 + N_6 \tilde{\beta}_{s2},$$

where  $N_i$ ,  $i = 1\dots6$  are the interpolation functions:

$$N_1 = \frac{s_2 - s}{s_2 - s_1}, \quad N_2 = -\frac{s_1 - s}{s_2 - s_1}, \quad (17.43)$$

$$N_3 = \frac{(s - s_2)^2(3s_1 - s_2 - 2s)}{(s_2 - s_1)^3}, N_4 = \frac{(s - s_2)^2(s_1 - s)}{(s_2 - s_1)^2},$$

$$N_5 = \frac{(s - s_1)^2(3s_2 - s_1 - 2s)}{(s_2 - s_1)^3}, N_6 = -\frac{(s - s_1)^2(s_2 - s)}{(s_2 - s_1)^2},$$

and:

$$\underline{u} = \begin{bmatrix} u \\ w \end{bmatrix} = \begin{bmatrix} N_1 & 0 & 0 & N_2 & 0 & 0 \\ 0 & N_3 & N_4 & 0 & N_5 & N_6 \end{bmatrix} \underline{\tilde{u}}_e = \underline{\underline{N}} \underline{\tilde{u}}_e. \quad (17.44)$$

The strain components in matrix form are:

$$\underline{\varepsilon} = \begin{bmatrix} \varepsilon_s \\ \varepsilon_\varphi \end{bmatrix} = \underline{\underline{B}} \underline{u}_e, \quad (17.45)$$

where the strain-displacement matrix is:

$$\underline{\underline{B}} = \begin{bmatrix} \frac{\partial N_1}{\partial s} & 0 & 0 & \frac{\partial N_2}{\partial s} & 0 & 0 \\ \frac{N_1 \sin \theta}{r} & \frac{N_3 \cos \theta}{r} & \frac{N_4 \cos \theta}{r} & \frac{N_2 \sin \theta}{r} & \frac{N_5 \cos \theta}{r} & \frac{N_6 \cos \theta}{r} \end{bmatrix}. \quad (17.46)$$

We collect also the curvatures in matrix form:

$$\underline{\kappa} = \begin{bmatrix} \kappa_s \\ \kappa_\varphi \end{bmatrix} = \underline{\underline{H}} \underline{\tilde{u}}_e, \quad (17.47)$$

where:

$$\underline{\underline{H}} = \begin{bmatrix} 0 & -\frac{\partial^2 N_3}{\partial s^2} & -\frac{\partial^2 N_4}{\partial s^2} & 0 & -\frac{\partial^2 N_5}{\partial s^2} & -\frac{\partial^2 N_6}{\partial s^2} \\ 0 & -\frac{\sin \theta}{r} \frac{\partial N_3}{\partial s} & -\frac{\sin \theta}{r} \frac{\partial N_4}{\partial s} & 0 & -\frac{\sin \theta}{r} \frac{\partial N_5}{\partial s} & -\frac{\sin \theta}{r} \frac{\partial N_6}{\partial s} \end{bmatrix}. \quad (17.48)$$

Based on the constitutive law the vector of stress components is:

$$\underline{\sigma}_0 = \underline{\underline{C}} \underline{\varepsilon} = \underline{\underline{C}} \underline{\underline{B}} \underline{\tilde{u}}_e, \quad (17.49)$$

$$\underline{\sigma}_1 = -z \underline{\underline{C}} \underline{\kappa} = -z \underline{\underline{C}} \underline{\underline{H}} \underline{\tilde{u}}_e.$$

The vectors of strain components and curvatures contain only two elements, therefore the constitutive matrix reduces to:

$$\underline{\underline{C}} = \frac{E}{1-\nu^2} \begin{bmatrix} 1 & \nu \\ \nu & 1 \end{bmatrix}. \quad (17.50)$$

Taking the former back into the total potential energy (similarly to the cylindrical shell element) we can calculate the element stiffness matrix in the local coordinate system:

$$\underline{\underline{\tilde{K}}}_e = \int_{s_1}^{s_2} (t \cdot \underline{\underline{B}}^T \underline{\underline{C}}^T \underline{\underline{B}} + \frac{t^3}{12} \underline{\underline{H}}^T \underline{\underline{C}}^T \underline{\underline{H}}) \cdot 2\pi r ds = \int_0^l (t \cdot \underline{\underline{B}}^T \underline{\underline{C}}^T \underline{\underline{B}} + \frac{t^3}{12} \underline{\underline{H}}^T \underline{\underline{C}}^T \underline{\underline{H}}) \cdot 2\pi(s \sin \theta + r_1) ds. \quad (17.51)$$

In the above expression it was considered that  $s_1 = 0$  and  $s_2 = l$  and so  $r = s \cdot \sin \theta$ . The exact computation of the stiffness matrix is quite complicated, and consequently the finite element codes implement numerical methods, e.g. the Gauss rule presented in section 12 is suitable to calculate the matrix components. The force vector is composed by two terms. The vector of concentrated forces can be constructed based on the nodal degrees of freedom:

$$\underline{\underline{\tilde{F}}}_{ec}^T = [F_{s1} \quad F_{n1} \quad M_1 \quad F_{s2} \quad F_{n2} \quad M_2], \quad (17.52)$$

where  $F$  refers to the concentrated force,  $M$  is a concentrated moment about the same direction tan that of  $\beta_s$ . The force vector from the distributed load is calculated based on the work of the load:

$$W_e = \int_0^l (p_s u + p_n w) 2\pi r ds = \underline{\underline{\tilde{u}}}_e^T \int_0^l \underline{\underline{N}}^T \begin{bmatrix} p_s \\ p_n \end{bmatrix} \cdot 2\pi r ds = \underline{\underline{\tilde{u}}}_e^T \underline{\underline{\tilde{F}}}_{ep}, \quad (17.53)$$

accordingly:

$$\underline{\underline{\tilde{F}}}_{ep} = \int_0^l \underline{\underline{N}}^T \begin{bmatrix} p_s \\ p_n \end{bmatrix} \cdot 2\pi(s \sin \theta + r_1) ds. \quad (17.54)$$

Considering that  $l \cdot \sin \theta = r_2 - r_1$  and assuming that both  $p_s$  and  $p_n$  are constants, we obtain:

$$\tilde{\underline{F}}_{ep} = \begin{bmatrix} \frac{1}{3} p_s \pi d (2r_1 + r_2) \\ \frac{1}{10} p_n \pi d (7r_1 + 3r_2) \\ \frac{1}{30} p_n \pi d^3 (3r_1 + 2r_2) \\ \frac{1}{3} p_s \pi d (r_1 + 2r_2) \\ \frac{1}{10} p_n \pi d (3r_1 + 7r_2) \\ -\frac{1}{30} p_n \pi d^3 (2r_1 + 3r_2) \end{bmatrix}. \quad (17.55)$$

In the local coordinate system the nodal displacement and reactions are calculated from the usual:

$$\tilde{\underline{K}}_{\underline{\underline{e}}} \tilde{\underline{u}}_e = \tilde{\underline{F}}_e \quad (17.56)$$

equation, where:

$$\tilde{\underline{F}}_e = \tilde{\underline{F}}_{ec} + \tilde{\underline{F}}_{ep}. \quad (17.57)$$

For a finite element structure we need the structural equation given by Eq.(14.86). Since the elements are connected under a given angle, the local displacement coordinates should be transformed into the global cylindrical coordinate system with longitudinal axis given by Z. The transformation can be performed based on Fig.17.3:

$$\begin{bmatrix} u \\ w \\ \beta_s \end{bmatrix} = \begin{bmatrix} \cos \theta & -\sin \theta & 0 \\ \sin \theta & \cos \theta & 0 \\ 0 & 0 & 1 \end{bmatrix} \begin{bmatrix} \tilde{u} \\ \tilde{w} \\ \tilde{\beta}_s \end{bmatrix} = \underline{\underline{L}}^T \tilde{\underline{u}}. \quad (17.58)$$

Based on the former the transformation of the stiffness matrix becomes:

$$\underline{\underline{K}}_e = \underline{\underline{\lambda}}^T \tilde{\underline{\underline{K}}} \underline{\underline{\lambda}}, \quad (17.59)$$

where:

$$\underline{\underline{T}} = \begin{bmatrix} \underline{\underline{L}}^T & 0 \\ 0 & \underline{\underline{L}}^T \end{bmatrix}, \quad (17.60)$$

is an orthogonal transformation matrix. The transformed force vector is:

$$\underline{\underline{F}}_e = \underline{\underline{T}} \tilde{\underline{\underline{F}}}_e . \quad (17.61)$$

For a single element the finite element equation in the global system is:

$$\underline{\underline{K}}_e \underline{u}_e = \underline{F}_e , \quad (17.62)$$

Moreover, for the whole structure we have:

$$\underline{\underline{K}} \underline{U} = \underline{F} . \quad (17.63)$$

In the finite element literature there are more element types, e.g. curved axisymmetric shell element [4,5,6], which operates similarly to the conical shell element.

#### 17.4. Thick-walled shell elements

For the solution of three-dimensional problems we can apply the spatial (SOLID type) elements. Fig.17.4 shows a 20 node isoparametric element. Isoparametric representation means that the geometry and the displacement field is described by the same set of interpolation functions [1,4,5]:

$$\begin{bmatrix} x \\ y \\ z \end{bmatrix} = \sum_{i=1}^{20} N_i(\xi, \eta, \zeta) \begin{bmatrix} x_i \\ y_i \\ z_i \end{bmatrix}, \begin{bmatrix} u \\ v \\ w \end{bmatrix} = \sum_{i=1}^{20} N_i(\xi, \eta, \zeta) \begin{bmatrix} u_i \\ v_i \\ w_i \end{bmatrix}. \quad (17.64)$$

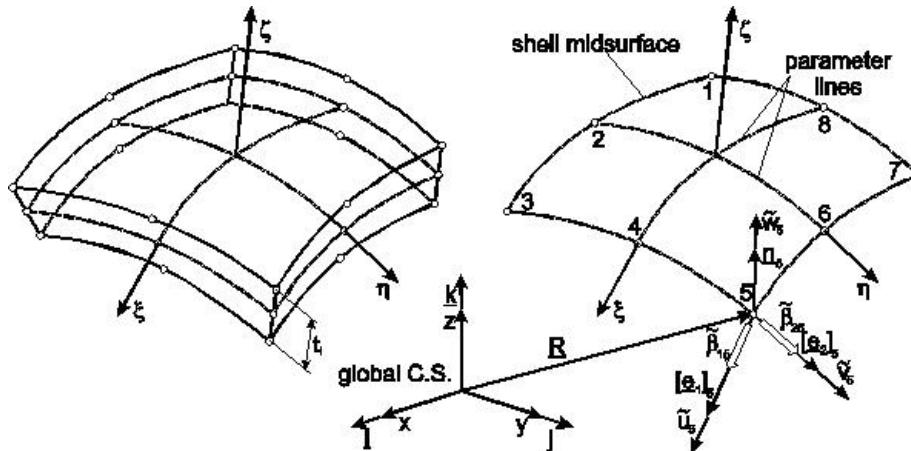


Fig.17.4. Quadratic two and three dimensional elements.

The thick-walled shell elements are constructed in accordance with isoparametric formulation, in this respect we point out that the sides perpendicularly to the shell midsurface are straight, i.e. the interpolation in the thickness direction is linear. The element is determined by the 8 nodes of the  $\zeta = 0$  midsurface. As it can be seen in Fig.17.4 the direction of the unit basis vectors changes from point to point, therefore the nodal number is indicated by subscript „ $i$ ”.

The coordinates of the points on the midsurface of the thick-walled shell element are given by:

$$\begin{bmatrix} x \\ y \\ z \end{bmatrix} = \sum_{i=1}^8 N_i(\xi, \eta) \begin{bmatrix} x_i \\ y_i \\ z_i \end{bmatrix} + \sum_{i=1}^8 N_i(\xi, \eta) \frac{\zeta}{2} t_i \underline{n}_i, \quad (17.65)$$

where  $\underline{n}_i$  are the column vector of normal vectors at the midsurface nodes,  $t_i$  is the thickness in the actual node,  $N_i$  are the interpolation functions, respectively. The interpolation functions are the same as those of the quadratic isoparametric plane membrane element (see section 12). The compact form of the interpolation function is:

$$N_i = \frac{1}{4} (1 + \xi \xi_i)(1 + \eta \eta_i)(\xi \xi_i + \eta \eta_i - 1), \quad i = 1, 3, 5, 7, \quad (17.66)$$

$$N_i = \frac{1}{2} \xi_i^2 (1 + \xi \xi_i)(1 - \eta^2) + \frac{1}{2} \eta_i^2 (1 + \eta \eta_i)(1 - \xi^2), \quad i = 2, 4, 6, 8,$$

where  $\xi_i$  and  $\eta_i$  are the local nodal coordinates. On the midsurface the  $\xi$  and  $\eta$  coordinate lines are orthogonal, therefore the basis vectors are calculated as:

$$\underline{n}_i = \frac{\underline{R}_{i,\xi} \times \underline{R}_{i,\eta}}{|\underline{R}_{i,\xi} \times \underline{R}_{i,\eta}|}, \quad \underline{e}_{2i} = \frac{\underline{R}_{i,\eta}}{|\underline{R}_{i,\eta}|}, \quad \underline{e}_{1i} = \underline{e}_{2i} \times \underline{n}_i. \quad (17.67)$$

The nodal displacement parameters are the  $u_i, v_i, w_i$  displacements and the  $\beta_{1i}$  and  $\beta_{2i}$  angle of rotations. In the case of eight nodes it means that the element has 40 degrees of freedom. Vector  $\underline{n}_i$  can be formulated by using the rotations and the basis vectors  $\underline{e}_{1i}, \underline{e}_{2i}$ :

$$\underline{n}_i = \tilde{\beta}_2 \underline{e}_{1i} - \tilde{\beta}_1 \underline{e}_{2i}, \quad (17.68)$$

which is the term capturing the transverse shear deformation, it causes an increment in  $u$  and  $v$ . According to the isoparametric representation the displacement field becomes:

$$\begin{bmatrix} u \\ v \\ w \end{bmatrix} = \sum_{i=1}^8 N_i(\xi, \eta) \begin{bmatrix} \tilde{u}_i \\ \tilde{v}_i \\ \tilde{w}_i \end{bmatrix} + \sum_{i=1}^8 N_i(\xi, \eta) \frac{\zeta}{2} t_i (\tilde{\beta}_{2i} \underline{e}_{1i} - \tilde{\beta}_{1i} \underline{e}_{2i}). \quad (17.69)$$

To calculate the stiffness matrix we have to establish the strain-displacement relationship. The derivatives of the displacement parameters with respect to the local coordinates are:

$$\begin{bmatrix} \frac{\partial u}{\partial \xi} \\ \frac{\partial u}{\partial \eta} \\ \frac{\partial u}{\partial \zeta} \end{bmatrix} = \sum_{i=1}^8 \begin{bmatrix} \frac{\partial N_i}{\partial \xi} [1 & -\frac{1}{2} t_i \zeta e_{2i}^x & \frac{1}{2} t_i \zeta e_{1i}^x] \\ \frac{\partial N_i}{\partial \eta} [1 & -\frac{1}{2} t_i \zeta e_{2i}^x & \frac{1}{2} t_i \zeta e_{1i}^x] \\ N_i [0 & -\frac{1}{2} t_i e_{2i}^x & \frac{1}{2} t_i e_{1i}^x] \end{bmatrix} \begin{bmatrix} \tilde{u}_i \\ \tilde{\beta}_{1i} \\ \tilde{\beta}_{2i} \end{bmatrix}. \quad (17.70)$$

For the other two components we obtain similar equations. The further computations require the Jacobi matrix and determinant [1,4,5]:

$$\begin{bmatrix} \frac{\partial}{\partial \xi} \\ \frac{\partial}{\partial \eta} \\ \frac{\partial}{\partial \zeta} \end{bmatrix} = \underline{J} \begin{bmatrix} \frac{\partial}{\partial x} \\ \frac{\partial}{\partial y} \\ \frac{\partial}{\partial z} \end{bmatrix}, \text{ and: } \begin{bmatrix} \frac{\partial}{\partial x} \\ \frac{\partial}{\partial y} \\ \frac{\partial}{\partial z} \end{bmatrix} = \underline{J}^{-1} \begin{bmatrix} \frac{\partial}{\partial \xi} \\ \frac{\partial}{\partial \eta} \\ \frac{\partial}{\partial \zeta} \end{bmatrix}. \quad (17.71)$$

The elements of the Jacobi matrix can be obtained using Eq.(17.65). Also, the derivatives of the displacement components can be determined in the global coordinate system. For example, the derivatives of the component  $u$  in matrix form are:

$$\begin{bmatrix} \frac{\partial u}{\partial x} \\ \frac{\partial u}{\partial y} \\ \frac{\partial u}{\partial z} \end{bmatrix} = \begin{bmatrix} J_{11}^{(-1)} & J_{12}^{(-1)} & J_{13}^{(-1)} \\ J_{21}^{(-1)} & J_{22}^{(-1)} & J_{23}^{(-1)} \\ J_{31}^{(-1)} & J_{32}^{(-1)} & J_{33}^{(-1)} \end{bmatrix} \begin{bmatrix} \frac{\partial u}{\partial \xi} \\ \frac{\partial u}{\partial \eta} \\ \frac{\partial u}{\partial \zeta} \end{bmatrix}, \quad (17.72)$$

where  $J_{ij}^{(-1)}$  are the elements of the inverse Jacobi matrix. Based on Eq.(17.70) we obtain the following:

$$\begin{aligned} \frac{\partial u}{\partial x} &= \sum_{i=1}^8 (J_{11}^{(-1)} \frac{\partial N_i}{\partial \xi} + J_{12}^{(-1)} \frac{\partial N_i}{\partial \eta}) \tilde{u}_i - \frac{1}{2} t_i e_{2i}^x \left\{ \zeta (J_{11}^{(-1)} \frac{\partial N_i}{\partial \xi} + J_{12}^{(-1)} \frac{\partial N_i}{\partial \eta}) + J_{13}^{(-1)} N_i \right\} \tilde{\beta}_{1i} + \\ &+ \frac{1}{2} t_i e_{1i}^x \left\{ \zeta (J_{11}^{(-1)} \frac{\partial N_i}{\partial \xi} + J_{12}^{(-1)} \frac{\partial N_i}{\partial \eta}) + J_{13}^{(-1)} N_i \right\} \tilde{\beta}_{2i} = \sum_{i=1}^8 \frac{\partial N_i}{\partial x} \tilde{u}_i + G_i^x (g_{1i}^x \tilde{\beta}_{1i} + g_{2i}^x \tilde{\beta}_{2i}), \end{aligned} \quad (17.73)$$

where:

$$G_i^x = \zeta (J_{11}^{(-1)} \frac{\partial N_i}{\partial \xi} + J_{12}^{(-1)} \frac{\partial N_i}{\partial \eta}) + J_{13}^{(-1)} N_i, \quad (17.74)$$

and:

$$\underline{g}_1^i = -\frac{1}{2}t_i e_{2i}, \underline{g}_2^i = \frac{1}{2}t_i e_{1i}. \quad (17.75)$$

The derivatives with respect to the other two coordinates are:

$$\begin{aligned} \frac{\partial u}{\partial y} &= \sum_{i=1}^8 (J_{21}^{(-1)} \frac{\partial N_i}{\partial \xi} + J_{22}^{(-1)} \frac{\partial N_i}{\partial \eta}) \tilde{u}_i - \frac{1}{2} t_i e_{2i}^x \left\{ \zeta (J_{21}^{(-1)} \frac{\partial N_i}{\partial \xi} + J_{22}^{(-1)} \frac{\partial N_i}{\partial \eta}) + J_{23}^{(-1)} N_i \right\} \tilde{\beta}_{1i} + \\ &+ \frac{1}{2} t_i e_{1i}^x \left\{ \zeta (J_{21}^{(-1)} \frac{\partial N_i}{\partial \xi} + J_{22}^{(-1)} \frac{\partial N_i}{\partial \eta}) + J_{23}^{(-1)} N_i \right\} \tilde{\beta}_{2i} = \sum_{i=1}^8 \frac{\partial N_i}{\partial y} \tilde{u}_i + G_i^y (g_{1i}^x \tilde{\beta}_{1i} + g_{2i}^x \tilde{\beta}_{2i}), \end{aligned} \quad (17.76)$$

$$\begin{aligned} \frac{\partial u}{\partial z} &= \sum_{i=1}^8 (J_{31}^{(-1)} \frac{\partial N_i}{\partial \xi} + J_{32}^{(-1)} \frac{\partial N_i}{\partial \eta}) \tilde{u}_i - \frac{1}{2} t_i e_{2i}^x \left\{ \zeta (J_{31}^{(-1)} \frac{\partial N_i}{\partial \xi} + J_{32}^{(-1)} \frac{\partial N_i}{\partial \eta}) + J_{33}^{(-1)} N_i \right\} \tilde{\beta}_{1i} + \\ &+ \frac{1}{2} t_i e_{1i}^x \left\{ \zeta (J_{31}^{(-1)} \frac{\partial N_i}{\partial \xi} + J_{32}^{(-1)} \frac{\partial N_i}{\partial \eta}) + J_{33}^{(-1)} N_i \right\} \tilde{\beta}_{2i} = \sum_{i=1}^8 \frac{\partial N_i}{\partial z} \tilde{u}_i + G_i^z (g_{1i}^x \tilde{\beta}_{1i} + g_{2i}^x \tilde{\beta}_{2i}), \end{aligned}$$

where:

$$G_i^y = \zeta (J_{21}^{(-1)} \frac{\partial N_i}{\partial \xi} + J_{22}^{(-1)} \frac{\partial N_i}{\partial \eta}) + J_{23}^{(-1)} N_i, \quad (17.77)$$

$$G_i^z = \zeta (J_{31}^{(-1)} \frac{\partial N_i}{\partial \xi} + J_{32}^{(-1)} \frac{\partial N_i}{\partial \eta}) + J_{33}^{(-1)} N_i.$$

Written in matrix form we have:

$$\begin{bmatrix} \frac{\partial u}{\partial x} \\ \frac{\partial u}{\partial y} \\ \frac{\partial u}{\partial z} \end{bmatrix} = \sum_{i=1}^8 \begin{bmatrix} \frac{\partial N_i}{\partial x} & G_i^x g_{1i}^x & G_i^x g_{2i}^x \\ \frac{\partial N_i}{\partial y} & G_i^y g_{1i}^x & G_i^y g_{2i}^x \\ \frac{\partial N_i}{\partial z} & G_i^z g_{1i}^x & G_i^z g_{2i}^x \end{bmatrix} \begin{bmatrix} \frac{\partial u}{\partial \xi} \\ \frac{\partial u}{\partial \eta} \\ \frac{\partial u}{\partial \zeta} \end{bmatrix}. \quad (17.78)$$

The derivatives of the other two components can be provided similarly. Using the derivatives we can calculate matrix  $\underline{\underline{B}}$ , which is the relationship between the strain components and the nodal displacement parameters:

$$\underline{\underline{\varepsilon}} = \underline{\underline{B}} \underline{\underline{\tilde{u}}}_e, \quad (17.79)$$

where  $\underline{\underline{\tilde{u}}}_e$  is the vector of nodal parameters in the local coordinate system. The vectors of strain and stress components in the global system are:

$$\underline{\underline{\varepsilon}}^T = [\varepsilon_x \quad \varepsilon_y \quad \varepsilon_z \quad \gamma_{xy} \quad \gamma_{yz} \quad \gamma_{xz}], \quad (17.80)$$

$$\underline{\underline{\sigma}}^T = [\sigma_x \quad \sigma_y \quad \sigma_z \quad \tau_{xy} \quad \tau_{yz} \quad \tau_{xz}].$$

Hooke's law in the local system can be written as:

$$\underline{\underline{\tilde{\sigma}}} = \underline{\underline{C}} \underline{\underline{\tilde{\varepsilon}}}, \quad (17.81)$$

where  $\underline{\underline{C}}$  is the constitutive matrix:

$$\underline{\underline{C}} = \frac{E}{1-\nu^2} \begin{bmatrix} 1 & \nu & 0 & 0 & 0 & 0 \\ \nu & 1 & 0 & 0 & 0 & 0 \\ 0 & 0 & 0 & 0 & 0 & 0 \\ 0 & 0 & 0 & \frac{1-\nu}{2} & 0 & 0 \\ 0 & 0 & 0 & 0 & k \frac{1-\nu}{2} & 0 \\ 0 & 0 & 0 & 0 & 0 & k \frac{1-\nu}{2} \end{bmatrix}. \quad (17.82)$$

The matrix above differs from the general three dimensional case in accordance with the followings. The stress normal to the shell surface is zero (3<sup>rd</sup> row, 3<sup>rd</sup> column). Since the element is thick-walled it considers also the effect of transverse shear deformation, but only in the form of an average stress. The constant in the elements of the 5<sup>th</sup> row, 5<sup>th</sup> column, and the 6<sup>th</sup> row, 6<sup>th</sup> column is a shear correction factor,  $k = 5/6$  [1,4,5]. The reason for that is the real distribution of the shear stresses is assumed to be parabolic over the thickness, and it is not constant as considered in the shell model. The correction factor  $k$  is the ratio of the strain energies from the two different distributions. Based on the transformation of local stress and strain components we can write the followings:

$$\underline{\underline{\tilde{\sigma}}} = \underline{\underline{T}} \underline{\underline{\sigma}}, \underline{\underline{\sigma}} = \underline{\underline{T}}^T \underline{\underline{\tilde{\sigma}}}, \quad (17.83)$$

$$\underline{\underline{\tilde{\varepsilon}}} = \underline{\underline{T}} \underline{\underline{\varepsilon}}, \underline{\underline{\varepsilon}} = \underline{\underline{T}}^T \underline{\underline{\tilde{\varepsilon}}},$$

where  $\underline{\underline{T}}$  is the transformation matrix for general spatial stress and strain states. The calculation of  $\underline{\underline{T}}$  is possible using the definitions given by Eq.(11.62). Taking back Eq.(17.83) into Hooke's law we have:

$$\underline{\underline{\tilde{\sigma}}} = \underline{\underline{C}} \underline{\underline{\tilde{\varepsilon}}}. \quad (17.84)$$

The premultiplication with  $\underline{\underline{T}}^{-1}$  leads to:

$$\underline{\underline{T}}^{-1} \underline{\underline{T}} \underline{\sigma} = \underline{\underline{T}}^{-1} \underline{\underline{C}} \underline{\underline{T}} \underline{\varepsilon}. \quad (17.85)$$

Since  $\underline{\underline{T}}$  is an orthogonal matrix we can write that:  $\underline{\underline{T}}^{-1} \underline{\underline{T}} = \underline{\underline{E}}$ , and  $\underline{\underline{T}}^T = \underline{\underline{T}}^{-1}$ , viz.:

$$\underline{\sigma} = \underline{\underline{T}}^T \underline{\underline{C}} \underline{\underline{T}} \underline{\varepsilon}. \quad (17.86)$$

The transformation matrix is [4]:

$$\underline{\underline{T}} = \begin{bmatrix} l_{1i}^2 & m_{1i}^2 & n_{1i}^2 & l_{1i}m_{1i} & m_{1i}n_{1i} & n_{1i}l_{1i} \\ l_{2i}^2 & m_{2i}^2 & n_{2i}^2 & l_{2i}m_{2i} & m_{2i}n_{2i} & n_{2i}l_{2i} \\ l_{3i}^2 & m_{3i}^2 & n_{3i}^2 & l_{3i}m_{3i} & m_{3i}n_{3i} & n_{3i}l_{3i} \\ 2l_{1i}l_{2i} & 2m_{1i}m_{2i} & 2n_{1i}n_{2i} & l_{1i}m_{2i} + l_{2i}m_{1i} & m_{1i}n_{2i} + m_{2i}n_{1i} & n_{1i}l_{2i} + n_{2i}l_{1i} \\ 2l_{2i}l_{3i} & 2m_{2i}m_{3i} & 2n_{2i}n_{3i} & l_{2i}m_{3i} + l_{3i}m_{2i} & m_{2i}n_{3i} + m_{3i}n_{2i} & n_{2i}l_{3i} + n_{3i}l_{2i} \\ 2l_{3i}l_{1i} & 2m_{3i}m_{1i} & 2n_{3i}n_{1i} & l_{3i}m_{1i} + l_{1i}m_{3i} & m_{3i}n_{1i} + m_{1i}n_{3i} & n_{3i}l_{1i} + n_{1i}l_{3i} \end{bmatrix}, \quad (17.87)$$

where  $l_i$ ,  $m_i$  and  $n_i$  are the direction cosines of the unit basis vectors at the actual point [4,7]:

$$l_{1i} = \cos(i, e_{1i}), m_{1i} = \cos(j, e_{1i}), n_{1i} = \cos(k, e_{1i}), \quad (17.88)$$

$$l_{2i} = \cos(i, e_{2i}), m_{2i} = \cos(j, e_{2i}), n_{2i} = \cos(k, e_{2i}),$$

$$l_{3i} = \cos(i, e_{3i}), m_{3i} = \cos(j, e_{3i}), n_{3i} = \cos(k, e_{3i}).$$

The transformation matrix should be evaluated in the nodes, moreover due to the numerical integration even in the integration points. The stiffness matrix in the global coordinate system can be calculated using Eq.(15.17):

$$\underline{\underline{K}}_e = \int_{V_e} \underline{\underline{B}}^T \underline{\underline{T}} \underline{\underline{C}}^T \underline{\underline{T}}^T \underline{\underline{B}} dV = \int_{V_e} \underline{\underline{B}}^T \underline{\underline{T}} \underline{\underline{C}}^T \underline{\underline{T}}^T \underline{\underline{B}} J d\xi d\eta d\zeta, \quad (17.89)$$

where  $J$  is the Jacobi determinant, which can be calculated using Eqs.(17.65) and (17.71). For the determination of the force vector we recall the displacement vector field in the usual form:

$$\underline{u}(\xi, \eta, \zeta) = \underline{\underline{N}} \tilde{\underline{u}}_e, \quad (17.90)$$

where  $\underline{\underline{N}}$  is the matrix of interpolation polynomials. As a result, the vectors of body, surface and line forces in the global coordinate system are:

$$\tilde{\underline{F}}_{eb} = \int_{V_e} \underline{\underline{N}}^T \underline{p}_b dV = \int_{V_e} \underline{\underline{N}}^T \underline{p}_b J d\xi d\eta d\zeta, \quad (17.91)$$

$$\tilde{\underline{F}}_{ep} = \int_{A_e} \underline{\underline{N}}^T \underline{p}_p dA = \int_{A_e} \underline{\underline{N}}^T \underline{p}_p J d\xi d\eta,$$

$$\tilde{\underline{F}}_{el} = \int_S \underline{\underline{N}}^T \underline{p}_l dS,$$

which can be determined by transformation into the global system in a similar way to that presented in section 16. In the nodes concentrated forces may act, the relevant vector can be obtained in the same way as that shown in plate elements. Because of the high number of nodes it is not detailed here. The finite element equilibrium equation is formed in the usual way, for a single element it is:

$$\underline{\underline{K}}_e \underline{u}_e = \underline{F}_e, \quad (17.92)$$

where  $\underline{F}_e$  is the sum of the vectors of body, surface, line and concentrated forces. Finally, the structural equation is:

$$\underline{\underline{K}} \underline{U} = \underline{F}. \quad (17.93)$$

### 17.5. A shell-solid transition element

In complex structures sometimes there is the necessity of the simultaneous application of solid and thick-walled shell elements. These elements can not be connected directly, because the nodal degrees of freedom are not identical. In these cases it is reasonable to use a transition element between the solid and shell elements [1,4,5]. A quadratic transition element is shown in Fig.17.5, where the nodes 1-8 are located in the solid side, nodes 10-12 care located in the shell side of the element.

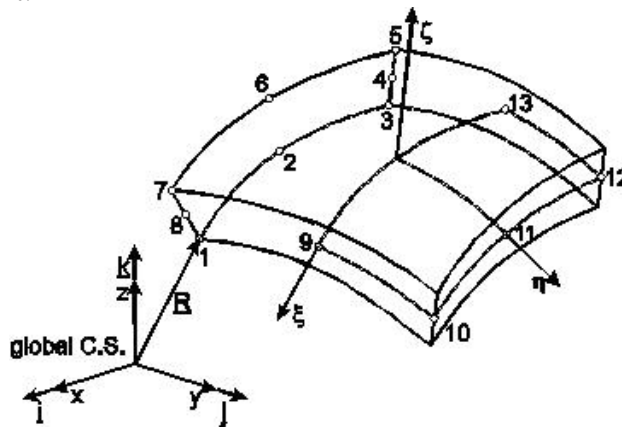


Fig.17.5. A shell-solid transition element.

The geometry of the transition element is captured by the function below:

$$\begin{bmatrix} x \\ y \\ z \end{bmatrix} = \sum_{i=1}^8 N_i(\xi, \eta, \zeta) \begin{bmatrix} x_i \\ y_i \\ z_i \end{bmatrix} + \sum_{i=9}^{13} N_i(\xi, \eta) \begin{bmatrix} x_i \\ y_i \\ z_i \end{bmatrix} + \sum_{i=9}^{13} N_i(\xi, \eta) \frac{\zeta}{2} t_i \underline{n}. \quad (17.94)$$

The indices  $i = 1 \dots 8$  refer to the interpolation function of the solid element given by Eq.(17.64), if  $i = 9 \dots 13$  then the actual interpolation functions of the thick-walled shell elements are referred to in accordance with Eq.(17.65). The composed system of functions satisfies the following conditions [1]:

$$\sum_{i=1}^8 N_i(\xi, \eta, \zeta) + \sum_{i=9}^{13} N_i(\xi, \eta) = 1, \quad (17.95)$$

$$N_i(\xi_j, \eta_j, \zeta_j) = \begin{cases} 0, & \text{if } i \neq j \\ 1, & \text{if } i = j \end{cases},$$

$$N_i(\xi_j, \eta_j) = \begin{cases} 0, & \text{if } i \neq j \\ 1, & \text{if } i = j \end{cases},$$

where  $\xi_j$ ,  $\eta_j$  and  $\zeta_j$  are the nodal coordinates in the local coordinate system. Similarly to the thick-walled shell elements the displacement field is expressed by:

$$\begin{bmatrix} u \\ v \\ w \end{bmatrix} = \sum_{i=1}^8 N_i(\xi, \eta, \zeta) \begin{bmatrix} \tilde{u}_i \\ \tilde{v}_i \\ \tilde{w}_i \end{bmatrix} + \sum_{i=9}^{13} N_i(\xi, \eta) \begin{bmatrix} \tilde{u}_i \\ \tilde{v}_i \\ \tilde{w}_i \end{bmatrix} + \sum_{i=8}^{13} N_i(\xi, \eta) \frac{\zeta}{2} t_i (\tilde{\beta}_{2i} e_{1i} - \tilde{\beta}_{1i} e_{2i}). \quad (17.96)$$

The degrees of freedom in nodes 1-8 are equal to three, in nodes 9-13 there are five degrees of freedom. Consequently the transition element has 49 degrees of freedom. The further calculations can be performed in similar fashion to that presented in the thick-walled shell element.

## 17.6. Bibliography

- [1] Imre Bojtár, Gábor Vörös, *Application of the finite element method to plate and shell structures*. Technical Book Publisher, 1986, Budapest (in Hungarian).
- [2] Gábor Vörös, *Lectures and practices of the subject Applied mechanics, manuscript*, Budapest University of Technology and Economics, Faculty of Mechanical Engineering, Department of Applied Mechanics, 1978, I. semester, Budapest (in Hungarian).
- [3] Singiresu S. Rao, *The finite element method in engineering – fourth edition*, Elsevier Science & Technology Books, 2004,
- [4] Klaus-Jürgen Bathe, *Finite element procedures*. Prentice Hall, Upper Saddle River, 1996, New Jersey 17458.
- [5] Thomas J. Hughes, *The finite element method – Linear static and dynamic finite element analysis*. Prentice Hall Inc., A division of Simon & Schuster, Englewood Cliffs, 1987, New Jersey 07632.
- [6] O.C. Zienkiewicz, R.L. Taylor. *The finite element method – fifth edition, Volume 2: Solid mechanics*. Butterworth-Heinemann, 2000, Oxford, Auckland, Boston, Johannesburg, Melbourne, New Delhi.

- [7] Pei Chi Chou, Nicholas J. Pagano, *Elasticity – Tensor, dyadic and engineering approaches*. D. Van Nostrand Company, Inc., 1967, Princeton, New Jersey, Toronto, London.

## 18. ANALYSIS OF 3D PROBLEMS WITH FINITE ELEMENT BASED PROGRAM SYSTEMS. INTRODUCTION OF 3D ELEMENTS.

In several cases, the geometry of a structure or a body cannot be modeled as a line or surface. In that special case it has to be modeled as a body. Bodies like these can only be approximated by 3D elements in order to prevail neglecting important parts. Complex geometry appears in simple structures as well. For example, if a welded beam structure is modeled, then it is suitable to use beam elements which is able to analyze the stress state of the structure. If the stress state has to be analyzed in the joints of a structure, then shell model must be applied. If the weld coalescences have to be examined as well, then 3D model must be applied. Naturally, the more precise modeling which involves more nodes, increases the amount of calculations as well.

The 3D elements can be hexahedrons, tetrahedron, less often pentahedron (these elements can be derived from hexahedrons) which can be described by linear-, quadratic or higher degree of basis functions.

### 18.1. Hexahedron elements

The hexahedron elements are mapped to a cube with unit length of two. Depending on the degree of the approximating polynomial, elements with 8, 20 or 32 nodes can be used as well.

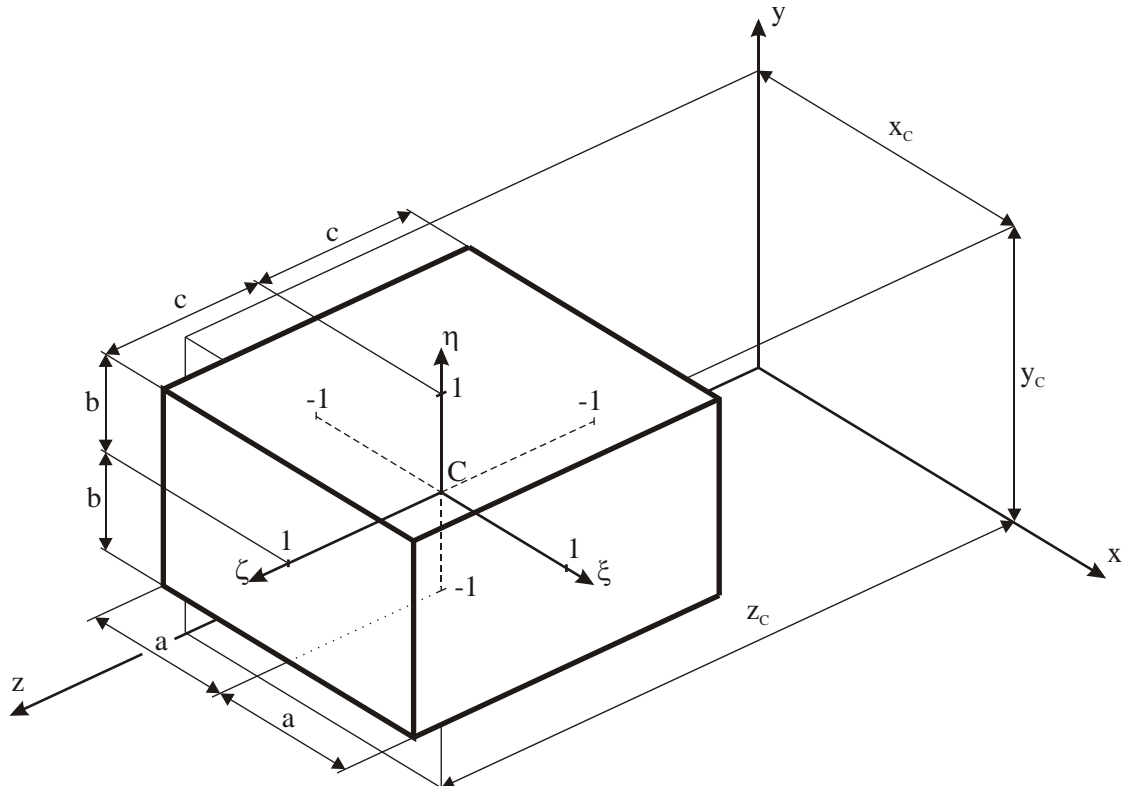


Figure 18.1.: Local coordinate system of the Hexahedron

The local coordinate system is derived from the global coordinates and the  $2a$ ,  $2b$ ,  $2c$  lengths of the cube. These coordinates are:

$$\xi = \frac{x - x_c}{a}, \quad (18.1)$$

$$\eta = \frac{y - y_c}{b} \text{ and} \quad (18.2)$$

$$\zeta = \frac{z - z_c}{c}. \quad (18.3)$$

Then the derivatives:

$$d\xi = \frac{dx}{a}, \quad (18.4)$$

$$d\eta = \frac{dy}{b} \text{ és} \quad (18.5)$$

$$d\zeta = \frac{dz}{c}. \quad (18.6)$$

#### 18.1.1. Hexahedron element with 8 nodes

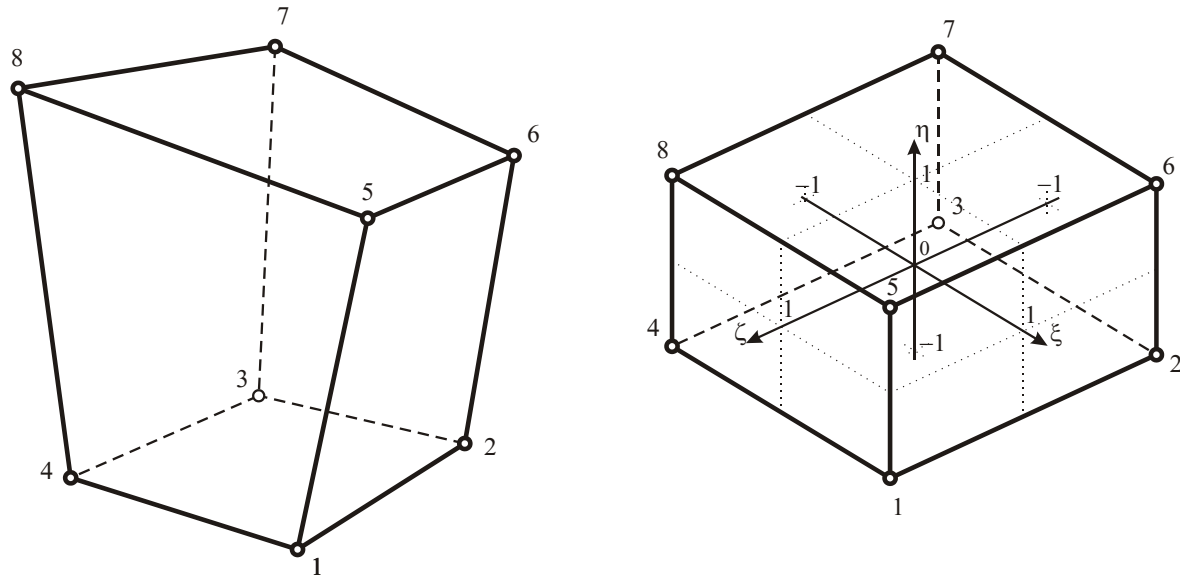


Figure 18.2.: Hexahedron with 8 nodes and the mapped cube

If the investigated body is to be analyzed by linear hexahedrons, then elements with 8 nodes must be used. The element is approximated by:

$$x = \sum N_i(\xi, \eta, \zeta) \cdot x_i, \quad (18.7)$$

$$y = \sum N_i(\xi, \eta, \zeta) \cdot y_i \text{ and} \quad (18.8)$$

$$z = \sum N_i(\xi, \eta, \zeta) \cdot z_i \quad (18.9)$$

formulas, where  $N_i(\xi, \eta, \zeta)$  is the basis function of the  $i^{th}$  node:

$$N_i = \frac{1}{8}(1 + \xi \xi_i)(1 + \eta \eta_i)(1 + \zeta \zeta_i), \quad (18.10)$$

where  $\xi_i, \eta_i, \zeta_i$  are the local coordinates of  $i^{th}$  node.

The  $\underline{\underline{J}}$  Jacobi-matrix determines the relationship between the local and global derivatives of the basis function:

$$\partial_{loc} N_i(\xi, \eta, \zeta) = \underline{\underline{J}} [\partial_{glob} N_i(\xi, \eta, \zeta)], \text{ where} \quad (18.11)$$

$$\underline{\underline{J}} = \begin{bmatrix} \frac{\partial x}{\partial \xi} & \frac{\partial y}{\partial \xi} & \frac{\partial z}{\partial \xi} \\ \frac{\partial x}{\partial \eta} & \frac{\partial y}{\partial \eta} & \frac{\partial z}{\partial \eta} \\ \frac{\partial x}{\partial \zeta} & \frac{\partial y}{\partial \zeta} & \frac{\partial z}{\partial \zeta} \end{bmatrix}. \quad (18.12)$$

The basis functions, similarly to (3.20) equation, are interpolation functions. These functions can be used to approximate the displacement of the element, thus there is no need to introduce new interpolation functions but to apply the (18.10) basis functions in case of a hexahedron element with 8 nodes.

$$u = \sum N_i(\xi, \eta, \zeta) \cdot u_i,$$

$$v = \sum N_i(\xi, \eta, \zeta) \cdot v_i,$$

$$w = \sum N_i(\xi, \eta, \zeta) \cdot w_i.$$

The described elements are named as **isoparametric** elements.

### 18.1.2. Hexahedron element with 20 nodes

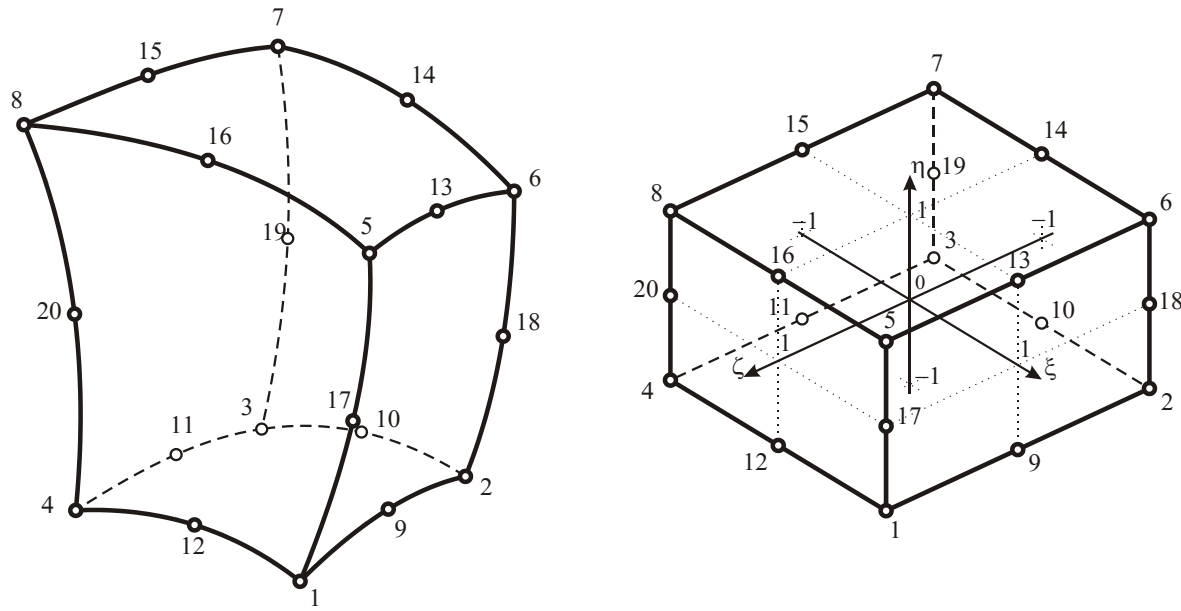


Figure 18.3.: Hexahedron with 20 nodes and the mapped cube

If the investigated body is to be described by quadratic hexahedrons, then elements with 20 nodes must be used. The element is approximated by:

$$x = \sum N_i(\xi, \eta, \zeta) \cdot x_i,$$

$$y = \sum N_i(\xi, \eta, \zeta) \cdot y_i \text{ and}$$

$$z = \sum N_i(\xi, \eta, \zeta) \cdot z_i$$

formulas, where  $N_i(\xi, \eta, \zeta)$  is the basis function of the  $i^{th}$  node. In case of an element with 20 nodes, the nodes in the corners and the nodes in the middle of the sides must be distinguished.

In case the node is located in a corner, the basis function is:

$$N_i = \frac{1}{8} (1 + \xi \xi_i)(1 + \eta \eta_i)(1 + \zeta \zeta_i)(\xi \xi_i + \eta \eta_i + \zeta \zeta_i - 2), \quad (18.13)$$

where  $\xi_i, \eta_i, \zeta_i$  are the local coordinate of corner  $i$ .

In case the node is located at the middle of a side, the basis function is:

If  $\xi_i = 0$ , then

$$N_i = \frac{1}{4} (1 - \xi^2)(1 + \eta \eta_i)(1 + \zeta \zeta_i). \quad (18.14)$$

If  $\eta_i = 0$ , then

$$N_i = \frac{1}{4} (1 + \xi \zeta_i) (1 - \eta^2) (1 + \zeta \zeta_i). \quad (18.15)$$

If  $\zeta_i = 0$ , then

$$N_i = \frac{1}{4} (1 + \xi \zeta_i) (1 + \eta \eta_i) (1 - \zeta^2), \quad (18.16)$$

where  $\xi, \eta, \zeta$  are the local coordinates of node  $i$  at the middle of the side.

Similarly to the element with 8 nodes, the  $\underline{\underline{J}}$  Jacobi-matrix determines the relationship between the local and global derivatives of the basis function:

$$\partial_{loc} N_i(\xi, \eta, \zeta) = \underline{\underline{J}} [\partial_{glob} N_i(\xi, \eta, \zeta)], \text{ where}$$

$$\underline{\underline{J}} = \begin{bmatrix} \frac{\partial x}{\partial \xi} & \frac{\partial y}{\partial \xi} & \frac{\partial z}{\partial \xi} \\ \frac{\partial x}{\partial \eta} & \frac{\partial y}{\partial \eta} & \frac{\partial z}{\partial \eta} \\ \frac{\partial x}{\partial \zeta} & \frac{\partial y}{\partial \zeta} & \frac{\partial z}{\partial \zeta} \end{bmatrix}.$$

If (18.13)-(18.16) basis functions are used to approximate the displacement of a hexahedron with 20 nodes, then the elements are named as **isoparametric** elements as well.

### 18.1.3. Hexahedron element with 32 nodes

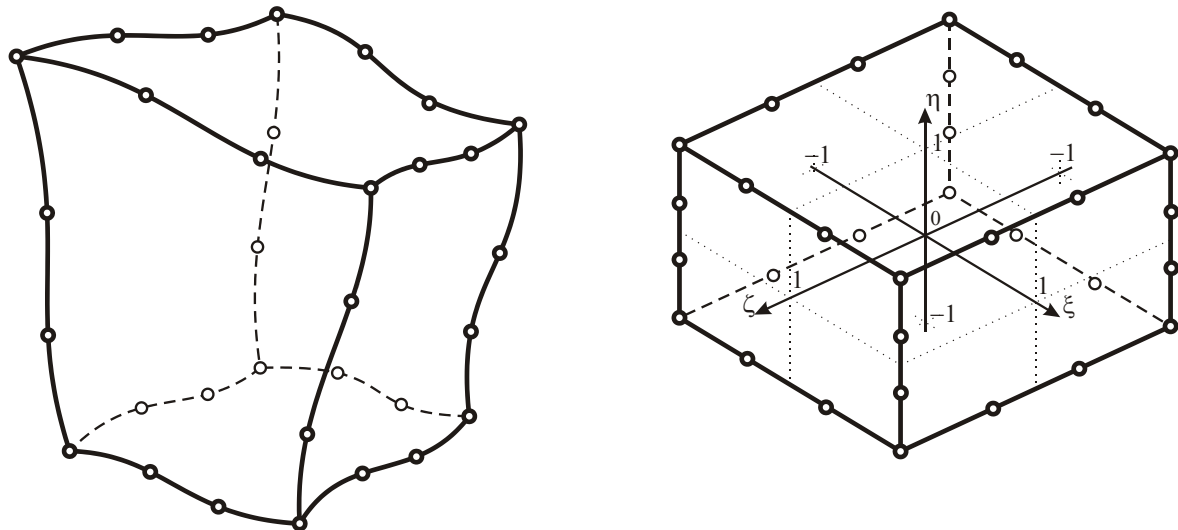


Figure 18.4.: Hexahedron with 32 nodes and the mapped cube

If the investigated body is to be described by cubic hexahedrons, then elements with 32 nodes must be used. The element is approximated by:

$$x = \sum N_i(\xi, \eta, \zeta) \cdot x_i,$$

$$y = \sum N_i(\xi, \eta, \zeta) \cdot y_i \text{ and}$$

$$z = \sum N_i(\xi, \eta, \zeta) \cdot z_i$$

formulas, where  $N_i(\xi, \eta, \zeta)$  is the basis function of the  $i^{th}$  node. In case of an element with 32 nodes, the nodes in the corners and the nodes along the sides must be distinguished.

In case the node is located in a corner, the basis function is:

$$N_i = \frac{1}{64} (1 + \xi \xi_i) (1 + \eta \eta_i) (1 + \zeta \zeta_i) [9(\xi^2 + \eta^2 + \zeta^2) - 19], \quad (18.17)$$

where  $\xi_i, \eta_i, \zeta_i$  are the local coordinates of corner  $i$ .

The basis functions at the point of the third length of the side:

If  $\xi_i = \pm \frac{1}{3}$ , then

$$N_i = \frac{9}{64} (1 - \xi^2) (1 + 9\xi \xi_i) (1 + \eta \eta_i) (1 + \zeta \zeta_i). \quad (18.18)$$

If  $\eta_i = \pm \frac{1}{3}$ , then

$$N_i = \frac{9}{64} (1 + \xi \xi_i) (1 - \eta^2) (1 + 9\eta \eta_i) (1 + \zeta \zeta_i). \quad (18.19)$$

If  $\zeta_i = \pm \frac{1}{3}$ , then

$$N_i = \frac{9}{64} (1 + \xi \xi_i) (1 + \eta \eta_i) (1 - \zeta^2) (1 + 9\zeta \zeta_i), \quad (18.20)$$

where  $\xi_i, \eta_i, \zeta_i$  are the local coordinates of node  $i$  along the side.

Similarly to the earlier, the  $\underline{\underline{J}}$  Jacobi-matrix determines the relationship between the local and global derivatives of the basis function:

$$\partial_{lok} N_i(\xi, \eta, \zeta) = \underline{\underline{J}} [\partial_{glob} N_i(\xi, \eta, \zeta)], \text{ where}$$

$$\underline{\underline{J}} = \begin{bmatrix} \frac{\partial x}{\partial \xi} & \frac{\partial y}{\partial \xi} & \frac{\partial z}{\partial \xi} \\ \frac{\partial x}{\partial \eta} & \frac{\partial y}{\partial \eta} & \frac{\partial z}{\partial \eta} \\ \frac{\partial x}{\partial \zeta} & \frac{\partial y}{\partial \zeta} & \frac{\partial z}{\partial \zeta} \end{bmatrix}.$$

If (18.17)-(18.20) basis functions are used to approximate the displacement of a hexahedron with 32 nodes, then the elements are named as **isoparametric** elements as well.

#### 18.1.4. Pentagon elements

Among the pentagon elements mostly the prism and the pyramid is used, which are described as a degenerated hexahedron.

### 18.2. Tetrahedron elements

Basis functions can be described in two kinds of coordinate systems in case of tetrahedron elements: in a coordinate system where the element is mapped as a tetrahedron with unit lengths, or in a so-called volume coordinate system (same as in the ANSYS). Both way of description will be introduced.

In case of the first description, the origin of the local coordinate system is allocated in one corner of the tetrahedron (Figure 18.5.).

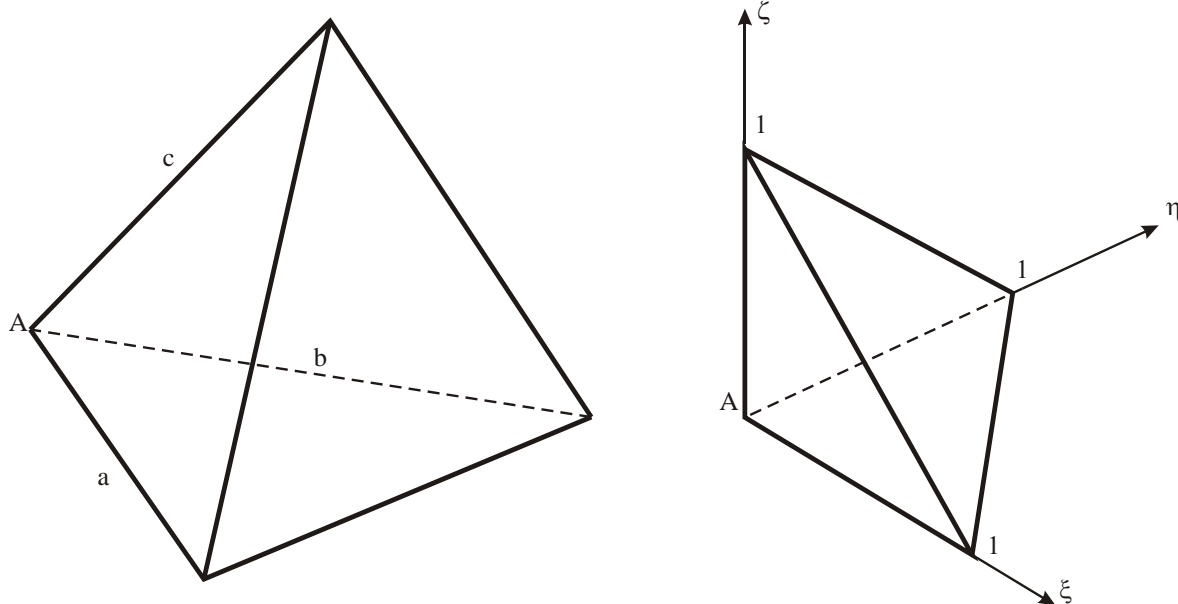


Figure 18.5.: Tetrahedron in the unit length coordinate system

In this origin, the local coordinates are described by the  $a, b, c$  lengths:

$$\xi = \frac{x - x_A}{a}, \quad (18.21)$$

$$\eta = \frac{y - y_A}{b} \text{ and} \quad (18.22)$$

$$\zeta = \frac{z - z_A}{c}. \quad (18.23)$$

The volume coordinate system is defined by the following equation system:

$$\begin{aligned} x &= L_1 x_1 + L_2 x_2 + L_3 x_3 + L_4 x_4, \\ y &= L_1 y_1 + L_2 y_2 + L_3 y_3 + L_4 y_4 \\ z &= L_1 z_1 + L_2 z_2 + L_3 z_3 + L_4 z_4 \\ 1 &= L_1 + L_2 + L_3 + L_4 \end{aligned} \quad (18.24)$$

$x, y, z$  are the global coordinates of an inner point,  $x_1, \dots, z_4$  are the global coordinates of the corners,  $L_1, \dots, L_4$  are the volume coordinates. By solving the (18.24) equation system the volume coordinates are:

$$L_1 = \frac{a_1 + b_1 x + c_1 y + d_1 z}{6V},$$

$$L_2 = \frac{a_2 + b_2 x + c_2 y + d_2 z}{6V},$$

$$L_3 = \frac{a_3 + b_3 x + c_3 y + d_3 z}{6V},$$

$$L_4 = \frac{a_4 + b_4 x + c_4 y + d_4 z}{6V}, \text{ where}$$

$a_1, \dots, d_4$  are constants, and  $V$  is the volume of the tetrahedron. By setting and simplifying the formulas, the single coordinates can be calculated at any inner  $P$  point of the tetrahedron, if the original body is divided into four tetrahedrons with respect of point  $P$ .

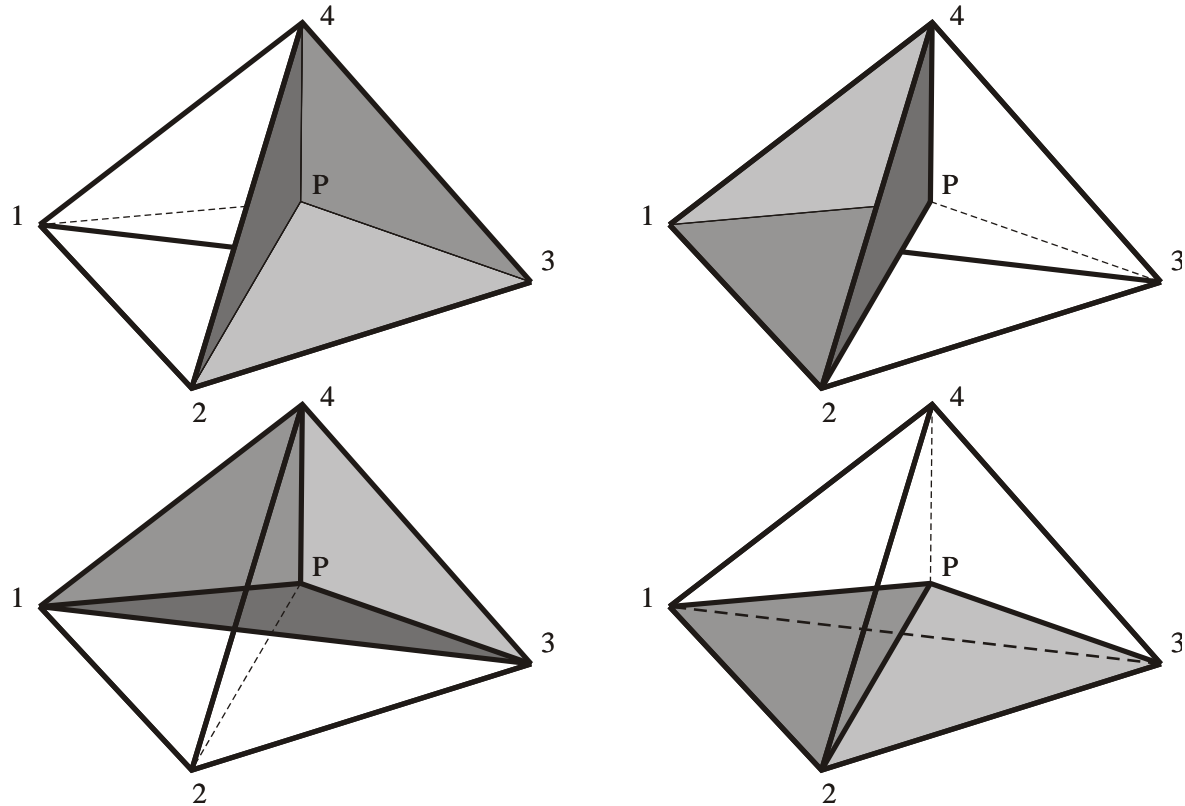


Figure 18.6.: Discretization of tetrahedron for volume coordinates

Thus the volume coordinates of  $P$  – related to each corner – can be obtained as the ratio of the opposite volume of the examined small tetrahedron and the volume of the original tetrahedron:

$$L_1 = \frac{V_{P234}}{V}, \quad L_2 = \frac{V_{P134}}{V}, \quad L_3 = \frac{V_{P124}}{V}, \quad L_4 = \frac{V_{P123}}{V}. \quad (18.25)$$

### 18.2.1. Tetrahedron element with 4 nodes

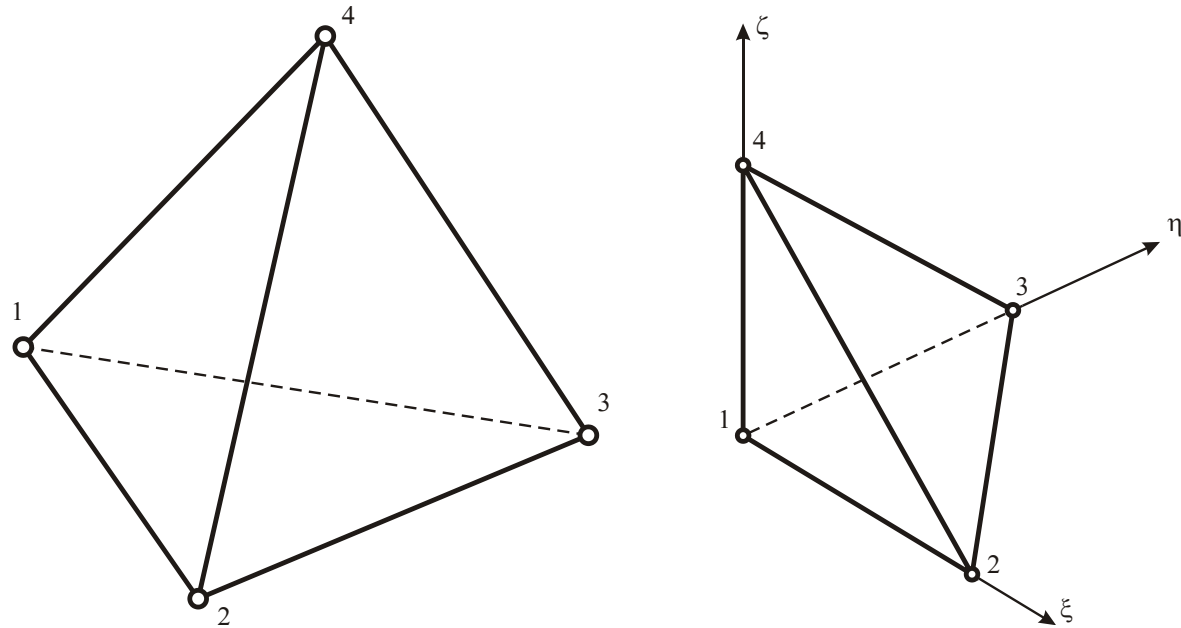


Figure 18.7.: Map of tetrahedron element with 4 nodes to  $\xi, \eta, \zeta$  coordinates

If the investigated geometry of the body is to be described by linear tetrahedrons, then elements with 4 nodes must be used. In a  $\xi, \eta, \zeta$  coordinate system the element is approximated by:

$$x = \sum N_i(\xi, \eta, \zeta) \cdot x_i,$$

$$y = \sum N_i(\xi, \eta, \zeta) \cdot y_i \text{ and}$$

$$z = \sum N_i(\xi, \eta, \zeta) \cdot z_i,$$

where  $N_i(\xi, \eta, \zeta)$  is the basis function related to the  $i$  node:

$$N_1 = 1 - \xi - \eta - \zeta, \quad (18.26)$$

$$N_2 = \xi, \quad (18.27)$$

$$N_3 = \eta, \quad (18.28)$$

$$N_4 = \zeta. \quad (18.29)$$

In volume coordinate system the shape is approximated by:

$$x = \sum N_i(L_1, L_2, L_3, L_4) \cdot x_i,$$

$$y = \sum N_i(L_1, L_2, L_3, L_4) \cdot y_i \text{ and}$$

$$z = \sum N_i(L_1, L_2, L_3, L_4) \cdot z_i$$

Formulas, where  $N_i(L_1, L_2, L_3, L_4)$  is the basis function of  $i$  node:

$$N_1 = L_1, \quad (18.30)$$

$$N_2 = L_2, \quad (18.31)$$

$$N_3 = L_3, \quad (18.32)$$

$$N_4 = L_4. \quad (18.33)$$

### 18.2.2. Tetrahedron element with 10 nodes

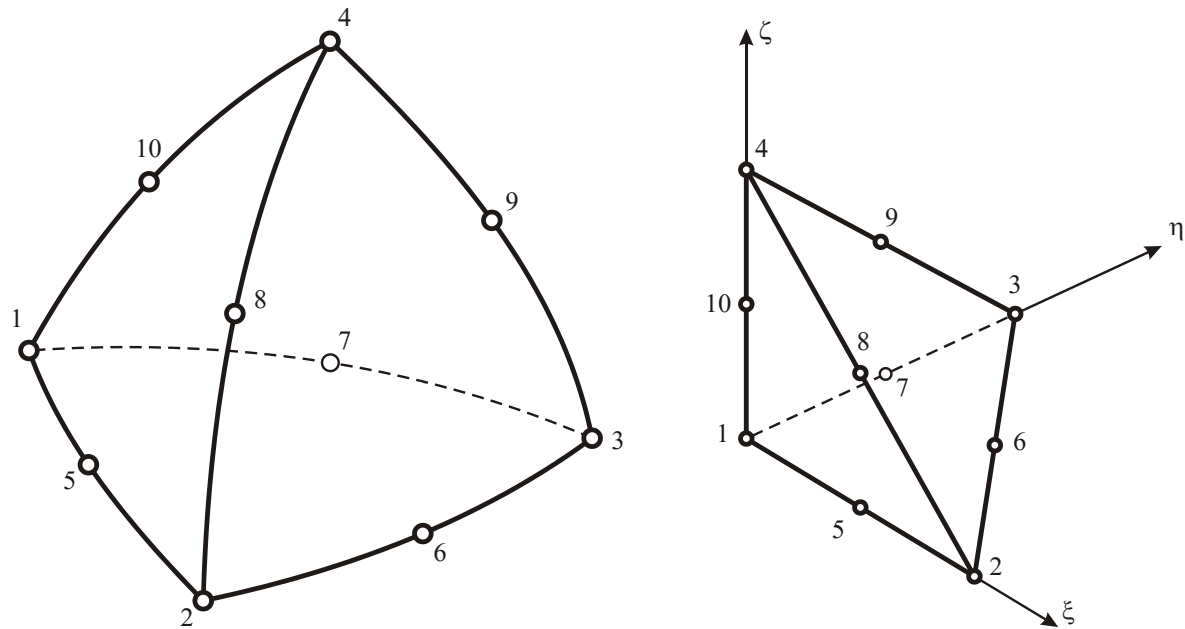


Figure 18.8.: Map of tetrahedron element with 10 nodes to  $\xi, \eta, \zeta$  coordinates

If the investigated geometry of the body is to be described by quadratic tetrahedrons, then elements with 10 nodes must be used. In a  $\xi, \eta, \zeta$  coordinate system the element is approximated by:

$$x = \sum N_i(\xi, \eta, \zeta) \cdot x_i,$$

$$y = \sum N_i(\xi, \eta, \zeta) \cdot y_i \text{ and}$$

$$z = \sum N_i(\xi, \eta, \zeta) \cdot z_i$$

where  $N_i(\xi, \eta, \zeta)$  is the basis function related to the  $i$  node in the corners:

$$N_1 = 1 - \xi - \eta - \zeta - 2\xi(1 - \xi - \eta - \zeta) - 2\eta(1 - \xi - \eta - \zeta) - 2\zeta(1 - \xi - \eta - \zeta),$$

$$N_2 = \xi - 2\xi(1 - \xi - \eta - \zeta) - 2\xi\eta - 2\xi\zeta,$$

$$N_3 = \eta - 2\xi\eta - 2\eta(1 - \xi - \eta - \zeta) - 2\eta\zeta,$$

$$N_4 = \zeta - 2\xi\zeta - 2\eta\zeta - 2\zeta(1 - \xi - \eta - \zeta).$$

The nodes in the middle of the sides:

$$N_5 = 4\xi(1 - \xi - \eta - \zeta),$$

$$N_6 = 4\xi\eta,$$

$$N_7 = 4\eta(1 - \xi - \eta - \zeta),$$

$$N_8 = 4\xi\zeta,$$

$$N_9 = 4\eta\zeta,$$

$$N_{10} = 4\zeta(1 - \xi - \eta - \zeta).$$

In volume coordinate system the shape is approximated by:

$$x = \sum N_i(L_1, L_2, L_3, L_4) \cdot x_i,$$

$$y = \sum N_i(L_1, L_2, L_3, L_4) \cdot y_i \text{ and}$$

$$z = \sum N_i(L_1, L_2, L_3, L_4) \cdot z_i$$

where  $N_i(L_1, L_2, L_3, L_4)$  is the basis function related to the  $i$  node.

Basis functions in the corners:

$$N_1 = L_1(2L_1 - 1),$$

$$N_2 = L_2(2L_2 - 1),$$

$$N_3 = L_3(2L_3 - 1),$$

$$N_4 = L_4(2L_4 - 1).$$

In the middle of the sides:

$$N_5 = 4L_1L_2,$$

$$N_6 = 4L_2L_3,$$

$$N_7 = 4L_1L_3,$$

$$N_8 = 4L_2L_4,$$

$$N_9 = 4L_3L_4,$$

$$N_{10} = 4L_1L_4.$$

The advantage of the volume coordinate system becomes more obvious since the basis functions are simple and similar to each other.

### 18.2.3. Tetrahedron element with 20 nodes

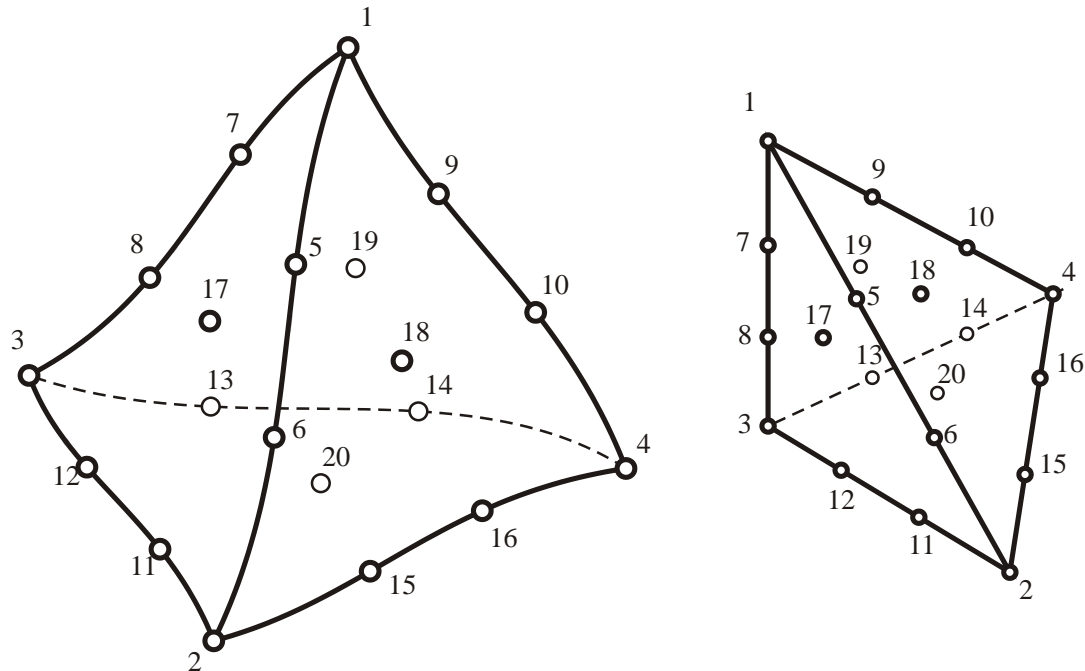


Figure 18.9.: Tetrahedron element with 20 nodes

If the investigated geometry of the body is to be described by cubic tetrahedrons, then elements with 20 nodes must be used.

Since the volume coordinate description has a simpler form, only this method will be presented. In volume coordinate system the shape is approximated by:

$$x = \sum N_i(L_1, L_2, L_3, L_4) \cdot x_i,$$

$$y = \sum N_i(L_1, L_2, L_3, L_4) \cdot y_i \text{ and}$$

$$z = \sum N_i(L_1, L_2, L_3, L_4) \cdot z_i$$

where  $N_i(L_1, L_2, L_3, L_4)$  is the basis function related to the  $i$  node.

Basis functions in the corners:

$$N_1 = \frac{1}{2} L_1(3L_1 - 1)(3L_1 - 2),$$

$$N_2 = \frac{1}{2} L_2(3L_2 - 1)(3L_2 - 2),$$

$$N_3 = \frac{1}{2} L_3(3L_3 - 1)(3L_3 - 2),$$

$$N_4 = \frac{1}{2} L_4(3L_4 - 1)(3L_4 - 2).$$

Basis functions in the middle of the sides:

$$N_5 = \frac{9}{2} L_1 L_2 (3L_1 - 1), \quad N_6 = \frac{9}{2} L_1 L_2 (3L_2 - 1),$$

$$N_7 = \frac{9}{2} L_1 L_3 (3L_1 - 1), \quad N_8 = \frac{9}{2} L_1 L_3 (3L_3 - 1),$$

$$N_9 = \frac{9}{2} L_1 L_4 (3L_1 - 1), \quad N_{10} = \frac{9}{2} L_1 L_4 (3L_4 - 1),$$

$$N_{11} = \frac{9}{2} L_2 L_3 (3L_2 - 1), \quad N_{12} = \frac{9}{2} L_2 L_3 (3L_3 - 1),$$

$$N_{13} = \frac{9}{2} L_3 L_4 (3L_3 - 1), \quad N_{14} = \frac{9}{2} L_3 L_4 (3L_4 - 1),$$

$$N_{15} = \frac{9}{2} L_2 L_4 (3L_2 - 1), \quad N_{16} = \frac{9}{2} L_2 L_4 (3L_4 - 1).$$

Middle of the surface:

$$N_{17} = 27 L_1 L_2 L_3,$$

$$N_{18} = 27 L_1 L_2 L_4,$$

$$N_{19} = 27 L_1 L_3 L_4,$$

$$N_{20} = 27 L_2 L_3 L_4.$$

### 18.3. Hierarchic basis functions

In case of elements with higher degree, hierarchic basis functions can be used, which has the original degree of the function in the corners but lower degree along the sides and the surfaces.

### 18.4. Definition of stiffness matrix and nodal loads

#### 18.4.1. Numerical Gauss integration method

In order to solve a finite element problem, the elements of the stiffness equation (stiffness matrix, nodal loads) must be determined. These elements can be obtained by integration as it is shown in Chapter 3.5. Most of the times the integrals cannot be solved analytically, thus numerical integration techniques must be applied. In case of a three dimensional  $F(x, y, z)$  function with respect to a  $V$  volume, by the use of the Gauss integration method:

$$\int_V F(x, y, z) dV = \iiint F(x, y, z) dx dy dz = \sum_i \sum_j \sum_k w_i w_j w_k F(x_i, y_j, z_k),$$

where:

- $w_i, w_j, w_k$ : weight factors,
- $x_i, y_j, z_k$ : Gauss coordinates.

If we choose to use  $\xi, \eta, \zeta$  local coordinates, then:

$$\iiint F(x, y, z) dx dy dz = \iiint F(\xi, \eta, \zeta) \det J(\xi, \eta, \zeta) d\xi d\eta d\zeta =$$

$$= \sum_i \sum_j \sum_k W_i W_j W_k \det J(\xi_i, \eta_j, \zeta_k) F(\xi_i, \eta_j, \zeta_k),$$

where:

- $W_i, W_j, W_k$ : Gauss weight factors,
- $\xi_i, \eta_j, \zeta_k$ : Gauss (local) coordinates,
- $\underline{\underline{J}}$ : Jacobi-matrix.

#### 18.4.2. Definition of stiffness matrix in case of 3D elements

In case of isoparametric elements the (3.23.) stiffness matrix must be defined as:

$$\underline{\underline{K}}_e = \int_{V_e} [\underline{\underline{B}}_e(\underline{r})]^T \underline{\underline{C}} \underline{\underline{B}}_e(\underline{r}) dV, \text{ where}$$

$$\underline{\underline{B}}_e(\underline{r}) = \underline{\underline{\partial N}}_e(\underline{r}).$$

Let  $\underline{\underline{F}}_e(x, y, z)$  be defined as function:

$$\underline{\underline{F}}_e(x, y, z) = [\underline{\underline{B}}_e(x, y, z)]^T \underline{\underline{C}} \underline{\underline{B}}_e(x, y, z),$$

Then the stiffness matrix of a hexahedron element:

$$\begin{aligned} \underline{\underline{K}}_e &= \int_{V_e} \underline{\underline{F}}_e(x, y, z) dV = \int_{-1}^1 \int_{-1}^1 \int_{-1}^1 \underline{\underline{F}}_e(\xi, \eta, \zeta) \det \underline{\underline{J}}(\xi, \eta, \zeta) d\xi d\eta d\zeta = \\ &= \sum_i \sum_j \sum_k W_i W_j W_k \det \underline{\underline{J}}(\xi_i, \eta_j, \zeta_k) \underline{\underline{F}}_e(\xi_i, \eta_j, \zeta_k) \end{aligned}$$

#### 18.4.3. Derivation of nodal loads from distributed force system on volume

The nodal loads are derived from the distributed force system on a volume or surface. According to (3.24) the load from the distributed force system on a volume:

$$\underline{\underline{F}}_{qe} = \int_{V_e} [\underline{\underline{N}}_e(\underline{r})]^T \underline{q} dV.$$

Introducing the  $\underline{f}_{qe}(x, y, z)$  function:

$$\underline{f}_{qe}(x, y, z) = [\underline{\underline{N}}_e(\underline{r})]^T \underline{q},$$

Deriving the nodal load from the distributed force system on a volume of a hexahedron element:

$$\begin{aligned} \underline{F}_{qe} &= \int_{V_e} \underline{f}_{qe}(x, y, z) dV = \int_{-1-1-1}^1 \int_{-1-1}^1 \int_{-1}^1 \underline{f}_{qe}(\xi, \eta, \zeta) \det \underline{\underline{J}}(\xi, \eta, \zeta) d\xi d\eta d\zeta = \\ &= \sum_i \sum_j \sum_k W_i W_j W_k \det \underline{\underline{J}}(\xi_i, \eta_j, \zeta_k) f_{qe}(\xi_i, \eta_j, \zeta_k) \end{aligned}$$

#### 18.4.4. Derivation of nodal loads from distributed force system on surface

According to (3.25) the load from the distributed force system on a surface:

$$\underline{F}_{pe} = \int_{A_{ep}} [\underline{\underline{N}}_e(r)]^T \underline{p} dA.$$

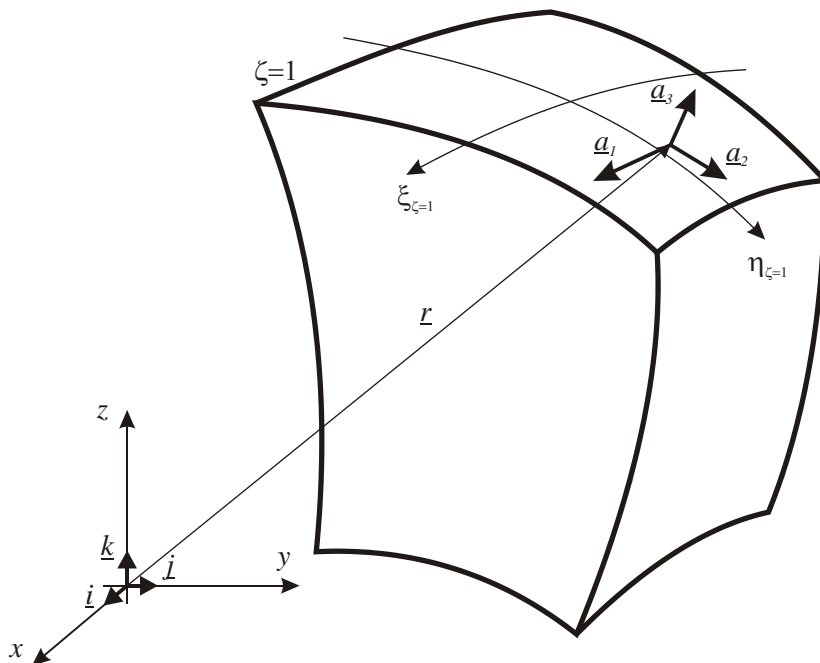


Figure 18.10.: Determination of the normal of a surface

In an arbitrary point of  $\zeta = 1$  coordinate the  $\underline{a}_1$  and  $\underline{a}_2$  tangents can be determined as:

$$\underline{a}_1 = \frac{\partial \underline{r}}{\partial \xi} \text{ és } \underline{a}_2 = \frac{\partial \underline{r}}{\partial \eta}.$$

By knowing these tangents, the normal  $\underline{a}_3$  vector is:

$$\underline{a}_3 = \underline{a}_1 \times \underline{a}_2.$$

The basis function is limited to the surface:

$$N_i(\xi, \eta) = N_i(\xi, \eta, \zeta = 1).$$

Then the tangents are:

$$\underline{a}_1 = \frac{\partial \underline{r}}{\partial \xi} = \sum \frac{\partial N_i(\xi, \eta)}{\partial \xi} x_i \cdot \underline{i} + \sum \frac{\partial N_i(\xi, \eta)}{\partial \xi} y_i \cdot \underline{j} + \sum \frac{\partial N_i(\xi, \eta)}{\partial \xi} z_i \cdot \underline{k},$$

$$\underline{a}_2 = \frac{\partial \underline{r}}{\partial \eta} = \sum \frac{\partial N_i(\xi, \eta)}{\partial \eta} x_i \cdot \underline{i} + \sum \frac{\partial N_i(\xi, \eta)}{\partial \eta} y_i \cdot \underline{j} + \sum \frac{\partial N_i(\xi, \eta)}{\partial \eta} z_i \cdot \underline{k}.$$

And the force vector on an infinitesimal surface is defined as:

$$\underline{p} dA = -\underline{p} \cdot d\underline{A} = -\underline{p} (\underline{a}_1 \times \underline{a}_2) d\xi d\eta = -\underline{p} \underline{a}_3 d\xi d\eta.$$

Substituting this into (3.25):

$$\underline{F}_{pe} = \int_{A_{ep}} [\underline{\underline{N}}_e(r)]^T \underline{p} dA = - \int_{-1-1}^{1-1} [\underline{\underline{N}}_e(\xi, \eta)]^T \underline{p} \underline{a}_3 d\xi d\eta.$$

Introducing  $\underline{f}_{pe}(\xi, \eta)$  function:

$$\underline{f}_{pe}(\xi, \eta) = [\underline{\underline{N}}_e(\xi, \eta)]^T \underline{p} \underline{a}_3,$$

Deriving the nodal load from the distributed force system on a surface of a hexahedron element:

$$\underline{F}_{pe} = - \int_{-1-1}^{1-1} \int_{-1-1}^{1-1} \underline{f}_{qe}(\xi, \eta) d\xi d\eta = \sum_i \sum_j W_i W_j \underline{f}_{qe}(\xi_i, \eta_j).$$

## **19. ANALYSIS OF 3D PROBLEMS WITH FINITE ELEMENT BASED PROGRAM SYSTEMS. APPLICATION OF 3D ELEMENTS.**

### **19.1. Creation of geometric model**

The geometric models of three-dimensional bodies are identical with the original 3D bodies if 3D elements are used during the creation. With the capacity of the modern computers even the most complex structures (linear material law, static problem) can be solved in reasonable time. Although, in many cases the complete, detailed analysis is irrelevant. The computational time can be decreased, and in case of non-linear problems the modification of the original shape of the body can be an essential condition. The importance of these questions will be presented in the following chapter.

There are two ways to import the geometry of a body into a finite element program: we either use to construct the model with the basic design module of the finite element program, or we use a commercial design program to create and import the geometry of a body.

#### *19.1.1. Editing the original geometry*

During the creation of the geometric model – the pure digitalization of the geometry is not sufficient – special surfaces must be created where:

- Loads and constraints can be applied,
- The mesh can be modified,
- Results can be plotted.

Further on, these routines can be only undertaken, if the appointed surfaces exist and are available to refer in the program.

In Figure 19.1 an example is shown about the definition of surfaces. On the original geometry the surface of the cylinder is a compact domain, but the load is applied on only one individual surface. That surface has to be separated, since it will be treated as a reference surface in case of defining force, pressure or deflection.

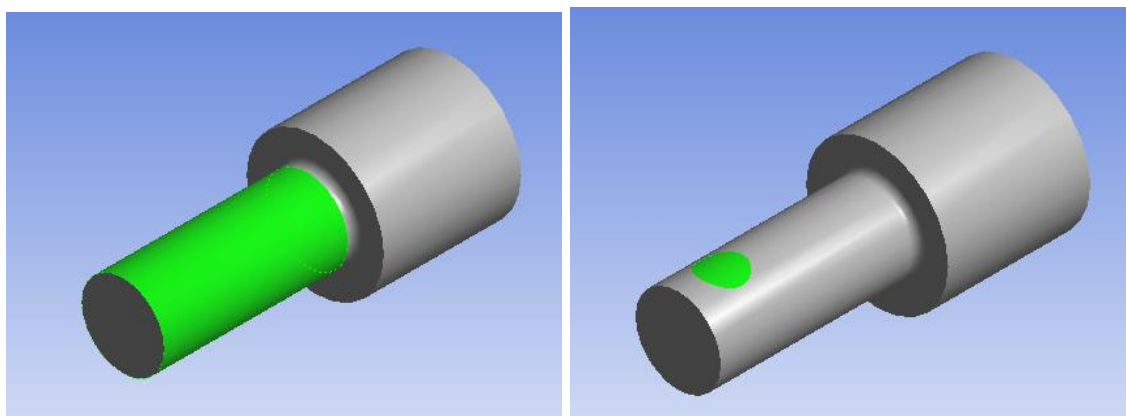


*Figure 19.1.: Creation of surface on a cylinder*

### 19.1.2. Modeling sides and corners

3D models include the geometry of sides and chamfered or rounded corners. On the other hand, it is recommended to decrease the computational time by selecting the essentially important parts for modeling and neglecting the ones which are less important related to the analysis. As a general engineering rule of thumb, if we suspect peak stresses in a certain area, then a more detailed model has to be used, while in case of an unloaded area the same model is irrelevant. In case of Figure 19.2 we assume that the loads and constraints are located at the ends of the shaft. Using rounded corners (signed as red) in this particular case only increases the complexity of the model without adding more information. In contrary, the rounded green part on the model has valid influence on the peak stresses, thus neglecting it would cause great unreliability in the calculation.

In case of this problem, the green rounded radius is given and appears in the model, while the corners – signed with red color – is neglected and also not represented on the model.

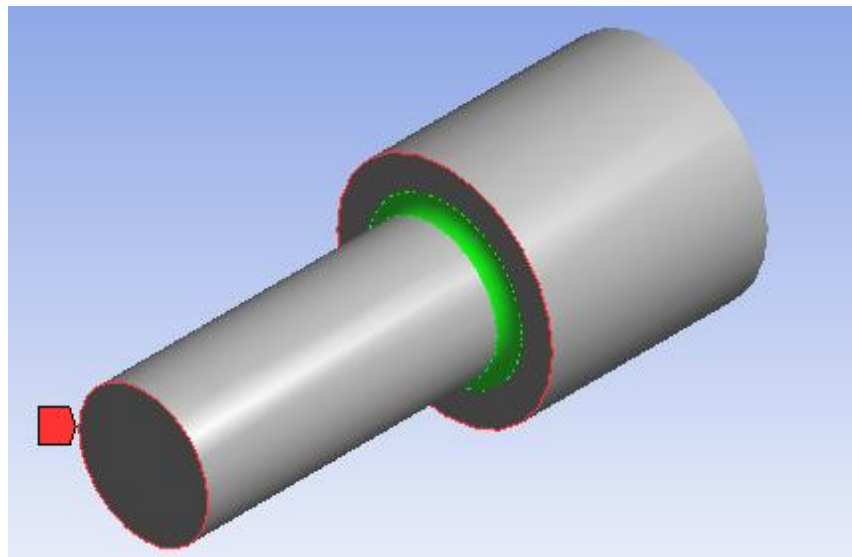


Figure 19.2.: Modeling sides and corners

### 19.1.3. Modeling unloaded parts

During the modeling the unloaded parts can be neglected. If it is known that a decoration of information board will be bolted to the crankshaft in Figure 19.3, then its influence can be neglected, and the handle can be skipped in the model.

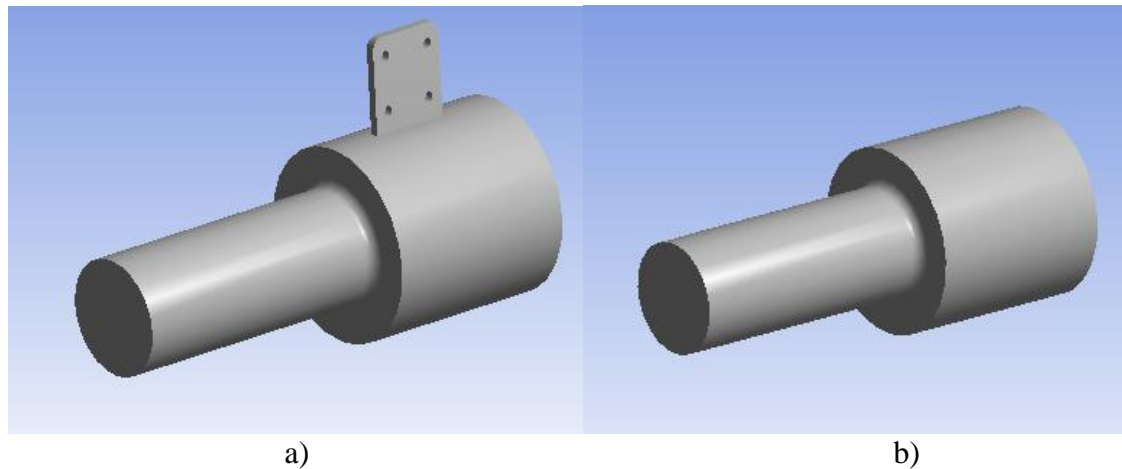


Figure 19.3: Modeling unloaded parts

#### 19.1.4. Modeling symmetric parts

In case of modeling a machine element, the symmetry itself can be utilized if the load is symmetric as well. It is sufficient to use the half of the geometry in case of single symmetry while the one-fourth of the geometry in case of double symmetry, while the proper constraints have to be applied on the intersected surfaces in order to model the neglected parts (Figure 19.4). This method is correct in case of strength calculation and analysis, while in case of stability and eigenfrequency can only be used with some restrictions.

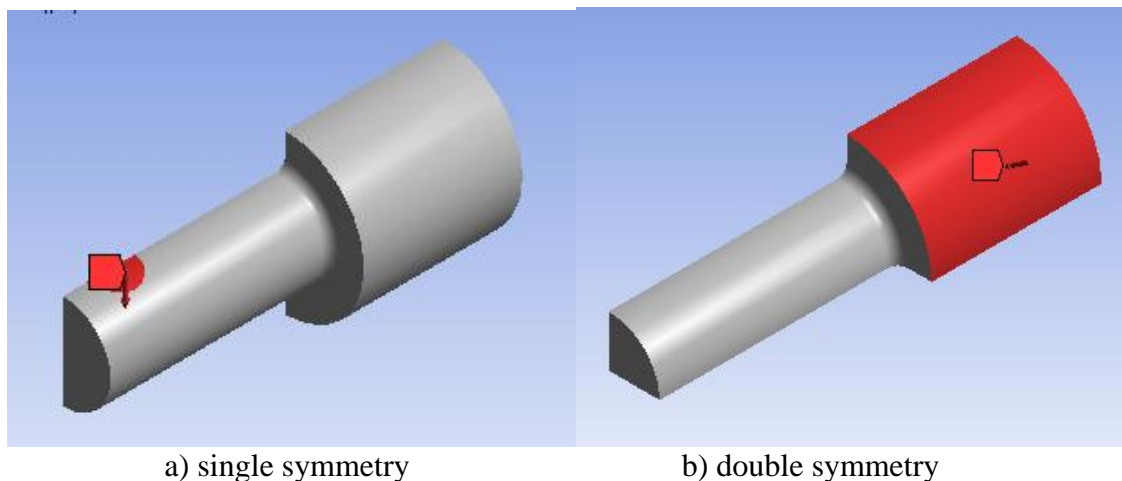


Figure 19.4: Utilization of symmetry properties

## 19.2. Creation of finite element model

The geometry of the bodies are discretized to finite elements according to method and presented element types in Chapter 18. The discretization of the body is called meshing. The meshing is carried out by the software although some parameters have to be specified (or the default parameters modified). The two most important parameters are the type and the size of the elements.

### 19.2.1. Defining the mesh

In case of classic, commercial software the element type has to be chosen, which is followed by the size or the numbers of the elements. After these steps comes the concrete meshing. Modern software is able to mesh the geometry without setting any parameters. In this special case the program uses a default setting which is appropriate for a rough estimation although this only gives the user a line on the results. In most cases we can only give capital credit to the mesh (feasible and appropriate) if the settings are well chosen. In the following chapter we shall investigate the influence of the element type and size.

### 19.2.2. Influence of element size

Earlier, a crankshaft was examined – under different settings – with fixation applied on one end and concentrated force applied on the other end. In Figure 19.5, the meshing was carried out with the default setting. As it is seen, the application of tetrahedrons results a coarse mesh, with maximal reduced stress of 48MPa.

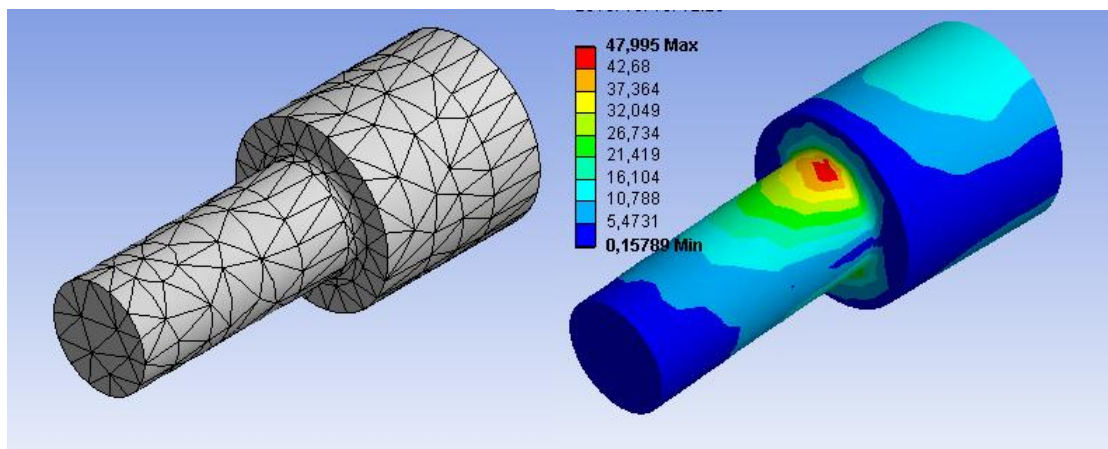


Figure 19.5: FEM mesh with default settings and calculated reduced stress (MPa)

Let us define the average element size to 5mm, which results finer mesh while the reduced stress increases to 55MPa.

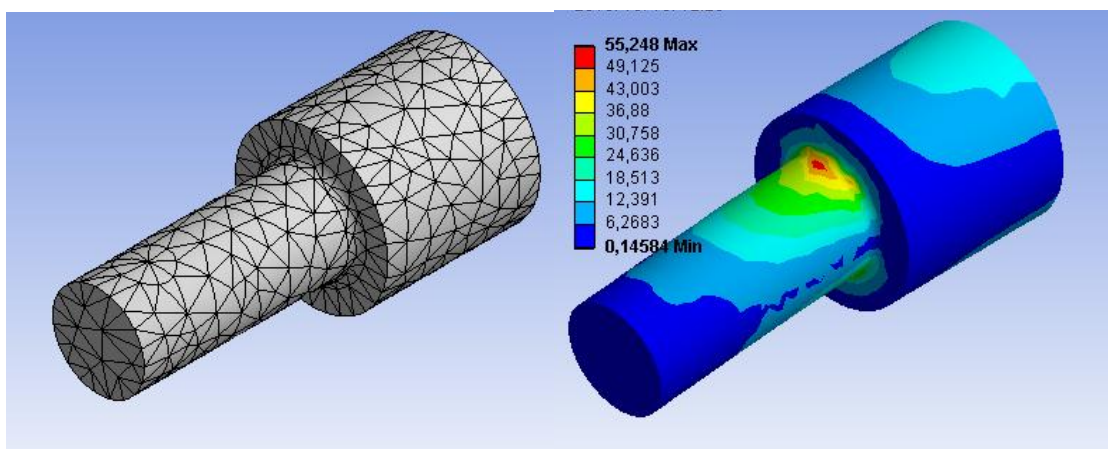
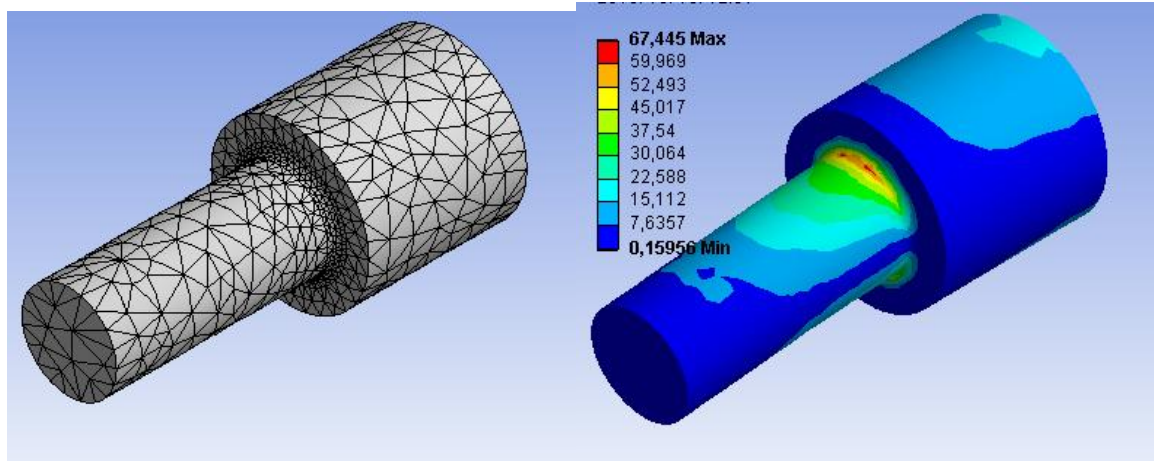


Figure 19.6: Calculated reduced stress in case of 5 mm average element size (MPa)

It appears very visibly that the critical part is located at the transition of the diameters, at the rounded corner. If we are already aware of the critical segments, the further refinement of the mesh on the complete geometry is irrelevant. Let us reduce the element size, but only in the critical segment, and investigate the additional influence.

Let us reduce the size the element size to 2 mm in the critical segment while the average element size remains 5mm in other segments.



*Figure 19.7: 5 mm of average element size, 2 mm of reduced element size in the critical segment and the calculated reduced stress (MPa)*

In Figure 19.7 it is seen, that further refinement in the mesh resulted additional 12MPa of stress increment in the calculation. As long as the results are so sensitive to the mesh, the correct solution is not even close, thus let us reduce the element size to 1 mm in the critical segment.

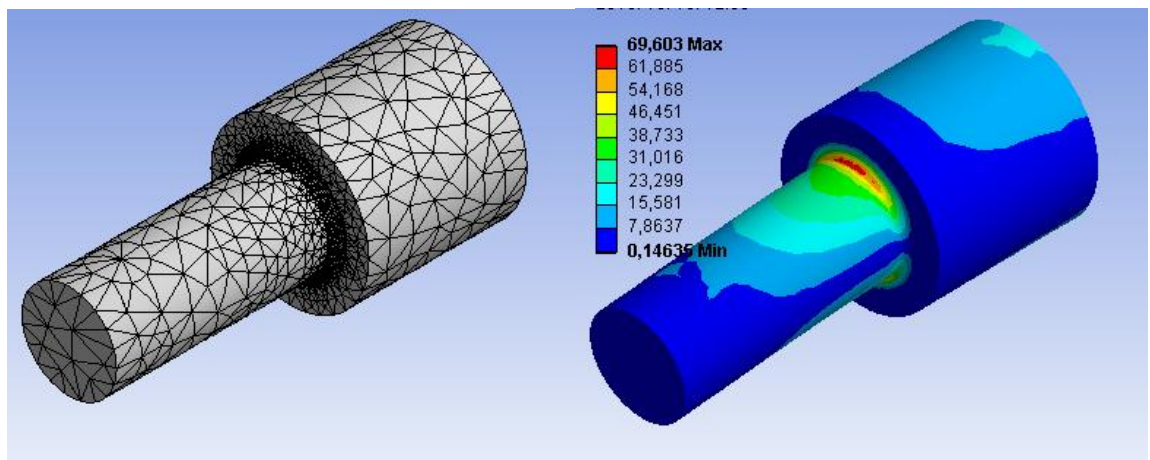


*Figure 19.7: 5 mm of average element size, 1 mm of reduced element size in the critical segment and the calculated reduced stress (MPa)*

The further refinement in the mesh caused no relevant difference, thus the result started converging. The solution is approximated and further refinement in the mesh will not have considerable influence on the result. (Note, that the element size was halved, which causes powered

increment in the element number. In three dimensions it increases the order of magnitude in the critical segment with closely one.)

As a validation, let us consider a much finer mesh with 0.5 mm of element size in the critical segment. In Figure 19.8 it is seen that this mesh causes less than 0.5 % difference in the result.

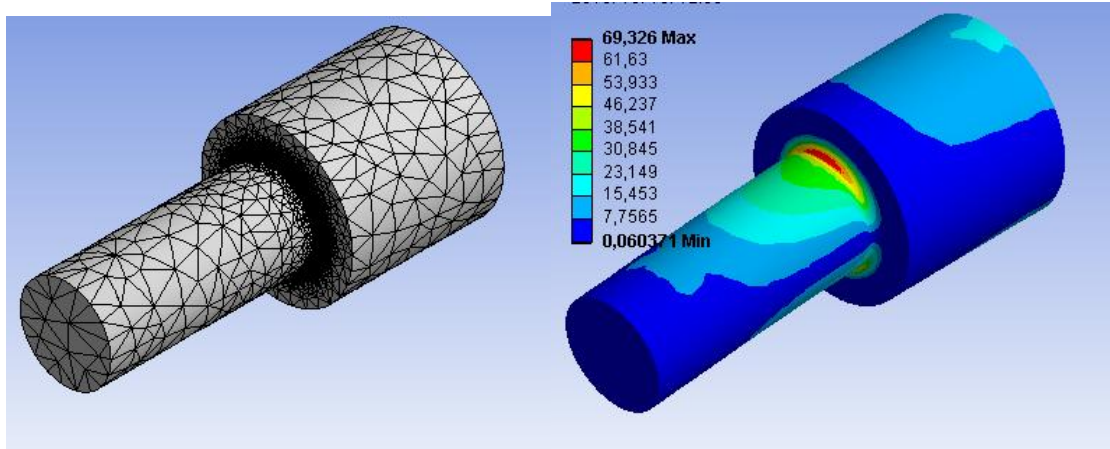


Figure 19.8: 5 mm of average element size, 0.5 mm of reduced element size in the critical segment and the calculated reduced stress (MPa)

### 19.2.3. Influence of element type

Let us investigate the influence of the tetrahedron elements with 4 nodes (linear approximation) compared to the earlier presented tetrahedron elements with 10 nodes (quadratic approximation). Very likely, the decrease of the order of approximate functions will have negative influence on the results. The element type remains tetrahedron, only the nodes in the element are reduced. The meshes are not presented (identical with Figure 19.5-8), only the reduced stresses are compared in case of identical mesh, element size and different (10 or 4) nodes.

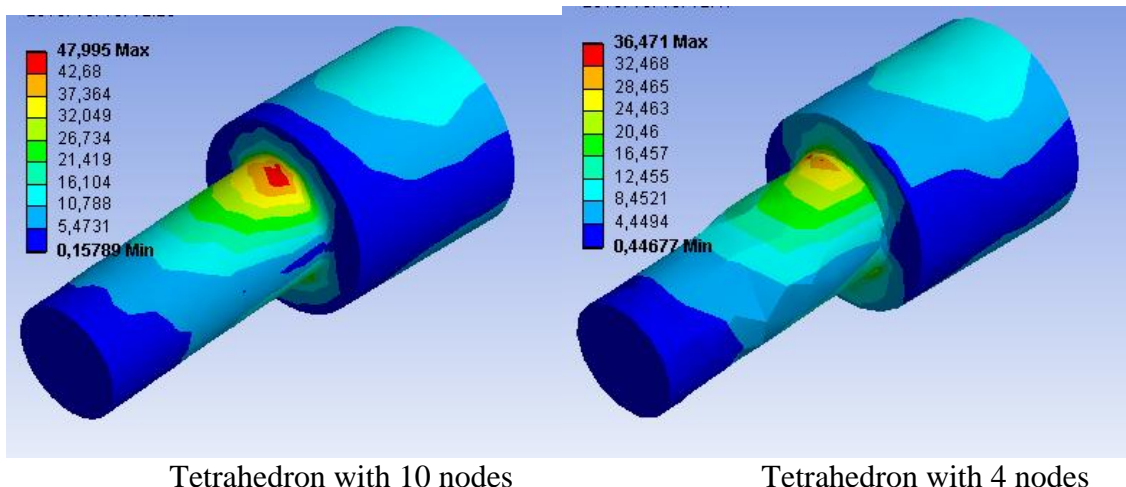
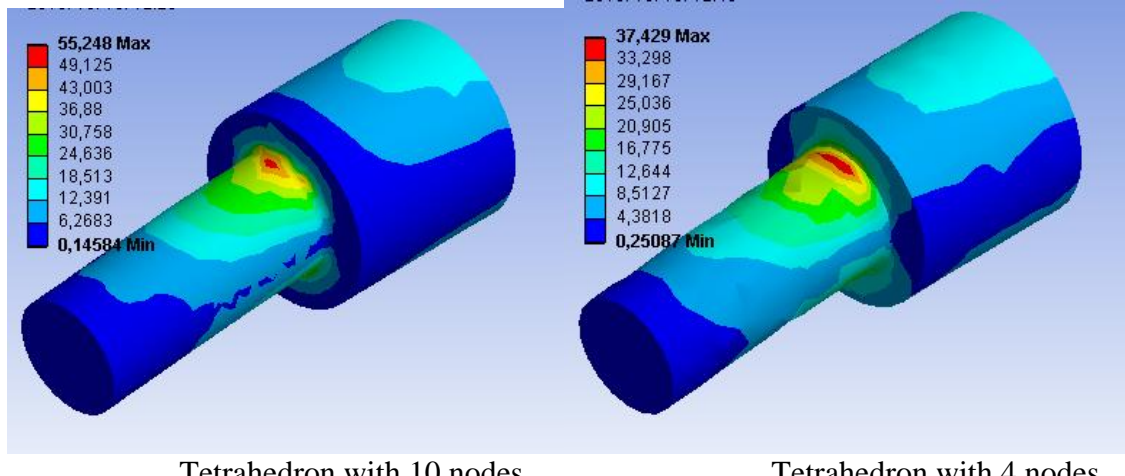


Figure 19.9: Calculated reduced stress (MPa) in case of different tetrahedrons, element size is default.

In Figure 19.9 it is seen, that the tetrahedron with 4 nodes cannot approximate properly the cylindrical geometry, since the side of certain elements are a plane due to the linear approximate functions, in contrast with the 10 nodes element which can model the sides as well.



*Figure 19.10: Calculated reduced stress (MPa) in case of different tetrahedrons, average element size is 5 mm*

The rounding radius was set to 3 mm, thus the maximum stress did not change significantly compared to the default setting. In the next step, the rounding radius is set to 2 mm, which will very likely enhance the accuracy of the result.

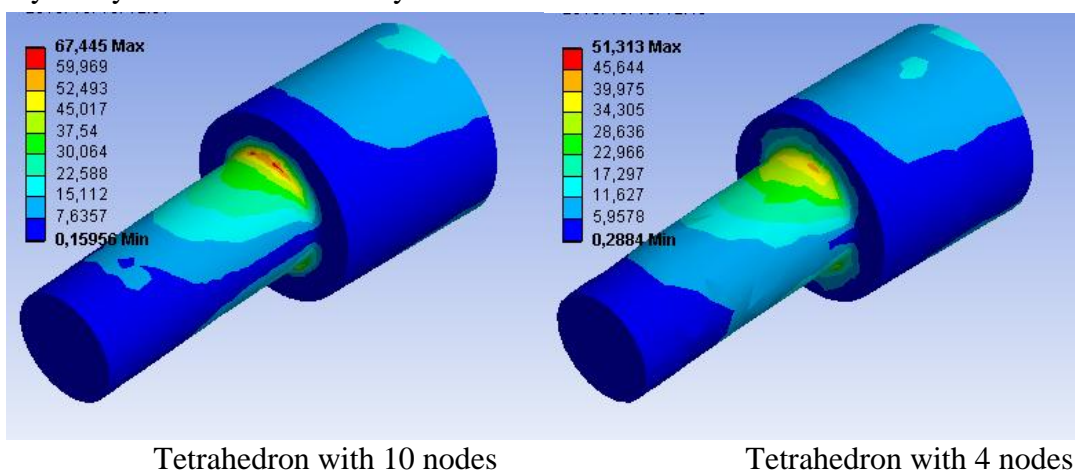


*Figure 19.11: Calculated reduced stress (MPa) in case of different tetrahedrons, average element size is 5 mm, element size in the critical segment is 2 mm*

In Figure 19.11 it is seen, that the results are highly refined if we use smaller elements than the rounding radius. While the valid result was already approximated with the 10 nodes element, the solution given by the 4 nodes element had relevant difference. Let us refine the mesh – which was already appropriate for the elements with 10 nodes – and observe the influence on the elements with 4 nodes.

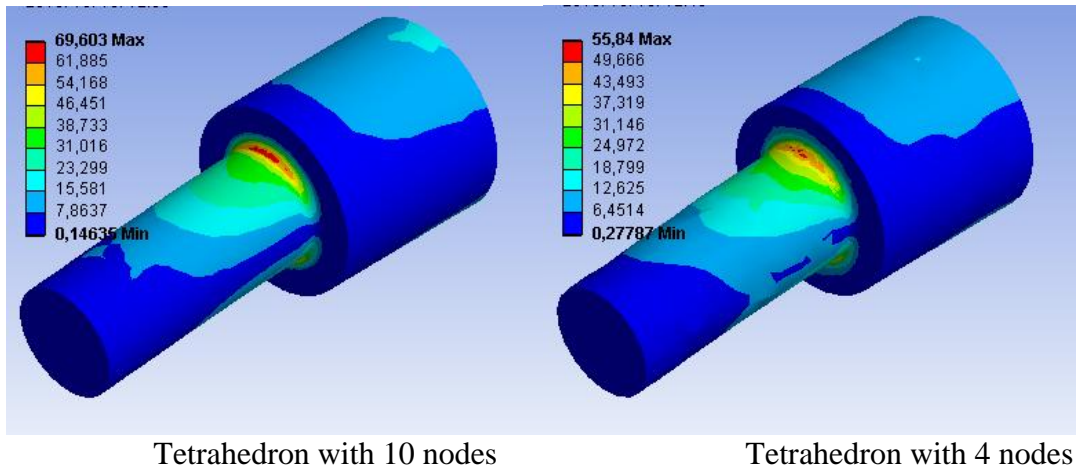


*Figure 19.12: Calculated reduced stress (MPa) in case of different tetrahedrons, average element size is 5 mm, element size in the critical segment is 1 mm*

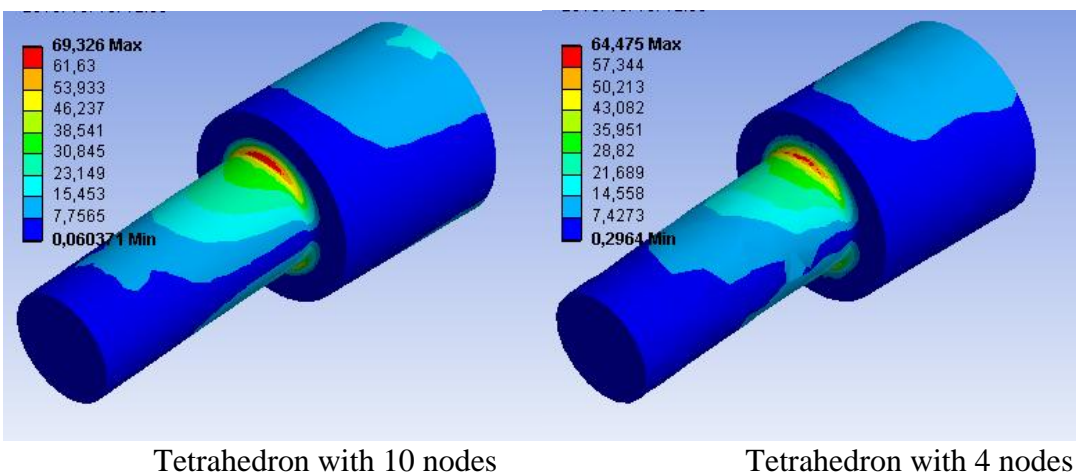


*Figure 19.13: Calculated reduced stress (MPa) in case of different tetrahedrons, average element size is 5 mm, element size in the critical segment is 0.5 mm*

In Figure 19.12 and 19.13 it is seen, that the elements with 4 nodes do not converge to the valid solution even if the mesh is very fine. In case of tetrahedron elements with 10 nodes we obtain an acceptable solution with fewer elements than the order of magnitude of two. We can draw the following conclusions: the use of elements with 4 nodes has to be avoided if the modeled body includes curved geometry. This means practically most cases.

### 19.3. Boundary conditions

Another most important part of FEM modeling is the proper settings of the boundary conditions. We cannot make faults by using approximate functions with higher order or a very fine mesh. That might relevantly increase the computational time, but the solution will be ultimately valid. The fault of boundary conditions settings will appear independently from the fine mesh. Many cases, the error due to the wrong boundary conditions is increased by the finer mesh.

### 19.3.1. Loads

Real bodies are subjected to distributed loads on their surface or volume. Loads can be concentrated in a point or distributed along a line if the modeling dimension is lower. The application of these loads is a fault in the 3D modeling, which proportionally increases the error in the solution by the refinement of the mesh.

In Figure 19.14 a cube is plotted with 20 mm of side length, and 100 N of concentrated force is applied on the middle of its upper plane. The other lower plane of the cube is fixed. Let us examine the stresses as a function of element size.

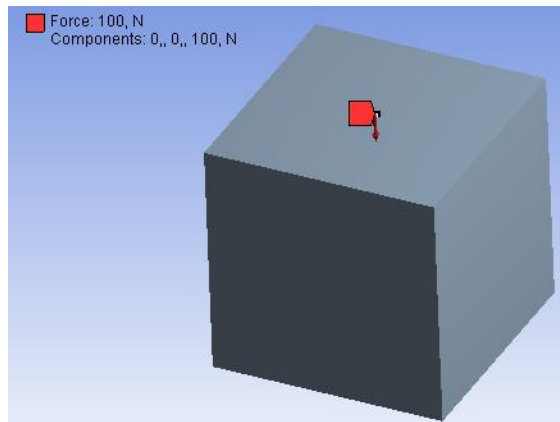


Figure 19.14: Cube loaded on the middle of its upper plane

If the force is acted on the total plane as a pressure:

$$\sigma = \frac{F}{A} = \frac{100N}{20mm \cdot 20mm} = 0,25MPa$$

Then normal stress appears in the total cross section. If we make the following fault by applying a concentrated force in the middle of the upper plane instead of a pressure, then we obtain different reduced stresses as a function of element numbers.

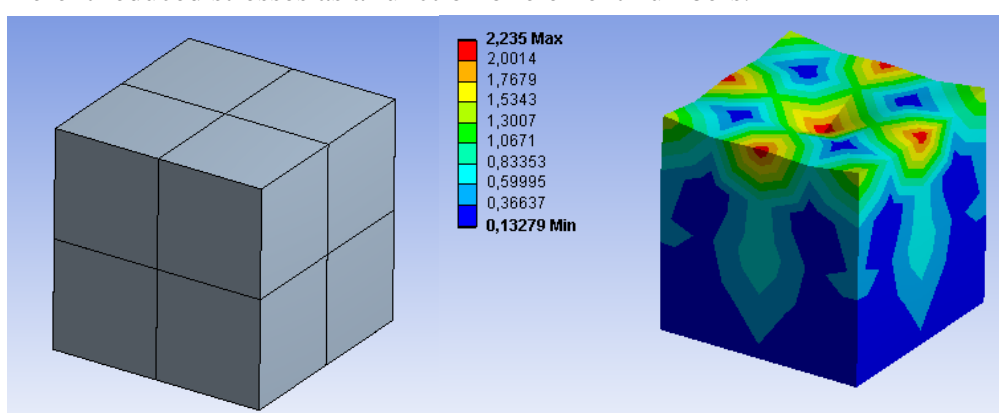


Figure 19.15: Calculated stresses (MPa) in a cube loaded in a point with concentrated force (element size 10 mm)

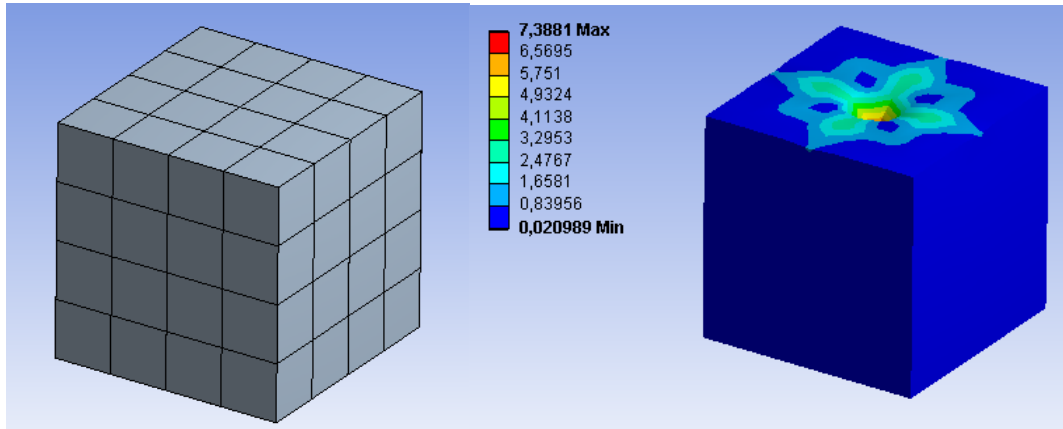


Figure 19.16: Calculated stresses (MPa) in a cube loaded in a point with concentrated force, (element size 5 mm)

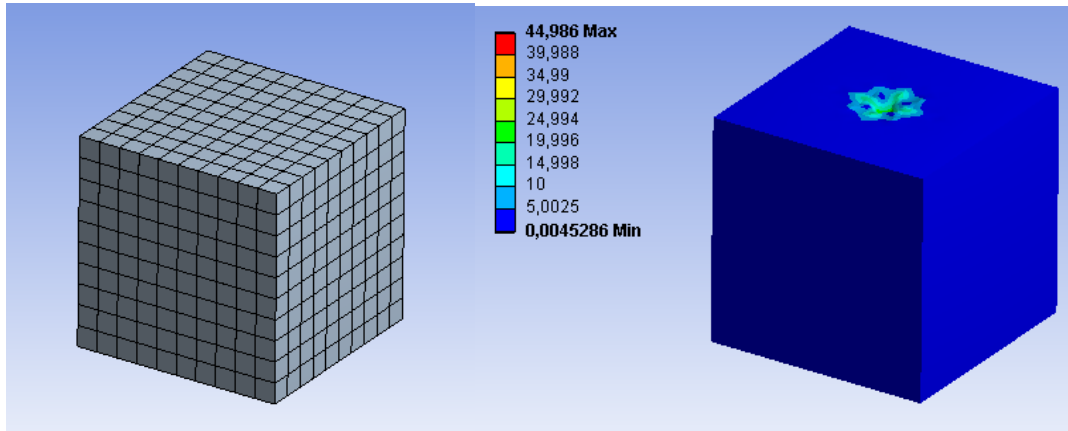


Figure 19.17: Calculated stresses (MPa) in a cube loaded in a point with concentrated force, (element size 2 mm)

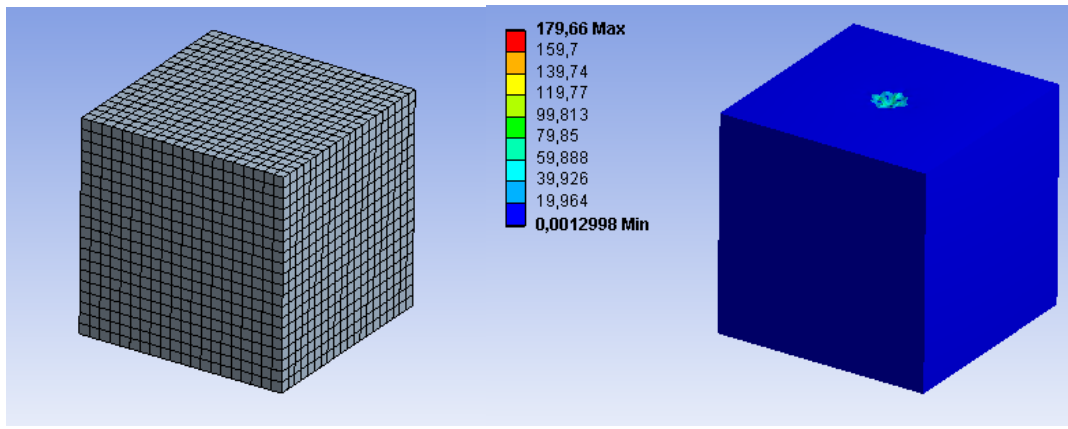


Figure 19.18: Calculated stresses (MPa) in a cube loaded in a point with concentrated force, (element size 1 mm)

We can observe that the decrease of the element size constantly (and increase of the element number) increases the reduced stress (Figure 19.19). By the decrease of the element size we

step by step approximate the theoretical concentrated load which results infinite stress. We obtain similar result if we apply distributed load along a line.

**In case of 3D modeling we can only apply distributed loads on the surfaces and the volumes.** We do not analysis further the problem, but the similar problem appears if a line- or shell element is directly connected to a 3D body.

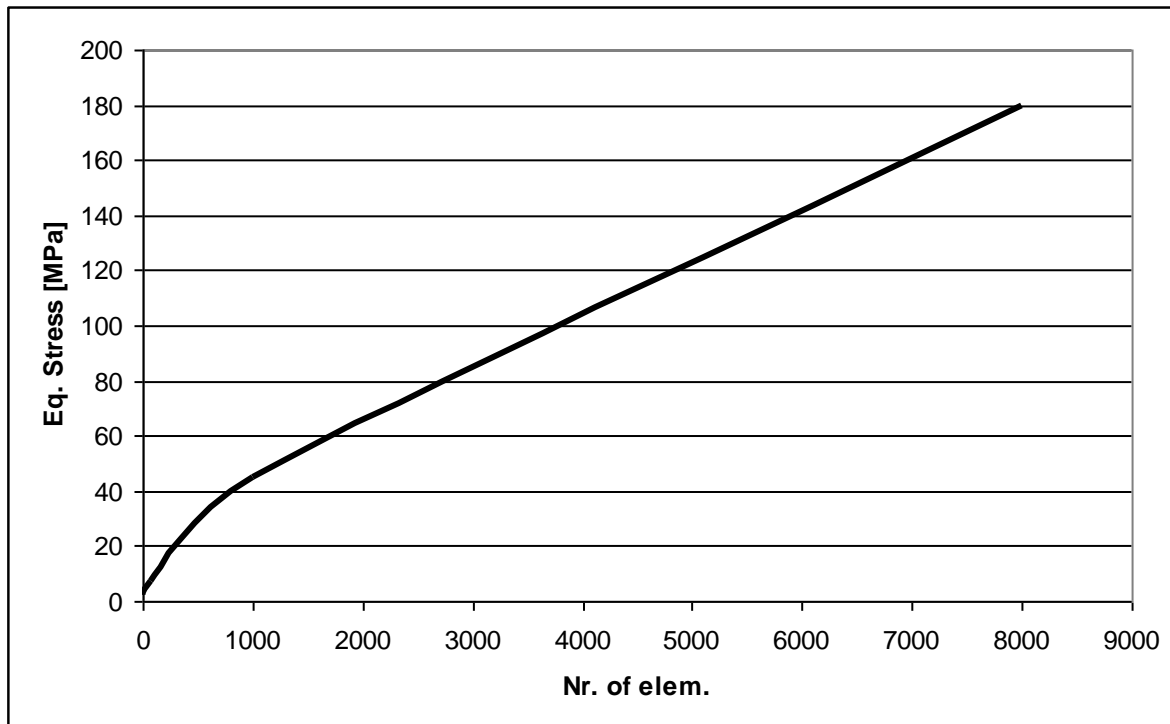


Figure 19.19: Reduced stress as a function of element number

### 19.3.2. Constraints

We have to pay special attention to the constraints if we model 3D bodies. Since the constraints are infinitely rigid, they might result unexpected and unrealistic stresses and deformation in the calculations. Although, this problem does not appear always so directly as it was demonstrated with the concentrated force in the earlier section. Due to this fact it can cause problems since it is hard to notice. Let us examine a beam fixed in one end and loaded with a concentrated force in the other end (Figure 19.20).

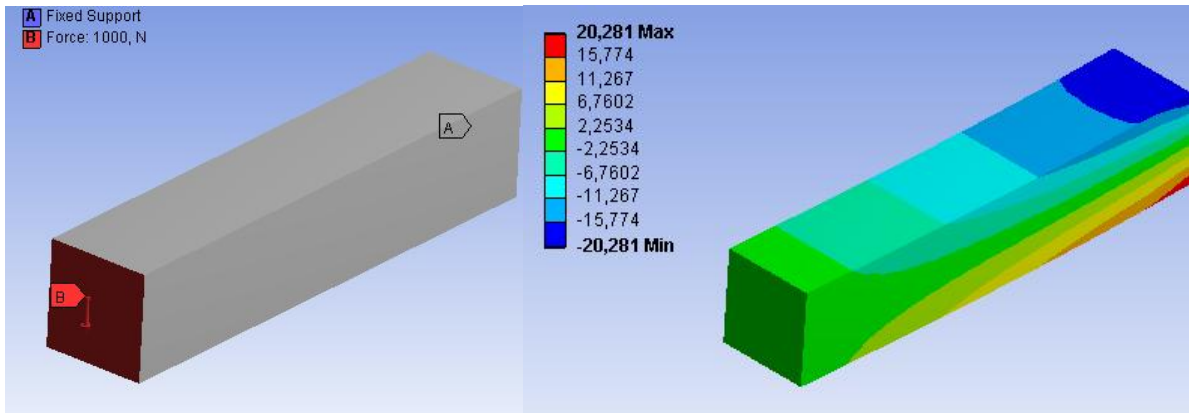


Figure 19.20: Normal stresses (MPa) in a fixed beam, hexahedron elements with 10 mm

Calculated stress from pure bending:

$$\sigma = \frac{F \cdot l}{K} = \frac{6 \cdot 1000N \cdot 200mm}{20^3 mm^3} = 18,75 MPa$$

The calculated stress in the body is summarized in a table as a function of element type, element number and number of nodes:

| Type                                  | Size      | Number of nodes | Number of element | Max. normal stress [MPa] | Max. reduced stress [MPa] |
|---------------------------------------|-----------|-----------------|-------------------|--------------------------|---------------------------|
| Tetrahedron with 4 nodes              | 10 (def.) | 218             | 513               | 16,2                     | 11                        |
|                                       | 5         | 876             | 2747              | 21,4                     | 15                        |
|                                       | 4         | 1306            | 4265              | 24,7                     | 16,9                      |
|                                       | 3         | 2814            | 10359             | 26                       | 18,4                      |
|                                       | 2         | 7325            | 29154             | 30,4                     | 22,2                      |
|                                       | 1         | 35861           | 156570            | 38,9                     | 27,8                      |
| Tetrahedron with 4 nodes (structured) | 10 (def.) | 442             | 1394              | 17,4                     | 13                        |
|                                       | 5         | 2361            | 9270              | 21,1                     | 16                        |
|                                       | 4         | 3948            | 16038             | 22                       | 16,5                      |
|                                       | 3         | 6935            | 27324             | 23,6                     | 17,9                      |
|                                       | 2         | 16758           | 69312             | 26,2                     | 20,3                      |
|                                       | 1         | 78573           | 341083            | 32,4                     | 26,4                      |
| Tetrahedron with 10 nodes             | 10 (def.) | 1149            | 513               | 25,5                     | 19                        |
|                                       | 5         | 5182            | 2747              | 31,8                     | 24,2                      |
|                                       | 4         | 7860            | 4265              | 34,6                     | 26,3                      |
|                                       | 3         | 17814           | 10359             | 38,8                     | 29,7                      |
|                                       | 2         | 47927           | 29154             | 44,6                     | 34,4                      |
|                                       | 1         | 243813          | 156570            | 57,8                     | 44,4                      |
| Hexahedron with 8 nodes               | 10 (def.) | 525             | 320               | 20,3                     | 18,7                      |
|                                       | 5         | 3321            | 2560              | 23,2                     | 20,2                      |
|                                       | 4         | 6171            | 5000              | 24,5                     | 21                        |
|                                       | 3         | Could not mesh  |                   |                          |                           |
|                                       | 2         | 44541           | 40000             | 30                       | 24,6                      |
| Hexahedron with 20 nodes              | 10 (def.) | 1865            | 320               | 23,6                     | 19,5                      |
|                                       | 5         | 12465           | 2560              | 28,8                     | 24,5                      |
|                                       | 4         | 23441           | 5000              | 31                       | 26,5                      |
|                                       | 3         | 59710           | 13538             | 34,6                     | 29,8                      |
|                                       | 2         | 173481          | 40000             | 39,5                     | 34,1                      |
|                                       | 1         | 1333361         | 320000            | 51                       | 44,1                      |

By observing the results we can derive that the solution does not converge, but the increase of the error is not as significant as it was with the concentrated force. This fault causes unreliability during the validation of the results, since the calculated higher stresses are unrealistic due to the rigid fixation. Even higher stresses are resulted if the kinematic constraint is defined only on a segment instead of the total surface.

The unrealistic stresses can be decreased by coarsening the mesh in the area of the ideal constraints. This is only a emergency solution, if we do not have the possibility to model contact or realistic constraints.

## 20. PRINCIPLES ABOUT MODELING, ACCURACY AND APPLICABILITY. COMPARISON OF DIFFERENT FINITE ELEMENT MODELS, ANALYSIS OF RESULTS.

### 20.1. Modeling beams

Multiple models can be used in a finite element system in case of beams with constant cross sectional area. Short beams can be modeled as 1D beam, 3D body while thin-walled structures even as shells. In the followings, we are going to investigate that depending on the conditions, which model is applicable. In order to compare the results, simple problems will be solved by the use of different models.

#### 20.1.1. Analysis of a beam with circular cross section

Let us consider a beam with circular cross section with 50 mm of radius and 1000 mm of length. All rotations and translations are constrained at one side, while on the other side a force with the magnitude of 1200 N is applied. Let us determine the maximum stress in the beam. Two models will be applied to solve the problem. Applying line elements the beam is modeled by its neutral axis (Fig. 20.1.a). In this case one end of the beam is fixed and the other end is loaded by a single force. By using 3D elements, the geometric model is a cylinder which is loaded by a distributed force system at one end. At the other end no fixation is applied, because the constraint of deformation would cause additional stresses beside the bending stress. Instead, the same distributed load is applied – with opposite direction – at the other end, while the axial displacement is prescribed to zero (Fig. 20.1.b.).

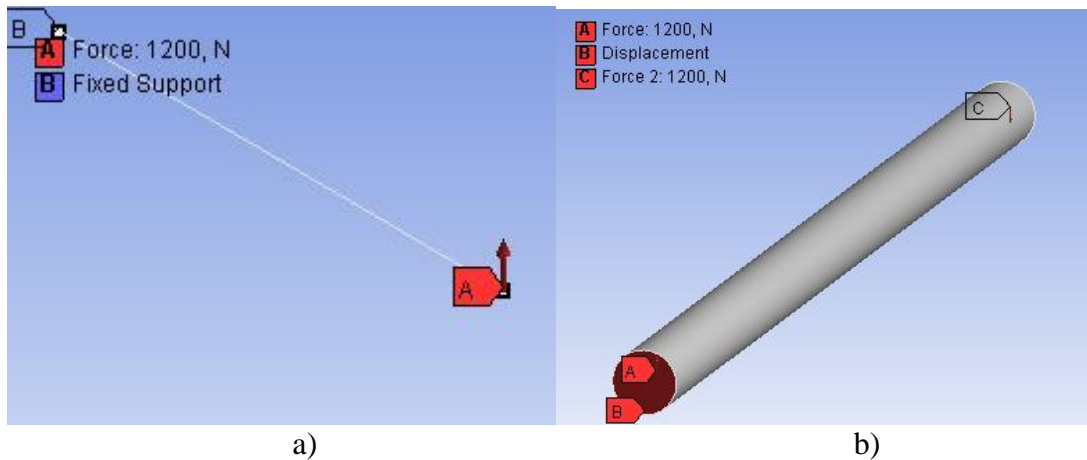


Figure 20.1.: Geometric model of the beam

The most important advantage of the 1D modeling related to the FEM is the reduced computation. The element itself is far simpler than the 3D elements, and beside the similar accuracy, less element is needed in the modeling. The meshed models are shown in Fig. 20.2.

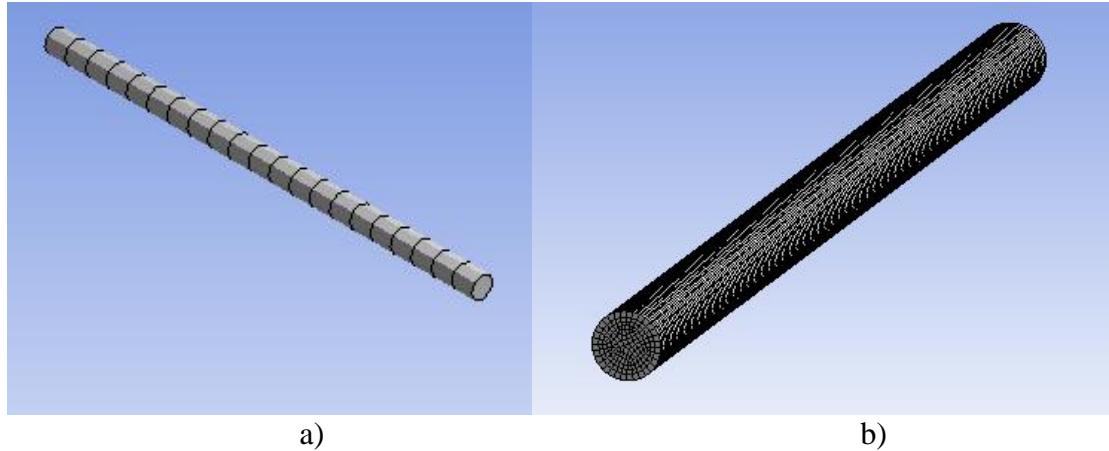


Figure 20.2.: FEM mesh with 1D and 3D elements

In case of beam elements 21 or 43 nodes are sufficient; while 33048 and 142911 nodes are required to create an appropriately precise model with 3D elements. The number of 3D nodes can be reduced if the elements are elongated axially, but ultimately far more are required; if not 1D elements are used.

The stresses are determined analytically as well in order to compare it to the later numerical results. In case of a fixed beam with circular cross section, the maximum stress calculated from the bending moment is:

$$\sigma = \frac{M_h}{K} = \frac{32 \cdot F \cdot l}{d^3 \pi} = \frac{32 \cdot 1200N \cdot 1000mm}{50^3 mm^3 \cdot \pi} = 97,78 MPa,$$

where:

$\sigma$  : Stress,

$M_h$  : Maximum bending moment,

$F$  : Concentrated force,

$K$  : Section modulus,

$d$  : Diameter of the cross section.

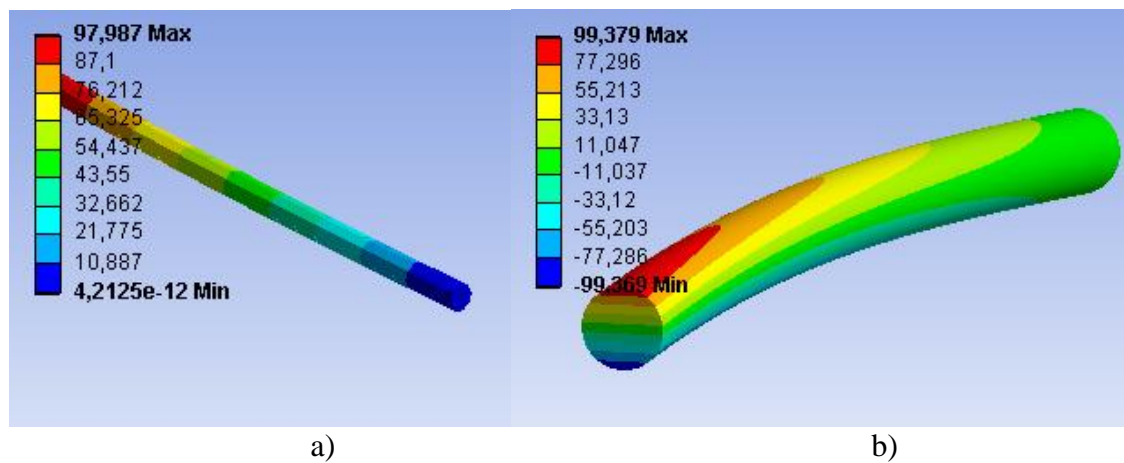


Figure 20.3.: Calculated normal stresses in MPa

The stresses are plotted in Fig. 20.3. The result related to the beam model is approximately the same as the analytical result. The difference between the analytical result and the result of the 3D model is less than 2%, which is practically acceptable.

The application of beam elements could be useful if we wish to model large structures with fine mesh, ignoring the use of 3D elements due to the limit of computational time or it is simply beyond possibility. If the boundary conditions are properly given, the result is reliable. Still, we have to be aware of the limit of beam elements. Fixed constraints, contact stresses, cross section transitions cannot be realistically modeled with it. The calculated stresses cannot be so described in details as good as if the geometry of the cross section is involved in the model.

### 20.1.2. Modeling of thin-walled beams

Let us consider the beam in the previous section as a thin-walled rectangular cross section with dimension of 60x60x4 and material of steel. In the modeling, now we have the possibility to use shell elements beside the 1D and 3D elements. It is clearly seen in Figure 20.4 that the beam is modeled and described as *a*) line element, *b*) surface element, *c*) or body.

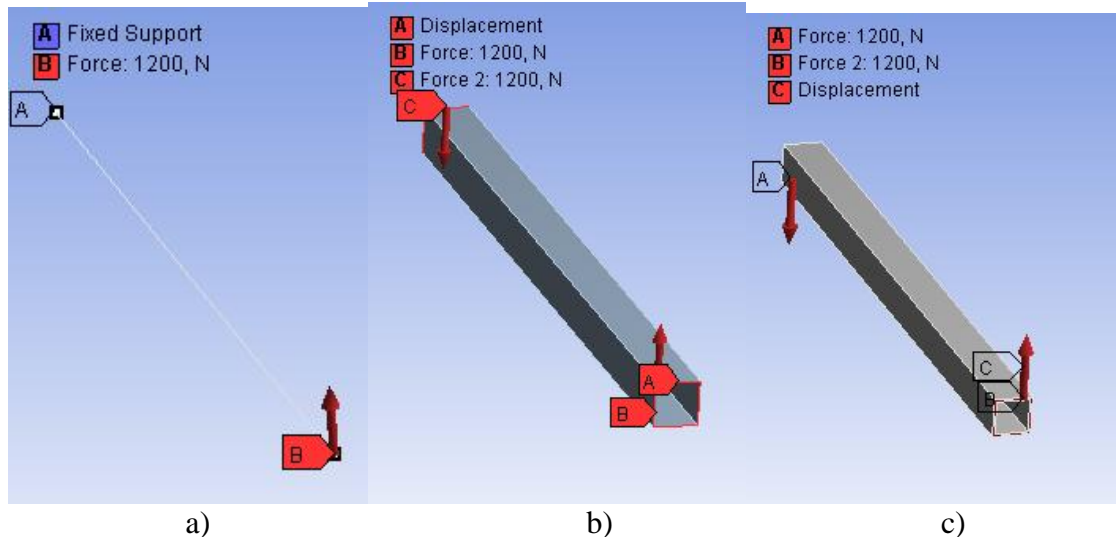


Figure 20.4: Geometric model of the beam with its constraints and loads

Similarly to the previous models, fixation is only applied in case of line elements. In case of shell and body model, couple and axial constraint are applied since only the stresses from the bending are demanded. By meshing each geometric models, we obtain the finite element models (Figure 20.5).

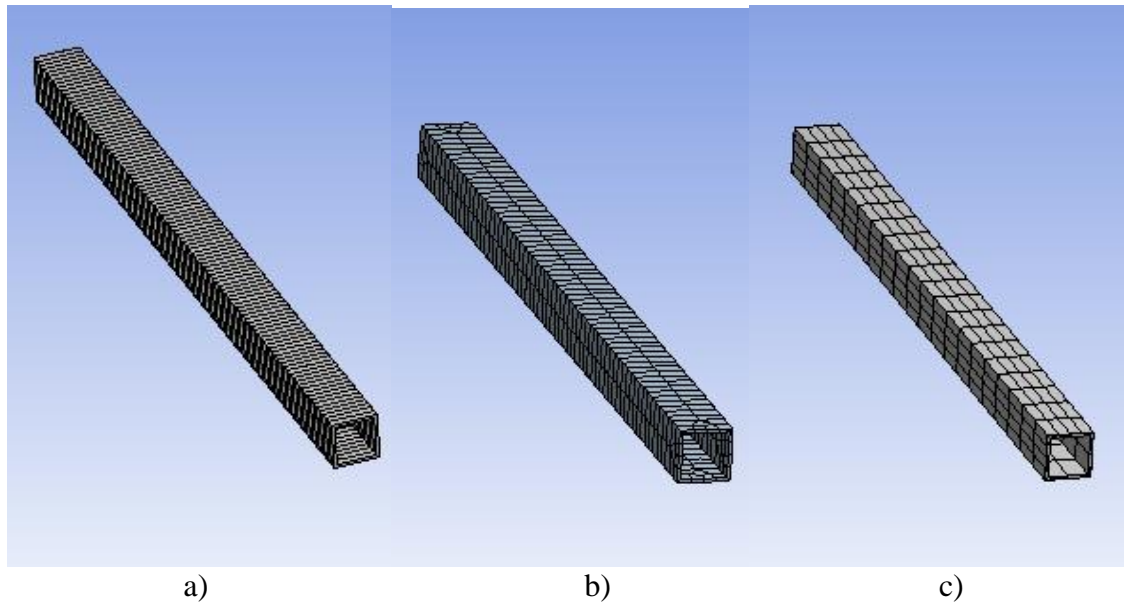


Figure 20.5: 1D, 2D and 3D finite element models

The model – built from line elements – is in Figure 20.5.a includes 100 elements and 201 nodes. The model – built from shell element – includes 530 elements and 1622 nodes in Figure 20.5.b which is significantly more compared to the line elements. In case of the body model – in Figure 20.5.c – the mesh is sparse axially, still 340 elements and 1907 nodes are used to build the model. As it was expected during the meshing, the models with higher order required proportionally more computational time due to the need of multiple elements and nodes.

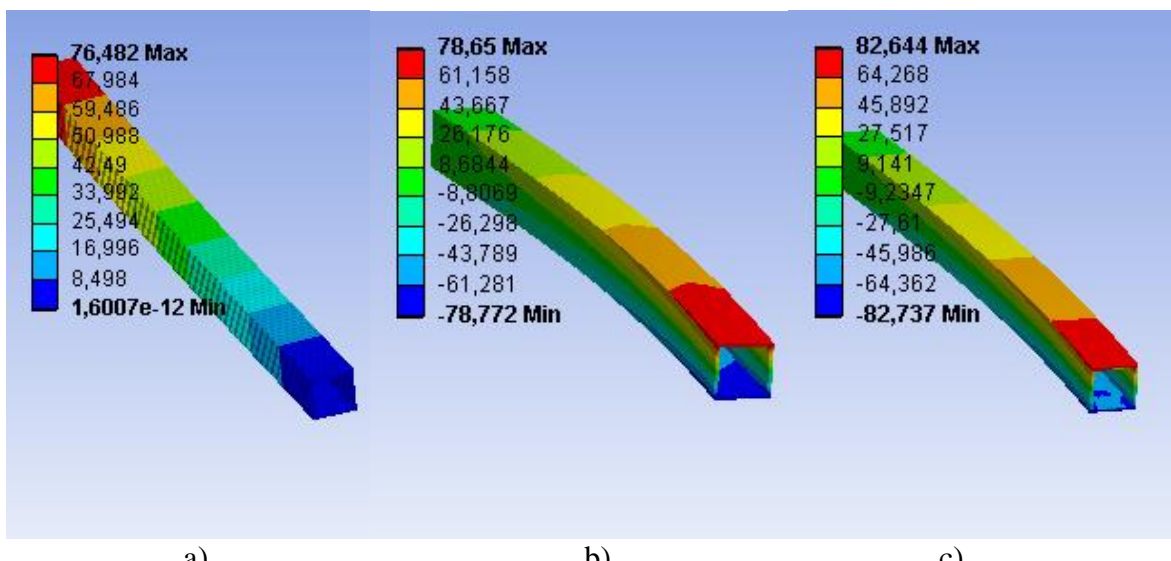


Figure 20.6: Calculated stresses of 1D, 2D and 3D finite element models in MPa

The maximum stress calculated from the bending moment is:

$$\sigma = \frac{M_h}{I_z} e = \frac{6 \cdot F \cdot l \cdot a}{a^4 - (a - 2v)^4} = \frac{6 \cdot 1200N \cdot 1000mm \cdot 60mm}{60^4 mm^4 - 52^4 mm^4} = 76,48 MPa,$$

where:

- $\sigma$  : Stress,
- $M_h$  : Maximum bending moment,
- $F$  : Concentrated force,
- $I_z$  : Second moment of area,
- $a$  : Height, width of the cross section,
- $v$  : Thickness of the cross section,
- $e$  : Distance from the neutral axis.

In Figure 20.6.a it is seen that the result of the beam model completely corresponds with the analytical solution, which is expected since the analytical solution is derived from the theory of the beam model. The result – given by the shell mode – in Figure 20.6.b shows closely 3% of increment, while in Figure 20.6.c this difference is 8%. The difference can be deduced from the inequality of axial stresses in thin-walled cross sections, and only higher ordered models can properly describe this phenomenon.

#### 20.1.3. Modeling of thin-walled open cross section beams

In the followings, we shall investigate the error if simple beam model is used to model thin-walled open cross section beams. The most significant difference is caused by the warping effect, since most models are unable to describe this phenomenon. Let us use – similarly to the previous example – a beam with 1000mm of length, while the dimension of the cold formed U section is 100x100x4. The beam is loaded with one single force with 1200 N of magnitude. First, let us determine the normal stresses analytically (the shear stresses are neglected although we are aware that they cause additional increment in the equivalent stress).

*The maximum stress calculated from the bending moment is:*

$$\sigma = \frac{M_h}{I_z} e = \frac{1200N \cdot 1000mm}{2103829mm^4} 50mm = 28,52MPa ,$$

where:

- $\sigma$  : Normal stress,
- $M_h$  : Maximum bending moment,
- $F$  : Concentrated force,

$$I_z = \frac{a^4}{12} - \frac{(a-v)(a-2v)^3}{12} = \frac{100^4}{12} - \frac{96 \cdot 92^3}{12} = 2103829mm^4 : \text{second moment of area},$$

- $a$  : Height, width of the cross section,
- $v$  : Thickness of the cross section,
- $e$  : Distance from the neutral axis.

*Calculation of maximum normal stress from warping moment:*

Sectorial second moment of area of thin-walled open cross section:

$$I_c = \frac{1}{3} \sum v_i s_i = \frac{1}{3} (4mm)^3 (2 \cdot 98mm + 96mm) = 6229,3mm^4,$$

where:

$v_i$ : Thickness of the flanges,

$s_i$ : Breadth of the flanges.

The sectorial coordinate function:

$$\omega = \int d\omega = \int_s^z y dz - \int_{y_0}^y z dy,$$

where:

$y, z$ : are the coordinates of the cross section contour.

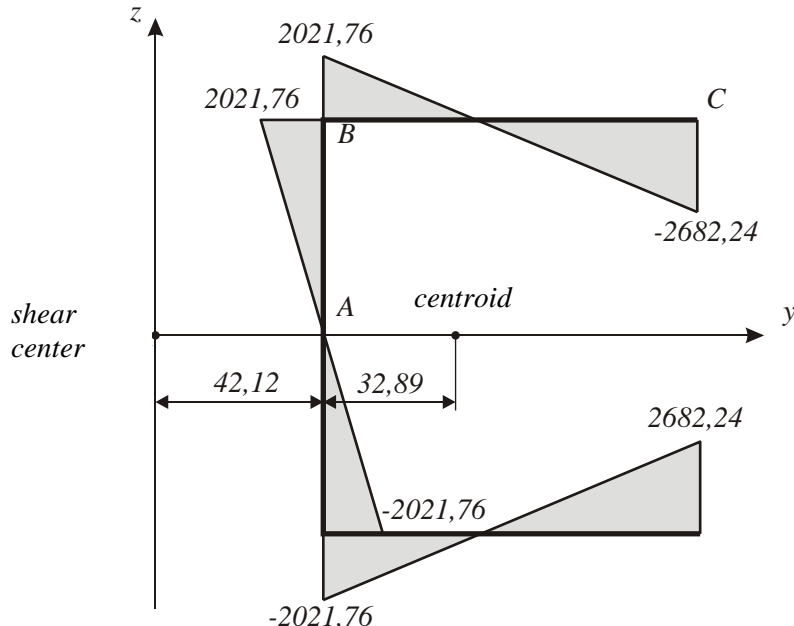


Figure 20.7:  $\omega$  function with respect to the pole ( $mm^2$ -ben)

The sectorial coordinate function is calculated with respect to the pole. By integrating the square root of the function we obtain the second moment of area of the cross section with respect to the pole:

$$I_\omega = \int_A \omega^2 dA = \int_s \omega^2 v ds = v \int_s \omega^2 ds = 4 \cdot \left[ \int_0^{48} (42,12s)^2 ds + \int_0^{98} (2021,76 - 48s)^2 ds \right] \cdot 2 = 2,054 \cdot 10^9 mm^6$$

Introducing:

$$\alpha = \sqrt{\frac{G \cdot I_c}{E \cdot I_\omega}} = \sqrt{\frac{80GPa \cdot 6229,3mm^4}{210GPa \cdot 2,054 \cdot 10^9 mm^6}} = 0,00107477 mm^{-1},$$

where:

$G = 80 \text{ GPa}$ : Shear modulus,

$E = 210 \text{ GPa}$ : Young-modulus.

Relative angular displacement of the cross section with respect to the pole along the axis [Csizmadia: Modellalkotás]:

$$\vartheta(x) = c_1 \cdot \operatorname{sh}(\alpha \cdot x) + c_2 \cdot \operatorname{ch}(\alpha \cdot x) + \frac{M_c}{G \cdot I_c} (1 - \operatorname{ch}(\alpha \cdot x)),$$

where:

$M_c$ : torsion with respect to the pole,

$x$ : coordinate of the axis of the beam,

$c_1, c_2$ : constants.

The derivatives:

$$\frac{d\vartheta(x)}{dx} = \alpha c_1 \cdot \operatorname{ch}(\alpha \cdot x) + \alpha c_2 \cdot \operatorname{sh}(\alpha \cdot x) - \alpha \frac{M_c}{G \cdot I_c} \operatorname{sh}(\alpha \cdot x).$$

At the free end of the beam:

$$\frac{d\vartheta(x)}{dx} = 0, \text{ thus: } c_1 = 0.$$

At the fixed end of the beam:

$$\vartheta(x) = 0, \text{ thus: } c_2 = \frac{M_c}{G \cdot I_c} \left( 1 - \frac{1}{\operatorname{ch}(\alpha \cdot l)} \right).$$

By substituting the obtained constants, the relative angular displacement of a one-end-fixed beam:

$$\vartheta(x) = \frac{M_c}{G \cdot I_c} \left( 1 - \frac{\operatorname{sh}(\alpha \cdot x)}{\operatorname{ch}(\alpha \cdot l)} \right).$$

The derivative of relative angular displacement:

$$\frac{d\vartheta(x)}{dx} = -\alpha \frac{M_c}{G \cdot I_c} \frac{\operatorname{sh}(\alpha \cdot x)}{\operatorname{ch}(\alpha \cdot l)}.$$

Normal stress with respect to the bimoment due to the warping:

$$\sigma_\omega = -\frac{B_\omega}{I_\omega} \omega,$$

where:

$$B_\omega = EI_\omega \frac{d\vartheta(x)}{dx} : \text{bimoment.}$$

In our case:

$$B_\omega = EI_\omega \left( -\alpha \frac{M_c}{G \cdot I_c} \frac{sh(\alpha \cdot x)}{ch(\alpha \cdot l)} \right) = -\frac{M_c}{\alpha} \frac{sh(\alpha \cdot x)}{ch(\alpha \cdot l)},$$

The maximum of the function is at the fixation  $x = l$ , van:

$$B_\omega = -6,6267 \cdot 10^7 \text{ Nmm}^2.$$

Then the stress in the corner of the U section due to bimoment in Figure 20.7, point „B” ( $\omega = 2021,76 \text{ mm}^2$ ) is:

$$\sigma_{\omega B} = 65,21 \text{ MPa},$$

At the end of the U section in Figure 20.7, point „C” ( $\omega = -2682,24 \text{ mm}^2$ ):

$$\sigma_{\omega C} = -86,52 \text{ MPa}.$$

Then the sum of stresses – caused by bending moment and bimoment – is:  
 $\sigma_B = \sigma + \sigma_{\omega B} = 93,73 \text{ MPa},$

$$\sigma_C = \sigma + \sigma_{\omega C} = -58 \text{ MPa}.$$

#### *Normal stresses calculated by VEM models*

Let us compare the analytically obtained stresses to the finite element models in case of line-, shell- and body elements. The geometric models are described as the axis of the beam (Figure 20.8.a), middle plane (Figure 20.8.b) or its complete cross section (Figure 20.8.c).

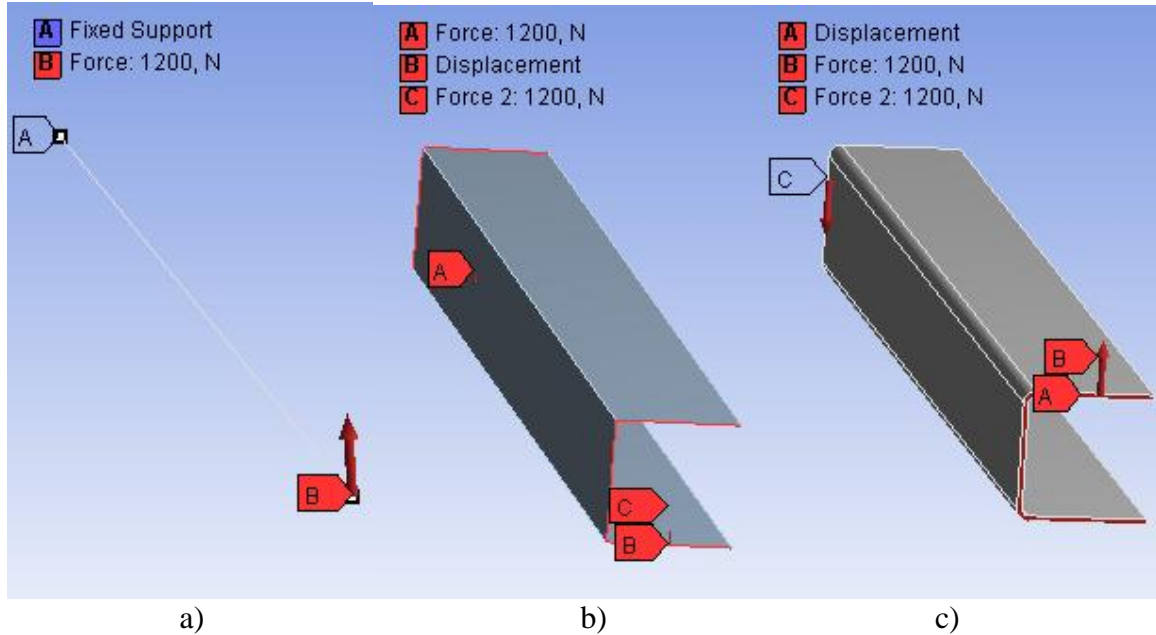


Figure 20.8: Geometric model of the beam with its constraints and loads

Similarly to the previous models, fixation is only applied in case of line elements while in case of shell and body models, couple and axial constraint are used.

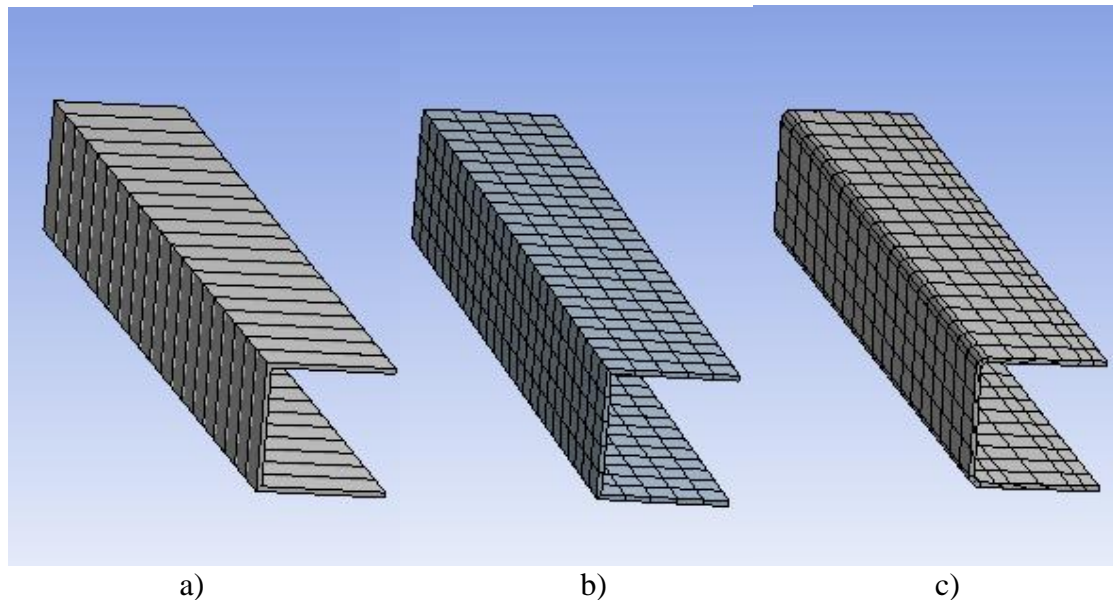


Figure 20.9: 1D, 2D and 3D finite element models

The model – built from line elements shown in Figure 20.9.a – includes 20 elements and 41 nodes. The model – built from shell element shown in Figure 20.9.b – includes 375 elements and 1206 nodes, while in case of the body model – in Figure 20.5.c – 420 elements and 3148 nodes are used to build the model.

In Figure 20.10 the calculated stresses are plotted in MPa. It is obviously seen that simple beam model with line elements takes only the bending into consideration, and neglects the

bimoment (note: some commercial software are able to model warping with line elements, but point of application in the cross section has to be defined by the user). The estimated results given by the shell and body models are higher than the analytical results. The reason is originated to the analytical description, since the stresses were calculated with respect to the middle plane, and considered constant along the thickness of the flanges, while the finite element models calculated the change along the thickness as well.

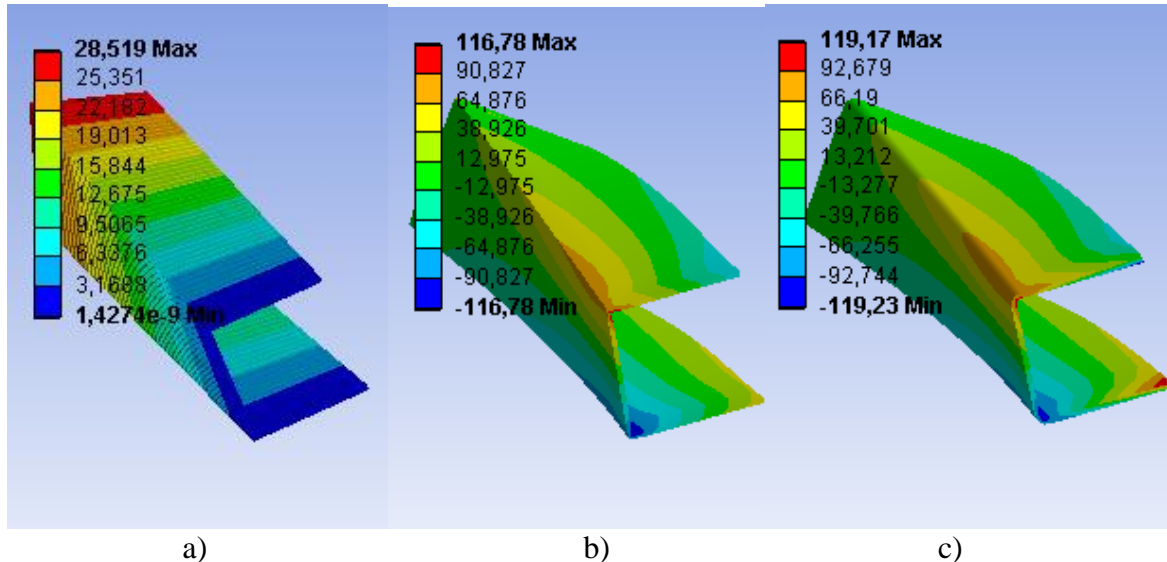


Figure 20.10: Calculated stresses in MPa in case of 1D, 2D and 3D finite element models

If we look at the stresses in the middle plane of the shell elements (Figure 20.11), that the results ( $\sigma_B = 93,73 \text{ MPa}$ ,  $\sigma_C = -58 \text{ MPa}$ ) correlate with small error.

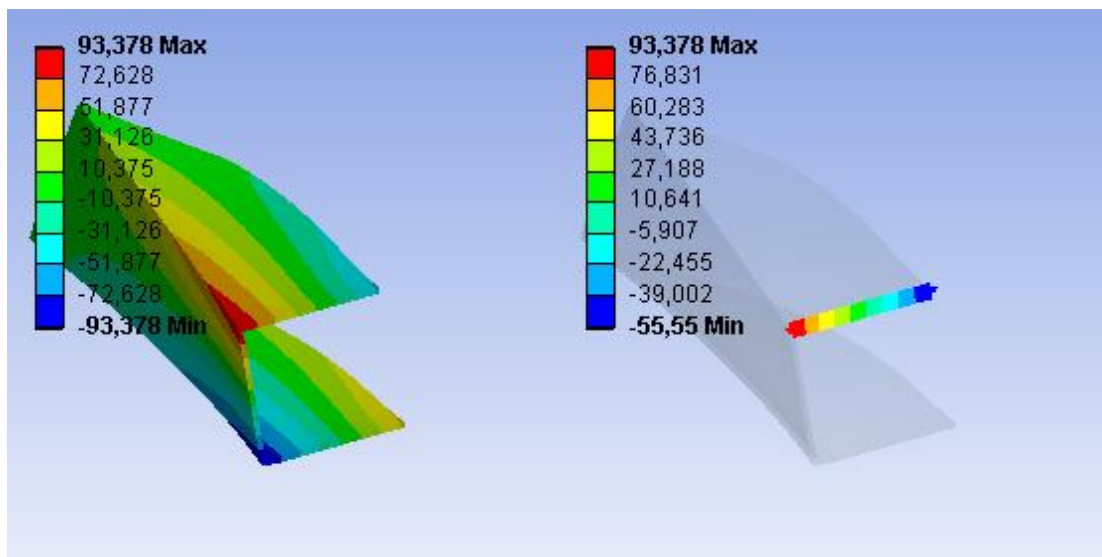


Figure 20.11: Calculated stresses (MPa) in the middle plane in case of shell

#### 20.1.4. Modeling of thick-walled cylinders, tubes

Let us examine a tube with 60mm of inside- and 120mm of outside diameter – while 30MPa of internal pressure is acting in it – and determine how precisely the phenomenon can be describe with different models.

##### Analytical model

In the thick-walled tubes the distribution of the longitudinal stresses is assumed constant, while they change along the radius as a function of quadratic hyperbole. The tube diagrams are commonly plotted as a function of relative reciprocate radius:

$$\rho = \left( \frac{r}{r_b} \right)^2,$$

where:

$r$ : the radius of the tube (variable),

$r_b$ : the internal radius of the tube.

In our case the number of  $\rho_k$  – considering the external and internal radius – is:

$$\rho_k = \left( \frac{r_k}{r_b} \right)^2 = \left( \frac{60}{30} \right)^2 = 0,25,$$

$$\rho_b = \left( \frac{r_b}{r_b} \right)^2 = 1.$$

According to these numbers the tube diagram:

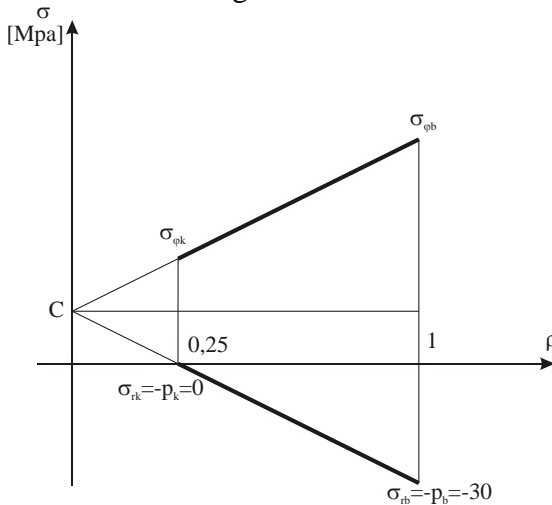


Figure 20.12: Tube diagram

The radial stress in the external and internal wall equals the external and internal pressure. By utilizing the proportionality of the stresses, the tangential stresses can be obtained

as:  $\sigma_{\phi b} = 50 \text{ MPa}$ ,  $\sigma_{\phi k} = 20 \text{ MPa}$ . The longitudinal stress depends on the fact whether the tube is closed or open, thus having a constant value of  $C$  or 0. Let us observe the results given by each finite element model!

### *Finite element models*

A thick-walled, pressurized tube can be properly described with either 2D or 3D models. Simplification is also possible in case of the 3D model by utilizing the fact that the longitudinal stresses are constant, thus only a short part of the original tube has to be analyzed. If the symmetry is also utilized, then only the half or one-fourth of the original tube is sufficient to analyze, although we have to be aware of prescribing the correct constraints at the cut-off part, according to the symmetry.

There are two possibilities to describe the tube with 2D models. We assume, that all cross sections of the tube are under the same planar deformation, thus the tube can be modeled as only one cross section. Here we can also utilize the symmetry by only using the half or one-fourth ring of the original cross section, carefully prescribing the correct constraints at the cut-off part. The other option, is to utilize the axis-symmetric geometry and load, and selecting a 2D axis-symmetric model. Then it is sufficient to model only a segment of the complete tube.

In order to compare the results, three models will be solved and presented from the multiple choices.

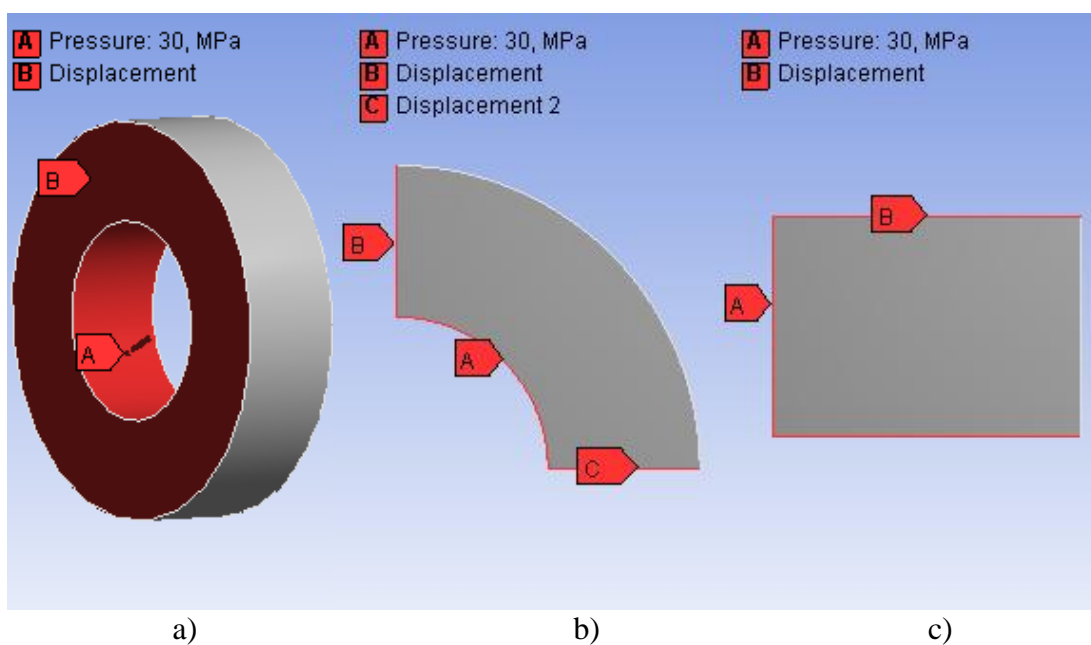


Figure 20.13: Modeling options of thick-walled tubes, loads, constraints

In Figure 20.13.a only a short segment of the tube is considered with the 3D model, the cut-off parts are substituted by constraints: no axial translation is available on the intersected surface (B). 30 MPa of pressure is defined on the internal surface of the tube.

In Figure 20.13.b the one-fourth part of the cross section is modeled, thus we have to define planar deformation in the 2D model. On line „B” and „C”, the perpendicular displacement is inhibited by utilizing the symmetric geometry. The 30 MPa of load is applied on line „A”.

In Figure 20.13.c the longitudinal section of the beam is modeled with 2D axis-symmetric elements. The construction of the geometric model is carried out by setting 30 mm of distance (the internal radius) between surface „A” and the axis of rotation. Vertical displacement is inhibited on line „B” and on the other additional lines beside it as well. This is how the tube is modeled furthermore. 30 MPa of pressure is applied on surface „A” as a constantly distributed force system.

In Figure 20.14 the finite element models are shown, each of them built from predetermined elements. The original complete finite element model – built from 3D elements – includes 44756 elements and 69542 nodes (Figure 20.14.a). The 2D model with planar deformation condition is shown in Figure 20.14.b while the mesh includes 1104 elements and 3455 nodes. The axis-symmetric model in Figure 20.14.c is built from 2D elements as well and the mesh includes 1887 elements and 5838 nodes. During the comparison it is worthy to note that using elements with the same number and size, the nodes of the models can be reduced one-fifth or even one-twentieth (in case of axis-symmetric modeling) of the original complete 3D model, while the same precision is obtained. According to these calculations, the best (requiring the least computational time) approximate finite element model is the axis-symmetric, second is the planar deformation and the last one is the original body model.

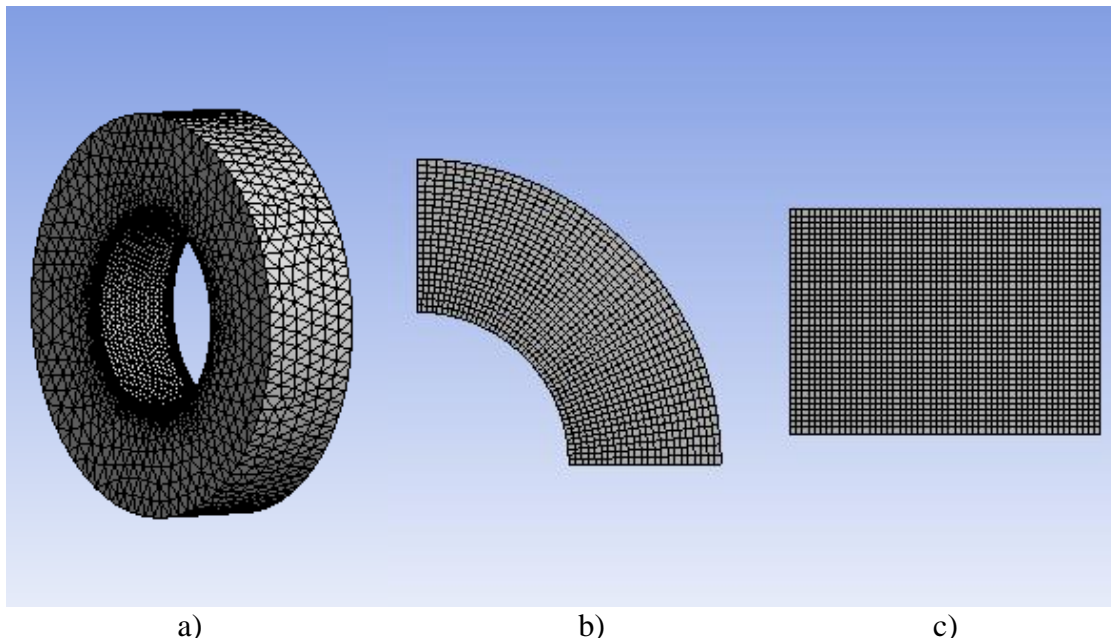


Figure 20.14: 3D, 2D planar deformation and 2D axis-symmetric models

Tangential stresses calculated by different models are shown in Figure 20.15.

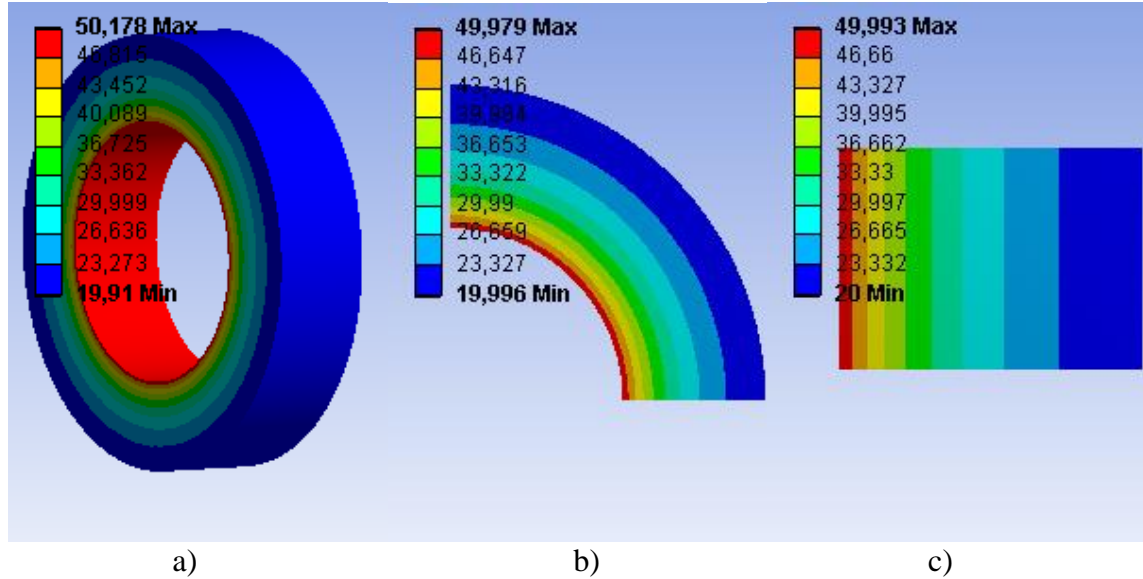


Figure 20.15: Tangential stresses calculated by 3D, 2D planar deformation and 2D axis-symmetric models in MPa

By comparing the results to each other and to the analytical solution, the following conclusions can be drawn; the best approximation is given by the axis-symmetric model although none of the models performed more error than 0,5% compared to the analytical solution. The difference can be emphasized better if the element size of the three models is determined to fit to 5% of error. In this specific case, we have to utilize the double symmetry of the body model.

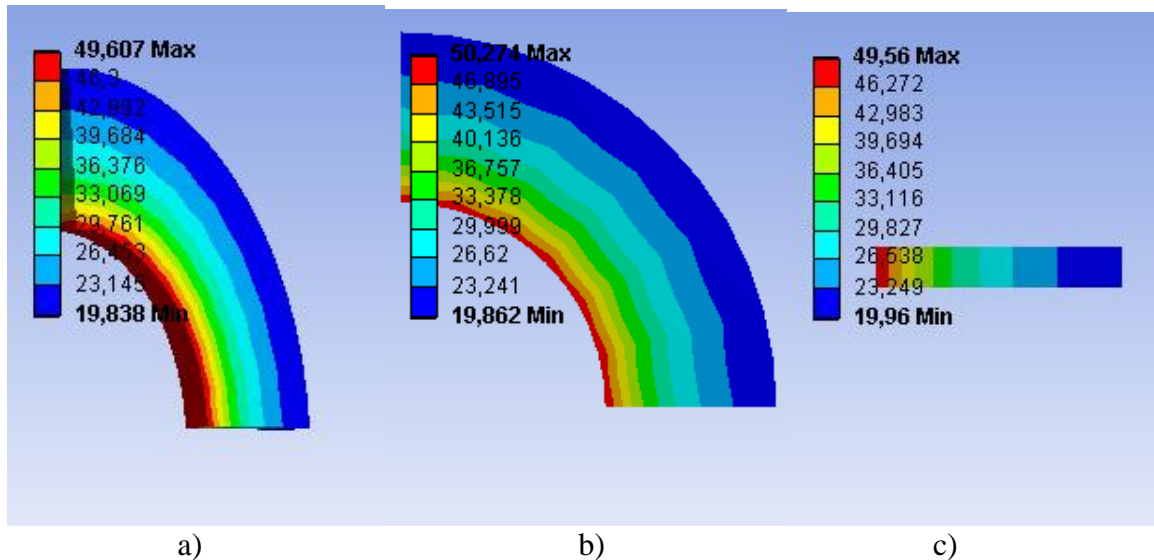


Figure 20.16: 3D, 2D planar-deformation, and the minimum number of element in case of 2D axis-symmetric model with respect of 5% of error in the tangential normal stresses in MPa

The stresses in Figure 20.16 were obtained by continuously modifying the mesh until it reached the 5% of error in the range of the theoretical 50 MPa. These coarse meshes are shown in Figure 20.17.

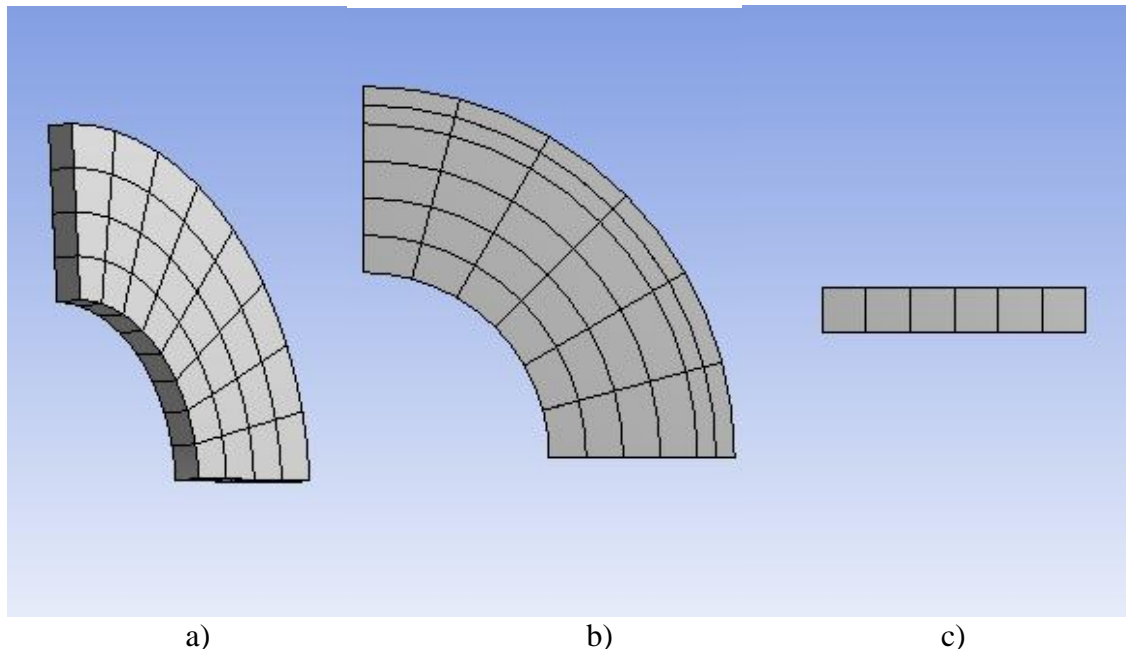


Figure 20.17: 3D, 2D planar-deformation, and the minimum number of element in case of 2D axis-symmetric model with respect of 5% of error

The number of elements and nodes related to each models:

| Model type            | Number of elements | Number of nodes |
|-----------------------|--------------------|-----------------|
| Body                  | 32                 | 287             |
| 2D planar deformation | 36                 | 133             |
| 2D axis-symmetric     | 6                  | 33              |

According to these results we can draw the same conclusions as earlier: the axes-symmetry model provides the most precise result with the least computation time.

## **21. EVALUATION AND APPLICATION OF COMPUTATIONAL RESULT IN DESIGN AND QUALIFICATION RELATED MECHANICAL ENGINEERING TASKS. RELATIONSHIP BETWEEN FINITE ELEMENT METHOD AND STANDARDIZED STRENGHT BASED DESIGN.**

### **21.1. Precision of Finite Element Method**

The Finite Element method is adequate to obtain approximation result about an engineering problem. The necessary accuracy of the approximation depends on the application and production of the structure or body, and it determines the quantity of the calculation. Considering the practice, the appropriate accuracy of the result should be in the range of 5% of error, although some cases demand even more accurate solution. In many cases, not even the loads are known precisely, thus this error appears in the solution independently from the method of calculation. Now, we are going to investigate the accuracy of calculation in case of given boundary conditions. The accuracy of the result could be easily calculated if we knew the exact solution, unfortunately apart from some simple problems, these exact solutions cannot be obtained thus we have to estimate the error. If we know the magnitude of the error and it does not meet the requirements, then the accuracy can be still improved. Mainly, there are two methods to improve the accuracy. The first one – already introduced in the earlier chapter – is based on the size reduction of the elements, which is called  $h$ -type approximation. The other method is based on choosing higher-order approximating polynomials, then we are talking about  $p$ -type approximation. The reduction of the element size and the increase of polynomial order can be combined as well ( $hp$ -type approximation).

The attainable accuracy of a given boundary value problem – solved by finite element method – is mainly determined by the applied parameters (element type, size) during meshing. In order to determine the accuracy of the solution, we have to calculate the difference between the exact  $\underline{u}$  displacement field and the  $\underline{u}_{FEM}$  displacement field which is calculated by finite element method.

The question is, that if the exact solution is unknown, how can we determine

$$\underline{e} = \underline{u} - \underline{u}_{VEM} \quad (21.1)$$

error? The problem can be solved by investigating the relationship between the degree of freedom ( $N$ ) of the finite element model and the norm of the error.

The energy norm of the displacement function can be defined as follows:

$$\|\underline{u}\| = \sqrt{U} . \quad (21.2)$$

Where  $U$  is the deformation energy:

$$U = \frac{1}{2} \int_V [\underline{\varepsilon}]^T \underline{\sigma} dV .$$

We can utilize the geometric equation:

$$\underline{\varepsilon} = \underline{\underline{\partial}} \underline{u}$$

and the constitutive equation:

$$\underline{\sigma} = \underline{\underline{C}} \underline{\varepsilon} = \underline{\underline{C}} \underline{\underline{\partial}} \underline{u} .$$

Where

$\underline{\underline{\partial}}$  : matrix of differential orders,

$\underline{\underline{C}}$  : matrix of material constants.

Then the deformation energy:

$$U = \frac{1}{2} \int_V [\underline{\varepsilon}]^T \underline{\sigma} dV = \frac{1}{2} \int_V [\underline{\underline{\partial}} \underline{u}]^T \underline{\underline{C}} \underline{\underline{\partial}} \underline{u} dV . \quad (21.3)$$

The energy norm of the exact solution:

$$\|\underline{u}\| = \sqrt{U} = \left( \frac{1}{2} \int_V [\underline{\underline{\partial}} \underline{u}]^T \underline{\underline{C}} \underline{\underline{\partial}} \underline{u} dV \right)^{\frac{1}{2}} . \quad (21.4)$$

And the energy norm of the error:

$$\|\underline{e}\| = \left( \frac{1}{2} \int_V [\underline{\underline{\partial}} \underline{e}]^T \underline{\underline{C}} \underline{\underline{\partial}} \underline{e} dV \right)^{\frac{1}{2}} . \quad (21.5)$$

With the finite element method we need a kinematically admissible displacement field (sum of functions with finite variable), which provides energy minimum. This requirement satisfies the following equation as follows:

$$\|\underline{u} - \underline{u}_{VEM}\| = \min \left\| \underline{u} - \underline{u}^* \right\| , \quad (21.6)$$

Thus:

$$\|\underline{e}\| = \min \left\| \underline{u} - \underline{u}^* \right\| . \quad (21.7)$$

Where according to  $\underline{u}^*$  and (21.7)  $\|\underline{e}\|$  depends on the element size and the order of the applied polynomials, thus it contains  $N$  unknown parameters. Depending on the choosing the increase of polynomial order or the decrease of element size, the result – given by the finite element method – converges differently to the exact solution.

### 21.1.1. Estimation of error in case of h-type approximation

The  $h$ -type approximation means that – during the discretization – we reduce the element size but we do not vary the order of the approximate polynomials. Let us investigate how the error varies as a function of element size in case of a beam with  $l$  length! Let us discretize the beam to  $N$  number of elements with identical length. The length of one element is:

$$h = \frac{l}{N}. \quad (21.8)$$

The approximate solution of  $u(x)$  exact displacement field is  $u_{VEM}(x)$ , which is a piecewise function. This function provides equal values with the exact solution in the interpolation points.

$$u(jh) = u_{VEM}(jh), \quad j = 0, 1, \dots, N. \quad (21.9)$$

The error of approximation in the  $i^{\text{th}}$  element:

$$e_i(x) = u(x) - u_{VEM}(x), \quad x \in [(i-1)h; ih], \quad i = 1, 2, \dots, N. \quad (21.10)$$

If the solution is continuously differentiable, then the error function as well. According to (21.9) the error is zero in the boundaries of the elements, and this continuity follows that the error function will have an extrema inside the element. The location of the  $|e_i|$  error is denoted with  $x_i$  (Figure 21). In this point

$$e'_i(x_i) = 0. \quad (21.11)$$

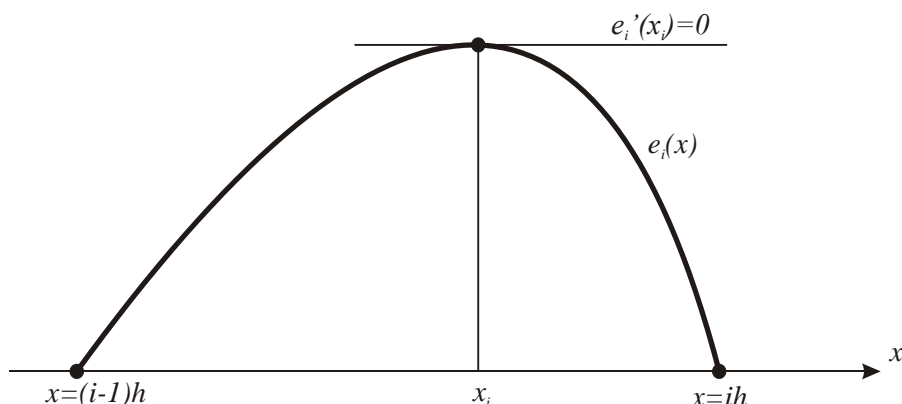


Figure 21.1: Error function in the  $i^{\text{th}}$  element

$u_{VEM}(x)$  linear, thus  $u_{VEM}''(x) = 0$ , then

$$e_i'(x) = \int_{x_i}^x e_i''(\xi) d\xi = \int_{x_i}^x u''(\xi) d\xi, \quad x \in [(i-1)h; ih].$$

If  $|u''| \leq C$ , then

$$|e_i''(x)| \leq C, \quad x \in [(i-1)h; ih], \text{ and} \quad (21.12)$$

$$\max(e_i'(x)) \leq C \cdot h, \quad x \in [(i-1)h; ih]. \quad (21.13)$$

Let us expand the  $e_i(x)$  function in the  $x_i$  point into Taylor series (using the Lagrange form of the remainder as well):

$$e_i(x) = e_i(x_i) + (x - x_i)e_i'(x_i) + \frac{(x - x_i)^2}{2} e_i''(\xi). \quad (21.14)$$

If the maximum of the error function is located in the second half of the element,

$$ih - x_i \leq \frac{h}{2}, \quad (21.15)$$

then:

$$e_i(ih) = 0 = e_i(x_i) + (ih - x_i)e_i'(x_i) + \frac{(ih - x_i)^2}{2} e_i''(\xi), \quad \xi \in [x_i; ih].$$

substituting (21.11) and (21.12):

$$0 = e_i(x_i) + (ih - x_i) \cdot 0 + \frac{(ih - x_i)^2}{2} e_i''(\xi). \quad (21.16)$$

from (21.16), utilizing (21.12) and (21.15):

$$\max|e_i(x_i)| = \max\left|\frac{(ih - x_i)^2}{2} e_i''(\xi)\right| \leq \frac{h^2}{8} C. \quad (21.17)$$

If the maximum of the error is located in the first half of the element, then the Taylor series have to be investigated at  $x = (i-1)h$ , where the value is zero, thus we obtain the (21.17) equation.

The deformation energy of the beam:

$$U(u) = \frac{1}{2} \int_0^l (AE(u')^2) dx, \quad (21.18)$$

The deformation energy of the error:

$$U(e) = \frac{1}{2} \int_0^l (AE(e')^2) dx = \frac{1}{2} \sum_{i=1}^n \int_{(i-1)h}^{ih} (AE(e'_i)^2) dx \leq \frac{1}{2} nh (AEC^2 h^2),$$

taking into consideration that  $n \cdot h = l$ , and the summing the constants the norm of the error is:

$$\|e\| = \sqrt{U(e)} \leq k_1 Ch. \quad (21.19)$$

In this formula the  $k_1$  constant is known, and by knowing the solution of the finite element model  $C$  can be estimated with small error.  $h$  stands as element size. In accordance with this result, the error of the solution is proportional to the element size. If we wish to estimate the error before solving the problem, then we have to summarize the constants. Then the maximum value of the error cannot be calculated due to not knowing  $C$  constant, but the convergence of the result will be visible. From (21.19) and (21.8):

$$\|e\| \leq \frac{k}{N}. \quad (21.20)$$

In many problems related to the practice, the displacement functions are not smooth functions. Then the relationship between the norm of the error and the number of elements changes as follows:

$$\|e\| \leq \frac{k}{N^\beta}, \quad (21.21)$$

where  $\beta$  depends on the  $p$  order of the approximate polynomials, and the  $\lambda$  character of the solution.

$$\beta = \frac{1}{2} \min(p, \lambda). \quad (21.22)$$

Stricter condition if not only the norm of the error, but the error itself is investigated on the total domain. In some cases it is possible that the norm of the error monotonically converges, but the solution is not monotonic. This can be only noticed if not only the global, but the local error is investigated.

In Figure 21.2 a thin plate is bent, and the energy and solution convergence is examined. The plate has 1mm thickness and 1Nm moment is applied on it. Since the load of the plate is co-planar, it is modeled as a planar stress problem as well.

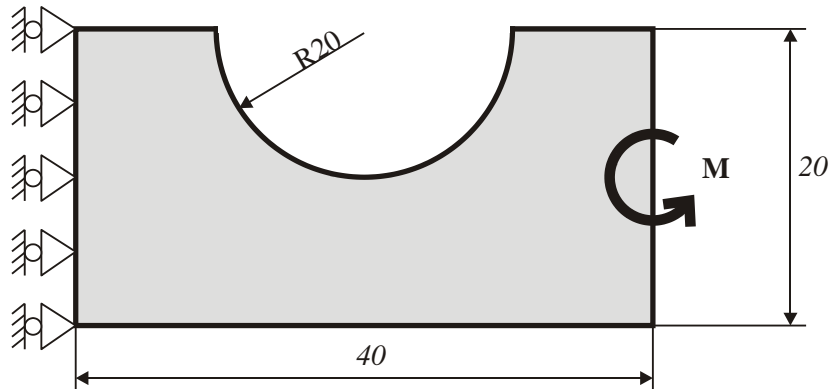


Figure 21.2: Bent plate

The finite element model is used to investigate the  $h$ -type convergence, thus the element size varies between 1 and 5 mm, while the order of the approximate polynomials stay unchanged. The convergence is examined with linear- and quadratic interpolation functions as well.

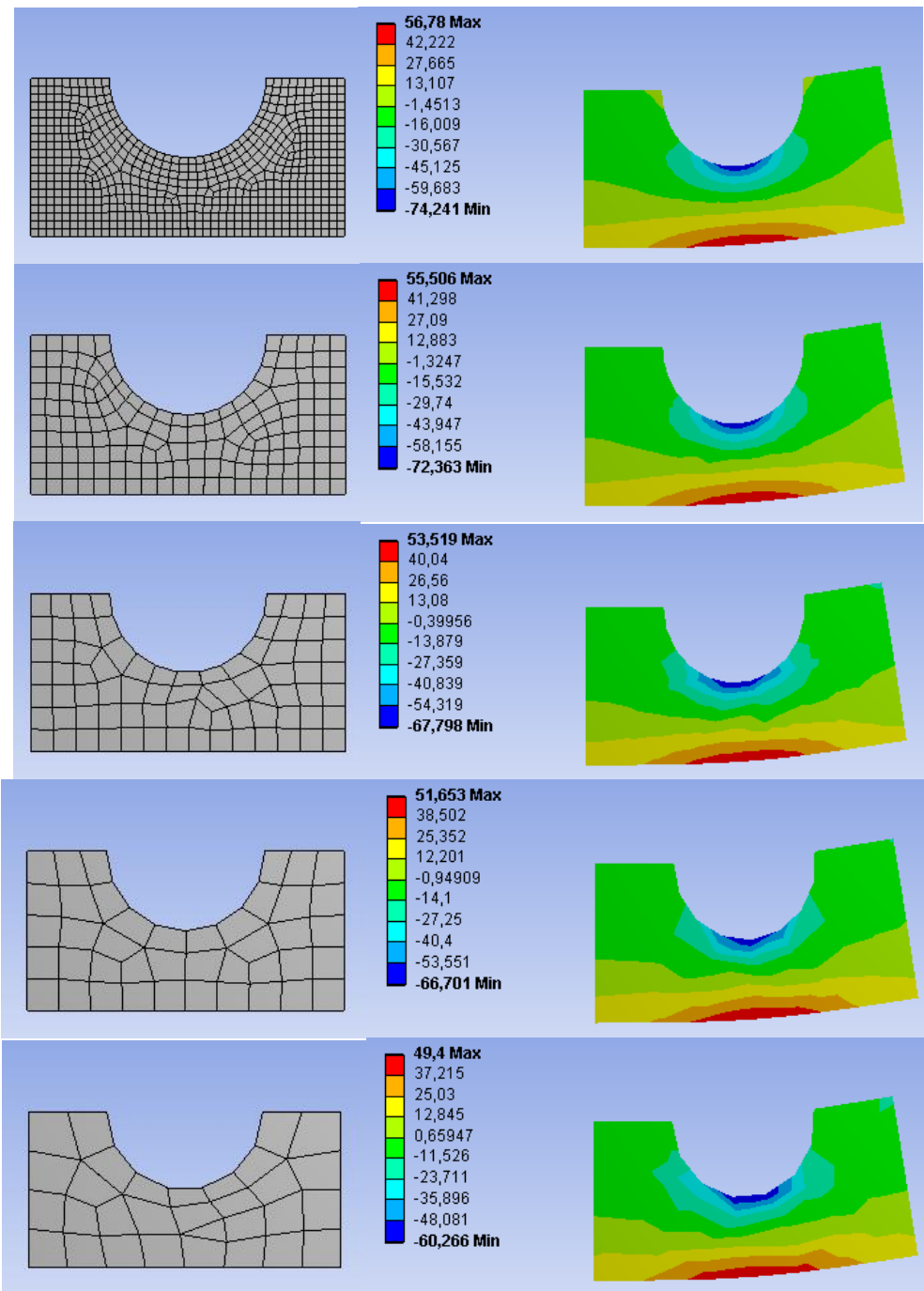


Figure 21.3: FEM mesh and normal stresses in MPa (element size of 1, 2, 3, 4, 5mm)

In the following table, the necessary parameters and results are summarized in order to examine convergence.

| Average element size [mm]             | N degree of freedom | Max. Stress [MPa] | Min. Stress [MPa] | Energy norm [ $\sqrt{mJ}$ ] |
|---------------------------------------|---------------------|-------------------|-------------------|-----------------------------|
| $p = 1$ (linear approximate function) |                     |                   |                   |                             |
| 1                                     | 2052                | 56,78             | -72,24            | 0,770136                    |
| 2                                     | 591                 | 55,51             | -72,36            | 0,766342                    |
| 3                                     | 306                 | 53,52             | -67,8             | 0,760592                    |
| 4                                     | 180                 | 51,65             | -66,7             | 0,754844                    |
| 5                                     | 135                 | 49,4              | -60,27            | 0,745319                    |

In this case, both the calculated stress and the energy norm monotonically converged by increasing the degree of freedom of the model (Figure 21.4).

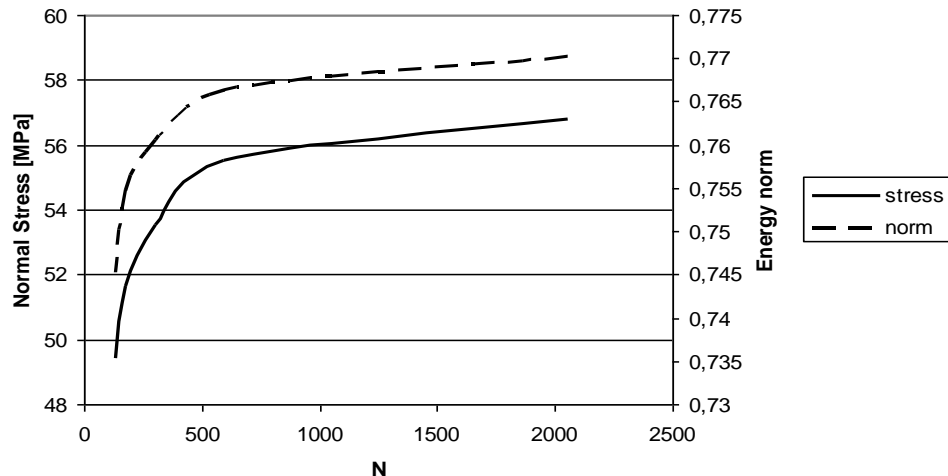


Figure 21.4: Result in the crucial point and the norm calculated on the complete domain

In this case, the error estimation can be determined according to the norm of the error function, thus it does not cause local problem.

Let us examine how the results change in case of quadratic approximate functions! The model was executed with the same parameters and element sizes as earlier (Figure 21.5).

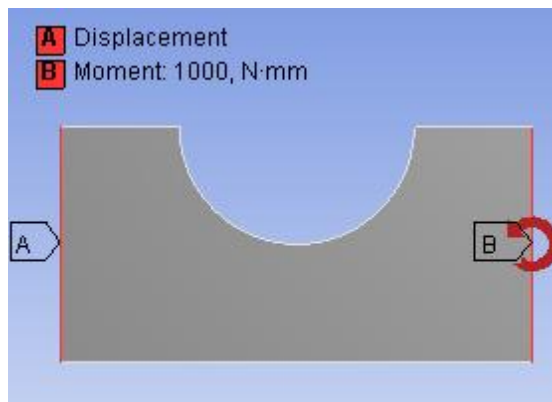


Figure 21.5: Model and boundary conditions

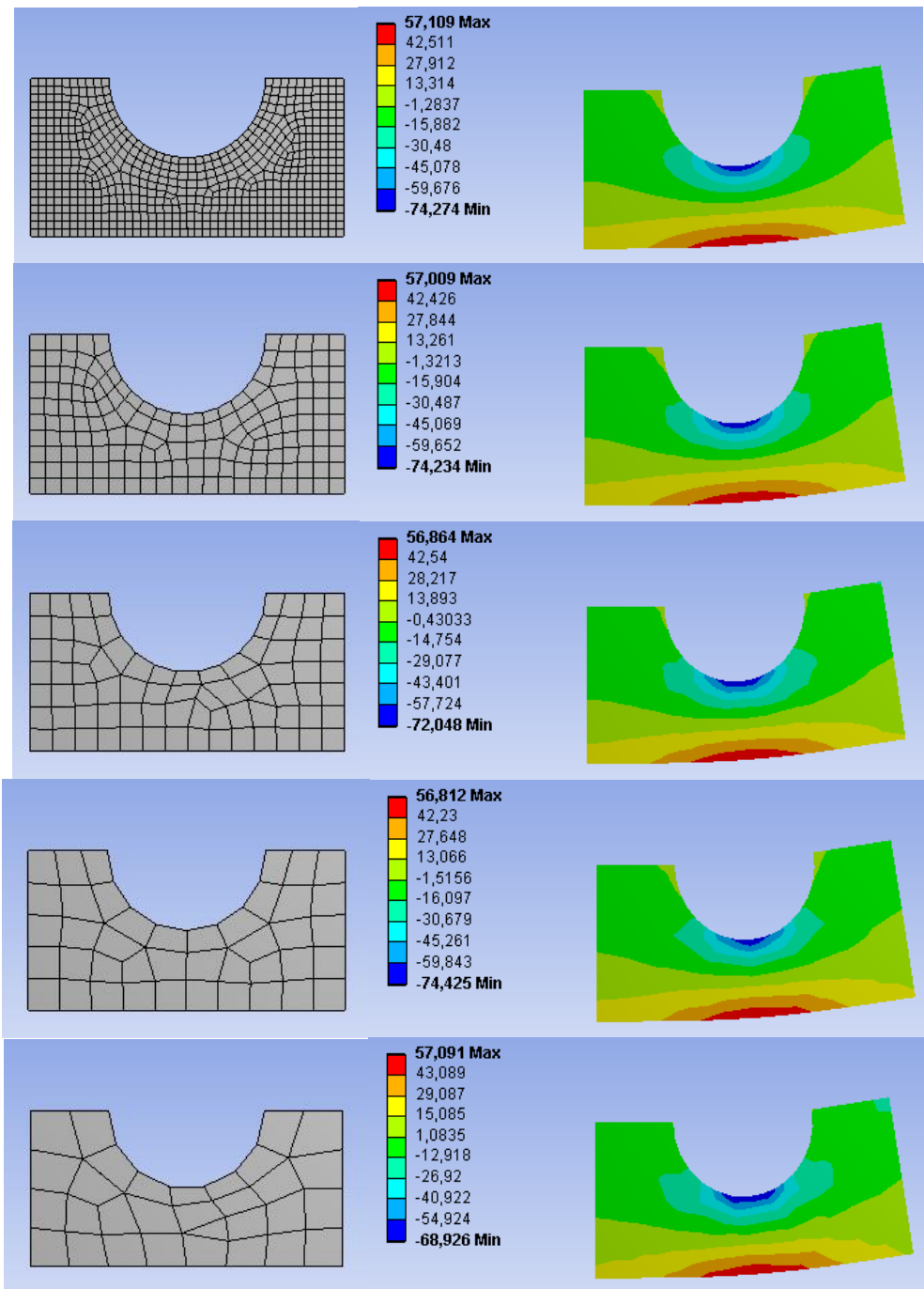


Figure 21.6: FEM mesh and normal stresses in MPa (element size of 1, 2, 3, 4, 5mm)

The obtained results with quadratic approximate function are summarized in the following table.

| Average element size [mm]                | N degree of freedom | Max. Stress [MPa] | Min. Stress [MPa] | Energy norm [ $\sqrt{mJ}$ ] |
|--|---------------------|-------------------|-------------------|-----------------------------|
| $p = 2$ (quadratic approximate function) |                     |                   |                   |                             |
| 1  | 5946                | 57,11             | -74,27            | 0,771466                    |
| 2  | 1623                | 57                | -74,23            | 0,77144                     |
| 3  | 843                 | 56,86             | -72,05            | 0,771349                    |
| 4  | 483                 | 56,81             | -74,43            | 0,771136                    |
| 5  | 360                 | 57,09             | -68,93            | 0,770824                    |

By examining the results we can draw the similar conclusion as earlier; the increase of the degrees of freedom resulted convergence. Although, while the norm monotonically converges through the complete domain, the stress converges with oscillation in the crucial point. (Figure 21.7). In this certain case, if we wish to estimate whether the solution is close to the exact or not, then it only up to luck how sever error we will make.

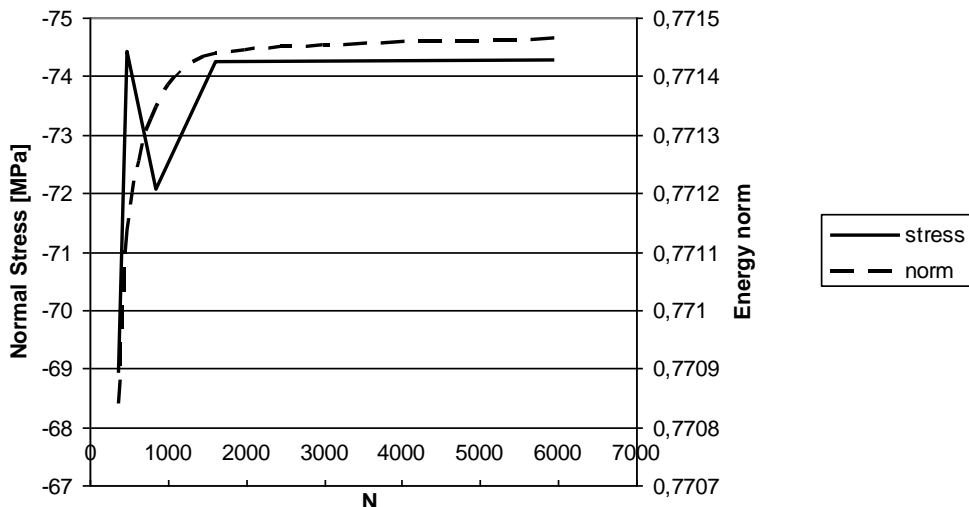


Figure 21.7: Result in the crucial point and the norm calculated on the complete domain

### 21.1.2. Calculation of error in case of h-type approximation

The error of an approximate solution cannot be exactly determined due to the unknown constant in (21.19). After the calculation, by knowing the approximate solution, the rela error can be determined.

According to (21.21):

$$\|e\| \leq kN^{-\beta},$$

and

$$\|\underline{e}\|^2 = \|\underline{u}\|^2 - \|\underline{u}_{VEM}\|^2, \quad (21.23)$$

then:

$$\|\underline{u}\|^2 - \|\underline{u}_{VEM}\|^2 \leq k^2 N^{-2\beta} \quad (21.24)$$

$k$  value is unknown, but by having the solution of the same problem with two different element sizes, the real error can be deduced.

Let us name the number of the unknown values at the first approximation as  $N_1$ , the approximate solution as  $\underline{u}_{VEM1}$ , and at the second approximation:  $N_2$  and  $\underline{u}_{VEM2}$ .

According to (21.24) both approximation are valid:

$$\|\underline{u}\|^2 - \|\underline{u}_{VEM1}\|^2 \leq k^2 N_1^{-2\beta}, \quad (21.25)$$

$$\|\underline{u}\|^2 - \|\underline{u}_{VEM2}\|^2 \leq k^2 N_2^{-2\beta}. \quad (21.26)$$

Let us deduce the energy of the exact solution from (21.25) in case of equilibrium:

$$\|\underline{u}\|^2 = \|\underline{u}_{VEM1}\|^2 + k^2 N_1^{-2\beta}, \quad (21.27)$$

and from (21.26) the  $k^2$  value:

$$k^2 = \frac{\|\underline{u}\|^2 - \|\underline{u}_{VEM2}\|^2}{N_2^{-2\beta}}. \quad (21.28)$$

Substituting (21.28) to (21.27) and setting the equation:

$$\|\underline{u}\|^2 = \frac{\|\underline{u}_{VEM1}\|^2 - \|\underline{u}_{VEM2}\|^2 \left( \frac{N_2}{N_1} \right)^{2\beta}}{1 - \left( \frac{N_2}{N_1} \right)^{2\beta}}. \quad (21.29)$$

By knowing the exact energy the real error can be determined from (21.23). This type of error estimation is called '*posteriori*' meaning '*estimation after calculation*'.

Let us examine the exact solution derived from the (21.29) formula, related to the problem in Figure 21.2. To determine  $\|\underline{u}\|^2$  value, the consecutive approximate solutions are taken into account:

$$\|\underline{u}\|^2 = \frac{\|\underline{u}_{VEMi}\|^2 - \|\underline{u}_{VEM(i-1)}\|^2 \left( \frac{N_{(i-1)}}{N_i} \right)^{2\beta}}{1 - \left( \frac{N_{(i-1)}}{N_i} \right)^{2\beta}} \quad (21.30)$$

The investigation is carried out by using linear approximate functions in case of  $\beta = 0,5$ . The results of the FEM approximation and the exact solution – calculated according to (21.30) formula – are summarized in the following table:

| i | Average element size [mm] | N degree of freedom | $\ \underline{u}_{VEMi}\ ^2$ [mJ] | $\ \underline{u}\ ^2$ [mJ] |
|---|---------------------------|---------------------|-----------------------------------|----------------------------|
| 1 | 0,5                       | 7788                | 0,59464                           | -                          |
| 2 | 1                         | 2052                | 0,59311                           | 0,595187                   |
| 3 | 2                         | 591                 | 0,58728                           | 0,595468                   |
| 4 | 3                         | 306                 | 0,5785                            | 0,596707                   |
| 5 | 4                         | 180                 | 0,56979                           | 0,590943                   |
| 6 | 5                         | 135                 | 0,5555                            | 0,61266                    |

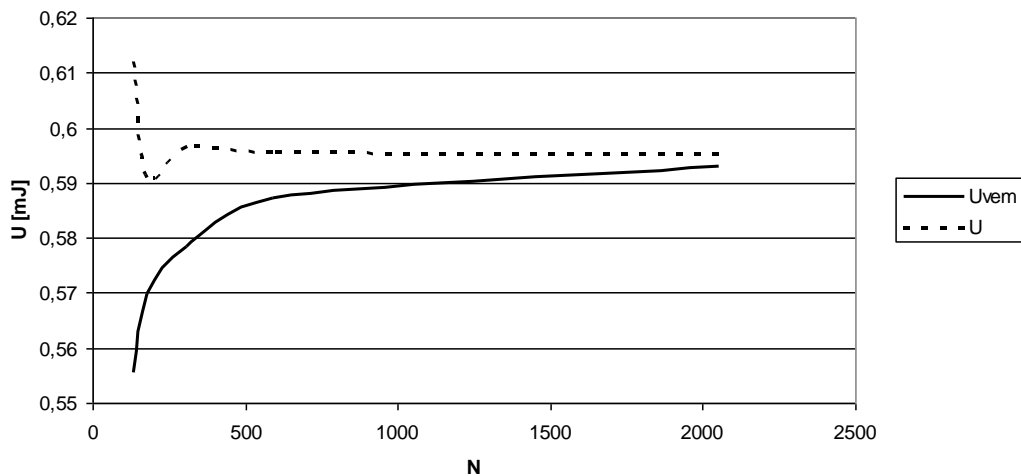


Figure 21.8: Approximate energy and the calculated exact energy as a function of N, linear approximation  $\beta = 0,5$

The calculated results are plotted in Figure 21.8, which shows that the exact solution can be derived from (21.29) with small error. The calculated result in case of rough discretization is not accurate, highly fluctuates, but soon it converges to the constant exact solution. By the increase of element numbers the solution has some deviation but does not alter significantly.

The results of the FEM approximation and the exact solution – calculated according to (21.30) formula – are summarized in the following table, with quadratic approximate function where,  $\beta = 1$ .

| i | Average element size [mm] | N degree of freedom | $\ \underline{u}_{VEMi}\ ^2$ [mJ] | $\ \underline{u}\ ^2$ [mJ] |
|---|---------------------------|---------------------|-----------------------------------|----------------------------|
| 1 | 1                         | 5946                | 0,59516                           | -                          |
| 2 | 2                         | 1623                | 0,59512                           | 0,595163                   |
| 3 | 3                         | 843                 | 0,59498                           | 0,595172                   |
| 4 | 4                         | 483                 | 0,59465                           | 0,595141                   |
| 5 | 5                         | 360                 | 0,59417                           | 0,59525                    |

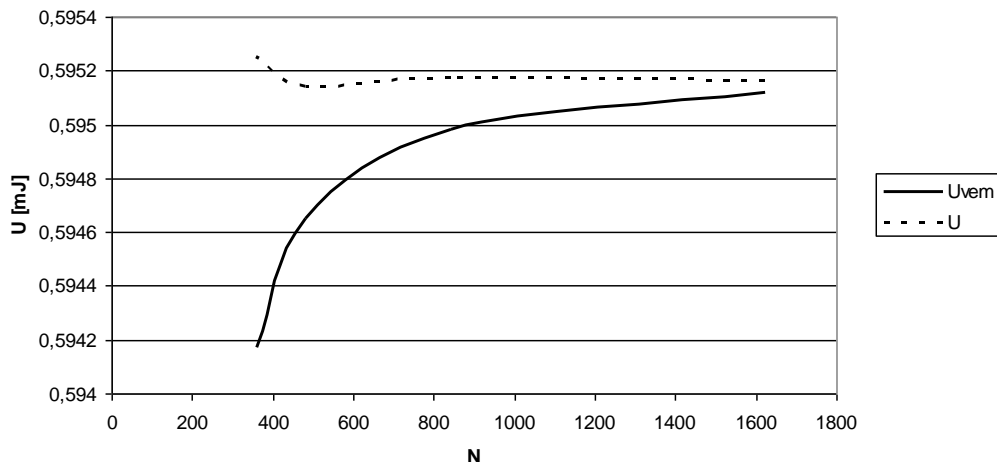


Figure 21.9: Approximate energy and the calculated exact energy as a function of  $N$ , quadratic approximation  $\beta = 1$

As it is seen in Figure 21.9, the calculated exact energy converges to a constant value sooner and with smaller error if quadratic approximate functions are used.

We can draw the following conclusion by comparing the results: the exact solution can be calculated by using two approximate solution – independently from the type of approximate functions – with small error.

### 21.1.3. $p$ -type approximation

The convergence of the solution particularly depends on the meshing, as we discussed earlier. The decrease of the element size in the mesh influences the accuracy of the solution as it was demonstrated earlier. If we do not change the element size, but increase the order of the interpolation functions, then we are talking about  $p$ -type approximation. The convergence of this approximation is exponential:

$$\|\underline{u} - \underline{u}_{VEM}\| \leq \frac{k}{\exp(\gamma N^\delta)},$$

where,

$k$ ,  $\gamma$ ,  $\delta$  positive constants.

The  $p$ -type approximation proves to be much faster in convergence than the  $h$ -type. The combination of the two types – the so-called hp-type approximation – provides the fastest

convergence, when both the number of elements and the order of the approximate functions are increased.

#### 21.1.4. Convergence in singular locations

In case of singular locations, the earlier introduced error calculation method cannot be applied since the (21.14) equation only works with analytical functions. According to the discretization the problems are distinguished into three categories:

1. category:  $\underline{u}$  is analytic on every elements and their boundaries thus it can be expanded into Taylor series,
2. category: inside the element  $\underline{u}$  is analytic, except some points in the boundaries,
3. category: the singular point can be anywhere in the element.

The estimation of error in case of specific 2D cases is summarized in the following table [Páczelt 1999.]:

|                          | 1. category                                       | 2. category                                       | 3. category                               |
|--------------------------|---|---|---|
| $h$ -type approximation  | $\ \underline{e}\  \leq kN^{-p}$                  | $\ \underline{e}\  \leq kN^{-\beta}$              | $\ \underline{e}\  \leq kN^{-\beta}$      |
| $p$ -type approximation  | $\ \underline{e}\  \leq k \exp(-\gamma N^\delta)$ | $\ \underline{e}\  \leq kN^{-\lambda}$            | $\ \underline{e}\  \leq kN^{-0.5\lambda}$ |
| $hp$ -type approximation |   | $\ \underline{e}\  \leq k \exp(-\gamma N^\delta)$ |   |

#### 21.1.5. Modeling mistakes

In Chapter 21.1, the introduced error estimation and accuracy improving techniques are suitable to determine the error and enhance the accuracy related to the finite element – numerical – method. The modeling mistakes cover more than that, since the error due to the false mechanical model creation appears in the solution as well independently from the solving method.

### 21.2. Evaluation of the calculated results

#### 21.2.1. Stresses beyond yield strength

The linear elastic constitutive equation is not adequate to model stresses beyond the yield strength, plastic constitutive model is required. If we use a yield strength-based method, we intend to avoid stresses beyond the yield point. It is not all the time possible to fulfill this idea completely. One of these cases is the contact stress or so-called Hertz-stress. In this case, stresses beyond the critical value appear only in the direct contact area, causing plastic deformation on the surface, but not complete structural damage. If we use plastic constitutive model, the rate of this deformation can be determined and by knowing the operation conditions we can also decide if this deformation permissible or not. In case of highly complex models, when even the linear calculation is problematic, the nonlinear problems become simply impossible in those certain conditions. This problem requires simplification on some area of the model, and we have to decide whether the obtained results are more accurate or not.

Crossing the yield strength is sometimes part of the test operation in case of certain structures. Some manufacturers – in order to simplify the production – produce simple cylindrical heating covers for tanks. During the test, the heating cover is pressurized by several times greater pressure than the operation pressure. This loading causes plastic deformation, thus the cover takes on the ideal form. With this form the stresses will not cross the threshold of the yield stress during operation condition. This approach makes the linear model completely unsuitable even for rough approximation.

### 21.2.2. *Singular locations*

Geometric singularities generally appear during the geometric modeling. Real structures or bodies do not have sides or corners with zero radii. Although it appears many times that we have several sides and corners with small (sometimes unknown) radii, which we are not aware of or it is just simply not relevant to describe with precise geometry. In these cases we do not model these rounding, but we have to take them into consideration in the solution. At the edges, if there is no connection with other bodies than it causes no problem either, but if it is, then we have to deal with it.

The boundary conditions – especially the kinematical boundary conditions of ideal constraints – frequently cause singularity problems in the boundary of the domain. By defining a prescribed displacement on a certain surface, the displacement constraint on the edge of the surface vanishes without any transition. Singular location appears when the constraint does not reach the boundary of the body's surface. Then the body reacts as it was connected to an infinitely rigid and sharp body. This problem can be evaded by using the original elastic body instead of the constraint, although the computation time notably increases since the model is expended with a contact problem. In addition, if we wish to model this problem with realistic frictional relationship, then the small displacement theory cannot be used either. Due to these existing problems, many times we are forced to use some simpler models and taking the singularities into consideration.

Those singular locations where the stresses are small cause no problem, since they reduce the computation time and higher relative error can be also accepted. In the aspect of the load, problems occur due to the critical points of the structure, since the design is based on these hot-spots, thus the absolute error will be significant as well. In addition the solution will not converge in the close area of these problematic parts, and the more accurate finite element models will only result higher stresses and strains.

### 21.2.3. *Standardized methods and the FEM*

Standards provide mainly guidelines to determine boundary conditions. Applied loads in case of individual fields, safety factors, material constants are determined by experimentally or from practical fields rather for classic analytical methods.

The standardized values of loads assume that the required accurate method is not in hand. Typical example is the standardized wind-load. To determine the wind-load, the applicable wind velocity is prescribed. This is also required for the FEM. Although it is also prescribed what to apply in case of cylindrical, flat, truss, splay structures, and what concrete pressure distribution must be calculated with. These prescribed values were determined analytically or experimentally, naturally not functions but simplified tables and graphs are derived from them

and presented with the standard loads. During the application – in order to have a carry out safe design – the factors must involve the influence of the difference between the real structure and the standardized structure. If finite element method – related to the fluid dynamics – is used to determine the loads then we obtain more accurate results than the standardized. By using the prescribed factors, the safety factor will be higher than the one which is based on the standardized calculation. In such a case, the safety factor cannot be reduced arbitrary. If the standards took the FEM into consideration in case of wind-load modeling, then it would prescribe a turbulent model – with its own increase factor – beside the wind velocity and the wind density.

We can draw the general conclusion, that the standards do not satisfy or solve the special needs and upcoming questions in the practice of finite element method. The engineers still have to lean on their own experiences when they model a structure or prescribe the boundary conditions. This is the source of the upcoming problems in the practice of FEM.